CONFIDENTIAL

REFERENCE ONLY

UNIVERSITY OF LONDON THESIS

Degree PhD Year 2005 | Name of Author HUGHES, G.A

COPYRIGHT

This is a thesis accepted for a Higher Degree of the University of London. It is an unpublished typescript and the copyright is held by the author. All persons consulting the thesis must read and abide by the Copyright Declaration below.

COPYRIGHT DECLARATION

I recognise that the copyright of the above-described thesis rests with the author and that no quotation from it or information derived from it may be published without the prior written consent of the author.

LOANS

Theses may not be lent to individuals, but the Senate House Library may lend a copy to approved libraries within the United Kingdom, for consultation solely on the premises of those libraries. Application should be made to: Inter-Library Loans, Senate House Library, Senate House, Malet Street, London WC1E 7HU.

REPRODUCTION

University of London theses may not be reproduced without explicit written permission from the Senate House Library. Enquiries should be addressed to the Theses Section of the Library. Regulations concerning reproduction vary according to the date of acceptance of the thesis and are listed below as guidelines.

A. Before 1962. Permission granted only upon the prior written consent of the author. (The Senate House Library will provide addresses where possible).

B. 1962 - 1974. In many cases the author has agreed to permit copying upon completion of a Copyright Declaration.

C. 1975 - 1988. Most theses may be copied upon completion of a Copyright Declaration.

D. 1989 onwards. Most theses may be copied.

This thesis comes within category D.

☐ This copy has been deposited in the Library of _____

☑ This copy has been deposited in the Senate House Library, Senate House, Malet Street, London WC1E 7HU.

NOVEL, POTENT ANTAGONISTS OF CAPSAICIN

by

GLYN ALAN HUGHES

Thesis submitted in accordance with

the requirements of the University of London,

for the degree of Doctor of Philosophy.

Department of Chemistry,

University College, London

June 2005

ProQuest LLC
789 East Eisenhower Parkway
P.O. Box 1346
Ann Arbor, MI 48106-1346

Abstract

The aim of this project was to explore and refine the conformational rationale for the activity of capsazepine (CPZ) as a blocker of the ion channel TRPV1 (transient receptor potential vanilloid type 1), by the synthesis and biological evaluation of further conformationally constrained capsaicin analogues.

The resolution of the stereoisomers of *N*-(4-chlorophenethylthiocarbamoyl)-6,7-dihydroxy-1-methyl-1,2,3,4-tetrahydroisoquino-line **29**, *N*-(4-chlorophenethylthiocarbamoyl)-6,7-dihydroxy-3-methyl-1,2,3,4-tetra-hydroisoquinoline **30** and *N*-(4-chlorophenethylthiocarbamoyl)-6,7-dihydroxy-1,3-dimethyl-1,2,3,4-tetrahydroisoquinoline **31** by stereoselective synthetic methodology is described, and some of the more unusual and interesting mechanisms are discussed.

The novel asymmetric chemistry described includes the separation of the enantiomers of 2-(3,4-dimethoxyphenyl)-1-methylethylamine **38** by crystallisation with the enantiomers of mandelic acid, the use of sodium triacetoxyborohydride in the stereoselective reduction of 6,7-dimethoxy-1,3-dimethyl-3,4-dihydroisoquinoline **171**, to give the *cis*-diastereomers of 6,7-dimethoxy-1,3-dimethyl-1,2,3,4-tetrahydroisoquinoline **44**, and the novel stereoselective route to the *trans*-diastereomers of 6,7-dimethoxy-1,3-dimethyl-1,2,3,4-tetrahydroisoquinoline **44** from the enantiomers of 2-(3,4-dimethoxyphenyl)-1-methylethylamine **38** by the Michael addition of *N*-benzyl-2-(3,4-dimethoxyphenyl)-1-methylethylamine **155** to ethynyl-4-tolylsulfone **150**, followed by TFA-mediated cyclisation, single electron reductive desulfonylation and palladium-catalysed hydrogenolysis.

The results of investigations into the conformational behaviour of the resolved stereoisomers of **29**, **30** and **31** by techniques of NMR spectroscopy and molecular modelling, the evaluation of their biological activity at the rat and human orthologues of the ion channel TRPV1, and the attempted correlation of the two sets of data, with respect to the published conformational rationale for the activity of CPZ, are also described.

The biological evaluation of these compounds has identified one analogue **31(1*S*,3*R*)** with a similar activity profile to CPZ, which has allowed a more accurate definition of the requirements for biological activity akin to CPZ at the human and rat orthologues of TRPV1. In addition, four analogues (**29*S***, **30*R***, **30*S*** and **31(1*S*,3*S*)**) have been identified with potent antagonism (IC_{50}<100nM) of capsaicin-induced

activation of the human orthologue of TRPV1, and potent agonism (EC_{50}<60nM) of the rat orthologue of TRPV1. Compounds possessing opposing activities for different mammalian orthologues of TRPV1 have not been described previously in the literature.

Table of Contents

Index of Tables

Index of Figures

Acknowledgements

I would like to begin by expressing my gratitude to my supervisors.

At NIMS, Dr. C. S. J. Walpole for getting me started and Dr. A. J. Culshaw for his willingness to take up the reins of supervision, his patience and his tireless proof reading, and at UCL, Professor C. R. Ganellin for his guiding hand throughout this project.

Thanks to Alex Groarke, Clare Davis, Marcus Peacock, Nadia Korniotis and Wai Lee for their various contributions in providing me with the biological data; thanks to Grety Rihs for the X-ray crystal structure analysis and Tim Ritchie for some fruitful discussions about molecular modelling. I would also like to thank Peter McIntyre for his support and willingness to discuss the varied aspects of TRP biology with me.

More generally, I would like to thank the many members of staff at NIMS who, over the years, have provided me with results, information, support, coffee and biscuits.

Thanks to those weekend warriors who, over the years, have helped to make Sundays at NIMS more bearable, particularly Graham, Caroline, Sarah F and Sarah B.

Thank you to the Pitfield Brewery for their phenomenal XXXX Stock Ale, and the Beer Essentials in Horsham for stocking it.

Finally, to my long-suffering wife; Lisa, for everything, I thank you.

Abbreviations

5-HT	serotonin
AM	Acetoxymethyl
AMPA	α-amino-3-hydroxy-5-methyl-4-isoxazoleproprionate
ATP	adenosine triphosphate
BK	bradykinin
cDNA	complementary deoxyribonucleic acid
$[Ca^{2+}]_i$	intracellular calcium ion concentration
CaMKII	Ca^{2+}/calmodulin-dependent kinase II
CGRP	calcitonin gene-related peptide
CHO	Chinese hamster ovary
CIP	Cahn-Ingold-Prelog
CNS	central nervous system
COX	cyclooxygenase
CPZ	capsazepine
DRG	dorsal root ganglion
ECF	extracellular fluid
EI	electron impact ionisation
ESI	electron spray ionisation
FBS	foetal bovine serum
GPCR	G protein coupled receptor
HBSS	Hank's balanced salt solution
HCN	hyperpolarization-activated cyclic nucleotide-gated
HEK	human embryonic kidney
HETE	hydroxyeicosatetraenoic acid
HEPES	4-(2-hydroxyethyl)-1-piperazineethanesulfonic acid
HPETE	hydroperoxyeicosatetraenoic acid
HPLC	high performance liquid chromatography
HRMS	high resolution mass spectroscopy
HTM	high threshold mechanoreceptor
hTRPV1	human orthologue of TRPV1
HTS	high throughput screening
IASP	International Association for the Study of Pain

IBTU	*N*-(4-chlorobenzyl)-*N'*-(4-hydroxy-3-iodo-5-methoxybenzyl)thiourea
IR	infra red
LTM	low threshold mechanoreceptor
MEM	minimum essential medium
MES	2-(*N*-morpholino)ethanesulfonic acid
mRNA	messenger ribonucleic acid
MS	mass spectroscopy
NK1	neurokinin 1, the substance P receptor
NMDA	*N*-methyl-*D*-aspartate
NMR	nuclear magnetic resonance
PAN	primary afferent neurone
PDN	painful diabetic neuropathy
PG	prostaglandin
PHN	post-herpetic neuralgia
PMN	polymodal nociceptor
PNS	peripheral nervous system
rTRPV1	rat orthologue of TRPV1
RTX	resiniferatoxin
SAR	structure-activity relationship
TFA	trifluoroacetic acid
TLC	thin layer chromatography
TRP	transient receptor potential
TRPV1	transient receptor potential vanilloid type 1
VR1	vanilloid receptor, subtype 1

To my ladies

Lisa and Caitlin.

INTRODUCTION

Pain, Capsaicin and TRPV1

Pain is 'one of the most challenging problems in medicine and biology' Ronald Melzack and Patrick D Wall [1].

It is 'a more terrible lord of mankind than even death itself.' Albert Schweitzer[2]

'The conquest of pain remains...the most important task...of every medical man' Cornelius Medvei[3]

The briefest perusal of the relevant literature from just the past fifty years reveals the topic of pain to be of enormous interest and immensely complex, both in the proposed biological mechanisms contributing to the sensation of pain, and in the proposed means of intervention. Many journal papers, reviews, books and textbooks have been written on and around the subject, from a multitude of perspectives. Despite the wealth of ongoing research and available information, many aspects of the sensation of pain remain unchallenged by current therapies.

As of October 2002, the National Pain Education Council (www.npecweb.org) estimated that more than 50million Americans are partially or totally disabled by chronic pain, with 7-10million (15-20%) having no treatment for that pain.

An increasingly significant field for both academic and industrial research into understanding the underlying mechanisms of the sensation of pain, and developing new pain therapies, is the ion channel *transient receptor potential, vanilloid type 1* (TRPV1), also known as the *vanilloid receptor, subtype 1* (VR1), or the *capsaicin receptor*. Initially studied indirectly through the effects of its exogenous agonist capsaicin, this ion channel has been the focus of a considerable amount of attention for over forty years, with fresh research and in depth review articles appearing with increasing frequency. So, what is pain, and where does TRPV1 fit in?

The Sensation of Pain

Pain is a general term, covering a broad spectrum of sensation. The International Association for the Study of Pain (IASP) has given the concise, generic definition of pain as "an unpleasant sensory and emotional experience associated with actual or potential tissue damage, or described in terms of such damage"[4].

Pain has two distinct components: the sensory, and the emotional. At its simplest, a potentially damaging noxious stimulus is detected by the pain receptors, or *nociceptors*[5], of the peripheral nervous system (PNS), and is communicated to the higher brain centres of the central nervous system (CNS). Here it is analysed, interpreted and, if categorised as painful, a suitable response is formulated. The sensory aspect of pain, *i.e.* the detection of noxious stimuli and the cascade of physiological and biochemical events that this can trigger, are a consistent component of the sensation of pain. The emotional aspect of pain, *i.e.* the interpretation of these stimuli as pain, can be highly variable, and specific to the individual.

Pain has been categorised in various ways:

- qualitatively, according to severity, from mild discomfort to agony;
- temporally, as transient (accompanying a noxious stimulus), acute (accompanying the healing process), and chronic (prolonged, persisting beyond the normal time of healing);
- mechanistically, as physiological, or pathological[6], and more recently as nociceptive, inflammatory and neuropathic[7].

The final approach will be followed herein.

While attempting to cover the entire complexity of current pain knowledge would be impossible, a brief résumé of the more pertinent physiological and biochemical principles and mechanisms involved would be appropriate, with much of the basic foundations for the preparation of this overview being drawn from the following key textbooks:

Biochemistry, 2nd edition, L. Stryer, (1988);

Ion Channels in Excitable Membranes, 3rd edition, B. Hille (2001);

Molecular Biology of the Cell, 1st edition, B. Alberts, D. Bray, J. Lewis, M. Raff, K. Roberts and J. D. Watson (1983);

Neuroscience: Exploring the Brain, 2nd edition, M. F. Bear, B. W. Connors, and M. A. Paradiso (2001);

Sensory Mechanisms of the Spinal Cord, 2nd edition, W. D. Willis, Jr. and R. E. Coggeshall (1991);

Textbook of Pain, 4th edition, edited by P. D. Wall and R. Melzack (1999).

Pain in the Periphery - Nociception[8]

The detection of noxious stimuli is a function of the *somatic sensory nervous system*, a collective term for the parts of the nervous system dedicated to the senses of touch, temperature, proprioception and pain. Unlike the other senses, where the receptors are concentrated in small, specialised sense organs, the receptors of the somatosensory system are distributed throughout the body, being found in skin, bone, muscle, most internal organs, blood vessels, and the heart.

Stimulation of the peripheral receptors of the somatic sensory nervous system is communicated to the CNS via the sensory *primary afferent neurones* (PANs). PANs have processes, or *axons*, extending from the receptors in the periphery to the superficial layers of the spinal cord, where they terminate within the dorsal horn; their cell bodies lie outside the CNS, in the dorsal root ganglia (DRG) (see Figure 1).

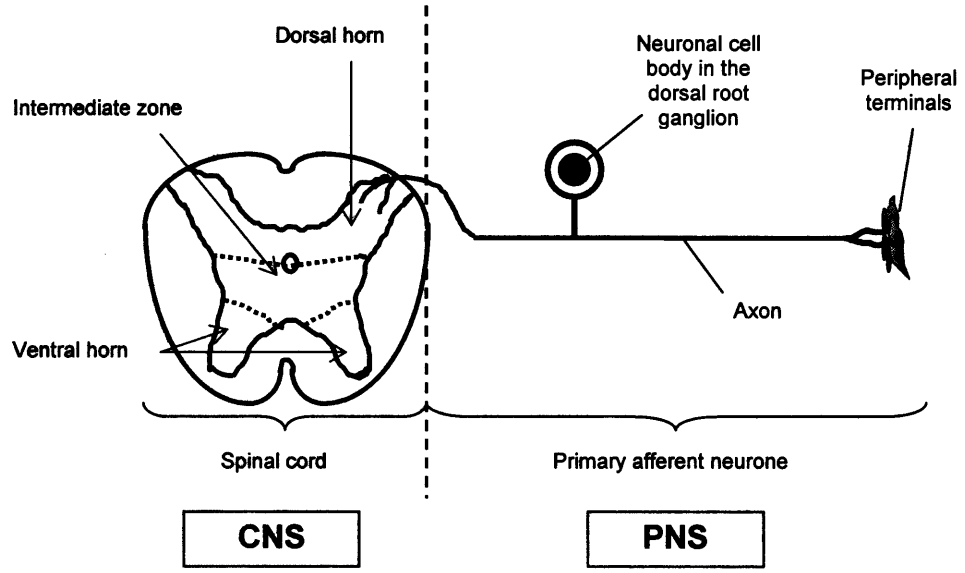

Figure 1: A schematic overview of PAN architecture, from the PNS to the CNS.

Subtypes of Primary Afferent Neurones of the Somatic Sensory System[8]

There are four categories of axon, divided according to diameter. The diameter is a function of the degree of myelination an axon has, and the greater the degree of myelination of an axon, the faster the speed of conductance of the action potential along that axon. The speed of conductance of an axon, and the type of sensory receptors they are associated with, are mutually interdependent, and determine the sensory function they perform. Three of the four categories of PAN, as described by axon diameter, have been determined to have a role in pain (see Figure 2).

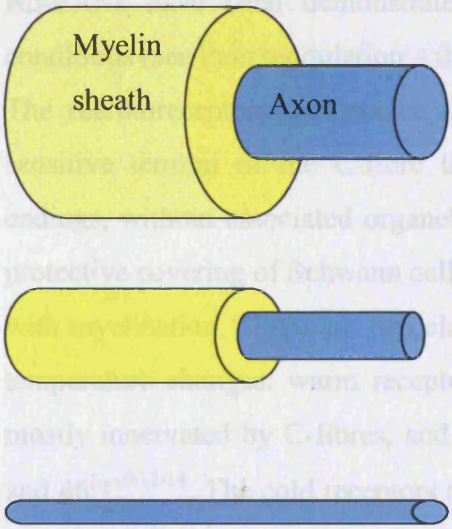

Aβ-fibres:
heavily myelinated;
6-12μM diameter;
conductance: 35–75ms^{-1}.

Aδ-fibres:
lightly myelinated;
1-5μM diameter;
conductance: 5–30ms^{-1}.

C-fibres:
unmyelinated;
0.2-1.5μM diameter;
conductance: 0.5–2ms^{-1}.

Figure 2: Schematic representation of subtypes of primary afferent neurones of the cutaneous somatic sensory system.

In addition to characterisation by cross-sectional diameter, the primary afferent neurones of the cutaneous somatic sensory system are also categorised by their response to different stimuli, the degree of stimulation (or threshold) necessary to cause activation, and thereby their presumed physiological role[9]. There are mechanoreceptors (responding to either innocuous (low threshold) or noxious (high threshold) pressure or displacement), thermoreceptors (activated by innocuous changes in temperature), and the 'pain' receptors. It has been noted that stimulation of the pain-sensing apparatus of the somatic sensory system does not itself constitute pain. To distinguish this stimulation of the pain-sensing apparatus from the emotional perception of pain, the term 'nociception' (from the Latin *nocere*-'to hurt') was adopted[5]. Neurones activated by noxious stimuli are therefore described as 'nociceptive receptors', or nociceptors.

The low threshold mechanoreceptors (LTM) and their associated organelles, (generally named after histologist who discovered them: *e.g.* Krause end bulbs, Merkel's discs, Meissner's corpuscles, Pacinian corpuscles, and Ruffini's endings) are predominantly innervated by Aβ-fibres, and, as the name suggests, they have a low threshold of activation, responding to non-noxious stimulation of the skin (touch)[10]. However, while not directly involved in the detection of noxious stimuli,

Aβ-PANs have been demonstrated to play a significant role in chronic pain conditions (see Pain modulation – the Gate-Control Theory of Pain).

The thermoreceptors and nociceptors are associated with Aδ- and C-fibres. The sensitive termini of the C-fibre thermoreceptors and nociceptors are free nerve endings, without associated organelles; those associated with Aδ-fibres may have a protective covering of Schwann cells[11], the non-neuronal glial support cell associated with myelination. There are two classes of thermoreceptor responding to innocuous temperature changes: warm receptors and cold receptors. The warm receptors are mostly innervated by C-fibres, and activate with increasing intensity between 30°C and 46°C[9;12-14]. The cold receptors are innervated by Aδ- or C-fibres, and respond to temperatures between 10°C and 35°C[9;14-16].

Capsaicin, an Exogenous Noxious Chemical Stimulus

Noxious stimuli can be broadly sub-divided into:

- *mechanical*, relating to pressure upon, and displacement of, the receptor;
- *thermal*, both hot and cold;
- *chemical*, both endogenous and exogenous in nature.

Of the exogenous chemical mediators of pain and nociception, one of the most widely investigated has been **capsaicin.** It is the principle pungent ingredient of the chilli peppers (*Capsicum spp.*), and the progenitor of the vanilloids (see Figure 3). This family of neuroexcitants is a diverse group of exogenous compounds with agonist activity at the capsaicin receptor (VR1/TRPV1). The name 'vanilloid' derives from the common vanillyl substitution pattern of the aromatic ring seen in the original members of the group:

- capsaicin, derived from chilli peppers (*Capsicum spp.*);
- piperine, derived from black pepper;
- zingerone, obtained from ginger; and, more recently,
- resiniferatoxin (RTX), obtained predominantly from the latex of *Euphorbia resinifera*[17].

RTX has proven itself to be of particular interest; it is frequently described as an 'ultrapotent vanilloid', being anything up to 10,000-fold more potent than capsaicin in some assays[17;18].

Once believed essential for activity, more recently discovered 'vanilloids' of fungal origin, including isovelleral[19] a terpenoid possessing a 1,4-dialdehyde moiety, and scutigeral[20] a non-pungent triprenyl phenol, demonstrated that the requirement for a vanillyl moiety is not absolute.

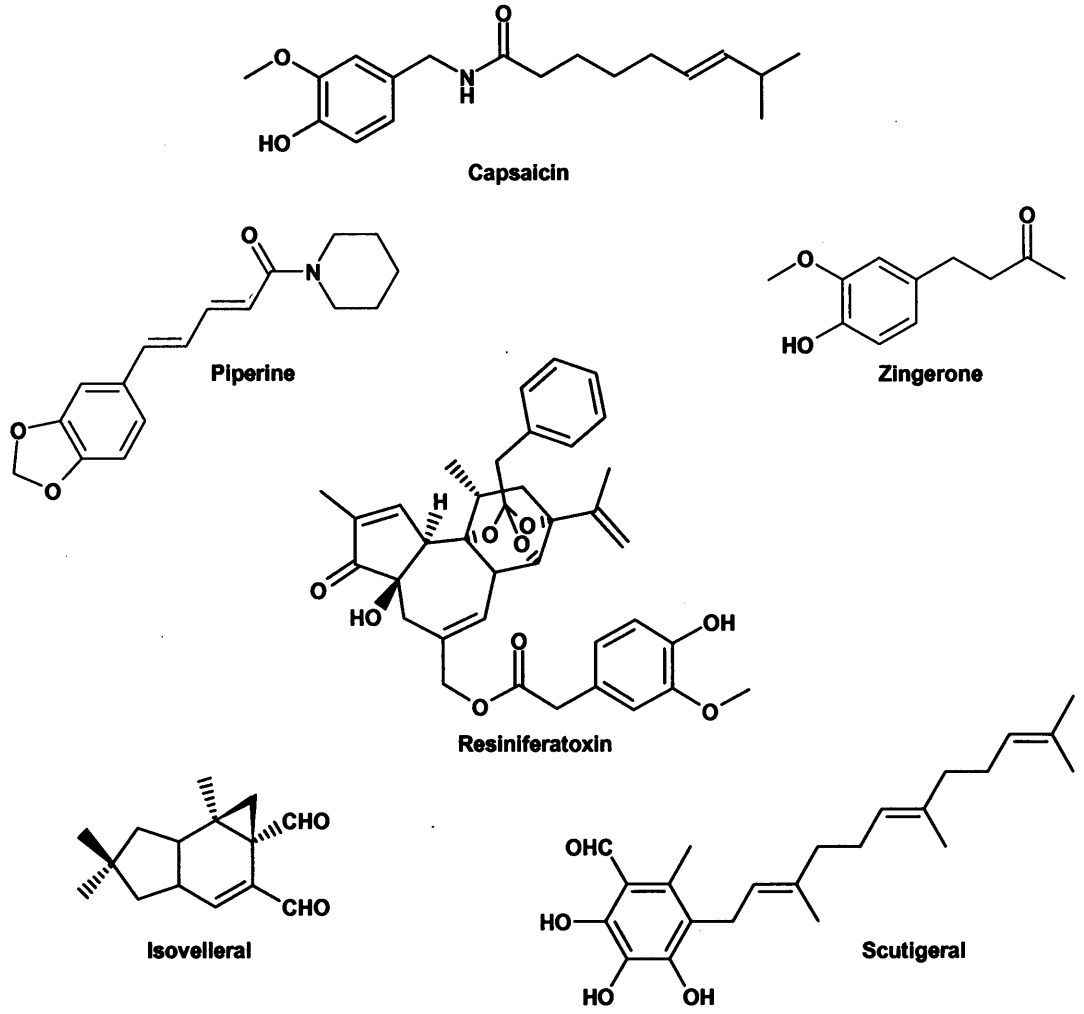

Figure 3: Examples of the vanilloids.

Early Vanilloid Pharmacology

Investigations into the isolation, structural elucidation and functional exploration of the vanilloid progenitor, capsaicin, began in the latter half of the nineteenth century. Derived from cayenne, this 'pungent principle' was first crudely isolated as a thick red oil, termed 'capsicol' (Buchheim, see Thresh[21]), from which was derived a colourless crystalline solid, termed 'capsaicin'[21-24].

During the original isolation of capsaicin, the extreme irritancy caused by exposure to the compound was noted. In the case of the mucous membranes, inhalation of the volatilised compound caused 'severe fits of coughing' and 'long continued fits of

sneezing'[21]. In the direct application of a capsaicin solution to the skin, the application to the arm of lint soaked in a solution of one part capsaicin to forty parts of spirit and glycerine caused 'an unbearable sensation of warmth and reddened inflammation, without blistering'[22]. The results of the ingestion of one-eighth of a grain dose of capsaicin in a coated pill were also reported, and two hours after ingestion, the subject experienced violent burning pains in the stomach, assuaged by 'copious drafts of demulcents'.

In 1878, it was reported that the burning sensation experienced when an alcoholic solution of the crude isolate capsicol was dropped on the skin was the result of a selective activation of sensory neurones (Högyes[25], from Szolcsányi[26]), and was reported to be accompanied by hyperaemia (an excess of blood at the site) (Högyes[25], from Toh *et al.*[27]).

These combined experiences illustrated the two aspects of painful sensation caused by exposure to capsaicin; firstly, exposure causes an acute nociceptive response, and secondly, a neurogenic inflammatory response.

Capsaicin has other *in vivo* biological effects. It has potent effects upon the cardiovascular and respiratory systems. Early experiments showed capsaicin to exert a potent hypotensive action in the anaesthetised dog[28], with later experiments extending these results. The *i.v.* administration of capsaicin to anaesthetised cats and dogs produced a 'triad' of hypotension (lowering of blood pressure), bradycardia (abnormally low rate of heart contraction) and apnoea (the temporary cessation of breathing)[27;29;30].

Capsaicin has a profound effect upon thermoregulation. It was reported that, while low doses of capsaicin induced a sudden transient drop in the rectal temperature of mice[31;32], rats and guinea pigs[33] (*hypothermia*)[34], higher doses of capsaicin actually *desensitise* the warmth response, such that thermoregulation is no longer possible for treated animals, even after one year[33;34].

Capsaicin and Sensory Neurones

The latter half of the nineteenth century saw the painful burning sensation resulting from exposure to capsaicin attributed to the specific actions of capsaicin upon sensory neurones[25]; it wasn't until the latter half of the twentieth century that further detailed explorations were made. The observation that nociceptive nerve endings were not only stimulated by capsaicin, but were disabled by high doses of capsaicin

(Janscó[35]; see Szolcsányi[26;36]) stimulated further exploration into the actions of capsaicin. The discovery of capsaicin's ability to *desensitise* sensory neurones to noxious chemical stimuli formed the basis for much of the later research into capsaicin, and analogues of capsaicin, as novel analgesics and anti-inflammatories.

Further experimentation demonstrated that parenterally (other than orally/rectally) or locally administered applications of high, prolonged or repeated doses of capsaicin cause animals to develop long-term, or even permanent, loss of sensitivity to a wide range of noxious chemical stimuli[37-42], as a result of selective degeneration of the capsaicin-sensitive primary afferent sensory neurones. This neurotoxic effect has allowed capsaicin to be widely used as a biological tool to investigate the properties of this discrete subset of PANs, by selectively damaging this neuronal subset and assessing the effects[43].

Nociceptor subtypes

As already noted, there are three broad categories of noxious stimuli, and the nociceptors are categorised according to the noxious stimuli that activate them. There are three main populations of nociceptor:

- those responding to 'damaging mechanical stimulation of the skin' only [44]; these high threshold mechanoreceptors, or HTMs, can be innervated by Aδ-fibres (hence Aδ-HTM)[44] [45] or C-fibres (C-HTM). Studies using rat skin found approximately 20% of Aδ-fibres, and 10-15% of C-fibres examined were HTMs[46;47]. Although normally insensitive to stimulation by noxious chemical or thermal stimulation, it is possible for a sub-population of these receptors to *become* heat sensitive, after repeated application of noxious heat[48]. These nociceptors are *unaffected* by capsaicin.
- those responding to noxious mechanical, thermal and chemical stimuli. Because of their multiple modalities of activation, these nociceptors are termed the polymodal nociceptors[49], or PMNs. They are predominantly innervated by C-fibres, although there is a small and significant sub-population innervated by Aδ-fibres[50;51]. The majority of the cutaneous nociceptors are polymodal; the polymodal nociceptors are the primary conduit for relaying the detection of nociception in the periphery to the CNS.

- those that are unresponsive to acute noxious stimulation, but can become 'sensitised' to respond to noxious chemical stimulation following tissue injury as a result of the inflammatory response (see Peripheral Sensitisation). These are the 'silent' nociceptors[52].

During the period that these nociceptors were being defined and described, the Hungarian laboratories working with capsaicin had begun to use the term 'capsaicin-sensitive afferents[53]. Comparative studies in rat[51;54], rabbit[55] and monkey[56] demonstrated that:

a) the capsaicin-sensitive afferents were comprised of polymodal nociceptors and warmth receptors, and
b) all of the polymodal nociceptors are capsaicin-sensitive, so much so that sensitivity to capsaicin is recognised as a pharmacological signature of the polymodal nociceptors.

For a fuller understanding of the actions of capsaicin, a consideration of the molecular components of nervous functioning, with particular reference to pain, is required.

Key Features of the Neuronal Membrane

As previously described, the PANs of the somatosensory nervous system, including the PMNs, have their cell bodies outside the CNS, in the DRGs. They have processes, or axons, extending from the receptors in the periphery to the superficial layers of the spinal cord, where they terminate within the dorsal horn (see Figure 1). The axons are essentially sealed hollow tubes, with the internal contents of the axon, or axoplasm, separated from the extracellular fluid (ECF), by the neuronal membrane. This membrane between the two fluids has as its basic structure the *phospholipid bilayer*[57;58]. As its name suggests, this barrier is composed of a double layer of phospholipids, a category of biological building block which is exemplified by the phosphoglycerides (see Figure 4). These molecules have a central glycerol molecule, to which is attached a charged functionality, in the form of a phosphorylated alcohol, and two long chain fatty acids (usually 14 to 24 carbons long), bound to the glycerol as esters. Individual phospholipids are therefore amphipathic, having a hydrophilic 'head' region and a hydrophobic 'tail' region.

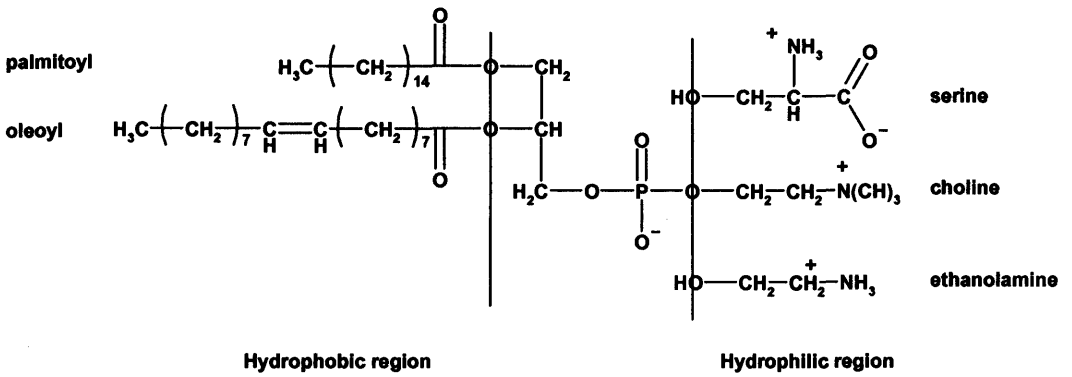

Figure 4: Representation of the more common components of the phosphoglycerides.

In an aqueous environment, their amphipathic characteristics require such molecules to form composite structures that effectively exclude water from the non-polar hydrophobic domains, while allowing the polar hydrophilic domain to continue to associate with the water. One such composite structure is a sheet, of two molecules in thickness, with the hydrophilic heads forming the outer surfaces of the sheet, sandwiching the hydrocarbon tails. The hydrophobic interior of this phospholipid bilayer makes it effectively impermeable to ions.

Embedded within this phospholipid bilayer are two categories of biological macromolecular complex which span the membrane and permit the passage of ions across the membrane. These are the *ion pumps* and the *ion channels*. These membrane proteins are constrained within the plane of the membrane, but are free to diffuse laterally within the membrane in a 'fluid mosaic'[59].

Ion Pumps

The hydrophobic interior of the phospholipid bilayer makes it effectively impermeable to ions, allowing different concentrations of ions to exist on either side of the membrane, resulting in a difference in electrical potential across the membrane, which is key to neuronal function. Defined as the inside potential minus the outside potential[60], this *transmembrane voltage potential difference* (V_m) can be measured by inserting a microelectrode into the neurone. The value in the 'resting' axon is –65mV[57].

While the phospholipid bilayer is essentially impermeable to ions, there is leakage of ions in both directions. The resting value of V_m is maintained by the *ion pumps*, constructed from specialised transmembrane proteins that are 'dissolved' within the plasma membrane. The ion pumps *actively* carry ions across the membrane, *against*

existing gradients, to establish and maintain such gradients, at the expense of metabolic energy, generally in the form of adenosine triphosphate (ATP).

There are two ion pumps in particular that are key to neuronal function, These are:

- the sodium-potassium pump (for a review, see Skou[61]), which exchanges internal sodium ions for external potassium ions at the expense of ATP, ensures that the resting neurone has a much higher cytosolic than extracellular potassium ion concentration, and a much higher extracellular than cytosolic sodium ion concentration;
- the ATP-dependent calcium ion/proton exchange pump (for a review, see Carafoli[62]), which actively pumps calcium ions out of the neurone. This and other mechanisms responsible for sequestering intracellular calcium within calcium-binding proteins and organelles ensure that the level of calcium ions within the resting axon is extremely low (<0.2μM), while the extracellular concentration might be as high as 1mM.

These concentration differences mean that, at rest, the inside of the axon has a negative charge with respect to the outside of the cell. It is the function of these ion pumps to maintain or, when disrupted, restore the resulting electrical potential difference (V_m) to the resting potential of –65mV.

Ion Channels

A typical functional ion channel requires the association of four to six similar transmembrane protein subunits, to form a pore between them. Such pores are not simply holes in the membrane through which there is free and random movement for any passing chemical entity; the nature of the protein subunits determines the nature of the pore and its properties. Many ion channels are selectively permeable to a particular ion, giving preferential passage to their selected ion through the membrane. Also, most ion channels are not permanently open, as the movement of ions through ion channels must be a controlled process. The majority of ion channels are 'gated', opening and closing in response to conformational changes in their tertiary and quaternary structure caused by specific changes in their immediate microenvironment. When this change is a result of a change in the immediate transmembrane potential difference, the channel is said to be *voltage-gated.* If it is the result of interaction with a specific chemical entity, the channel is said to be *ligand-gated.*

In contrast to the ion pumps, the movement of ions through an open ion channel is passive and bidirectional. The net direction of the movement of ions is determined by the *electrochemical gradient*. This gradient is a combination of:

- the concentration gradient, with ions moving from a solution of a higher to a lower concentration; and
- the transmembrane voltage potential (V_m), with ions 'pulled' to the side of the membrane possessing the opposite charge.

Where these two gradients are contradictory, ions move to establish an equilibrium that balances these contributory factors, such that the diffusional and electrical forces are equal and opposite. For cations such as sodium and, in particular, calcium, where there is a steep concentration gradient into the cell and V_m of the resting membrane is negative, the driving force for the passive entry of these ions into the cell is extremely high.

Generation and Propagation of the Action Potential[63;64]

The first step in the detection of any stimulus requires the presence of that stimulus to be converted into the neuronal common currency of the *action potential*, by the process of *transduction*. The action potential is a brief, self-propagating *depolarisation* and *repolarisation* of the axonal membrane, during which V_m rises from –65mV, to +40mV (*depolarisation*), before dropping back again (*repolarisation*), over approximately 2 milliseconds[63]. The capacity to generate and conduct action potentials defines the membranes of neuronal cells as *excitable*[64]. The modern understanding and interpretation of the events occurring during the generation and conductance of an action potential arise from the classical analysis of ionic currents in the squid giant axon performed by Hodgkin and Huxley[65]. They were the first to recognise that the observed membrane currents of the excited squid giant axon required controlled, separate, voltage-dependent changes in membrane permeability toward different ions, specifically sodium and potassium. The agents of these permeability changes have been established to be the voltage-gated sodium ion channels and the voltage-gated potassium ion channels.

It has been noted that the internal concentration of ions in the resting neurone is maintained by ion pumps to ensure that:

- the concentration of potassium ions is higher internally than externally;

- the concentration of sodium and calcium ions is much lower internally than externally.

When an action potential is triggered, the voltage-gated sodium ion channels open, allowing a large influx of sodium ions into the cell. These channels are only open for approximately one millisecond, but this is long enough for V_m to rise from –40mV to +40mV. This change of membrane polarity, or *depolarisation* of the membrane, then *inactivates* the voltage-gated sodium channels, and stimulates the opening of the voltage-gated potassium channels. The resulting large efflux of potassium ions from the axon causes a *repolarisation* of the membrane, with V_m rapidly dropping back to below the resting potential of –65mV. This repolarisation closes the potassium channels, and is followed by the gradual restoration of V_m to the resting potential by the ATP-dependent sodium-potassium ion pumps, which work throughout to restore the original ionic concentration gradients.

Once generated, the action potential is communicated from the periphery to the CNS, by *conductance* of the action potential along the axons of the primary afferent neurones. The triggering of an action potential causes the opening of the voltage-gated sodium channels. The influx of sodium ions depolarises the adjacent section of membrane, until that too reaches threshold, and generates its own action potential. In this way, the action potential is propagated along the axon, as each action potential generates an action potential in the membrane adjacent to it. The direction of conductance is *orthodromic*, or unidirectional, away from the site of stimulation and toward the CNS, because the voltage-gated sodium channels at the site of an action potential are unable to open again until V_m has returned to the resting value of –65mV, resulting in the sodium channels 'behind' the action potential being inactivated until the local value for V_m has returned to the resting value of –65mV.

It is important that minor fluctuations in V_m either side of the resting potential do not stimulate an action potential. Therefore, for an action potential to be generated, it must be triggered by a rise in V_m from the resting potential of –65mV to above the *threshold* value of ≈–40mV. This initial change in the value of V_m requires a dedicated influx of cations, and this is the role of transduction. Noxious stimuli, whether mechanical, thermal or chemical, act to trigger the action potential by either directly or indirectly causing the opening of cation-selective channels in the neuronal membrane, resulting in an influx of cations (generally calcium and sodium) into the

cell, causing the value of V_m rises. A sufficiently large stimulus will cause a large enough influx of cations to cause V_m to rise beyond the *threshold*, and an action potential is triggered.

Capsaicin, the Capsaicin Receptor and TRPV1

In vitro mechanistic studies of the capsaicin-induced activation of PMNs, made using cultured DRG neurones and isolated PANs, demonstrated that exposure to capsaicin initiated an increase in membrane cation permeability, particularly to calcium and sodium[42;66-68]. As described, an increase in the non-selective cation permeability of the resting neuronal membrane results in a net movement of cations into the neurone, and a sufficiently large influx of cations triggers an action potential.

How does capsaicin do this? The highly selective nature of capsaicin's activity upon sensory neurones, coupled with the strict requirements for analogues of capsaicin to retain activity, implied mediation by a specific receptor. The first hypothetical pharmacological receptor for capsaicin, based upon SAR studies indicating critical moieties for binding, was presented by Szolcsányi and Jancsó-Gábor in 1975[69] (see Figure 5).

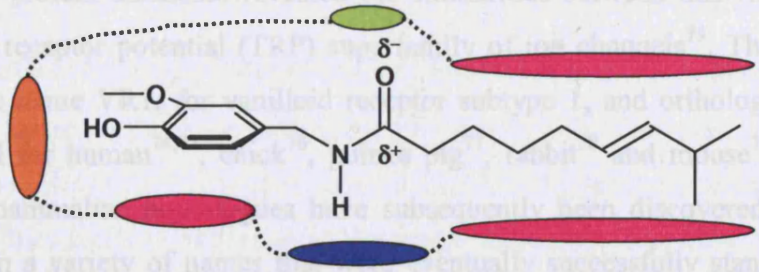

Key:							
●	H-bonding site for OH group	●	Electropositive site for the carbonyl oxygen	●	Electronegative site for the H of the NH group and the δ+ carbon	●	Apolar areas bound by van der Waals forces

Figure 5: Schematic representation of the hypothetical capsaicin receptor (after Szolcsányi and Jancsó-Gábor [69]).

Further evidence for the existence of a specific receptor to capsaicin came with the experimental evidence for capsaicin's activation of polymodal nociceptors occurring via the opening of a non-selective cation channel[42;66-68;70], and the discovery of the *competitive* antagonist to capsaicin-induced activation of the polymodal nociceptors, capsazepine (CPZ; see Figure 6)[71,72] (see The Discovery of Capsazepine - the First Competitive Antagonist of the Neuroexcitatory Action of Capsaicin).

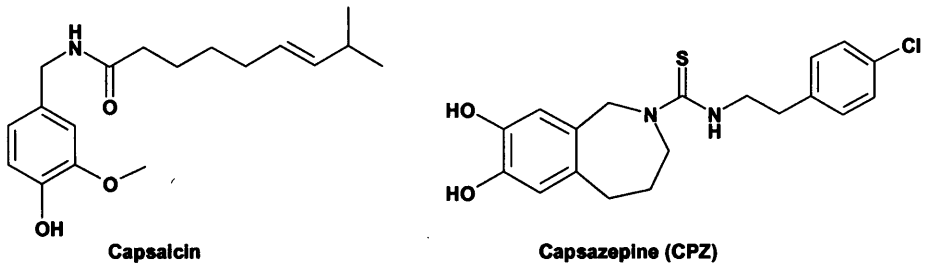

Figure 6: Capsaicin and the first competitive antagonist of capsaicin-induced activation of the polymodal nociceptors, capsazepine (CPZ).

The identity of the capsaicin receptor was determined by using a cDNA library constructed from rat DRG-derived mRNA to successfully isolate, clone and express a capsaicin-sensitive non-specific cation channel for the rat[73]. A homology search of available protein databases revealed the similarities between this receptor and the transient receptor potential (TRP) superfamily of ion channels[73]. The receptor was given the name VR1, for vanilloid receptor subtype 1, and orthologues have been identified for human[74;75], chick[76], guinea pig[77], rabbit[78] and mouse[79]. Five closely related mammalian homologues have subsequently been discovered (see Table 1), and given a variety of names that were eventually successfully standardised under the umbrella of the transient receptor potential vanilloid (TRPV) family of the TRP superfamily of ion channels, numbered one through six. As the progenitor of this branch, VR1 has become the transient receptor potential vanilloid type 1 (TRPV1) ion channel[80]. Despite the name, none of the other TRPV ion channels are sensitive to activation by capsaicin, or any of the vanilloids.

Unified nomenclature[80]	Alternative nomenclatures	
TRPV1	VR1	Vanilloid receptor subtype 1[73]
TRPV2	VRL-1	Vanilloid receptor-like 1[81]
TRPV3[82]		[83;84]
TRPV4	VR-OAC	vanilloid receptor-related osmotically activated channel[85];
	TRP12	Transient receptor potential 12[86]
	OTRPC4	Osm-9-like transient receptor potential channel 4[87]
TRPV5	ECaC1	Epithelial calcium channel 1
	CaT2	Calcium transporter 2
TRPV6	ECaC2	Epithelial calcium channel 2
	CaT1	Calcium transporter 1

Table 1: Members of the mammalian TRPV subfamily.

The Transient Receptor Potential (TRP) Superfamily of Ion Channels

The TRP superfamily of ion channels have recently been described as 'the vanguard of our sensory systems'[88], with individual TRP homologues responding to a range of thermal, mechanical and chemical stimuli allowing responses to changes in temperature, touch, pain, osmolarity, pheromones and taste[88;89]. With a couple of exceptions, the TRP channels have been found to be non-selective Ca^{2+} permeable cation channels. Many of the TRP channels are found to be expressed in neuronal membranes. As already described, the concentration of calcium ions within neurones is maintained at an extremely low level, by means of the ATP-dependent calcium pump and intracellular calcium sequestering. $[Ca^{2+}]_i$ can be as much as 20,000 fold lower than extracellular concentrations[90]. This extreme concentration gradient and electrical potential difference across the plasma membrane of the resting neurone constitute a powerful driving force for calcium ions to enter the cell. When TRP ion channels open in response to their respective aforementioned stimuli, the resulting influx of calcium ions leads to a sharp and decisive rise in $[Ca^{2+}]_i$, and with it the

value of V_m. As such, these ion channels are molecular transducers, translating changes in the extracellular environment into changes in the value of V_m, thereby elevating V_m to beyond the threshold value, 'kick-starting' the action potential (see Generation and Propagation of the Action Potential).

The existence of the first TRP channel was extrapolated from behavioural studies of a *Drosophila melanogaster* mutant. Despite exhibiting normal behaviour in dim light, this mutant strain appeared as though blind in bright light[91]. Electroretinograms, which record the changes in extracellular current flow in the eye in response to light, revealed that, while the wild-type fly has a constant change in receptor potential as a result of exposure to continuous bright light, the mutant shows only a temporary, or transient, change in receptor potential, hence *trp* mutant[91]. The mutation was deduced to be the result of a gene deletion[92], coding for a transmembrane protein[93], which was later demonstrated to be an ion channel[94].

Homologues of this ion channel have been found throughout the animal kingdom. The sequencing of entire genomes, coupled with advances in techniques of gene isolation and identification, have led to examples of TRP ion channels being identified in yeast[95-97], nematodes[98] and several mammalian species. With the identification of the first human homologue of the TRP ion channel (TRPC1)[99;100] and six TRP-related genes in the mouse genome[101] came a deluge of publications revealing new mammalian TRP ion channels. At the last count, there are upward of twenty eight human genes coding for TRP monomers[88;89], organised into six families, according to sequence homology.

As the number of recognised human TRP channels has increased, so the requirement for a unifying nomenclature for the TRP channels increased. Unlike most other ion channels, the TRP channels are not grouped according to their functional roles which, where they have been determined, are diverse. These channels are classified by identity in homologous regions of their sequence, some of which are highly conserved. The first attempt was based upon the 13 TRP channels of the nematode *Caenorhabditis elegans*, and divided the TRP channels into STRPCs (Short), LTRPCs (Long) and OTRPCs (Osm-9-like), as all TRPs known at the time could be grouped according to these three subfamilies[102]. As further TRPs were identified, the present generally accepted system was proposed and adopted[80]. The three original families of STRPC, OTRPC and LTRPC became TRPC (Canonical, or Classical), TRPV (Vanilloid) and TRPM (Melastatin) respectively, and these have been joined

by the TRPA (Ankyrin transmembrane protein), TRPP (Polycystins) and the TRPML (MucoLipins)[89].

None of the TRP proteins have been crystallised, so no crystal structures exist as yet. The currently accepted model for the generic TRP channel architecture has been deduced from the derived primary sequences of amino acids encoded for by the TRP genes, with regions of hydrophobicity and putative secondary structural organisation, as well as other recognised motifs, having been identified. Although the initial hydrophobicity analysis of the *Drosophila* TRP channel predicted eight transmembrane domains[93], subsequent analyses of the second *Drosophila* TRP (*trpl*, for *trp*-like)[103] and the first published human TRP channel (TRPC1)[99;104] revised the number of transmembrane domains to six. The currently accepted model has six hydrophobic domains that span the membrane (6TM), with an hydrophobic loop between the fifth and sixth transmembrane domains forming a putative pore domain (see Figure 7). An apparent lack of cell recognition sequences has led to the conclusion that the C and N termini are located intracellularly[102;105].

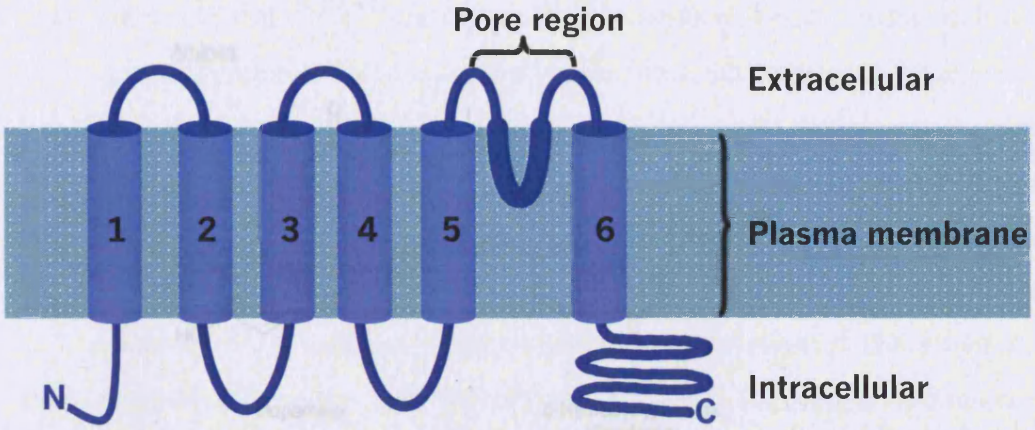

Figure 7: Diagrammatic representation of the putative architecture of the TRP channels.

The nature of these cytoplasmic regions is more varied, both in length and recognisable motifs. The TRPC and TRPM channels have a proline-rich region immediately after the sixth putative transmembrane sequence, and the TRPC, TRPV and TRPA channels have varying numbers of ankyrin-like repeats in the N-terminal region before the first transmembrane sequence[105]. The ankyrins are a family of proteins that 'coordinate interactions between various integral membrane proteins and cytoskeletal elements'[106]. Presumably the ankyrin-like repeats of the TRP channels fulfil a similar role. Their presence and number is one of the identifying

markers for characterising members of the TRP subfamilies (TRPC and TRPV have three or four; TRPA has fourteen[88]).

Comparison with the voltage-gated Ca^{2+} and Na^{+} ion channel families has also been used to predict the active TRP ion channel as homo- or heterotetrameric, comprised of four single TRP subunits[102].

Pain from the PNS to the CNS - Synaptic Transmission[107]

The axons of the primary sensory afferent neurones enter the spinal cord, via the *dorsal root*, and terminate within the superficial layers of the *dorsal horn* of the spinal cord. Here any action potential is relayed to *second-order neurones*, also called *projection neurones*, because they have axons which project up the spinothalamic tract to the higher centres of the CNS.

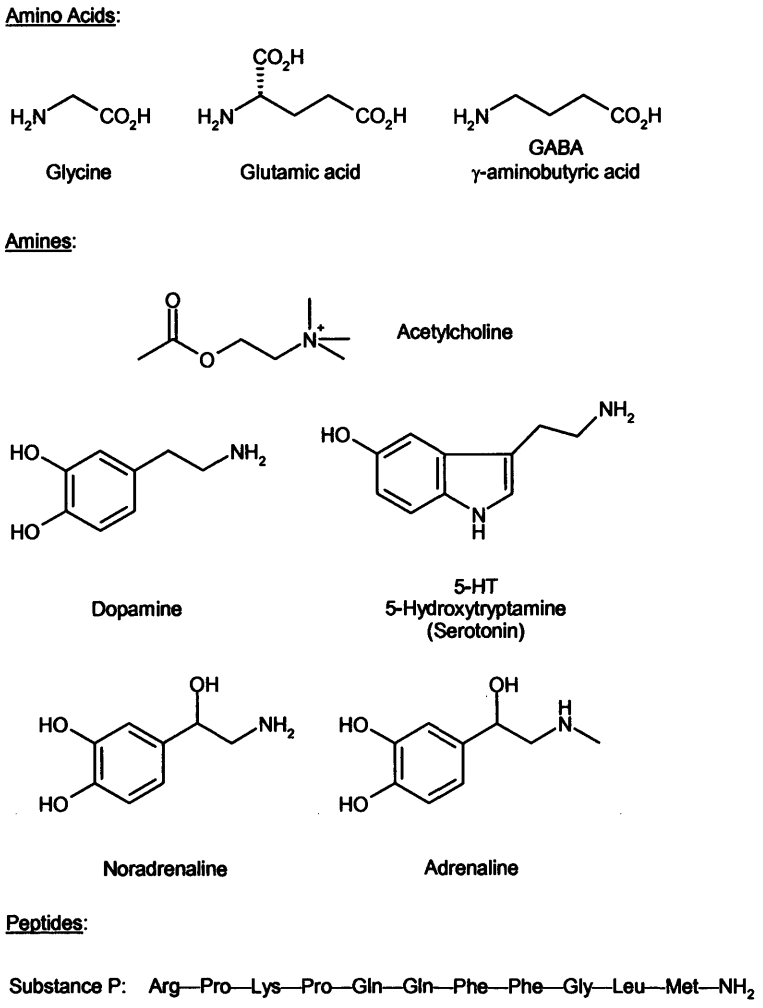

Figure 8: Some neurotransmitters.

In general, neurones do not actually touch; there is a gap or space maintained between them, and communication between neurones across this gap, or *synapse*, is

almost exclusively chemical in nature. When an action potential arrives at a synapse, it stimulates the opening of voltage-gated calcium ion channels in the membrane. The resulting influx of calcium ions from the extracellular fluid stimulates the rapid release (within 0.2 milliseconds) of *neurotransmitters*, specialist chemicals which cross the synapse and bind to dedicated receptors on the surface of the adjacent neurone. These neurotransmitters can be excitatory or inhibitory, and fall into one of three chemical classes: amines, amino acids and peptides (for examples, see Figure 8).

Of these transmitters, the following have all been identified as being located within the nociceptors, and have been confirmed as being released from nociceptors following activation by capsaicin:

- glutamic acid[108-111] is an excitatory amino acid, generally accepted as the principle excitatory neurotransmitter in the spinal cord[112-114]. It has been demonstrated that stimulation by capsaicin causes the release of glutamic acid from isolated rat DRG neurones[109] and from rat dorsal horn slices[115;116].
- substance P is[108;117-122] an 11 amino acid residue peptide of the tachykinin group of proteins. There is compelling evidence that substance P is one of the key neurotransmitters in central nociceptive signalling and central sensitisation. When applied to the dorsal horn, it has been shown to excite CNS neurones that respond to noxious peripheral stimuli[123;124], with increased levels of substance P resulting in increased sensitivity to noxious stimuli[119;125]. In addition, antagonists of the activation of the substance P receptor (NK1) are anti-hyperalgesic[126;127], and the selective removal of spinal neurons expressing NK1 leads to a reduction in responses to noxious stimuli[128]. It has been demonstrated that stimulation by capsaicin causes the release of substance P from the hemisected rat spinal cord[129] and from slices of the spinal cord of the rat[130] and the guinea pig[131].
- calcitonin gene-related peptide (CGRP) is a 37 amino acid residue peptide[132;133] and has been reported to have a role in the transmission of nociceptive information, and central sensitisation[134-137]. CGRP has been reported to potentiate substance P release[138] and to attenuate the nociceptive actions of substance P and capsaicin[139]. It has been demonstrated that

stimulation by capsaicin causes the release of CGRP in slices of the guinea pig dorsal spinal cord[140].

There are two principle types of receptor for neurotransmitters: the transmitter-gated ion channels, and the G protein-coupled receptors (GPCRs). The transmitter-gated ion channels are ligand-gated ion channels, and operate as already described (see Ion Channels). The GPCRs are much more complex and diverse in function, forming a large superfamily of homologous transmembrane proteins found in most cell types. They are activated by a variety of different classes of ligand, such as hormones, neurotransmitters and calcium ions[141;142]. GPCRs are formed by a single protein, comprising an extracellular N-terminus, a serpentine portion containing seven transmembrane helices connected by intracellular and extracellular loops, and an intracellular C-terminus. Rather than the 'simple' action of directly opening a pore, the GPCRs are much more diverse in their effects, mediating their actions via the activation of intracellular G proteins. The G-protein is comprised of three non-identical subunits, α, β and γ; when activated, the G-protein splits into two parts, G_α and $G_{\beta\gamma}$; these are each capable of activating a third group of effector proteins. These effector proteins may be G-protein-gated ion channels in the membrane, or they may be G-protein-activated enzymes which can trigger an elaborate cascade of biochemical reactions, via second messenger systems. These second messenger systems ultimately alter neuronal function, either by the regulation of ion channel function, or by altering cellular metabolism. The same G-protein has the potential to be activated by any one of several GPCRs; each GPCR is capable of activating several G-proteins. This potential is dependent upon gene expression within the cell. Hence, the same neurotransmitter can have different effects, in different synapses, depending upon the nature of the G-proteins present in the neuronal membrane. Over 100 GPCRs have thus far been described in the literature. The preferred substance P receptor (Neurokinin 1, or NK1) and the CGRP receptor are both GPCRs; their location within the superficial dorsal horn has been confirmed by radioactive ligand binding experiments[143]. There are GPCRs for glutamate, the metabotropic glutamate receptors (mGluR), and these have also been localised to the superficial dorsal horn[144].

Nociceptive Action of Capsaicin - Summarised

The sequence of events by which the nociceptive effects of capsaicin are transmitted from the periphery to the neurones of the CNS would appear to be:

- transduction, from noxious chemical to action potential by the activation of TRPV1 at the PMN cell surface, causing the opening of the non-specific, calcium permeable cation channel, leading to an influx of cations, particularly calcium, triggering an action potential;
- conductance of the action potential to the central synapse in the dorsal horn;
- release of excitatory neurotransmitters, such as substance P, CGRP and glutamic acid, into the synapse, stimulating the second order neurones of the CNS.

Pathological Pain

The information so far summarises the underlying mechanism of nociception, with particular reference to the nociceptive action of capsaicin. If this was all there was to the sensation of pain, then the same noxious stimulus, applied in the same way, would produce the same sensation, every time. This is not the case. When there is actual tissue damage, as a result of disease or trauma, the somatosensory system can be subject to a host of induced alterations, resulting in either an enhancement or a disruption of normal sensory mechanisms. When the responses of the neurones of the somatosensory nervous system concerned with pain are altered, the resulting pain states have been generally categorised as *pathological pain*[6]. Several different mechanisms underlie the pathological pain states, which may include any or all of the following conditions:

- *hyperalgesia*, an amplification of responsiveness to noxious stimuli[145];
- *allodynia*, pain resulting from a normally non-noxious stimulus[145];
- *hyperpathia*, an abnormally painful and prolonged reaction to noxious stimuli[145];
- spontaneous nociceptor activation.

Key pathological pain states are inflammatory and neuropathic pain.

Inflammatory Pain

Actual tissue damage can be accompanied by inflammation (*oedema*) of the injured tissue. This is due to changes in the local blood flow (*vasodilatation*) and vascular

permeability, leading to the leakage of plasma into the surrounding tissues (*extravasation*). These changes also lead to reddening (*erythema*) of the injured tissue and the surrounding area. This is generally accompanied by an increase in pain sensitivity (*sensitisation*), as a result of the lowering of pain thresholds in the nociceptors at the site of injury. This *inflammatory hyperalgesia* serves a protective function, to limit further damage, and is part of the healing process of tissue repair[146;147].

Neurogenic Inflammation

In addition to peripheral PMN stimulation causing the central release of excitatory neurotransmitters via the generation of an action potential, an accompanying peripheral release at the site of tissue damage (linked to increase $[Ca^{2+}]_i$) has been reported for glutamic acid[148], substance P and CGRP[149-151]. This local release of excitatory neurotransmitters is a key component of the inflammatory response to tissue damage. The co-release of substance P and CGRP in particular has a co-operative inflammatory effect. Substance P and particularly CGRP are potent vasodilators, increasing blood flow in the site of tissue damage. Substance P also causes plasma extravasation, conceivably enhanced by the simultaneous increase in blood flow caused by the vasodilation[149;150;152-160].

Vasodilatation and plasma extravasation caused by neuropeptide stimulation is termed *neurogenic inflammation.*

Peripheral Sensitisation

In addition to the neurotransmitters already mentioned, a vast array of other chemicals are released into the ECF in response to tissue damage, forming an '*inflammatory soup*' of endogenous chemical mediators[146;161] that serve to sensitise the nociceptors and enhance the pain response. As well as their role in neurogenic inflammation, substance P and CGRP have also been linked to other aspects of inflammatory hyperalgesia[146;161;162]. Mast cells are stimulated by substance P to release histamine and serotonin. Substance P and CGRP attract other inflammatory cells (monocytes, neutrophils, basophils) to the site of injury, where they are stimulated to release a plethora of peptides and lipids with roles as mediators of inflammation[146;161;163;164]. The peptidic mediators are collectively known as the cytokines, and include the interleukins (IL), the interferons (IFN) and tumour

necrosis factor (TNF). The many lipid mediators of inflammation are predominantly the products of the oxidative metabolism of arachidonic acid, itself the product of the phospholipase A_2 catalysed cleavage of membrane phospholipids, and are collectively known as the eicosanoids. There are two main classes of oxidative enzymes (oxygenases):

- the cyclooxygenases, which give rise to the prostanoids (particularly prostaglandins E_2 (PGE_2) and I_2 (PGI_2)); and
- the lipoxygenases, which produce the hydroperoxyeicosatetraenoic acids (HPETE), the hydroxyeicosatetraenoic acids (HETE), the hepoxilins, the lipoxins and the leukotrienes.

In addition, damaged cells release their intracellular contents, including inflammatory mediators that have an identified role in pain and hyperalgesia, including protons[165;166], potassium ions and adenosine triphosphate (ATP). Bradykinin (BK), a potent pain-producing and pro-inflammatory substance, is produced by the cleavage of high molecular weight kininogens by proteases at the site of tissue injury[167].

Many of these inflammatory mediators act to either excite or sensitise nociceptors, either by direct interaction (opening ion channels to boost the nociceptive signal), or by acting via GPCR-mediated second messenger systems to release other mediators which act directly upon the nociceptors[161;163;168]. They are also responsible for recruiting the 'silent' nociceptors[52;169;170], neurones which, under normal circumstances, do not respond to noxious stimuli, but under inflammatory conditions, respond to chemical mediators such as BK[169], thereby magnifying the nociceptive signal.

This is *peripheral sensitisation*, the activation of the local somatosensory afferents, including the nociceptive pathways, in such a way as to generate an abnormal response to both noxious and non-noxious stimuli.

TRPV1 in Inflammatory Pain

As already described (see Early Vanilloid Pharmacology), accompanying the 'unbearable sensation of warmth' of the topical application of capsaicin was 'reddened inflammation, without blistering'[22], and when an alcoholic solution of the crude isolate capsicol was dropped on the skin, the pain was accompanied by an excess of blood at the site[25]. These early experiments clearly demonstrated a

capsaicin-induced neurogenic inflammation. In the classical afferent nociceptive action of capsaicin already described, the capsaicin-induced increase in $[Ca^{2+}]_i$ in the peripheral termini of the PMN triggers an action potential, ultimately causing a central release of the excitatory neurotransmitters substance P, CGRP and glutamic acid in the CNS. The rise in $[Ca^{2+}]_i$ also causes the *local* release of the same neurotransmitters from the *peripheral* termini of the PMNs[171]. Implicit in these actions of capsaicin is a major role in inflammatory pain for TRPV1, both as the initiator of neurogenic inflammation, and a key target for peripheral sensitisation, and this has been demonstrated *in vivo* for inflammatory hyperalgesia, where $TRPV1^{-/-}$ knockout mice demonstrate a severely impaired response to *in vivo* models of thermal inflammatory hyperalgesia[172;173].

Many of the inflammatory mediators already described have been demonstrated to have an effect upon the activation of TRPV1, either by direct excitation or indirectly, by sensitisation, lowering the threshold of TRPV1 to direct activation.

Protons

Extracellular acidosis is a feature of inflamed tissues, with damaged cells releasing protons into the ECF, thereby reducing the extracellular pH to below the normal physiological level. Prior to the cloning of TRPV1, protons were identified as activating capsaicin-sensitive DRG neurones isolated from the rat[174;175], and the human[176]. Protons and capsaicin have also been demonstrated to share a common mechanism of neuronal activation[177]. The sensitivity of the capsaicin receptor to activation by protons was used in the original characterisation of the TRPV1 ion channel[73], where, in addition to activation by capsaicin, TRPV1 was shown to be activated in the absence of capsaicin by a reduction in extracellular pH, from 7.6 to 5.5.

Low pH has also been shown to facilitate responses to capsaicin in isolated rat DRG neurones[73;178-180]. In addition to the direct stimulation of PMNs, it has been demonstrated that decreasing pH, from 7.3 to 6.3, enhanced the capsaicin-induced current in rat DRG neurones by 7-fold[178]. A reduction in pH, from 7.6 to 6.3, potentiates the response to a submaximal dose of capsaicin[73]; these results suggest that protons have an allosteric effect, lowering the threshold of activation of the channel, presumably by protonation of the ion channel. An extracellular Glu residue within the putative TRPV1 pore region has been demonstrated to be key to these pH-mediated effects[181].

Lipid mediators

Several of the lipid mediators of inflammation derived from the lipoxygenase-mediated metabolism of arachidonic acid (see Figure 9) have been demonstrated to be weak agonists at TRPV1[182]. The potency and efficacy of these compounds are such that each is unlikely to activate TRPV1 in isolation, but might act synergistically to enhance activation of the ion channel.

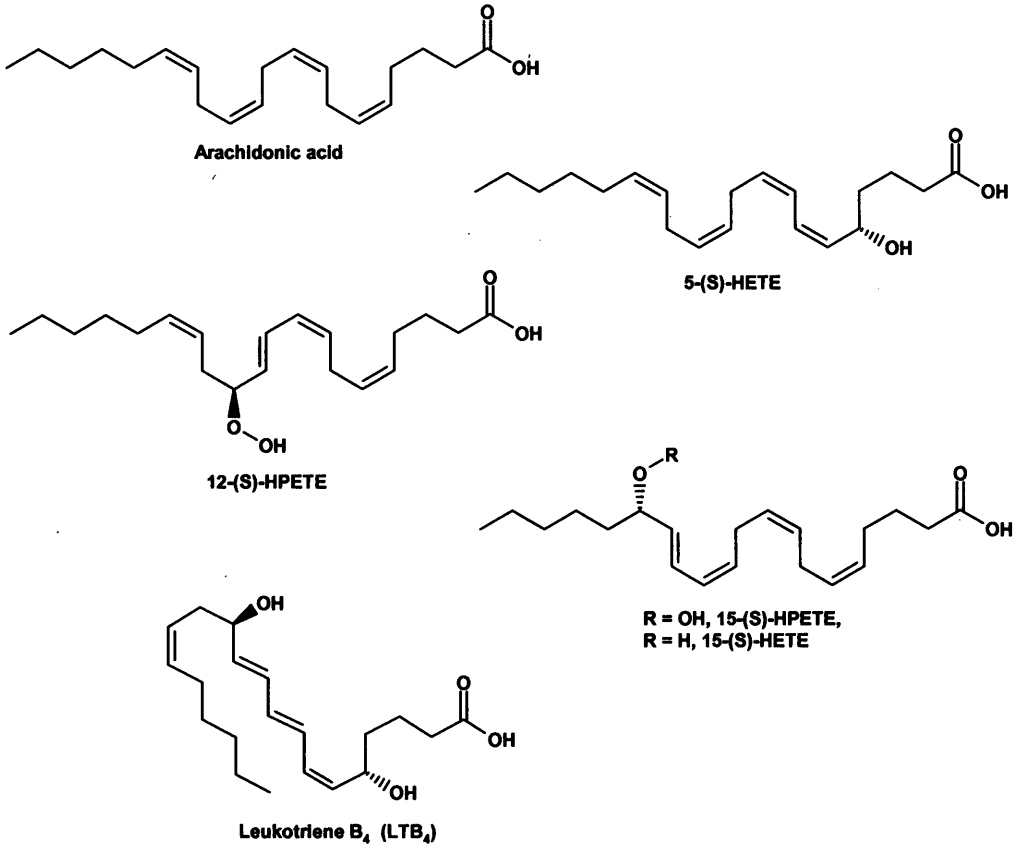

Figure 9: Arachidonic acid and the lipoxygenase-mediated metabolites with TRPV1 agonist activity[182].

Other endogenous arachidonic acid derivatives have also been demonstrated to have agonist activity at TRPV1 (see Figure 10). The endogenous cannabinoid receptor agonists *N*-arachidonoylethanolamide (anandamide)[183] and *N*-arachidonoyl-dopamine[184] are also full agonists at TRPV1[185-187] with potent vasodilatory/vasorelaxant activity[188-190].

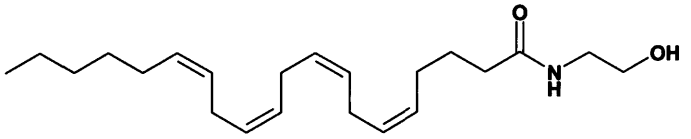

Anandamide

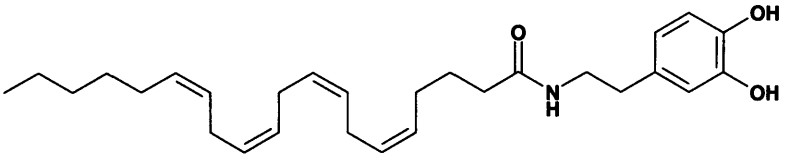

NADA

Figure 10: Other derivatives of arachidonic acid with full agonist activity at TRPV1: *N*-arachidonoylethanolamine (Anandamide) and *N*-arachidonoyldopamine (NADA)

Bradykinin, Serotonin and PGE_2

Other inflammatory mediators, such as BK, PGE_2 and serotonin (5-HT) have been shown to act in concert to facilitate activation of the TRPV1 ion channel at acidic pH[191;192]. 5-HT may act independently of the TRPV1 channel, via its own $5\text{-}HT_3$ ion channel[193]. BK does not act directly upon TRPV1, but binds to its own bradykinin B_2 receptor. This receptor is a GPCR, and BK's sensitisation of the TRPV1 ion channel is achieved via second messenger signalling within the neurone[194;195]. PGE_2 has also been identified as acting upon TRPV1 via a GPCR-mediated second messenger signalling cascade[193].

TRPV1 and Noxious Heat

As already described, the PMNs respond to noxious mechanical, thermal and chemical stimuli. Further studies have demonstrated the sensitivity of a sub-population of freshly dissociated[196] and cultured[197] rat DRG neurones to both noxious heat and capsaicin, with the activation by noxious heat being significantly reduced in the presence of the competitive antagonist of capsaicin-mediated PMN stimulation, capsazepine[198].

Not surprisingly therefore, in addition to the ligand-induced activation already described, TRPV1 is also sensitive to noxious heat, being activated by an increase in temperature into the noxious range (>43°C)[73]. TRPV1 is therefore capable of transducing both noxious chemical and noxious thermal stimuli (two of the three categories of stimulation that activate PMNs). Consequentially, TRPV1 has been

described as a molecular integrator of chemical and physical stimuli that elicit pain[180].

Some of the chemical activators of TRPV1 have been demonstrated to effect the activation of the ion channel by temperature. Capsaicin has been demonstrated to enhance the heat response in rat DRG neurones[196]. Acidosis can lower the threshold of TRPV1 to temperatures as low as 35°C[180], potentially resulting in the TRPV1 ion channel being continually opened in inflamed tissue.

Pain in the CNS – Central Sensitisation

What happens after the nociceptive signal has been passed on to the neurones of the CNS? The perception of pain is a highly variable, complex and subtle process, with the same level of nociceptor activity producing quite different individual pain states. This process has been attributed to *neuronal plasticity*, the ability of neurones to change their function down to the metabolic level in response to external influence. Excitatory examples include *wind up* and *secondary hyperalgesia.*

Secondary Hyperalgesia

The peripheral sensitisation described so far does not explain the full extent of changes occurring in inflammatory pain. The phenomenon of hyperalgesia has two components. There is *primary* hyperalgesia, where increased responsiveness to heat and mechanical stimuli occurs at the site of injury. This is adequately explained by peripheral sensitisation. There is also the mechanical allodynia displayed by surrounding uninjured tissue, termed *secondary* hyperalgesia, which peripheral sensitisation does not explain[6;199;200]. This secondary hyperalgesia has been attributed to changes within the CNS, that result in the input from Aβ primary afferent fibres responding to normally innocuous stimuli being interpreted as nociceptive[201-203]. This *central sensitisation* is probably mediated by excitatory amino acids acting at the NMDA receptor[204].

Capsaicin has been used to explore this phenomenon; intradermal injections of capsaicin produces an intense, but transient, pain, followed by heightened sensitivity outside the region of the capsaicin injection to pinprick (secondary hyperalgesia) and brush (secondary allodynia)[205;206].

Wind-up

Wind up was first described in the mid-1960s as a frequency-dependent facilitation of spinal cord neuronal responses mediated by afferent C-fibres[207], but not Aβ-fibres[208]. The repeated stimulation of a C-fibre, at an identical intensity, induces a sudden marked increase in the response from the second-order neurones, which persists beyond the cessation of the initial C-fibre stimulus. The most widely accepted hypothesis for wind-up[209] relies upon the neurotransmitter glutamic acid, its function as a substrate for both the α-amino-3-hydroxy-5-methyl-4-isoxazoleproprionate (AMPA) and N-methyl-D-aspartate (NMDA) receptors, and the connectivity of the second-order neurones that bear them.

While the AMPA receptor ion channels are free to open in response to the presence of glutamic acid, the NMDA receptor ion channels are not. Under normal physiological conditions, the ion channel is blocked by magnesium ions[210]. This blockade is voltage-dependent[209]. When the Aβ-fibres are activated by low-threshold, innocuous stimulation, the glutamic acid released acts upon second-order neurones of the CNS with AMPA receptors, the stimulation of which is registered as 'innocuous'. PMNs contain glutamic acid and substance P[108], and release both in response to noxious stimulation[109;115;116;129;131;211]. Wind up is the result of repeated PMN stimulation, with each stimulation causing the release of glutamic acid and substance P. With the repeated release of substance P comes a gradual, cumulative depolarisation of the plasma membrane in the second-order neurone, mediated via the NK1 tachykinin receptor. The voltage-dependent affinity of magnesium ions for the NMDA receptor gradually lessens, until the ion channel is no longer blocked. Glutamic acid can now open the ion channel, and sodium and calcium ions flood into the neurone, resulting in a high firing frequency of action potentials. In addition, the originally innocuous Aβ-fibre-mediated release of glutamic acid now registers as noxious, with the net result that a prolonged painful stimulus can become more painful over time.

This phenomenon has been simulated by repeated exposure to noxious heat[212].

Neuropathic Pain

Neuropathic pain is a generic term, defined by the IASP as 'pain initiated or caused by a primary lesion or dysfunction in the nervous system'[145]. In contrast to nociceptive and inflammatory pain, neuropathic pain and suffering are the result of

ongoing nervous system dysfunction that serves no apparent biological purpose[213]. The sensation of pain has been described as alternately burning, aching, throbbing, shooting, and stabbing. The sources of potentially painful neuropathies are manifold; some examples are:

- direct injury to the nerves, by trauma or avulsion;
- indirect injury to the nerves, by compression or entrapment;
- ischaemia;
- metabolic (*e.g.* diabetes);
- vitamin deficiency (B_1, B_6, B_{12}, E);
- infectious pathogens (*e.g. herpes zoster*, HIV);
- neurodegeneration (*e.g.* multiple sclerosis);
- stroke.

The mechanisms of these associated neuropathic pain conditions, where established, are equally as varied, but all involve damage to the tissues of nervous system. The normally long term nature of this category of pain defines it as chronic pain. Neuropathic pain is the least understood, and as a result, the least amenable to current pharmaceutical intervention. In particular, painful diabetic neuropathy (PDN), post-herpetic neuralgia (PHN) and painful HIV-associated neuropathy are all considered to be insensitive to current therapies.

Endogenous pain modulation and analgesia

The perception of pain is a highly variable, complex and subtle process. The same level of nociceptor activity is capable of producing quite different individual pain states. In addition to the enhanced and exaggerated pain states already described, the reverse is also seen, with the nervous system able to moderate the sensation of pain and, in extreme cases, disregard it altogether. There must be considerable modulation and regulation of the nociceptive information both prior to and post its ascension of the spinothalamic tract.

The most successful hypothesis for this regulation came with the gate-control theory of pain, proposed in 1965 by Ronald Melzack and Patrick D. Wall[1;214]; its success lies in its emphasis of the mechanisms of the CNS that control the perception of a noxious stimulus. While subsequent research has filled in many of the gaps and modified the details, it has yet to be seriously contradicted.

Pain modulation – the Gate-Control Theory of Pain[1;214]

In summary, nociceptive information is relayed from the periphery to the spinal cord by the small diameter Aδ- and C-fibre nociceptors, which transmit this information, via chemical synapse, to the second-order neurones of the CNS. The nociceptive information is transmitted onward to the higher centres of the brain, for interpretation and response, but not without first being 'tweaked' by other parts of the nervous system. In the gate-control theory of pain, Melzack and Wall hypothesised that, in addition to the primary nociceptors, and the second-order neurones, there are interneurones, which serve as a focus for **modulation** of the nociceptive message within the CNS (see Figure 11). The interneurones have synapses with the second-order neurone and, when stimulated, inhibit the stimulation of the second order neurone by the nociceptors. The nociceptors also synapse to the interneurone, and can in turn inhibit the stimulation of the interneurone, and thereby inhibit the inhibition of the second-order neurone by the interneurone.

The stimulation of the inhibitory interneurones comes from two sources:

- *afferent regulation*. The simultaneous stimulation of nociceptive fibres and the low-threshold Aβ-fibre mechanoreceptors of the peripheral nervous system can reduce the pain that would be evoked by the sole stimulation of nociceptors (for a practical example, consider the relief associated with rubbing a pinch). The Aβ-fibres conceivably synapse to the interneurone, and stimulation of the Aβ-fibres causes excitation of the interneurone, with subsequent inhibition of the second-order neurone.
- *descending regulation*. Electrical stimulation of areas of the midbrain can lead to the successful suppression of nociceptive signalling and behavioural analgesia in a variety of mammalian species[215-218]. This analgesia is the result of the stimulation of neuronal filaments found to extend from the midbrain to the areas of the dorsal horn associated with nociception, and the secretion of serotonin (5-hydroxytryptamine, or 5-HT)[219-222], and noradrenaline[219;220], from these descending neuronal filaments. The secretion of these neurotransmitters causes neurones within the dorsal horn to secrete further *inhibitory neurotransmitters*, with the subsequent inhibition of the responses within the dorsal horn to noxious stimuli.

Serotonin has quite a broad range of effects within the CNS, probably due to the many different receptor subtypes distributed throughout the CNS[223;224]

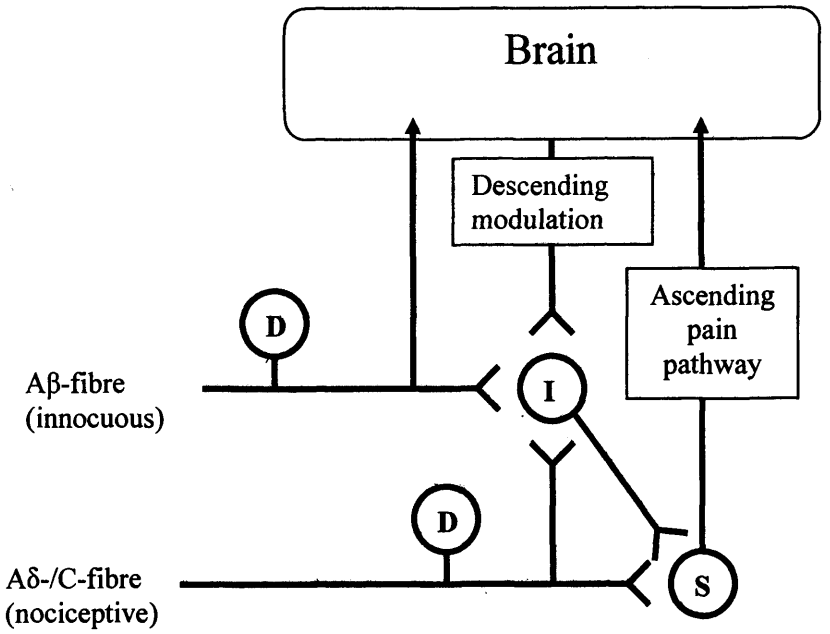

Figure 11: A schematic representation of Melzack and Wall's gate-control theory of pain (D = dorsal root ganglion; I = interneurone; S = second-order neurone).

Inhibitory Neurotransmitters

Many neurotransmitters have been found to have an inhibitory effect upon nociceptive transmission (for reviews, see Fürst (1999)[225] and Millan (2002)[226]). The receptors for these neurotransmitters are widely distributed throughout the CNS, but are concentrated in regions associated with pain perception[227]. The receptors are found both presynaptically, where they inhibit the release of excitatory neurotransmitters, and post-synaptically, where they inhibit the generation of action potentials in the second-order neurone.

The more common inhibitory neurotransmitters found in nociception include:

1. the inhibitory amino acids gamma-aminobutyric acid (GABA) and glycine[228]. GABA is the main inhibitory transmitter in the CNS[229]; GABA secreting neurones have been found throughout the dorsal horn of rats[230] and monkeys[231;232]. Two receptor subtypes that bind GABA have been described in the rat dorsal horn. The $GABA_A$ receptor is a transmitter-gated ion channel, comprised of four different subunits that combine to form a chloride permeable ion channel; the $GABA_B$ receptor is a GPCR.[233-235]. Glycine acts via a post-synaptic transmitter-gated chloride ion-permeable channel (the

glycine receptor, GlyR)[227;236]. It has been found to be co-localised with GABA in primary afferents[237;238]; GlyR and the $GABA_A$ receptor have also been found co-localised in the rat spinal cord[239], implying some form of co-operative inhibition.

2. the endogenous opioids. Four opioid receptors and their endogenous ligands have been identified. The μ opioid receptor is activated by β-endorphin, the δ opioid receptor responds to enkephalins, the κ opioid receptor binds dynorphins, and the most recently recognised member of the group, the opioid orphan receptor (ORL-1) binds nociceptin (also known as orphaninFQ)[240-246]. Opioid receptors are predominantly present on the presynaptic terminals; their activation either causes potassium channels to open (μ, δ, and ORL-1) or calcium channels to close (κ);
3. adenosine. Adenosine has both inhibitory and facilitatory effects upon the transmission of nociceptive stimuli[247]. Of the four recognised neuronal adenosine receptors (A_1, A_{2A}, A_{2B} and A_3)[248;249], the adenosine A_1 receptor has been localised to the dorsal horn[250;251], and identified as mediating the antinociceptive effects[252;253];
4. somatostatin. Somatostatin is released by primary afferent neurones in the dorsal horn in response to noxious thermal stimulation[254;255]; the somatostatin receptors (SSTR1-5) are GPCRs coupled to inhibitory cellular signalling systems. The conclusion is that this sub-population of C-fibres containing somatostatin have an inhibitory effect upon thermal nociception;
5. acetylcholine (ACh)[227]. Both nicotinic acetylcholine receptors (nAChR)[256;257] and muscarinic acetylcholine receptors (mAChR)[258] have been shown to have antinociceptive involvement.

As with the excitatory neurotransmitters, neurones are frequently found to contain more than one inhibitory neurotransmitter, leading to the supposition that the modulation of nociception is the result of several neurotransmitters working in concert to achieve the desired effect.

The antinociceptive effect of the activation of inhibitory receptors is produced by the hyperpolarisation of the neuronal membrane, *i.e.* the value of V_m is **lowered**, to below –65mV, either by opening chloride permeable channels, thus allowing chloride to enter the neurone, closing calcium channels, thereby preventing calcium

ions from entering the cell, or opening potassium channels, thus allowing potassium ions to leave the neurone.

Contemporary Pharmaceutical Analgesia

So far, this brief description of the best understood mechanisms of the nervous system and their involvement in the complexity of the sensation of pain has described some of the myriad of transmitters and receptors that have been shown to have a role in the sensation of pain. This section should have served to introduce the sensation of pain as an incredibly complex area of study, which continues to expand. There are many potential 'points of intervention' that might offer opportunities for the design of new analgesics. Despite this, current drug therapies are largely reliant upon the development of therapies that have been in place for thousands of years, namely the non-steroidal anti-inflammatory drugs (NSAIDs) and the opioids.

The NSAIDs

The use of proto-NSAIDs has its origins in the writings of the Assyrians and ancient Egyptians, with evidence of the use of infusions of myrtle and willow leaves for joint pain[259], and Hippocrates is frequently cited as recommending the use of the leaves of willow trees and the juice of poplar trees for eye diseases and in childbirth[259-261].

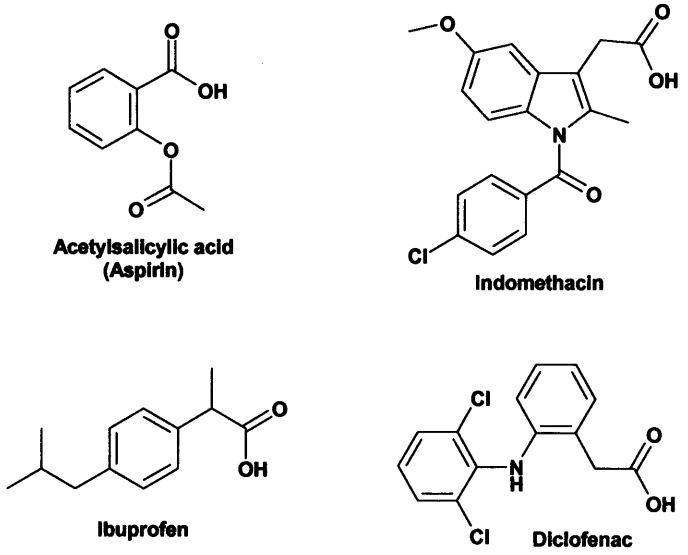

Figure 12: Some examples of the chemically diverse non-steroidal anti-inflammatory drugs.

The analgesic activity of this broad class of chemical structures (see Figure 12), stems primarily from their disruption of the biosynthesis of the prostanoids, via the inhibition of the enzyme cyclooxygenase (COX)[260;262]. As described in the section on

Peripheral Sensitisation, there are two principle pathways of arachidonic acid metabolism by which lipid mediators of inflammation are biosynthesised. In addition to the lipoxygenase based metabolism, and the TRPV1 agonists already described[182] (see TRPV1 in Inflammatory Pain), the cyclooxygenase-mediated metabolism of arachidonic acid produces the prostanoids. Many of these (thromboxane (TXA_2), prostaglandin D_2, (PGD_2), E_2 (PGE_2), $F_{2\alpha}$ ($PGF_{2\alpha}$) and prostacyclin (prostaglandin I_2; PGI_2)) have been identified as present in the inflammatory soup of chemical mediators released or produced in the periphery as a result of tissue damage. PGE_2 in particular is prevalent as the major metabolite of arachidonic acid[146].

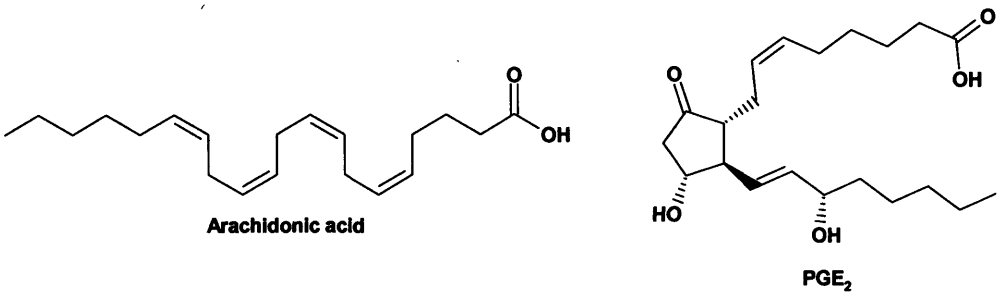

Figure 13: Arachidonic acid, and the principle inflammatory COX metabolite, PGE_2.

Unfortunately for the NSAIDs, the prostanoids are found throughout the body, fulfilling several biological functions beyond their role in inflammatory pain. COX is the first enzyme in the biosynthetic pathway from arachidonic acid, so the inhibition of COX has resulted in the classical NSAIDs having a range of well known adverse effects[263]. TXA_2 is a thrombotic agent and a vasoconstrictor; PGD_2 is an inhibitor of platelet aggregation and a vasodilator; $PGF_{2\alpha}$ is a bronchoconstrictor and a mediator of myometrial contraction; and PGI_2 is an inhibitor of platelet aggregation, a vasodilator and a hyperalgesic[264]. The most abundant inflammatory prostanoid, PGE_2 also has a range of other effects, including the contraction of bronchial and gastrointestinal smooth muscle, the stimulation of intestinal fluid secretion, the stimulation of gastric mucus secretion, and the inhibition of gastric acid secretion. In addition to the inhibition of inflammation and pain, some normal tissue function can also be compromised, leading to the recognized side effects of gastrointestinal bleeding and ulcers, renal impairment, and platelet function abnormalities[263].

More recently, the search for new, side-effect free NSAIDs received a boost with the discovery that COX has two isoforms (COX-1 and COX-2)[265-268]. COX-2 was reported to be an inducible isoform of COX expressed by macrophages and other

cells at sites of inflammation[269-272], with little expression elsewhere. The assumption that selectivity for COX-2 will only inhibit prostanoid synthesis at the site of inflammation, thereby minimising the inhibition of prostanoid activity outside the site of inflammation and significantly reducing adverse side effects[273], has led to the search for COX-2 selective NSAIDs. Although there are differences in the binding pocket when compared with COX-1[274-276], the classical NSAIDs have been shown to be fairly non-specific between COX-1 and COX-2. Subsequent drug discovery programs have given rise to a new generation of COX-2 selective NSAIDs, such as celecoxib[277] (Celebrex®, Searle), rofecoxib[278] (Vioxx®, Merck) and lumiracoxib[279] (Prexige®, Novartis) (see Figure 14), with much improved side effect profiles reported[280]. The sudden withdrawal of Vioxx® (as of September 2004), citing increased risk of stroke and heart attack in long term users, has put a significant dent in the confidence of the market in this drug class[281-283].

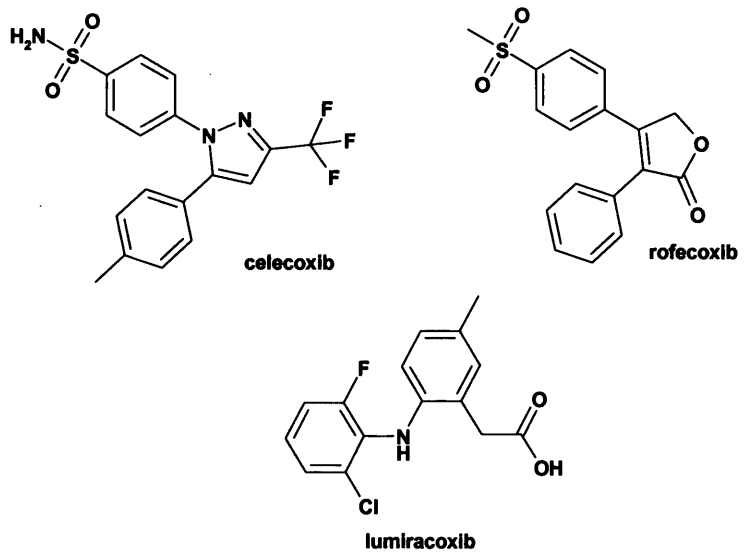

Figure 14: Some COX-2 inhibitors.

One very popular analgesic frequently included within the NSAIDs is the antipyretic analgesic acetaminophen (paracetamol; see Figure 15), although there is still some debate over its mechanism of action. Despite some *in vivo* inhibition of PG synthesis being reported, the analgesic mechanism of action of acetaminophen is unclear[284], as acetaminophen does not exhibit anti-inflammatory or anticoagulant activity. While it does exhibit weak inhibition of COX-1 and COX-2 *in vitro*[285], there is also literature evidence for the presence of inducible, acetaminophen-sensitive variants of both COX-1 (called COX-3[286]) and COX-2[287].

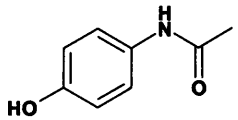

Paracetamol

Figure 15: The structure of paracetamol.

The Opioids

Awareness of the opioids can be traced back to the Babylonians, the ancient Egyptians, even to the Sumerian culture of 3000 B.C.[288]. The earliest documented medical use for opium comes from the Ebers papyrus (1550 B.C.), where it is recommended for calming crying children[1]! Opium itself is obtained from the opium poppy *Papaver somniferum*, and three active components have been isolated: morphine, codeine and thebaine (see Figure 16).

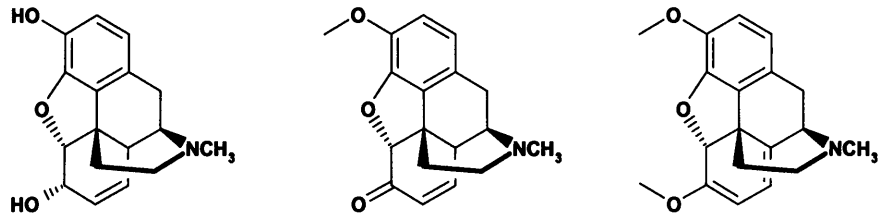

Morphine Codeine Thebaine

Figure 16: Structures of the opioid analgesics isolated from opium.

As already described, there have so far been four opioid receptors identified: the μ-, δ- and κ-opioid receptors, and ORL-1[241-244;246]. While all have been reported as having a role in the inhibition of nociception, experiments with μ-opioid receptor knockout mice have shown that morphine and its analogues mediate their analgesic effect via the μ-opioid receptor[289]. However, as with the NSAIDs, a diverse range of adverse side effects are found with opioid usage, as the opioid receptors occur throughout the CNS, serving to modulate synaptic transmission in a variety of neuronal pathways other than nociception. Side effects include euphoria, sedation, respiratory depression and constipation, with the additional complications of addiction and tolerance. Numerous attempts have been made to isolate receptor subtypes, and synthesise analogues to separate the analgesic effects from the adverse effects, with little success.

Analgesic Adjuvants

Neither of the two classical classes of analgesic are particularly effective against neuropathic pain. However, several other diverse medicines are in widespread use as analgesics. This group of largely unrelated compounds are drugs with a primary therapeutic indication other than analgesia, that have been found to be effective against neuropathic pain conditions, particularly PDN and PHN[290-293]. Since analgesia is a secondary indication for these drugs, side effects can be anticipated. These *analgesic adjuvants* (see Figure 17) include selected tricyclic antidepressants such as amitryptiline and desipramine[294-298] and antiepileptic/anticonvulsant medicines, including carbamazepine[299] and gabapentin[300]. Pfizer's follow up to gabapentin, pregabalin[301], is in phase III trials in fibromyalgia, a condition typified by non-specific pain in the soft fibrous tissues of the body, the muscles, ligaments, and tendons.

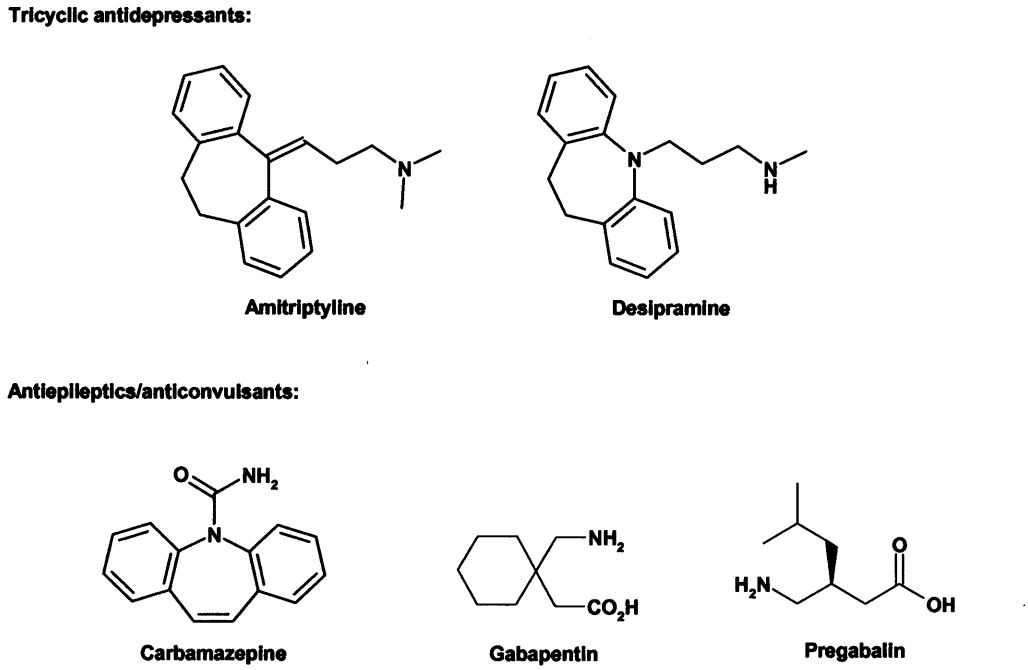

Figure 17: Some examples of analgesic adjuvants.

Capsaicin, TRPV1 and Agonist Analgesia

Current drug therapies are largely reliant upon the developments of therapies that have been in place for thousands of years, despite the myriad of transmitters and receptors that have been shown to have a potential role in the sensation of pain. This is not for lack of effort, with both industry and academia exploring the many potential 'points of intervention' that offer opportunities for pharmaceutical-based analgesia. Of the modulatory neurotransmitters and inflammatory mediators already

described, most have been the target for exploration toward analgesic exploitation at some time, and the more successful approaches have been reviewed extensively elsewhere[290;291;293;302;303].

Of particular relevance to this thesis is the TRPV1 ion channel, and its role in nociception. Over the last forty years, the effects of capsaicin have been used extensively to investigate aspects of acute and chronic pain sensation. TRPV1 appears to occupy a significant role in peripheral nociception and neurogenic inflammation. Exposure to capsaicin is painful, it's activation of the TRPV1 ion channel provokes nociception, peripheral sensitisation via neurogenic inflammation, central sensitisation and wind-up. The development of $TRPV1^{-/-}$ knockout mice has confirmed that the ion channel is essential for the development of some pathological pain conditions[172;173]. As has already been touched upon (see Early Vanilloid Pharmacology), the seed for the eventual appreciation of the importance of the TRPV1 ion channel was sown in the mid-nineteenth century, with the works of Högyes[26;27;304] and Thresh[21-24], since when capsaicin and its actions, both in nociception and as an instigator of neurogenic inflammation, have continued to intrigue.

Structural Elucidation of Capsaicin

After the successful isolation of capsaicin by Thresh[21-24], initial attempts at deducing the composition by elemental analysis failed to detect the presence of nitrogen within the atomic composition and gave capsaicin the erroneous empirical formula $C_9H_{14}O_2$. Later structural analyses established the presence of nitrogen in the molecule, as well as one hydroxyl substituent and one methoxy substituent. Thermal decomposition of capsaicin yielded a vanilla-like odour, and it was concluded that capsaicin was a derivative of vanillin (4-hydroxy-3-methoxybenzaldehyde). After further elemental analysis, capsaicin was given the impossible empirical formula of $C_{18}H_{28}NO_3$[305;306], which was later corrected to $C_{18}H_{27}NO_3$ by Nelson[307].

The isolation of 50g of capsaicin from 50lbs of 'very hot' cayenne pepper, and subsequent chemical degradation, revealed capsaicin as an amide of vanillylamine and a decenoic acid[307]. In an attempt to ascertain the geometry of the decenoic acid, several analogues were synthesised[308]; unfortunately, their similar potency (by taste!) shed no light on the nature of the decenoic acid. The first partial synthesis of capsaicin was from synthetic vanillylamine and the decenoyl chloride derived from

the hydrolysis of capsaicin[309]; the decenoic acid was eventually correctly identified as 8-methylnon-6-enoic acid of unspecified geometry[310].

The first complete synthesis of capsaicin, of undefined alkene geometry, was published by Spath and Darling[311], with the final piece of the jigsaw, the nature of the geometrical isomerism, being resolved in 1955. The information was published, along with a selective total synthesis of the correct isomer, by Crombie *et al.*[312].

SAR Studies of Capsaicin Analogues

To facilitate the consideration of capsaicin analogue SAR, it is useful to adopt a modular consideration of the molecule, dividing it into three regions: A, B and C[313-315] (see Figure 18).

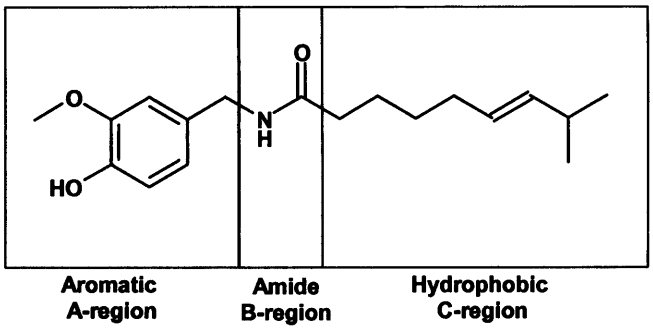

Figure 18: A modular consideration of capsaicin substructure[313-315]

Interest in capsaicin and its inherent pungency led to the publication of several SAR studies, where analogues of capsaicin were synthesised and tested to determine the structural requirements for pungency. The earliest, while initiated to determine the exact geometry of the decenoic acid portion of capsaicin[308;316], established the optimal unbranched chain length for pungency of 9 carbons. Further studies[317-327] proposed the following requirements as optimal for pungency.

For the aromatic A-region:

- the parent vanillyl substitution pattern for the aromatic ring, with any substitution of the 4-hydroxyl eliminating pungency (the aromatic ring can be replaced by a n-propyl chain, with some loss of pungency);
- the number of methylenes between the aromatic ring and the amide must be 0 or 1;

For the amide B-region/ hydrophobic C-region:

- a free NH is required;
- $C_9 - C_{11}$ straight chain carboxamides are the most pungent.

Antinociceptive Action of Capsaicin

Rather than becoming a pharmacological footnote, capsaicin's potential began to blossom from the mid-twentieth century onwards with the serendipitous discovery that it also has an **anti**nociceptive effect. Large, repeat doses of topically or systemically applied capsaicin proved to be ultimately analgesic in rodents[37-39]. This capsaicin-evoked desensitisation of the animals to noxious stimulation was seen as a result of chronic exposure to capsaicin over several days, with chronic dosing of experimental animals with capsaicin causing the loss of response to noxious thermal and chemical stimuli. This was manifested as raised thresholds to stimulation by noxious chemicals and nociceptive pressure, long after dosing with capsaicin had ceased[41]. Studies have shown that the repeated *in vivo* application of capsaicin over a period of days by subcutaneous injection depletes the nociceptive neurones of substance P[328], and has been ascribed to the blockade of 'axoplasmic transport'[329]. Primary afferent neurones have their cell bodies located in the DRG, with axonal processes extending to the periphery and into the dorsal horn. Axons and the axonal termini cannot construct the biomolecules necessary for their function. Biosynthesis of the cellular macromolecules of neuronal function, such as substance P, occurs in the cell body, and the products of biosynthesis are transported from the cell body within the axon to the axonal termini. When the axoplasmic transport is interrupted, presynaptic stocks of neurotransmitter are not replenished[330].

However, *in vitro* studies of the effects of capsaicin on isolated rat sciatic nerve demonstrated rapid desensitisation with repeated application[331], and the acute *in vivo* dosing of rats with capsaicin has also been shown to be antinociceptive for a few hours[332;333]. It is this acute desensitisation that is reported to be responsible for capsaicin's analgesic and anti-inflammatory effects[334]. Some early studies on the acute desensitising action of capsaicin indicated the site of action to be at the peripheral nerve endings[335]. Studies on isolated DRG neurones have demonstrated this acute desensitisation to be in response to the capsaicin-induced increase in the concentration of intracellular calcium ($[Ca^{2+}]_i$), resulting from the influx of calcium ions from the extracellular fluid[336;337]. One effect of the increase in $[Ca^{2+}]_i$ is to promote the activity of the calcium-dependent cytosolic phophatase 2B (calcineurin). Specific inhibition of calcineurin has been shown to inhibit capsaicin-evoked desensitisation[338], implying that the capsaicin-evoked desensitisation of polymodal

nociceptors to noxious stimuli is, at least in part, a result of the dephosphorylation of the capsaicin receptor-gated calcium-selective cation channel by calcineurin. A more recent study has confirmed the desensitisation of the capsaicin receptor in cultured rat DRG neurones by calcineurin, and reported that the desensitisation can be reversed while the $[Ca^{2+}]_i$ is still high, by phosphorylation of the capsaicin receptor by Ca^{2+}/calmodulin-dependent kinase II (CaMKII)[339]. Despite the identification, cloning and successful expression of a functional capsaicin-sensitive ion channel[73], the precise molecular mechanism for capsaicin-evoked desensitisation still remains elusive. TRPV1 activation does appear to be under exquisitely fine control via mechanisms of $[Ca^{2+}]_i$ dependent phosphorylation and dephosphorylation, with sequences corresponding to active sites of phosphorylation for protein kinase A (PKA)[340], protein kinase C (PKC)[341] and Ca^{2+}/calmodulin-dependent kinase II (CaMKII)[339] having been identified.

So, capsaicin has a diverse range of effects, mediated via activation of the polymodal nociceptors. Depending upon dose, frequency of exposure and age of the animal at exposure, capsaicin can be:

- excitatory, (algesic/ algogenic/ nociceptive);
- desensitising (analgesic/ antihyperalgesic/ antinociceptive);
- neurotoxic (neuronal cell death; see Capsaicin and Sensory Neurones).

Capsaicin and Agonist Analogues as Analgesics

TRPV1 has a central role in peripheral nociception and neurogenic inflammation. It has a highly specific distribution, being predominantly associated with the PMNs, and is an appropriate target for analgesic intervention, with minimal foreseeable side-effects. The phenomenon of the capsaicin-induced desensitisation/antinociception of TRPV1 has great potential for analgesia, and topical creams containing capsaicin have been used in the treatment of PHN and PDN, as well as psoriasis, osteoarthritis and rheumatoid arthritis[342;343]. Unfortunately, repeated applications are usually required to achieve analgesia, and the initial excitatory effects of burning pain and reddening of the skin inherent in the topical application of capsaicin[22;25] are often too great, with patients frequently abandoning treatment before analgesia is achieved. Some effect has been achieved with co-administration of a local anaesthetic with

large doses of capsaicin[344], however. Although the antinociceptive actions of capsaicin has great appeal as a putative analgesic with a novel mode of action, the intensely painful response to initial exposure makes capsaicin itself unattractive, except in the most extreme cases.

A successful analgesic based upon capsaicin's mechanism of action would need to minimise the acute excitatory effects, while promoting the desensitisation of the sensory neurone. In addition, other biological effects, such as apnoea, bradycardia, hypotension and hypothermia (see Early Vanilloid Pharmacology) would all have to be addressed. Capsaicin's actions upon the polymodal nociceptors have promoted decades of research into understanding the mechanisms behind the two physiological actions of the initial acute excitatory and algesic effect, and the subsequent analgesic effect of desensitisation to noxious stimuli. The pharmaceutical industry has focussed upon attempts to separate these two effects and exploit the beneficial analgesia.

Of the other vanilloids, the ultrapotent capsaicin analogue RTX has provoked some pharmaceutical interest. While *in vivo* measures of acute nociception have revealed RTX to have a similar potency to capsaicin[17], the potency of RTX with respect to other aspects of vanilloid pharmacology, such as hypothermia, neurogenic inflammation and desensitisation of PMNs, is several orders of magnitude higher than capsaicin[17;18;345]. Unfortunately, detailed investigations have been hampered by the limited availability of RTX, which can only be obtained either via purification from natural sources, or via a low-yielding 26 step synthesis[346]. However, RTX pharmacology has demonstrated that the separation of nociception and desensitisation is possible.

Several attempts to separate the antinociceptive effects of synthetic capsaicin analogues from their nociceptive and other biological actions have been published. Of these structure-activity relationship (SAR) studies[69;313-315;347-350], while some divergence in the structural requirements for pungency and desensitisation was achieved, none achieved total separation. One attempt to separate capsaicin's antinociceptive properties from its hypothermic properties [332], also failed. It was only when very specific changes to the 4-substituent of the A-ring were made that a significant reduction in pungency was achieved[351-354]. The A-region 4-hydroxyl substituent has been repeatedly demonstrated as pivotal for pungency[69]; its modification was essential to the amelioration of pungency[351]. Procter & Gamble[353;354], and the Novartis Institute for Biomedical Research, London (formerly

the Sandoz Institute of Medical Research)[313-315;352] both discovered analogues with reduced pungency, yet with sufficient *in vivo* analgesic activity to enter development. The common feature of both strategies was to replace the 4-hydroxy substituent of pungent analogues with a 2-aminoethoxy moiety (see Figure 19); neither of these compounds have survived the rigours of subsequent drug development. A Korean academic group have followed a similar route, patenting an assortment of *N*-arylalkylphenylacetamides possessing excellent analgesic and anti-inflammatory activities, and a greatly reduced level of skin irritation and toxicity[355;356]. The lead compound, **DA-5018** (see Figure 19), has been taken into clinical trials by Dong-A Pharmaceutical of South Korea.

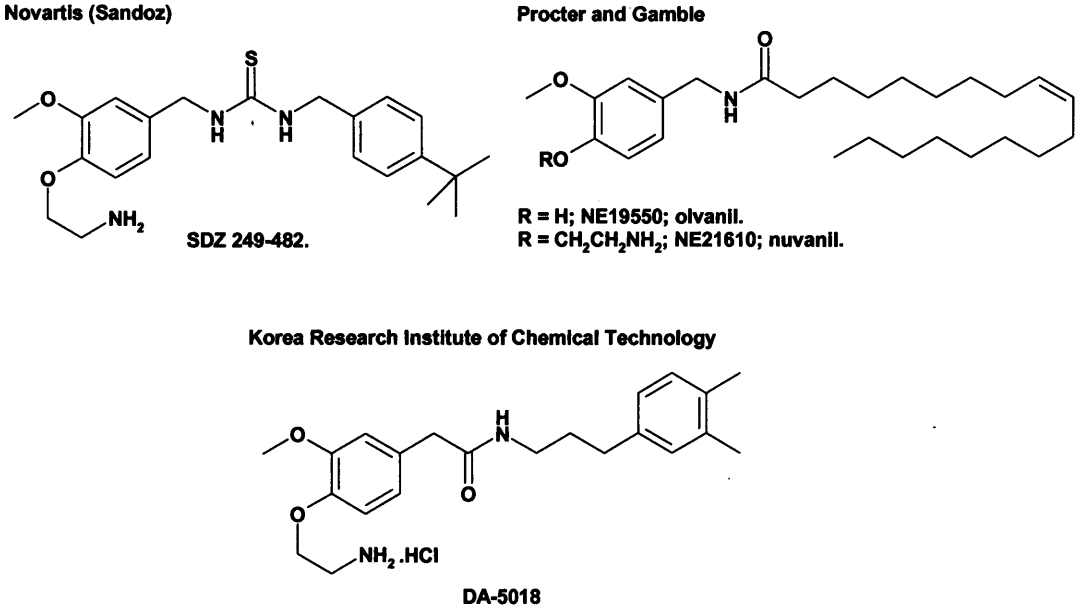

Figure 19: Capsaicin analogues entering clinical development[352;354]

Lastly, a second Korean group have focussed upon increasing the potency of capsaicin analogues such as SDZ 249-482 and DA 5018 by introducing structural features to mimic key potential pharmacophores from the tricyclic diterpene C-region of RTX[357-361], with some success (see Figure 20). Of the compounds shown, *N*-(3-*tert*-butanoyloxy-2-(3,4-dimethylbenzyl)propyl)-*N'*-(4-hydroxy-3-methoxybenzyl) thiourea (**1**) and *N*-(3-*tert*-butanoyloxy-2-(4-*tert*-butylbenzyl)propyl)-*N'*-(4-hydroxy-3-methoxybenzyl) thiourea (**2**) are respectively reported as 280- and 480-fold more potent than capsaicin in a [^{3}H]RTX binding assay, while *N*-(3-*tert*-butanoyloxy-2-(3,4-dimethylbenzyl)propyl)-*N'*-(4-(2-

aminoethoxy)-3-methoxybenzyl) thiourea (**3**) is described as a 'potent analgesic', based upon results from the acetic acid-induced writhing test in mice.

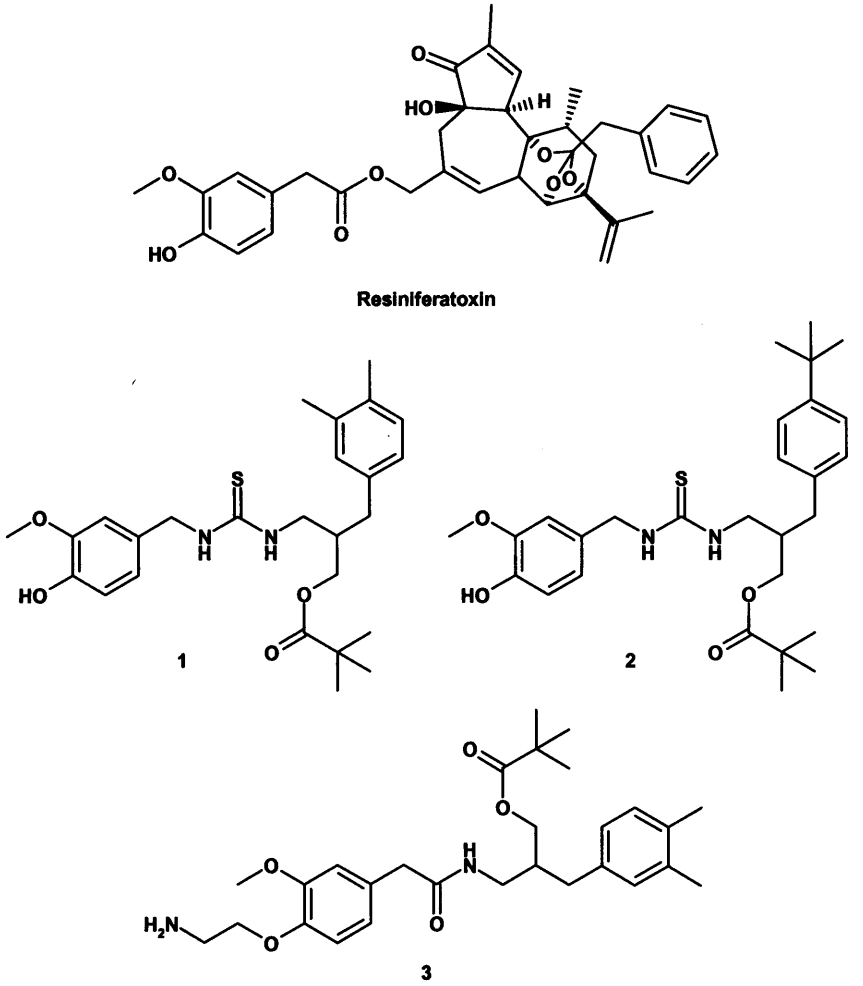

Figure 20: Potent synthetic capsaicin analogues, derived from modelling of the putative pharmacophores of RTX[357-361].

The Discovery of Capsazepine - the First Competitive Antagonist of the Neuroexcitatory Action of Capsaicin[71;72]

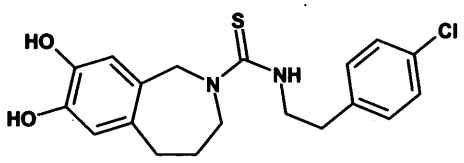

Figure 21: The competitive capsaicin antagonist, capsazepine (CPZ).

First synthesised in 1988 at the Sandoz Institute for Medical Research (now the Novartis Institute for Biomedical Research, London), capsazepine (**CPZ**, see Figure 21) was synthesised as part of the ongoing drug discovery project to produce agonist analogues of capsaicin with antinociceptive activity. Prior to the

successful identification, cloning and expression of the TRPV1 ion channel[73], various *in vitro* and *in vivo* assays had been employed at various times to assess the activity of capsaicin analogues, including the evaluation of capsaicin-like pungency by taste! With respect to the published SAR studies of capsaicin analogues at the Sandoz Institute for Medical Research from the early 1990s[72;313-315;352], the primary screen for analogue activity required the monitoring of the analogue-induced influx of radioactive $^{45}Ca^{2+}$ ions into cultured, isolated neonatal rat DRG neurones[66].

During the project, a short series of capsaicin analogues were synthesised and tested in which a conformational constraint was introduced to assess the effect upon activity that controlling the orientation of the A- and B-regions of the molecule with respect to each other would have. In addition to the conformational tether, there are other structural differences between these compounds and capsaicin. Rather than using capsaicin as the parent, parallel investigations had produced a synthetically more accessible, slightly more potent progenitor. The key structural stepping stones on the way from capsaicin to the constrained analogues, complete with their activities in the calcium efflux assay, are illustrated in Figure 22.

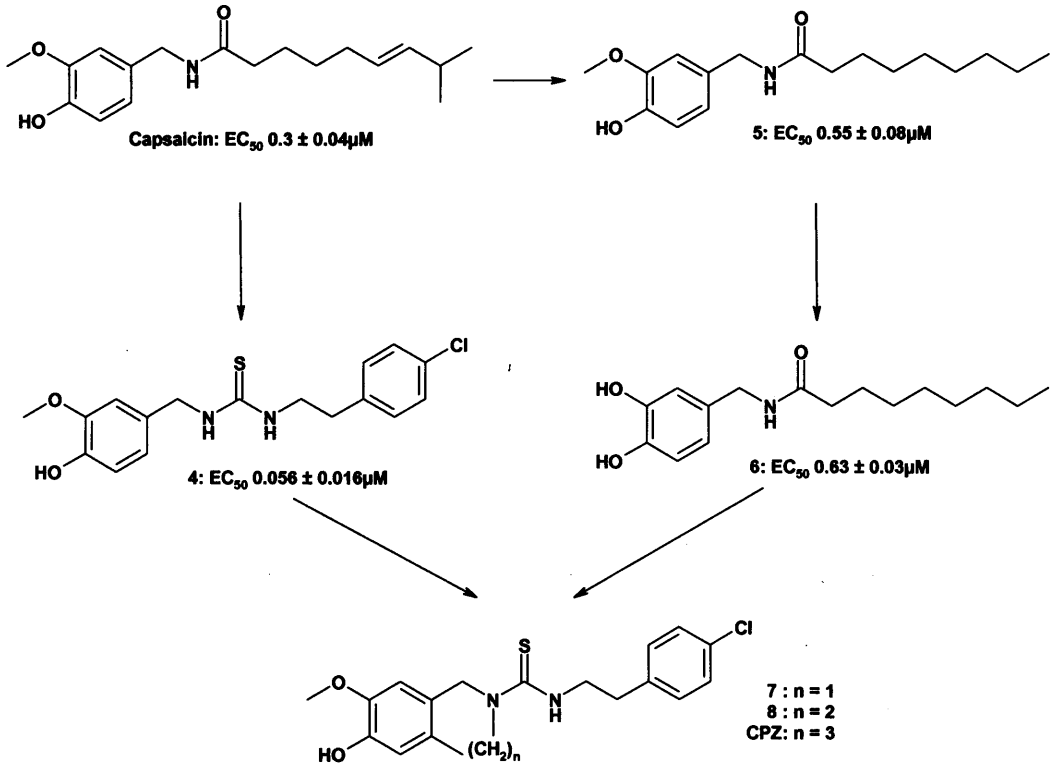

Figure 22: Key steps in development, from capsaicin to CPZ.

To summarise, the drug discovery project had produced *N*-(2-(4-chlorophenyl)ethyl)-*N'*-(4-hydroxy-3-methoxybenzyl) thiourea (**4**) as the lead compound, with a 6-fold greater agonist potency than capsaicin[352]. It retained the optimal A-ring vanillyl substitution pattern[313], but had replaced the B-region amide with a thiourea[314], and the C-region aliphatic chain with the 2-(4-chlorophenyl)ethyl moiety[315]. Parallel investigations had also demonstrated that the replacement of the 4-hydroxy-3-methoxy substitution pattern of the vanillyl ring in an analogue with the 3,4-catechol produced an analogue of similar potency, as exemplified by comparison of *N*-(4-hydroxy-3-methoxybenzyl)nonanoyl amide (**5**) and *N*-(3,4-dihydroxy benzyl)nonanoyl amide (**6**)[313]. This substitution pattern for the A-ring was adopted for synthetic expediency in the constrained molecules. To incorporate a degree of conformational constraint into the molecules, a tether of 1 to 3 methylenes between the benzylic nitrogen and the 6-position of the vanillyl ring was introduced, to give *N*-(5,6-dihydroxy-1,3-dihydroisoindole-2-thiocarboxy)-2-(4-chlorophenyl)ethyl-amine (**7**), *N*-(6,7-dihydroxy-3,4-dihydro-1H-isoquinoline-2-thiocarboxy)-2-(4-chlorophenyl)ethylamine (**8**) and *N*-(7,8-dihydroxy-1,3,4,5-tetrahydrobenzo[c]-azepine-2-thiocarboxy)-2-(4-chlorophenyl)ethylamine (capsazepine, CPZ). Of the conformationally restrained compounds, the isoindoline (**7**) and the tetrahydroisoquinoline (**8**) showed agonist potency of the same order of magnitude as capsaicin, whereas the tetrahydrobenzazepine (CPZ) was totally inactive as an agonist (see Table 2). However, further testing revealed CPZ to be a moderately potent, *competitive antagonist* of the capsaicin-induced $^{45}Ca^{2+}$ influx, with an IC_{50} of 0.420 ± 0.046 μM (see Table 2)[71].

Compound	$^{45}Ca^{2+}$ influx EC_{50} (μM)	Inhibition of capsaicin (500nM)-induced $^{45}Ca^{2+}$ influx IC_{50} (μM)
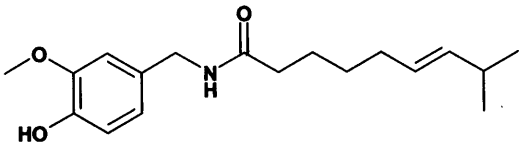 **Capsaicin**	0.3 ± 0.04	NT
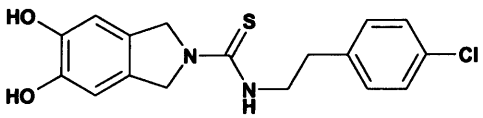 **7**	0.55 ± 0.08	NT
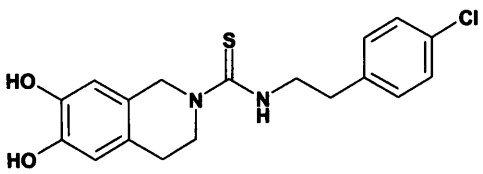 **8**	0.29 ± 0.04	NT
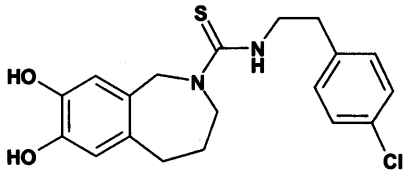 **Capsazepine, CPZ**	>100	0.42 ± 046

Table 2: Primary biological data for the conformationally constrained capsaicin analogues (NT = not tested)[71;72].

The magnitude of this discovery, and its contribution to the field of vanilloid and vanilloid receptor research cannot be overestimated. Ruthenium red, an inorganic microscopic stain[362], had been demonstrated to have *functional* antagonism of

capsaicin activity as an inhibitor of both capsaicin-evoked stimulation and desensitisation of sensory neurones[363].[364;365] This action had been determined to be *non*-competitive[71;366], and was deemed a result of ruthenium red's general actions as a blocker of calcium ion channels, rather than a specific interaction with the capsaicin receptor.

As the first competitive antagonist of capsaicin-evoked activation of polymodal nociceptors, CPZ has been used widely as a pharmacological tool to investigate PMN functionality, with respect to the actions of capsaicin. Using SciFinder to search the CAplus database for references to 'capsazepine' produced 400 hits.

As a pharmacological tool, CPZ has proven a little promiscuous in its actions, having some activity at other ion channels. These include the blockade of voltage-activated calcium channels in sensory neurones[367] and of cold and menthol-activated channels (probably TRPM8) in rat DRG neurones[368], the inhibition of nicotinic acetylcholine receptors (nAChR)[369] and of human hyperpolarization-activated cyclic nucleotide-gated 1 (HCN1) channel[370], and the activation of the δ-subunit of the human amiloride-sensitive epithelial Na+ channel (ENaC)[371], albeit at multiple millimolar concentrations. Despite this, antagonism by CPZ continues to be a standard by which potential ligands for the TRPV1 ion channel are measured and defined.

Conformational Hypothesis for the Activity of Capsazepine

If we refer back to the original paper in the Journal of Medicinal Chemistry that described the discovery of CPZ[72] and the section entitled *The Discovery of Capsazepine - the First Competitive Antagonist of the Neuroexcitatory Action of Capsaicin*, the three constrained analogues **7**, **8** and CPZ, while at first glance are structurally very similar, have very different activities. To reiterate, **7** and **8** are agonists of a similar potency to capsaicin, whereas CPZ is an antagonist. The techniques of NMR spectroscopy, X-ray crystallographic analysis, and molecular modelling were used to study, compare and contrast the conformational behaviour of CPZ with respect to **8** as the agonist exemplar, and a rationale for the difference in activity was proposed. By considering the aromatic ring of the A-region and the thiourea of the B-region as each being planar, and the angle between these planes as α (see Figure 23), it is possible to envisage the length of the conformational tether as determining the value of α for each of the analogues.

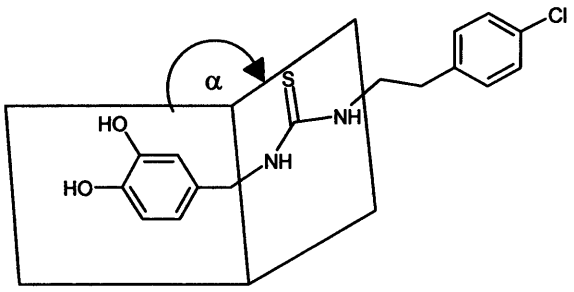

Figure 23: Definition of the angle α[72]

For **8**, the heterocyclic ring displays some degree of flexibility, which is reflected in the NMR spectra, with no single favoured conformation. Even so, the A/B-region of the molecule maintains an extended conformation, with α held at 180°±30°. The heterocyclic ring of CPZ, on the other hand, adopts four discrete and quite rigid conformations, with 92% of the conformations populating one of two 'pseudochair' forms. These serve to hold the two planes almost orthogonal to one another, with α at ~±90°. As a result, it was postulated that, while both compounds possess the pharmacophores for activity, CPZ was unable to attain the necessary conformation for agonism. The antagonist activity was envisaged as resulting from the different disposition of the pharmacophores utilising a different binding mode to the agonist, but with some overlap in the binding motifs of the receptor ensuring antagonism. The distinctive orientation of the pharmacophores in CPZ might provide a template for the design of a second generation of antagonists. The accessible low energy conformations from the molecular dynamics simulations performed at the time for each of **8** and CPZ are reproduced in Figure 24, by kind permission of the authors.

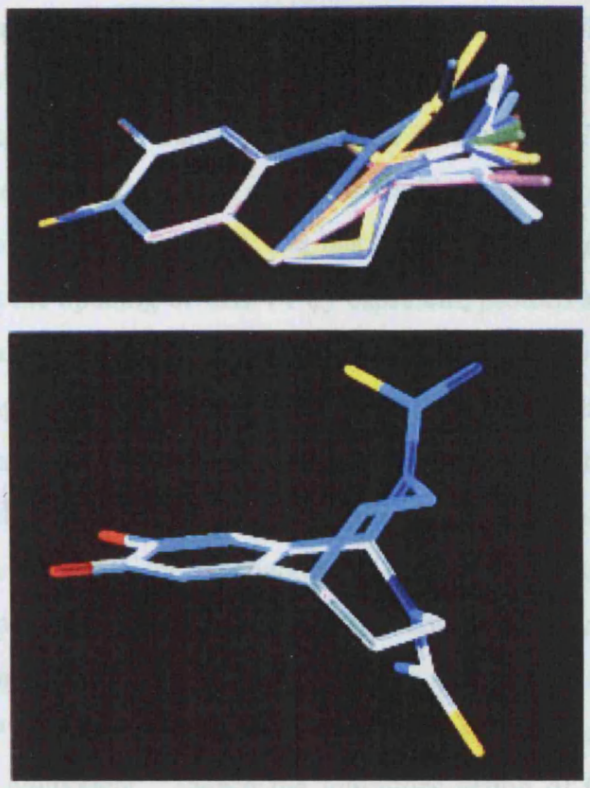

Figure 24: Accessible low energy conformations of **8** (top) and CPZ (bottom), as described by Walpole *et al*, with the C-region side chains omitted for clarity[72]

CPZ as an Analgesic

Consideration of the mechanism of the activation of TRPV1 by capsaicin, with the central role TRPV1 appears to have in peripheral nociception and neurogenic inflammation, would suggest that antagonists of such activation would be efficient analgesics. As such, they would be preferable to the desensitisation of the agonists, as an antagonist would not have the acute excitatory effects associated with agonism. Rather tragically, early studies on capsazepine concluded that capsaicin antagonists would be unlikely to be useful as analgesics, as early experimental pharmacology demonstrated that CPZ lacked any antihyperalgesic activity in *in vivo* models of acute and chronic pain in the rat[372]. It wasn't until subsequent studies showed CPZ to have an antinociceptive effect in inflammatory pain models in the mouse[373;374], and that CPZ could effect reversal of mechanical hyperalgesia in models of inflammatory and neuropathic pain in the guinea pig[375] that interest in the potential for TRPV1 antagonists as analgesics was renewed. This begs the question; why is CPZ analgesia species specific?

The most likely answer came as the identification, cloning and expression of various orthologues for mammalian TRPV1, particularly the rat[73], the human[74;75] and the

guinea pig[77], occurred, allowing CPZ's behaviour in each of these species to be explored. CPZ was demonstrated to inhibit the capsaicin-induced activation of them all, with higher potency in the human[75] (see Table 3). However, TRPV1 is not only activated by chemical mediators such as the vanilloids, it is also activated by acidic pH (~5.5)[73] and noxious heat (>43°C)[73]. It has been demonstrated that, while CPZ successfully blocks the opening of TRPV1 by capsaicin, protons and noxious heat in the guinea pig[77] and the human[75], CPZ does **not** block the proton-induced activation of the rat orthologue of TRPV1[75] (see Table 4) and is much less effective at inhibiting the noxious heat-induced activation of TRPV1 in the rat[75] (data not shown). This would seem to imply that the inhibition of capsaicin-induced activation of TRPV1 alone is not sufficient for analgesia. The determinants of this variance in activity between species appears to be the responsibility of only a few amino acid residues, as demonstrated by the ability to confer human-like activity on the rat orthologue of TRPV1 by point mutation of only three amino acid residues to the human orthologue equivalent[376]. Since the inhibitory action of CPZ in the human orthologue more closely resembles that seen in the guinea pig over the rat, might CPZ, or close analogues, be analgesic in the human?

IC_{50} (μM) for CPZ vs. capsaicin-induced activation of orthologues of TRPV1		
Rat[75]	Guinea pig[77]	Human[75]
0.478	0.324	0.186

Table 3: IC_{50} values for CPZ vs. capsaicin-induced activation of TRPV1 orthologues.

IC_{50} (μM) for CPZ vs. activation of orthologues of TRPV1 by low pH.		
Rat[75]	Guinea pig[77]	Human[75]
>10	0.355	0.180

Table 4: IC_{50} values for the inhibition by CPZ of the activation of orthologues of TRPV1 by low pH.

Further Vanilloid-derived Analogues with Antagonist Activity at TRPV1

Other vanilloid-derived antagonists of the capsaicin-induced activation of TRPV1 have been published. After CPZ, the next to be reported as a potential antagonist of capsaicin activity was capsazocaine[377], and only antagonism of capsaicin-induced

activity was reported. Described as a 'molecular fusion product of irritant synthetic capsaicin and the local anaesthetic benzocaine', capsazocaine incorporates structural features of benzocaine and synthetic capsaicin, a synthetically more amenable, yet equipotent, analogue of capsaicin, in which the branched and unsaturated aliphatic C-region sidechain of capsaicin has been replaced with an n-octyl chain. The synthesis and similar potency of this simplified capsaicin analogue were first reported in 1925[317]; and has more recently appeared in other SAR studies[315] (see Figure 25).

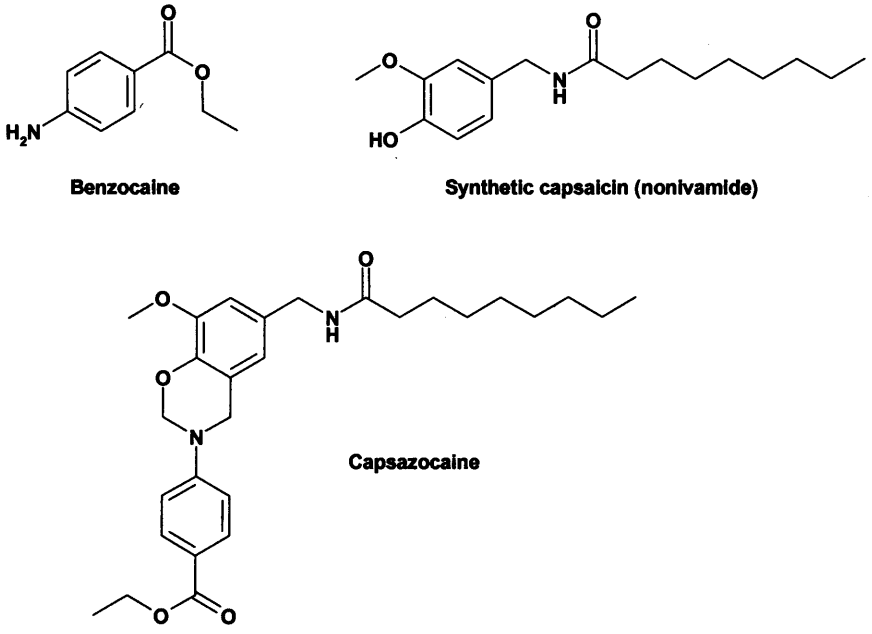

Figure 25: Capsazocaine[377]

Simple iodination appears to convert specific agonists to antagonists (see Figure 26). RTX is an ultrapotent vanilloid[17], with in excess of 6500-fold greater potency than capsaicin in a given assay[378]. The 5-iodo analogue (I-RTX) is a highly potent *ant*agonist, at least 40-fold more potent CPZ against capsaicin-induced currents in *Xenopus laevis* oocytes expressing the rat orthologue of TRPV1[378] and 800-fold more potent than CPZ when assayed against capsaicin-induced currents in human embryonic kidney cells (HEK) expressing rat TRPV1[379]. I-RTX also inhibited both proton-induced and heat-induced currents in rat TRPV1-HEK cells[379], and intrathecal administration of I-RTX blocked pain responses induced by the injection of capsaicin into the paw of the mouse[378]. However, the local sub-cutaneous injection of I-RTX did not inhibit the capsaicin-induced nociceptive response of the rat, as modelled by capsaicin-induced paw flinching[379].

Similarly, N-(4-chlorobenzyl)-N'-(4-hydroxy-3-methoxybenzyl)thiourea (**9**)[352] is an approximately 5-fold more potent TRPV1 agonist than capsaicin, as assessed by influx of radioactive $^{45}Ca^{2+}$ ions into cultured, isolated neonatal rat DRG neurones[66]. The similar addition of an iodo-substituent to the compound produced N-(4-chlorobenzyl)-N'-(4-hydroxy-3-iodo-5-methoxybenzyl)thiourea (IBTU), a 5-fold more potent antagonist than CPZ, as assessed by the inhibition of capsaicin-induced uptake of $^{45}Ca^{2+}$ ions by Chinese hamster ovary (CHO) cells heterologously expressing the rat orthologue of TRPV1[380]. IBTU was not tested against other modalities of TRPV1 activation.

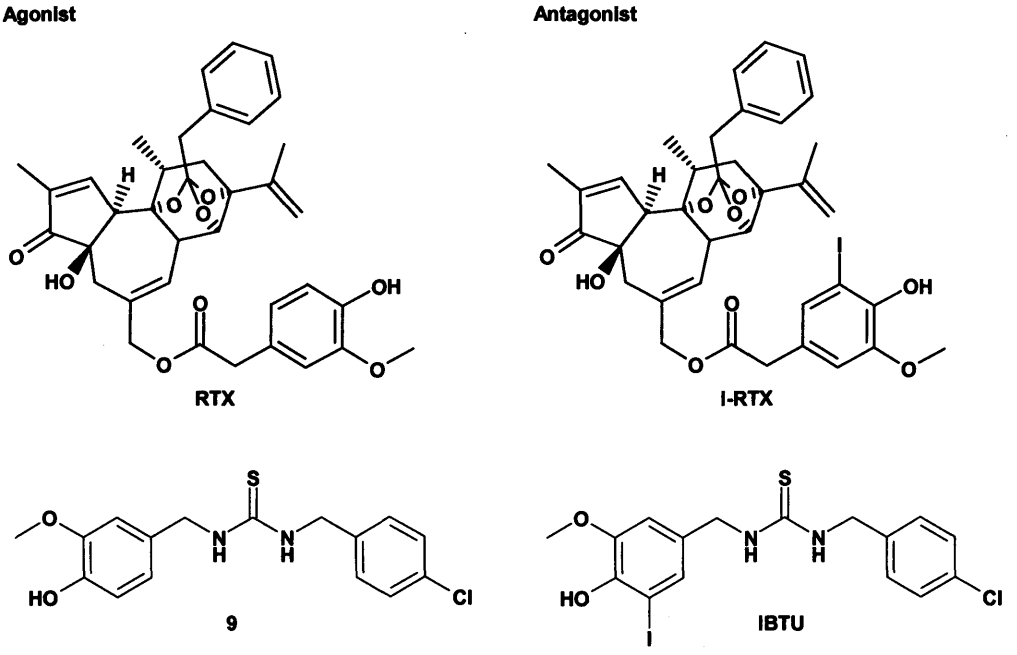

Figure 26: Iodinated vanilloid analogues with antagonism of capsaicin-induced activation of TRPV1, and their agonist progenitors.

In addition to increasing the potency of capsaicin analogues such as SDZ 249-482 and DA 5018 by introducing structural features to mimic key potential pharmacophores from the tricyclic diterpene C-region of RTX (see Capsaicin and Agonist Analogues as Analgesics), Lee and co-workers at the Seoul National University have also explored several other approaches to synthesising antagonists of capsaicin-induced activation of the rat TRPV1 ion channel. Their first approach explored the effect of combining their modified 3-acyloxy-2-benzylpropyl C-regions with the conformationally constrained A/B-regions of **8** and CPZ[381]. Intriguingly, both the tetrahydrobenzazepine analogue (**10**) and the tetrahydroisoquinoline

analogue (**11**) are antagonists of similar potency to CPZ, while minor structural changes to the C-region substitution produced full agonists of submicromolar potency. Clearly, the requirements for agonism vs. antagonism are finely balanced in this series.

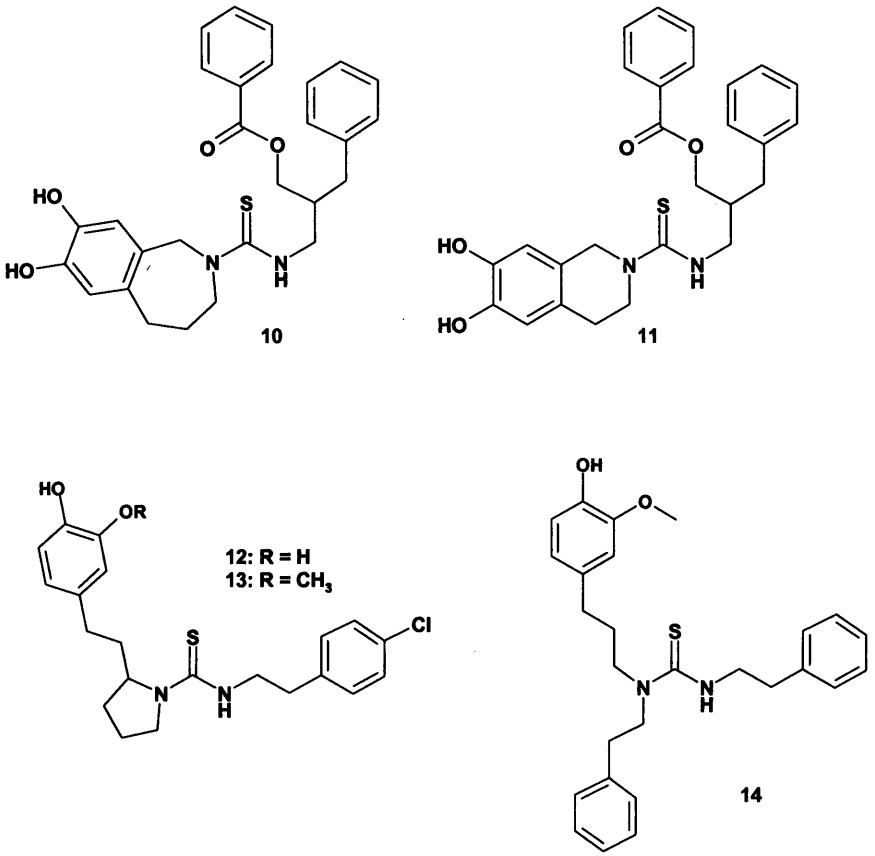

Figure 27: Some vanilloid-derived TRPV1 antagonists of similar potency to CPZ.

The second approach explored the potential in opening the tetrahydrobenzazepine ring of CPZ between the benzene ring and the benzylic methylene, then re-introducing constraint in the form of a pyrrolidine[382] (**12** and **13**) to produce micromolar antagonists, or in the form of steric bulk (*e.g.* **14**) to produce antagonists of submicromolar potency, similar to that of CPZ[383] (see Figure 27).

A third approach was discovered during investigations into the effect of varying the substitutents of the A-region away from the parent vanillylamine upon already potent agonists such as **1** and **2**, and included the isosteric replacement of the phenolic oxygen beyond the 2-aminoethoxy alternative already seen in PKF249-482 and **3** (see Capsaicin and Agonist Analogues as Analgesics). This approach ultimately yielded antagonists with nanomolar activity (see Figure 28), with **15**[384] clearly

derived from **1** (see Figure 20) and **SC0030**[385-389] clearly derived from Novartis's PKF249-482 (see Figure 19).

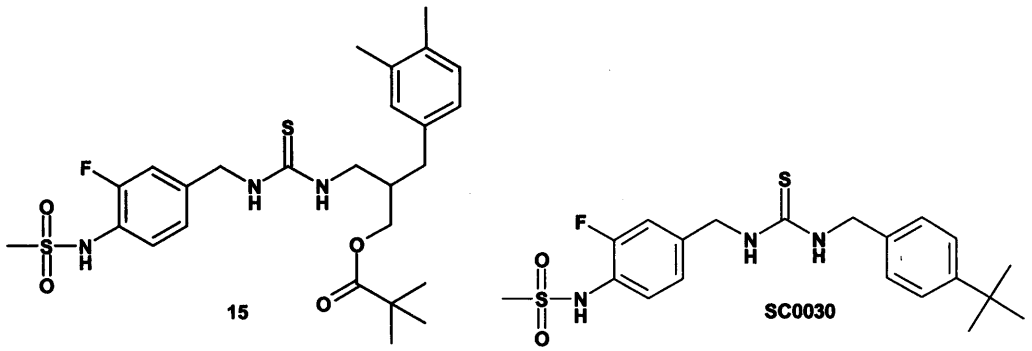

Figure 28: Nanomolar antagonists of TRPV1 activation.

Of the vanilloid-derived antagonists **10-15** and SC0030, only SC0030 was reported to also inhibit activation by acidic pH and noxious heat in the rat orthologue of TRPV1[386;387], and to exhibit analgesia in the parabenzoquinone-induced writhing test in mice of similar potency to the COX inhibitor indomethacin [388]. Although the antagonist activity of **15** was only reported for capsaicin-induced activation of the rat orthologue of TRPV1, it was reported to have dramatically enhanced analgesic potency over ketorolac (another COX inhibitor) in the acetic acid-induced writhing test in mice[384].

Non-Vanilloid-derived Antagonists of TRPV1 Activation

With the demonstration that TRPV1 antagonists can be analgesic in rodents came a change in the drug discovery approach to analgesics acting via the capsaicin receptor, from partial agonist desensitisers to antagonists. Initial research centred around antagonists based upon capsaicin and other vanilloids. The subsequent successful identification, cloning and expression of assorted mammalian orthologues of TRPV1, particularly the rat[73] and the human[74;75], coupled with advances in high throughput screening (HTS) technologies and assay development, has allowed companies to exploit both their in-house and commercially available compound collections, using such technologies to identify structurally novel antagonists of TRPV1 activation. Most pharmaceutical companies have or have had projects devoted to developing TRPV1 channel blockers as analgesics, and the last few years have seen numerous publications to this effect. The 'building block' nature of such compound libraries has resulted in some recurring structural motifs. In particular, compounds featuring a

central piperazine with pendant aryl groups plus linkers have been patented or published by Purdue Pharma (4-(3-chloropyridin-2-yl)piperazine-1-carboxylic acid (4-tert-butyl-phenyl)amide, BCTC, **16**)[390;391], Neurogen ((R)-4-(3-chloro-pyridin-2-yl)-2-methylpiperazine-1-carboxylic acid (4-trifluoromethyl-phenyl)amide, **17**)[392], Euro-Celtique (*N*-(4-tert-butylphenyl)-*N'*-cyano-4-(3-chloropyridin-2-yl)piperazine-1-carboxamidine, **18**)[393], Amgen (2-[4-(3-chloro-pyridin-2-yl)piperazin-1-yl]-6-trifluoromethyl-1H-benzoimidazole, **19**)[394] and Johnson and Johnson (4-(3-trifluoromethylpyridin-2-yl)piperazine-1-carboxylic acid (5-trifluoromethylpyridin-2-yl)amide, **20**)[395] (see Figure 29).

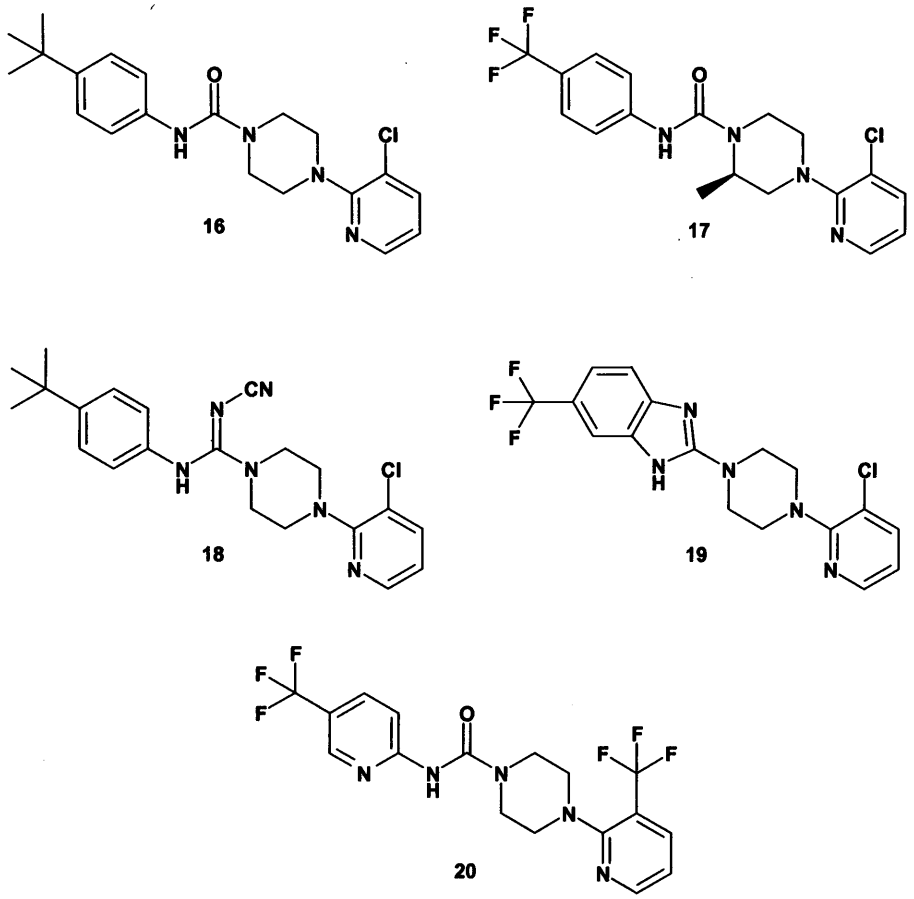

Figure 29: Diarylpiperazine antagonists of TRPV1.

SmithKlineBeecham, now GlaxoSmithKline (GSK), have patented/published on a series of N,N'-substituted ureas (see Figure 30), exemplified by compounds **21**[396;397], **22**[398] and **23**[399-401]. These compounds are clearly related to the diarylpiperazines described above.

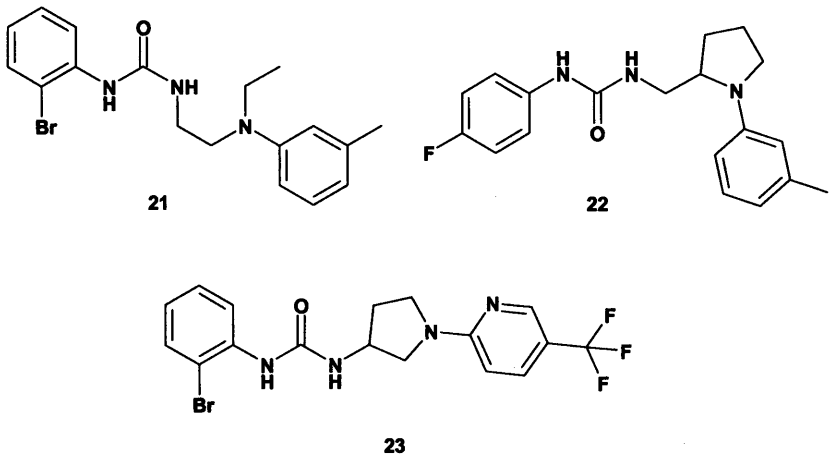

Figure 30: N,N'-substituted ureas antagonists of TRPV1 from GSK.

Quinazoline cores have also appeared as a common structural motif, as exemplified by 3-[4-[(4-trifluoromethylphenyl)amino]-7-(3-trifluoromethylpyridin-2-yl)quinazolin-2-yl]propionic acid (**24**) from Neurogen[402-404], and 6-(4-Chloro-3-cyclopropylmethoxyphenyl)-7-isopropyl-2-methyl-3H-quinazolin-4-one (**25**) from Novartis[405] (see Figure 31)

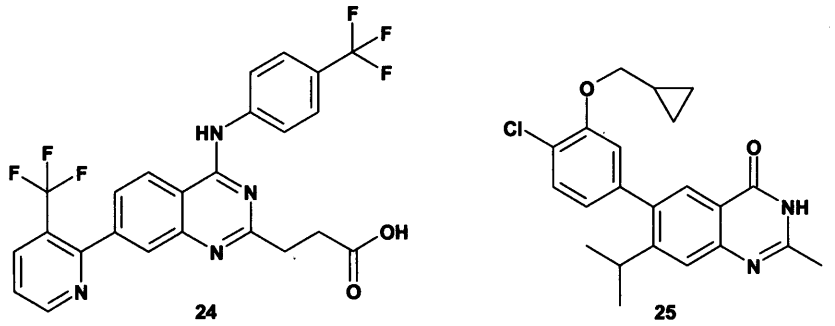

Figure 31: Quinazoline-derived TRPV1 antagonists.

Amgen and GSK have both described *N*-aryl cinnamides (see Figure 32), with Amgen publishing a detailed SAR study[406;407], featuring (*E*)-*N*-quinolin-7-yl-3-(6-trifluoromethyl-2-(piperidin-1-yl)pyridin-3-yl)acrylamide (**26**) and (*E*)-*N*-quinolin-7-yl-3-(6-trifluoromethyl-2-(morpholin-4-yl)pyridin-3-yl)acrylamide (**27**) as their most potent antagonists of TRPV1 activation, and GSK reporting the discovery of (*E*)-*N*-(3-methoxyphenyl)-3-(4-chlorophenyl)acrylamide (**SB-366791**)[408;409].

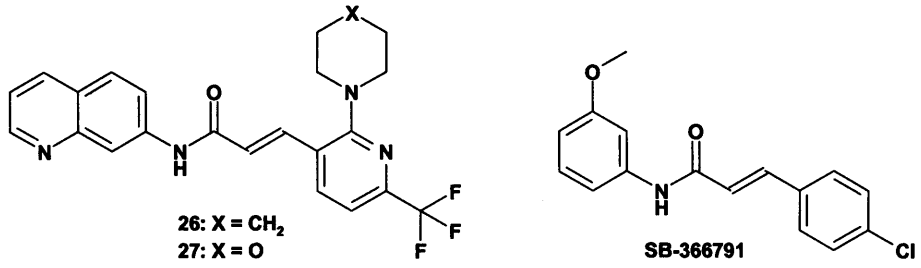

Figure 32: *N*-aryl cinnamide-derived TRPV1 antagonists

Finally, Purdue Pharma have improved upon the pharmaceutical and pharmacological profile of **16**, with the recent disclosure of (R)-4-(6-Chloro-4-methylpyridazin-3-yl)-2-methylpiperazine-1-carboxylic acid (6-fluorobenzothiazol-2-yl)amide (**28**)[410] (see Figure 33).

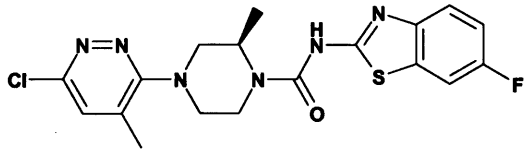

28

Figure 33: (*R*)-4-(6-Chloro-4-methylpyridazin-3-yl)-1-(6-fluoro-benzothiazol-2-yl)carbamoyl-2-methylpiperazine **28**[410].

AIMS

Further Conformationally Constrained Antagonists

During the drug discovery phase that produced CPZ, several other conformationally constrained analogues were also synthesised. In particular, three analogues (**29**, **30** and **31**) of the tetrahydroisoquinoline derivative **8** were synthesised and tested (see Table 5).

Compound	Ca^{2+}-influx assay (μM)	
	agonist EC_{50}	antagonist IC_{50}
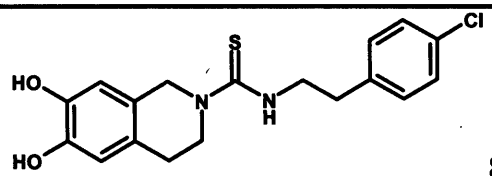 **8**	0.29 ± 0.04	NT
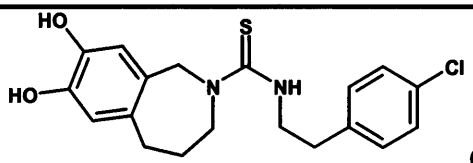 **CPZ**	>100	0.420 ± 0.046
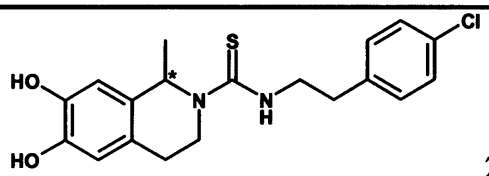 **29**	>100	1.07
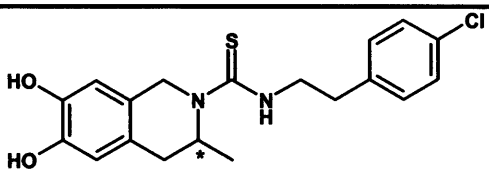 **30**	>100	0.18
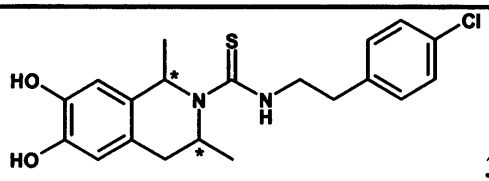 **31**	>100	0.63

Table 5: Biological activities of 1-, 3- and 1,3- substituted analogues of **8**.

Interestingly, **29**, **30** and **31** were found to be totally inactive as agonists, at concentrations up to 100μM, as determined by the stimulation of uptake of $^{45}Ca^{2+}$ ions by neonatal rat DRGs, while **8** was already established as an agonist of similar potency to capsaicin. Further investigation revealed these compounds to act as *ant*agonists of the capsaicin-induced uptake of $^{45}Ca^{2+}$ ions by neonatal rat DRGs, with potencies of a similar magnitude to CPZ (see Table 5).

Stereoisomerism

Marked with a * in Table 5, **29**, **30** and **31** each possess one or more tetrahedral carbon atom(s), to which four different substituents are attached. These *chiral centres*[411] allow each analogue to exhibit *stereoisomerism*, *i.e.* each has *non-superimposable* isomers of identical constitution, which differ in their conformation and/or configuration (the arrangement of their atoms in space)[411] (see Figure 34). Compounds with one chiral centre, such as **29** and **30**, have two possible stereoisomers; these are mirror images of each other, and are referred to as *enantiomers*. For compounds with more than one chiral centre such as **31**, the situation is more complex. While some pairs of stereoisomers are mirror images of one another, and hence are still termed *enantiomers*, others are *not* mirror images of one another; these are referred to as *diastereomers*.

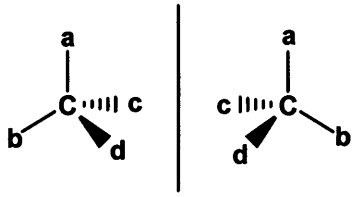

Figure 34: Illustration of the non-superimposability of tetrahedral chiral centres (Cabcd).

To distinguish between these stereoisomers and others throughout this thesis, the author has employed the commonly used Cahn-Ingold-Prelog (CIP) system for the specification of absolute molecular configuration. This system uses the *chiral descriptors R* and *S* to denote the absolute configuration at a chiral centre[412-414]. Briefly, to assign the correct descriptor, the four substituents at the chiral centre are ranked, or *prioritised*, from highest to lowest, according to rules based upon the material properties (atomic number and mass number) and the structural properties of topology and geometry, as described in the cited references[412-414].

Once ranked, it is necessary to then consider the chiral centre and its substituents 3-dimensionally. The molecule is oriented such that it is possible to look down the bond between the central atom and the lowest priority ligand, with the lowest priority ligand 'behind' the central atom. The remaining three ligands form a triangular array, with two possible directions of rotation when moving from highest to lowest priority. If the direction is *clockwise*, the descriptor used is *R*; if anticlockwise, then *S* is used (see Figure 35).

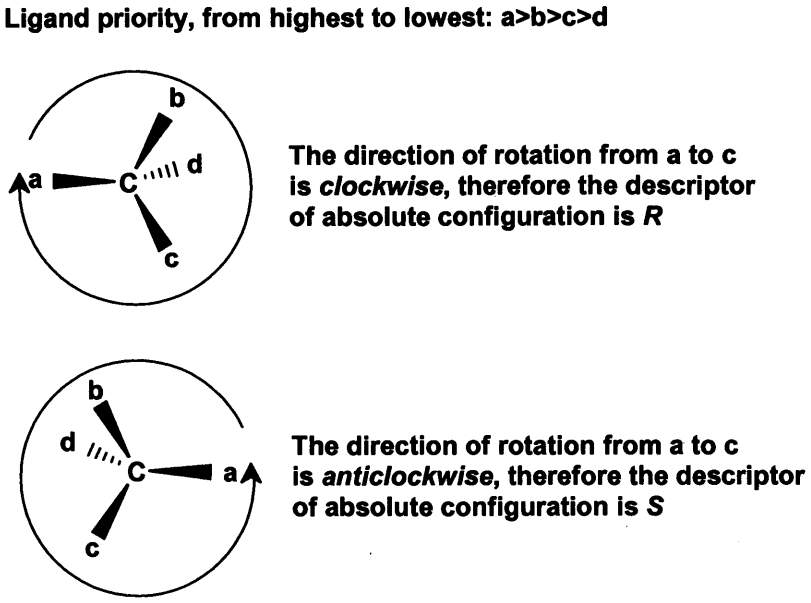

Figure 35: Chiral descriptors of absolute configuration, as defined by the CIP system[412-414].

Further points of relevance:

- When there is a mixture of stereoisomers, and both configurations at a chiral centre are present, both descriptors are used *i.e.* when both enantiomers of **29** are present in a mixture, the material would be more accurately labelled as **29*RS***.
- When more than one chiral centre exists in a molecule, each is identified by positional numbering (see Figure 36) *i.e.* the mixture of stereoisomers comprising **31** is more accurately described by the identifier **31(1*RS*,3*RS*)**.

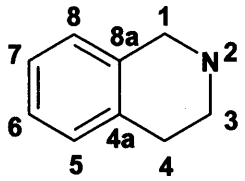

Figure 36: Numbering of the isoquinoline ring system.

Aims

For reasons of synthetic expediency, **29**, **30** and **31** were originally synthesised without regard to stereoisomerism, and were subsequently tested as mixtures of stereoisomers (*i.e.* as **29*RS***, **30*RS*** and **31(1*RS*,3*RS*)**). The aim of this research project was to develop enantio- and diastereoselective synthetic routes to each stereoisomer of **29**, **30** and **31** (see Figure 37), to investigate their *in vitro* biological activity at the TRPV1 ion channel, to explore their conformational behaviour, and possibly extrapolate these findings to the activity of CPZ.

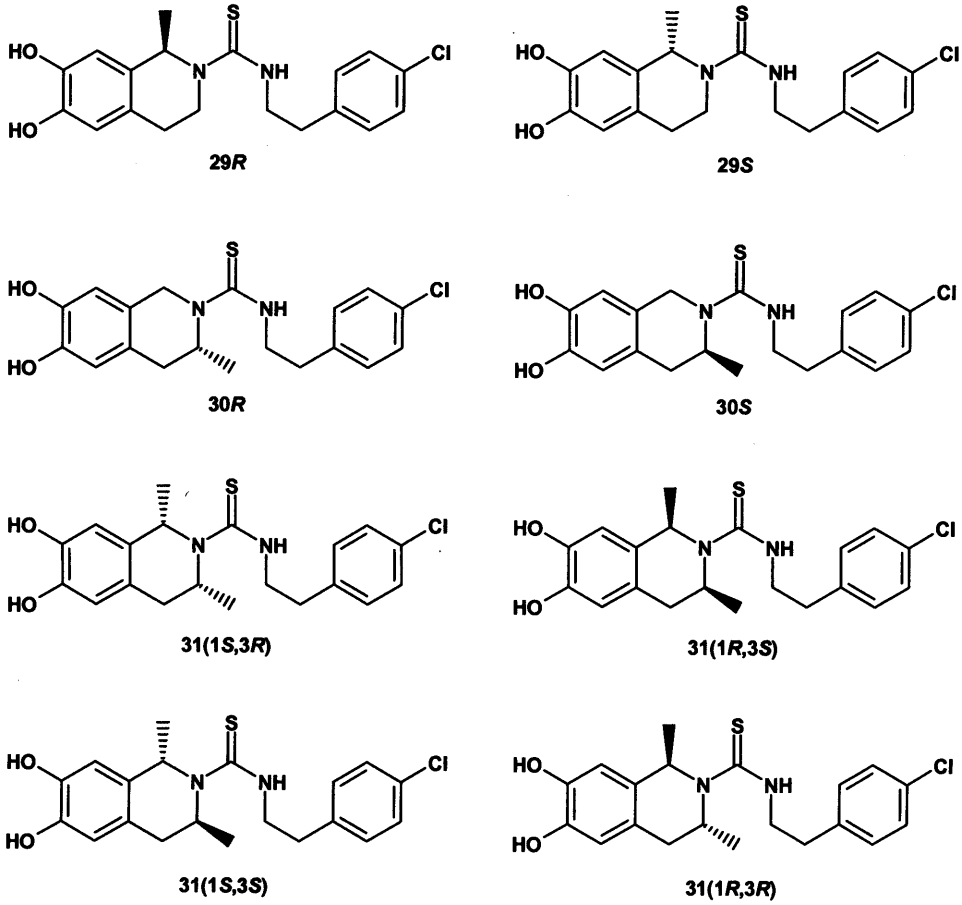

Figure 37: The desired stereoisomers of **29, 30** and **31**.

RESULTS AND DISCUSSION

Chemistry

Synthesis of the Stereoisomeric Mixtures of 29*RS*, 30*RS* and 31(1*RS*,3*RS*)

The common final step in the established achiral routes to **29*RS***, **30*RS*** and **31(1*RS*,3*RS*)** was the formation of the thiourea moiety by the coupling of an unresolved tetrahydroisoquinoline precursor (**33*RS***, **34*RS*** or **35(1*RS*,3*RS*)**) with the the commercially available 2-(4-chlorophenyl)ethyl isothiocyanate **32** (see Figure 38).

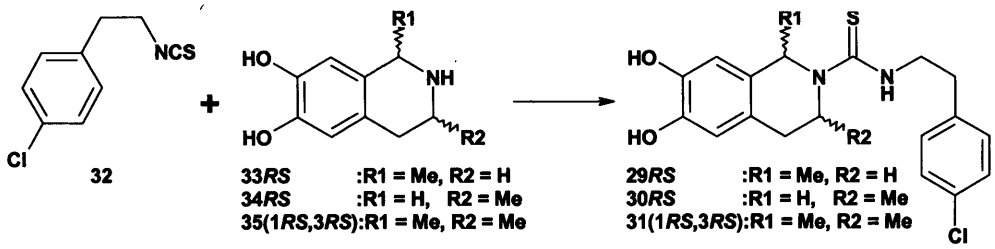

Figure 38: The generic final step in the synthesis of analogues of **8**.

The synthesis of **29*RS*** had been simplified by the commercial availability of the racemate of 6,7-dihydroxy-1-methyl-1,2,3,4-tetrahydroisoquinoline **33*RS*** (known trivially as (±)-salsolinol), allowing the synthesis of **29*RS*** to be achieved in one step (see Figure 39).

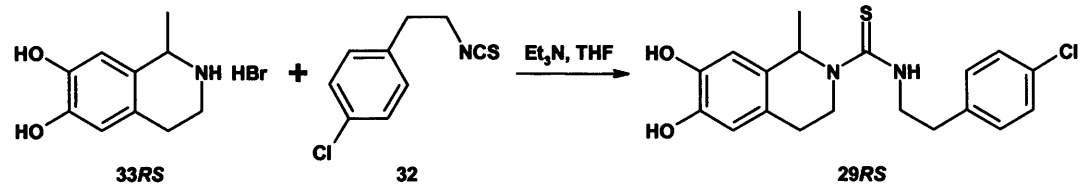

Figure 39: The synthesis of **29*RS***.

By comparison, neither **34*RS***, the 3-methyl analogue tetrahydroisoquinoline precursor to **30*RS***, nor **35(1*RS*,3*RS*)**, the 1,3-dimethyl tetrahydroisoquinoline precursor to **31(1*RS*,3*RS*)**, were commercially available. Each was synthesised from the commercially available 3,4-dimethoxyphenylacetone **36** (see Figure 40). Reaction of ketone **36** with methoxylamine hydrochloride gave the O-methyl oxime **37**, the reduction of which with borane-tetrahydrofuran complex gave the racemic amine **38*RS***. Cleavage of the methyl ethers with refluxing hydrobromic acid gave the racemic hydrobromide salt of 2-(3,4-dihydroxyphenyl)-1-methylethylamine **39*RS***,

and the tetrahydroisoquinolines **34*RS*** and **35(1*RS*,3*RS*)** were formed by reaction of **39*RS*** with either formaldehyde or acetaldehyde, using classical Pictet-Spengler tetrahydroisoquinoline synthesis methodology[415]. The final products **30*RS*** and **31(1*RS*,3*RS*)** were synthesised by coupling these unresolved tetrahydroisoquinolines with the isothiocyanate **32** (see Figure 40).

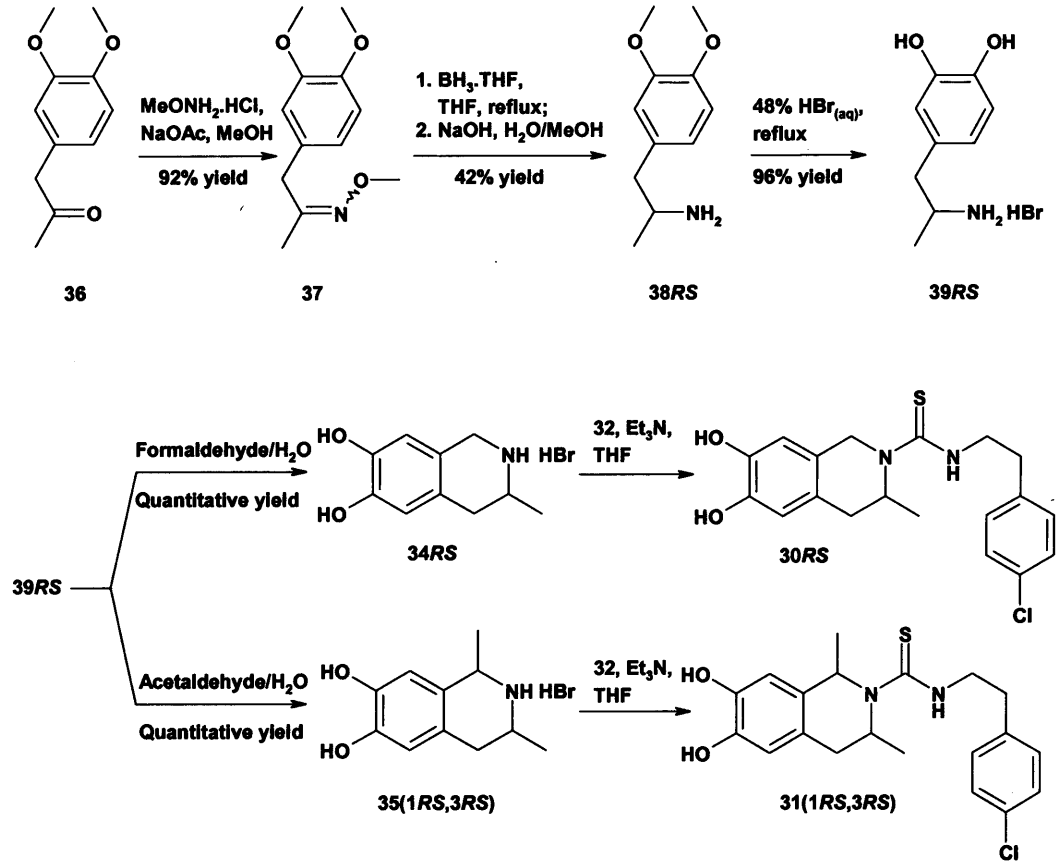

Figure 40: Syntheses of **30*RS*** and **31(1*RS*,3*RS*)**, and the tetrahydroisoquinoline precursors **34*RS*** and **35(1*RS*,3*RS*)**.

Retrosynthesis Common to 29, 30 and 31

The initial retrosynthetic analysis for each of the target full structures confirmed the most appropriate first disconnection to be of the carbon–nitrogen bond between the 2-position tetrahydroisoquinoline nitrogen and the thiocarbonyl carbon of the thiourea (see Figure 41; see Figure 36 for numbering of the tetrahydroisoquinoline ring). In addition to its commercial availability, the isothiocyanate **32** could be readily synthesised from 2-(4-chlorophenyl) ethylamine **40** and thiophosgene **41**, and a large batch was prepared in this way.

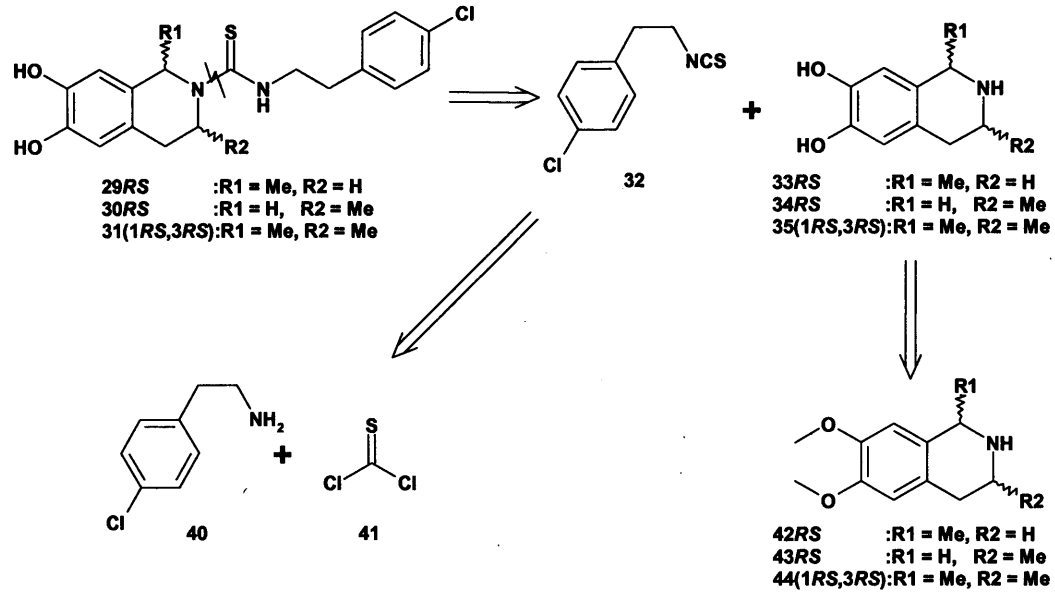

Figure 41: The initial retrosynthesis of the full structure targets:

Catechols are quite reactive, and can be difficult to store. Their reactivity in particular can impose limitations for many potential synthetic manipulations, due to putative side reactions. While determining asymmetric syntheses for the each of the stereoisomers of the tetrahydroisoquinolines **33**, **34** and **35** and their appropriate precursors, it was decided to perform the bulk of the synthetic work with the catechols protected as the methyl ethers, with deprotection as the penultimate step, prior to coupling with the isothiocyanate (see Figure 41).

The investigative synthetic work therefore concentrated upon routes to synthesise/resolve the pure (*R*)- and (*S*)-enantiomers of tetrahydroisoquinoline **42**, the pure (*R*)- and (*S*)-enantiomers of tetrahydroisoquinoline **43**, the pure (1*R*,3*S*)- and (1*S*,3*R*)-diastereomers of the *cis*-isomer of tetrahydroisoquinoline **44**, and the pure (1*R*,3*R*)- and (1*S*,3*S*)-diastereomers of the *trans*-isomers of tetrahydroisoquinoline **44**, as key intermediates. Through the exploitation and the modification of literature precedent, and the development of new methodology, the synthesis of each of these key intermediates, and hence each of the eight target full structures, was achieved.

Approaches to the Synthesis of Tetrahydroisoquinolines

There are traditionally three approaches to the synthesis of isoquinolines, each of which have proven amenable to enantioselective modification, much of which has been reviewed elsewhere[416;417]. Each approach requires an appropriately substituted benzene ring, from which the heterocycle is formed by means of a cyclisation step. They are respectively the Pictet-Spengler synthesis[415], which gives the 1,2,3,4-

tetrahydroisoquinoline directly, the Bischler-Napieralski synthesis[418], which gives the generally isolable 3,4-dihydroisoquinoline, and requires a subsequent reduction to the 1,2,3,4-tetrahydroisoquinoline, and the Pomeranz-Fritsch synthesis[419-423], which gives the fully aromatic isoquinoline, but which, via the Bobbitt modification[424], gives the 1,2,3,4-tetrahydroisoquinoline via the *in situ* reduction of a generally unstable 1,2-dihydroisoquinoline.

These classical approaches to isoquinoline synthesis were comprehensively reviewed in separate chapters in the 1951 edition of Organic Reactions[425-427].

Pictet-Spengler Tetrahydroisoquinoline Synthesis[415]

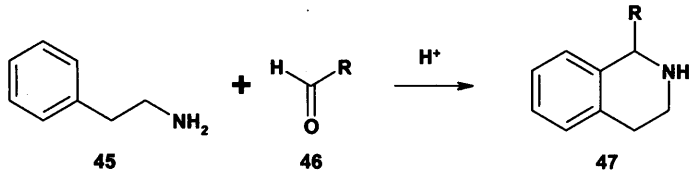

Figure 42: Pictet-Spengler tetrahydroisoquinoline synthesis[415].

The classical Pictet-Spengler reaction (see Figure 42) has been comprehensively reviewed elsewhere[426]. The tetrahydroisoquinoline **47** is formed by the condensation of a 2-phenylethylamine **45** with an aldehyde **46**, and can be considered to be a special example of the Mannich reaction (see Figure 43).

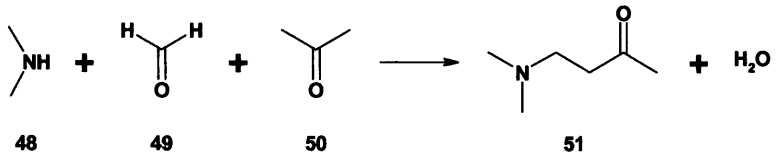

Figure 43: Comparison of the Mannich and Pictet-Spengler reactions.

These reactions are generally carried out in acidic media (*e.g.* hydrochloric acid, acetic acid), and are considered to occur in two steps:

1. the amine (**45/48**) reacts with the aldehyde (**46/49**) to form an iminium ion,
2. the iminium ion is then susceptible to attack by a carbon nucleophile to form a new carbon–carbon bond.

For the generic Mannich reaction shown, the carbon nucleophile is the ketone **50**, and the product is a 4-aminobutan-2-one **51**; for the Pictet-Spengler reaction, this second step occurs intramolecularly, with the new bond formation occurring between the iminium carbon and the ring carbon *ortho* to the ethyl chain, to join carbon-1 and

carbon-8a of the newly formed tetrahydroisoquinoline **47** (see Figure 36 for the numbering of the tetrahydroisoquinoline ring).

The mechanism of the Pictet-Spengler reaction is detailed in Figure 44 and Figure 45. In Figure 44, the mechanism of imine formation is described. Both **45** and **46** exist in equilibrium between their protonated and unprotonated forms. The formation of the imine **52** requires the nucleophilic attack of the lone pair of the neutral amine nitrogen onto the carbonyl carbon of the protonated aldehyde. The carbon-oxygen bond of the aldehyde is polarised, due to the greater electronegativity of the oxygen atom; the carbonyl carbon is therefore suited to nucleophilic addition. Protonation of the carbonyl oxygen increases the positive character of the carbon atom, facilitating nucleophilic attack. The neutrality of the nitrogen is restored by the loss of a proton. This is repeated; protonation of the hydroxyl induces the loss of the remaining proton from the nitrogen atom, and a transfer of electrons to form the imine. The imine itself is readily protonated, and the resulting iminium ion is highly reactive to nucleophiles.

In Figure 45 the mechanism of ring closure is described. The cyclisation step with an unactivated aromatic ring can be slow and require forcing conditions; it can be facilitated by increased electron density at the point of ring closure, and most literature examples have an electron-donating substituent, such as an alkoxyl or hydroxyl moiety, *para* to the point of ring closure. Therefore, for exemplification purposes, an appropriately placed methoxy group is included in Figure 45. Protonation of the nitrogen of imine **53**, to form the iminium ion, also facilitates nucleophilic attack on the iminium carbon atom. The oxygen donates a lone pair of electrons into conjugation with the aromatic ring, increasing the electron density at the point of ring closure; nucleophilic attack on the iminium carbon restores the neutrality of the nitrogen, with the loss of a proton restoring both the aromaticity of the benzene portion of the tetrahydroisoquinoline core and the neutrality of the oxygen substituent, to give the neutral product **54**.

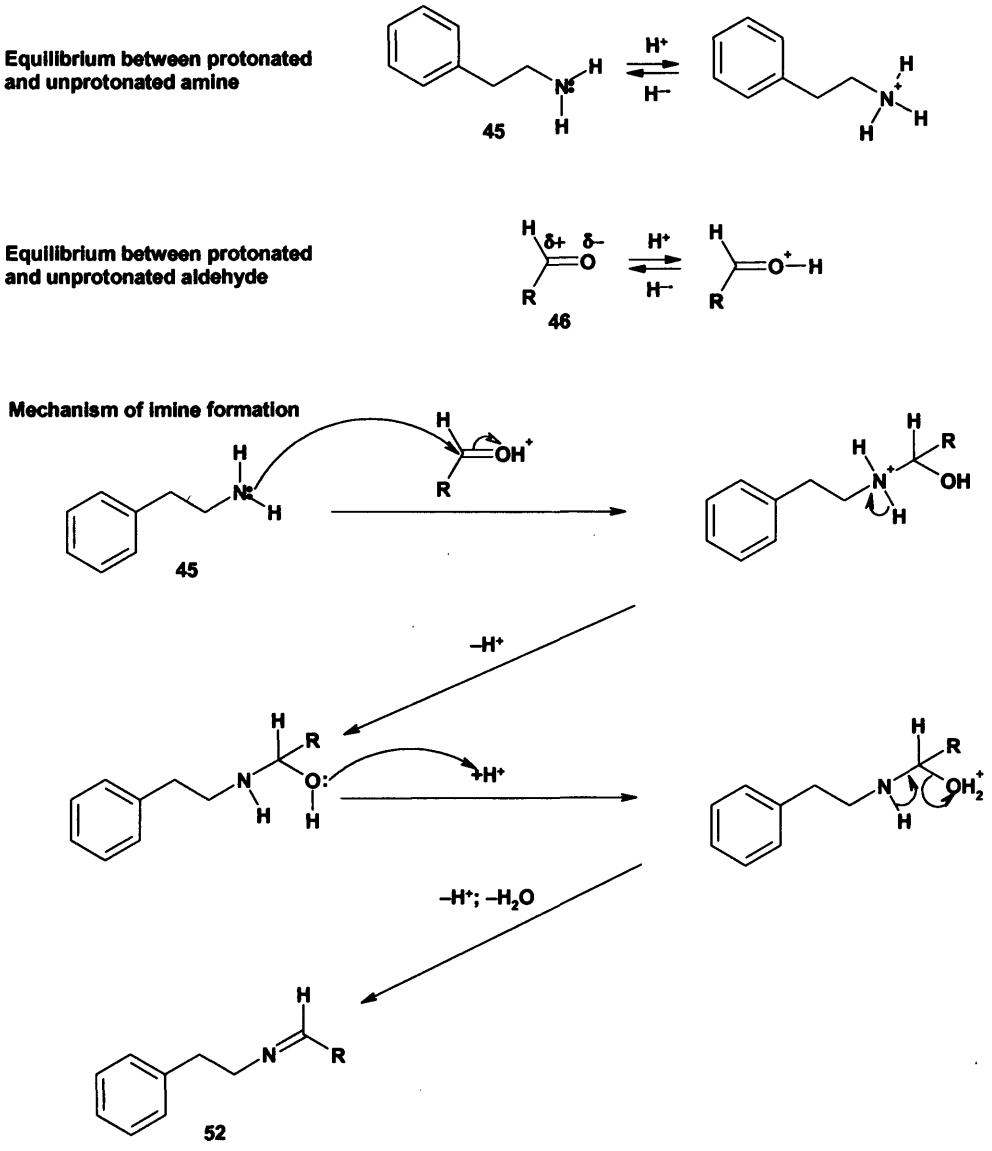

Figure 44: The mechanism of imine formation in the Pictet-Spengler tetrahydroisoquinoline synthesis.

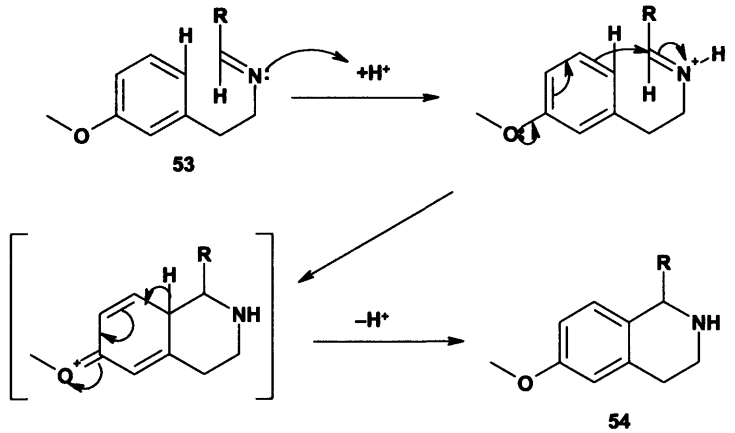

Figure 45: The mechanism of ring closure in the Pictet-Spengler tetrahydroisoquinoline synthesis.

Bischler-Napieralski Tetrahydroisoquinoline Synthesis[418]

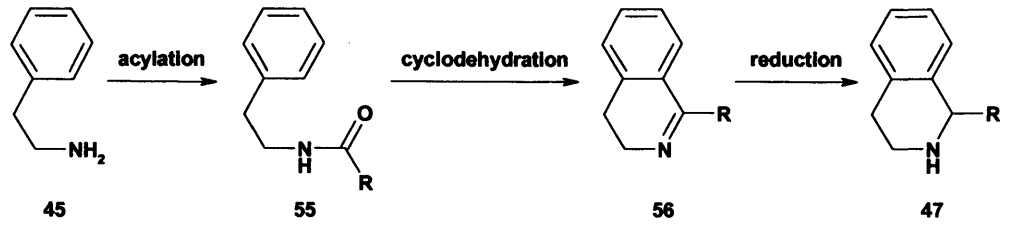

Figure 46: The Bischler-Napieralski tetrahydroisoquinoline synthesis

The classical Bischler-Napieralski reaction (see Figure 46) has been comprehensively reviewed elsewhere[425]. As in the Pictet-Spengler synthesis of 1,2,3,4-tetrahydroisoquinolines, the Bischler-Napieralski synthesis requires a 2-phenylethylamine **45** as its starting point. Rather than making an imine and cyclising the iminium salt, the amine **45** is acylated to an amide **55**, and cyclised in anhydrous solvent in the presence of a dehydrating agent, such as phosphorus pentoxide, anhydrous zinc chloride or, more commonly, phosphorus oxychloride. As before, carbon-carbon bond formation occurs between a ring carbon *ortho* to the ethyl chain, and the activated electrophilic carbon alpha to the nitrogen, to join carbon-1 and carbon-8a of the newly formed tetrahydroisoquinoline **47** (see Figure 36 for the numbering of the tetrahydroisoquinoline ring). The product of the ring closure is the 3,4-dihydroisoquinoline **56**, and a subsequent reduction is required to give the desired 1,2,3,4-tetrahydroisoquinoline **47**, with sodium borohydride in methanol a popular choice.

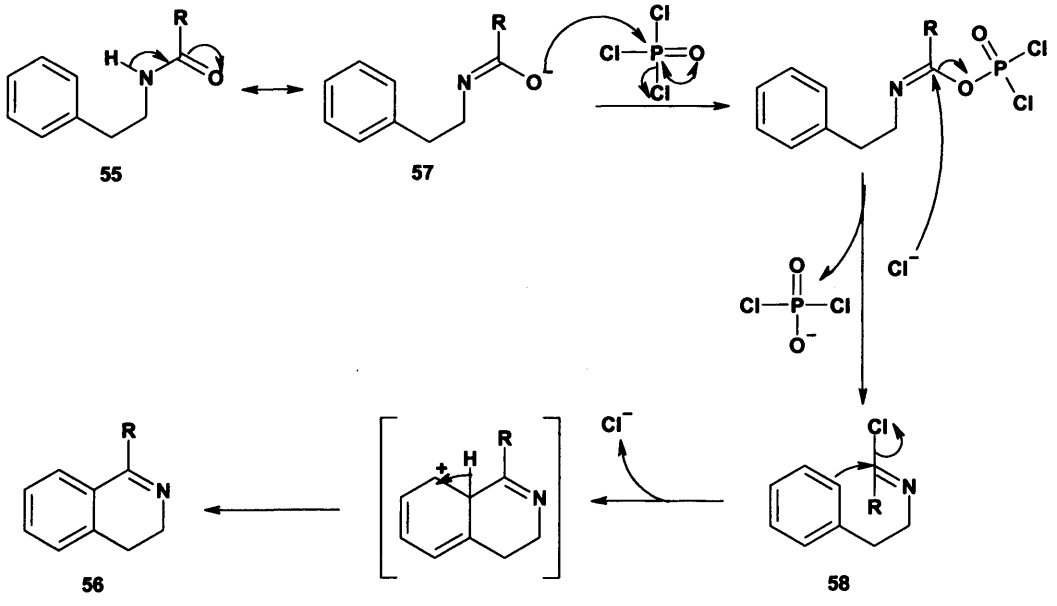

Figure 47: The accepted mechanism of the cyclodehydration step of the Bischler-Napieralski synthesis of 3,4-dihydroisoquinolines **56**.

The probable mechanism of the cyclodehydration step is represented in Figure 47. The amide can be considered as having two tautomeric forms, the amide **55** and the imidic acid **57**. The oxygen of the imidate **57** performs a nucleophilic attack upon the phosphorus atom, with the formation of a new phosphorus–oxygen bond at the expense of cleavage of a phosphorus-chorine bond as the driving force. The dichlorophosphinyl group formed is an excellent leaving group; the imide carbon is susceptible to nucleophilic attack. The liberated chloride ion returns to attack this carbon, and release the dichlorophosphinic acid. The imidoyl chloride **58** is the accepted reactive precursor for the ring closure step of the Bischler-Napieralski isoquinoline synthesis[428]. The electron rich carbon in the ortho-position of the benzene ring attacks the carbon of the imidoyl chloride **58**, and displaces the chloride ion, to form a new six-membered heterocyclic ring. The loss of the proton from the ortho carbon restores aromaticity to the benzene ring portion of the molecule.

Pomeranz-Fritsch Tetrahydroisoquinoline Synthesis[419-423]

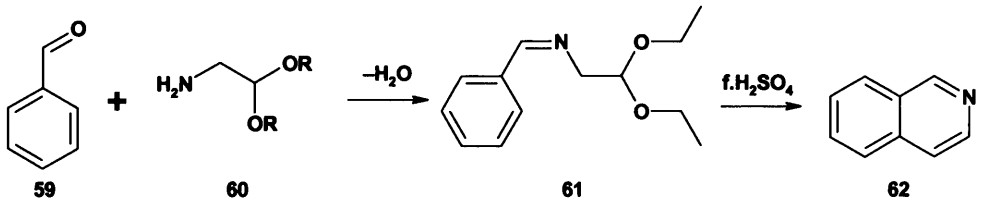

59 60 61 62

Figure 48: The Pomeranz-Fritsch isoquinoline synthesis.

The classical Pomeranz-Fritsch isoquinoline synthesis (see Figure 48) has been comprehensively reviewed elsewhere[427]. In contrast to the two approaches already discussed, this synthesis does not involve the use of 2-phenylethylamine **45** as the starting point; rather, the carbon-carbon bond formation occurs between carbon-4 and carbon-4a of the newly formed isoquinoline ring. The original synthesis required the condensation of a benzaldehyde **59** and an aminoacetal **60**, to give an imine **61**, the sulphuric acid-catalysed cyclisation of which gave the fully aromatic isoquinoline **62** (see Figure 48). In the Schlittler-Muller modification[429], an alternative imine **65** can be obtained from the condensation of a benzylamine **63** and dimethoxyacetaldehyde **64**, and cyclised under identical conditions, to give the same fully aromatic isoquinoline **62** (see Figure 49).

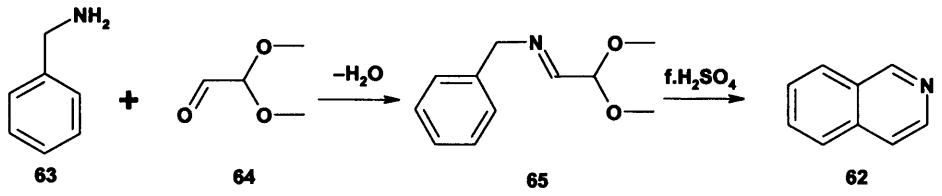

Figure 49: The Schlittler-Muller modification of the Pomeranz-Fritsch isoquinoline synthesis.

To obtain the 1,2,3,4-tetrahydroisoquinoline **47** requires the utilisation of the Bobbitt modification[424;430] of these isoquinoline syntheses, in which the imines **61/65** are reduced to the secondary amine **66** prior to cyclisation. The resulting 1,2-dihydroisoquinolines **67** are inherently unstable, with disproportionation to a mixture of the fully aromatic isoquinoline **62** and the tetrahydroisoquinoline **47** frequently seen. This is resolved by utilisation of an *in situ* reduction of the 1,2-dihydroisoquinoline **67** with hydrogen over palladium on carbon, to give the 1,2,3,4-tetrahydroisoquinoline **47** (see Figure 50).

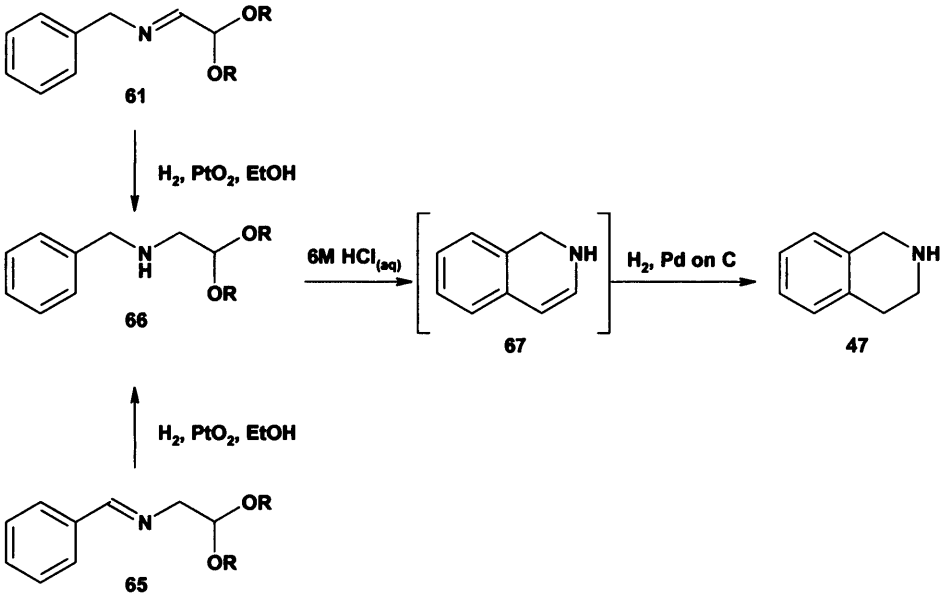

Figure 50: The Bobbitt modification of the Pomeranz-Fritsch/Schlittler-Muller isoquinoline syntheses, to obtain 1,2,3,4-tetrahydroisoquinolines, such as **47**.

Stereogenic Synthesis

The synthetic approaches to each of the requisite stereoisomers of the tetrahydroisoquinoline cores requires at least one stereogenic step. There are three general approaches to obtaining pure stereoisomers.

- Utilise an appropriate isomerically pure stereogenic starting material from the 'chiral pool', such as an amino acid.

- Introduce the new stereogenic centre into your target compound non-selectively, to form a mixture, then separate the stereoisomers. When forming a new stereogenic centre in a molecule that already contains one or more stereogenic centres, this separation may occur readily, as the diastereomers produced will have different physical properties and can normally be separated based upon these properties. For a racemic mixture of enantiomers, the standard approach is to use a *resolving agent*, *i.e.* one enantiomer of a chiral compound that can be combined with the racemate, to form a mixture of diastereomers. Once separation of the diastereomers is achieved, the resolving agent can be removed to leave the resolved enantiomers. Two examples of this approach were used in the course of this research.
- Form the new stereogenic centre stereoselectively. This may involve the use of a chiral catalyst to bias the formation of the new stereogenic centre to the required asymmetry. More usually for enantiomers, a chiral auxiliary or adjuvant is used. This is temporarily covalently bound to the achiral starting material and used to guide the formation of the new stereogenic centre of the target compound, ideally to the exclusion of the undesired stereoisomer. The auxiliary is then removed to leave the desired enantiomer with a high degree of enantiopurity. For diastereomers, the same approach may be taken, or a more 'atom efficient' and elegant approach will utilise the existing stereogenic centre(s) within the starting material to guide the stereogenicity of the new centre. Two examples of this approach were used in the course of this research.

Naturally Occurring Tetrahydroisoquinolines

The 1-substituted- and 1,3-disubstituted-1,2,3,4-tetrahydroisoquinoline cores occur widely within the realm of the plant alkaloids[431-433]. It has also been proposed that tetrahydroisoquinolines may form in trace amounts in mammalian tissues, via Pictet-Spengler-like cyclisation[415] of the products of the direct, non-enzymatic condensation of endogenous amines and amino acids, such as dopamine, adrenaline, noradrenaline, tryptamine, serotonin, L-DOPA, tryptophan and 5-hydroxytryptophan, with metabolic or exogenous carbonyl compounds, such as acetaldehyde and α-keto acids. The putative existence of these 'mammalian alkaloids'[434-438] and their potential pharmacological activity, has encouraged detailed research into their synthesis, first

as racemates, then as enantiomers. Of particular interest to this thesis are the synthetic approaches made to the plant alkaloids shown in Figure 51, which is discussed in detail below.

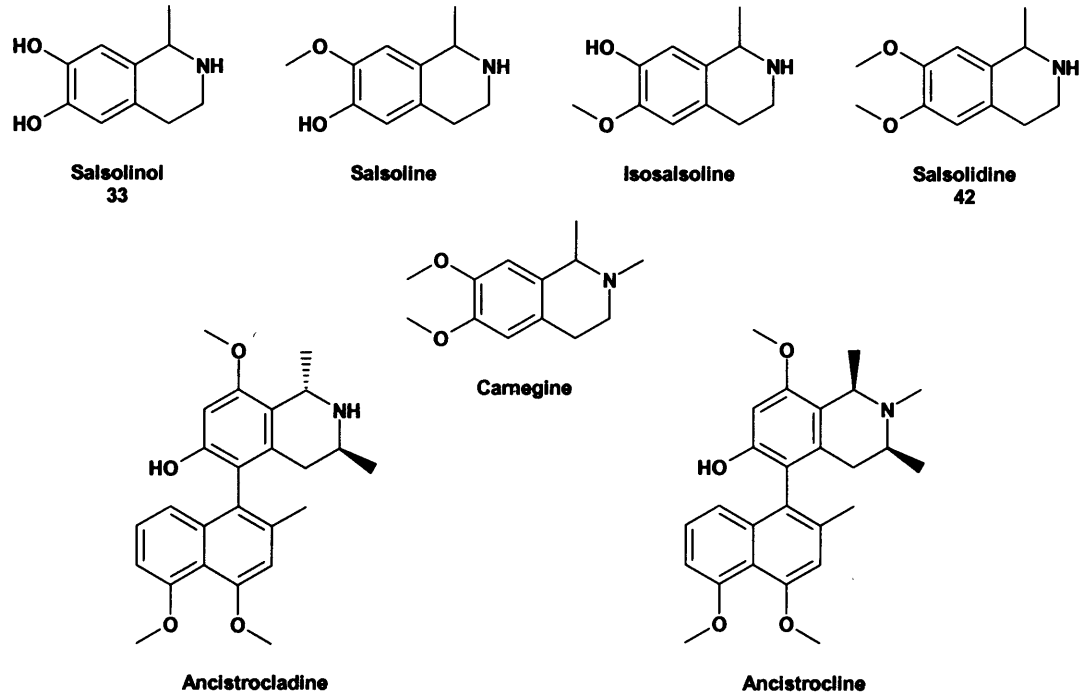

Figure 51: Some tetrahydroisoquinoline-containing plant alkaloids.

Investigations into the Synthesis of the Enantiomers of 6,7-Dimethoxy-1-methyl-1,2,3,4-tetrahydroisoquinoline (42)

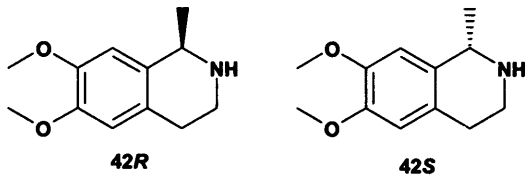

Figure 52: The desired enantiomers of 6,7-dimethoxy-1-methyl-1,2,3,4-tetrahydroisoquinoline (**42*R*** and **42*S***).

When this project commenced, while the racemic 6,7-dihydroxy-1-methyl-1,2,3,4-tetrahydroisoquinoline **33** ((±)-salsolinol) was commercially available, the enantiomers were not. We therefore required a protocol for the synthesis/resolution, of either **33**, or of an appropriate 6,7-dioxygenated precursor, such as **42** (see Figure 53).

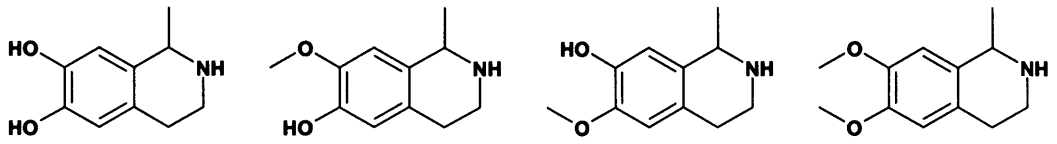

Salsolinol 33 | **Salsoline** | **Isosalsoline** | **Salsolidine** 42

Figure 53: Some 6,7-dioxygenated-1-methyl-1,2,3,4-tetrahydroisoquinoline cactus alkaloids.

These and other 1-substituted-6,7-dialkoxy/dihydroxy-1,2,3,4-tetrahydroisoquinolines have been the subject of chemical and pharmacological interest for several years, as:

- potential metabolites of biogenic primary amines, such as L-tryptophan, L-5-hydroxytryptophan, dopamine and L-DOPA[434-437], with pharmacological significance as neurotoxins;
- inhibitors of human monoamine oxidases[439]; and
- bronchodilators[440].

As a result, several literature approaches to producing the desired enantiomers of **33** have been reported, and these have recently been reviewed[441]. Although the resolution of suitable racemic precursors to **33*R*** and **33*S*** by recrystallisation with chiral acids has been reported[442], these were generally low yielding. More attractive were two routes to the enantiomers of 6,7-dimethoxy-1-methyl-1,2,3,4-tetrahydroisoquinoline **42** (see Figure 52).

The first offered an enantioselective route to **42*S*** from 3,4-dimethoxyphenyl acetic acid **68**[443] (see Figure 54). The route used (*S*)-1-(2,6-dichlorophenyl)ethylamine **69*S*** as a chiral auxiliary, and the reaction of **68** with **69*S*** to form amide **70** as the first step. Reduction of the carbonyl of **70** gave the secondary amine **71**, and acetylation with acetic anhydride gave a chiral tertiary amide **72**. Cyclodehydration under Bischler-Napieralski conditions gave a chiral iminium ion **73** which, when reduced with sodium borohydride, was capable of inducing stereoselectivity in the new stereogenic centre of the 1-methyl tetrahydroisoquinoline **74**. The auxiliary was removed by hydrogenation over palladium on carbon, to give **42*S***. Presumably the enantiomer of the chiral auxiliary **69*R*** could be used to acquire **42*R***. This approach was rejected in favour of the route chosen, because it required the synthesis of the chiral auxiliaries **69*R*** and **69*S***.

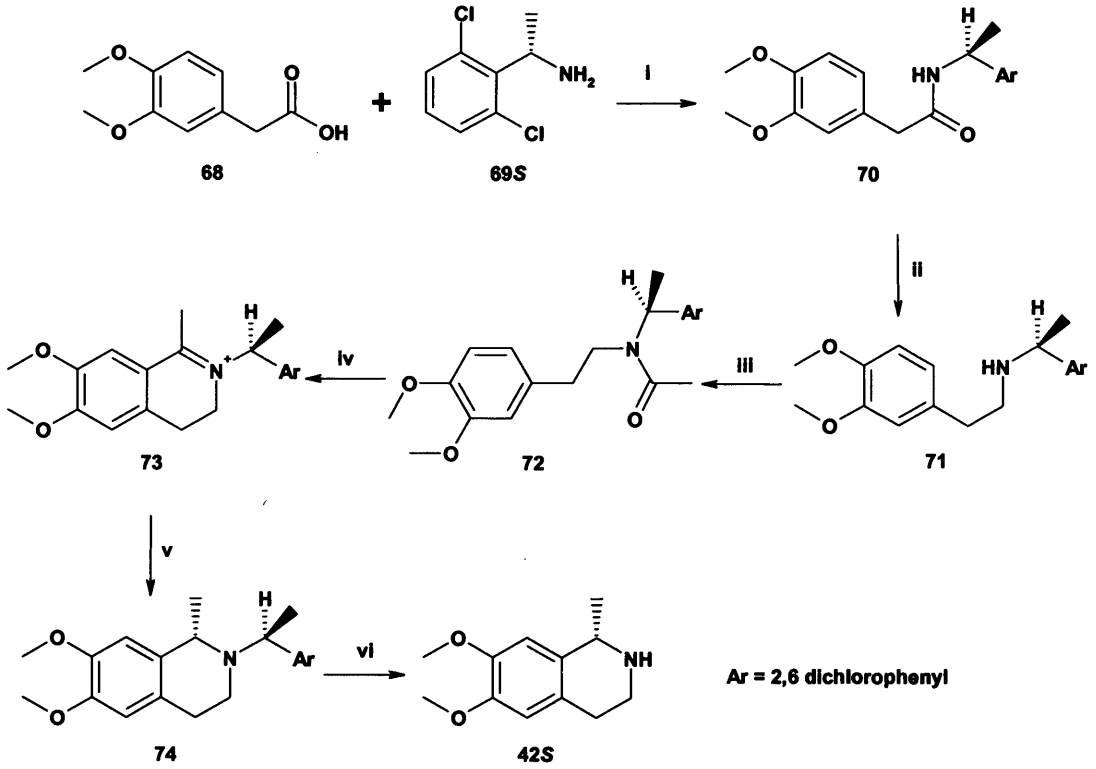

i. 1.2 eq. 1,1'-carbonyldiimidazole, THF, 0°C to r.t.;ii. 2.5 eq. BH_3-THF, 0.4eq BF_3•Et_2O, THF, reflux;
iii. 1.5 eq. Ac_2O, 0.1 eq DMAP, 1.2 eq Et_3N, CH_2Cl_2; iv. 2:1 benzene-$POCl_3$, 90°C;
v. 4-5 eq. $NaBH_4$, added in portions, –78°C; vi. H_2, 10% Pd/C, EtOH-EtOAc, 10% HCl.

Figure 54: An enantioselective synthesis of (–)-**42**[443].

Synthesis of the Enantiomers of 42

The route chosen followed an elegant literature synthesis[444], with the key resolution of racemic **42**, to the pure enantiomers **42*R*** and **42*S*** being performed by reaction of the racemic **42** with the chiral auxiliary (*R*)-(1-phenylethyl)isocyanate **75*R***, thereby creating a diastereomeric mixture of (*S*)-2-((*R*)-1-phenylethyl)carbamoyl-6,7-dimethoxy-1-methyl-1,2,3,4-tetrahydroisoquinoline **76(1*S*,α*R*)** and (*R*)-2-((*R*)-1-phenylethyl)carbamoyl-6,7-dimethoxy-1-methyl-1,2,3,4-tetrahydroisoquinoline **76(1*R*,α*R*)**. This route had the advantage over the route using the enantiomers of the chiral auxiliary **69**, in that:

a. both enantiomers of **42** were reported as resolved by using the one enantiomer of **75**,
b. the pure enantiomers of **75** were commercially available.

The creation of diastereomers frequently allows enantiomers with identical physical properties to be separated as diastereomers with differing physical properties. In this case[444], separation was achieved by recrystallisation of the diastereomeric mixture[444]. **76(1*S*,α*R*)** was reported as being readily obtained as a crystalline solid,

and repeated recrystallisation of the residue from the mother liquor removed all trace of **76(1*S*,α*R*)**, to leave the pure, non-crystalline **76(1*R*,α*R*)**. The enantiomers of **42** were reported to be obtained by the thermal decomposition of each urea in refluxing 2M sodium butoxide in butan-1-ol[444], with no loss of enantiopurity (see Figure 55).

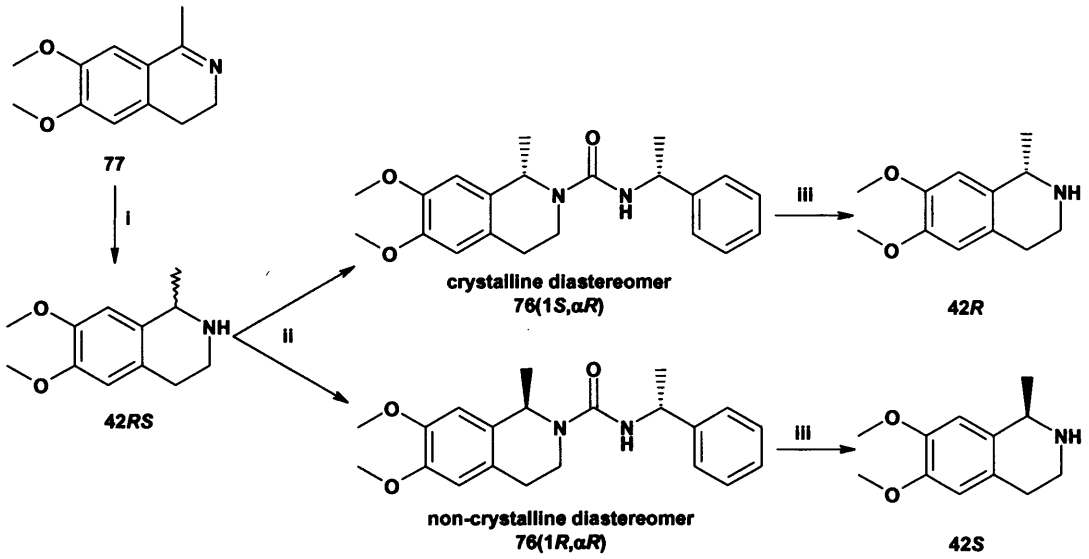

I. $NaBH_4$, MeOH, 0°C - r.t.; II. (*R*)-(1-phenylethyl)isocyanate (75*R*), Et_3N, CH_2Cl_2; III. 2M NaOBu/BuOH, reflux

Figure 55: Selected literature resolution of **42**[444].

Although eventually successful, some modification proved necessary during the synthesis. Reduction of the commercially available achiral 6,7-dimethoxy-1-methyl-3,4-dihydroisoquinoline **77** with sodium borohydride gave racemic **42*RS***, which was characterised as the hydrochloride salt. Subsequent reaction with **75*R*** gave the diastereomeric mixture of **76(1*RS*,α*R*)**. It was not possible to distinguish between these diastereomers by analytical HPLC using the conditions detailed in the literature[444]; baseline separation was eventually achieved using a chiral stationary phase (Anachem CHI-D-PGC-250A (250 x 4.6mm)) and isocratic elution (20% propan-2-ol in n-hexane; 210nm). In addition, the diastereomers were clearly distinguishable by ^{1}H- and ^{13}C-NMR, with ^{13}C-NMR becoming the method of choice for determining diastereomeric purity (see Figure 56, spectrum A). Repeated recrystallisation of the mixture of diastereomers, once from ethyl acetate, then dichloromethane/ propan-2-ol, gave the crystalline **76(1*S*,α*R*)** to analytical purity (see Figure 56, spectrum B). As a point of interest, the optical rotation of the diastereomer thus obtained ($[\alpha]_D^{20}$ +75.0° (*c* 0.7, chloroform)) was consistently higher than that given in the literature (*c.f.* $[\alpha]_D^{r.t.}$ +48.0° (*c* 0.7, chloroform)[444]).

Unfortunately[444], it was not possible to purify the non-crystalline **76(1*R*,α*R*)** beyond a *d.e.* of ~90% by HPLC, despite repeated recrystallisation, with the ^{13}C-NMR spectrum confirming the presence of residual **76(1*S*,α*R*)** (see Figure 56, spectrum C).

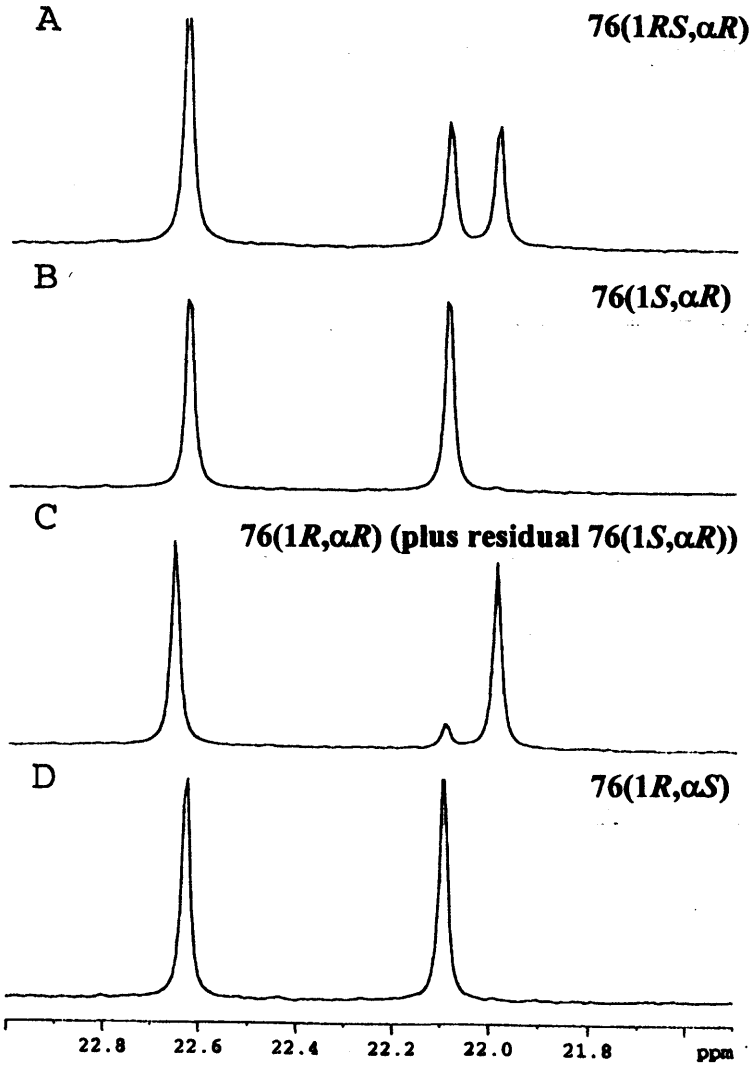

Figure 56: Expansions from the ^{13}C-NMR spectra of diastereomers of **76**, showing the peaks corresponding to the methyl groups attached to each of the stereogenic centres.

The commercial availability of the enantiomer of the chiral auxiliary **75*S*** meant that this complication was readily overcome. Thermal decomposition of the enriched mixture of 95% **76(1*R*,α*R*)**, plus 5% residual **76(1*S*,α*R*)**, by refluxing in 2M sodium butoxide in butan-1-ol[444], gave an enriched mixture of 95% **42*R***, plus 5% **42*S***. Reaction with **75*S*** gave a mixture of 95% **76(1*R*,α*S*)**, contaminated with 5% of the **76(1*S*,α*S*)**. As **76(1*R*,α*S*)** is the enantiomer of the crystalline **76(1*S*,α*R*)**, it was readily purified to analytical purity (for ^{13}C-NMR spectroscopy;

see Figure 56 spectrum D) ($[\alpha]_D^{22}$ –75.1° (*c* 0.7, chloroform)) by recrystallisation from dichloromethane/ propan-2-ol. The absolute stereochemistry of **76(1*R*,α*S*)** was confirmed by X-ray crystallography (for a representation of the X-ray crystallographic image of **76(1*R*,α*S*)**, see Figure 57; for the crystal co-ordinates, see Appendix 1).

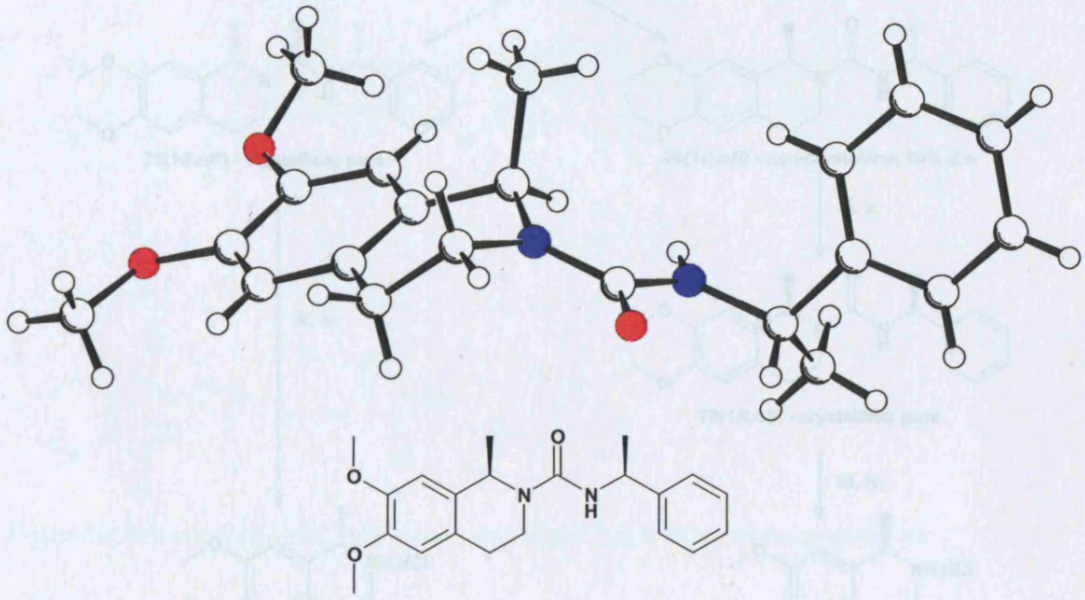

Figure 57: An X-ray crystallographic image of **76(1*R*,α*S*)**.

The pure enantiomers of **42*R*** and **42*S*** were obtained by thermal decomposition of the analytically pure, crystalline diastereomers **76(1*R*,α*S*)** and **76(1*S*,α*R*)** in refluxing 2M sodium butoxide in butan-1-ol[444]; the product tetrahydroisoquinolines (**42*R*** and **42*S*** respectively) were purified and characterised as the recrystallised hydrochloride salts. The full synthetic route, from commercially available achiral **77** to enantiopure **42*R*** and **42*S*** is shown in Figure 58.

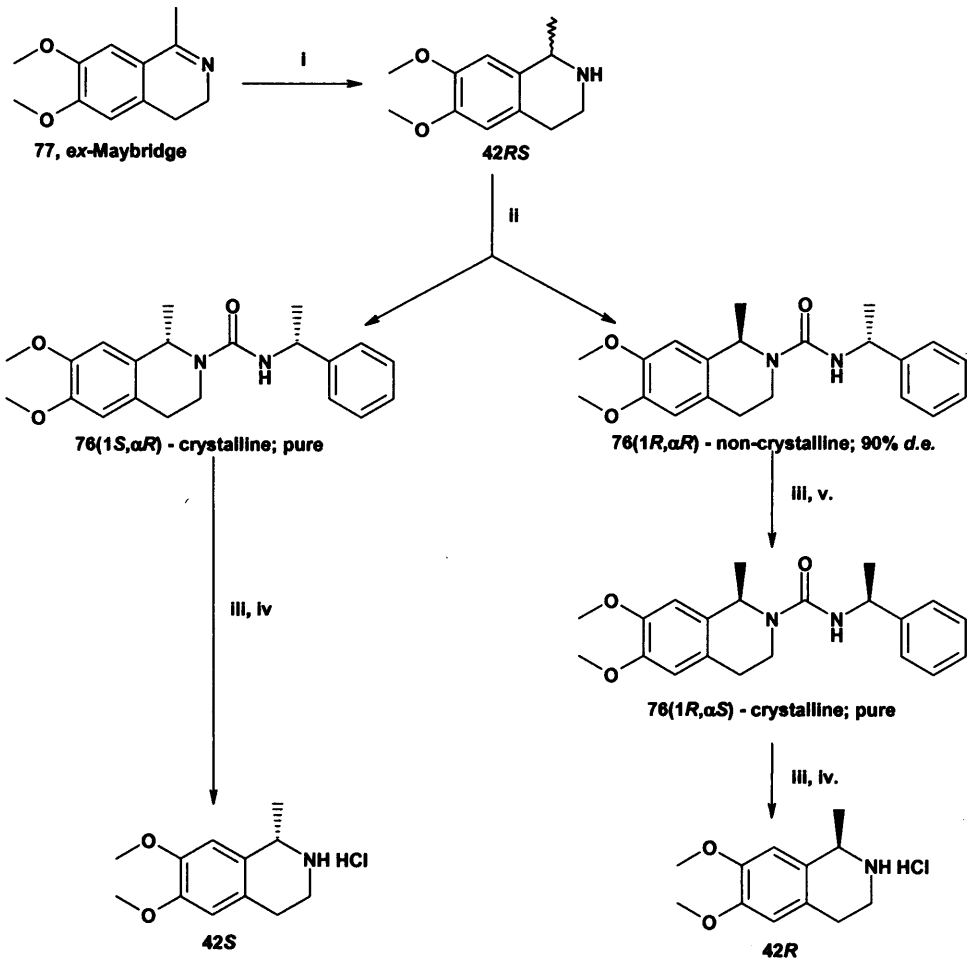

i. $NaBH_4$, MeOH, 0°C - r.t.; ii. (*R*)-(1-phenylethyl)isocyanate **75*R***, Et_3N, CH_2Cl_2;
iii. 2M NaOBu/BuOH, reflux; iv. hydrogen chloride, 1,4-dioxane/methanol;
v.(*S*)-(1-phenylethyl)isocyanate **75*S***, Et_3N, CH_2Cl_2.

Figure 58: Synthetic route to the pure (*R*)- and (*S*)-enantiomers of **42**.

Investigations into the Synthesis of the Enantiomers of 6,7-Dimethoxy-3-methyl-1,2,3,4-tetrahydroisoquinoline (43)

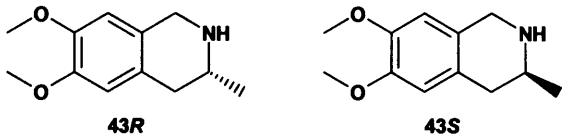

Figure 59: The desired enantiomers of 6,7-dihydroxy-3-methyl-1,2,3,4-tetrahydroisoquinoline (**43*R*** and **43*S***)

When this project commenced, neither the enantiomers nor the racemate of **43** were commercially available. While there were numerous approaches in the literature toward the synthesis of the enantiomers of the 1-methyl tetrahydroisoquinoline **42**, this was not the case for the enantiomers of the 3-methyl regioisomer **43**. Retrosynthetic analysis of **43** (see Figure 60) suggested two possible routes:

1. via a Pomeranz-Fritsch-Bobbitt type synthetic approach, using 3,4-dimethoxybenzaldehyde **79** (veratraldehyde) and either the racemate or the enantiomers of an appropriate 2,2-dialkoxy-1-methylethylamine **80**;
2. via a Pictet-Spengler type of synthetic approach, from either the racemate or the enantiomers of 2-(3,4-dimethoxyphenyl)-1-methylethylamine **38**.

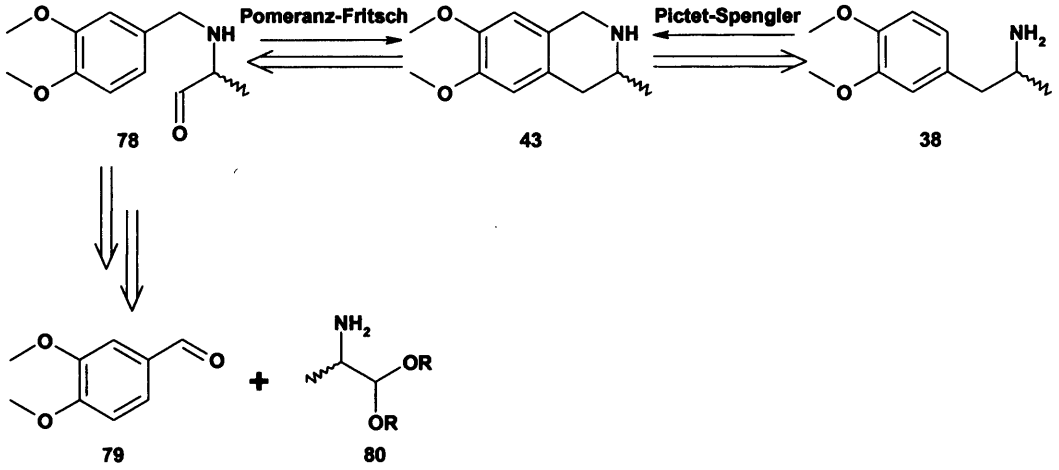

Figure 60: Retrosynthesis of 6,7-dimethoxy-3-methyl-1,2,3,4-tetrahydroisoquinoline **43**.

Neither of the required chiral starting materials were commercially available, so either the resolution of **43**, or the resolution/ enantioselective synthesis of either **80** or **38** was required.

With respect to the synthesis of the enantiomers of **80**, literature precedent[445] describes how to prepare these useful reagents from 1,1-dialkoxy-2-propanones **81**, by the asymmetric reduction of the chiral imines **83**, formed by condensation of **81** with the enantiomers of 1-phenylethylamine **82*R*** and **82*S***, to give the diastereomeric secondary amines **84**. The benzyl group from the chiral auxiliary can then be cleaved by palladium-catalysed transfer hydrogenation, to give **80** (see Figure 61).

The desired enantiomers of **43** could then be accessed by the reductive alkylation of **80** with **79** and sodium borohydride in methanol, followed by cyclisation in 6M hydrochloric acid, and *in situ* reduction with hydrogen over 5% palladium on carbon (see Figure 62).

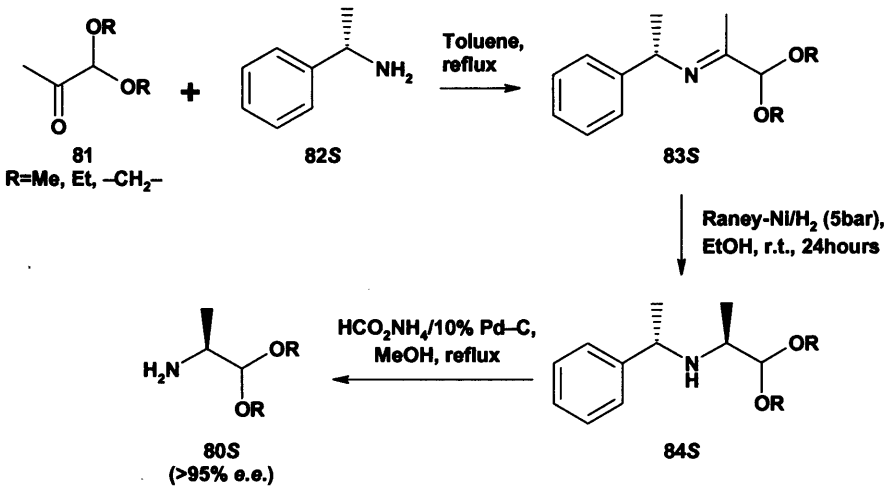

Figure 61: Synthesis of (*S*)-1,1-dialkoxy-2-propanamines **80*S***[445]

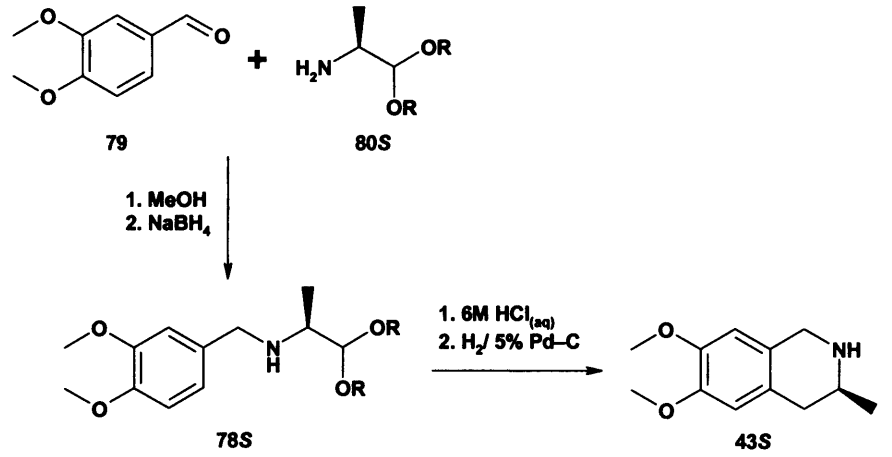

Figure 62: Putative Pomeranz-Fritsch-Bobbitt route to (*S*)-6,7-dimethoxy-3-methyl-1,2,3,4-tetra-hydroisoquinoline (**43*S***).

The alternative approach to the enantiomers of **43**, via a Pictet-Spengler cyclisation of the pure enantiomers of amine **38**, was given priority as, once in hand, the enantiomers of **38** would not only give access to the desired enantiomers of **43**, but were also envisaged as a useful starting point to gain access to the four diastereomers of the 1,3-dimethyl analogue **44** (see Figure 63).

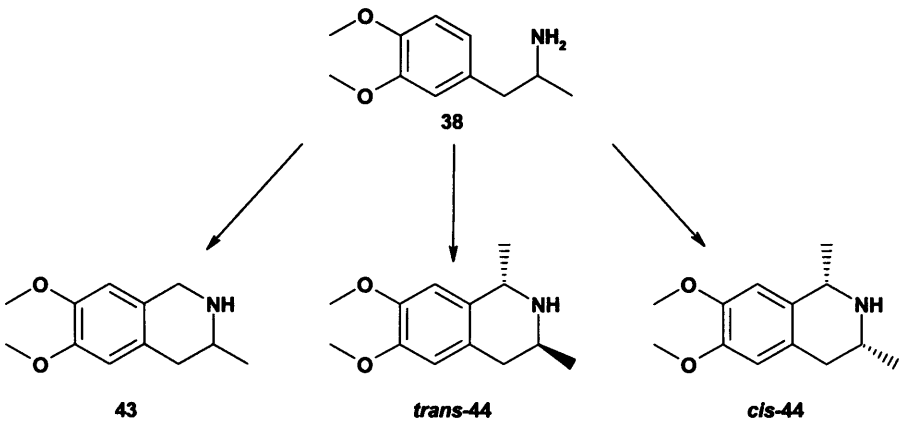

Figure 63: **38** as a common intermediate to **43** and **44**.

Investigations into the Synthesis of the Enantiomers of 2-(3,4-Dimethoxyphenyl)-1-methylethylamine (38)

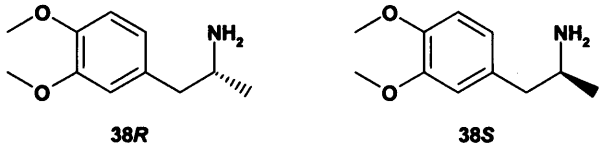

Figure 64: Key intermediates **38*R*** and **38*S***.

The literature offered four approaches to the desired enantiomers of the stereogenic amine **38**, although three were unsatisfactory for various reasons (see below). The one attractive approach utilised commercially available starting materials from the chiral pool, namely the enantiomers of alanine **85*R*** and **85*S***[446]. The use of such starting materials to provide the stereogenic centre of the enantiomers of **38** would provide products of known absolute configuration. The reaction scheme for this approach is illustrated in Figure 65.

The first step required the synthesis of *N*-trifluoroacetyl-(*L*)-alanine **86*S***, and this was achieved in good yield by the literature reaction of ethyl trifluoroacetate with **85*S***[447]. The next sequence of reactions were carried out in one pot. Firstly, the conversion of **86*S*** to *N*-trifluoroacetyl alaninoyl chloride **87*S***, by reaction with oxaloyl chloride in dichloromethane with a catalytic amount of *N,N*-DMF, followed by the *in situ* Friedel-Crafts acylation of 1,2-dimethoxybenzene **88**, to give (*S*)-*N*-trifluoroacetyl-1-(3,4-dimethoxybenzoyl)ethylamine **89*S***. Had this step proven reproducible, all that would be required to obtain the key stereogenic intermediate **38*S*** would be the triethylsilane-mediated reduction of the carbonyl group[448] to give

(*S*)-*N*-trifluoroacetyl-2-(3,4-dimethoxyphenyl)-1-methylethylamine **90*S***, followed by basic hydrolysis of the amide.

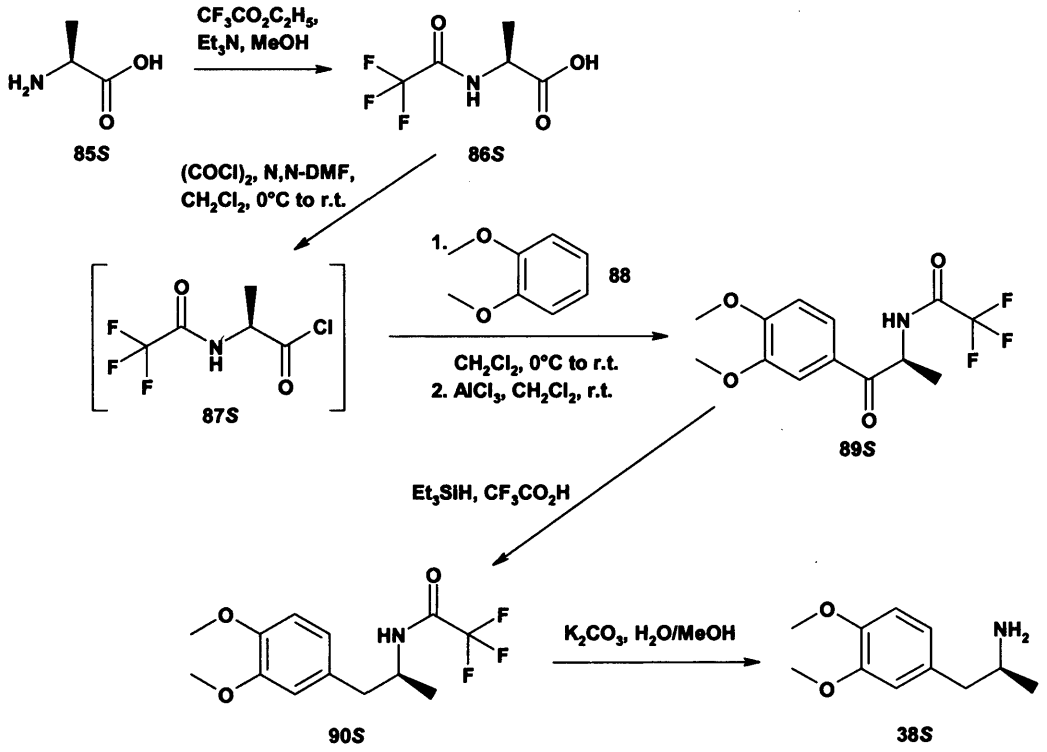

Figure 65: Proposed route to the enantiomers of amine **38** from alanine **85**, as exemplified for **38*S*** from **85*S***[446;449]

Unfortunately, despite scrupulously following the literature procedure[446;449], the conversion of **86*S*** to **89*S*** proved unreliable and highly variable, with only a small amount of the desired product formed from four attempts at the reaction and total consumption of **86*S*** seen each time. The most likely side reaction is that of formation of the oxazolone **91**[450](see Figure 66). The reactive polarised complex intermediate formed between the acid chloride **87*S*** and the Lewis acid catalyst[451] would conceivably facilitate this reaction. This side reaction is suppressed with carbamate protecting groups, but these do not lend themselves to Friedel-Crafts reactions, with decarbamoylation readily occurring[452]. Of the two published carbamate-protected alanine derivatives used to successfully acylate aromatic systems via a Friedel-Crafts reaction, *N*-methoxycarbonylalanine[453] was only tried for benzene, and *N*-ethoxycarbonylalanine[452] did not work with methoxybenzene, and would not, therefore, be anticipated to work with **88**.

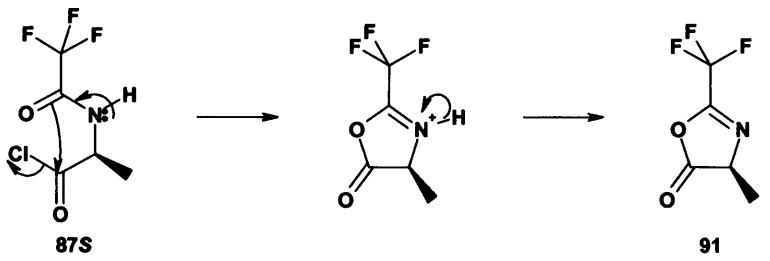

Figure 66: Side reaction of amino acid chlorides.

Of the three alternative literature procedures, one utilised the asymmetric reductive amination of ketone **36** with amine **82*S*** under an atmosphere of hydrogen over Raney nickel at 100 atmospheres pressure to give [(*S*)-2-(3,4-dimethoxy-phenyl)-1-methylethyl]-((*S*)-1-phenylethyl)amine **92(1*S*,1'*S*)**, followed by cleavage of the benzyl group by palladium-catalysed hydrogenolysis. While this approach appeared highly efficient, no facilities to achieve the required pressure were available to us at the time (see Figure 67)[454].

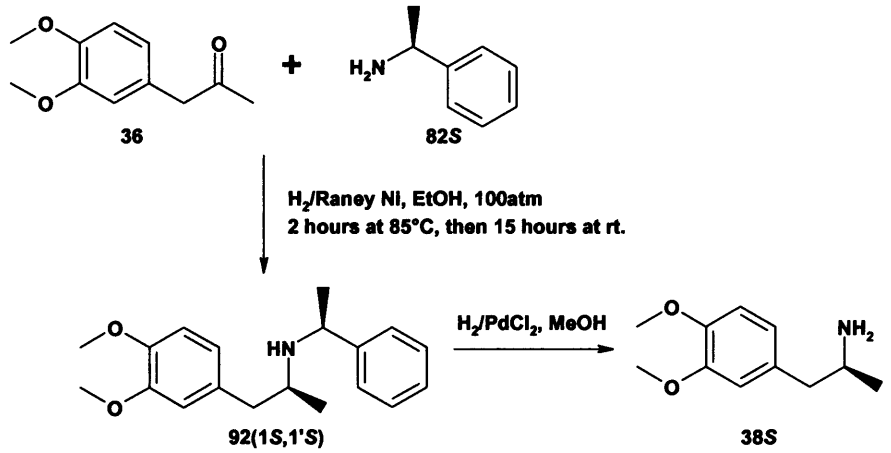

Figure 67: The Weinges and Graab synthesis of **38*S***[454].

The remaining literature routes, while unattractive, were useful in that they provided evidence for the absolute configuration of the product amines **38*R*** and **38*S***. The earliest route was rejected, as it required the synthesis and enantiomeric resolution of 3-(3,4-dimethoxyphenyl)-2-methylpropionic acid **93**[455]. The procedure isolated **(+)-93** as diastereomeric salt by recrystallisation of the racemate **93*RS*** with quinine **94**, with subsequent isolation of **(–)-93** from the enriched mixture of enantiomers obtained from the mother liquor using a diastereomeric salt of the popular chiral auxiliary amine **82*S***. The pure **(–)-93** thus obtained was reported as being readily converted to **(–)-38** via a Curtius rearrangement, and hence with retention of configuration (see Figure 68)[455].

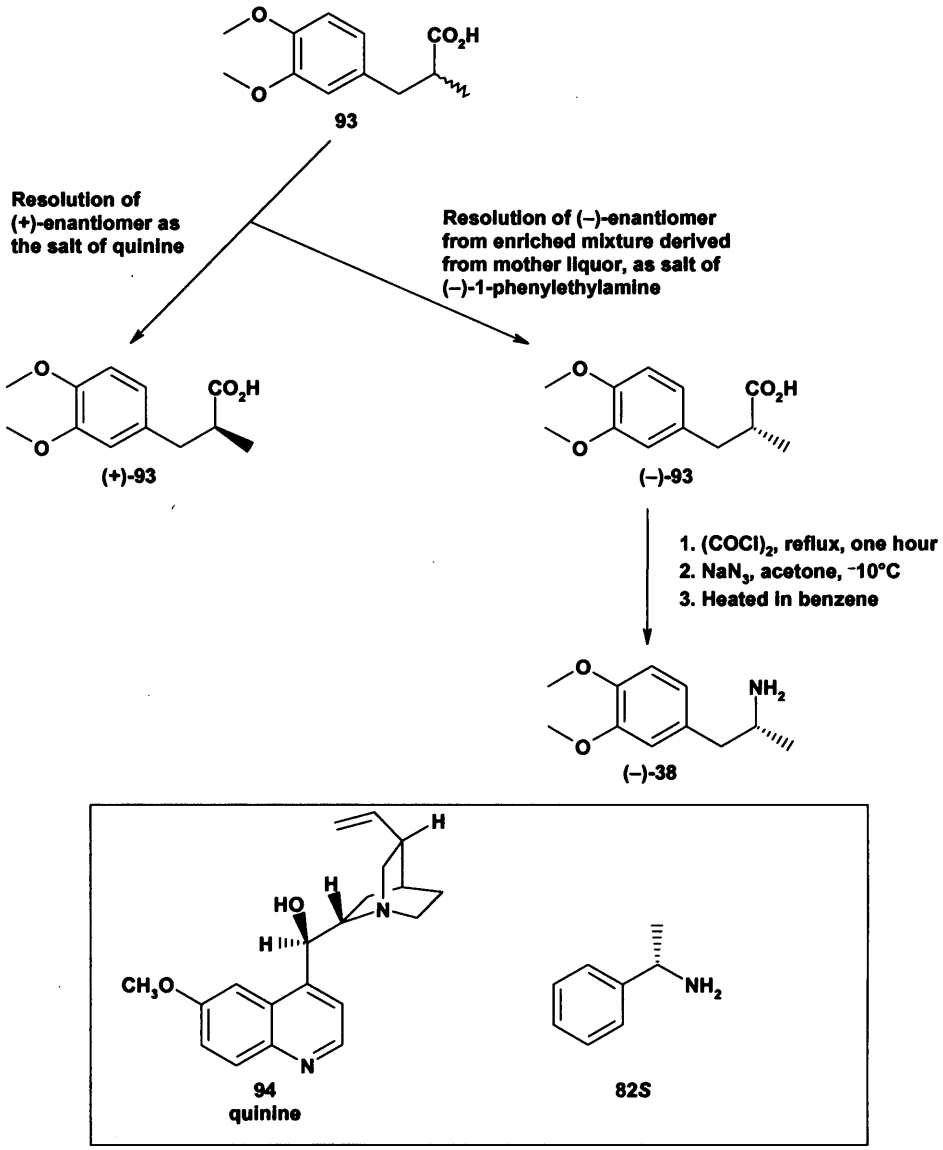

Figure 68: Schrecker's synthesis of **(–)-38**[455].

The absolute configuration of **(–)-38** was demonstrated in a companion paper[456], in which the tosylation of the **(–)-38** gave (–)-*N*-tosyl-2-(3,4-dimethoxyphenyl)-1-methylethylamine **(–)-95**. (*S*)-3,4-dihydroxyphenylalanine **96*S***, a natural amino acid of established absolute configuration, can also be converted, via intermediates **97**, **98**, **99** and **100** and with retention of configuration, to **(–)-95**, thereby establishing the absolute configuration of **(–)-95**, and of **(–)-38**, as ***R*** (see Figure 69).

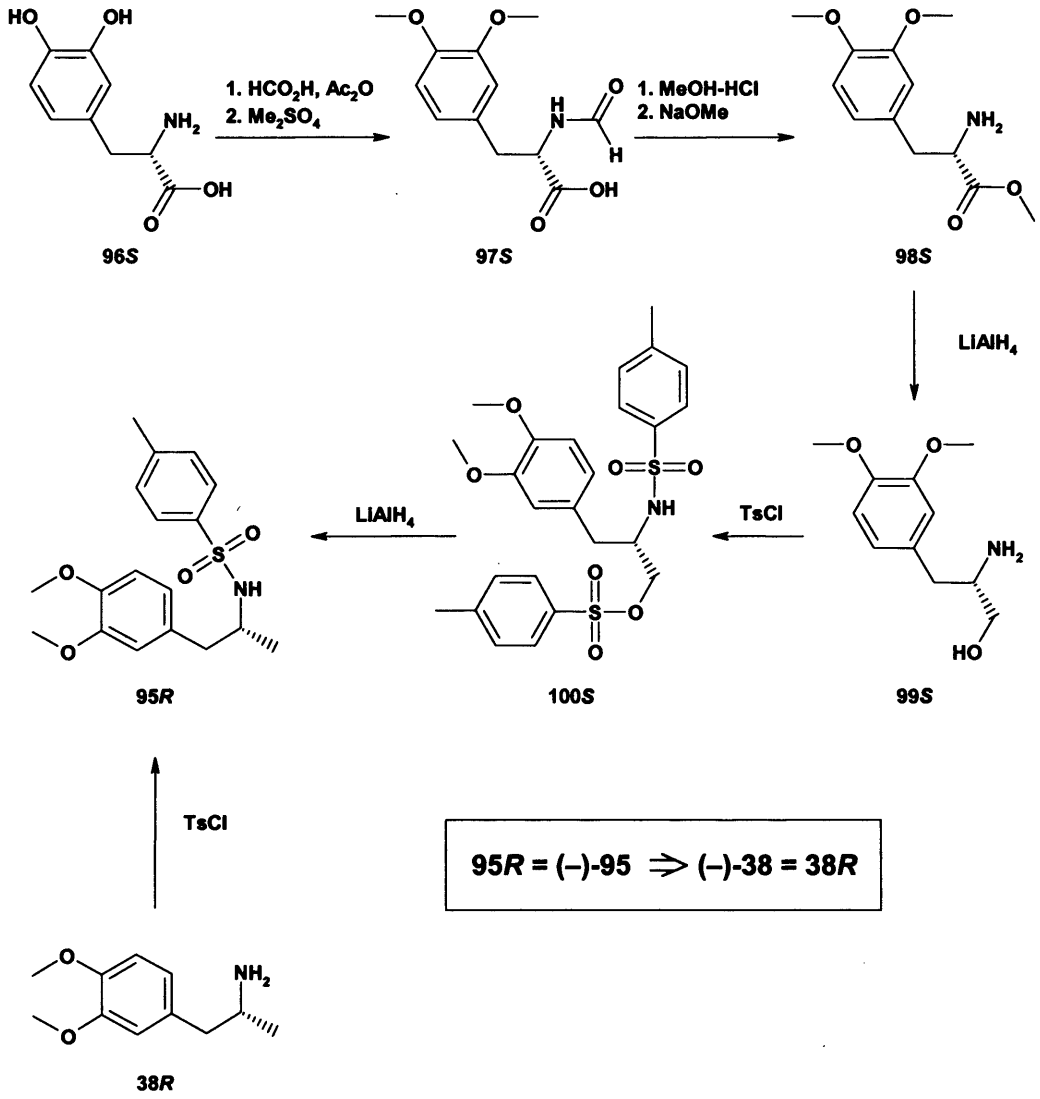

Figure 69: Literature route to establish the absolute configuration of (–)-38 as *R*, by the synthesis of **96*S*** from chiral starting materials of known absolute configuration[456].

The final literature route also utilised the available chiral pool of starting materials, synthesising (–)-**38** from (*L*)-alanine **85*R*** (see Figure 70). However, some racemisation was reported in the product of the Friedel-Crafts acylation to give ketone **101*R*** and the reduction with aluminium isopropoxide to give the diastereomeric alcohol **102*R***[457]. Although these impurities were crystallised out, it was felt that this was undesirable in our synthetic route. However, by synthesising **(–)-38** from **85*R***, via a series of transformations that left the stereogenic centre largely unaffected, **(–)-38** was again confirmed as having the (*R*)-configuration[457].

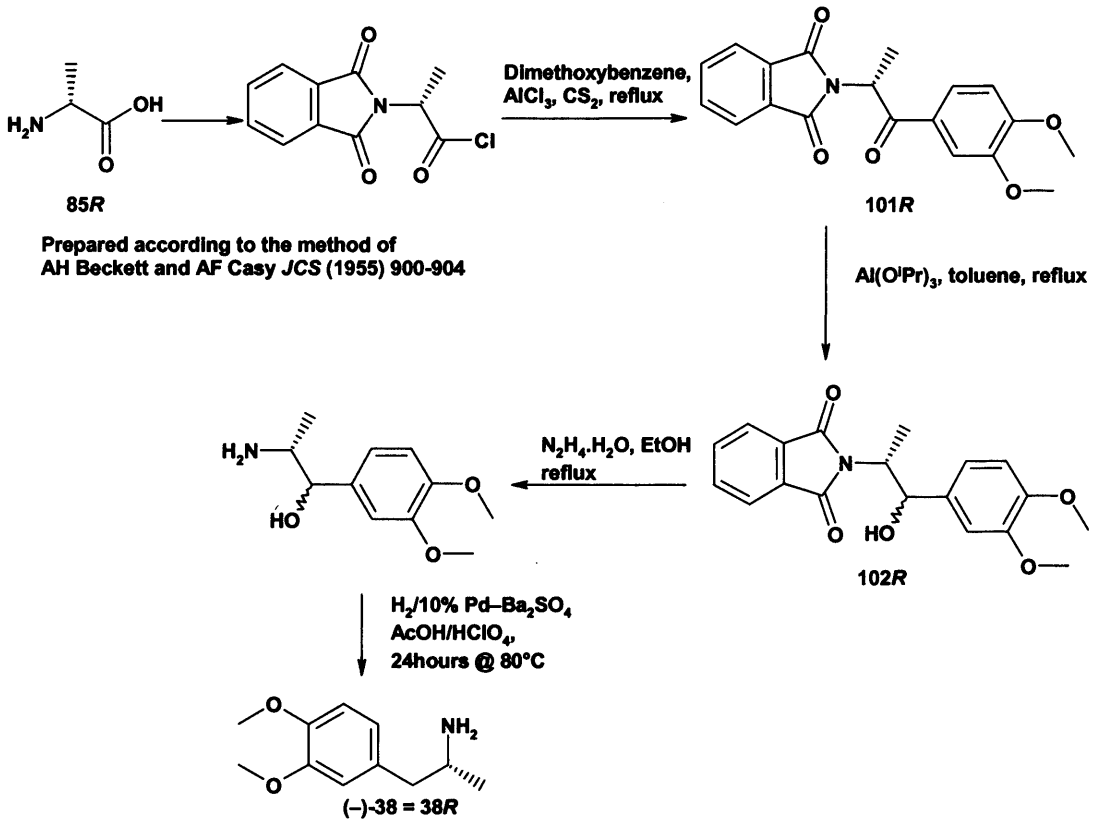

Figure 70: Literature route to **(–)-38** from **85*R***, establishing the absolute configuration as ***R***[457;458].

Synthesis of the Enantiomers of 38

The enantiomers of our key intermediate amine **38** were eventually obtained, albeit in low yields, via a classical resolution of the racemate **38*RS*** (see Figure 73), using one enantiomer of a chiral acid to form a diastereomeric salt mixture, and separating the diastereomers based upon differences in solubility[459]. The racemic amine **38*RS*** was synthesised as described previously (see Figure 40) from ketone **36**; the racemic amine **38*RS*** was purified and characterised as the hydrochloride salt.

When resolving enantiomers, it is necessary to be able to follow the success, or otherwise, of the resolution. A widely used method for establishing the degree of enantiomeric purity of amines, and particularly amino acids, employs the reaction of the amine with *N*-α-(2,4-dinitro-5-fluorophenyl)-(*L*)-alaninamide **104*S*** (Marfey's reagent, see Figure 71)[460;461]. The diastereomers generated can then be analysed for analytical differences, with reverse-phase analytical HPLC normally adequate[462].

To establish whether this method could be used for following the resolution of amine **38**, a sample of the racemate **38*RS*** was reacted with an excess of **104*S***, to form **105(*R*,*S*-ala)** and **105(*S*,*S*-ala)** as a mixture of diastereomers. This mixture was analysed by reverse-phase analytical HPLC at 340nm, as Marfey's reagent and the

product diastereomers are bright yellow. **105(*R,S*-ala)** and **105(*S,S*-ala)** were separated at the baseline (see Figure 72B), therefore Marfey's reagent **104*S*** was demonstrated as suitable for following the attempted resolution of amine **38**.

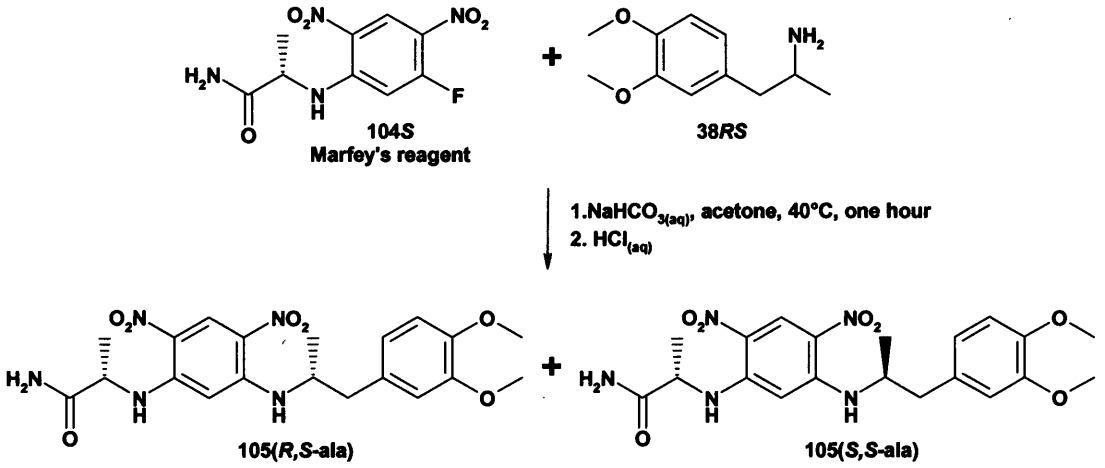

Figure 71: Scheme to show the diastereomers produced by the reaction of racemic **38** and Marfey's reagent **104*S***.

Resolution of **38*S*** was achieved by combining the free base of **38*RS*** with a stoichiometric amount of (*R*)-mandelic acid **103*R*** in boiling propan-2-ol, which crystallised as the diastereomeric salt mixture upon cooling. Repeated recrystallisation of this mixture from ethyl acetate/methanol 2:1 eventually gave one enantiomer of **38** to enantiomeric purity, as the salt of **103*R*** (see Figure 73). Enantiomeric enrichment at each stage of recrystallisation, as well as the eventual enantiomeric purity of the resolved amine, was determined by the method of Marfey[460;461] (for a comparison of the HPLC traces, see Figure 72).

Once the pure enantiomer was obtained as the salt of **103*R***, a sample was converted to the free base and crystallised from n-pentane as waxy low melting point solid. The value for the standardised optical rotation of plane polarised light by the amine was recorded, and the absolute configuration was assigned by comparison with the literature values ($[\alpha]_D^{22}$ +32.5 (*c* 4.02, EtOH); *c.f.* $[\alpha]_D^{21}$ +32.1 (*c* 3.98, EtOH)[455]). This established that the enantiomer of **38** resolved by crystallisation with **103*R*** was **(+)-38**, with the absolute configuration ***S***.

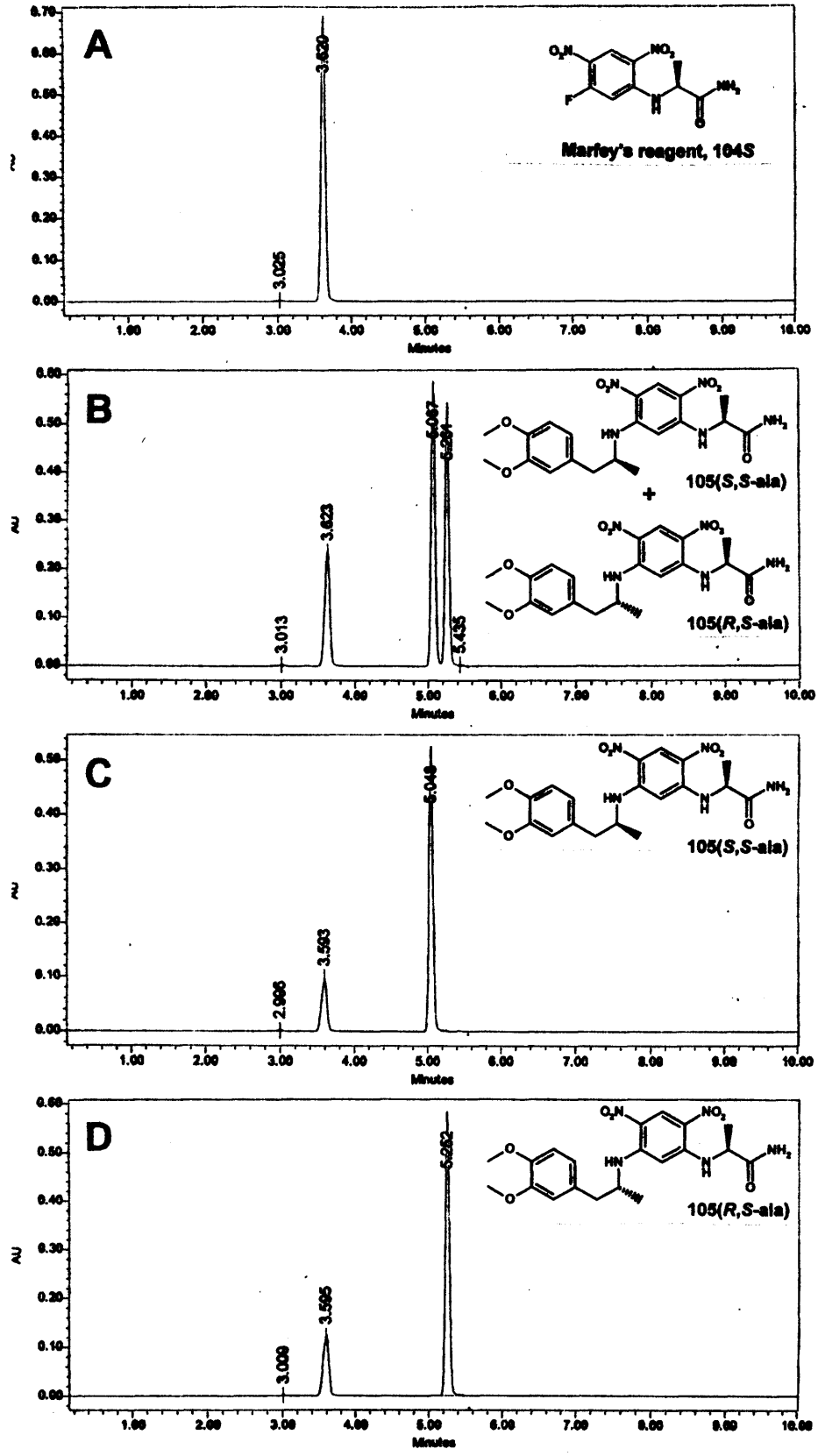

Figure 72: HPLC confirmation of the successful resolution of the enantiomers of **38**.
A shows the trace for **104*S*** alone;
B shows the trace after the reaction of **38*RS*** and **104*S***;
C shows the trace after the reaction of resolved **38*S*** and **104*S***;
D shows the trace after the reaction of resolved **38*R*** and **104*S***.

The enantiomer **38*R*** was obtained by combining the mother liquors from the recrystallisations performed to obtain **38*S***, and removing the solvents under reduced pressure to yield a colourless crystalline mixture of **38*R*** and **38*S*** salts of **103*R***. This mixture was dissolved in water, and the (*R*)-enriched amine **38** was liberated as the free-base by basification of the aqueous solution with sodium hydroxide, and extraction into dichloromethane. Removal of the dichloromethane under reduced pressure gave a colourless syrup; combination with stoichiometric (*S*)-mandelic acid **103*S*** in boiling propan-2-ol yielded the diastereomeric salt mixture as a colourless crystalline solid upon cooling. Repeated recrystallisation of the colourless crystalline mixture of salts from ethyl acetate/methanol 2:1 gave the pure colourless diastereomeric salt **38*R*+103*S***, with the enantiomeric enrichment of **38** established after each recrystallisation by reaction of the free amine with **104*S*** as already described, until enantiomeric purity, to the limit of detection, was achieved (for the HPLC trace, see Figure 72).

As for **38*S***, a sample of the resolved **38*R*** was converted to the free base and crystallised from n-pentane as waxy low melting point solid. The optical rotation was recorded, and compared with the literature value ($[\alpha]_D^{21}$ –32.8 (*c* 4.00, EtOH); *c.f.* $[\alpha]_D^{21}$ –32.1 (*c* 4.00, EtOH), –31.8 (*c* 3.80, EtOH)[455]). The resolution of **38*R*** and **38*S*** is summarised in Figure 73.

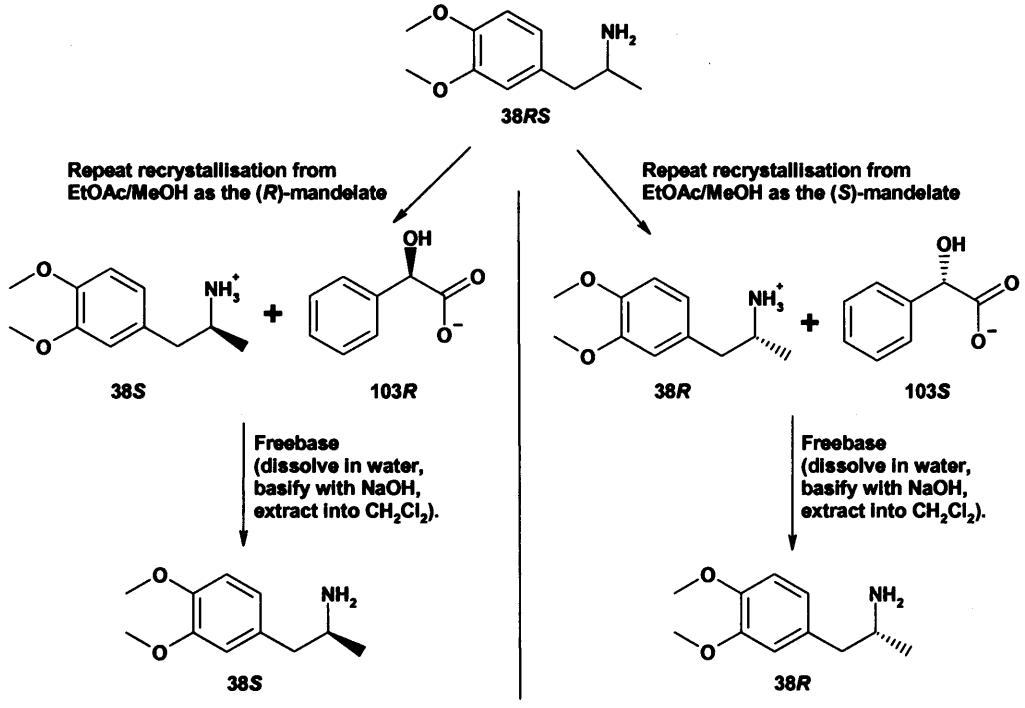

Figure 73: Synthesis and resolution of the enantiomers of the key intermediates **38*R*** and **38*S***.

Synthesis of the Enantiomers of 43

With the resolved enantiomers of amine **38** in hand, the enantiomers of tetrahydroisoquinoline **43** were readily synthesised by a variation of the Pictet-Spengler tetrahydroisoquinoline synthesis[415]. The reaction of each enantiomer of amine **38** with paraformaldehyde in glacial acetic acid and purification by recrystallisation from n-hexane gave the desired enantiomers of **43** as a cream coloured crystalline solid (see Figure 74).

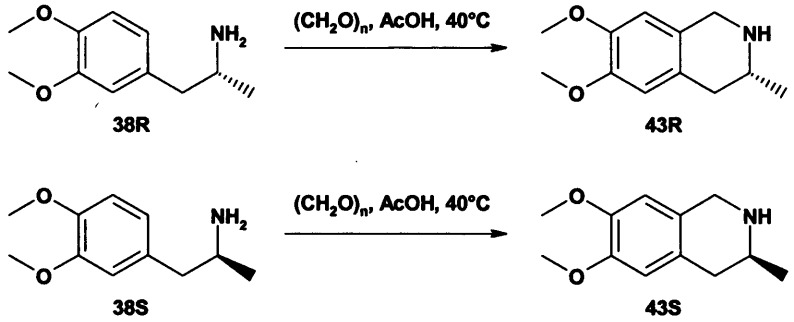

Figure 74: Synthesis of the enantiomers of **43** from the enantiomers of **38**.

Establishing the Enantiopurity of 43*R* and 43*S*

Although racemisation was not anticipated during ring closure, it was considered prudent to confirm that no racemisation had occurred during the cyclisation step of the tetrahydroisoquinoline synthesis. The high enantiopurity of the tetrahydroisoquinoline enantiomers **43*R*** and **43*S*** was confirmed by ^{1}H-NMR spectroscopy, using a *chiral solvating agent*[463]. The ^{1}H-NMR spectra were recorded for each enantiomer, and a racemic mixture, in the absence and the presence of 2 equivalents of the chiral solvating agent (*S*)-(+)-1-(9-anthryl)-2,2,2-trifluoroethanol **106*S*** ((*S*)-TFAE; see Figure 75)[463;464].

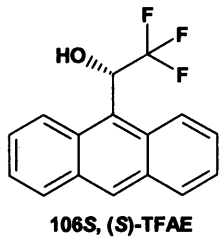

Figure 75: Structure of (*S*)-(+)-1-(9-anthryl)-2,2,2-trifluoroethanol **106*S*** ((*S*)-TFAE)[464].

While some resolution of the separate enantiomers was seen with one equivalent of **106*S***, the incomplete separation apparent for most of the substituted tetrahydroisoquinoline signals necessitated the addition of two equivalents,

whereupon baseline separation for most of the signals of interest was observed. In particular, the doublets corresponding to the methyl group attached to the stereogenic carbon, the doublet of doublets corresponding to each of the protons of the adjacent methylene, and the singlets corresponding to the aromatic protons of the tetrahydroisoquinoline were clearly realised for each enantiomers (see Figure 76).

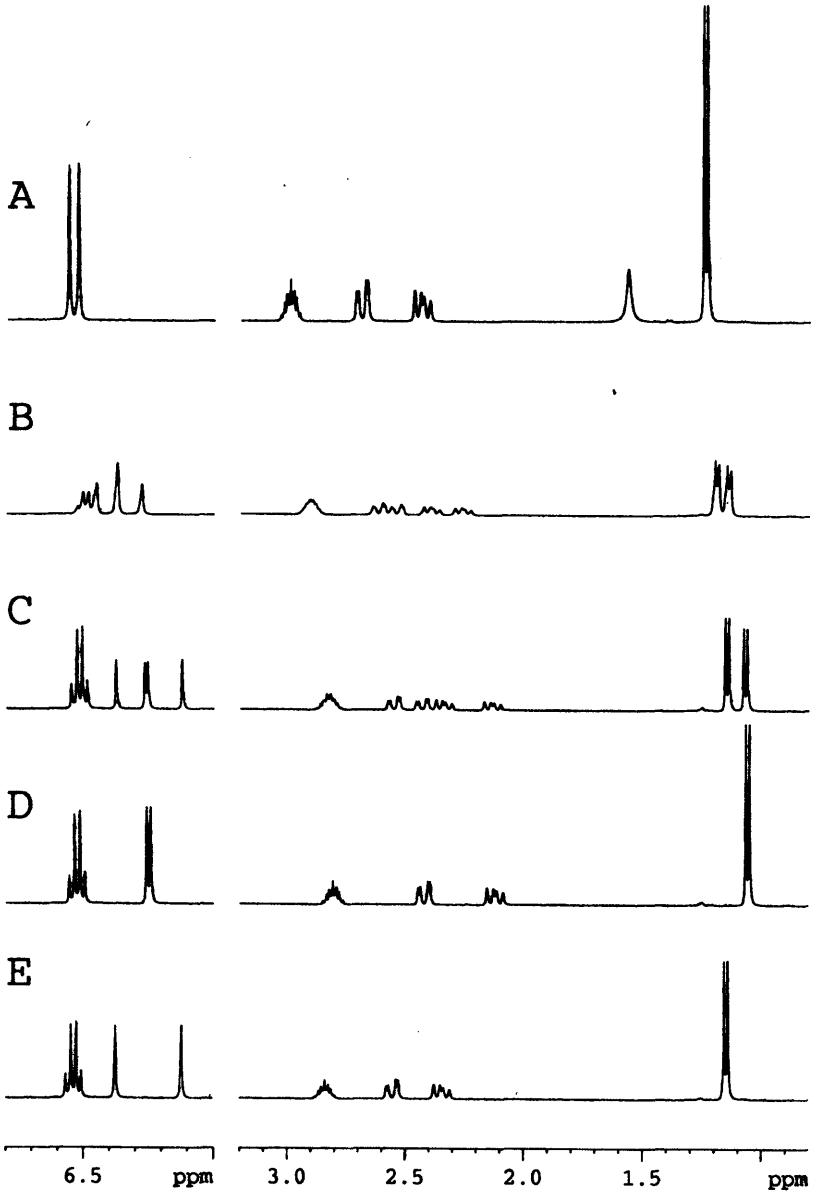

Figure 76: Comparative ^{1}H-NMR spectra, confirming the enantiopurity of the enantiomers of **43**: A. **43*RS***; B. **43*RS*** + 1 eq. **106*S***; C. **43*RS*** + 2 eq. **106*S***; D. **43*S*** + 2 eq. **106*S***; E. **43*R*** + 2 eq. **106*S***.

Investigations into the Synthesis of the Enantiomers of the *cis*- and the *trans*-diastereomers of 6,7-dimethoxy-1,3-dimethyl-1,2,3,4-tetrahydro-isoquinoline (44)

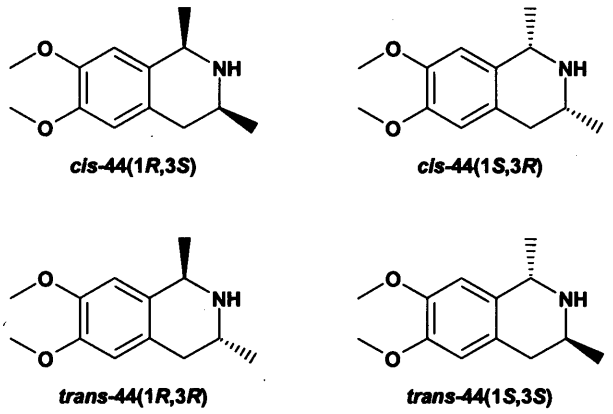

Figure 77: The four desired diastereomers of 6,7-dimethoxy-1,3-dimethyl-1,2,3,4-tetrahydroisoquinoline (*cis*-**40**(1*R*,3*S*), *cis*-**40**(1*S*,3*R*), *trans*-**40**(1*R*,3*R*) and *trans*-**40**(1*S*,3*S*))

Figure 77 shows the four possible diastereomers of the key intermediate tetrahydroisoquinoline **44**, the enantio- and diastereoselective syntheses of which was a key objective of this thesis. Ideally, and with the resolved enantiomers of amine **38** as a starting point, the synthesis of each pair of diastereomers was to be achieved by the stereoselective insertion of a 2-carbon unit to form the ring and the methyl group of the 1-position. Direct stereoselective insertion required an asymmetric Pictet-Spengler synthesis of the tetrahydroisoquinoline, while an indirect approach, via acetylation to give the amide **107** and ring closure under Bischler-Napieralski conditions to give the 3,4-dihydroisoquinoline intermediate **108**, followed by a stereoselective reduction, offered a viable synthetic alternative (see Figure 78). Given that we could start from **38*R*** and **38*S***, the use of a Pomeranz-Fritsch-Bobbitt approach to tetrahydroisoquinoline synthesis was not considered.

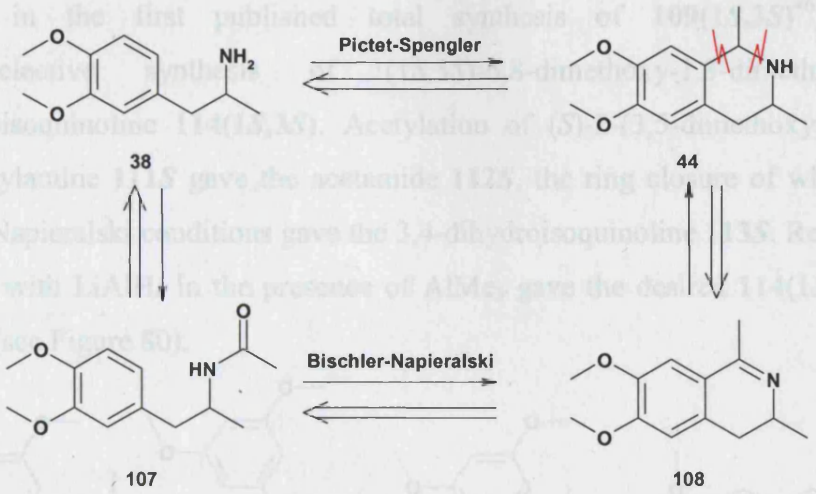

Figure 78: Retrosynthetic analysis of approaches to **44** form **38**.

Investigations into the Synthesis of the Stereoisomers of 44, via Modification of the Bischler-Napieralski Tetrahydroisoquinoline Synthesis[418]

At the commencement of this project, few diastereoselective synthetic approaches to 1,3-dimethyl-1,2,3,4-tetrahydroisoquinolines had been published, and none contained the desired 6,7-dioxygenated substitution pattern; a recent review has confirmed that this is still the case[417]. However, the requisite *cis*- and *trans*-1,3-dimethyl-1,2,3,4-tetrahydroisoquinoline cores are found in the naturally occurring naphthylisoquinoline alkaloids[433], with representatives being isolated from tropical lianas of the families *Ancistrocladaceae* and *Dionchophyllaceae*. These include (–)-ancistrocladine **109(1*S*,3*S*)**[465] and (+)-isoancistrocladine **110(1*R*,3*S*)**[466] (see Figure 79).

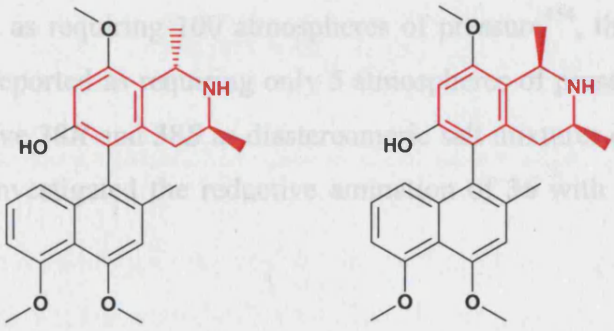

Figure 79: Some examples of naturally occurring alkaloids containing 1,3-dimethyl-1,2,3,4-tetrahydroisoquinoline cores (in red).

Included in the first published total synthesis of **109(1*S*,3*S*)**[467] was a diastereoselective synthesis of (1*S*,3*S*)-6,8-dimethoxy-1,3-dimethyl-1,2,3,4-tetrahydroisoquinoline **114(1*S*,3*S*)**. Acetylation of (*S*)-2-(3,5-dimethoxyphenyl)-1-methylethylamine **111*S*** gave the acetamide **112*S***, the ring closure of which under Bischler-Napieralski conditions gave the 3,4-dihydroisoquinoline **113*S***. Reduction of the imine with $LiAlH_4$ in the presence of $AlMe_3$ gave the desired **114(1*S*,3*S*)** with 92% *d.e.* (see Figure 80).

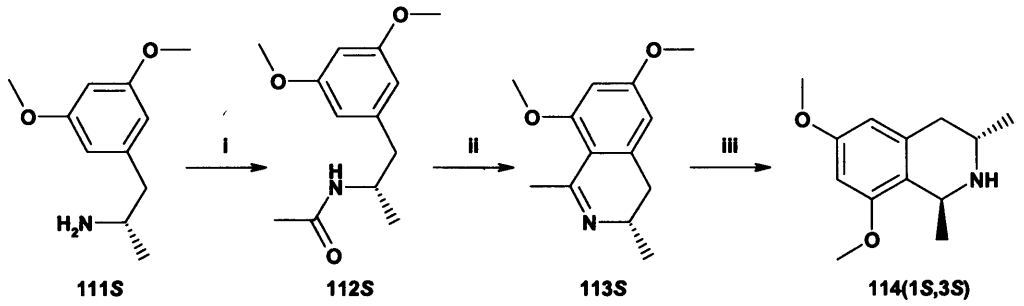

Reagents and conditions: I. H_3CCOCl, Et_3N, CH_2Cl_2; II. $POCl_3$, MeCN, reflux; III. $LiAlH_4/AlMe_3$, THF, –78°C to 0°C

Figure 80: Diastereoselective synthesis of **114(1*S*,3*S*)**[467].

Interestingly, this synthesis required the synthesis of the pure enantiomer **111*S***, which was obtained by the stereoselective two step reductive amination of 3,5-dimethoxyacetophenone **115** with **82*S*** to give the diastereomeric amine **117(1*S*,1'*S*)**, via the imine **116*S***. Hydrogenolysis of the benzylamine of **117(1*S*,1'*S*)** gave **111*S*** (see Figure 81). This synthesis is directly comparable to the route to the enantiomers of **38** published by Weinges and Graab already discussed (see Figure 67). However, whereas the reduction of imine formed between **36** and **82*S*** was reported as requiring 100 atmospheres of pressure[454], the reduction of the imine **116*S*** was reported as requiring only 5 atmospheres of pressure. If we had not been able to resolve **38*R*** and **38*S*** as diastereomeric salt mixtures of **103*R*** and **103*S***, we would have investigated the reductive amination of **36** with **82*S*** under similar conditions.

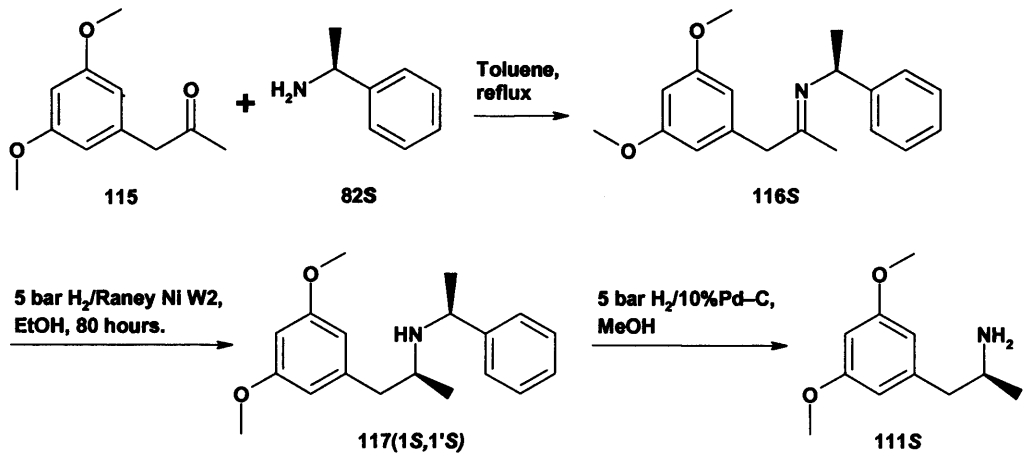

Figure 81: Stereoselective synthesis of **111*S***[467]

Seven years after the publication of the total synthesis of **109(1*S*,3*S*)**[467], a subsequent publication from the same group gave synthetic approaches to all four diastereomers of **114**[468]. The key synthetic revelation of the paper was that, while confirming that the use of $LiAlH_4/AlMe_3$ in the reduction of **113** gave *trans*-**114** to greater than 90% *d.s.*, the use of sodium borohydride in the same step gave predominantly *cis*-**114**, to greater than 95% *d.s.* (see Figure 82).

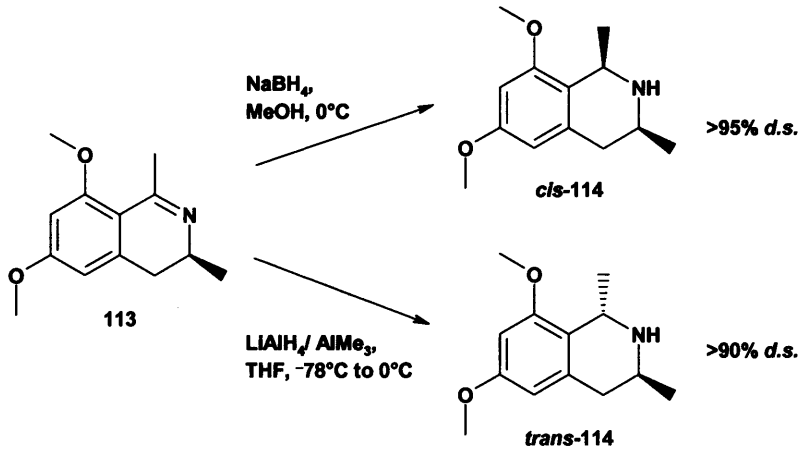

Figure 82: Diastereodivergent stereoselective synthesis of *cis*- and *trans*-**114**[468].

When the same methodology was applied in the literature to the synthesis of the 5,6,7,8-unsubstituted-1,3-dimethyl-1,2,3,4-tetrahydroisoquinoline **119**[469] however, some problems arose. While the enantiomers of *cis*-**119** could be successfully obtained by the reduction of the enantiomers of 1,3-dimethyl-3,4-dihydroisoquinoline **118** with $NaBH_4$, the reduction of the enantiomers of **118** with $LiAlH_4/AlMe_3$ not only gave a mixture of *cis*-**119** and *trans*-**119**, but also caused the loss of chiral integrity at the 3-position (see Figure 83). The diastereomers *cis*-**119**

and *trans*-**119** were separated by column chromatography, and the enantiomers of *trans*-**119** by recrystallisation as diastereomeric salts with the enantiomers of dibenzoyl tartaric acid[469]. It was postulated that the oxygen moiety at the 8-position in the synthesis of **114**[467] was essential for both the stereoselectivity, and lack of racemisation seen in the $LiAlH_4/AlMe_3$ reduction step.

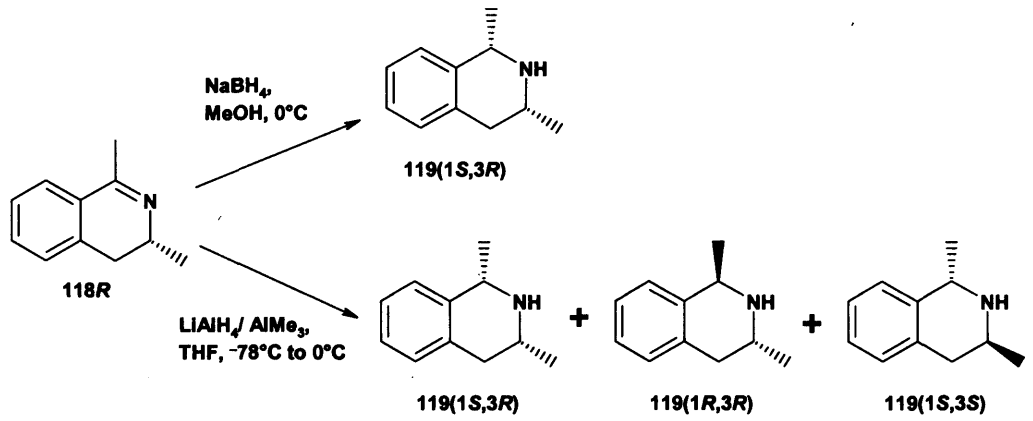

Figure 83: The effects of using different reducing agents upon the diastereoselectivity of the reduction of **118*R***[469].

Our 3,4-dihydroisoquinoline **108** does not have the apparently requisite oxygen moiety at the 8-position. Rather than explore the diverse range of available reducing agents for *trans*-diastereoselectivity, we decided to explore the potential for using a chiral auxiliary to introduce the 1-position methyl group asymmetrically by the most direct route, via a Pictet-Spengler type reaction with the enantiomers of **38**. By using each enantiomer of the chiral auxiliary, it would be possible to selectively insert the 2-carbon subunit into the 1-position of the tetrahydroisoquinoline in either the ***R*** or ***S*** absolute configuration. In conjunction with the enantiomers of **38**, this would give access to all four diastereomers of **44**, ideally with a high degree of diastereoselectivity.

Stereoisomerism (2)

It is perhaps worth emphasising at this point that the capacity to act as a chiral centre is not confined to tetrahedral carbon atoms; the appropriate substitution of any quadriligant (four-coordinate) and sexiligant (six-coordinate) atom, as well as the pyramidal triligant (three-coordinate) atoms, such as N and P, can produce chirality[412;414]. The stability and potential for isolation of these putative stereoisomers is dependent upon any barrier to rotation; frequently the barrier is too low for the existence of such stereoisomers to be anything other than hypothetical.

Suitably substituted triligant sulfur compounds having pyramidal structure, such as sulfonium salts, sulfoxides and sulfinate esters, contain a chiral sulfur atom[470]. In particular, sulfoxides can have three sterically and stereoelectronically different types of substituent pendant to the chiral sulfur: the lone pair of electrons, the oxygen atom, and two alkyl/aryl groups. As such, sulfoxides are frequently stable to thermal racemisation to beyond 200°C[470], and the use of the enantiomers of chiral sulfoxides in asymmetric carbon-carbon bond formation is well established[470].

For the purposes of the CIP-system descriptor assignment, the three ligands of sulfoxides (and other triligant centres) are prioritised according to the established rules[412-414], as touched upon briefly in the section entitled '**Stereoisomerism**'. The fourth "absent" ligand in these pyramidal triligant systems, usually a lone pair of electrons, is considered to have atomic number zero, and therefore lowest prioritised rank[414]. It is this ligand that is therefore projected away from the viewer when assigning the CIP-descriptor. Finally, for clarity, especially with multiple chiral centres of more than one atom type, it has proven useful to subscript the descriptors for atoms other than carbon with the appropriate atomic symbol. This is summarised for the enantiomers of 4-tolylmethylsulfoxide **120** in Figure 84.

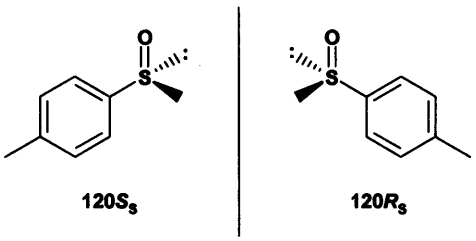

120S_S **120R_S**

Figure 84: Illustrating the application of the CIP-system descriptors to sulfoxides.

Investigations into the Synthesis of the Stereoisomers of 44, via Modification of the Pictet-Spengler Tetrahydroisoquinoline Synthesis[415]

The published synthesis of (*R*)-(+)-carnegine **125*R*** (*N*-methylated-**42*R***)[471] included the enantioselective insertion of the desired 2-carbon unit into the 1-position of the tetrahydroisoquinoline, by the reaction of the (R_S)-enantiomer of the chiral acetylenic sulfoxide **121** with 2-(3,4-dimethoxyphenyl)ethylamine **122** (see Figure 85). This appeared[472] to be an attractive starting point in the search for an appropriate chiral auxiliary to introduce the 1-position methyl group asymmetrically via a Pictet-Spengler type reaction with the enantiomers of **38**.

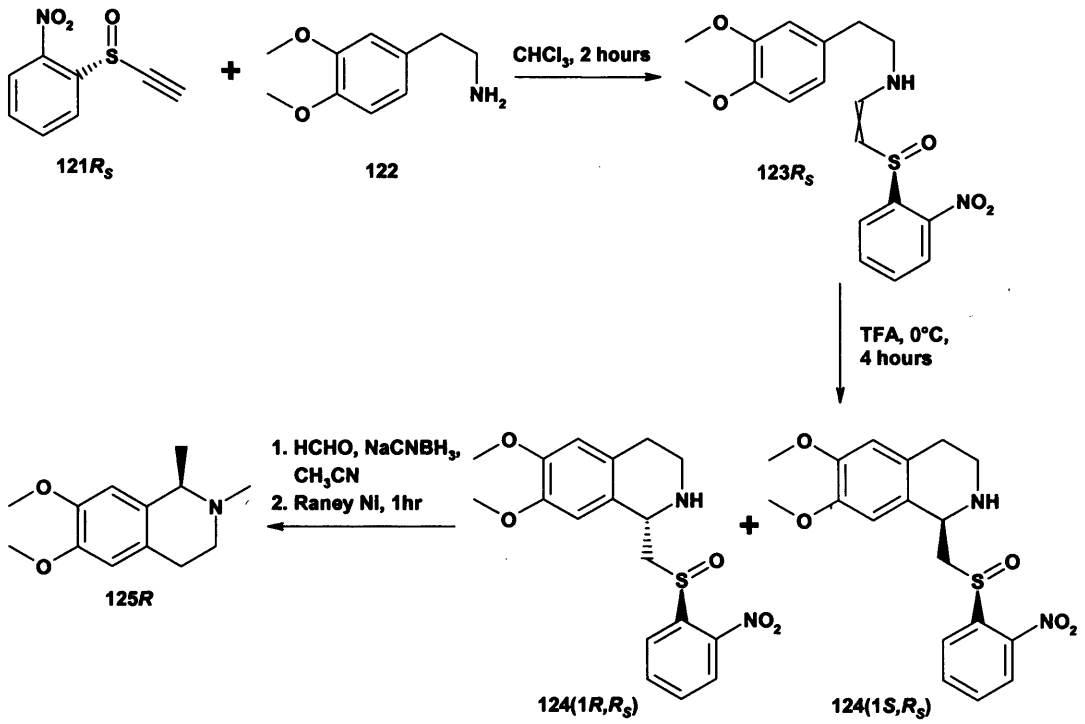

Figure 85: Total synthesis of **125*R***, using the chiral acetylenic sulfoxide **121*R*$_S$**[471;472]

In the published synthesis of **125*R***[471], the Michael addition of 2-(3,4-dimethoxyphenyl)ethylamine **122** to (*R*S)-ethynyl-2-nitrophenylsulfoxide **121*R*S** formed the β-aminovinylsulfoxide **123*R*S**, the acid-mediated ring closure of which gave only one diastereomer of the product 1-substituted tetrahydroisoquinoline **124(1*R*,*R*S)**. The reaction was repeated with an alternative chiral acetylenic sulfoxide ((*S*S)-ethynyl-4-tolylsulfoxide), and a 2:1 mixture of diastereomers was formed[472]. Methylation of the tetrahydroisoquinoline nitrogen, and subsequent reductive cleavage of the sulfur-carbon bond, gave the desired alkaloid **125*R***[472].. The rationalisation for the diastereoselectivity ring closure reaction proposed the acid-mediated formation of a conformationally constrained iminium intermediate **126*R*S**, stabilised by hydrogen bond formation between the sulfoxide oxygen and the iminium hydrogen, to form a six-membered ring (see Figure 86). This intermediate determines the orientation of the ring closure. The presence of the 2-nitro substituent enhances the diastereoselectivity by stabilising the hydrogen bond[472].

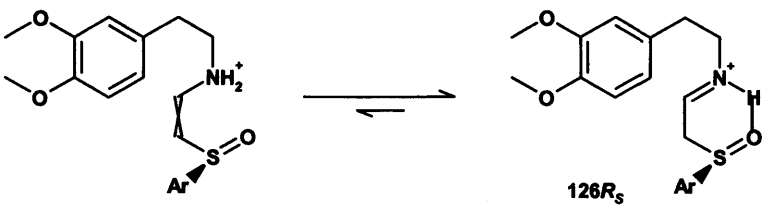

Figure 86: The reactive intermediates of the acid-mediated cyclisation of $123R_S$, with the iminium intermediate $126R_S$ proposed as the predominant species. The conformationally constrained, hydrogen bond containing six-membered ring was speculated to determine the orientation of the ring closure[472].

To investigate the applicability of using the (R_S)- and (S_S)-enantiomers of **121**[472] in the synthesis of the enantiomers of ***cis*-44** and ***trans*-44**, a synthetic approach to the pure (R_S)- and (S_S)-enantiomers of **121**[472] was required. Attempts to reproduce the stereoselective synthesis and purification of $121R_S$[472] described in the literature[471] (see Figure 87) proved highly variable, and not without complication.

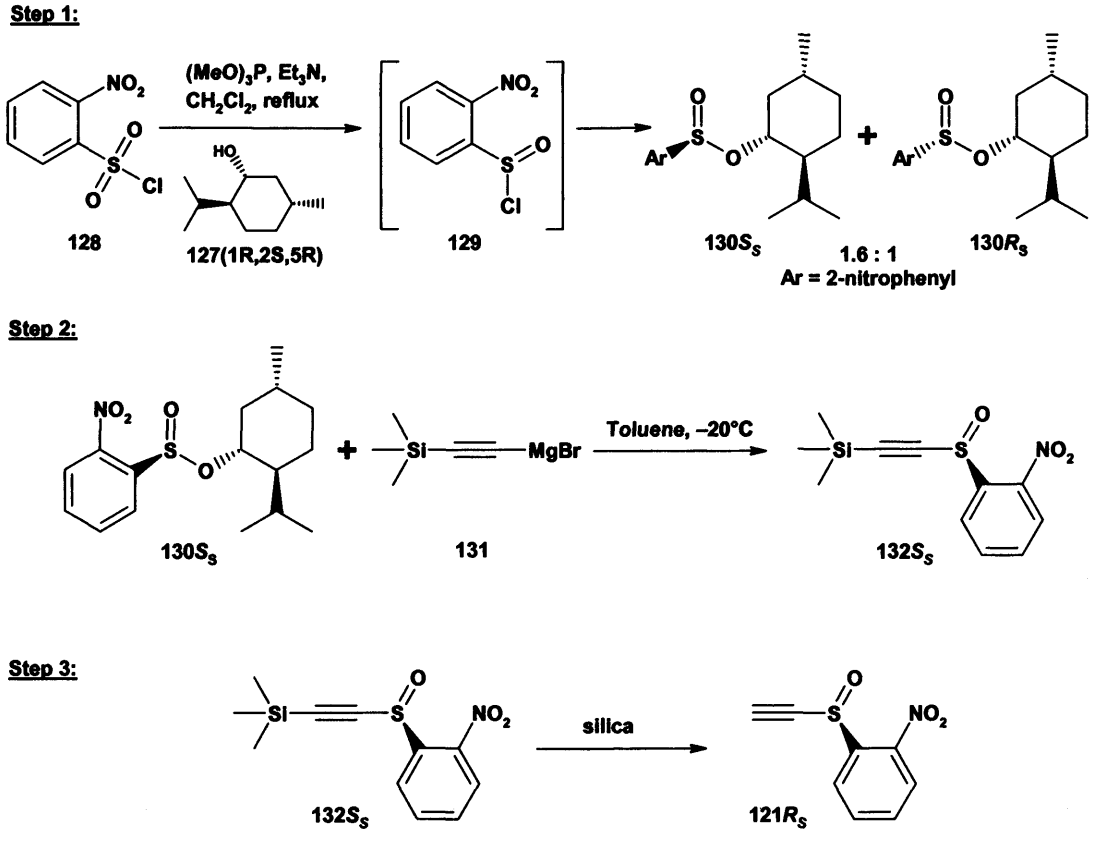

Figure 87: Literature synthetic route to $121R_S$[471,472]

In the literature approach to $125R$[472], the pure enantiomer of the chiral sulfoxide $121R_S$ was synthesised via resolution of the menthyl sulfinate ester $130S_S$, following the classical route developed by Andersen[473] (see Figure 87). Firstly, trimethyl phosphite was used to reduce 2-nitrobenzenesulfonyl chloride **128** to 2-nitrobenzenesulfinyl chloride **129**, using methodology developed by Klunder and

Sharpless[474], whereupon **129** was trapped *in situ* by reaction with (1*R*,2*S*,5*R*)-menthol **127(1*R*,2*S*,5*R*)**, to give the menthyl sulfinate ester **130*R*$_S$*S*$_S$** as a mixture of diastereomers. [472]Some degree of stereoselectivity was reported in the formation of the diastereomers of the menthyl sulfinate ester **130**[471], with **130*S*$_S$** and **130*R*$_S$** being produced as either a 1.6:1 mixture, separable by column chromatography[472], or a 3:1 mixture, resolved by crystallisation from ethanol[471].

Presumably the presence of **127(1*R*,2*S*,5*R*)** created a chiral environment that, during the formation of **129**, introduced some asymmetry into the reduction of **128**, prior to ester formation between **129** and **127(1*R*,2*S*,5*R*)**. The small degree of diastereoselectivity and reported 'ease' of separation were attractive as, in order to obtain both enantiomers at the tetrahydroisoquinoline 1-position (and thereby the four diastereomers of **44**), both **121*R*$_S$** and **121*S*$_S$** would be required.

In step two, the Grignard reagent trimethylsilylethynylmagnesium bromide **131** was generated *in situ* from trimethylsilylacetylene and ethylmagnesium bromide[475], and reacted with the purified diastereomer of **130*S*$_S$**, to give the acetylenated sulfoxide **132*S*$_S$**. This reaction proceeded with total inversion at the sulfur atom, ensuring retention of optical purity and absolute configuration. The final step saw the removal of the trimethylsilyl group from **132*S*$_S$** by hydrolytic cleavage, reportedly achieved during column chromatography, to give the desired chiral acetylenic sulfoxide **121*R*$_S$**.

Some subtleties of the CIP system, and the care that must be taken when assigning descriptors are apparent from this reaction sequence. Despite the conversion of producing inversion at the chiral sulfur atom, the chiral descriptor remained ***S*$_S$** for both **130** and **132**, as the menthyl group, of higher priority than the sulfoxide oxygen, was replaced with an acetylene, of lower priority than the sulfoxide oxygen. In contrast, despite no change in the configuration at the chiral sulfur atom in the conversion of **132** to **121**, the chiral descriptor changed, from ***S*$_S$** to ***R*$_S$**, because the loss of the silicon atom altered the priority of the acetylenic substituent with respect to the aryl substituent. This is illustrated in Figure 88.

Direction of rotation, from highest (1) to lowest (3) ranking substituent:

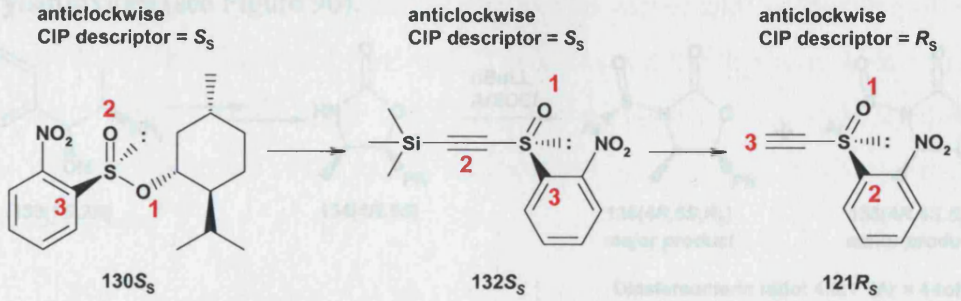

Figure 88: Absolute configuration, substituent prioritisation and CIP descriptors[412;413].

However, following the literature procedure[471;472] to the pure enantiomers of **121** proved problematical. While the addition of a mixture of trimethyl phosphite and triethylamine to a solution of **127** and **128** in dichloromethane yielded the predicted diastereomeric mixture of **130*R*$_S$** and **130*S*$_S$**, neither diastereomer of **130** could be isolated to the necessary degree of diastereomeric purity. Repeated attempts at purification by flash column chromatography and preparative HPLC were unsuccessful. The similarity of R_f values and HPLC retention times for each of the diastereomers led only to incomplete separation, although some enriched fractions for each diastereomer were obtained. Repeated recrystallisations also failed to significantly increase the *d.e.*. To test the applicability of the chiral acetylenic sulfoxides to the planned synthesis, we decided to push through material of a sufficiently high *d.e.* and react it with the Grignard reagent **131**. However, the reaction between **130** and **131** also proved low yielding, with significant quantities of unreacted **130** recovered.

To improve these aspects of the synthesis, alternative chiral auxiliaries were sought. One literature source described the use of separate *N*-sulfinyloxazolidinones **135(4*R*,5*S*,*R*$_S$)** and **138(4*S*,*S*$_S$)** as chiral sulfinyl transfer reagents to obtain the opposite enantiomers of synthetically useful arylsulfoxides[476]. Originally derived from (1*S*,2*R*)-2-amino-1-phenylpropan-1-ol **133(1*S*,2*R*)** ((1*S*,2*R*)-norephedrine)[477], the now commercially available (4*R*,5*S*)-4-methyl-5-phenyloxazolidin-2-one **134(4*R*,5*S*)** can be readily converted to the *N*-sulfinyloxazolidinones **135(4*R*,5*S*,*R*$_S$)**, from which (S_S)-enantiomers of arylsulfoxides can be synthesised (see Figure 89). Similarly, the commercially available (S)-4-benzyl-oxazolidin-2-one **137*S***, itself originally derived from (*S*)-phenylalanine **136*S***[478], can be readily converted to the *N*-

sulfinyloxazolidinones **138(4*S*,S_S)** which can be converted into the (R_S)-enantiomers of arylsulfoxides (see Figure 90).

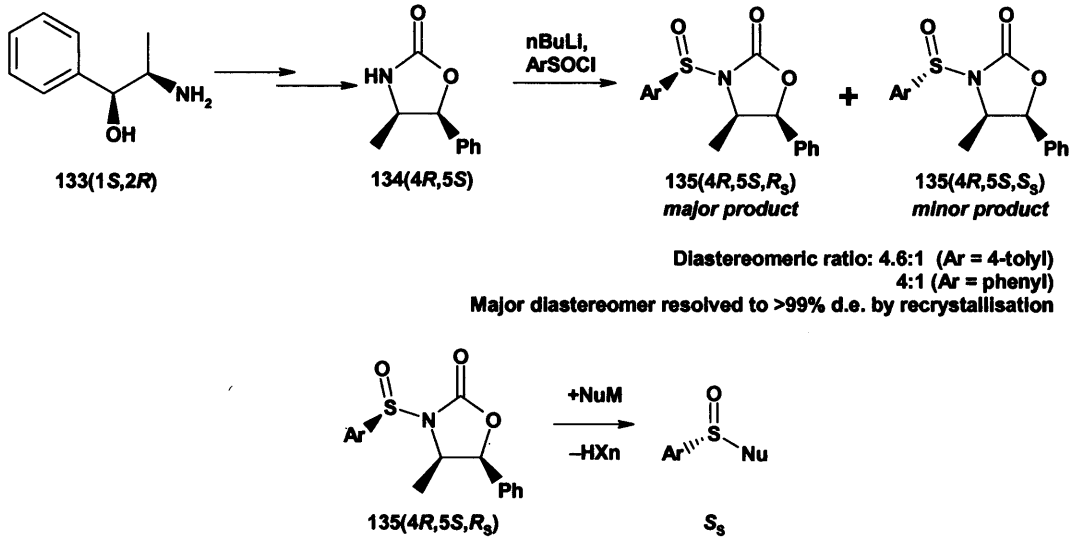

Figure 89: Synthesis of (S_S)-sulfoxides from (1*S*,2*R*)-norephedrine **133(1*S*,2*R*)**[476;477].

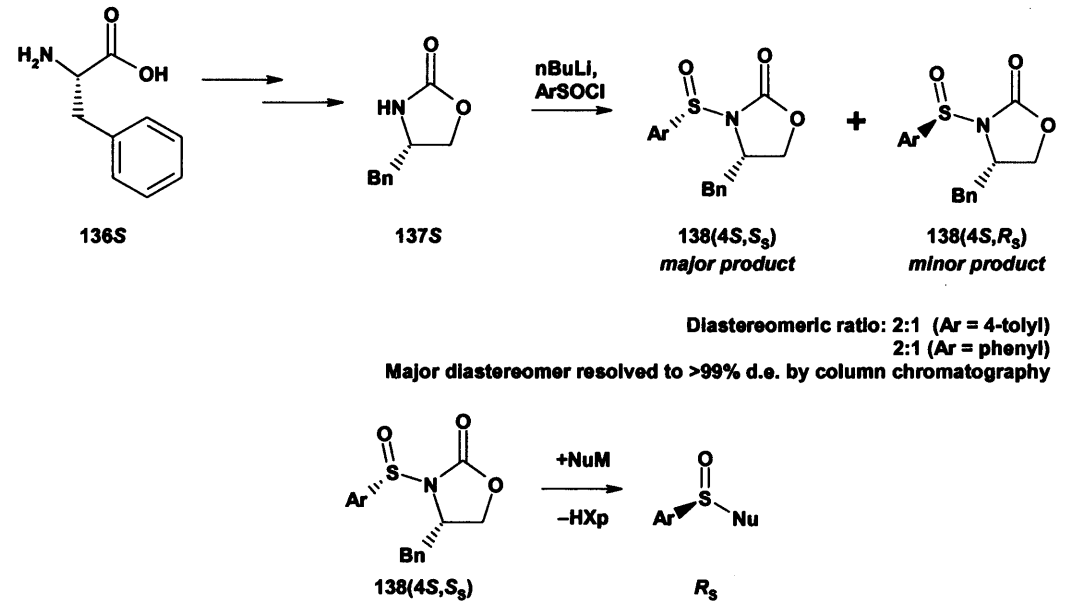

Figure 90: Synthesis of (R_S)-sulfoxides from (*S*)-phenylalanine **136*S***[476;478].

The reported advantages in using the oxazolidinones **134(4*R*,5*S*)** and **137*S*** included greater ease of diastereomeric resolution, either by recrystallisation or chromatographic separation, and a 100-fold increased reactivity with Grignard reagents over the menthyl sulfinates such as **130**[476]. The synthesis of (*S*)-4-benzyl-3-((*S*)-2-nitrobenzenesulfinyl)oxazolidin-2-one **140(4*S*,S_S)** from **137*S*** required the generation of 2-nitrophenylsulfinyl chloride **129**. Two approaches were taken: the previously employed *in situ* reduction of 2-nitrophenylsulfonyl chloride **128** with

trimethyl phosphite[474], and an alternative literature preparation from 2-nitrophenyldisulfide **139**, using sulfuryl chloride in acetic acid[479]. Reaction of either preparation of the **129** with the lithiated **137*S*** gave multiple products, with no useful quantities of either **140(4*S*,S_S)** or **140(4*R*,S_S)** being isolated. This may be a reflection of the inherent instability of the anticipated products, as described in a footnote in the original protocol[476].

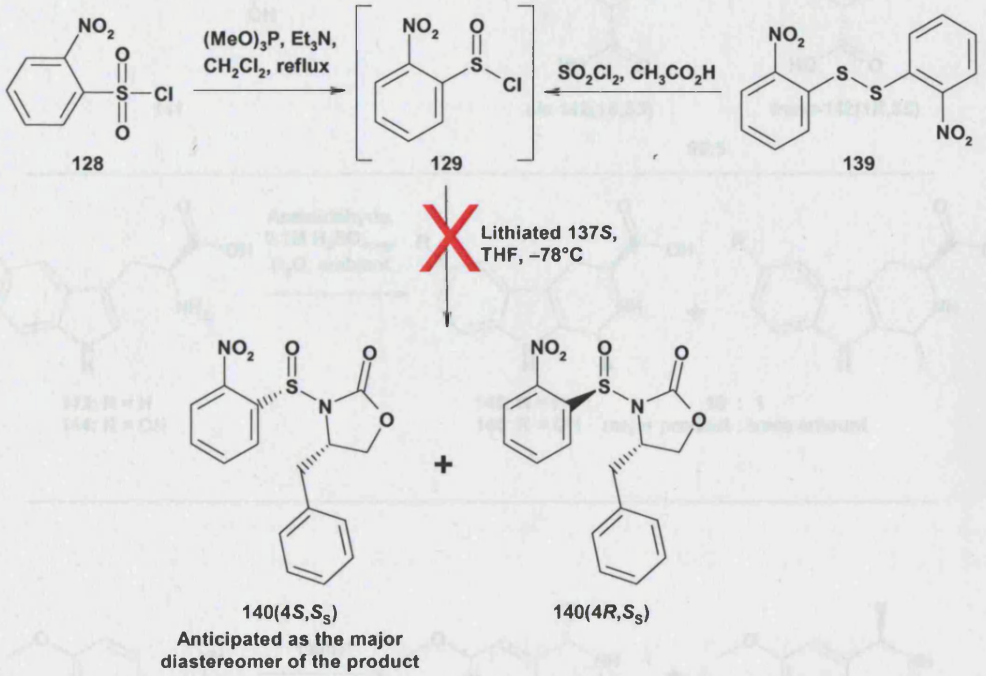

Figure 91: The unsuccessful route to **140(4*S*,S_S)**.

The difficulty in obtaining the pure (R_S)- and (S_S)-enantiomers of **121**[472] was proving to be a detrimental to the synthetic effort, necessitating a reappraisal of the synthetic approach to the pure diastereomers of **44**. Rather than using an additional stereogenic centre to induce stereoselectivity at the 1-position, a search of the literature provided ample evidence that the existing 3-position stereogenic centre could exert some degree of stereoselective induction at the 1-position (see Figure 92). The cyclisation of L-DOPA **141** with acetaldehyde in the presence of a mineral acid was reported to give the 1-methyl-3-carboxylic acid tetrahydroisoquinoline product **142** in a 95:5 ratio of the ***cis*-142(1*S*,3*S*)** to the ***trans*-142(1*R*,3*S*)**[434]. The same authors reported similar results with Pictet-Spengler cyclisations of acetaldehyde with L-tryptophan **143** to give tetrahydroisoquinoline **145** and of acetaldehyde with L-5-hydroxytryptophan **144** to give tetrahydroisoquinoline **146**, with both producing the *cis*-analogues as the major diastereomer[436]. It has also been reported that the

formation of 1-substituted-3-aryltetrahydrosioquinolines **148** by the classical Pictet-Spengler cyclisation[415] of 1,2-bis(3,4-dimethoxyphenyl)ethylamine **147** with acetaldehyde gave the *cis*-products as the major diastereomer[480].

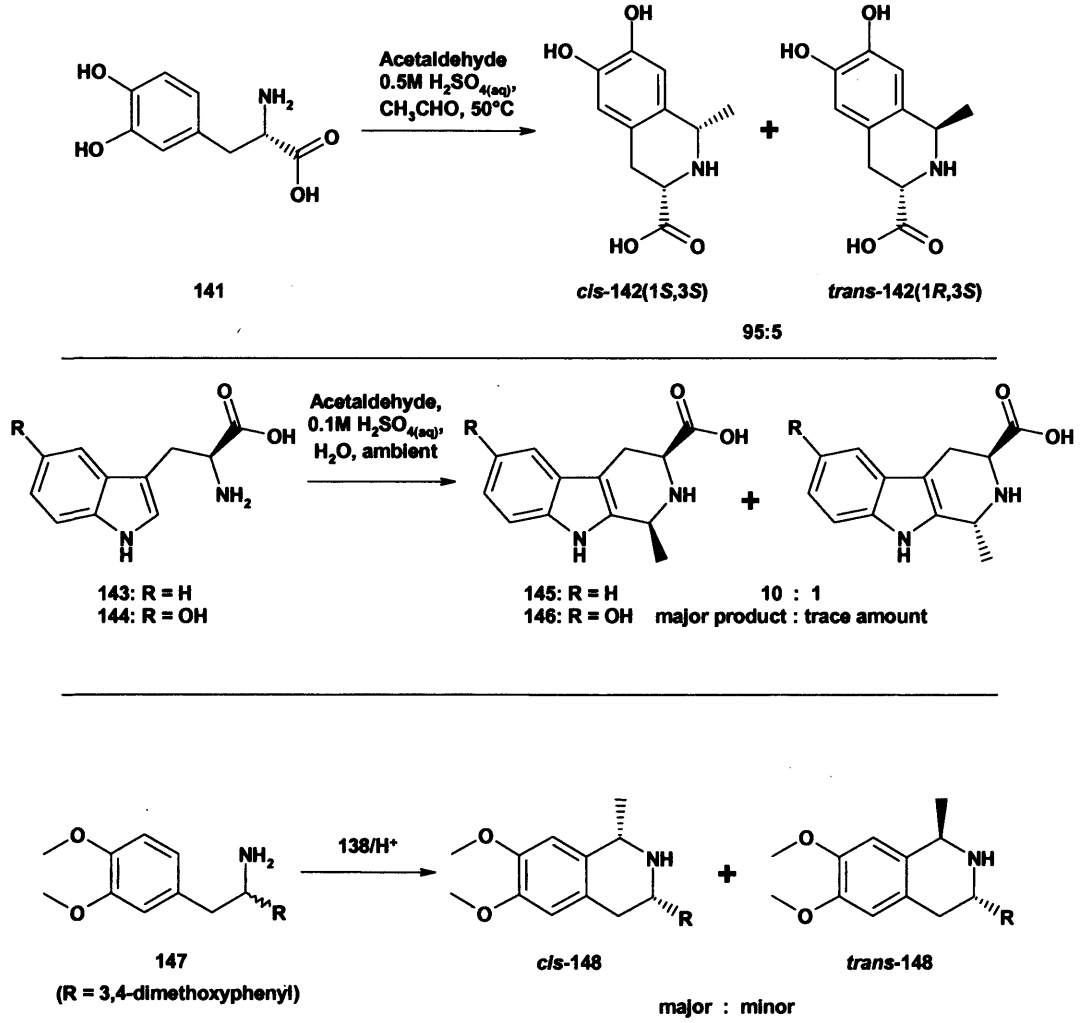

Figure 92: Literature examples of diastereoselective Pictet-Spengler cyclisations of 1-substituted 2-arylethylamines with acetaldehyde[434;436;480].

A review of the ^{1}H-NMR spectrum of **31(1*RS*,3*RS*)** revealed that the original full structure mixture of diastereomers, rather than an equal 1:1:1:1 mixture of **31(1*R*,3*R*)**, **31(1*S*,3*S*)**, **31(1*R*,3*S*)** and **31(1*S*,3*R*)**, was a 6:1 mixture of *cis* and *trans* diastereomers, as seen from the peaks corresponding to the 1- and 3-methyl substituents (see Figure 93).

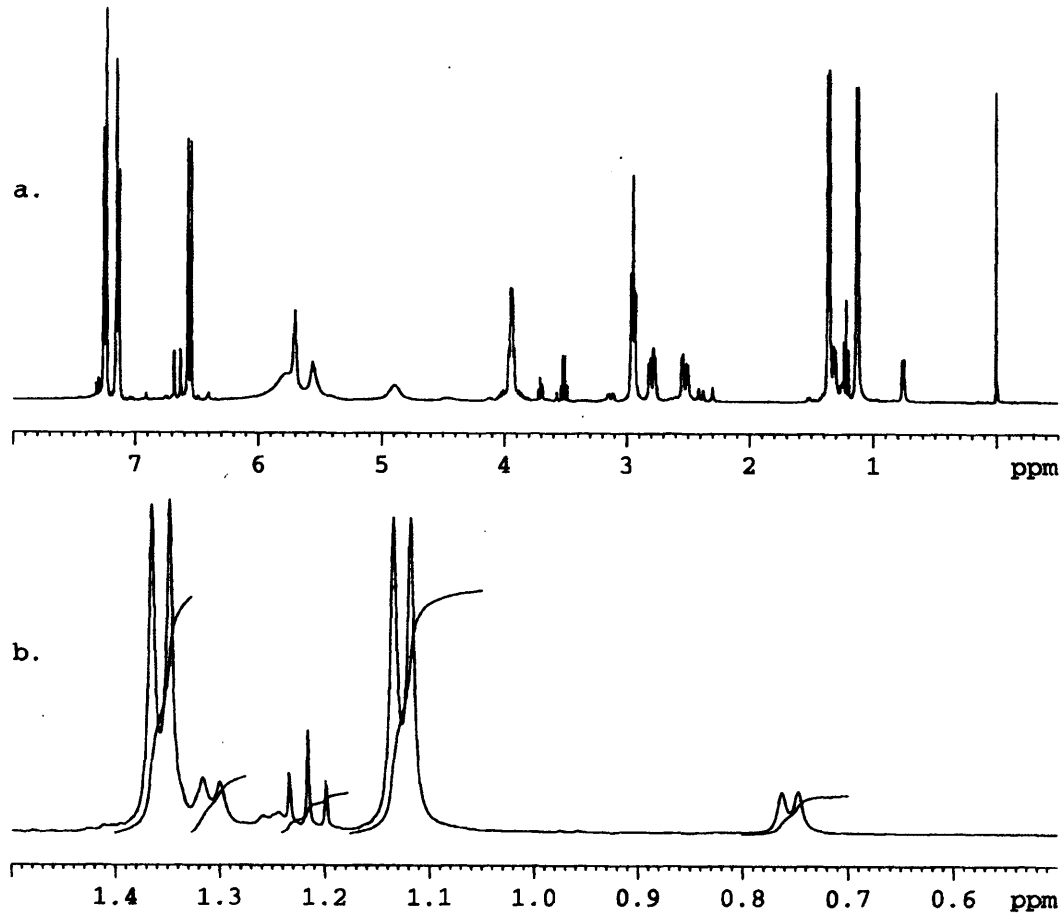

Figure 93: a. ^{1}H-NMR spectrum of the racemic mixture of diastereomers of **31(1*RS*,3*RS*)**;
b. Expansion of the region 0.5-1.5ppm, showing the doublets corresponding to the 1- and 3-methyl groups, with a diastereomeric ratio of approximately 6:1 (plus a triplet corresponding to the CH_3 of diethyl ether).

In the synthesis of **31(1*RS*,3*RS*)**, the 1-position stereogenic centre was introduced via a Pictet-Spengler cyclisation[415] of amine **39*RS*** and acetaldehyde in water to give tetrahydroisoquinoline **35(1*RS*,3*RS*)** (see Figure 40). The existing 3-position stereogenic centre must exert some degree of chiral induction at this point.

For comparative purposes, a trial reaction was carried out between amine **38*RS*** and acetaldehyde in hydrochloric acid under reflux. The ^{1}H-NMR spectrum of the crude product **44(1*RS*,3*RS*)** confirmed the tetrahydroisoquinoline product mixture to be formed with a degree of diastereoselectivity, in an approximately 3:1 mixture of diastereomers (see Figure 94).

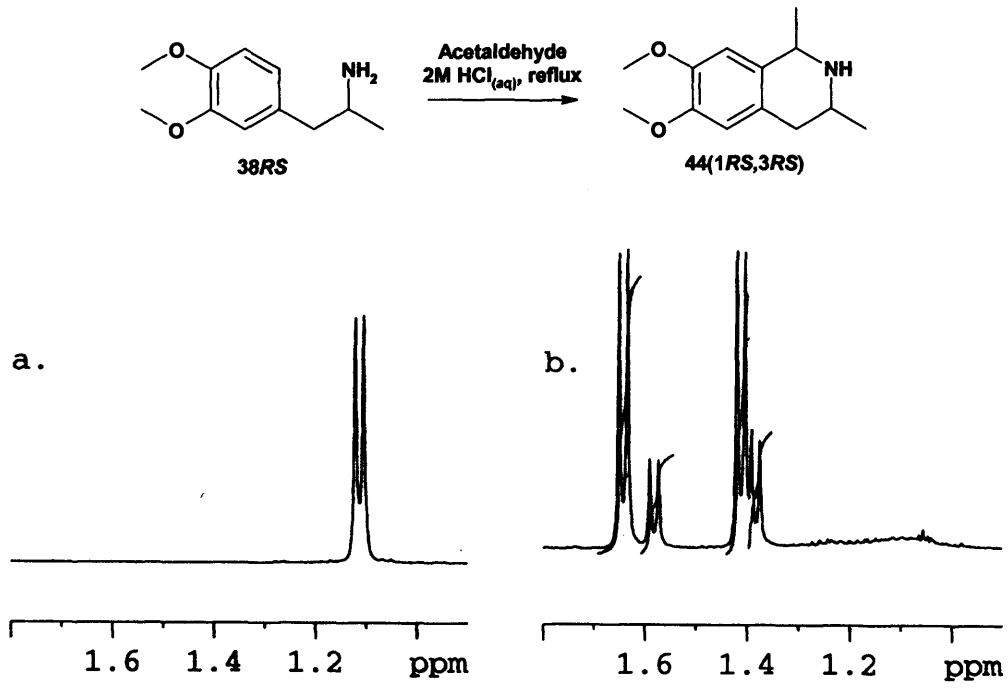

Figure 94: Trial synthesis of **44** as a mixture of diastereomers from **38*RS*** and acetaldehyde under Pictet-Spengler conditions, with expansions from ^{1}H-NMR spectra to show the doublets corresponding to the aliphatic methyl groups of **a.** **38*RS***, and **b.** the crude product.

Consideration of the reaction mechanism from a 3-dimensional perspective should allow the rationalisation of the indicated diastereoselectivity (see Figure 95). The key step of the synthesis, in which the orientation of the substituent at position 1 of the tetrahydroisoquinoline is determined, is when the electrons from the electron-rich carbon at position 6 of the benzene ring attack the electron-poor carbon of the iminium ion **149**. The iminium precursor would be expected to have the thermodynamically more stable (*E*)-configuration about the C=N bond. As the electrons from C-6 carbon attack the electron-poor carbon of the iminium ion, the carbon-nitrogen double bond will become increasingly single bond in character, with both atoms undergoing a transformation from a planar *sp2*-hybridised centre, to a tetrahedral *sp3*-hybridised centre. As the new carbon-carbon bond is formed, the transition state for forming the new ring would be required to adopt a half-chair conformation (*c.f.* cyclohexene[481]). There are two such transition state conformations available to the molecule, with the methyl group of the existing stereogenic centre lying either pseudoaxially or pseudoequatorially. With the methyl group in the pseudoequatorial position, the formation of the new carbon-carbon bond would lead

to the *cis*-diastereomer; with the methyl group in the pseudoaxial position, the *trans*-diastereomer would form. The preferred conformation has the methyl group held in the pseudoequatorial conformation (*c.f.* 4-substituted cyclohexenes[481]), although not exclusively, as some of the *trans*-diastereomer is formed.

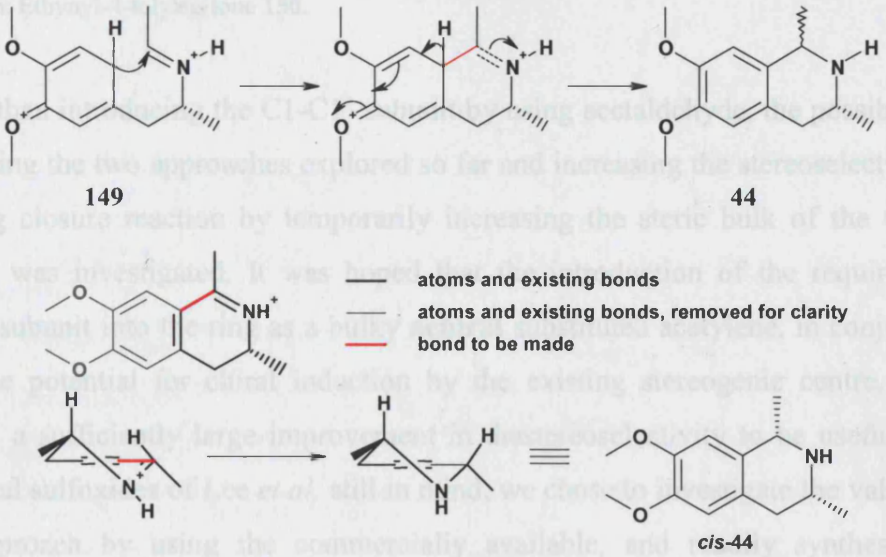

Figure 95: Diagrammatical representation of the conformations available during the heterocyclic ring formation of tetrahydroisoquinoline **44**, from the Pictet-Spengler cyclisation of **38** with acetaldehyde.

A similar rationalisation was proposed by Dominguez *et al* for the diastereoselectivity seen in the Pictet-Spengler cyclisation of **147** with acetaldehyde, to form **148** (see Figure 92)[480;482]. As expected, the steric effect of having a larger aryl substituent in the 3-position disfavours the transition state conformation with the axial disposition, thereby enhancing the stereoselectivity of the ring closure. In the cited example[480], having a 3,4-dimethoxybenzyl substituent in the 3 position resulted in an 8:1 ratio of *cis*:*trans* diastereomers.

In our example, the *cis*- and *trans*-diastereomers of **44** proved inseparable by either reverse-phase analytical HPLC or normal phase TLC. The derivatised BOC-protected amine was no better, and accessing the separate pairs of diastereomers via this route was not feasible.

Using Ethynyl-4-tolylsulfone (150) to Introduce the C1-C1' Subunit.

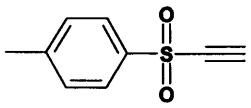

150

Figure 96: Ethynyl-4-tolylsulfone **150**.

Rather than introducing the C1-C1' subunit by using acetaldehyde, the possibility of combining the two approaches explored so far and increasing the stereoselectivity of the ring closure reaction by temporarily increasing the steric bulk of the C1-C1' subunit was investigated. It was hoped that the introduction of the required two carbon subunit into the ring as a bulky **achiral** substituted acetylene, in conjunction with the potential for chiral induction by the existing stereogenic centre, would provide a sufficiently large improvement in diastereoselectivity to be useful. With the chiral sulfoxides of Lee *et al.* still in mind, we chose to investigate the validity of this approach by using the commercially available, and readily synthesised[483], ethynyl-4-tolyl sulfone **150** (see Figure 96), which has been used as both a Michael acceptor[484] and a Diels-Alder dienophile[485].

A further potentially useful investigative aspect to the synthesis was included at this point. In addition to the published synthesis of **125*R***, using the primary amine **122** and **121*R*$_S$** (see Figure 85), a route to the enantiomer **125*S*** has also been published by the same group[486]. Using the **same** enantiomer of the acetylenic sulfoxide **121*R*$_S$**, but this time with a range of *N*-substituted analogues of **122**, there was an effective **reversal** of stereoselectivity seen in the ring closure step (see Figure 97).

It was hoped these observations might be used to good effect in this latest approach to the stereoisomers of **44**. To this end, the synthetic work now focussed upon the use of both the primary amine **38** and the *N*-benzylated secondary analogue **155** (for the initial routes investigated, see Figure 98). The Michael addition of the amines **38** and **155** to the alkyne **150** was anticipated to give the β-aminovinylsulfones **156** and **157** respectively. The acid-mediated ring closure of **156** should provide the desired 1,3-disubstituted-1,2,3,4-tetrahydroisoquinoline **159** directly, while the transformation of **157** to **159** would occur via **158**, with an extra deprotection/cleavage step required. The subsequent reductive cleavage of the sulfone should yield the desired tetrahydroisoquinoline **44**.

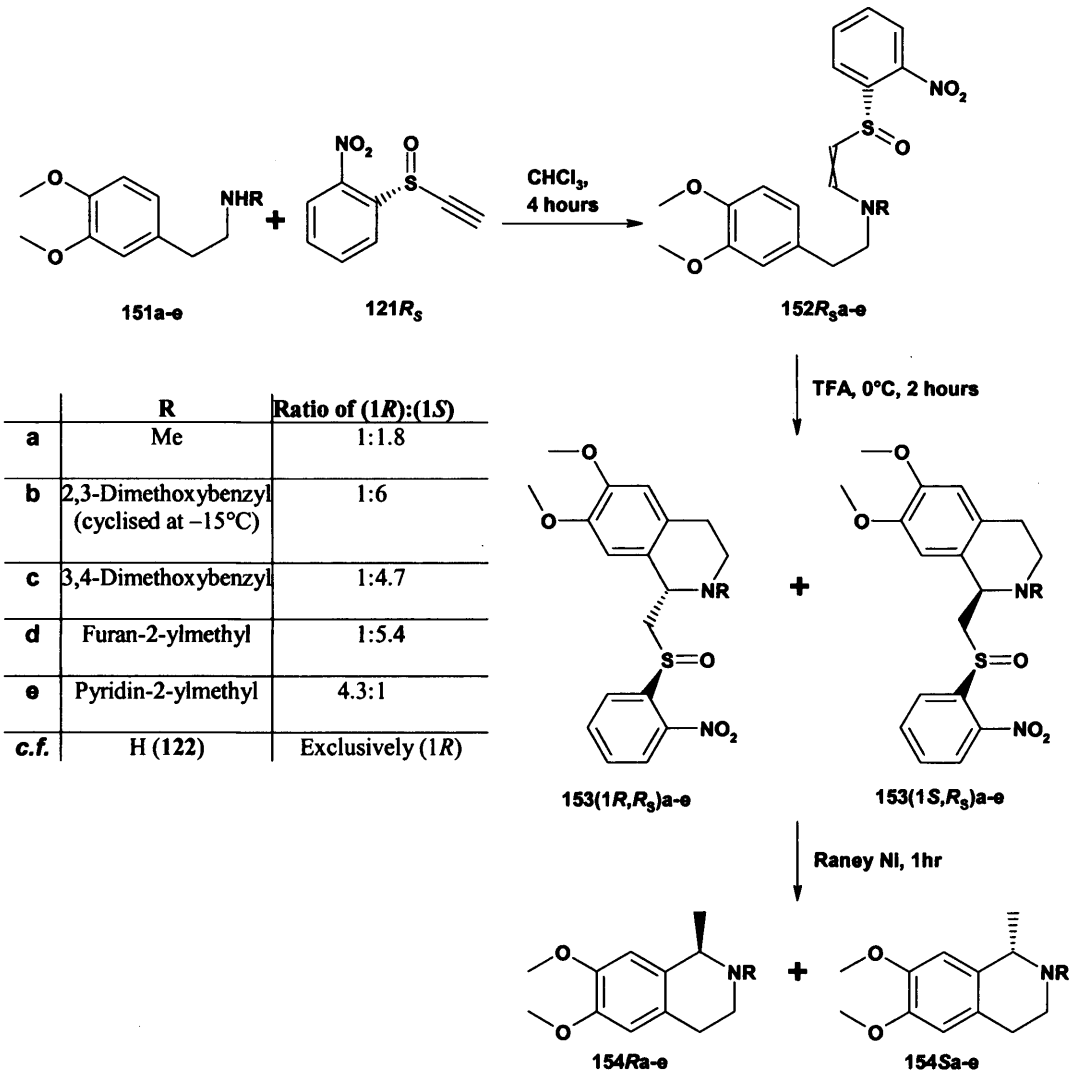

	R	Ratio of (1*R*):(1*S*)
a	Me	1:1.8
b	2,3-Dimethoxybenzyl (cyclised at −15°C)	1:6
c	3,4-Dimethoxybenzyl	1:4.7
d	Furan-2-ylmethyl	1:5.4
e	Pyridin-2-ylmethyl	4.3:1
c.f.	H (122)	Exclusively (1*R*)

Figure 97: Literature investigations into the reaction of secondary amines **151a-e** with **121*R*$_S$**, and the effects upon the stereoselectivity of the subsequent cyclisation[472;486].

The pure enantiomer **38*S*** was used as the starting point throughout, as the use of X-ray crystallographic methods was anticipated in the determination of the absolute stereochemistry of the products. Such determinations are facilitated when the absolute stereochemistry of one chiral centre is known.

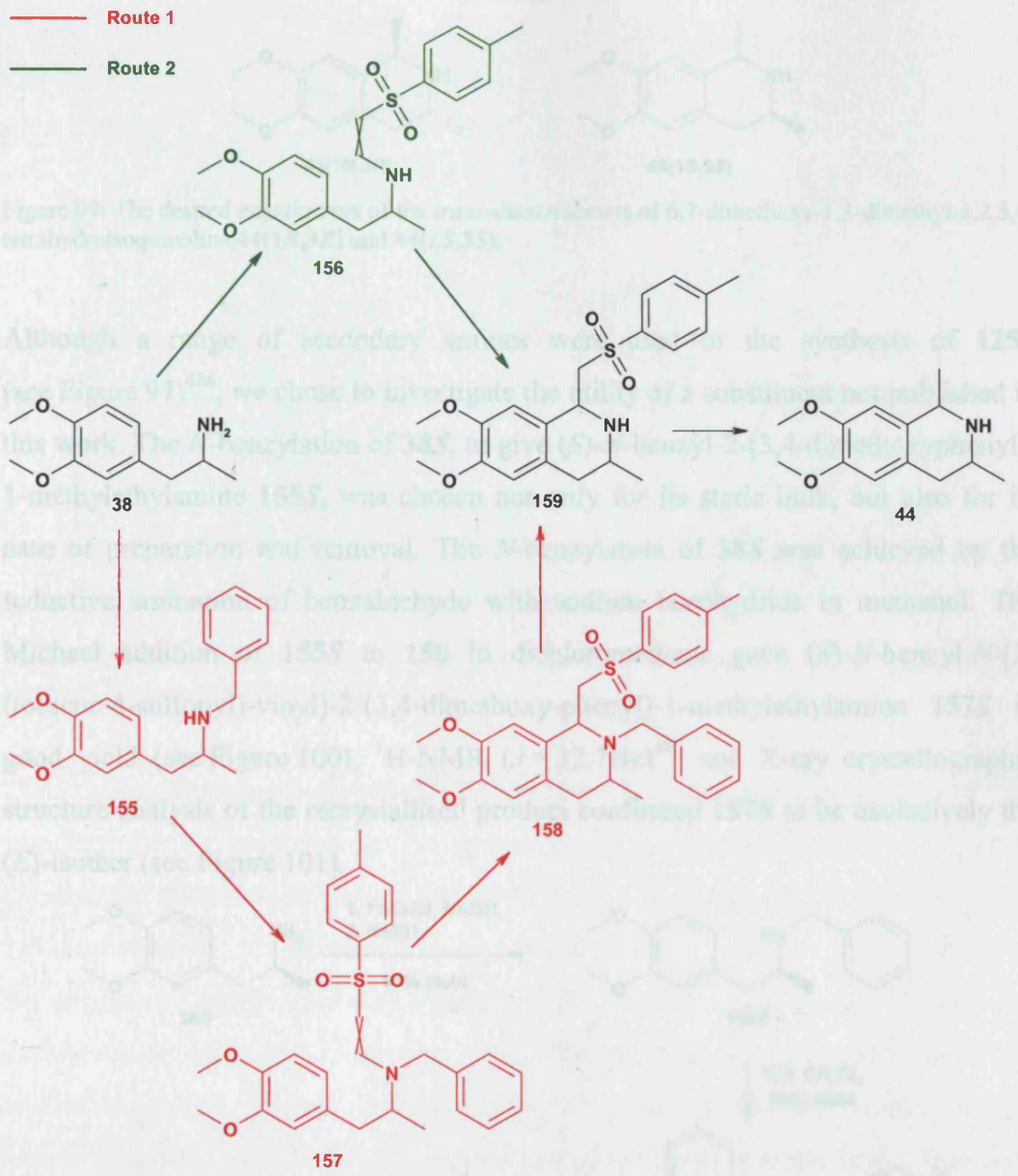

Figure 98: Proposed alternative routes to the isomers of tetrahydroisoquinoline **44** from the enantiomers of **38**, using **150** to introduce the C1-C1' subunit.

Exploring the potential of Route 1, and Its Application to the Synthesis of the *trans*-Diastereomers of 44

The first route investigated (route 1, see Figure 98), from **38** to **44** via the secondary amine, became the route of choice for the synthesis of the *trans*-diastereomers of **44** (see Figure 99).

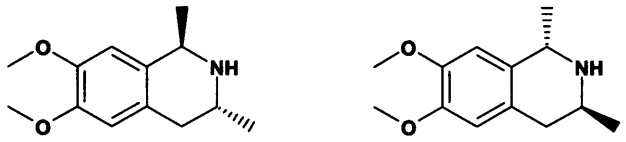

44(1*R*,3*R*) 44(1*S*,3*S*)

Figure 99: The desired enantiomers of the *trans*-diastereomers of 6,7-dimethoxy-1,3-dimethyl-1,2,3,4-tetrahydroisoquinoline **44(1*R*,3*R*)** and **44(1*S*,3*S*)**.

Although a range of secondary amines were used in the synthesis of **125*S*** (see Figure 97)[486], we chose to investigate the utility of a substituent not published in this work. The *N*-benzylation of **38*S***, to give (*S*)-*N*-benzyl-2-(3,4-dimethoxyphenyl)-1-methylethylamine **155*S***, was chosen not only for its steric bulk, but also for its ease of preparation and removal. The *N*-benzylation of **38*S*** was achieved by the reductive amination of benzaldehyde with sodium borohydride in methanol. The Michael addition of **155*S*** to **150** in dichloromethane gave (*S*)-*N*-benzyl-*N*-[2-(toluene-4-sulfonyl)-vinyl]-2-(3,4-dimethoxy-phenyl)-1-methylethylamine **157*S*** in good yield (see Figure 100). ^{1}H-NMR ($J = 12.7$Hz)[487] and X-ray crystallographic structure analysis of the recrystallised product confirmed **157*S*** to be exclusively the (*E*)-isomer (see Figure 101).

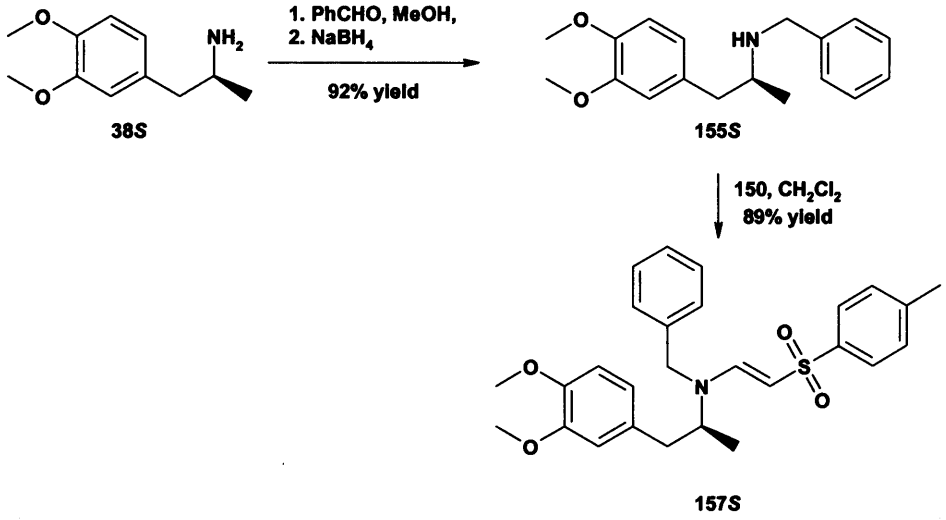

38*S* 155*S* 157*S*

Figure 100: Route 1, from **38*S*** to **157*S***.

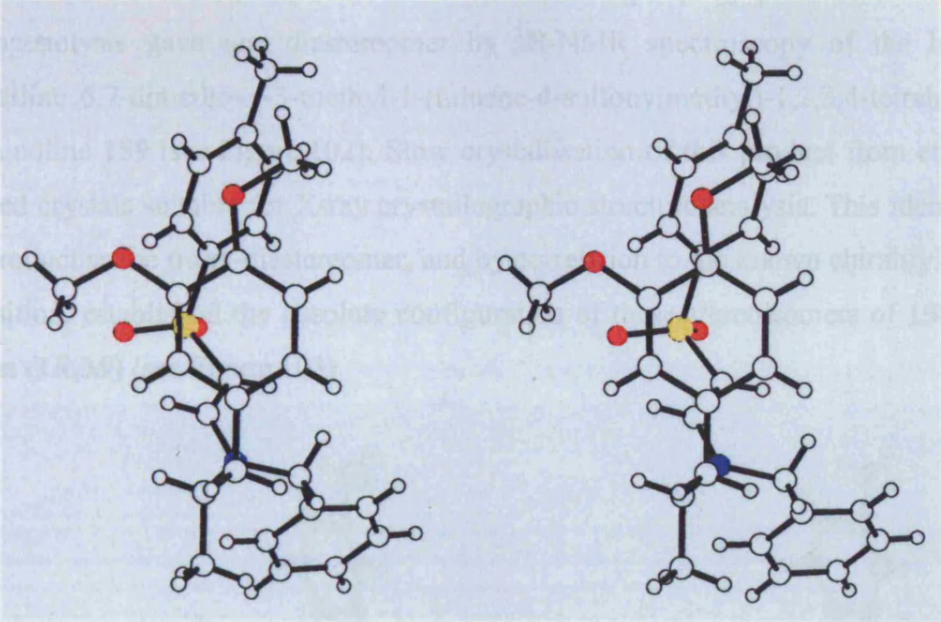

Figure 101: Stereo plot of the X-ray crystallographic structure analysis of **157*S***, confirming the geometry of the β-aminovinylsulfone as (*E*).

The cyclisation protocol described for the syntheses of the enantiomers of **125**[472,486] was successfully employed for the cyclisation of the Michael adduct **157*S***. When dissolved in dichloromethane and chilled to –15°C, cyclisation of **157*S*** to the desired 1,3-disubstituted-1,2,3,4-tetrahydroisoquinoline **158** was achieved in good yield by the addition of a large excess of similarly chilled trifluoroacetic acid, with **only one diastereomer evident**, to the limit of NMR detection. It was hoped that NMR studies exploiting Nuclear Overhauser Effect (NOE) differences would indicate which diastereomer had been formed, but these were inconclusive. The non-crystalline nature of **158** did not allow for the determination of the absolute configuration of the newly formed stereogenic centre at C-1 by X-ray crystallographic structure analysis.

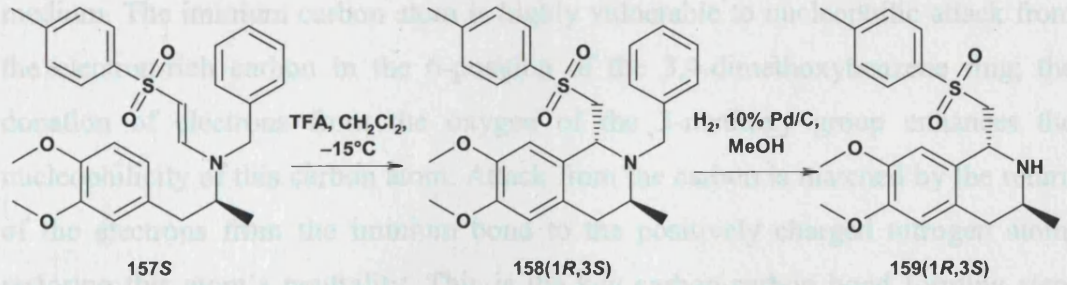

Figure 102: Synthesis of the ***trans***-diastereomer **159(1*R*,3*S*)**, from **157*S***.

Fortunately, the subsequent removal of the benzyl group by palladium-catalysed hydrogenolysis gave one diastereomer by ^{1}H-NMR spectroscopy of the highly crystalline 6,7-dimethoxy-3-methyl-1-(toluene-4-sulfonylmethyl)-1,2,3,4-tetrahydro-isoquinoline **159** (see Figure 102). Slow crystallisation of this product from ethanol yielded crystals suitable for X-ray crystallographic structure analysis. This identified the product as the ***trans***-diastereomer, and by correlation to the known chirality at the 3-position, established the absolute configuration of these stereoisomers of **158** and **159** as **(1*R*,3*S*)** (see Figure 103).

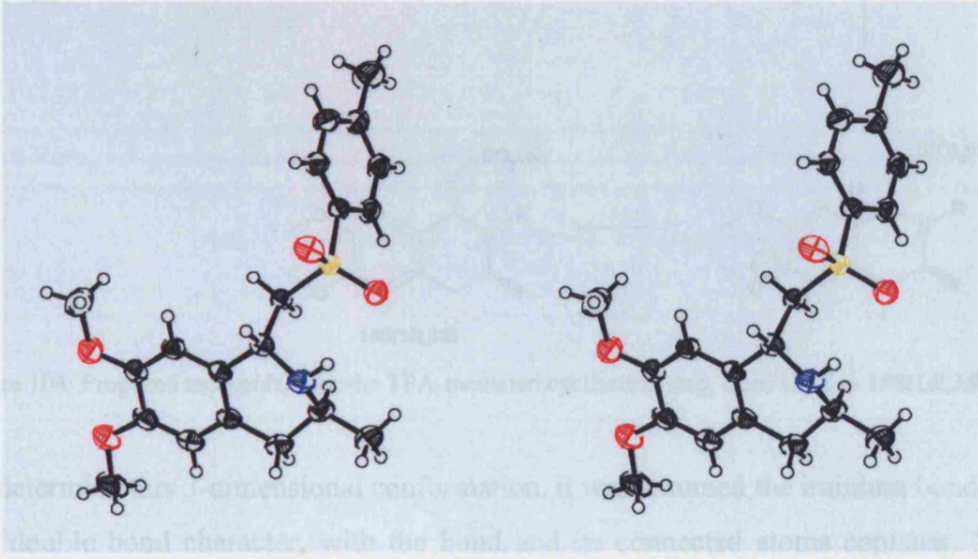

Figure 103: Stereo plot of the X-ray crystal structure analysis of **159(1*R*,3*S*)**, confirming the *trans* relationship between the 1- and 3- substituents of the tetrahydroisoquinoline.

Mechanism

One putative mechanism for the ring closure of **157** to **158** can be envisaged as following a Pictet-Spengler-like process (see Figure 104). In the first part of the reaction, the nitrogen lone pair feeds into the β-aminovinylsulfone to create an iminium ion **160*S***, as the β-carbon picks up a proton from the acidic reaction medium. The iminium carbon atom is highly vulnerable to nucleophilic attack from the electron-rich carbon in the 6-position of the 3,4-dimethoxybenzene ring; the donation of electrons from the oxygen of the 3-methoxy group enhances the nucleophilicity of this carbon atom. Attack from the carbon is matched by the return of the electrons from the iminium bond to the positively charged nitrogen atom, restoring this atom's neutrality. This is the key carbon-carbon bond forming step. With only the loss of the proton from carbon-8a of the tetrahydroisoquinoline ring needed to allow the benzene ring to rearomatise and the methoxy oxygen to return to

neutral, it is the step in which the diastereoselectivity of the reaction is determined by the 3-dimensional conformation of the intermediate.

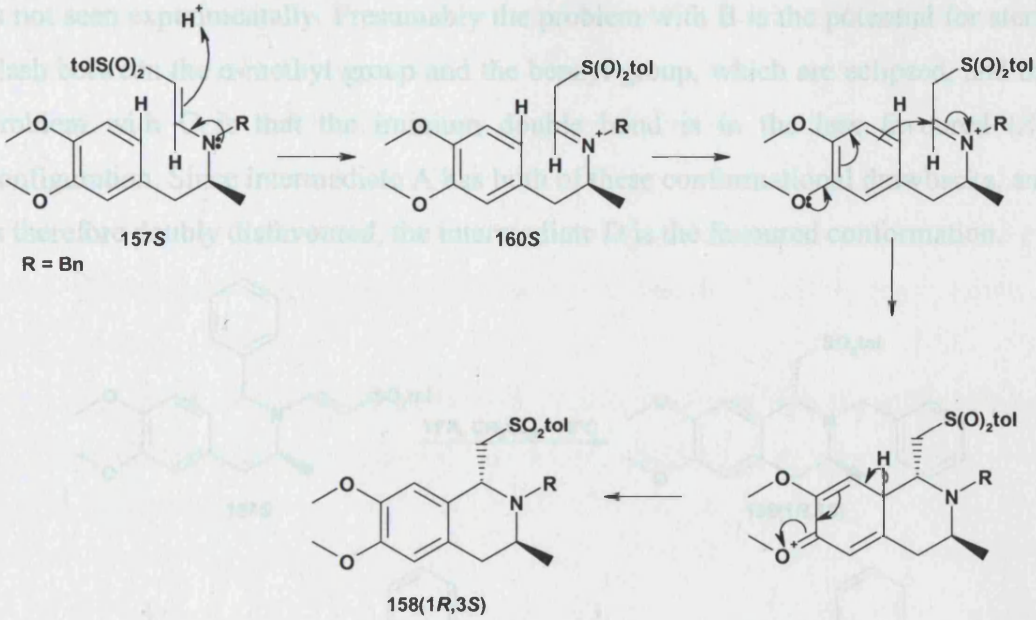

Figure 104: Proposed mechanism for the TFA-mediated cyclisation step, from **157*S*** to **158(1*R*,3*S*)**.

To determine this 3-dimensional conformation, it was assumed the iminium bond has full double bond character, with the bond and its connected atoms coplanar. This bond will therefore adopt either the (*E*)- and/or the generally less-favoured (*Z*)-configuration (see Figure 105).

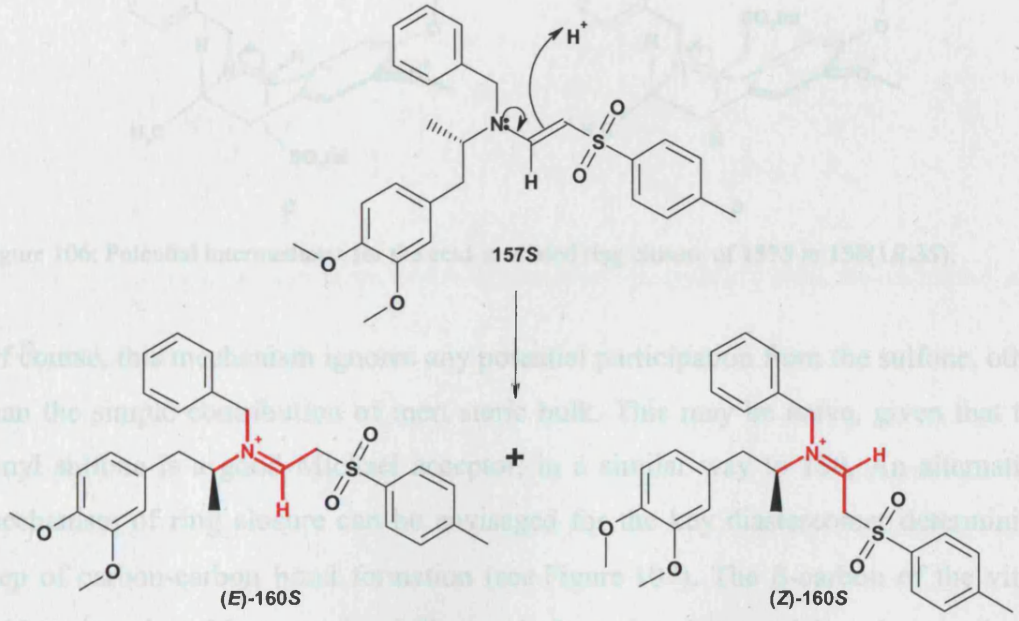

Figure 105: Formation and potential configurations of the iminium bond.

This assumption allows for four possible conformations for the ring closure intermediate (see Figure 106). Of the four, only A and D will give the correct 1,3-*trans* substituent configuration in the product, with B and C giving the *cis*, which is not seen experimentally. Presumably the problem with B is the potential for steric clash between the α-methyl group and the benzyl group, which are eclipsed, and the problem with C is that the iminium double bond is in the less favoured (*Z*)-configuration. Since intermediate A has both of these conformational drawbacks, and is therefore doubly disfavoured, the intermediate D is the favoured conformation.

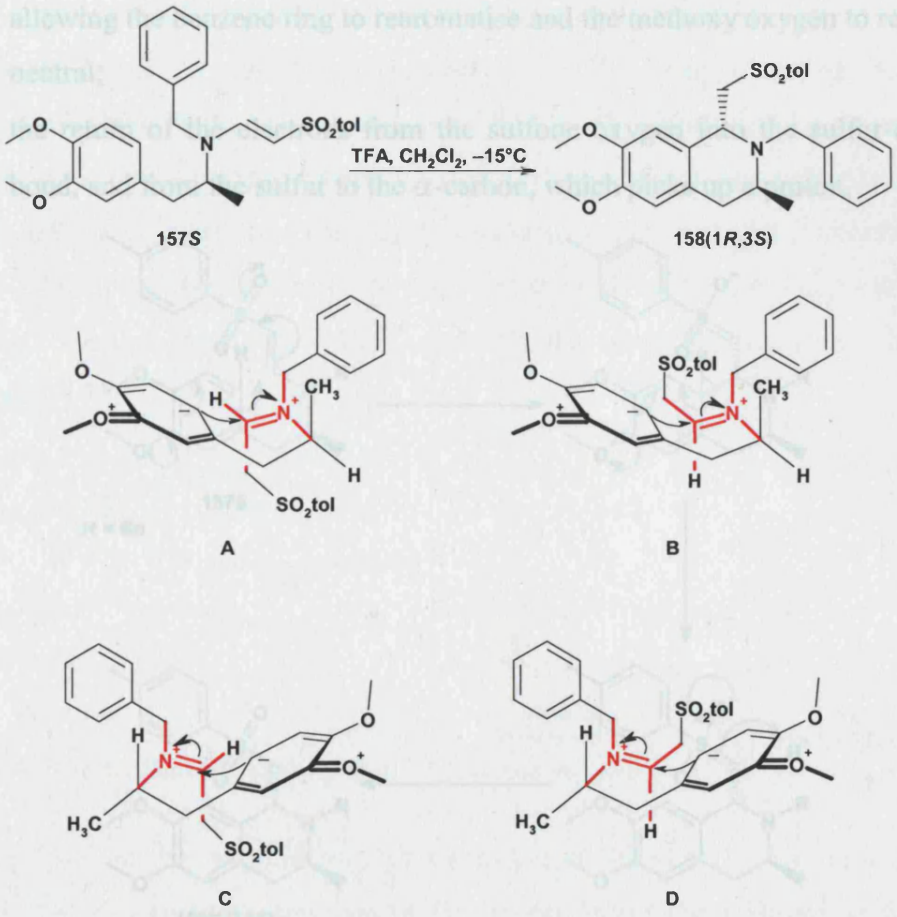

Figure 106: Potential intermediates for the acid-mediated ring closure of **157*S*** to **158(1*R*,3*S*)**.

Of course, this mechanism ignores any potential participation from the sulfone, other than the simple contribution of inert steric bulk. This may be naïve, given that the vinyl sulfone is a good Michael acceptor, in a similar way to **150**. An alternative mechanism of ring closure can be envisaged for the key diastereomer determining step of carbon-carbon bond formation (see Figure 107). The β-carbon of the vinyl sulfone is vulnerable to nucleophilic attack from the electron-rich carbon in the 6-

position of the 3,4-dimethoxybenzene ring. Again, the donation of electrons from the oxygen of the 3-methoxy group enhances the nucleophilicity of this C-6 carbon atom. Attack from the C-6 carbon is further facilitated by the favourable process of the movement of electrons into the carbon-sulfur bond, and from either of the sulfur-oxygen bonds onto the oxygen atom.

Once the new ring has formed, a return to neutrality within the molecule is realised by:

- the loss of the proton from carbon-8a of the tetrahydroisoquinoline ring, allowing the benzene ring to rearomatise and the methoxy oxygen to return to neutral;
- the return of the electrons from the sulfone oxygen into the sulfur-oxygen bond, and from the sulfur to the α-carbon, which picks up a proton.

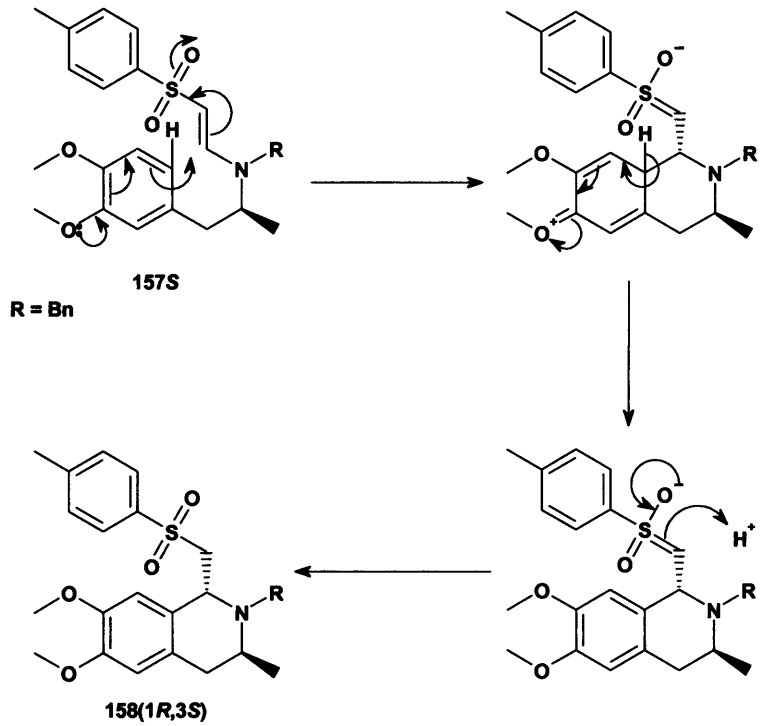

Figure 107: An alternative mechanism for the TFA-mediated cyclisation of **157*S***, to give **158(1*R*,3*S*)**.

Completing the Synthesis

The final step required the cleavage of the tolylsulfone from the methylene of **159(1*R*,3*S*)**, to leave the desired methyl group in the 1-position of the tetrahydroisoquinoline, and thereby obtain the key intermediate **44(1*S*,3*S*)**. Literature methods for the desulfonylation of sulfones abound, and are generally via the reductive cleavage of the alkyl sulfone bond by a single electron transfer reagent.

The most frequently used reagent is sodium-mercury amalgam, usually buffered in alcohol with disodium hydrogen phosphate and sodium dihydrogen phosphate[488-490 491]. Several other electron transfer reagents have been used, including magnesium in ethanol, with a catalytic amount of mercuric chloride[492], aluminium amalgam[493], lithium in ethylamine[488] sodium dithionite[494] and samarium diiodide[495]. Electrolytic reductive cleavage has also been used[496].

Trial reactions with commercially available sodium-mercury amalgams (5%, 10% and 20%) were low-yielding, slow and with multiple products. Of the alternative single electron transfer reagents available, lithium naphthalenide was investigated next, due to its stability and ease of preparation[497]. This reagent worked well, with rapid consumption of the starting material **159(1*R*,3*S*)**. Unfortunately, the reaction gave two products, with the desired 1,3-dimethyl tetrahydroisoquinoline **44(1*S*,3*S*)** formed as the **minor** product. The major product was identified as 6,7-dimethoxy-3-methyl-3,4-dihydroisoquinoline **161*S***, and confirmed as such by the comparison of ^{1}H-NMR spectral data with the commercially available racemate of **161** (see Figure 108).

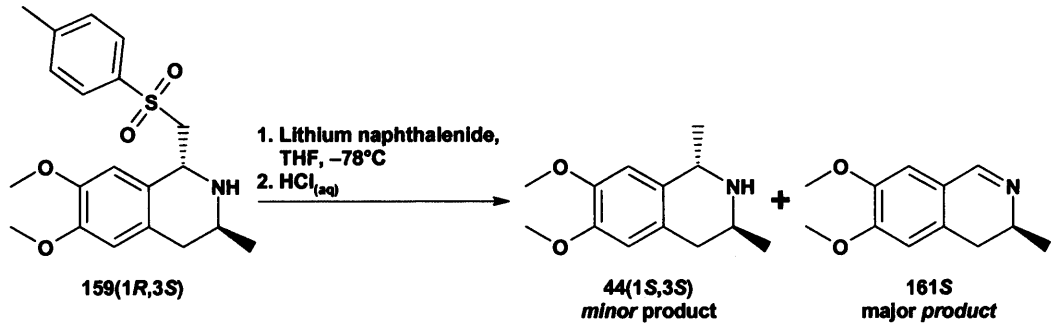

Figure 108: Desulfonylation of **159(1*R*,3*S*)** with lithium naphthalenide.

Consideration of the reaction mechanism suggests the initial steps toward both products share a common mechanism (see Figure 109). The addition of the first electron from the napthalenide anion reduces the alkyl sulfone **159** to the intermediate radical anion **162(1*R*,3*S*)**.

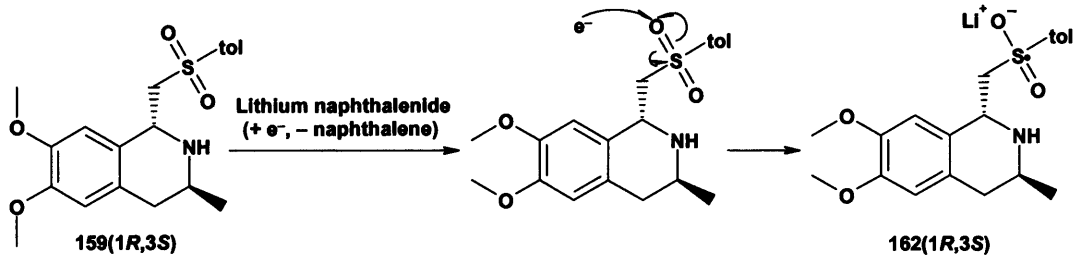

Figure 109: Mechanism for the formation of the intermediate **162(1*R*,3*S*)** common to the synthesis from **159(1*R*,3*S*)** of both **44(1*S*,3*S*)** and **161*S***.

To form the desired product **44(1*S*,3*S*)** requires the homolytic cleavage of the sulfur-alkyl bond to give the alkyl radical **163(1*S*,3*S*)** and the lithium tolylsulfinate **164** as shown, with the valency of the sulfur reducing from (VI) to (IV). The addition of a second electron to **163(1*S*,3*S*)** gives the alkyl anion **165(1*S*,3*S*)**, with lithium as the counter ion. Quenching with hydrochloric acid gives the desired methyl substituent at the 1-position, and **44(1*S*,3*S*)** (see Figure 110).

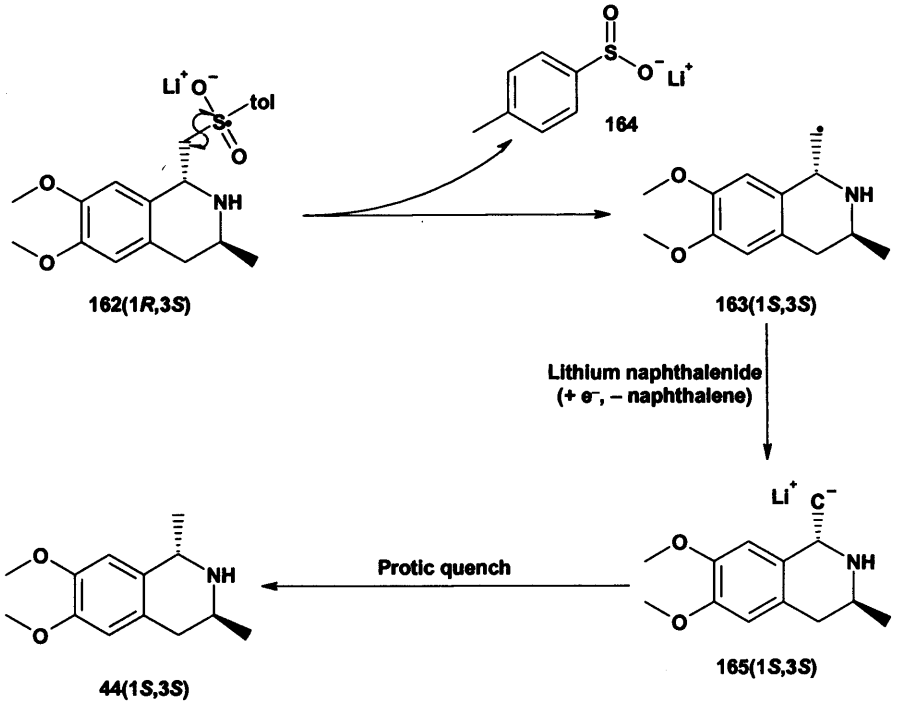

Figure 110: Putative mechanism for the conversion of **162(1*R*,3*S*)** to **44(1*S*,3*S*)**.

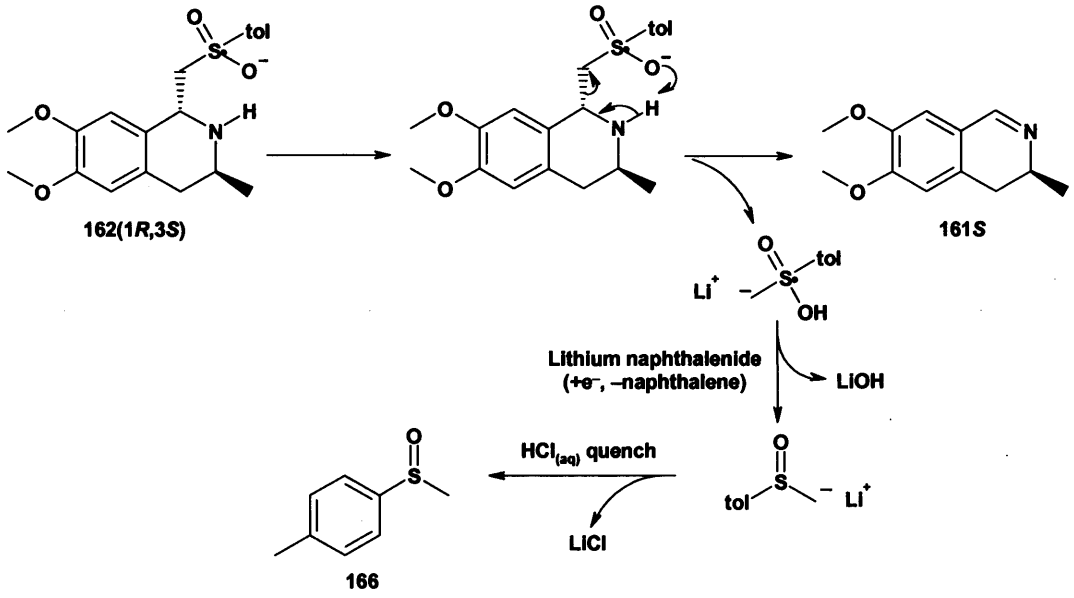

Figure 111: Putative mechanism for the conversion of **162(1*R*,3*S*)** to **161*S***.

The competing mechanism (see Figure 111) sees the charged oxygen atom of **162(1*R*,3*S*)** able to deprotonate the nitrogen of the tetrahydroisoquinoline, via a six-membered cyclic movement of electrons. This would give the identified side-product **161*S***, and, although not isolated, a second single electron transfer could give tolylmethylsulfoxide **166**.

With this proposed mechanism of by-product formation in mind, replacing the amine hydrogen with an appropriate protecting group should eliminate this side reaction. A simple yet effective solution to this problem was offered by revising the sequence of reactions from **158(1*R*,3*S*)** to **44(1*S*,3*S*)** (see Figure 112). By not removing the *N*-benzyl group until *after* the desulfonylation step, the side reaction to give **161*S*** was successfully eliminated. Desulfonylation of **158(1*R*,3*S*)** gave the *N*-benzyl-6,7-dimethoxy-1,3-dimethyl-1,2,3,4-tetrahydroisoquinoline **167(1*S*,3*S*)** in moderate yield. This material showed some degree of instability, with some brown discolouration of the colourless syrup soon apparent. Subsequent removal of the benzyl group by catalytic hydrogenolysis gave the desired *trans*-diastereomer of the intermediate tetrahydroisoquinoline **44(1*S*,3*S*)**.

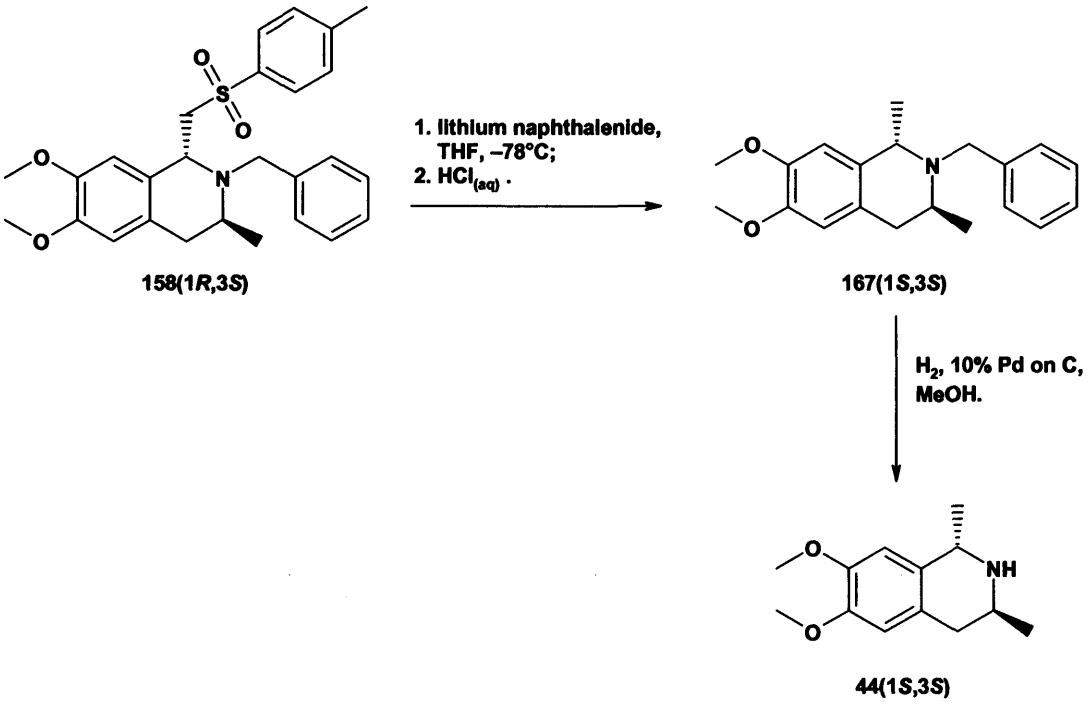

Figure 112: The synthetic route of choice, from **158(1*R*,3*S*)** to **44(1*S*,3*S*)**, avoiding the production of **161*S***.

Of note here is the potential to vary substituents at the 1-position; quenching the reductive desulfonylation with electrophiles other than protons would afford access

to a range of potential functionality at this position (*e.g.* quenching with alkyl halides for chain extension, or aldehydes to introduce an alcohol moiety, *etc.*)[498;499].

Synthesis of the *trans*-Diastereomers of 44

With the diastereospecific route to the resolved and enantiopure *trans*-diastereomers of **44** from the resolved enantiomers of **38** now successfully determined, it was possible to obtain gram quantities of **44(1*R*,3*R*)** and **44(1*S*,3*S*)** in a reproducible fashion. For each enantiomer of **38,** the primary amine was benzylated via a two-step, one-pot reductive alkylation reaction. Imine formation with a stoichiometric amount of benzaldehyde in methanol at –10°C (salt/ice bath) was followed by reduction with an excess of sodium borohydride, to give the enantiomers of the secondary amine **155** as colourless oils. Preliminary characterisation of the oils of **155** was followed by full characterisation of a small sample of each enantiomer as the hydrochloride salt. The next step required the formation of the β-aminovinylsulfone **(*E*)-157** by the addition of acetylene **150** to an ice cold solution of the free amine of **155** in dichloromethane on an ice/water bath. The enantiomers of **(*E*)-157** were isolated in good yield as colourless crystalline solids.

Formation of the tetrahydroisoquinoline core was achieved by the addition of a large excess of chilled TFA (–15°C, salt/ice bath) to a similarly chilled solution (–15°C, salt/ice bath) of **(*E*)-157** in dichloromethane. The cyclisation of the enantiomers of **(*E*)-157** gave the *trans*-diastereomers of tetrahydroisoquinoline **158** exclusively, which were isolated in good yield as colourless expanded foams. Desulfonylation with two equivalents of lithium naphthalenide in THF at –78°C and quenching with aqueous hydrochloric acid gave the *trans*-diastereomers of tetrahydroisoquinoline **167** as colourless syrups. These compounds proved to be moderately unstable, quickly discolouring to brown, and not surviving prolonged storage; characterisation was confined to NMR, accurate mass and the measurement of optical rotation. The removal of the benzyl groups by palladium-catalysed hydrogenolysis gave the target tetrahydroisoquinoline intermediates **44(1*R*,3*R*)** and **44(1*S*,3*S*)** as pale yellow syrups, with final purification and full characterisation achieved by conversion to, and recrystallisation of, the hydrochloride salts. Diastereomeric purity was confirmed by the absence of any peaks in the ^{1}H- and ^{13}C-NMR spectra, to the limit of detection, corresponding to the subsequently synthesised *cis*-diastereomers of **44**. Only the

desulfonylation step had a moderate yield (45%), with every other step yielding 89% or better.

The final synthetic reaction sequence, as applied to each enantiomer of **38**, is described for **38*R*** to **44(1*R*,3*R*)** in Figure 113.

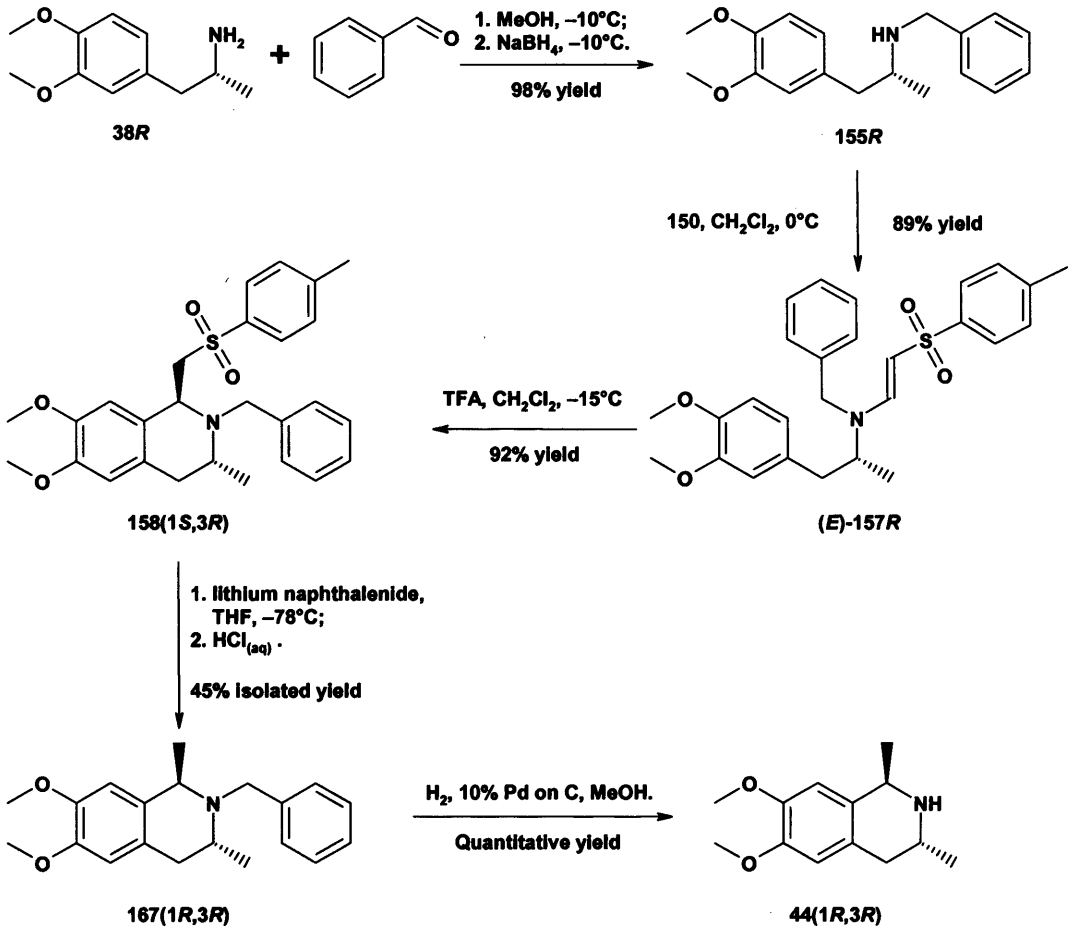

Figure 113: Route to the *trans*-diastereomers of 6,7-dimethoxy-1,3-dimethyl-1,2,3,4-tetrahydro-isoquinoline **44**, from the resolved enantiomers of **38**, as exemplified for **44(1*R*,3*R*)** from **38*R***.

Exploring the potential of Route 2, and Its Application to the Synthesis of the *cis*-Diastereomers of 44

Although a successful and, to the limits of detection, stereospecific route to the *trans*-diastereomers of **44** had been established, a route to the *cis*-diastereomers had still to be determined. It was hoped that the effective **reversal** of the stereoselectivity reported for the syntheses of both enantiomers of carnegine **125**[472;486], when secondary (**151a-e**) rather than primary (**122**) phenylethylamines were used (see Figure 85 and Figure 97), could be repeated here with the enantiomers of **38** and the ethynylsulfone **150** (route 2, see Figure 98). As for route 1, one enantiomer of **38** was used to facilitate any X-ray crystal structure analysis.

The Michael addition of **38*S*** to **150**, to form (*S*)-[2-(3,4-dimethoxy-phenyl)-1-methyl-ethyl]-[2-(toluene-4-sulfonyl)-vinyl]amine **156*S***, occurred readily at ambient temperature in dichloromethane, with removal of the volatiles under reduced pressure giving the desired product in good yield. In contrast to the product of the reaction of **155** with **150**, the product was quite clearly a mixture of (*E*)- and (*Z*)-isomers, as determined by ^{1}H-NMR spectroscopy. Comparison of the integrations and coupling constants of the signals corresponding to the vinyllic protons showed the ratio of *E*:*Z* to be ~10:1 (see Figure 114).

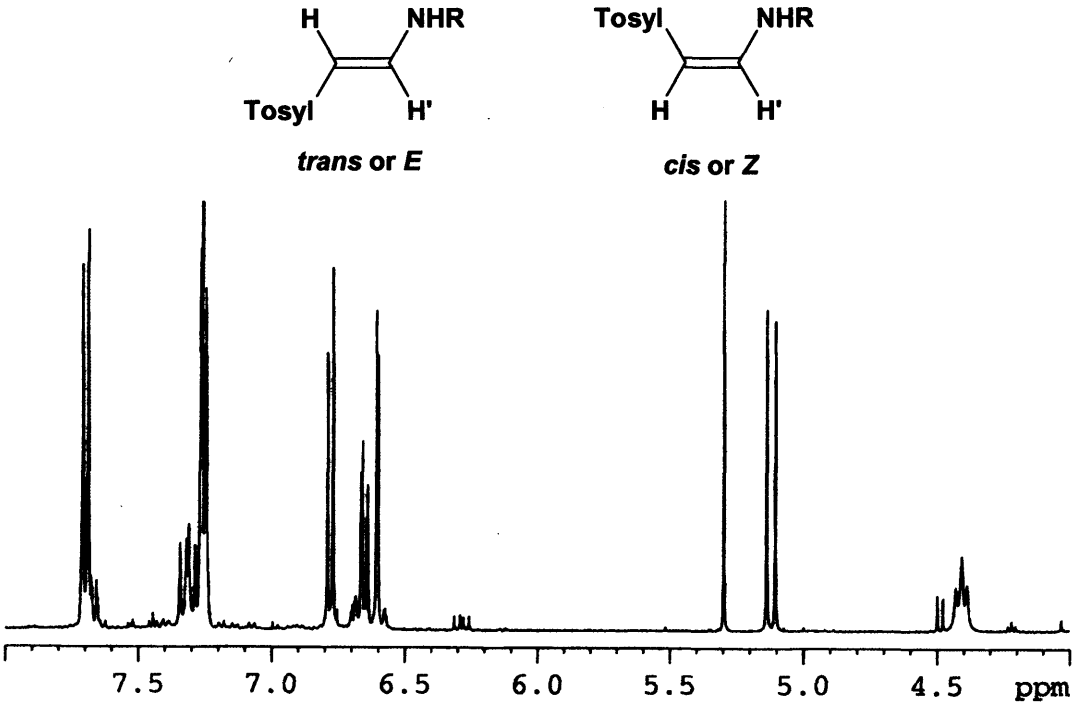

Isomer	Proton	δ_H in $CDCl_3$	Multiplicity	$J_{H,H'}$ (Hz)*
E	H	5.12	d	13.0
	H'	7.31	dd	13.0
Z	H	4.49	d	8.5
	H'	6.28	dd	8.5

Figure 114: Identification of key ^{1}H-NMR signals in the determination of the ratio of *E*:*Z* isomers in **156*S***. * Reference values for aliphatic *cis* and *trans* vicinal coupling constants are in the range 0-12Hz for *cis* (typically 8Hz) and 12-18Hz for *trans* (typically 15Hz)[487]

Recrystallisation of this crude product gave the (*E*)-isomer of **156*S*** as a colourless waxy crystalline solid. While recording the NMR spectrum of **156*S*** it was noted that it began to isomerise immediately, eventually equilibrating to a 3:1 mixture of *E*:*Z* within hours. Isomerisation of this double bond can be envisaged as occurring via an enamine-imine tautomerisation, with accompanying bond rotation (see Figure 115).

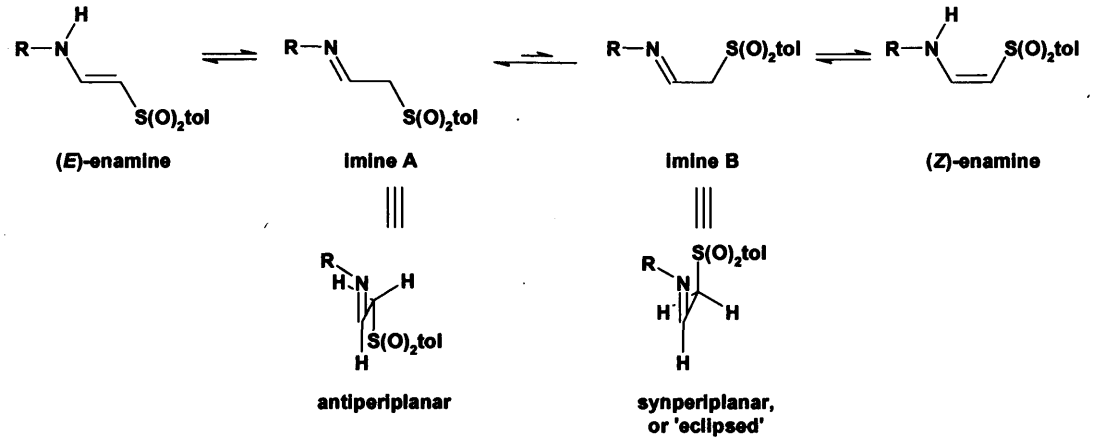

Figure 115: Proposed mechanism for the equilibration of (*E*)- and (*Z*)-configurations of **156*S***.

At first glance, the conversion of the thermodynamically more stable **(*E*)-156*S*** to the **(*Z*)-156*S*** was surprising. Although the tautomerisation of the (*E*)-enamine to imine A would allow free rotation about the carbon-carbon bond, such free rotation would be hindered by imine A having the sterically more favoured antiperiplanar conformation[500]. The tautomerisation of the (*Z*)-enamine would give imine B, with the sterically more hindered, and hence less favoured, synperiplanar[500], or eclipsed, conformation (see Figure 115). For ~25% of molecules to adopt the synperiplanar conformation, from which the (*Z*)-enamine is derived, there must be a significant external factor influencing the equilibrium, with the energy difference between the synperiplanar and antiperiplanar conformations of the imine being less than anticipated.

A closer examination of the (*Z*)-enamine reveals a possible explanation in the potential for the atoms of the amino-vinyl-sulfone moiety to adopt the conformational equivalent of an almost planar six membered ring, with either of the sulfone oxygens linking to the amine hydrogen via a hydrogen bonding interaction (see Figure 116). Such a hydrogen bond would serve to stabilise the (*Z*)-enamine, and would be anticipated to significantly reduce any conformational energy difference, with respect to the (*E*)-enamine.

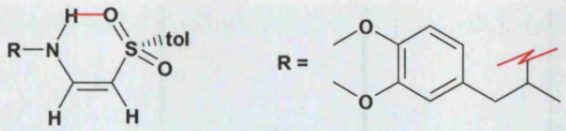

Figure 116: Proposed stabilising hydrogen bond of the (*Z*)-enamine of **156*S***.

To explore this equilibrium, the reaction of **38*S*** with **150** was performed on an NMR scale in deuterated dichloromethane. The ^{1}H-NMR spectrum for each of the starting materials was recorded, the samples were combined, and immediately returned to the spectrometer. In the time taken to load, tune the instrument and run the sample (less than ten minutes) the reaction had gone to completion. The ^{1}H-NMR spectrum revealed that the bond formed in the reaction was exclusively *Z* (literature precedent reports the nucleophilic addition of secondary amines to such electron deficient acetylenes as generally giving the (*E*)-conformer[484]). Further spectra were recorded at ten minute intervals, and isomerisation of this bond was seen to commence immediately; the ratio of *E*:*Z* reached 1:2 within 30 minutes, 1.25:1 within 100 minutes, and had achieved an equilibrium ratio of 3:1 *E*:*Z*. within 16 hours (see Figure 117). Some slight differences in chemical shift meant that the vinyllic proton α to the amine was not visible for the (*E*)-isomer, as it was overlapped by the peaks of the tosyl aromatic protons. However, the other vinyllic proton was clearly visible for both isomers, and was used to determine the isomeric ratio, in conjunction with the doublet corresponding to the aliphatic methyl group (δ_H 1.25 (*Z*) and 1.14 (*E*)), and the multiplet corresponding to the methine (δ_H 3.46-3.51 (*Z*) and 3.35-3.40 (*E*)).

As in the isomerisation of the NMR sample of the crystallised (*E*)-isomer, the equilibrium did not proceed beyond the 3:1 ratio of *E*:*Z*, in contrast to the 10:1 ratio of the dried residue from the crude reaction. Since the standard conditions for removal of the reaction solvent under reduced pressure include the use of elevated temperature (40°C water bath), this may have influenced the isomeric ratio of the crude reaction residue. However, the effect of temperature upon the isomeric equilibrium was not investigated.

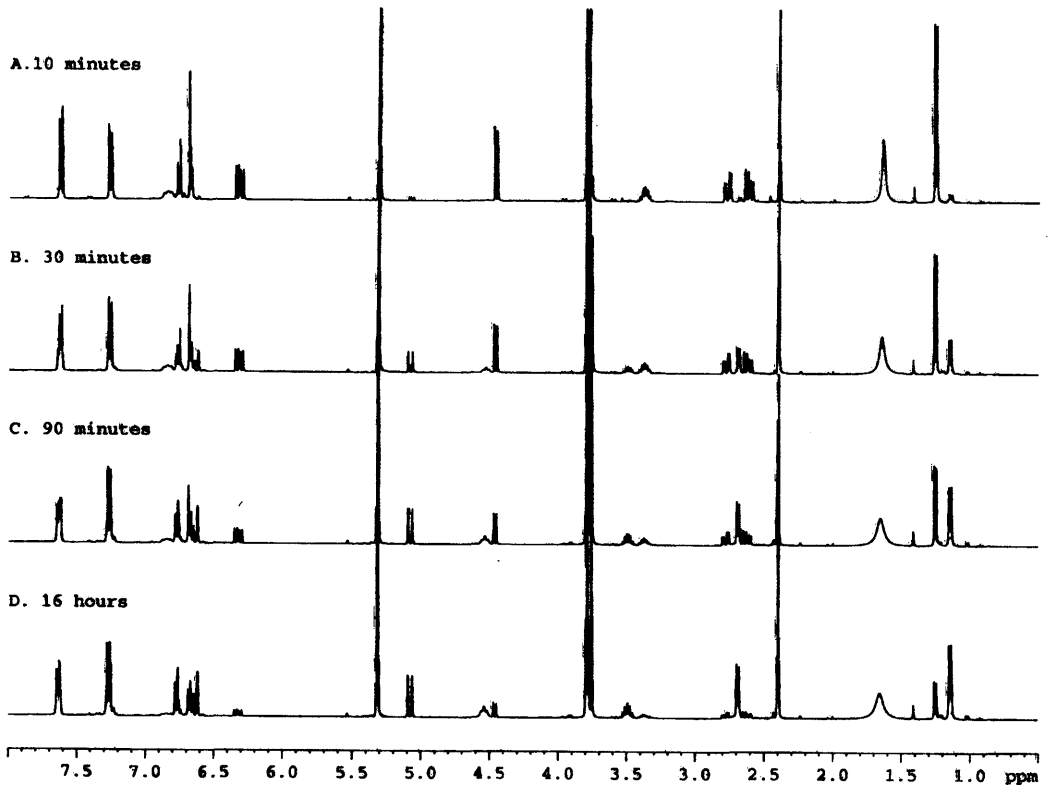

Figure 117: ^{1}H-NMR spectra, showing the isomerism of **156*S***, from 2-(3,4-dimethoxyphenyl)-1-methylethyl]-[2-(toluene-4-sulfonyl)vinyl]amine over time

The spectra from this NMR experiment illustrate other potentially important differences between the two isomers (the regions of particular interest in this sequence of spectra are expanded in Figure 118).

a) The difference between the respective chemical shifts of the broad peaks corresponding to the proton of the amine is striking and informative. In **(*E*)-156*S***, it appears at 4.5-4.6ppm; in **(*Z*)-156*S***, it is 2.3ppm downfield, at 6.8-6.9ppm. This is consistent with the extensive deshielding of an intramolecular hydrogen bond[501], and constitutes direct experimental evidence for the existence of the proposed hydrogen-bonded stabilisation of the (*Z*)-enamine.

b) The peaks corresponding to the benzylic methylene (shown in the expansion 2.45 to 2.85ppm) show that the two protons in **(*Z*)-156*S*** are quite clearly non-equivalent, having the complex coupling pattern of an ABX system, with the protons coupled to each other, and to the proton of the adjacent methine. In **(*E*)-156*S***, they are equivalent, with only the coupling to the proton of the adjacent methine apparent. This would appear to indicate that

the (*Z*)-configuration is conformationally constrained and comparatively inflexible.

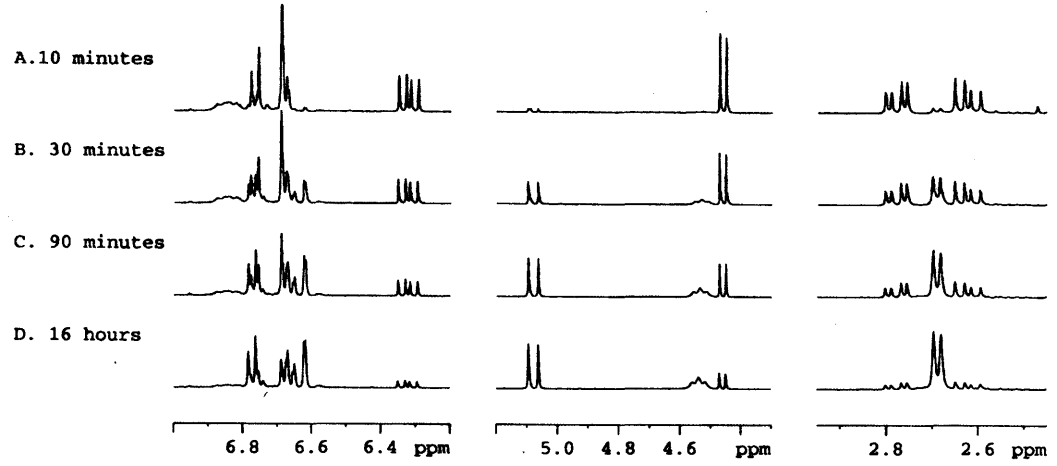

Figure 118: Expansion of the more interesting parts of the ^{1}H-NMR spectra of **156*S***, showing the evidence for the stabilising hydrogen bond and comparative rigidity of the (*Z*)-isomer.

This S=O···H-N hydrogen bond would also account for the (*Z*)-isomer being formed initially. As illustrated in Figure 119, the mechanism of this reaction requires the lone pair of electrons from the nitrogen of **38*S*** to attack the electropositive carbon of the primary acetylene of **150**, forming an ammonium ion. This is facilitated by the ability to push electrons from the alkyne into the carbon-sulfur bond and onto one of the oxygens, creating an intermediate vinylidene **168*S***. The electrons from this unstable intermediate return into the oxygen-sulfur bond and on to the alpha carbon, which picks up a proton. Concurrently, the ammonium nitrogen loses a proton, and returns to neutrality. In this example, the potential for the formation of a hydrogen bond between a sulfone oxygen and the amine hydrogen atom serves to direct the conformation of the intermediate vinylidene as the electrons return to the alpha carbon, forcing the reaction product into the (*Z*)-conformation. Once formed, the conformational equilibrium already postulated (see Figure 115) would allow the observed isomerisation.

This would make the (*Z*)-isomer the *kinetic* product of the reaction, and the (*E*)-isomer the *thermodynamic* product.

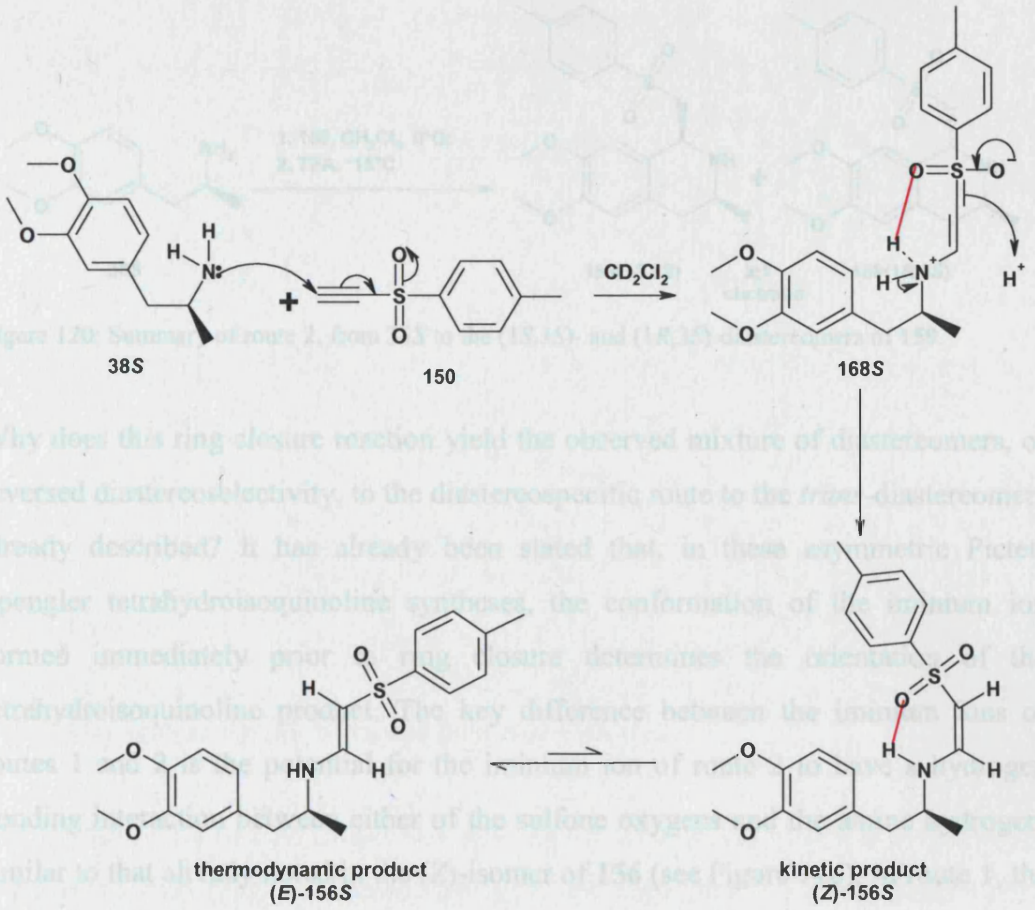

Figure 119: Mechanism for **(*Z*)-156*S*** as the kinetic product of the reaction of **38*S*** with **150**.

The TFA-mediated cyclisation of **156*S*** gave a good yield of the desired tetrahydroisoquinoline **159**, but as a 3:1 mixture of diastereomers. Although a mixture, some separation on TLC could be seen. Pure samples of each tetrahydroisoquinoline product diastereomer were obtained by column chromatography, although the majority of fractions still contained both. Of the pure samples, the major product was crystallised and characterised as the hydrochloride salt, while the inherently crystalline nature of the minor diastereomer allowed crystallisation and characterisation as the free base. Comparison of the ^{1}H-NMR spectra of these two products with the ^{1}H-NMR spectrum of the established *trans*-diastereomer **159(1*R*,3*S*)** confirmed this to be the **minor** product of the reaction. The **major** product of the TFA-induced cyclisation of **156*S*** was therefore the *cis*-diastereomer (see Figure 120).

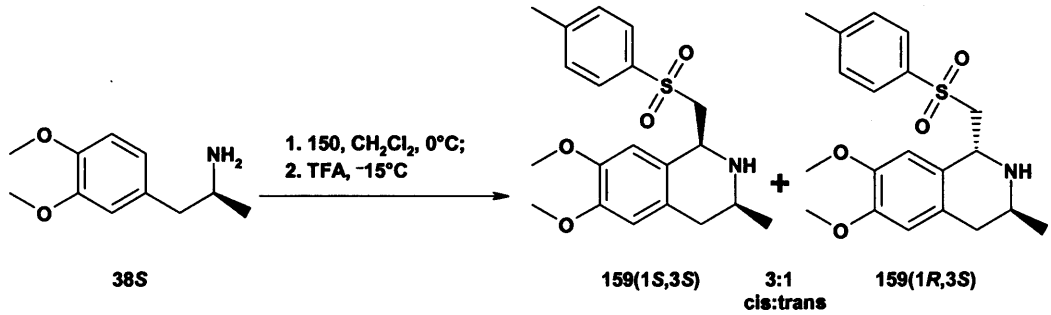

Figure 120: Summary of route 2, from **38*S*** to the (1*S*,3*S*)- and (1*R*,3*S*)-diastereomers of **159**.

Why does this ring closure reaction yield the observed mixture of diastereomers, of reversed diastereoselectivity, to the diastereospecific route to the *trans*-diastereomers already described? It has already been stated that, in these asymmetric Pictet-Spengler tetrahydroisoquinoline syntheses, the conformation of the iminium ion formed immediately prior to ring closure determines the orientation of the tetrahydroisoquinoline product. The key difference between the iminium ions of routes 1 and 2 is the potential for the iminium ion of route 2 to have a hydrogen bonding interaction between either of the sulfone oxygens and the amine hydrogen, similar to that already noted in the (*Z*)-isomer of **156** (see Figure 116). In route 1, the presence of the *N*-benzyl substituent precludes any such hydrogen bond formation. This potential hydrogen bond can therefore be assumed to have a key role in the diastereoselectivity of the cyclisation reaction.

The existence of a similar hydrogen bond was proposed in the literature synthesis of **125*R***[471;472] to explain the diastereoselectivity of the acid-mediated cyclisation of **123*R*$_S$**. The formation of a conformationally constrained iminium intermediate **169*R*$_S$** was proposed, with a hydrogen bond between the sulfoxide oxygen and the iminium hydrogen forming a six-membered ring (see Figure 121).

The diastereospecific nature of the reaction was ascribed to the stabilisation of the H-bond by the *ortho*-nitro substituent, as when the same reaction sequence was performed with (S_S)-ethynyl-*p*-tolylsulfoxide, a 2:1 ratio of product diastereomers was observed. This would imply that perhaps a greater degree of diastereoselectivity could have been achieved in this section of our work, by the use of ethynyl-2-nitrophenylsulfone to supply the 2-carbon unit. This reagent appears to be novel; it is neither commercially available, nor found in the literature.

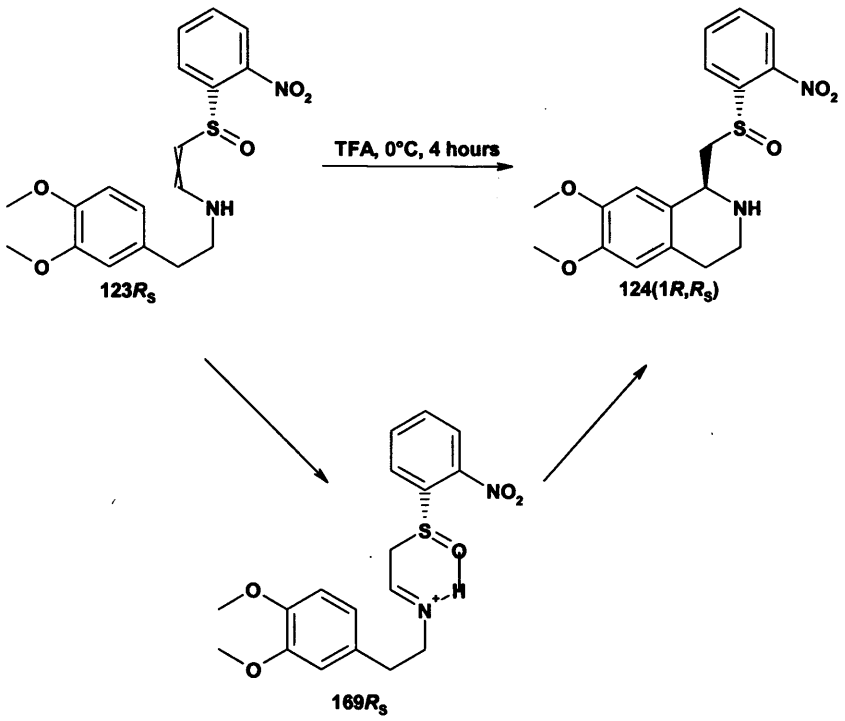

Figure 121: Hydrogen-bonded intermediate proposed by Lee et al[472].[471]

The isolated yield of **159(1*S*,3*S*)** was low. As for **159(1*R*,3*S*)**, attempts to cleave the tosyl group with lithium naphthalenide gave the undesired 3,4-dihydroisoquinoline **161*S*** as the major product, with the desired tetrahydroisoquinoline **44(1*R*,3*S*)** formed as the **minor** product (see Figure 122).

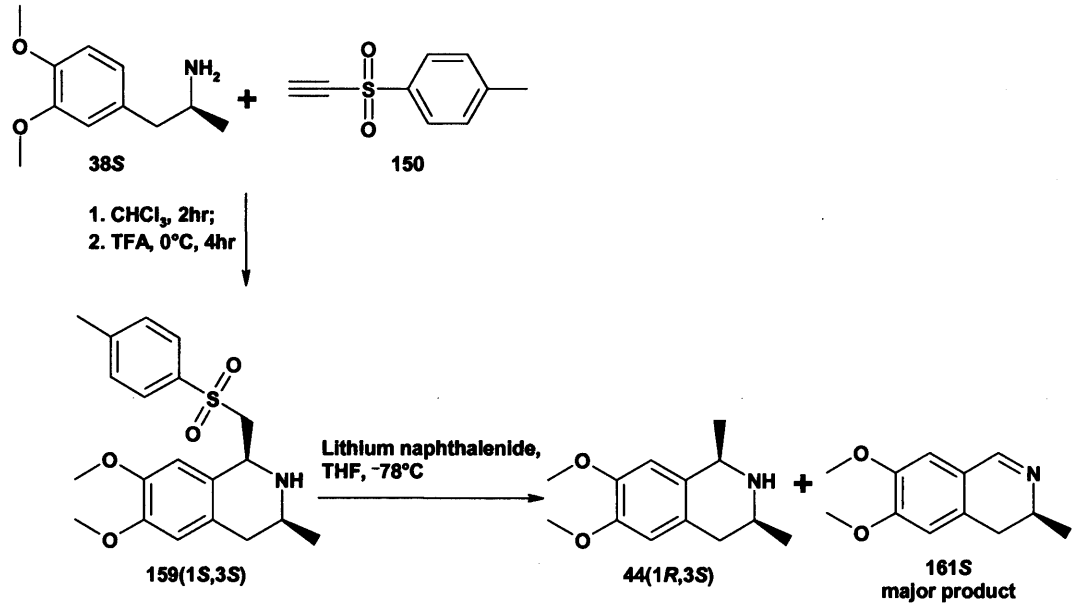

Figure 122: Route 2, from **38*S*** to **44(1*R*,3*S*)**, one *cis*-diastereomer of the key intermediate tetrahydroisoquinoline **44**.

In the same way that this side reaction was overcome for the synthesis of the *trans*-diastereomers, it was hoped to eliminate this by-product by *N*-benzylation of the nitrogen atom of **159(1*S*,3*S*)**. Despite numerous attempts and reagent variation, all attempts to benzylate **159(1*S*,3*S*)** failed. At this point, the decision was taken to abandon this approach to the *cis*-diastereomers, and to return to the literature to seek an alternative, higher yielding and more diastereoselective route.

Investigations into the Synthesis of the *cis*-Diastereomers of 44, via Modification of the Bischler-Napieralski Tetrahydroisoquinoline Synthesis[418]

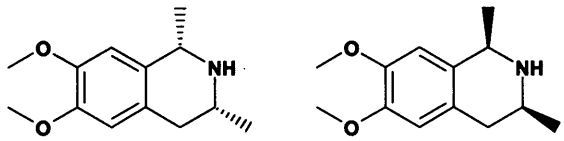

44(1*S*,3*R*) **44(1*R*,3*S*)**

Figure 123: The desired enantiomers of the *cis*-diastereomers of 6,7-dimethoxy-1,3-dimethyl-1,2,3,4-tetrahydroisoquinoline **44(1*S*,3*R*)** and **44(1*R*,3*S*)**.

There are several literature examples of synthetic approaches to compounds with *cis*-1,3-dimethyl-1,2,3,4-tetrahydroisoquinoline cores; some have already been touched upon. These have generally employed asymmetric reductions of 1,3-dimethyl-3,4-dihydroisoquinoline products of the Bischler-Napieralski isoquinoline synthesis[418], and include:

a. the reduction of the cyclic imine 6,8-dimethoxy-1,3-dimethyl-3,4-dihydroisoquinoline **113*S*** with sodium borohydride, which was reported to give the *cis*-6,8-dimethoxy-1,3-dimethyl-1,2,3,4-tetrahydroisoquinoline **114(1*S*,3*S*)** with a diastereoselectivity of greater than 95%[468];

b. the reduction of the parent 1,3-dimethyl-3,4-dihydroisoquinoline **118*R*** with sodium borohydride, which was reported to give a similar result, with a single recrystallisation of the hydrobromide salt giving the *cis*-1,3-dimethyl-1,2,3,4-tetrahydroisoquinoline **119(1*S*,3*R*)** exclusively[469];

c. catalytic hydrogenation of the 1,3-dimethyl-3,4-dihydroisoquinoline on 10% palladium on carbon was also reported to give the *cis* product exclusively by ^{1}H-NMR[502].

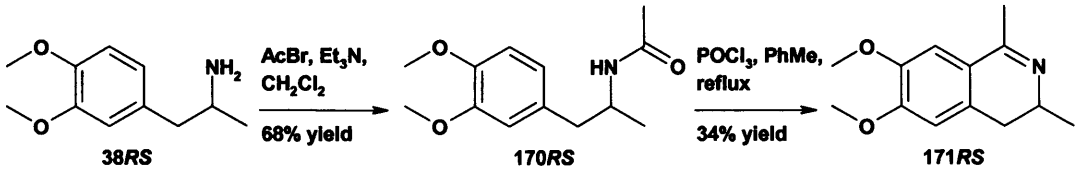

Figure 124: The synthesis of racemic **171*RS*** from **38*RS***.

To explore the application of this approach to the synthesis of the *cis*-diastereomers of **44**, racemic 6,7-dimethoxy-1,3-dimethyl-3,4-dihydroisoquinoline **171*RS*** was synthesised over two steps from **38*S*** in modest yield. Acetylation with acetyl bromide gave the acetamide **170*RS***, which was cyclised by dehydration using Bischler-Napieralski conditions of phosphorus oxychloride in toluene[425] (see Figure 124).

A trial reduction of **171*RS*** with sodium borohydride in methanol gave **44** in a 6:1 ratio of *cis*:*trans*, as determined by ^{1}H-NMR spectroscopy (see Figure 125). The 3-methyl group is exerting some stereofacial selectivity, by sterically hindering the approach of the borohydride moiety to the *cis* face of the dihydroisoquinoline **171*RS***, and thereby impeding the delivery of the hydride. The use of a hydride reducing agent of increased steric bulk would be anticipated to increase the degree of stereoselectivity. A trial reaction with sodium triacetoxyborohydride, following a literature protocol for reductive aminations with this reagent[503], gave a much improved ratio of 19:1 *cis*:*trans* (95% *d.s.*) by ^{1}H-NMR spectroscopy (see Figure 125). The successful utilisation of sodium triacetoxyborohydride to reduce 6,7-dimethoxy-3-**aryl**-1-methyl-3,4-dihydroisoquinolines to *cis*-6,7-dimethoxy-3-aryl-1-methyl-1,2,3,4-tetrahydroisoquinolines with a high degree of diastereoselectivity (95:5 *cis*:*trans*) has been published simultaneously to this investigation[482].

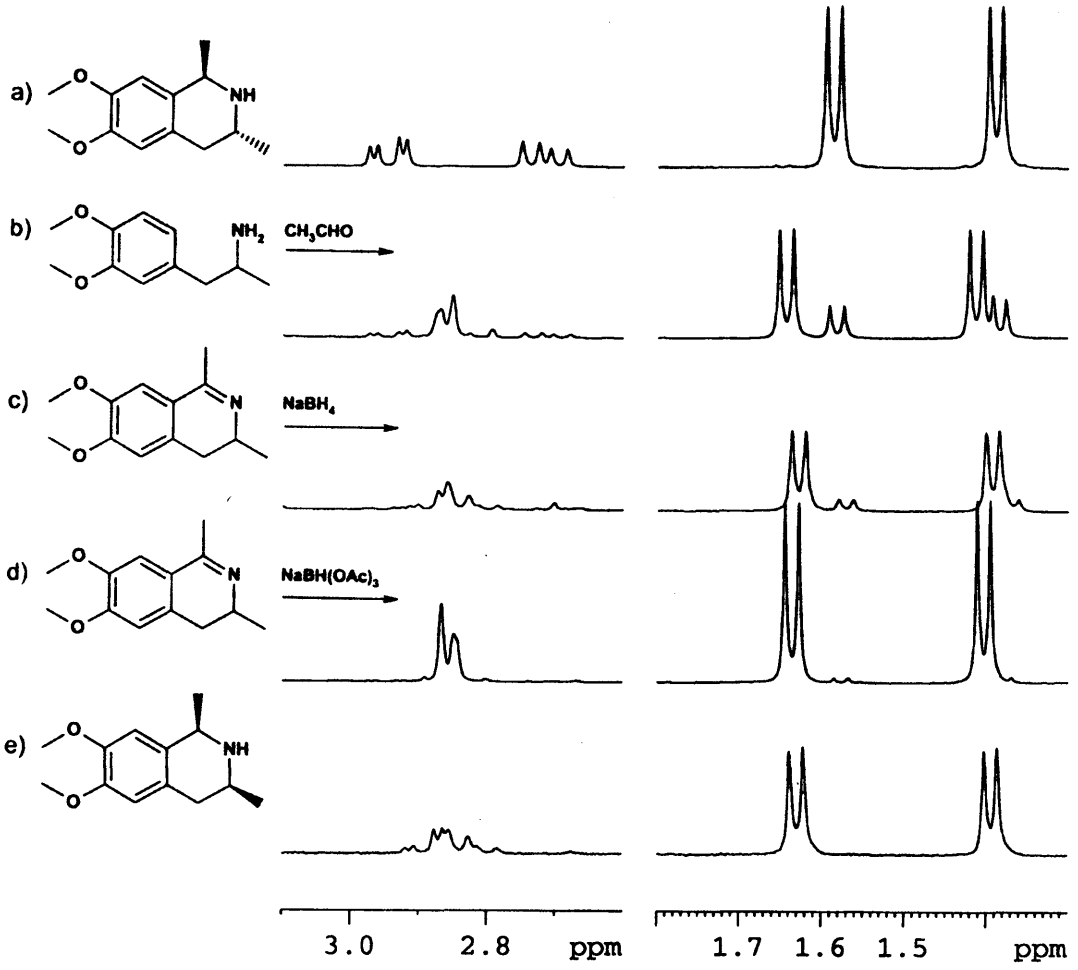

Figure 125: Comparison of expanded regions of ^{1}H-NMR spectra, demonstrating the contrasting diastereoselectivities of comparative synthetic routes from **38*RS*** to **44**:

a) **44(1*R*,3*R*)**, a pure *trans*-diastereomer;
b) crude product of the Pictet-Spengler reaction of **38*RS*** with acetaldehyde;
c) the reduction of **171*RS*** with sodium borohydride;
d) the reduction of **171*RS*** with sodium triacetoxyborohydride;
e) **44(1*R*,3*S*)**, a pure *cis*-diastereomer.

Synthesis of the *cis*-Diastereomers of 44

Given the high diastereoselectivity seen with sodium triacetoxyborohydride, this protocol was chosen for the synthesis of the separate (1*R*,3*S*)- and (1*S*,3*R*)-stereoisomers of **44**. When repeated with the pure enantiomers of **38**, recrystallisation of the products as the hydrochloride salt gave the *cis*-diastereomers as the only diastereomers detectable by ^{1}H-NMR spectroscopy (see Figure 125), and it was possible to obtain gram quantities of **44(1*R*,3*S*)** and **44(1*S*,3*R*)** in a reproducible fashion.

For each enantiomer **38**, a solution in dichloromethane with triethylamine was chilled to –15°C on a salt/ice bath, before acetyl bromide was added. The resulting

acetamides **170** were isolated in very good yield. Cyclisation to the enantiomers of **171** was accomplished under Bischler-Napieralski conditions, using phosphorus oxychloride in toluene at reflux. Reduction of the 3,4-dihydroisoquinolines with sodium triacetoxyborohydride gave the desired (1*R*,3*S*)- and (1*S*,3*R*)-enantiomers of **44**; the final route is illustrated for **44(1*S*,3*R*)** from **38*R*** (see Figure 126).

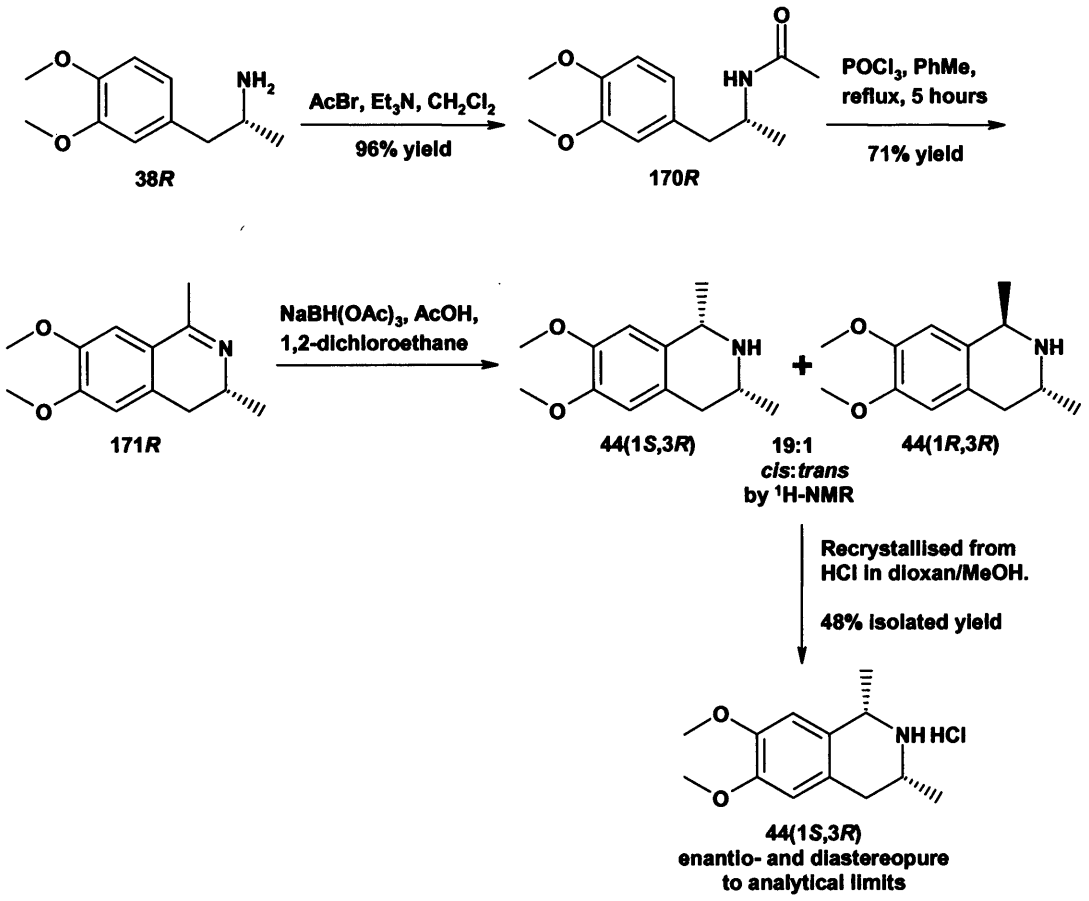

Figure 126: Route to **44(1*S*,3*R*)** hydrochloride from **38*R***.

The Final Steps in the Synthesis of the Full Structure Conformationally Constrained Analogues Of Capsaicin 29, 30 and 31

With each of the stereoisomers of the key tetrahydroisoquinoline intermediates **42**, **43** and **44** in hand, it was possible to access the full structure thioureas **29**, **30** and **31** by following a more generic route over two steps. The first step required the removal of the methyl groups protecting the catechol moiety. This was achieved by dissolving the compounds in refluxing 48% aqueous hydrobromic acid[435], usually overnight. The resulting catechols were all characterised as the hydrobromide salts (see Figure 127).

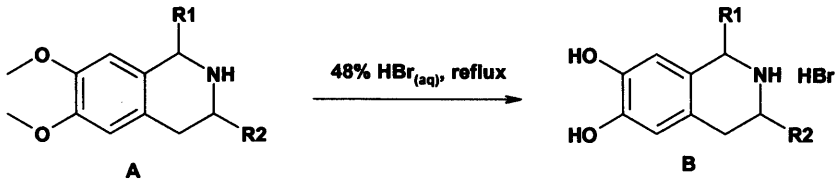

A B

Compound A	R1	R2	Compound B	Yield after crystallisation*
42*R*	Me	H	**33*R***	quantitative**
42*S*	Me	H	**33*S***	59%
43*R*	H	Me	**34*R***	4%
43*S*	H	Me	**34*S***	16%
44(1*R*,3*R*)	Me	Me	**35(1*R*,3*R*)**	55%
44(1*S*,3*S*)	Me	Me	**35(1*S*,3*S*)**	50%
44(1*R*,3*S*)	Me	Me	**35(1*R*,3*S*)**	84%
44(1*S*,3*R*)	Me	Me	**35(1*S*,3*R*)**	72%

Figure 127: Demethylation of the catechols (* the yield for this reaction was quantitative, with crystallisation of the product catechols performed for characterisation purposes; ** **33*R*** was not recrystallised, but was rather triturated from diethyl ether).

The final step of coupling the tetrahydroisoquinolines with the isothiocyanate **32** to give the desired thioureas, was achieved by reaction in the presence of triethylamine in a dry, aprotic solvent (see Figure 128).

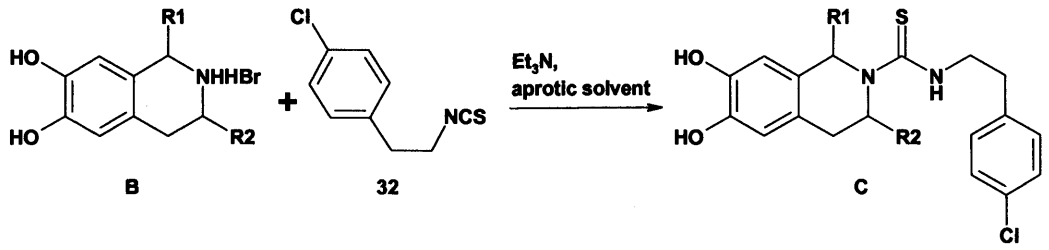

Compound C	R1	R2	Solvent	Yield
29*R*	Me	H	THF	89%
29*S*	Me	H	THF	80%
30*R*	H	Me	*N,N*-DMF	58%
30*S*	H	Me	DCM	64%
31(1*R*,3*R*)	Me	Me	*N,N*-DMF	82%
31(1*S*,3*S*)	Me	Me	*N,N*-DMF	73%
31(1*R*,3*S*)	Me	Me	*N,N*-DMF	67%
31(1*S*,3*R*)	Me	Me	*N,N*-DMF	72%

Figure 128: Final steps to the resolved stereoisomers of **29**, **30** and **31**.

Assessing the Purity of Final Products

Despite many of the intermediate compounds being crystalline, all of the final compounds resolutely defied every attempt to induce crystallisation. Each full structure was found to be a low melting amorphous solid and some residual solvent was found to be present in several of the final compounds. Where necessary, solvent impurities have been identified by comparative ^{1}H- and ^{13}C-NMR spectroscopy[504], and quantified by comparative integrations, as observed by ^{1}H-NMR spectroscopy. While successful elemental analyses were obtained for the 1-methyl and 3-methyl analogues, this was not possible for any of the dimethylated analogues, and the alternative option of using high resolution mass spectrometry to obtain an accurate mass value, in conjunction with the use of two separate analytical HPLC systems to assess compound purity, was used.

Determining the Optical Activity and the Optical Purity of Final Products 29, 30 and 31

The determination of the optical activity of the final products was confined to the measurement of optical rotation, *i.e.* with respect to this thesis, the ability of a solution of an optically active substance to rotate plane polarised light, as measured in a polarimeter. The observed angle of rotation is generally represented by the symbol α. It was determined in the early nineteenth century that the value of α for a given compound is proportional to:

a) the concentration c (measured in grams $100mL^{-1}$);
b) the path length l (measured in dm).

This was summarised as Biot's law[505]:

$$100\alpha = [\alpha]cl$$

with the value of the compound-specific proportionality constant $[\alpha]$ generally cited, as the compound's specific rotation. This value was later determined to be dependent upon wavelength (normally the sodium D-line of 589nm is used), temperature, concentration and solvent, all of which should be quoted with $[\alpha]$. Optical activity, in the form of calculated values for $[\alpha]$, was demonstrated for each of the final products (see Table 6).

Compound		Optical rotation
29*R*	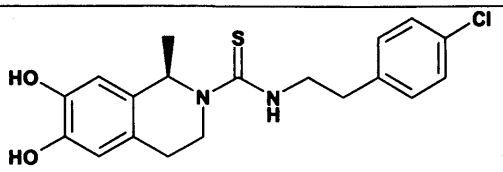	$[\alpha]_D^{24}$ –124.8 (c 1.0, $CHCl_3$)
29*S*	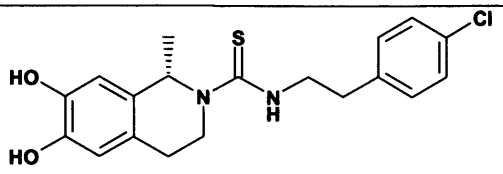	$[\alpha]_D^{24}$ +122.7 (c 1.0, $CHCl_3$)
30*R*	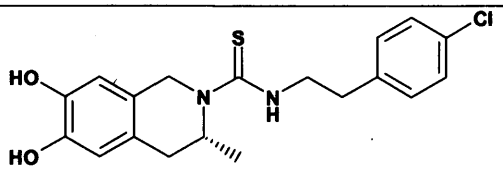	$[\alpha]_D^{25}$ +113.0 (*c* 1.05, $CHCl_3$)
30*S*	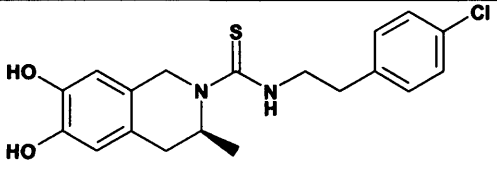	$[\alpha]_D^{25}$ –114.5 (*c* 1.04, $CHCl_3$)
31(1*R*,3*S*)	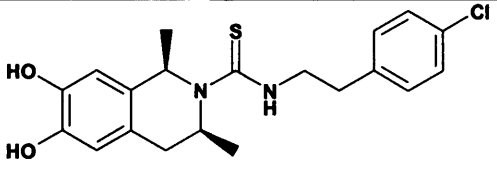	$[\alpha]_D^{23}$ –68.2 (c 1.00, CH_2Cl_2)
31(1*S*,3*R*)	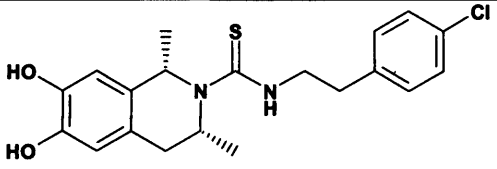	$[\alpha]_D^{23}$ +60.5 (c 1.01, CH_2Cl_2)
31(1*S*,3*S*)	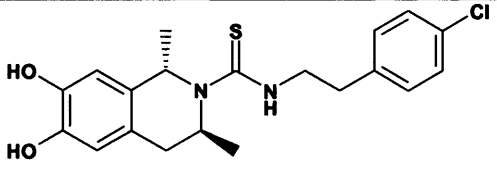	$[\alpha]_D^{21}$ –114.4 (c 0.52, CH_2Cl_2)
31(1*R*,3*R*)	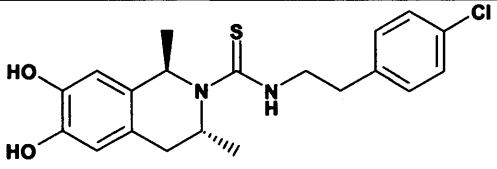	$[\alpha]_D^{21}$ +114.1 (c 0.54, CH_2Cl_2)

Table 6: Measured optical rotations for the enantiomers of **29** and **30**, and the diastereomers of **31**.

While the four pairs of enantiomers have similar rotations of opposing sign, the enantiomers of the *cis*-diastereomers **31(1*R*,3*S*)** and **31(1*S*,3*R*)** demonstrated a potentially significant difference in the numerical values of their respective rotations.

Rather than the result of stereomeric impurity, both enantiomers were seen to have differing amounts of cyclohexane present, as a result of the final steps taken in their purification. This could be seen in the ^{1}H- and ^{13}C-NMR spectra for each compound, with quantification possible from the ^{1}H-NMR. Compound **31(1*R*,3*S*)** still contained ~0.15 equivalents of cyclohexane, while compound **31(1*S*,3*R*)** had retained ~0.5 equivalents of cyclohexane. The calculation of the specific rotation [α] does not account for this, relying as it does upon the absolute weight of material used (*c*). Unfortunately, any attempt to further reduce the amount of trapped solvent by oven drying, even at low temperatures, led to decomposition. However, this inequality in effective molecular weight can be compensated for by calculating the **molar rotation** [Φ]:

$$[\Phi] = \frac{[\alpha].\text{Effective molecular weight}}{100}$$

The resulting values, while not equal and opposite, are within 5% (see Table 7).

Compound		Molar rotation
31(1*R*,3*S*)	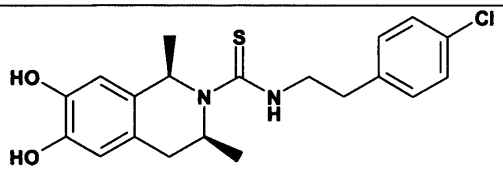	$[\Phi]_D^{23}$ –275.2 (c 1.00, CH_2Cl_2)
31(1*S*,3*R*)	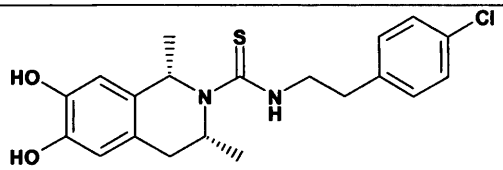	$[\Phi]_D^{23}$ +262.0 (c 1.01, CH_2Cl_2)

Table 7: Calculated values of molar rotation [Φ] for **31(1*R*,3*S*)** and **31(1*S*,3*R*)**.

While useful as an indicator of chirality in the product molecules, there are limitations with the use of optical rotation as a measure of optical purity. Enantiomers do not have to be pure for a solution to be optically active; any mixture of enantiomers will give a value for α. While the preparation of both enantiomers of a given compound should give equal values of opposing rotation, without pure samples for comparison, the measurement of optical rotation does not allow for the

possibility that each compound is similarly contaminated with its enantiomer *i.e.* samples of pure (*R*)- and pure (*S*)-enantiomers will give equal and opposite rotations, but so will *e.g.* 4:1 mixtures of (*R*):(*S*) and (*S*):(*R*) enantiomers.

An unequivocal measure of optical purity was therefore required for the final products. Analytical HPLC with a chiral column does not have the limitations of optical rotation. A chiral HPLC column has an optically active material covalently bound to the stationary phase. When passing through the column, each enantiomer of a pair can interact with this chiral stationary phase (CSP) to a greater or lesser extent, to be retarded to a greater or lesser extent, and therefore eluted from the column separately from its enantiomer. The quantity of each enantiomer can therefore be readily assessed. However, each compound class may also interact with the many and varied CSPs to a greater or lesser extent, requiring a sample of racemic material to be tried for enantiomeric separation against a range of analytical columns and CSPs. Of the available chiral HPLC columns, the Daicel Chemical Industries Chiralpak AD-H column (250 x 4.6mm) was found to successfully separate each of the synthesised pairs of enantiomers, by isocratic elution with mixtures of n-hexane/propan-2-ol containing 0.1% TFA and 0.1% diethylamine by volume.

Confirmation of the Enantiomeric Purity of 29*R* and 29*S*

The enantiomers of **29** were successfully resolved on the specified column (see the section entitled *Determining the Optical Activity and the Optical Purity of Final Products 29, 30 and 31*) by elution with a 3:1 mixture of n-hexane/propan-2-ol containing 0.1% TFA and 0.1% diethylamine by volume (see Figure 129).

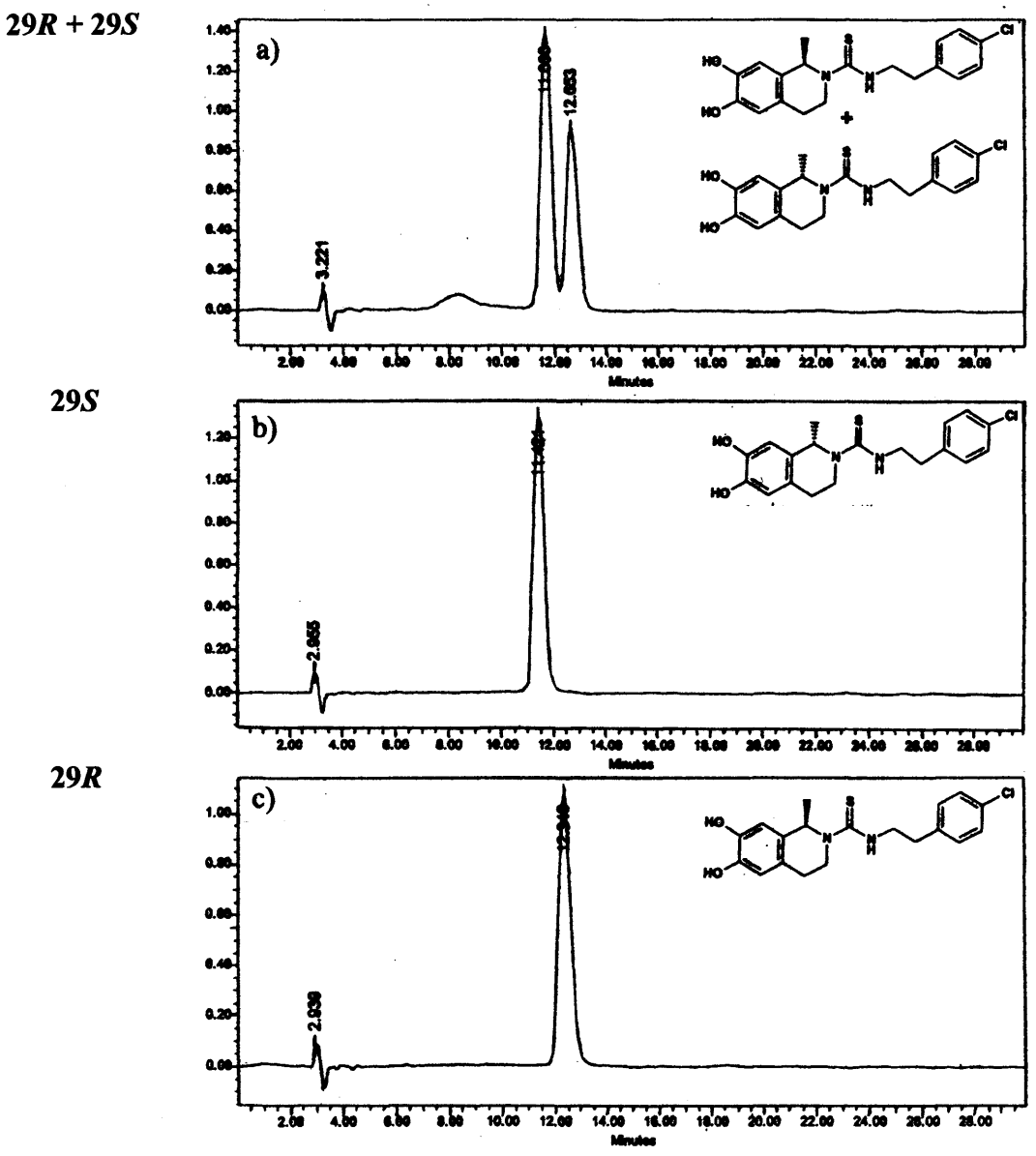

Figure 129: Chiral HPLC separation of the enantiomers of **29**.

Confirmation of the Enantiomeric Purity of 30*R* and 30*S*

The enantiomers of **30** were also successfully resolved on the specified column (see the section entitled *Determining the Optical Activity and the Optical Purity of Final Products 29, 30 and 31*) by elution with a 3:1 mixture of n-hexane/propan-2-ol containing 0.1% TFA and 0.1% diethylamine by volume (see Figure 130).

30*R* + 30*S*

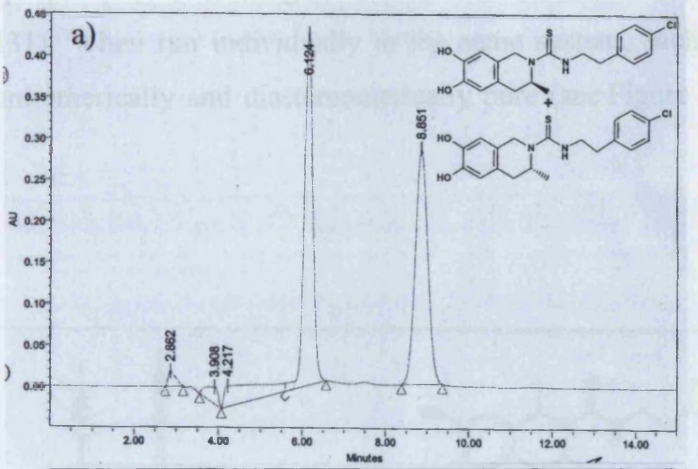

30*R*

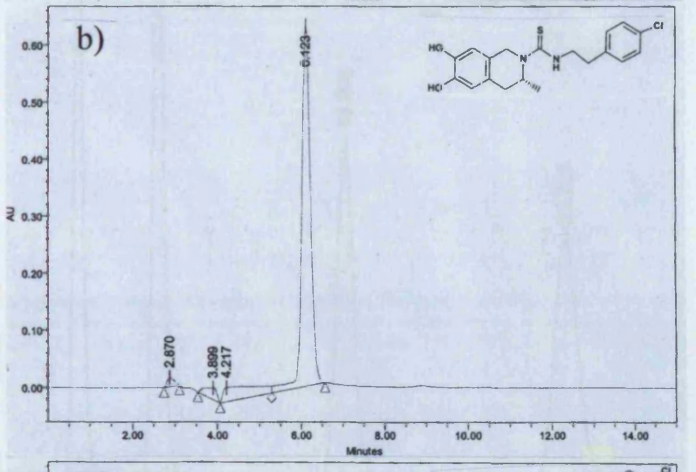

30*S*

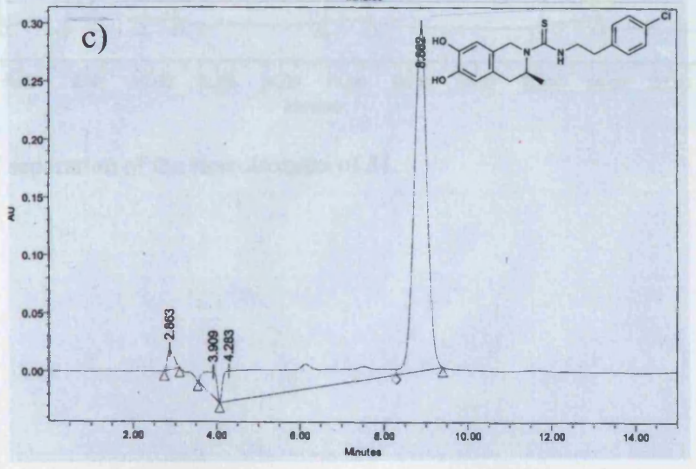

Figure 130: Chiral HPLC separation of the enantiomers of **30**.

Confirmation of the Enantiomeric and Diastereomeric Purity of the Stereoisomers of 31

The four stereoisomers of **31** were found to separate on the chosen chiral analytical HPLC column (see the section entitled *Determining the Optical Activity and the Optical Purity of Final Products 29, 30 and 31*). A sample containing an equal amount of each isomer gave baseline separation when eluted isocratically with a 4:1 mixture of n-hexane/propan-2-ol containing 0.1% TFA and 0.1% diethylamine by volume (see Figure 131). When run individually in the same system, each sample was shown to be enantiomerically and diastereomerically pure (see Figure 132 and Figure 133).

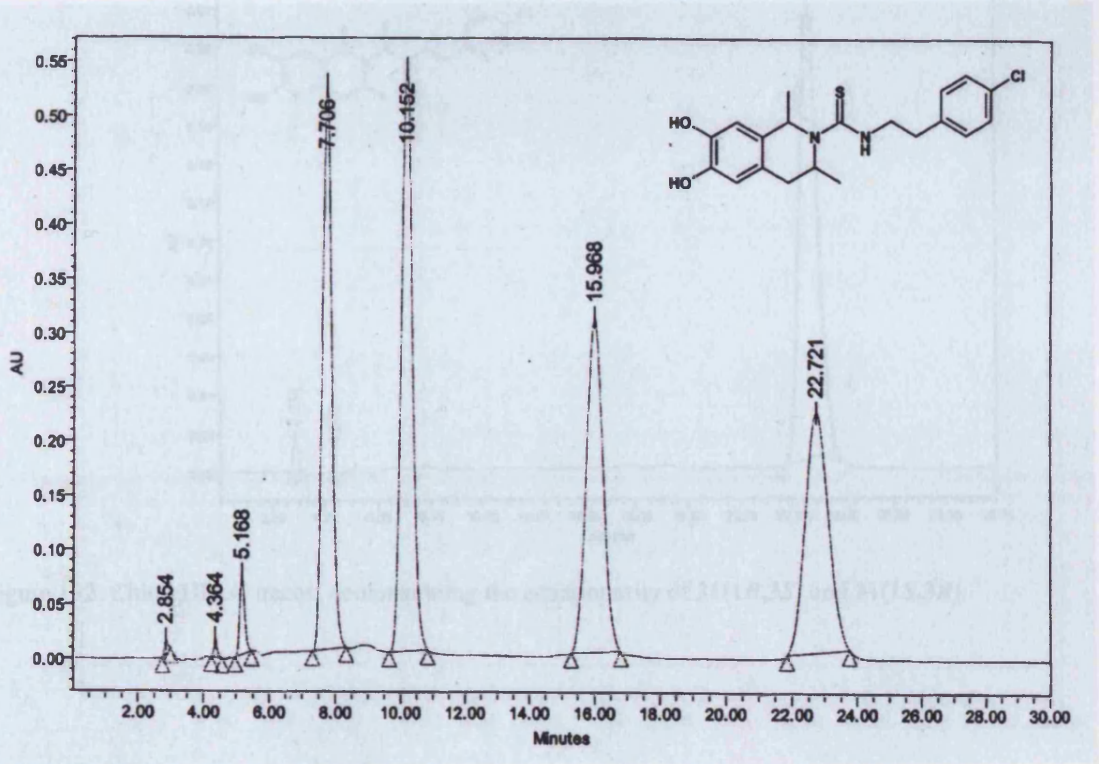

Figure 131: Chiral HPLC separation of the stereoisomers of **31**.

31(1*S*,3*R*)

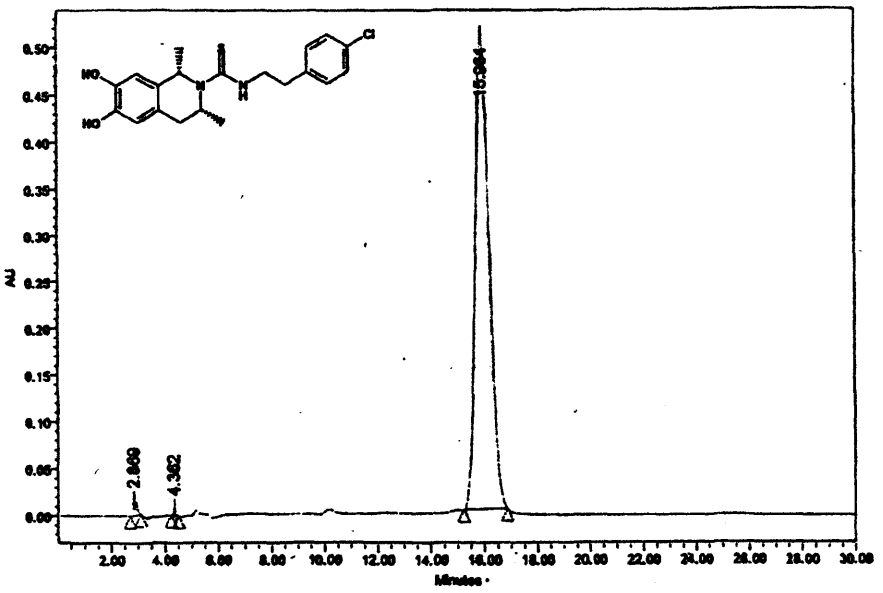

31(1*R*,3*S*)

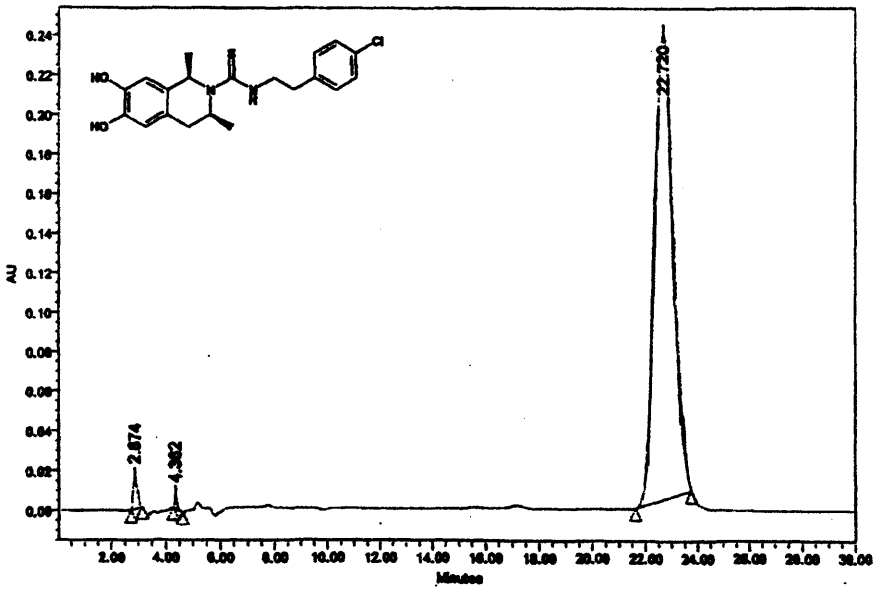

Figure 132: Chiral HPLC traces, demonstrating the enantiopurity of **31(1*R*,3*S*)** and **31(1*S*,3*R*)**.

31(1*S*,3*S*)

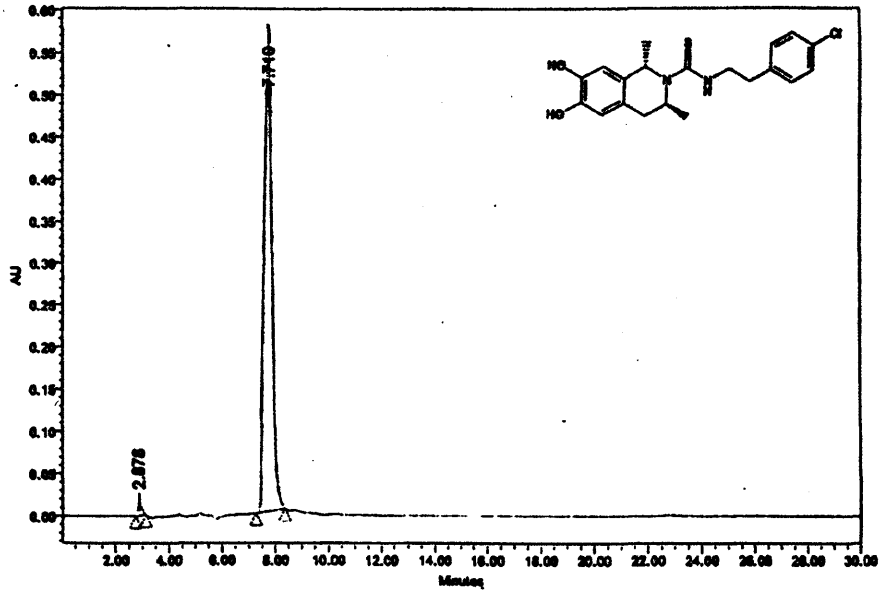

31(1*R*,3*R*)

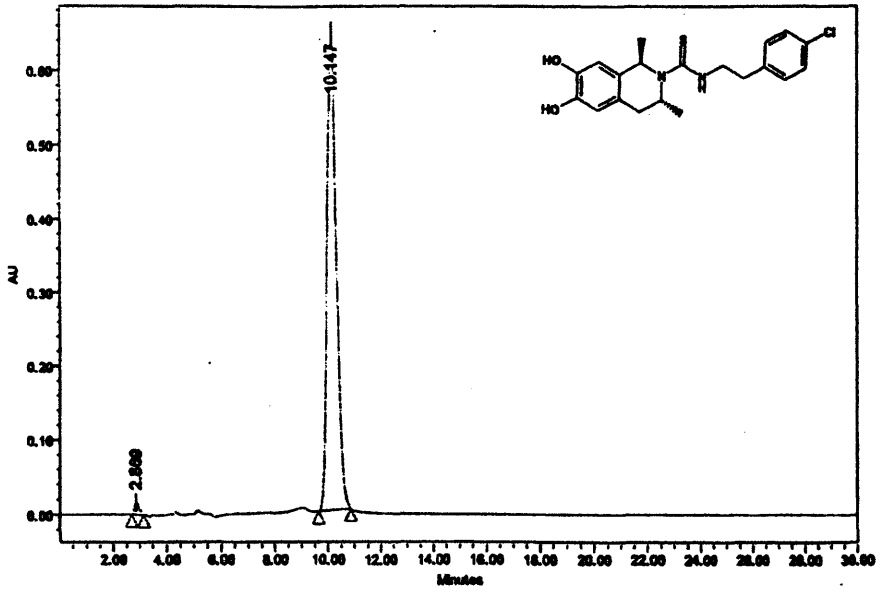

Figure 133: Chiral HPLC traces, demonstrating the enantiopurity of **31(1*R*,3*R*)** and **31(1*S*,3*S*)**.

In addition to analytical HPLC, the different physical properties of diastereomers allows diastereomeric purity to also be measured by NMR spectroscopy. Examination of the ^{1}H-NMR and ^{13}C-NMR spectra of the *trans*- and *cis*-diastereomers of *N*-(4'-chlorophenethylthiocarbamoyl)-6,7-dihydroxy-1,3-dimethyl-1,2,3,4-tetrahydroisoquinoline revealed several signals appropriate for comparative purposes as a measure of diastereomeric purity (see Table 8). None of the four compounds showed any of the opposing diastereomer, to the limit of detection (see Figure 134 and Figure 135).

	^{1}H-NMR		^{13}C-NMR	
	δ_H, multiplicity		δ_C	
	trans	*cis*	*trans*	*cis*
3-CH_3	0.77, d	1.14, d	18.43	20.37
1-CH_3	1.34, d	1.38, d	23.32	21.65
Ar**CH$_A$**CH$_B$CH	2.42, dd	2.55, dd		
ArCH$_A$**CH$_B$**CH	3.15, dd	2.81, dd		
3-H			50.63	49.27
1-H			55.45	53.52
C_{Ar}H-5	6.69, s	6.55, s	113.44	115.12
C_{Ar}H-8	6.71, s	6.57, s	115.86	112.97

Table 8: Comparison of ^{1}H- and ^{13}C-NMR peaks for the *cis* and *trans* diastereomers of **31**.

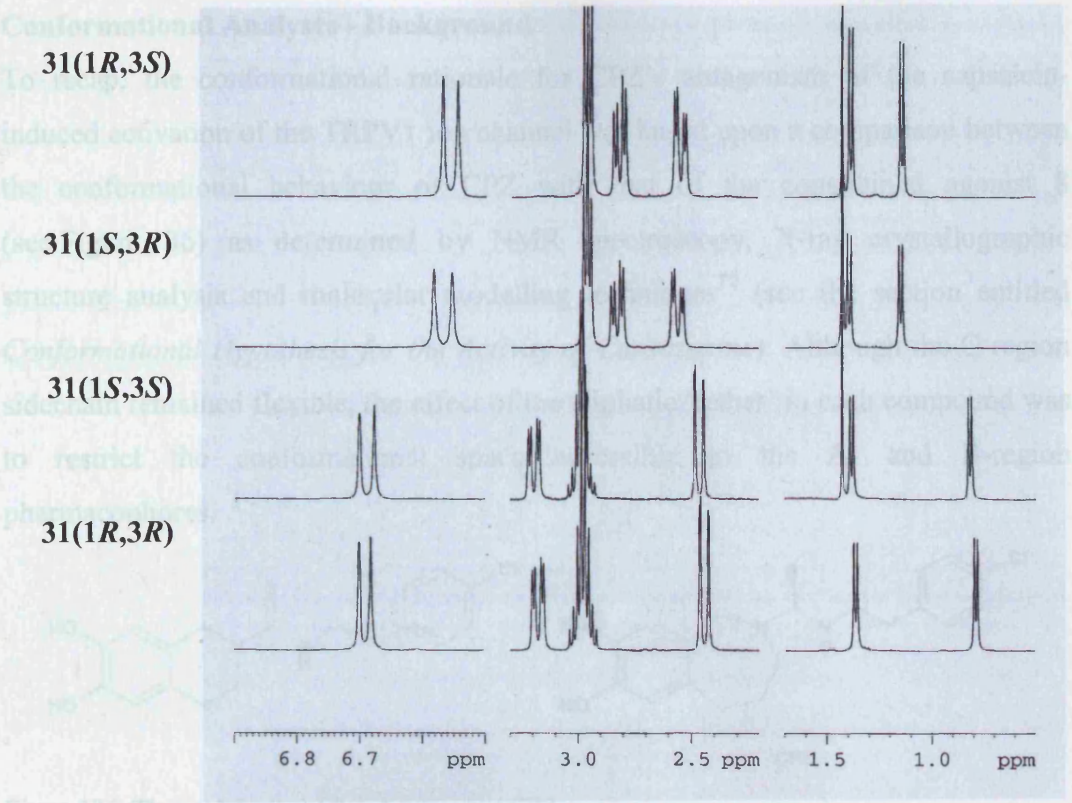

Figure 134: Comparison of ^{1}H-NMR spectra for the resolved diastereomers of **31**.

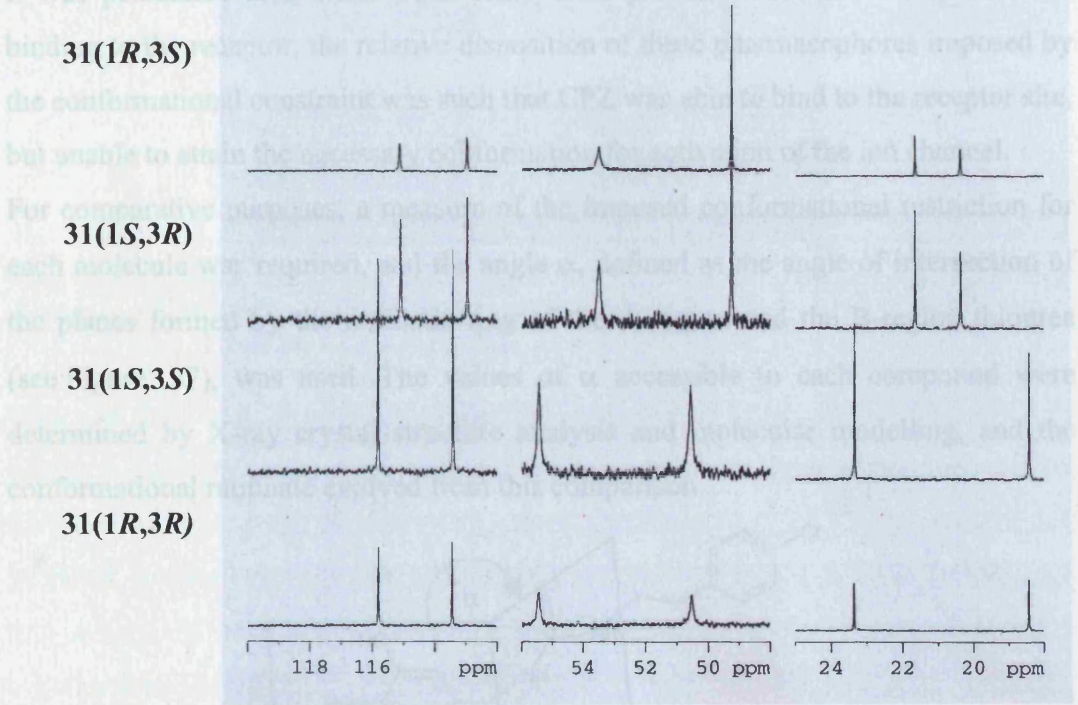

Figure 135: Comparison of the ^{13}C-NMR spectra for the resolved diastereomers of **31**.

Conformational Analyses - Background

To recap, the conformational rationale for CPZ's antagonism of the capsaicin-induced activation of the TRPV1 ion channel was based upon a comparison between the conformational behaviour of CPZ with that of the constrained agonist **8** (see Figure 136) as determined by NMR spectroscopy, X-ray crystallographic structure analysis and molecular modelling techniques[72] (see the section entitled *Conformational Hypothesis for the Activity of Capsazepine*). Although the C-region sidechain remained flexible, the effect of the aliphatic 'tether' in each compound was to restrict the conformational space accessible to the A- and B-region pharmacophores.

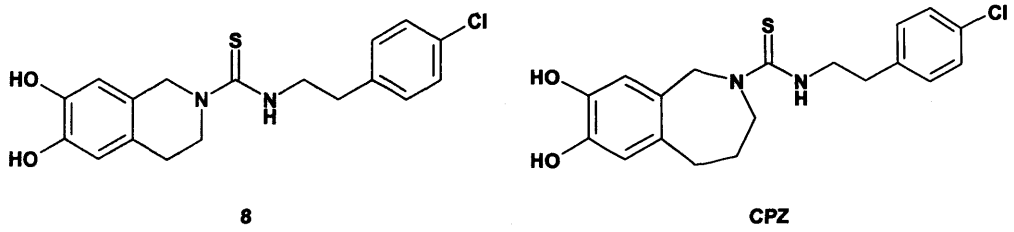

Figure 136: The model agonist **8** and antagonist CPZ.

It was postulated that, while both compounds possessed the pharmacophores for binding to the receptor, the relative disposition of these pharmacophores imposed by the conformational constraint was such that CPZ was able to bind to the receptor site, but unable to attain the necessary conformation for activation of the ion channel.

For comparative purposes, a measure of the imposed conformational restriction for each molecule was required, and the angle α, defined as the angle of intersection of the planes formed by the aromatic ring of the A-region and the B-region thiourea (see Figure 137), was used. The values of α accessible to each compound were determined by X-ray crystal structure analysis and molecular modelling, and the conformational rationale evolved from this comparison.

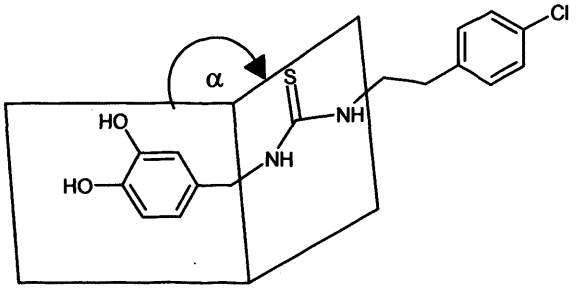

Figure 137: Definition of the angle α[72]

For **8**, the molecular modelling suggested the heterocyclic ring was flexible, with no particular conformation preferred, and α held within ±30° of co-planarity (see Figure 138). In comparison, molecular modelling gave four discrete and quite rigid conformations for the heterocyclic ring of CPZ, with 92% of the conformations populating one of two 'pseudochair' forms. These two conformations hold the two planes almost orthogonal to one another, with α at ~±90°. The X-ray crystal structure of CPZ gave a conformation with α equal to +93.5°.

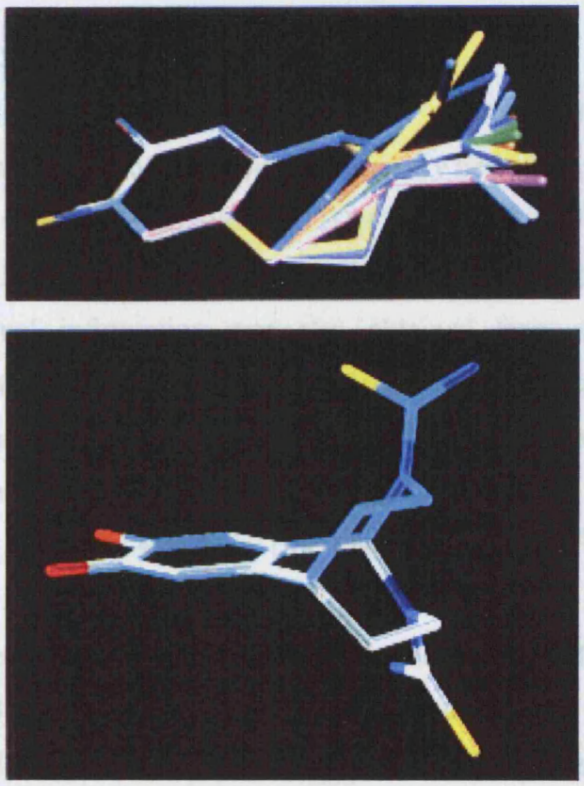

Figure 138: Accessible low energy conformations of **8** (top) and CPZ (bottom), reproduced from Walpole *et al*[72], with the C-region side chains omitted for clarity

Although the NMR spectroscopy experiments described in the original paper[72] were primarily for analysing the tautomeric ratio of two possible orientations of the thiourea, the anticipated rigidity of the seven-membered ring of CPZ was supported by NMR spectra from the low temperature experiment. While at room temperature the protons of each methylene of the conformational tether were magnetically equivalent and coincident; at 173K each proton gave rise to distinct signals, implying conformational rigidity. Similar experiments for **8** showed no distinction between these protons, and this was taken to confirm the highly flexible nature of the 'saturated' ring.

Conformational Analyses of the Stereoisomers of 29, 30 and 31.

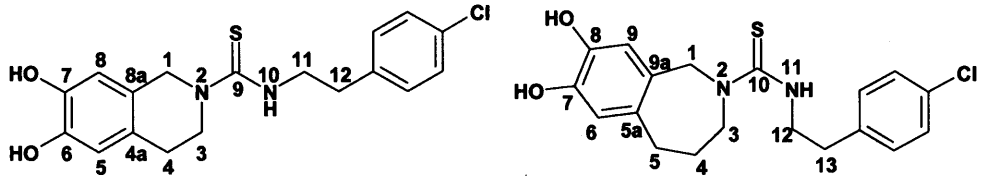

Figure 139: Atomic numbering for CPZ and the tetrahydroisoquinoline analogues **8**, **29**, **30** and **31**.

NMR Spectroscopy

The principle use of NMR spectroscopy was for structural characterisation and confirmation; the assignment of NMR signals for every new chemical entity included in this thesis was made after analysis by 1D (^{1}H-, ^{13}C- and ^{13}C-DEPT) and 2D (COSY, HMBC and HMQC) experiments (for definitions, see Experimental section). Some conformational information was also obtained from these experiments, primarily as a result of increased complexity of some signals in the ^{1}H-NMR spectra beyond first-order approximation, in particular of the signals corresponding to the protons of the methylenes and methines of the bicyclic ring systems, and the methylenes of the C-region sidechain (for the full ^{1}H- and ^{13}C-spectra of each stereoisomer of **29**, **30** and **31**, see Appendix 2).

For example, in the ^{1}H-NMR spectra of the enantiomers of **29**, if the protons of the methylenes at C-3 and C-4 (see Figure 139 for numbering) were magnetically equivalent, first order approximation would dictate that the corresponding signals of the ^{1}H-NMR spectrum would be predicted to be triplets, and the methine at C-1 would be a doublet. Further, the methylene at C-11 would be a doublet of triplets. This was not the case (see Figure 140). While C-4 was a triplet, the others were more complex. C-1 and one of the two protons at C-3 were broad with no splitting apparent, while the second proton at C-3 and the protons at C-11 had complex, second order splitting patterns.

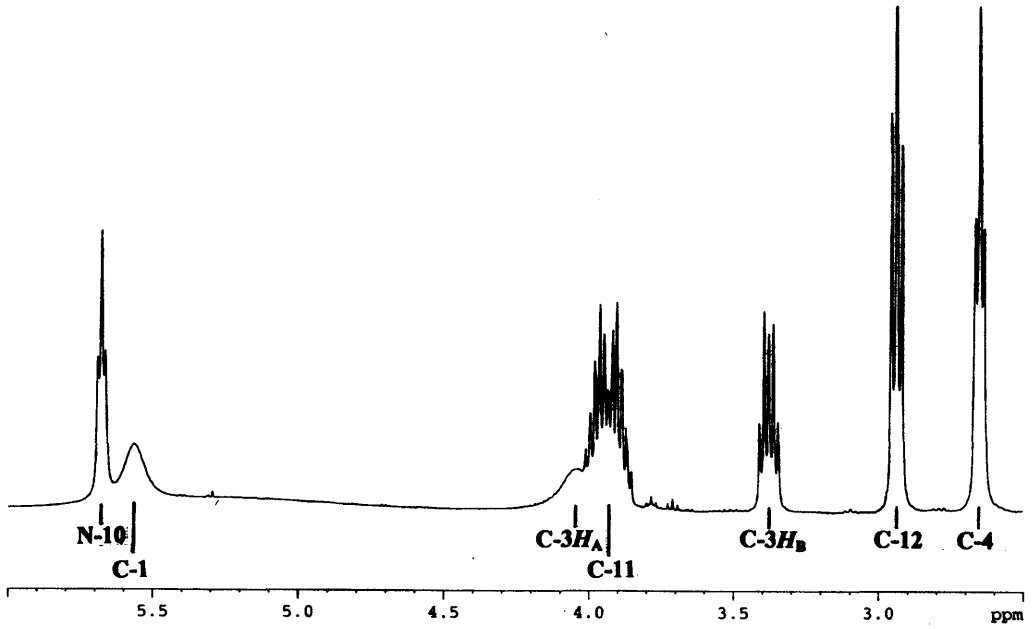

Figure 140: Region of the ^{1}H-NMR spectrum of 29*S*, showing the complexity beyond first order approximations of the signals corresponding to the protons of the methylenes at C-3 and C-11, and the methine at C-1.

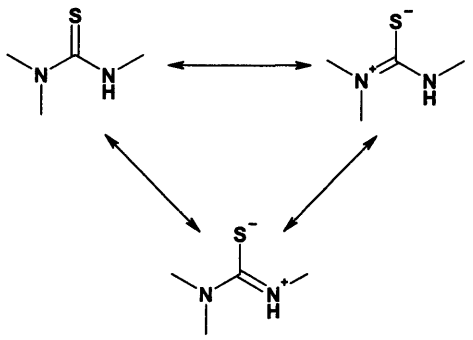

Figure 141: Resonance forms for the thiourea moiety.

There are two possible contributory factors[487]. One arises from the proximity of these protons to the thiourea moiety. As a result of the delocalisation of π-electrons within the moiety, each of the bonds between the carbon atom of the thiocarbonyl and the nitrogen atoms has a degree of double bond character (see Figure 141), leading to slow rotation about these two bonds. This would give rise to four slowly interconverting conformers (see Figure 142), with different magnetic environments for the protons concerned. Depending upon the rate of interconversion, these conformers may be observable within the NMR timeframe as increased complexity of the signal and possible line broadening. This phenomenon is known as

environmental exchange. Variable temperature NMR experiments (not available at NIMS beyond a narrow temperature range) would confirm this analysis.

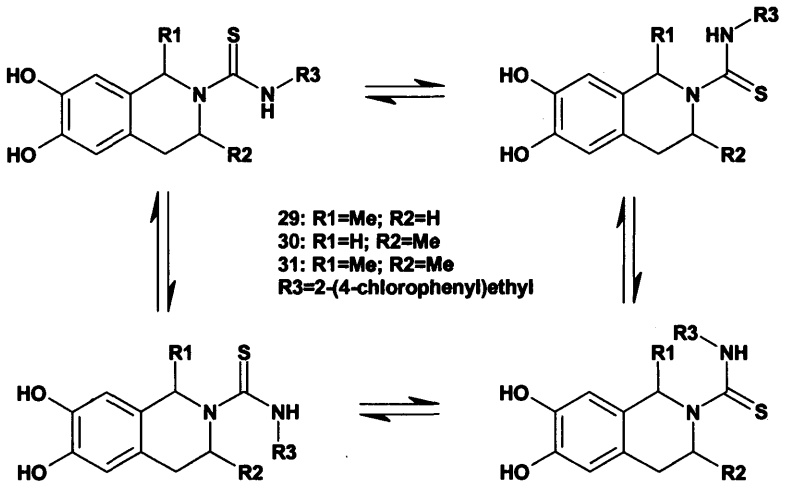

Figure 142: The four possible orientations of the thiourea moiety of **29**, **30** and **31**..

A second phenomenon of *efficient relaxation*, whereby protons that are close in space to one another can facilitate the relaxation from the high energy state to the low energy state of the NMR experiment, can also lead to line broadening. The presence of two such broad signals would lend credence to this explanation, and by extrapolation imply that the conformation of the constrained portion of the molecule is such as to hold these protons in the correct orientation and proximity to one another.

For the enantiomers of **30**, similarly complex signals were seen (see Figure 143). Rather than the signal corresponding to the methylene protons at C-1 appearing as a singlet, the protons were non-equivalent ($\Delta\delta = 0.37$), and a coupled pair of doublets were seen. The protons of the C-4 methylene were also non-equivalent ($\Delta\delta = 0.51$), and exhibited the classical ABX splitting pattern[487], coupled as they were with each other and with the proton of the methine at C-3. The *geminal coupling* between the two protons of C-1, and between the two protons of C-4, was a result of the conformational influence of the methyl group of the chiral centre at C-3. The methylene protons were magnetically non-equivalent, or *diastereotopic*[487].

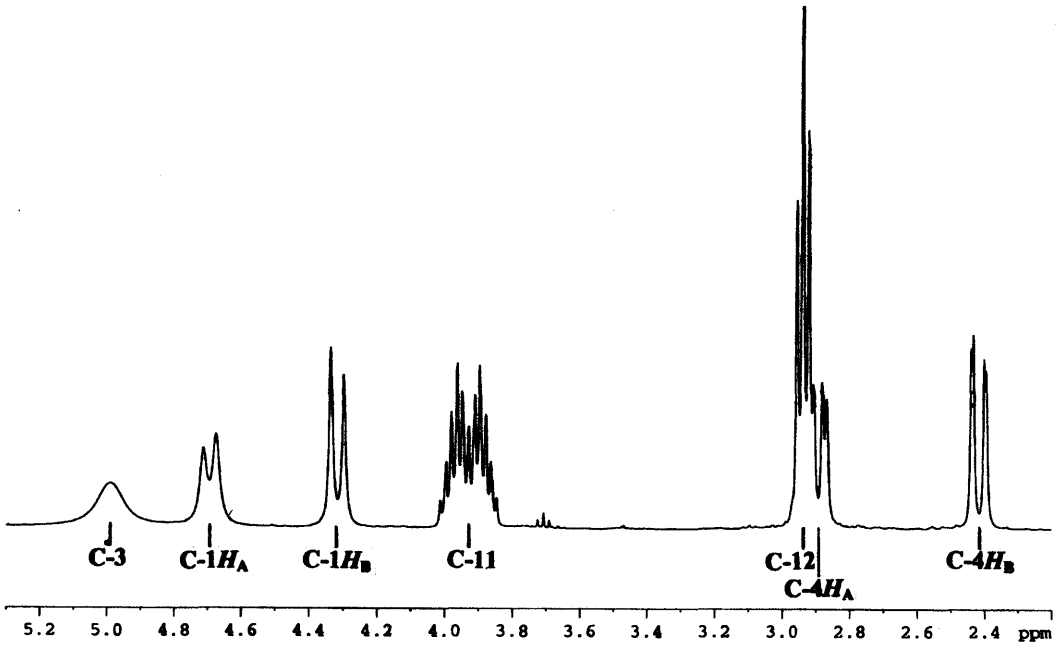

Figure 143: Region of the ^{1}H-NMR spectrum of **30*R***, showing the complexity beyond first order approximations of the signals corresponding to the protons of the methylenes at C-1 and C-11, and the methine at C-3.

In addition, the signals corresponding to the protons at C-1 and the methine proton at C-3 were broad, and the signal corresponding to protons of the methylene at C-11 was considerably more complex than a first order approximation would predict. The likely cause is aforementioned restricted rotation of the carbon-nitrogen bonds of the thiourea, with the four possible slowly interconverting conformers (see Figure 142), causing environmental exchange.

For the *trans*-diastereomers of **31** (see Figure 144), the supposed restricted rotation of the thiourea (see Figure 141) produced broadening of the signals corresponding to the C-1 and C-3 methine protons, and complexity beyond first order approximation to the methylenes at C-11 **and** C-12. In addition, the protons of the C-4 methylene were diastereotopic and magnetically non-equivalent ($\Delta\delta = 0.74$), due to one or both of the stereogenic centres at C-1 and C-3. They also had the classical ABX pattern in the ^{1}H-NMR spectrum, arising from the geminal coupling of the two protons at C-4 with each other, and vicinal coupling with the adjacent proton at C-3.

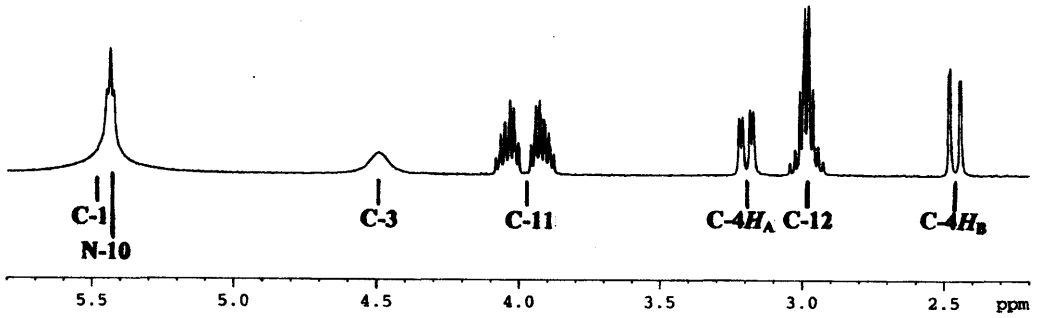

Figure 144: Region of the ^{1}H-NMR spectrum of the *trans*-diastereomer **31(1*S*,3*S*)**, showing the complexity beyond first order approximations of the signals corresponding to the protons of the methylenes at C-11 and C-12, the broadening of the signals corresponding to the protons of the methines at C-1 and C-3, and the non-equivalence and ABX splitting pattern of the signals corresponding to the methylene at C-4.

For the *cis*-diastereomers of **31** (see Figure 145), the supposed restricted rotation of the thiourea (see Figure 141) only produced broadening of the signals corresponding to the C-1 and C-3 methine protons. There was no apparent complication of the signals corresponding to the methylenes at C-11 and C-12 beyond the first order approximation of the splitting pattern. The protons of the C-4 methylene were also diastereotopic and magnetically non-equivalent ($\Delta\delta = 0.27$), and exhibited the classical ABX pattern in the ^{1}H-NMR spectrum seen in other analogues.

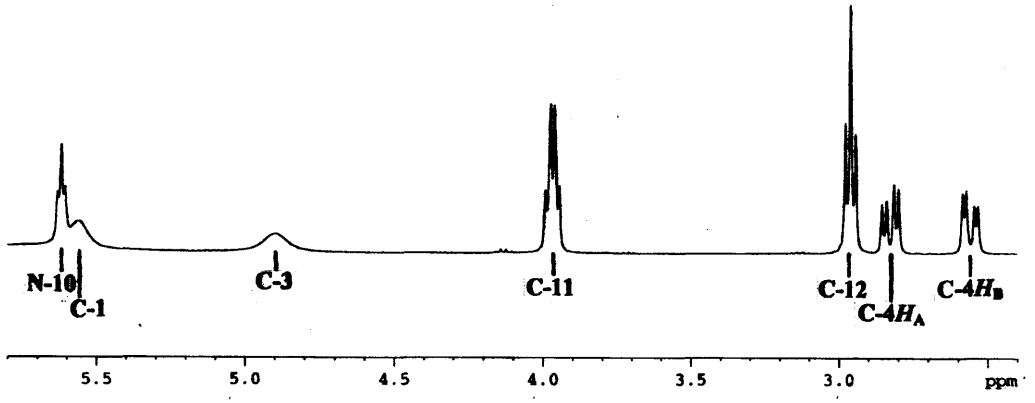

Figure 145: ^{1}H-NMR spectrum of the *cis*-diastereomer **31(1*S*,3*R*)**, showing the comparative simplicity of the signals corresponding to the protons of the methylenes at C-11 and C-12, the broadening of the signals corresponding to the protons of the methines at C-1 and C-3, and the non-equivalence and ABX splitting pattern of the signals corresponding to the protons of the methylene at C-4.

X-ray Crystallographic Structure Analysis

Unfortunately, the final products resisted all efforts at crystallisation, and this prevented any structural analysis via this technique.

Molecular Modelling

The principle basis for the conformational rationale was molecular modelling. Walpole et al. used molecular dynamics simulations to study the preferred conformations of **8** and CPZ from 251 energy minimised structures, and a measurement for α was taken for each[72]. A similar analysis was pursued for the new analogues, using the desktop molecular modelling package Spartan'02 (Wavefunction, Inc., Irvine, CA) to generate 100 conformers within 10kcal/mol of the lowest energy conformer.

It is important to recognise that, while such a modelling exercise can only give an indication of the range of possible conformations accessible by a compound, it should be possible to identify the nature of the molecule, its rigidity, and the major conformational classes available.

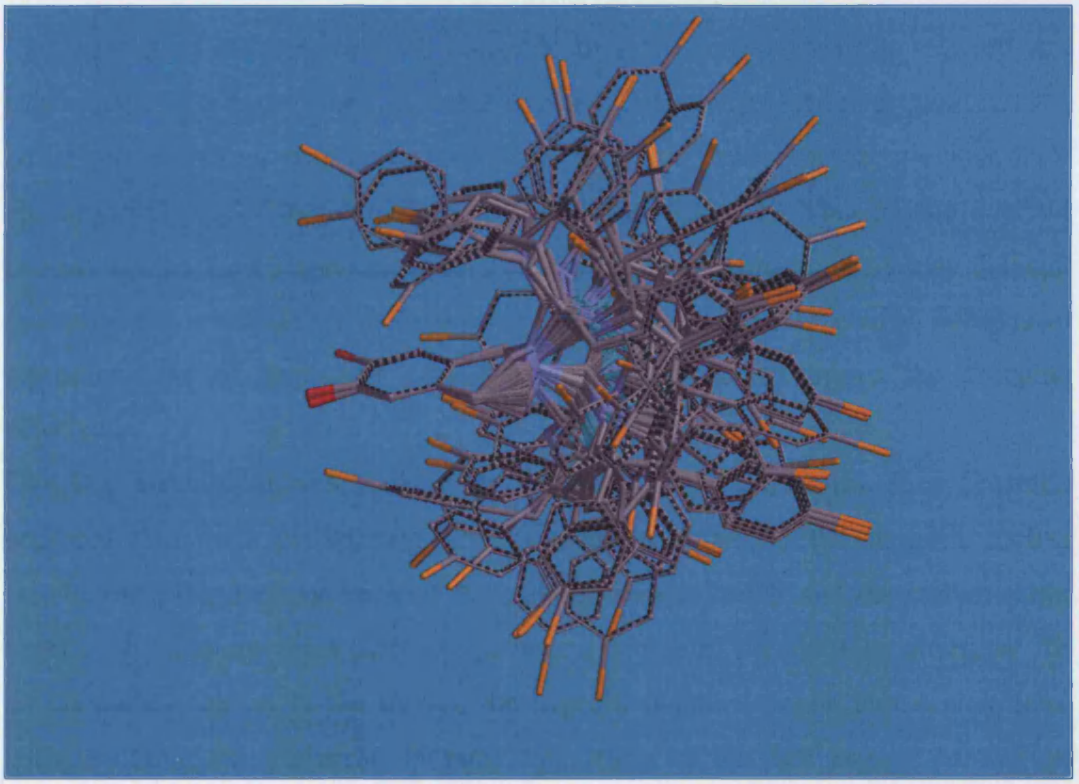

Figure 146: A representation of the conformations accessible to **8**, as determined by molecular modelling using Spartan'02.

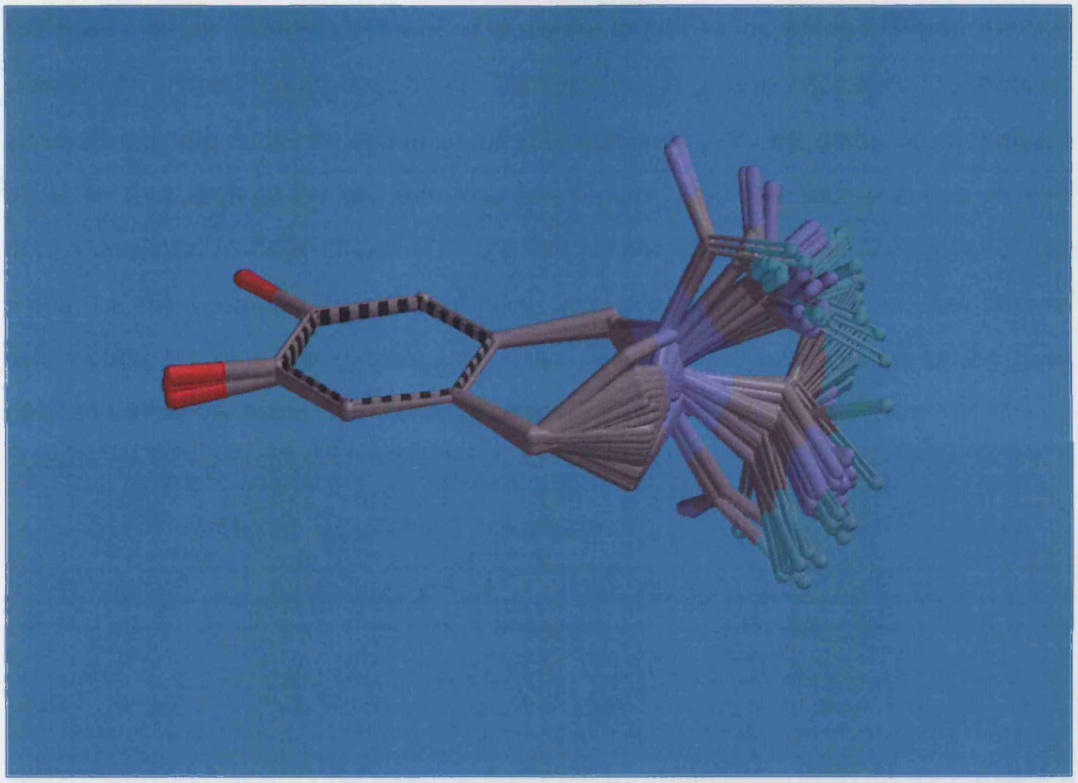

Figure 147: Figure 146, minus the C-region sidechains.

The portion of interest for each molecule in this exercise was the tethered and conformationally constrained A- and B-regions. In keeping with the original work[72], while the modelling was performed upon the intact molecule, the flexible 2-(4-chlorophenyl)ethyl C-region sidechains were removed when viewing the overlaid conformers, as their presence made examination of the conformer overlay difficult (compare the results for **8** in Figure 146 with Figure 147). For clarity, subsequent representations of accessible conformations are presented minus the C-region sidechains.

One key assumption was made when constructing the molecules. It is generally accepted that there is delocalisation of π-electrons within the thiourea moiety (see Figure 141), and that each of the carbon-nitrogen bonds and the carbon-sulfur bond of the thiourea must therefore possess a degree of double bond character. To accommodate this in to the model, the trigonal planar nitrogen atoms were used when building the molecule. Despite this, many of the low energy conformers demonstrated deformation of the planarity of the ring nitrogen atom, and frequent rotation about the bond between this nitrogen atom and the carbon atom of the thiocarbonyl moiety beyond the anticipated 0° and 180°. This in turn introduced

variation into the measured values of α, as the line of coincidence between the two planes was altered. To accommodate this variation, it proved necessary to define an alternative angle to α, independent of this bond rotation, by using an alternative plane to that defined by the thiourea (see Figure 148). The incorporation of two points common to both planes (*i.e.* the two carbon atoms of the heterocyclic ring alpha to the aromatic ring) eliminated any possible distortion in the line of intersection between the planes. Using the thiocarbonyl carbon atom as the third point to define the plane allowed comparison with the original work[72].

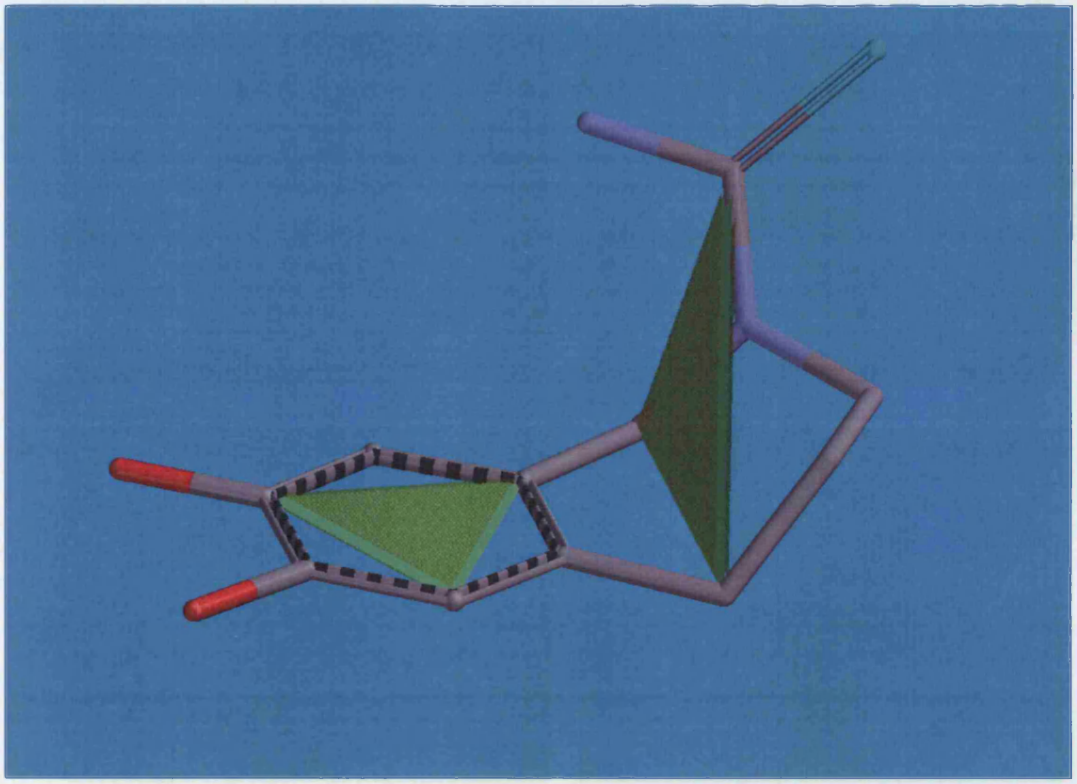

Figure 148: Revised planes to be used as a measure of conformational variation.

With the planes defined, the angle formed between these planes was defined as θ. When the thiocarbonyl carbon was in the plane of the aromatic ring, the value for θ was 0°. To distinguish between opposite sides of the molecule, with respect to the plane formed by the aromatic A-ring, it was necessary to define positive and negative values of θ. If the aromatic ring was held horizontally, with the catechol to the left, the heterocyclic ring to the right, and the benzylic carbon of C-1 on the far side of the molecule, anything above the plane of the aromatic ring was declared to have a positive value for θ and anything below the plane had a negative value for θ. The molecule in Figure 148 therefore had a positive value for θ.

Comparing 8 and CPZ

As an initial exercise, and to demonstrate the suitability of this approach, the modelling experiments for **8** and CPZ were reproduced.

Compound 8

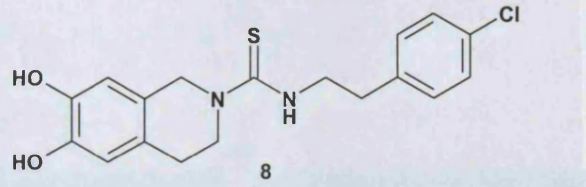

8

A

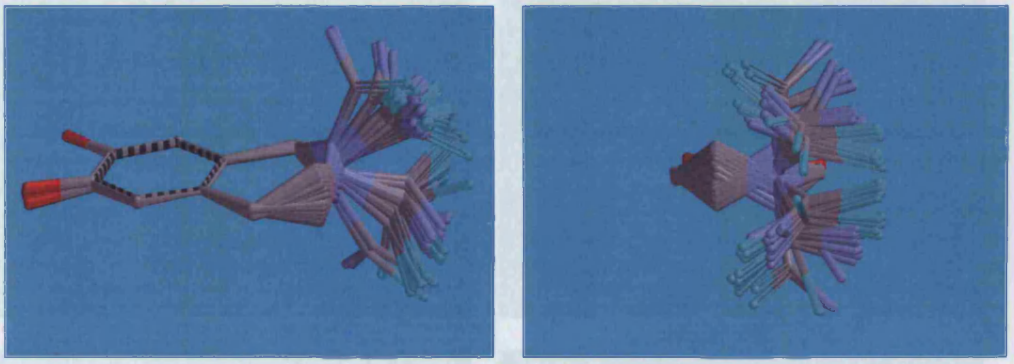

$-50.5° < \theta < -14.5°$; $14.8° < \theta < 47.6°$

B

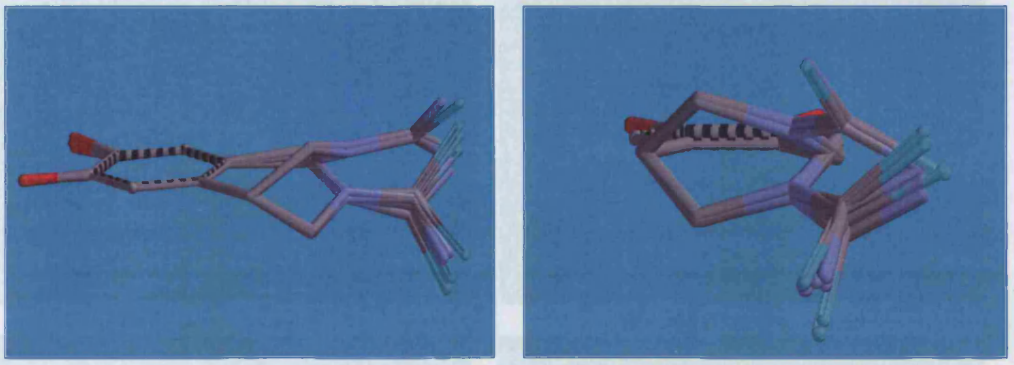

$-26.8° < \theta < -16.0°$; $15.8° < \theta < 16.6°$

Figure 149: A tabular representation of the conformations accessible to **8** (minus the C-region sidechain), as determined by molecular modelling using Spartan'02.

The molecular modelling experiment for **8** appeared to confirm the inherent flexibility of the aliphatic portion of the tetrahydroisoquinoline bi-cycle (see Figure 149). For approximately 90% of the generated conformers, the heterocyclic ring adopted the half-chair shape of A, as described by Olefirowicz and Eliel in their conformational analysis of *C*-methyl-1,2,3,4-tetrahydroisoquinolines[506]. This configuration placed the C-3 carbon atom and the N-2 nitrogen on opposite sides of the molecule, although there was also a significant minority (~10%) with these atoms on the same side of the molecule. Measured values for θ were between

$-50.0° < \theta < -15.1°$ and $14.8° < \theta < 47.4°$ either side of coplanarity, with no one conformation appearing preferred.

CPZ

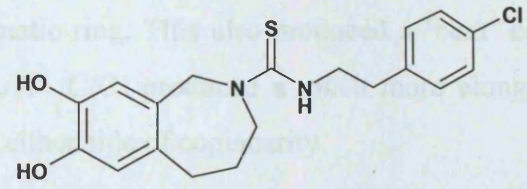

CPZ

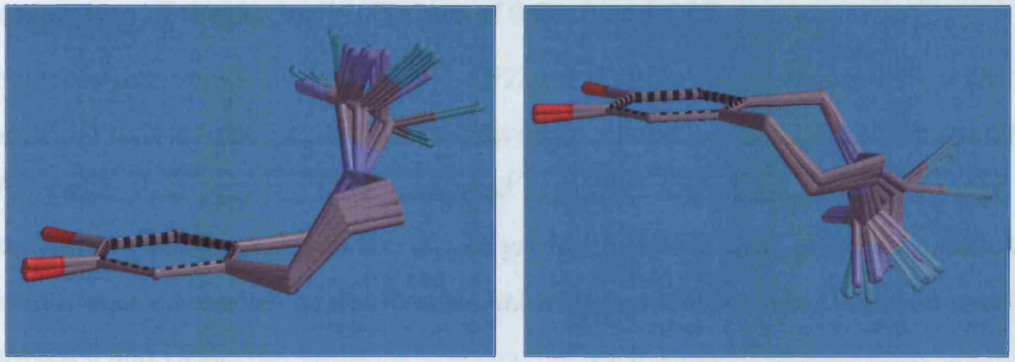

A: $56.0° < \theta < 79.4°$ **A'**: $-79.8° < \theta < -54.2°$

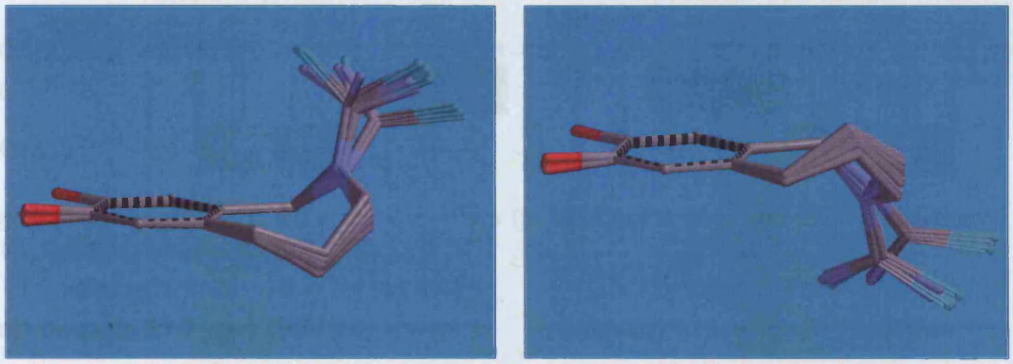

B: $47.5° < \theta < 64.5°$ **B'**: $-64.6° < \theta < -44.6°$

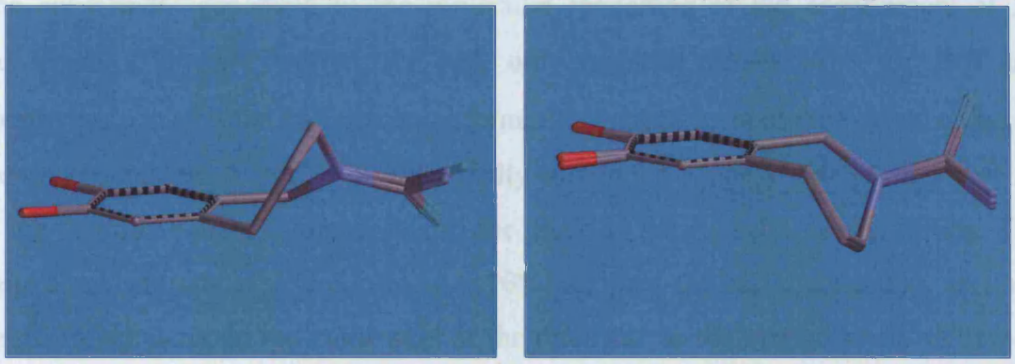

C: $7.3° < \theta < 11.3°$ **C'**: $-10.5° < \theta < -6.8°$

Figure 150: A tabular representation of the conformational classes accessible to CPZ (minus the C-region sidechain), as determined by molecular modelling using Spartan'02.

In comparison, CPZ had three quite distinct pairs of conformers (see Figure 150). The most populated (~60%) conformational class was the published[72] 'orthogonal'

conformation of A/A' with the atoms of the saturated tether positioned on the same face of the molecule, as defined by the A-region aromatic ring. In addition, there were two other conformations: B/B' (~35%) and C/C' (~5%). The B/B' conformation had the tether 'straddling' the two sides of the molecule, as defined by the plane of the aromatic ring. This also produced a 'bent' configuration, although not as extreme as A/A'. C/C' produced a much more elongated structure, with θ between ~7° and 11° either side of coplanarity.

Comparison of the Accessible Values of θ for 8 and CPZ

The accessible values of θ for **8** and CPZ are summarised in Figure 151, with the accessible ranges in black. By including every available low energy conformation for CPZ, rather than only the most populated[72], this broadened the accessible range of measured values for θ. Even so, it was gratifying to see that, in keeping with the general requirements of the conformational hypothesis, there was almost no overlap between **8** and CPZ.

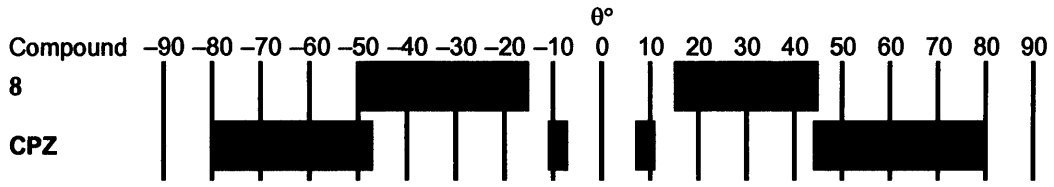

Figure 151: A summary of the accessible values (in black) of θ for **8** and CPZ, as determined by molecular modelling using Spartan'02.

Compounds 29*R* and 29*S*

The conformers generated in the molecular modelling of the enantiomers of **29** (see Figure 152) gave conformers with only negative values of θ for **29*R*** and positive values of θ for **29*S***. Each conformer was found to hold the methyl group of the stereogenic centre at C-1 **pseudoaxially** and on the opposite side of the molecule to the thiourea moiety, with respect to the plane of the A-region aromatic ring. The most abundant pair of A conformers (~90%) adopted the half-chair shape, and had the C-3 methylene on the **same** side of the molecule as the methyl group. A few of the generated conformers had the C-3 methylene on the **opposite** side of the molecule to the methyl group, giving rise to more extended conformations. The measured values for θ for these conformers fell into three discrete groupings (B, C and D; see Figure 152), although examples for all three were not seen for both enantiomers.

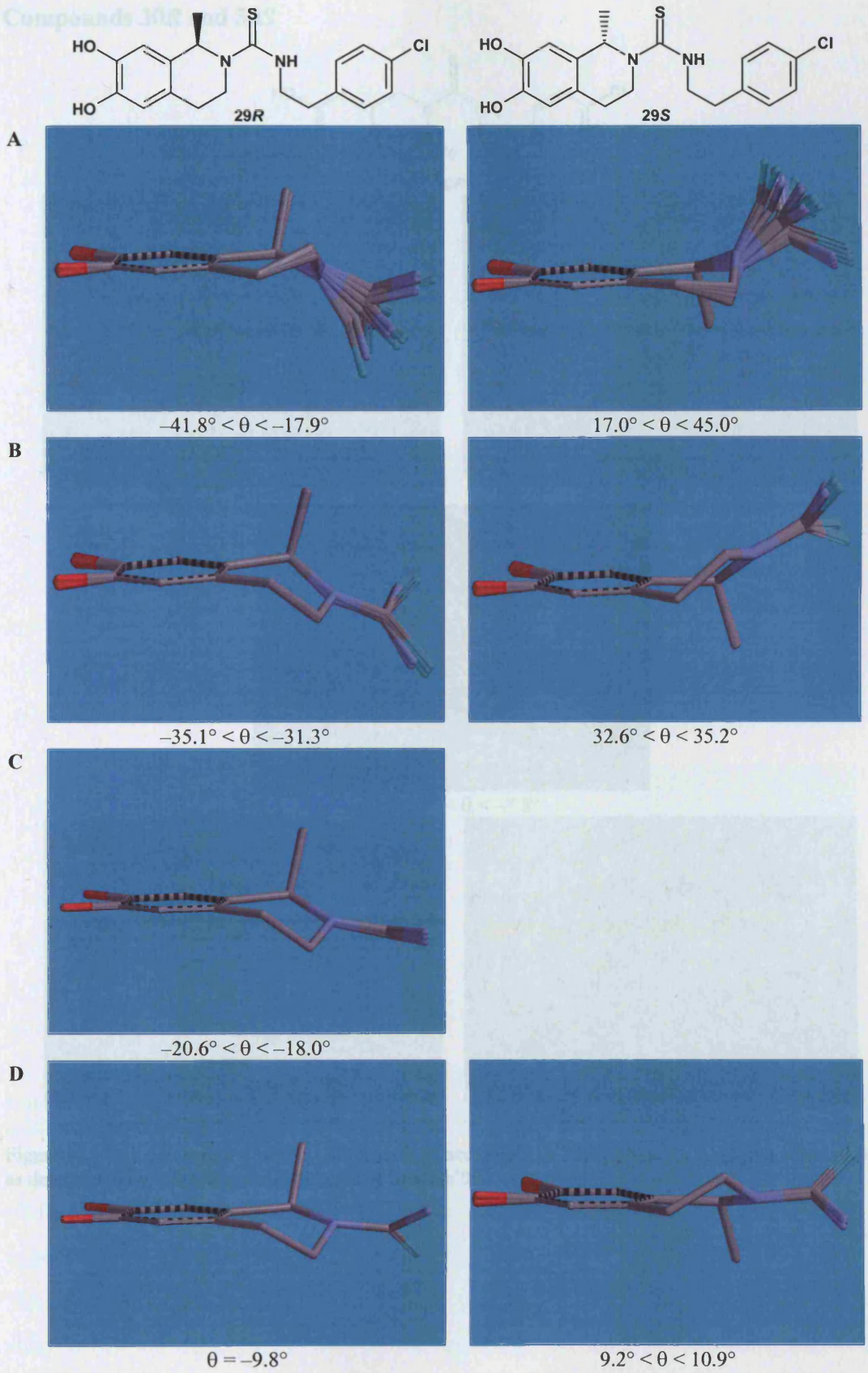

Figure 152: A tabular representation of the classes of conformation accessible to **29*R*** and **29*S*** (minus the C-region sidechain), as determined by molecular modelling using Spartan'02.

Compounds 30*R* and 30*S*

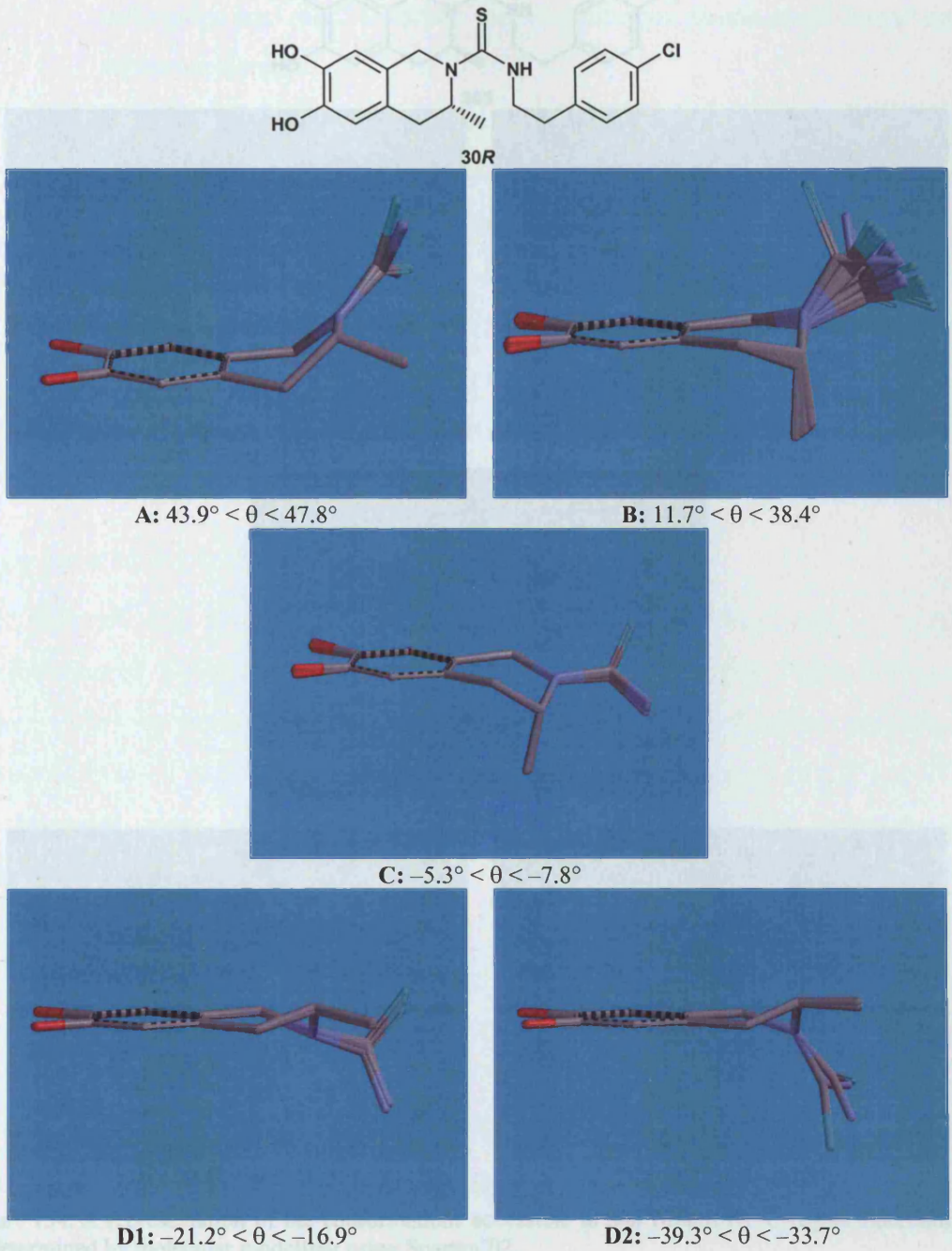

Figure 153: A representation of the conformations accessible to **30*R*** (minus the C-region sidechain), as determined by molecular modelling using Spartan'02.

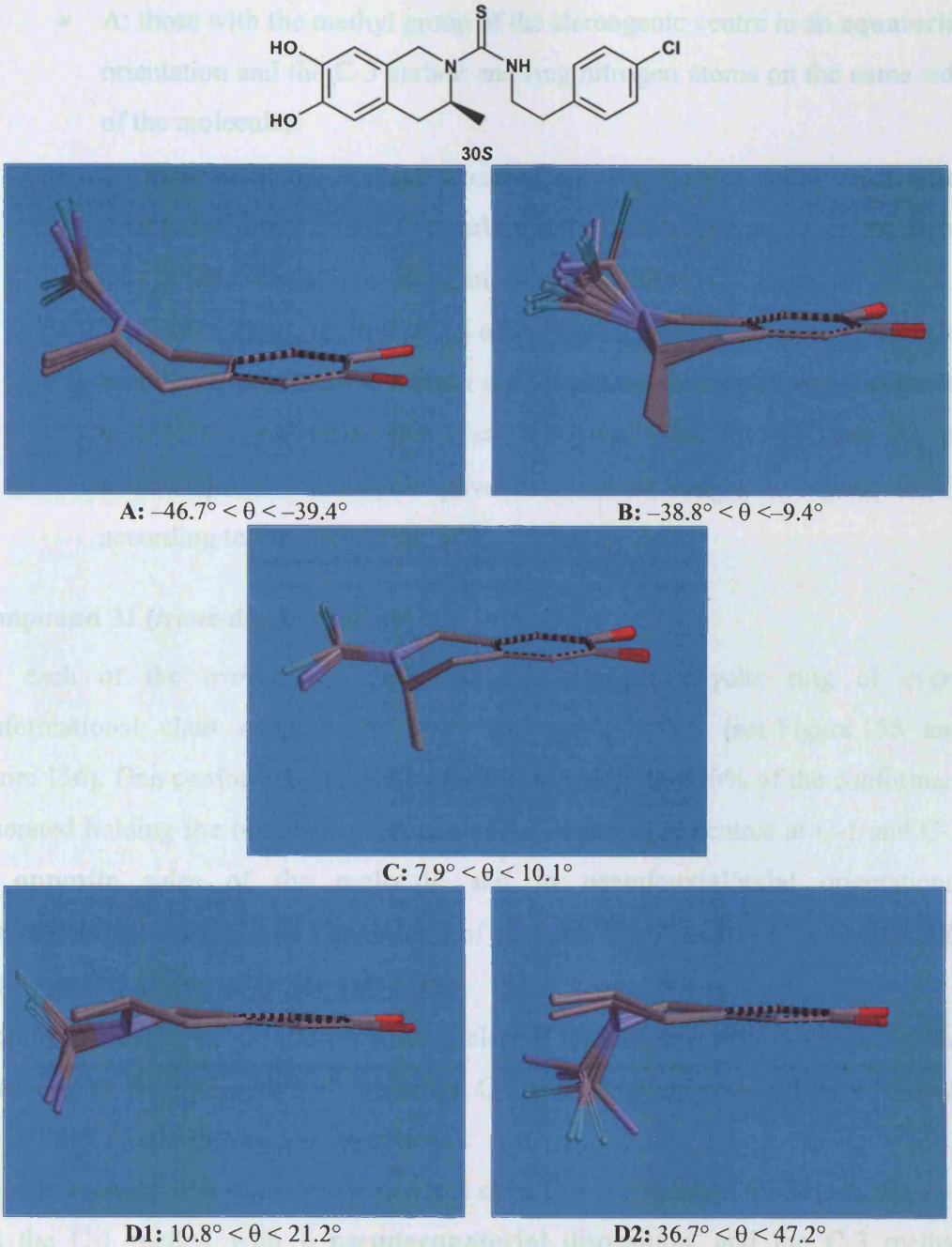

Figure 154: A representation of the conformations accessible to **30*S*** (minus the C-region sidechain), as determined by molecular modelling using Spartan'02.

The generated conformers of **30*R*** and **30*S*** gave a wide range of calculated values for θ, and four associated conformational classes (see Figure 153 and Figure 154).

The most populated class of conformers was B (~65%). These conformers also adopted the half-chair shape, and had the methyl group of the stereogenic centre in a **axial** orientation, and the C-3 carbon and ring nitrogen atoms on the **opposite** side of the molecule. The remaining conformers were evenly distributed between:

- A: those with the methyl group of the stereogenic centre in an **equatorial** orientation and the C-3 carbon and ring nitrogen atoms on the **same** side of the molecule;
- C: those with the methyl group of the stereogenic centre in a **axial** orientation, but with the C-3 carbon and ring nitrogen atoms on the **same** side of the molecule, resulting in a more extended conformation;
- D: those with the methyl group of the stereogenic centre in an **equatorial** orientation and the C-3 carbon and ring nitrogen atoms on the **opposite** side of the molecule. This class was subdivided into D1 and D2, as disposition of the bicycle gave two narrow ranges of values for θ, according to the disposition of the thiourea.

Compound 31 (*trans*-diastereomers)

For each of the *trans*-diastereomers of **31**, the heterocyclic ring of every conformational class adopted the half-chair configuration (see Figure 155 and Figure 156). One conformational class (**A**) dominated, with >90% of the conformers generated holding the two methyl groups of the stereogenic centres at C-1 and C-3 on **opposite** sides of the molecule and in **pseudoaxial/axial** orientations. Conformational class A gave values for θ of between –36.6° and –8.8° for **31(1*R*,3*R*)** and between 8.1° and 37.0° for **31(1*S*,3*S*)**.

In comparison, the minor conformational class B had the two methyl groups on the **same** side of the molecule and, while the C-1 methyl group was still **pseudoaxial**, the C-3 methyl group was now **equatorial**.

A single example of a third conformational class C was generated for **31(1*R*,3*R*)**, and had the C-1 methyl with a **pseudoequatorial** disposition, and the C-3 methyl oriented **axially**, again placing the methyl groups on opposite sides of the molecule. Presumably **31(1*S*,3*S*)** would also access this conformation.

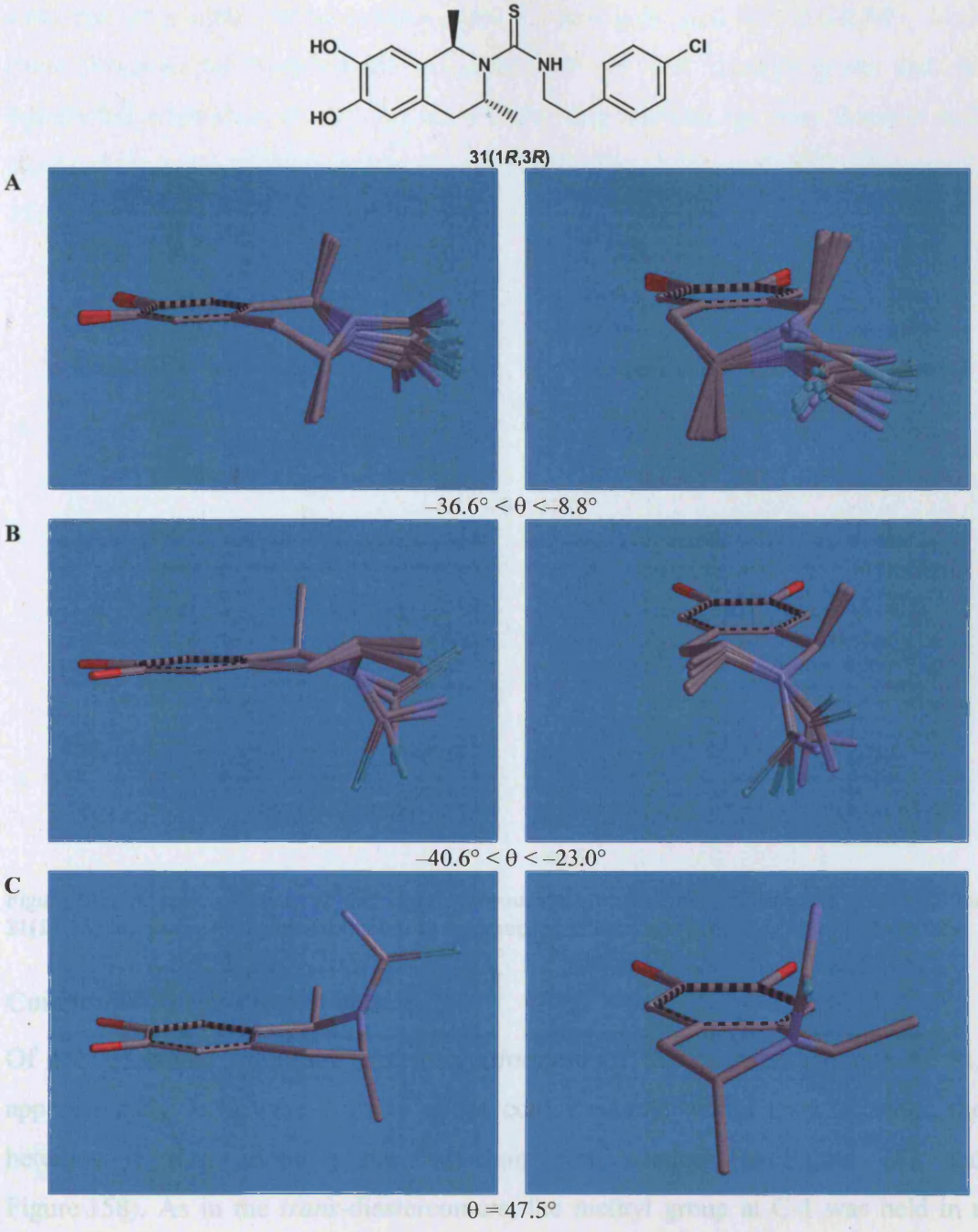

Figure 155: A representation of the three conformational classes of conformation generated for **31(1*R*,3*R*)** (minus the C-region sidechain), as determined by molecular modelling using Spartan'02.

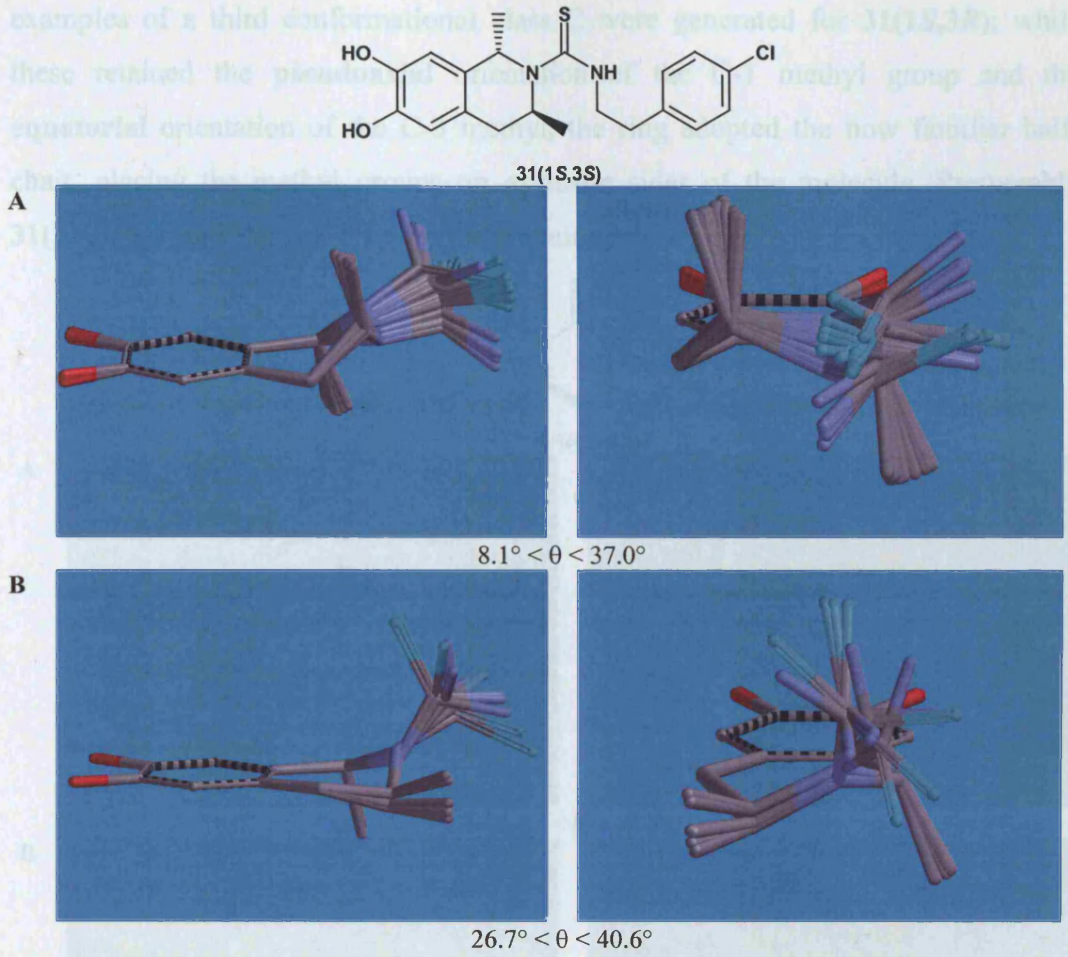

Figure 156: A representation of the two conformational classes of conformation generated for **31(1*S*,3*S*)** (minus the C-region sidechain), as determined by molecular modelling using Spartan'02.

Compound 31 (*cis*-diastereomers)

Of the generated minimum energy conformers of the *cis*-diastereomers of **31**, approximately 75% were seen to adopt conformations within class A with the heterocyclic ring adopting the half-chair configuration (see Figure 157 and Figure 158). As in the *trans*-diastereomers, the methyl group at C-1 was held in a **pseudoaxial** orientation, while the methyl group at C-3 was held in a genuinely axial orientation, but this time the methyl groups were held on the **same** side of the molecule, and the measured values for θ were between ~10° and 28° (negative for **31(1*R*,3*S*)**, positive for **31(1*S*,3*R*)**).

By comparison, the heterocyclic ring of the conformers in class B (20-25% of the generated conformations) appeared to be boat-shaped, with the two methyl groups of the stereogenic centres at C-1 and C-3 held on **opposite** sides of the molecule; with C-1 adopting an **pseudoaxial** orientation, and C-3 an **equatorial** one. Three

examples of a third conformational class C were generated for **31(1*S*,3*R*)**; while these retained the **pseudoaxial** orientation of the C-1 methyl group and the **equatorial** orientation of the C-3 methyl, the ring adopted the now familiar half-chair, placing the methyl groups on **opposite** sides of the molecule. Presumably **31(1*R*,3*S*)** would also access this conformation.

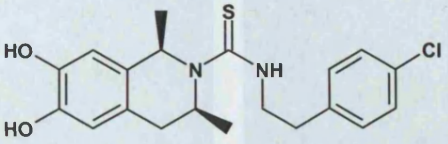

31(1*R*,3*S*)

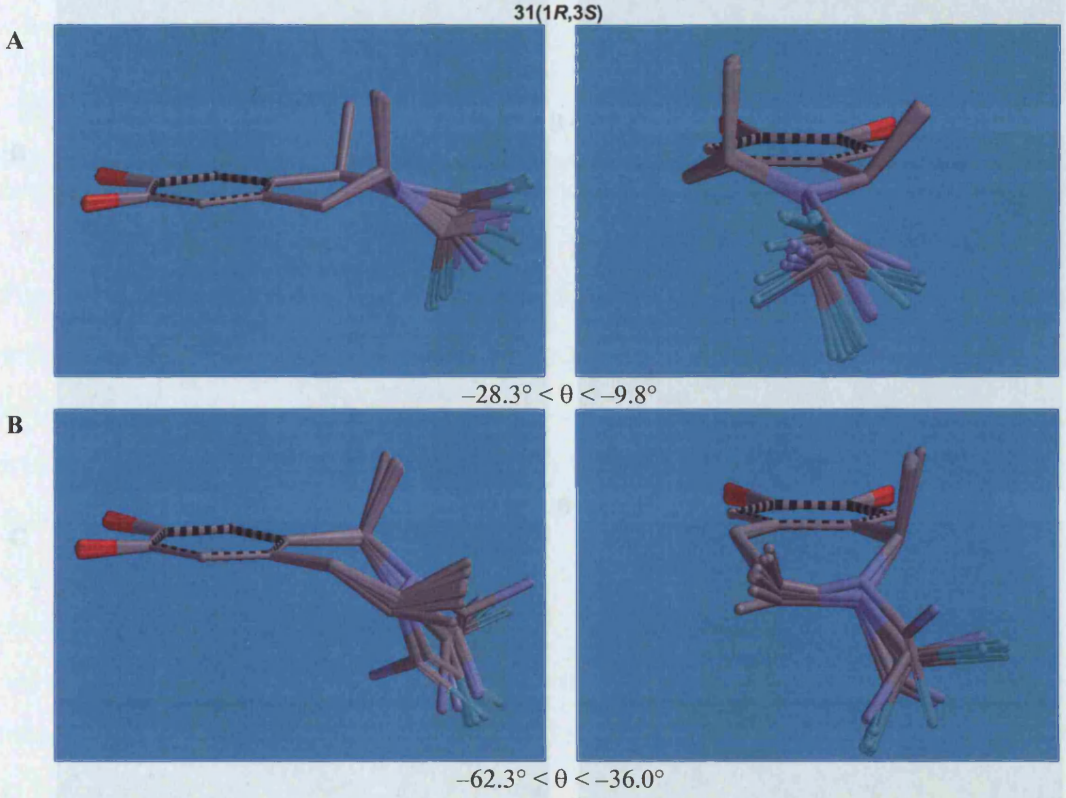

Figure 157: A representation of the two classes of conformation generated for **31(1*R*,3*S*)** (minus the C-region sidechain), as determined by molecular modelling using Spartan'02.

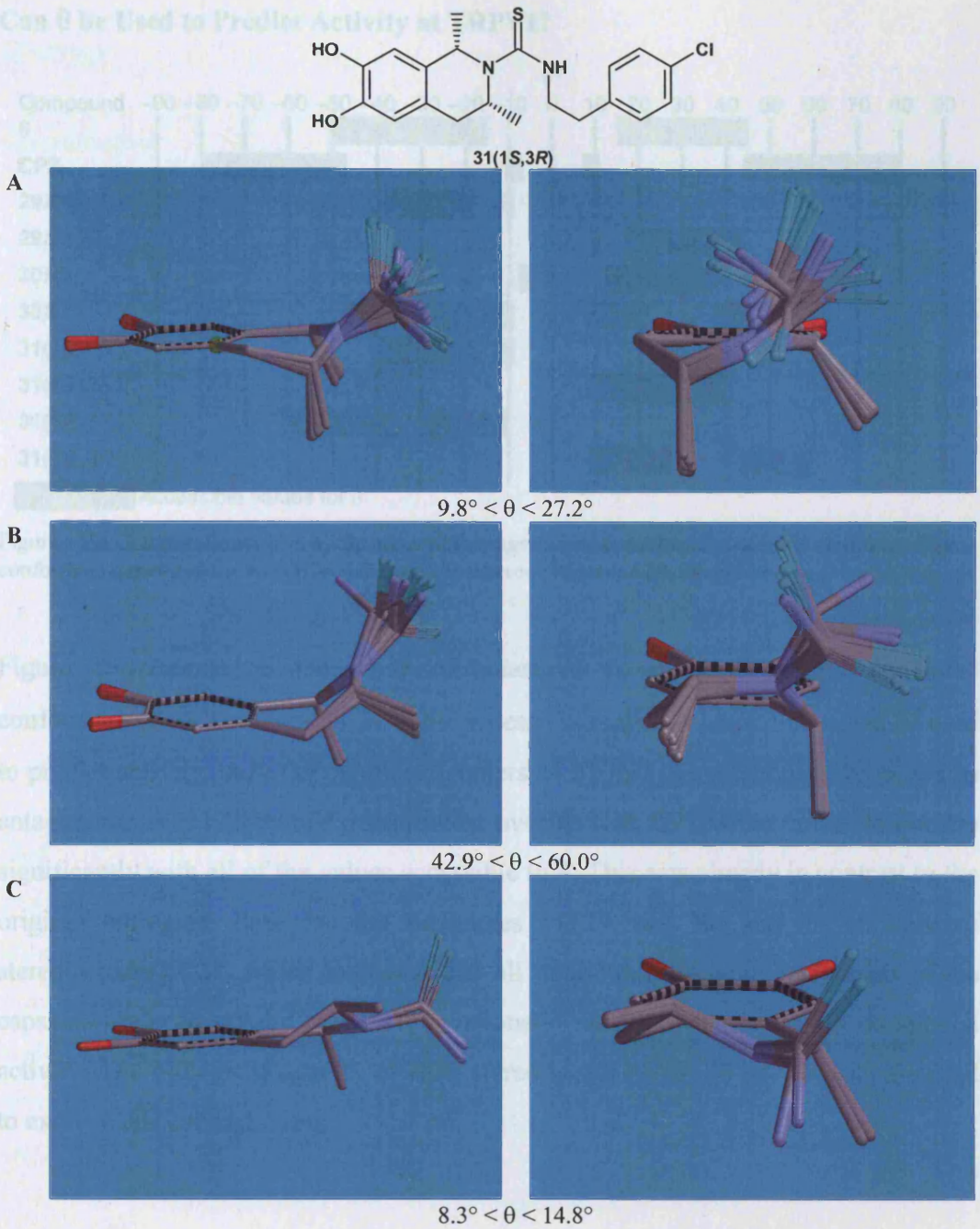

Figure 158: A representation of the three classes of conformation generated for **31(1*S*,3*R*)** (minus the C-region sidechain), as determined by molecular modelling using Spartan'02.

Can θ be Used to Predict Activity at TRPV1?

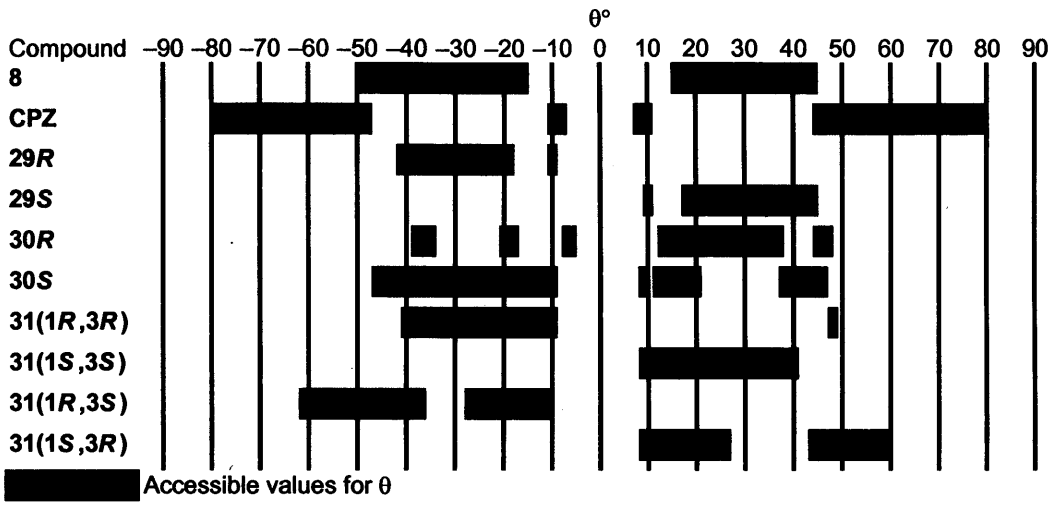

Figure 159: Graphic summation of the accessible ranges of measured values of θ for the low energy conformers generated for each of **8**, CPZ, and the stereoisomers of **29**, **30** and **31**.

Figure 159 summarises the range of measured values of θ for the generated conformers of each compound, with the accessible ranges in black. If θ could be used to predict activity, only the *cis*-diastereomers of **31** had the potential to be active as antagonists, as only they had a significant overlap with CPZ while failing to overlap significantly with all of the values accessible to **8**. This was already in contrast to the original biological data for the racemates of **29** and **30**, and the mixture of stereoisomers of **31**, which indicated that all three mixtures were antagonists of the capsaicin-induced uptake of $^{45}Ca^{2+}$ by neonatal rat DRG neurons, with no agonist activity. The biological activity of each stereoisomer of **29**, **30** and **31** was assessed to explore this contradiction.

Biology

Introduction

The primary assays for determining the activities of test compounds against TRPV1 were performed by the Biology Department of the Novartis Institute for Medical Sciences (NIMS) in London.

Key points:

- the opening of the TRPV1 ion channel causes changes in $[Ca^{2+}]_i$. This allows the activation of TRPV1, and inhibition of any such activation, to be followed by monitoring changes in $[Ca^{2+}]_i$;
- when testing compounds for antagonism, it is possible for potent agonist compounds to gave false readings as potent antagonists, through desensitisation of the TRPV1 ion channel (see *Antinociceptive Action of Capsaicin*). It was therefore necessary to initially test the synthesised stereoisomers of **29**, **30** and **31** for any agonism at TRPV1, before entering them into the antagonist assays.

The decision to resolve by synthesis the stereoisomers of **29, 30** and **31** was made based upon the biological activity of the unresolved mixtures of stereoisomers as antagonists of the capsaicin-induced influx of $^{45}Ca^{2+}$ ions into cultured neonatal rat DRG neurones[66] (see the section entitled *Further conformationally constrained antagonists*). The commencement of the synthetic phase of this research project was accompanied by a number of key advances in the study of the biological actions of capsaicin, including:

- the identification of the capsaicin receptor as TRPV1[73];
- the successful cloning and stable expression of TRPV1 orthologues for, amongst others, rat[73], guinea pig[77] and human[74;75].
- the identification of other activators of TRPV1, such as low pH and noxious heat[73].

These key advances resulted in the replacement at NIMS of the isolated, cultured DRG neurone with Chinese hamster ovary (CHO) cells expressing the required orthologue of TRPV1, cloned from DRG derived cDNA libraries[75]. Each cell line was fully characterised and validated as representative for native TRPV1 activity, using capsaicin, low pH and noxious heat[75].

While having the advantage of accurately representing the native state, the harvesting, isolation and culturing of DRG neurones from neonatal rats is time consuming, labour intensive and comparatively low yielding. CHO cells stably transfected with cDNA for TRPV1 orthologues are more stable, more robust and are amenable to being grown in culture, hence are ethically preferable.

In addition to changes in cells, the development of fluorimetric techniques to measure $[Ca^{2+}]_i$, have removed the requirement to use the radioactive isotope 45 of calcium in cell-based functional assays. The cytosolic concentration of calcium ions $[Ca^{2+}]_i$ can now be measured by using any one of a number of commercially available fluorimetric dyes. Generally, each dye incorporates a fluorophore, and selectively chelates calcium ions. The chelation of a calcium ion causes both a shift in the wavelength and an increase in the intensity of the fluorescence. The change in fluorescence is proportional to $[Ca^{2+}]_i$, thereby the measurement of changes in fluorescence allows the measurement of changes in $[Ca^{2+}]_i$. Two fluorimetric dyes were used for the assays at NIMS; the dye used in the agonist assay was fluo-4[507] (see Figure 160), and the dye used in the antagonist assays was fura-2[508] (see Figure 161). Each dye was loaded into intact cells by incubation with the membrane-soluble acetoxymethyl (AM) ester form (see Figure 160 and Figure 161); once incorporated into the cell, cytosolic esterases hydrolyse the ester groups, to leave the membrane-impermeable form of the dye 'trapped' within the cell.

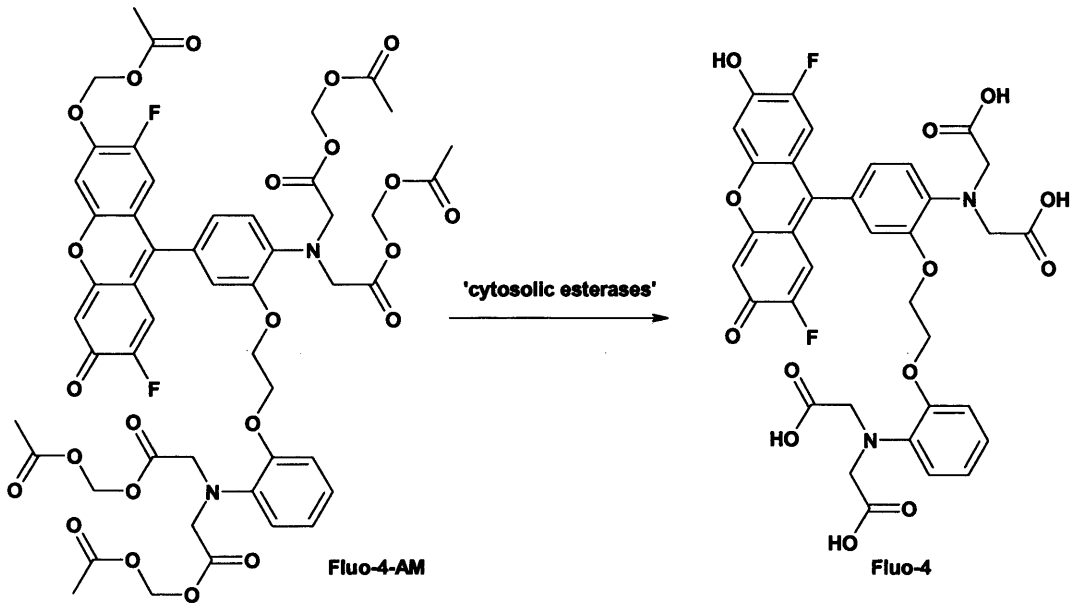

Figure 160: Structure of the fluorimetric dye fluo-4 and its membrane-permeable precursor fluo-4-AM[507].

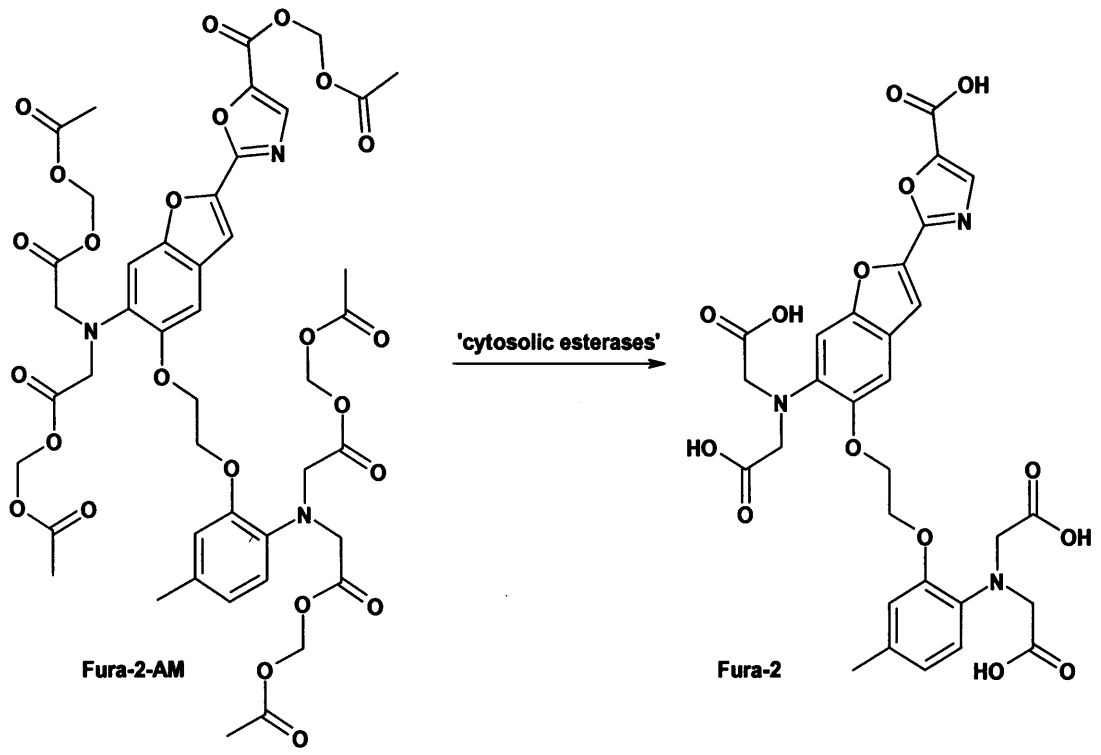

Figure 161: Structure of the fluorimetric dye fura-2 and its membrane-permeable precursor fura-2-AM[508].

Biological Assay Strategy and Data

Given the advances made since the original mixtures of stereoisomers of **29**, **30** and **31** were assayed, it was no longer possible have the resolved stereoisomers tested against neonatal rat DRG neurones. Instead, these compounds were initially tested as potential agonists at CHO cells expressing either rTRPV1 or hTRPV1, with the 1,3-unsubstituted analogue **8** included for comparison (see Table 9), and only compounds showing no, or very weak, agonist activity were subsequently tested as antagonists of both capsaicin-mediated and low pH-mediated activation of rTRPV1 and hTRPV1, with CPZ included for comparison (see Table 10).

As already described, CPZ is an antagonist of the capsaicin-induced activation of the rat[73], guinea pig[77] and human[75] orthologues of TRPV1. However, while CPZ also successfully blocks the opening of TRPV1 by protons and noxious heat in the guinea pig[77] and the human[75], CPZ does **not** block the proton-induced activation of TRPV1 in the rat[75], and is much less effective at inhibiting the noxious heat-induced activation of the same[75] (see section entitled *CPZ as an Analgesic*).

	Agonist assay data; EC_{50} in μM. (percentage of maximal capsaicin response)	
Compound	rTRPV1	hTRPV1
Capsaicin	0.0043±0.0003	0.0075±0.0005
8	0.0026±0.0008 (109.4±1.7)	0.0265±0.0121 (71.7±9.2)
CPZ	Not active @ 30μM	Not active @ 30μM
29*R*	0.1344±0.078 (109.0±5.5)	>21 (34.8±9.8)
29*S*	0.0122±0.011 (89.4±3.1)	Not active @ 30μM
30*R*	0.0505±0.0055 (77.7±4.4)	Not active @ 30μM
30*S*	0.0097±0.0036 (84.0±2.7)	Not active @ 30μM
31(1*R*,3*R*)	1.086±0.3129 (103.6±2.5)	13.34±3.62 (59.7±9.1)
31(1*S*,3*S*)	0.0452±0.0187 (58.9±2.5)	Not active @ 30μM
31(1*R*,3*S*)	13.93±6.7225 (72.6±3.3)	Not active @ 30μM
31(1*S*,3*R*)	Not active @ 30μM	Not active @ 30μM

Table 9: *In vitro* data for the resolved stereoisomers of **29**, **30** and **31** as agonists at hTRPV1 and rTRPV1.

	Antagonist assay data; IC_{50} in μM			
	rTRPV1		hTRPV1	
Compound	vs. pH	vs. capsaicin	vs. pH	vs. capsaicin
CPZ	>10	0.640±0.04	0.103±0.02	0.093±0.018
29*R*	Agonist, so not tested		>30	2.012±0.28
29*S*	Agonist, so not tested		>30	0.055±0.013
30*R*	Agonist, so not tested		>30	0.079±0.011
30*S*	Agonist, so not tested		0.166±0.045	0.017±0.0031
31(1*R*,3*R*)	Agonist, so not tested		>30	4.20±0.73
31(1*S*,3*S*)	Agonist, so not tested		No fit	0.021±0.010
31(1*R*,3*S*)	Agonist, so not tested		>30	0.767±0.133
31(1*S*,3*R*)	>30	0.161±0.014	0.390±0.085	0.045±0.0051

Table 10: *In vitro* data for the resolved stereoisomers of **29**, **30** and **31** as antagonists of capsaicin- and pH-induced activation of the rat (rTRPV1) and the human (hTRPV1) orthologues of TRPV1.

What was immediately apparent from the agonist data in Table 9 was that, despite the original $^{45}Ca^{2+}$/DRG assay identifying the racemates of **29** and **30** as having no agonist activity in the rat at up to 100μM (see the section entitled *Further Conformationally Constrained Antagonists*), the current protocol has identified the resolved enantiomers of each as moderate to potent agonists at rTRPV1. This was most unexpected, as the activities of capsaicin, **8** and CPZ were consistent across the agonist and antagonist assays (see Figure 162).

	agonist $EC_{50}(\mu M)$		antagonist vs. capsaicin $IC_{50}(\mu M)$	
	DRG/$^{45}Ca^{2+}$	CHO-rTRPV1 Fluo-4	DRG/$^{45}Ca^{2+}$	CHO-rTRPV1 Fura-2
Capsaicin	0.30±0.01	0.0043±0.0003	NT	NT
8	0.29 ± 0.04	0.0026±0.0008	NT	NT
CPZ	>100	>30	0.420 ± 0.046	0.640±0.04

Figure 162: Comparison of capsaicin, **8** and CPZ as agonists of rat DRG neurones and rTRPV1 expressed in CHO cells, and CPZ as an antagonist of the capsaicin-induced activation of rat DRG neurones and rTRPV1 expressed in CHO cells.

These contradictory data could not be reconciled with one another. Unfortunately, it was not possible to assay either the original mixtures of stereoisomers of **29**, **30** and **31** in the CHO cell-based functional assays, or the resolved stereoisomers as agonists of the capsaicin receptor in isolated, cultured neonatal rat DRG neurones, as the running of these assays has been discontinued at NIMS. One plausible explanation stems from the fact that ion channels such as TRPV1 do not work in isolation, but in conjunction with many accessory proteins that modulate the function of the ion channel. In the assays using CHO cells and recombinant DNA, although the cloned and expressed orthologue of TRPV1 is from the rat, the full complement of accessory proteins in CHO cells are the **hamster** equivalent. While this is unimportant for capsaicin, **8** and CPZ, it is enough to alter the functionality of the receptor complex, with respect to the resolved enantiomers of **29** and **30**, and possibly **31(1*S*,3*S*)**.

Whatever the reason, this difference in activity between the 'wild' type TRPV1 of the rat DRG neurone and the recombinant rat orthologue in CHO cells requires investigation.

Interestingly, the resolved diastereomers of **31** feature both a potent agonist of rTRPV1 in **31(1*S*,3*S*)**, and a potent capsaicin antagonist in **31(1*S*,3*R*)**. The mixture of stereoisomers of **31** also showed no agonist activity in the original $^{45}Ca^{2+}$/DRG assay, but this could be explained by the relative potencies and diastereomeric ratio in the mixture (6:1, *cis*:*trans*; see Figure 93).

What is also apparent from considering the agonist data from Table 9 and the antagonist data from Table 10 is there is a profound species difference in the activity of almost every one of the resolved compounds. Given that the only difference

between the two cell lines is the origin of the TRPV1 DNA, this must be the reason for the difference. Although there is some evidence for species selectivity in the activity of some compounds at these two orthologues of TRPV1 (*e.g.* phorbol-12-phenylacetate-13-acetate-20-homo-vanillate (PPAHV) shows some agonism of ratTRPV1, but is virtually inactive at human TRPV1[75], and CPZ is a more potent blocker of the capsaicin-induced activation of human TRPV1 than rat TRPV1[75]) **these are the first compounds to show agonism at one orthologue of TRPV1 and antagonism at another**. Such compounds could prove highly useful in the exploration of the functional differences between the active sites of rat TRPV1 and human TRPV1.

Analysis of the Biological Data, and its Comparison with θ

Rather than a direct comparison with the conformational rationale of Walpole *et al.*[72], is it possible to formulate a similar hypothesis for the resolved stereoisomers of **29**, **30** and **31** at the recombinant rat and human orthologues of TRPV1 in CHO cells?

Does θ predict biological activity in the rat?

By taking the conformational summary table of Figure 159, and colour coding each compound for biological activity at rTRPV1 (see Figure 163), patterns do emerge, and a conformational hypothesis formulated that θ does appear predictive. The comparatively low potency of CPZ against capsaicin at rTRPV1 might also be explained.

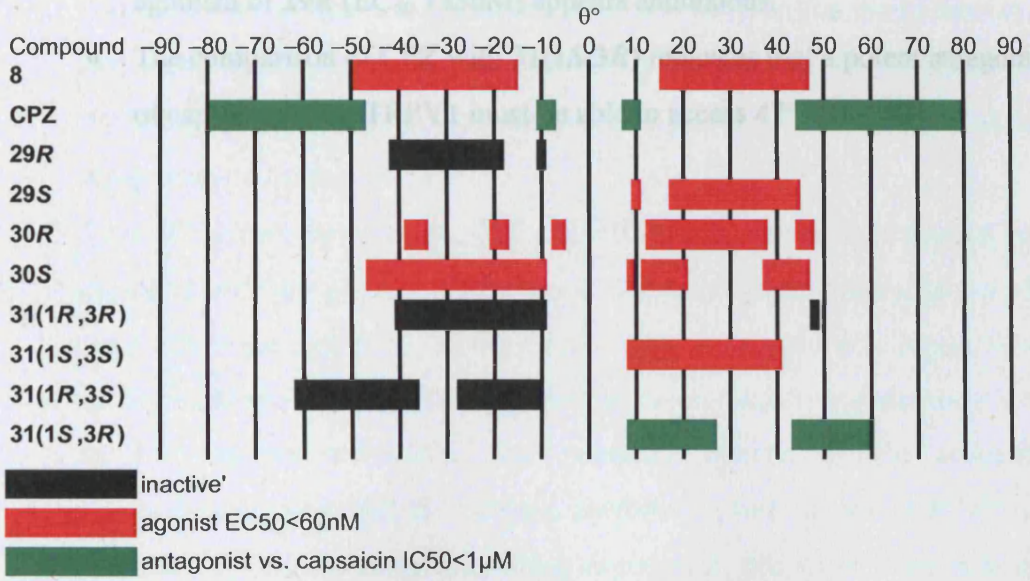

Figure 163: Figure 159, incorporating biological activity at rTRPV1.

- There is extensive overlap between the potent agonist analogues and **8**.
- For biological activity at rTRPV1 (*i.e.*, be it agonist EC_{50} <60nM, or antagonist IC_{50} <1μM), an analogue must be able to access conformations where θ is **positive**; all of the black 'inactive' compounds (*i.e.* **29*R***, **31(1*R*,3*R*)** and **31(1*R*,3*S*)**) have almost exclusively negative values for θ.
- Since half of the conformations of CPZ have values of θ < 0°, and the rigidity of the molecule described in the literature[72] would indicate the requirement of a high input of energy to flip the ring from a conformation with a negative values of θ to one with a positive values, would suggest that at any one time half of the molecules of CPZ are 'stuck' in an inactive conformation.
- Assuming neither CPZ nor **31(1*S*,3*R*)** can attain the necessary conformation for agonism, a comparison of **8** with **31(1*S*,3*R*)** indicates that a potent agonist must be able to access conformations such that 25° < θ < 43°, the only values of θ accessible to **8**, but not accessed by **31(1*S*,3*R*)**.
- Consideration of the values of θ accessed by the newly discovered agonists **29*S***, **30*R***, **30*S*** and **31(1*S*,3*S*)** narrows down this range to 37° < θ < 38°, although as stated earlier, 100 conformations is by no means an exhaustive and complete picture of the accessible conformations, and the agonism of **29*R*** (EC_{50} 135nM) appears anomalous.
- The comparison of CPZ with **31(1*S*,3*R*)** indicates that a potent antagonist of capsaicin at rat TRPV1 must be able to access 47° < θ < 60°.

Does θ predict biological activity in the human?

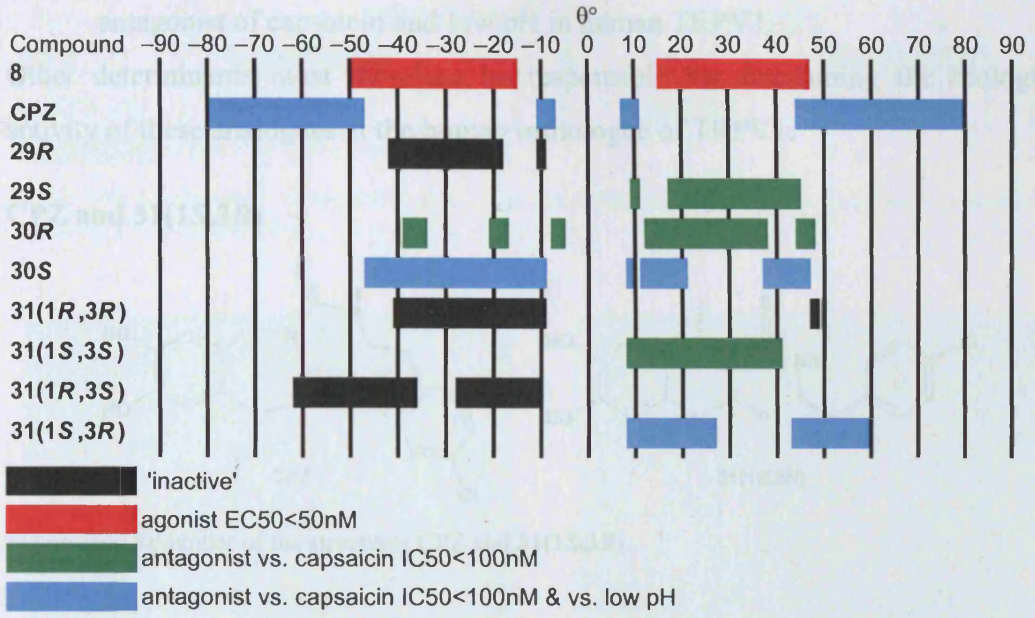

Figure 164: Figure 159, incorporating biological activity at hTRPV1, including data vs. low pH.

As for the rat data, the human data was plotted against θ by colour-coding the conformational summary table (Figure 159) for biological activity (see Figure 164).

- Biological activity (*i.e.*, be it agonist EC_{50} <50nM or antagonist IC_{50} <100nM) was confined to the same molecules that displayed biological activity in the rat orthologue assays.
- Of the four novel rat agonists (**29*S***, **30*R***, **30*S*** and **31(1*S*,3*S*)**), all were antagonists of capsaicin induced activity in the human. As a result, there was complete overlap between the values for θ accredited to the model agonist **8**, and compounds with potent antagonism, as represented by **29*S***, **30*R*** and **31(1*S*,3*S*)**; θ could not therefore be used to distinguish between agonism and antagonism in human TRPV1.
- Two of the new compounds, **30*S*** and **31(1*S*,3*R*)**, were antagonists of both capsaicin and low pH (*c.f.* CPZ) It was not possible to identify values of θ unique to these molecules that did not overlap with agonist **8**. Again, while the 100 conformations generated in the molecular modelling experiment were in no way an exhaustive and complete picture of the accessible conformations, and **30*S*** may access conformers with values of θ>47° not generated by the molecular modelling experiment, this experiment indicated

that θ could not be used to predict whether a compound would be a combined antagonist of capsaicin and low pH in human TRPV1.

Other determinants must therefore be responsible for fine-tuning the biological activity of these analogues at the human orthologue of TRPV1.

CPZ and 31(1*S*,3*R*)

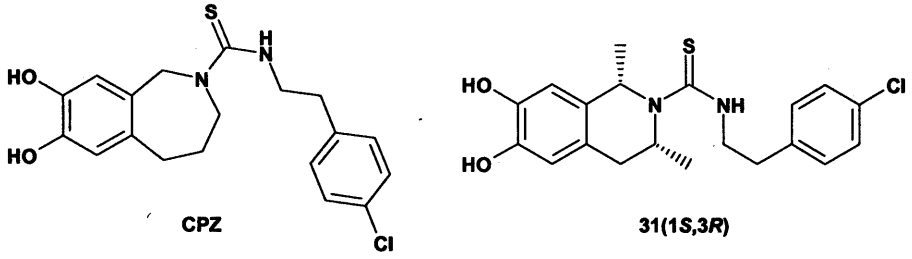

Figure 165: Reminder of the structures CPZ and **31(1*S*,3*R*)**.

Only one of the resolved conformationally constrained stereoisomers (**31(1*S*,3*R*)**) had a similar activity profile to CPZ, although the potencies differed (see Table 11). By comparing the accessible values of θ for CPZ and **31(1*S*,3*R*)** against each other and compound **8**, it was possible to identify the range of values of θ the active conformation of each of CPZ and **31(1*S*,3*R*)** must access as $47° < \theta < 60°$ (see Figure 166). By comparing this range of values for θ with the conformational classes generated for each compound (for CPZ, see Figure 150; for **31(1*S*,3*R*)**, see Figure 158), it was possible to identify the active conformation of CPZ as B_{CPZ}, and the active conformation of **31(1*S*,3*R*)** as $B_{31(1S,3R)}$ (see Figure 167).

	IC_{50} in μM			
	rTRPV1		hTRPV1	
Compound	vs pH	vs. capsaicin	vs pH	vs. capsaicin
CPZ	>10	0.640±0.04	0.103±0.02	0.093±0.018
31(1*S*,3*R*)	>30	0.161±0.014	0.390±0.085	0.045±0.0051

Table 11: *In vitro* data for CPZ and **31(1*S*,3*R*)** as antagonists of capsaicin- and pH-induced activation of the rat (rTRPV1) and the human (hTRPV1) orthologues of TRPV1.

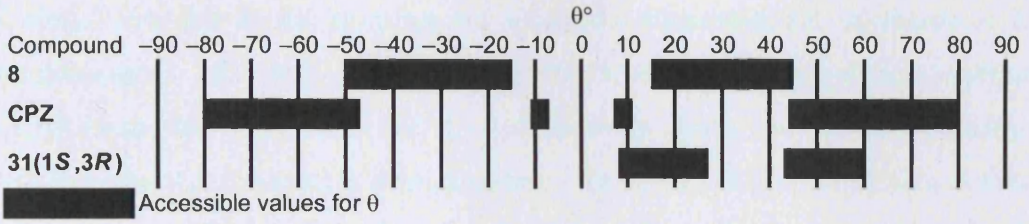

Figure 166: Comparison of the accessible values of θ for the low energy conformers generated for each of **8**, CPZ and **31(1*S*3*R*)**.

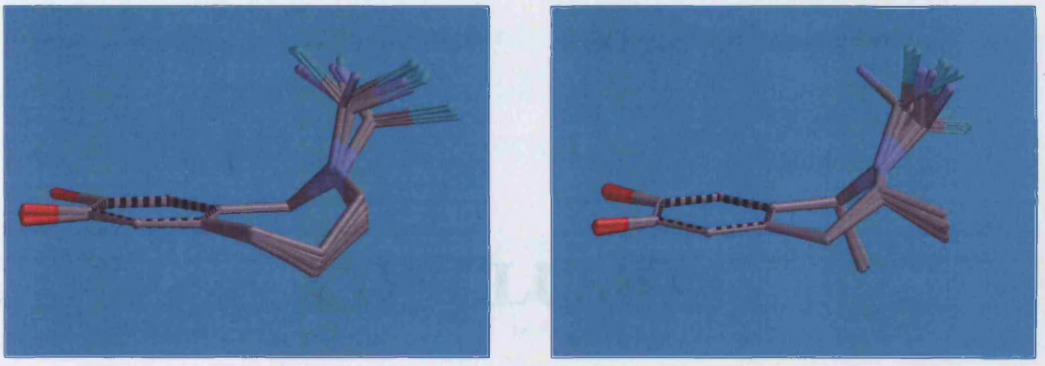

CPZ **31(1*S*,3*R*)**

Figure 167: The active conformations of CPZ and **31(1*S*,3*R*)** as generated by Spartan'02.

Since B_{CPZ} forms only 19% of the generated conformers for CPZ, and $B_{31(1S,3R)}$ forms only 25% of the generated conformers for **31(1*S*,3*R*)**, it would be interesting to identify, synthesise and test a more conformationally constrained analogue.

CONCLUSION

In conclusion, this thesis describes the successful stereoselective syntheses of the stereoisomers of *N*-(4-chlorophenethylthiocarbamoyl)-6,7-dihydroxy-1-methyl-1,2,3,4-tetrahydro-isoquinoline **29**, *N*-(4-chlorophenethylthio-carbamoyl)-6,7-dihydroxy-3-methyl-1,2,3,4-tetrahydroisoquinoline **30** and *N*-(4-chlorophenethylthio-carbamoyl)-6,7-dihydroxy-1,3-dimethyl-1,2,3,4-tetrahydroisoquinoline **31**, via the development of successful stereoselective routes to the intermediate 6,7-dimethoxy-1,2,3,4-tetrahydroisoquinoline precursors **42**, **43** and **44**.

The enantiomers of 6,7-dimethoxy-1-methyl-1,2,3,4-tetrahydroisoquinoline **42** were obtained by the modification of a literature route, employing the enantiomers of (1-phenylethyl)isocyanate as resolving agents (see Figure 168).

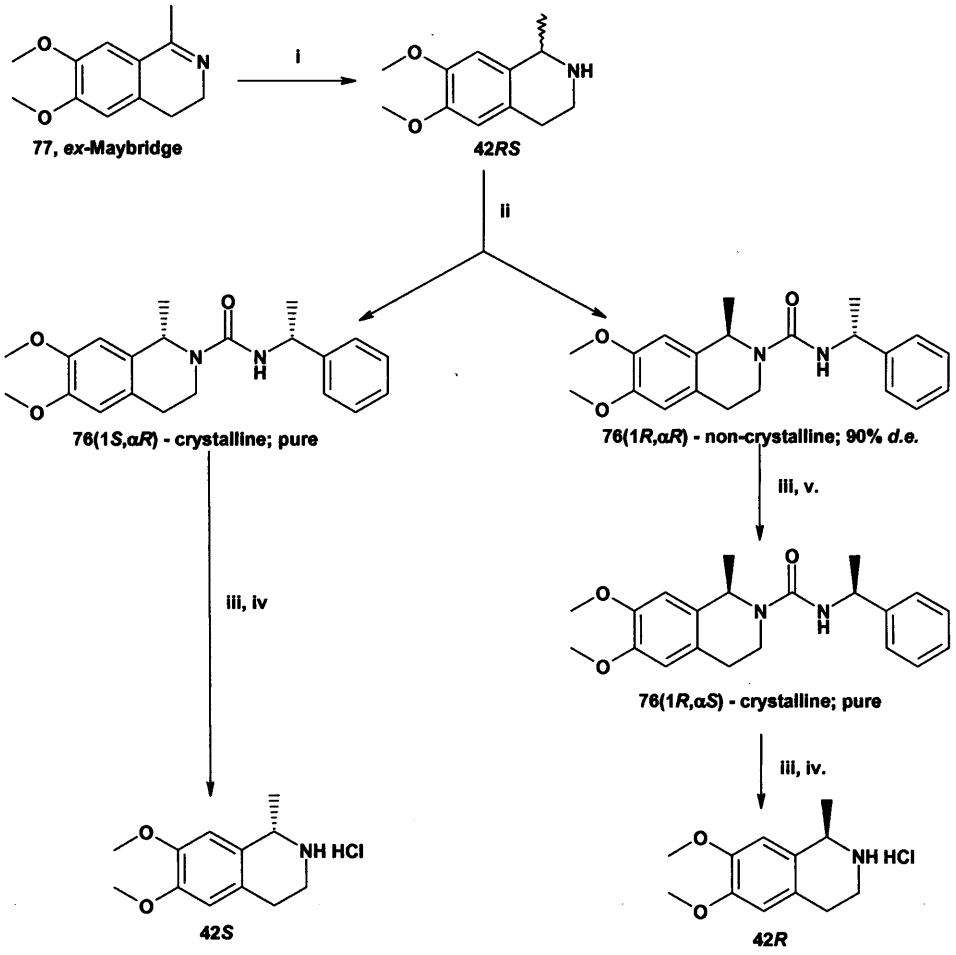

i. $NaBH_4$, MeOH, 0°C - r.t.; ii. (*R*)-(1-phenylethyl)isocyanate **75*R***, Et_3N, CH_2Cl_2;
iii. 2M NaOBu/BuOH, reflux; iv. hydrogen chloride, 1,4-dioxane/methanol;
v.(*S*)-(1-phenylethyl)isocyanate **75*S***, Et_3N, CH_2Cl_2.

Figure 168: Synthetic route to the pure (*R*)- and (*S*)-enantiomers of **42**.

The resolution of the stereogenic centre in the enantiomers of 6,7-dimethoxy-3-methyl-1,2,3,4-tetrahydroisoquinoline **43** was achieved by the separation of the enantiomers of 2-(3,4-dimethoxyphenyl)-1-methylethylamine **38** by crystallisation with the enantiomers of mandelic acid, and subsequent methylene insertion and ring closure under the conditions of the Pictet-Spengler tetrahydroisoquinoline synthesis[415;426] (see Figure 169).

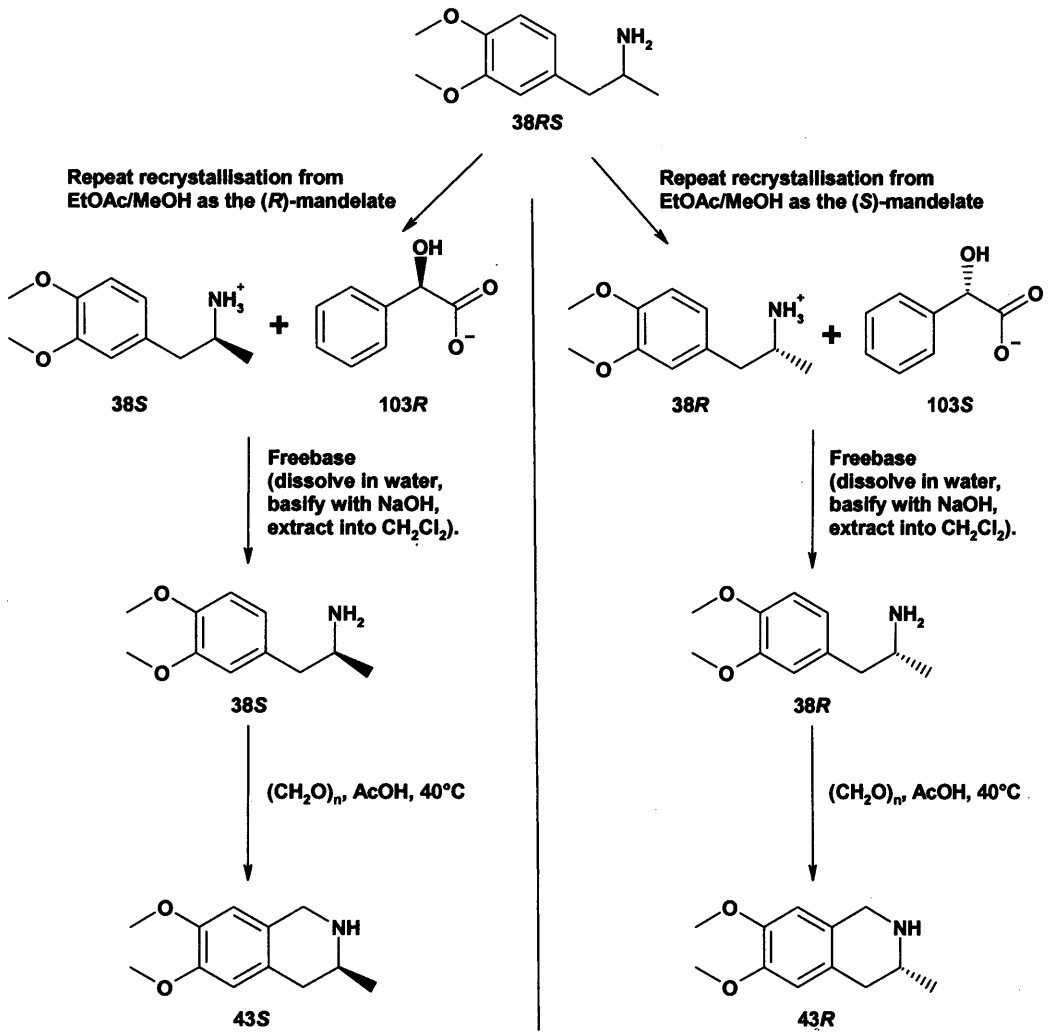

Figure 169: Synthesis of the enantiomers of **43** via the resolution of the enantiomers **38**.

The enantiomers of the *cis*-diastereomer of 6,7-dimethoxy-1,3-dimethyl-1,2,3,4-tetrahydroisoquinoline **44** were synthesised by the stereoselective reduction of the enantiomers of 6,7-dimethoxy-1,3-dimethyl-3,4-dihydroisoquinoline **171** with sodium triacetoxyborohydride. The enantiomers of **171** were synthesised from the resolved enantiomers of **38** via acetylation and cyclisation under Bischler-Napieralski conditions[418;425] (see Figure 170).

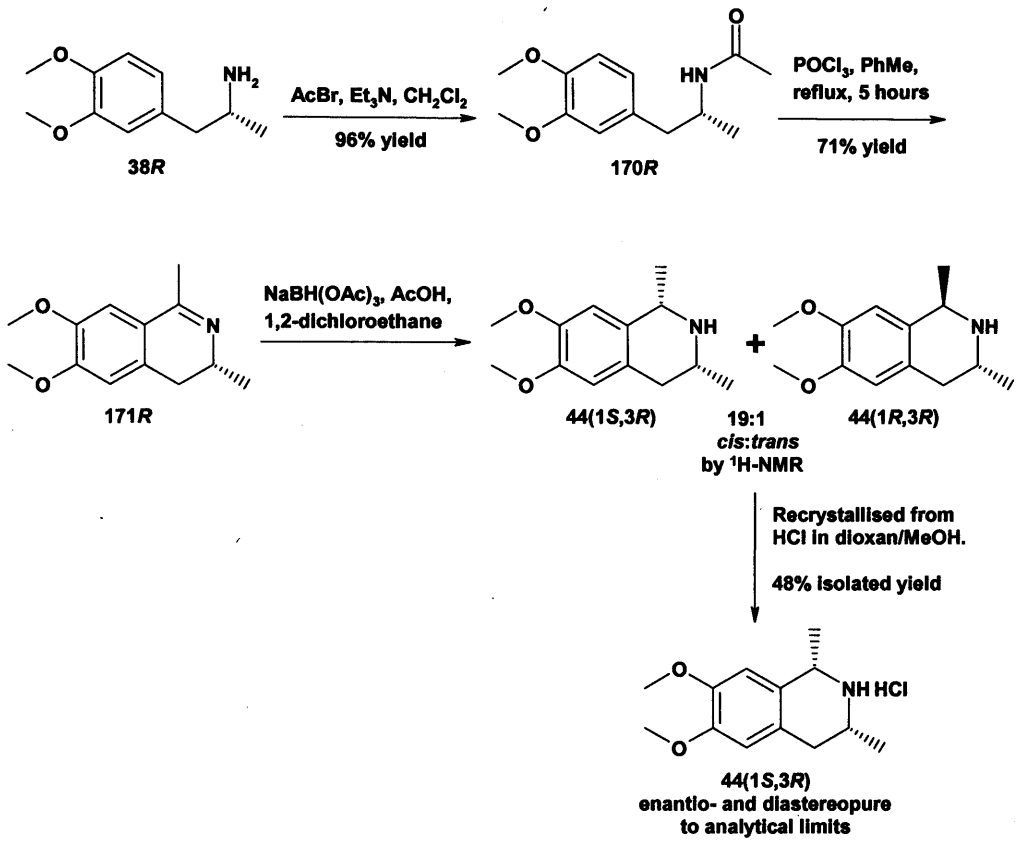

Figure 170: Route to **44(1*S*,3*R*)**, one enantiomer of the *cis*-diastereomer of **44**, from **38*R***.

The enantiomers of the *trans*-diastereomer of **44** were also synthesised from the enantiomers of **38**, via a novel, efficient and highly stereoselective route. The enantiomers of *N*-benzyl-2-(3,4-dimethoxyphenyl)-1-methylethylamine **155** were formed by reductive benzylation of the resolved enantiomers of **38** with benzaldehyde and sodium borohydride. Michael addition of **155** to ethynyl-4-tolylsulfone **150**, followed by TFA-mediated cyclisation, single electron reductive desulfonylation and palladium-catalysed hydrogenolysis, gave the desired enantiomers of the *trans*-diastereomers of 6,7-dimethoxy-1,3-dimethyl-1,2,3,4-tetrahydroisoquinoline **44** (see Figure 171).

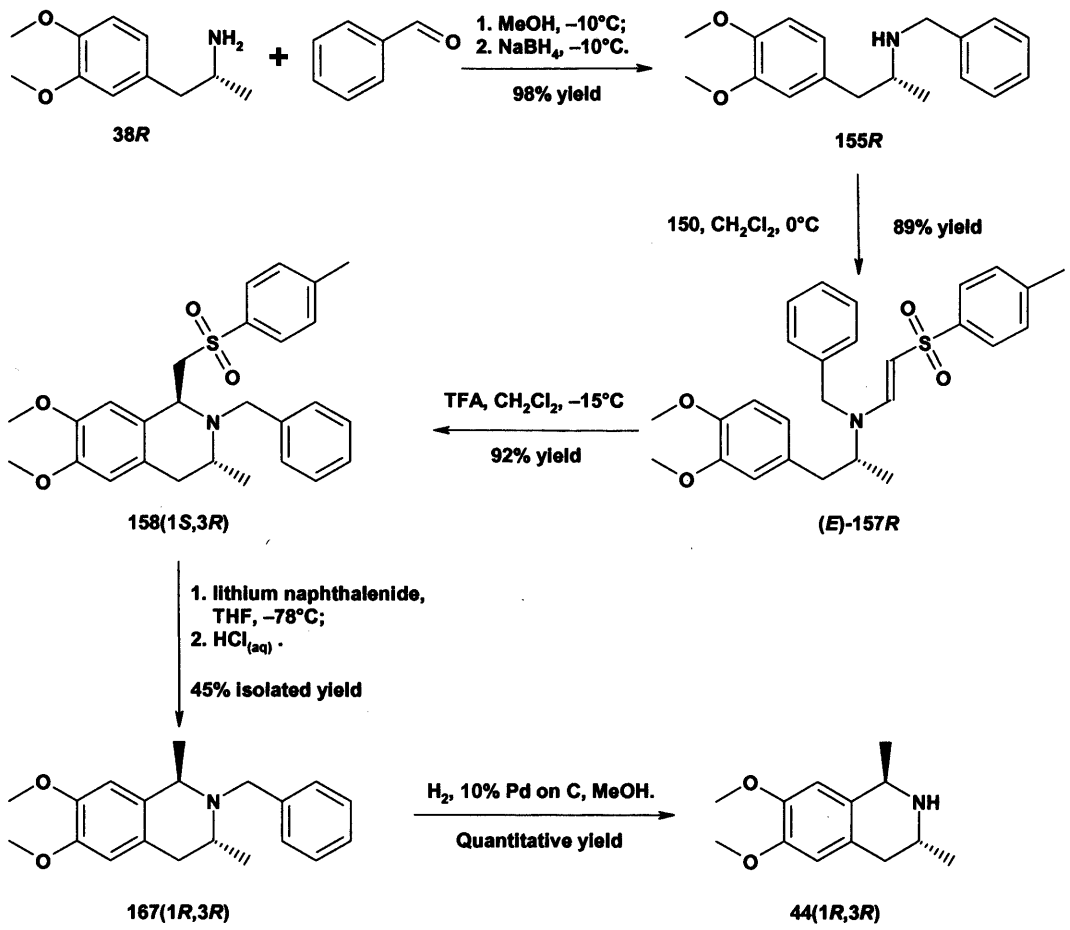

Figure 171: Route to the **44(1*R*,3*R*)**, one enantiomer of the *trans*-diastereomer of **44**, from **38*R***.

The results of investigations into the conformational behaviour of the resolved stereoisomers of **29**, **30** and **31** by techniques of NMR spectroscopy and molecular modelling, the evaluation of their biological activity at the rat and human orthologues of the ion channel TRPV1, and the attempted correlation of the two sets of data, with respect to the published conformational rationale for the activity of CPZ, are also described.

The use of the original conformational parameter α of Walpole *et al.*{Walpole, Bevan, et al. 1994 635 /id} proved to give variable results with the different molecular modelling software. This variability was overcome by defining a new parameter θ, and revising the conformational hypothesis accordingly.

The comparison of θ with the biological activity data demonstrated a general correlation between θ and the activity of the compounds tested for the rat orthologue of TRPV1, but **not** for the human orthologue. Of the compounds tested, **31(1*S*,3*R*)** had a similar activity profile to CPZ, and a comparison of the values of θ available to

each of **31(1*S*,3*R*)**, CPZ and **8** has suggested a target set of values of θ when aiming for future conformationally constrained capsaicin analogues with an activity profile akin to CPZ.

Finally, no less than **four** of the eight analogues (**29*S***, **30*R***, **30*S*** and **31(1*S*,3*S*)**) have been identified as potent antagonists (IC_{50}<100nM) of the capsaicin-induced activation of the human orthologue of TRPV1, while being potent agonists (EC_{50}<60nM) of the rat orthologue of TRPV1. Compounds possessing opposing activities for different mammalian orthologues of TRPV1 have not been previously described in the literature.

EXPERIMENTAL PROCEDURES

Instrumentation and methods

NMR:

^{1}H-NMR were measured at 400MHz, and recorded on a Bruker DPX400 spectrometer.

^{13}C-NMR were measured at 100MHz on the same instrument.

For samples in $CDCl_3$, CD_2Cl_2 and DMSO-d_6, tetramethylsilane was used as an internal reference to δ0.00, unless otherwise stated.

For samples in D_2O, the sodium salt of 3-(trimethylsilyl)propionic-2,2,3,3-d_4 acid was used as an internal reference to δ0.00, unless otherwise stated.

In addition to the usual 1-dimensional ^{1}H- and ^{13}C-NMR experiments, spectroscopic interpretation was facilitated by performing the following series of experiments for the majority of compounds synthesised:

^{13}C DEPT (**D**istortionless **E**nhancement by **P**olarisation **T**ransfer) is an experiment which uses polarisation transfer from protons to the ^{13}C nuclei to enhance signal strength. This experiment can also distinguish whether there are an odd or even number of protons attached to each carbon atom, and can separate CH and CH_3 peaks form CH_2. Peaks due to quaternary carbons do not appear;

H,H-COSY (**CO**rrelation **S**pectroscop**Y**) is a 2D experiment to identify coupled pairs of protons;

HMQC (**H**eteronuclear **M**ultiple **Q**uantum **C**oherence) is a 2D experiment which correlates the signals from the ^{13}C-NMR spectrum with those of the ^{1}H-NMR spectrum, to determine which carbons are directly bonded to which protons ($^{1}J_{CH}$).

HMBC (**H**eteronuclear **M**ultiple **B**ond **C**orrelation) is a 2D experiment to determine long range couplings between carbon atoms, and the protons attached via two ($^{2}J_{CH}$) or three ($^{3}J_{CH}$) bonds. Of note here is the observation that, particularly in aromatic systems, $^{3}J_{CH}$ can be considerably stronger than $^{2}J_{CH}$, as there is no simple relationship between the size of $^{n}J_{CH}$ and the number of intervening bonds This can lead to some confusion for the uninitiated, and accurate interpretation requires careful analysis of the spectrum in combination with other data[509].

IR:

IR spectra were recorded either at NIMS on a Nicolet Avatar 360 FT-IR spectrometer as a film (neat), or by Analytical Services at Novartis Pharma, Basle on a Bruker IFS 66 FT-IR spectrometer, either as KBr pellets or telquel film.

All values are given in cm^{-1}.

MS:

Mass spectral data were recorded at Novartis Pharma, Basle.

Electron impact ionisation mass spectra (EI) were recorded, using a Finnigan MAT 8430 spectrometer (acceleration voltage 3000V).

Electron spray ionisation mass spectra (ESI) were recorded on a Fisons VG Platform II (capillary voltage 3000V).

High resolution electron spray ionisation mass spectra (HRMS) were recorded as an average of 10 measurements, on a Finnigan MAT 900 S spectrometer (capillary voltage 4700V), against PEG 400 as the standard.

X-ray crystallography:

X-ray crystallography was performed at Novartis Pharma AG Basle. Data was collected using a Nonius CAD4 diffractometer, with the structures solved using SHELXS-86 and SHELXL-93.

Elemental analysis:

Elemental analyses were obtained from Solvias AG in Basle, and are within ±0.4% of calculated values.

Optical rotations:

Optical rotations were measured on an Optical Activity AA-100 polarimeter.

Melting points:

Melting points were recorded on a Thermovar Hot Stage microscope, and are uncorrected.

Thin layer chromatography (TLC):

Analytical TLC was performed on either Merck or Whatman 0.25mm silica gel 60-F plates.

Column chromatography:

Flash column chromatography was performed using the Biotage FLASH 12i or 40i systems.

Analytical high performance liquid chromatography (HPLC):

Reverse phase analytical HPLC was performed using either the Waters 600E system controller, 717 autosampler and 996 photodiode array detector and analysed using Waters Millennium software, or the Waters Alliance HPLC system, plus 2996 photodiode array, and analysed using Waters Empower software.

Analytical systems employed were:

	Column	Elution conditions	Wavelength
System 1	Phenomenex Luna 3μ C18 (30 x 4.6mm)	Gradient, from 10–100% acetonitrile in 0.08% aqueous formic acid at 3.0 ml/min over 10 minutes	254nm
System 2	Phenomenex Synergi 4μ MAX-RP (50 x 4.6mm)	Gradient, from 10–100% methanol in 0.1% aqueous TFA at 2.0 ml/min over 10 minutes	254nm
System 3	Hichrom Ltd Nucleosil 120-5C18-250A (250 x 4.6mm)	Gradient, from 10–100% acetonitrile in 0.1% aqueous TFA at 1.5 ml/min over 38 minutes	340nm
System 4	Phenomenex Kingsorb 3μ C18 (30 x 4.6mm)	Gradient, from 10–100% acetonitrile in 0.1% aqueous TFA at 3.0 ml/min over 10 minutes	340nm

All reactions were stirred by magnetic hotplate and follower under an atmosphere of either dry nitrogen or dry argon at room temperature, unless otherwise stated.

Molecular Modelling

Studies on the compounds **8**, CPZ, **29*R***, **29*S***, **30*R***, **30*S***, **31(1*R*,3*R*)**, **31(1*S*,3*S*)**, **31(1*R*,3*S*)** and **31(1*S*,3*R*)** were performed, using the desktop molecular modelling package Spartan'02 (Wavefunction, Inc., Irvine, CA). The molecules were constructed using the build element of Spartan'02, and a local minimum energy conformation generated using Molecular Mechanics Force Fields (MMFF94 – Merck Pharmaceuticals). A representative sample of the conformer distribution available to each compound was generated by applying the same force fields to the local minimum energy conformation to generate a 100 low energy conformers within 10kcal/mol of the lowest energy conformer. These were sorted into groups of similar conformation, overlaid and the C-region sidechains deleted for clarity. The parameter θ was measured for each, using Spartan'02 (for the definition of θ, see the section entitled *Molecular Modelling* within the section entitled *Conformational Analyses of the Stereoisomers of 29, 30 and 31.*).

Enantiomers of *N*-(4-chlorophenethylthiocarbamoyl)-6,7-dihydroxy-1-methyl-1,2,3,4-tetrahydroisoquinoline analogues (29*R* and 29*S*)

6,7-Dimethoxy-1-methyl-1,2,3,4-tetrahydroisoquinoline hydrochloride (42*RS*)

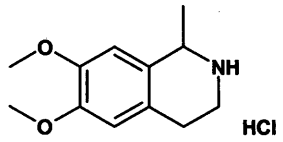

3,4-Dihydro-6,7-dimethoxy-1-methylisoquinoline **77** (*ex*-Maybridge Chemicals; 10g, 0.0488mol) was dissolved in methanol and cooled on an ice/water bath. Sodium borohydride (*ex*-Lancaster Synthesis; 5.54g, 0.1463mol, 3 equivalents) was added portionwise over fifteen minutes. Once addition was complete, the reaction was left to slowly come to room temperature overnight, when it was poured into 0.5M aqueous sodium hydroxide (500mL) and the product extracted into dichloromethane (2 x 250mL). The combined extractions were washed with brine (100mL), and dried over dried magnesium sulfate. Filtration, and the removal of solvent under reduced pressure, gave an orange syrup (10g). The residue was dissolved in dioxan (80mL); 4.0M hydrogen chloride in dioxan (20mL) was added with stirring. The resultant suspension was heated to boiling, and sufficient methanol (~25mL) was added to dissolve the precipitate; the solution was hot-filtered, and left to cool to room temperature overnight. Crystallisation was induced by sonication; the precipitate was filtered and washed with diethyl ether, to give a colourless crystalline solid (10.1g, 85%). Despite attempts to dry the compound (18hours/0.1mmHg/100°C), characterisation (^{1}H-NMR, IR and elemental analysis) revealed the presence of ~0.17 equivalents of water, assumed to be solvent of crystallisation from 'wet' methanol:

Characterisation:

TLC: *Rf* 0.23 (dichloromethane/ methanol/ 32% $AcOH_{(aq.)}$ 90:9:1);

Melting point: 194-5°C (literature 196-197°C{Spath & Dengel 1938 8 /id});

^{1}H-NMR (DMSO-d_6): δ_H 1.61 (3H, d, J = 6.8Hz, $CHCH_3$), 2.86-2.92 (1H, m, $ArCH_AH_BCH_2$), 2.96-3.02 (1H, m, $ArCH_AH_BCH_2$), 3.16-3.23 (1H, m, $CH_2CH_ACH_BN$) 3.30-3.39 (1H, m, $CH_2CH_ACH_BN$), 3.47 (H_2O), 3.73 (3H, s, $ArOCH_3$), 3.74 (3H, s, $ArOCH_3$), 4.41 (1H, quartet, J = 6.8Hz, $CHCH_3$), 6.77 (1H, s, Ar*H*-5), 6.84 (1H, s, Ar*H*-8), 9.75 (2H, br, NH_2^+);

^{13}C-NMR (DMSO-d_6):	δ_C 19.11 ($CH\boldsymbol{C}H_3$), 24.47 ($Ar\boldsymbol{C}H_2CH_2$), 38.16 ($CH_2\boldsymbol{C}H_2N$), 49.75 ($\boldsymbol{C}HCH_3$), 55.41 ($ArO\boldsymbol{C}H_3$), 55.61 ($ArO\boldsymbol{C}H_3$), 109.41 ($\boldsymbol{C}_{Ar}H$-8), 111.53 ($\boldsymbol{C}_{Ar}H$-5), 123.62 ($\boldsymbol{C}_{Ar}$-4a), 125.75 ($\boldsymbol{C}_{Ar}$-8a), 147.56 ($\boldsymbol{C}_{Ar}OMe$), 147.97 ($\boldsymbol{C}_{Ar}OMe$);
MS (EI) *m/z*:	M^+ 207(21), $[M\text{-}CH_3]^+$ 192(100), $[M\text{-}OCH_3]^+$ 176(18);
IR (KBr) *ν*/cm:	3430 (H_2O), 2543 (N^+–H), 1516 (C_{Ar}=C_{Ar}), 1226 (C_{Ar}–OMe);
Microanalysis (C,H,N):	Calculated for $C_{12}H_{18}NO_2Cl$(+0.17 H_2O): 58.42, 7.49, 5.68; Found: 58.39/58.41, 7.33/7.36, 5.72/5.82

2-((*R*)-1-Phenylethyl)carbamoyl-6,7-dimethoxy-1-methyl-1,2,3,4-tetrahydroisoquinoline (76(1*RS*,α*R*))[444]

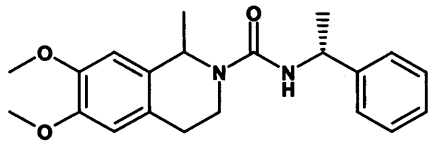

Racemic **42*RS*** (11.5g, 0.0472mol) was dissolved in dry dichloromethane (100mL) with triethylamine (7.23mL, 5.26g, 0.0520mol, 1.1 equivalents) and stirred under nitrogen. After cooling on an ice/water bath, (*R*)-(1-phenylethyl)isocyanate **75*R*** (6.62mL, 6.95g, 0.0472mol) was added, and the reaction was stirred at room temperature overnight.

The reaction was diluted to 500mL with dichloromethane, and washed consecutively with 2.0M hydrochloric acid (2 x 100mL), water (100mL) and brine (50mL), before drying over dried magnesium sulfate. Filtration and the removal of solvent under reduced pressure gave a brown foam (~17.0g, quantitative). Separation of the mixture of diastereomers formed was not apparent by TLC (one spot) or reverse phase HPLC (system 1: a single peak, with a retention time of 5.1 minutes). The separate diastereomers were visualised by:

1. an alternative normal phase analytical HPLC method (Anachem CHI-D-PGC-250A (250 x 4.6mm) column; isocratic elution 20% propan-2-ol in n-hexane; 210nm),
2. ^{1}H-NMR spectral analysis at each of the two aliphatic methyl signals, and
3. ^{13}C-NMR spectral analysis at the peaks corresponding to the racemic stereogenic carbon, the attached methyl group, and the tetrahydroisoquinoline ring methylenes.

Characterisation:

TLC: *Rf* 0.46 (cyclohexane/ethyl acetate 1:1)

^{1}H-NMR ($CDCl_3$): δ_H 1.43-1.46 (3H, 2 x d overlapping, J = 6.7Hz, tetrahydroisoquinoline CHC***H***$_3$), 1.49-1.52 (3H, 2 x d overlapping, J = 6.9Hz, PhCHC***H***$_3$), 2.67-2.73 (1H, m, ArC***H***$_A$H$_B$CH$_2$), 2.79-2.88 (1H, m, ArCH$_A$***H***$_B$CH$_2$), 3.23-3.30 (1H, m, CH$_2$C***H***$_A$H$_B$N), 3.83 (3H, s, ArOC***H***$_3$), 3.84 (3H, s, ArOC***H***$_3$), 3.91-3.97 (1H, m, CH$_2$CH$_A$***H***$_B$N), 4.71-4.77 (1H, m, N***H***), 4.99-5.09 (2H, m, overlapping tetrahydroisoquinoline C***H***CH$_3$ and PhC***H***CH$_3$), 6.57-6.60 (2H, br, Ar***H***-5, -8), 7.21-7.26 (1H, m, Ph***H***-4'), 7.30-7.36 (4H, m, Ph***H***-2', -3', -5', -6');

^{13}C-NMR ($CDCl_3$): δ_C 21.99, 22.09 (tetrahydroisoquinoline CH***C***H$_3$), 22.63 (PhCH***C***H$_3$), 28.35, 28.41 (tetrahydroisoquinoline Ar***C***H$_2$CH$_2$), 37.80, 37.84 (tetrahydroisoquinoline CH$_2$***C***H$_2$N), 49.99, 50.04 (tetrahydroisoquinoline ***C***HCH$_3$), 50.17 (Ph***C***HCH$_3$), 55.93, 56.03 (2 x ArO***C***H$_3$), 109.85 (***C***$_{Ar}$H-8), 111.36 (***C***$_{Ar}$H-5), 126.12 (***C***$_{Ar}$H-2', ***C***$_{Ar}$H-6'), 126.16 (***C***$_{Ar}$-4a), 127.04 (***C***$_{Ar}$H-4'), 128.58 (***C***$_{Ar}$H-3', ***C***$_{Ar}$H-5'), 130.71 (***C***$_{Ar}$-8a), 144.70 (***C***$_{Ar}$-1'), 147.64 (***C***$_{Ar}$OMe), 147.69 (***C***$_{Ar}$OMe), 156.14 (***C***=O);

(*S*)-2-((*R*)-1-Phenylethyl)carbamoyl-6,7-dimethoxy-1-methyl-1,2,3,4-tetrahydro-isoquinoline (76(1*S*,α*R*))[444]

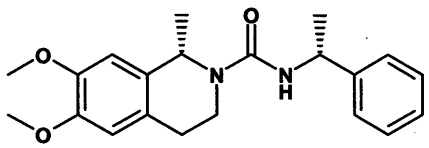

Initial separation of the diastereomers of **76(1*RS*,α*R*)** (~17.0g), was achieved by trituration of the foam with hot ethyl acetate (40mL); the suspension was alternately sonicated and heated, until a fine precipitate was apparent. Filtration gave a colourless powdered solid (8.3g, 50% from **42*RS***), which was seen to be predominantly one diastereomer of **76** by ^{1}H-NMR. The removal of solvent from the filtrate under reduced pressure gave a beige foam (8.2g, 49%); ^{1}H-NMR confirmed

this foam to be predominantly the other diastereomer of **76**. The precipitate was suspended in hot propan-2-ol (50mL); dichloromethane was added until everything was in solution (~85mL). The solution was cooled to room temperature, then refrigerated overnight. It was necessary to remove much of the dichloromethane under reduced pressure to induce crystallisation. Filtration gave a colourless crystalline solid (5.50g, 33% of a maximum possible 50%), confirmed as one diastereomer (*d.e.* 100% by HPLC, ^{1}H- and ^{13}C-NMR):

Characterisation:

TLC:	*Rf* 0.46 (cyclohexane/ethyl acetate 1:1);
Melting point:	210°C;
Optical rotation $[\alpha]_D^{20}$:	+75.0 (c 0.7, chloroform) (lit. +48.0 (c 0.7, chloroform)[444];
^{1}H-NMR ($CDCl_3$):	δ_H 1.44 (3H, d, J = 6.7Hz, tetrahydroisoquinoline CHC***H***$_3$), 1.50 (3H, d, J = 6.9Hz, PhCHC***H***$_3$), 2.67-2.73 (1H, m, ArC***H***$_A$H$_B$CH$_2$), 2.79-2.88 (1H, m, ArCH$_A$***H***$_B$CH$_2$), 3.23-3.30 (1H, m, CH$_2$C***H***$_A$H$_B$N), 3.83 (3H, s, ArOC***H***$_3$), 3.84 (3H, s, ArOC***H***$_3$), 3.91-3.97 (1H, m, CH$_2$CH$_A$***H***$_B$N), 4.75 (1H, d, J = 7.1Hz, N***H***), 4.99-5.09 (2H, m, overlapping tetrahydroisoquinoline C***H***CH$_3$ and PhC***H***CH$_3$), 6.57 (1H, s, Ar***H***-8), 6.59 (1H, s, Ar***H***-5), 7.21-7.26 (1H, m, Ph***H***-4'), 7.30-7.36 (4H, m, Ph***H***-2', -3', -5', -6');
^{13}C-NMR ($CDCl_3$):	δ_C 22.09 (tetrahydroisoquinoline CH***C***H$_3$), 22.63 (PhCH***C***H$_3$), 28.41 (Ar***C***H$_2$CH$_2$), 37.84 (CH$_2$***C***H$_2$N), 50.04 (tetrahydroisoquinoline ***C***HCH$_3$), 50.17 (Ph***C***HCH$_3$), 55.93, 56.03 (2 x ArO***C***H$_3$), 109.85 (***C***$_{Ar}$H-8), 111.36 (***C***$_{Ar}$H-5), 126.12 (***C***$_{Ar}$H-2', ***C***$_{Ar}$H-6'), 126.16 (***C***$_{Ar}$-4a), 127.04 (***C***$_{Ar}$H-4'), 128.58 (***C***$_{Ar}$H-3', ***C***$_{Ar}$H-5'), 130.71 (***C***$_{Ar}$-8a), 144.70 (***C***$_{Ar}$-1'), 147.64 (***C***$_{Ar}$OMe), 147.69 (***C***$_{Ar}$OMe), 156.14 (***C***=O);
MS (ESI positive) *m/z*:	MH$^+$ 355(35), [M+Na]$^+$ 377(100);
IR (KBr) *ν*/cm:	3422 (NH), 1642 (C=O), 1519 (C$_{Ar}$–C$_{Ar}$), 1252 (C$_{Ar}$–OMe);
Microanalysis (C,H,N):	Calculated for $C_{21}H_{26}N_2O_3$ 71.16, 7.39, 7.90; Found 70.91, 7.47, 7.84.

(*R*)-2-((*R*)-1-Phenylethyl)carbamoyl-6,7-dimethoxy-1-methyl-1,2,3,4-tetrahydro-isoquinoline (76(1*R*,α*R*))[444]

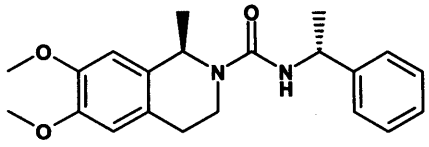

The mother liquors from the repeat recrystallisations to resolve the pure **76(1*S*,α*R*)** were combined, and the solvents were removed under reduced pressure, to give a beige foam; ^{1}H-NMR confirmed this to be predominantly **76(1*R*,α*R*)**, with a small amount of residual **76(1*S*,α*R*)**. Attempts to remove the residual **76(1*S*,α*R*)** by fractional crystallisation were unsuccessful. Despite repeated recrystallisations, a trace of the crystalline diastereomer was always apparent, both in the HPLC traces and the NMR spectra. NMR data for the major diastereomer, the non-crystalline **76(1*R*,α*R*)** is given:

Characterisation:

^{1}H-NMR ($CDCl_3$): δ_H 1.46 (3H, d, J = 6.7Hz, tetrahydroisoquinoline CHC***H***$_3$), 1.52 (3H, d, J = 6.8Hz, PhCHC***H***$_3$), 2.67-2.73 (1H, m, ArC***H***$_A$H$_B$CH$_2$), 2.79-2.88 (1H, m, ArCH$_A$***H***$_B$CH$_2$), 3.23-3.30 (1H, m, CH$_2$C***H***$_A$H$_B$N), 3.83 (3H, s, ArOC***H***$_3$), 3.84 (3H, s, ArOC***H***$_3$), 3.91-3.97 (1H, m, CH$_2$CH$_A$***H***$_B$N), 4.75 (1H, d, J = 7.1Hz, N***H***), 4.98-5.01 (1H, m, C***H***CH$_3$) 5.06-5.11 (1H, m, C***H***CH$_3$), 6.59-6.60 (2H, 2 x overlapping s, Ar***H***-5, Ar***H***-8), 7.21-7.26 (1H, m, Ph***H***-4'), 7.30-7.36 (4H, m, Ph***H***-2', -3', -5', -6');

^{13}C-NMR ($CDCl_3$): δ_C 21.96 (tetrahydroisoquinoline CH***C***H$_3$), 22.62 (PhCH***C***H$_3$), 28.32 (Ar***C***H$_2$CH$_2$), 37.71 (CH$_2$***C***H$_2$N), 49.95 (tetrahydroisoquinoline ***C***HCH$_3$), 50.10 (Ph***C***HCH$_3$), 55.88, 55.97 (2 x ArO***C***H$_3$), 109.71 (***C***$_{Ar}$H-8), 111.25 (***C***$_{Ar}$H-5), 126.09 (***C***$_{Ar}$H-2', ***C***$_{Ar}$H-6'), 126.16 (***C***$_{Ar}$-4a), 127.03 (***C***$_{Ar}$H-4'), 128.54 (***C***$_{Ar}$H-3', ***C***$_{Ar}$H-5'), 130.60 (***C***$_{Ar}$-8a), 144.49 (***C***$_{Ar}$-1'), 147.52 (***C***$_{Ar}$OMe), 147.64 (***C***$_{Ar}$OMe), 156.14 (***C***=O).

(*R*)-2-((*S*)-1-Phenylethyl)carbamoyl-6,7-dimethoxy-1-methyl-1,2,3,4-tetrahydro-isoquinoline (76(1*R*,α*S*))

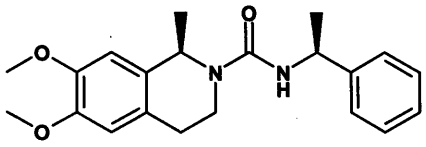

This material was synthesised in two steps from the impure **76(1*R*,α*R*)** (+ **76(1*S*,α*R*)**), obtained from the mother liquors of the resolution of the pure diastereomer **76(1*S*,α*R*)**.

i) Sodium spheres (3.45g, 0.15mol) were dissolved in dry butan-1-ol (75mL), in a flame-dried round-bottomed flask, under argon. The impure **76(1*R*,α*R*)** (+ **76(1*S*,α*R*)**) (10g, 0.0282mol) was dissolved in hot butan-1-ol (35mL), and added to the sodium butoxide solution. The resultant solution was stirred at reflux for six hours, cooled to room temperature, and poured into 2.0M aqueous hydrochloric acid (300mL) to quench residual sodium butoxide. The solution was washed with ether (2 x 100mL); the combined ether washes were washed with fresh 2.0M aqueous hydrochloric acid (100mL), then discarded. The aqueous layers were combined, basified by the addition of 5.0M aqueous sodium hydroxide (250mL), and the desired product was extracted into dichloromethane (3 x 100mL). The combined dichloromethane extractions were washed with brine (50mL), and dried over dried magnesium sulfate. The filtration and removal of solvent under reduced pressure gave a yellow syrup (6.2g, >100%).

The residue was purified by being dissolved in dioxan (30mL), to which concentrated hydrochloric acid (7.5mL, ~3 equivalents) was added. After 24 hours, crystallisation had to be induced by sonication for a few seconds in the sonic bath, whereupon an immediate dense colourless precipitate was produced. Filtration of the precipitate, washing with diethyl ether and drying gave a colourless powdered solid (4.15g, 60%), which ^{1}H-NMR confirmed as the pure hydrochloride salt of **42**.

Removal of the solvents from the mother liquor under reduced pressure gave a further 4.0g of material as a brown syrup; ^{1}H-NMR confirmed this syrup to contain the desired hydrochloride salt of **42** (maximum 2.73g, 0.011mol), contaminated with dioxan and minor unidentified impurities.

iia) The pure hydrochloride salt of **42** (4.0g, 0.0164mol) was suspended in dry dichloromethane with stirring, and 1.1 equivalents of triethylamine (2.5mL, 1.82g, 0.0180mol) were added. The mixture was stirred for ten minutes, after which time (*S*)-(1-phenylethyl) isocyanate **75*S*** (2.3mL, 2.41g, 0.0164mol) was added in dry dichloromethane (10mL) dropwise over five minutes. After three hours, the reaction was washed with dilute aqueous hydrochloric acid (2 x 50mL) and brine (50mL), and dried over dried magnesium sulfate. The filtration and removal of volatile components under reduced pressure gave a colourless foam (5.5g). ^{1}H-NMR confirmed this crude material to be predominantly the desired **76(1*R*,α*S*)** (by comparison with spectral details for **76(1*S*,α*R*)**).

iib) The impure residue was assumed to contain 0.011mol of the hydrochloride salt of **42**, and was dissolved in dry dichloromethane (100mL) with triethylamine (1.70g, 0.0168mol, 1.5 equivalents). A solution of **75*S*** (1.55mL, 1.61g, 0.011mol) in dry dichloromethane (10mL) was added. After eighteen hours, the solution was washed with dilute aqueous hydrochloric acid (2 x 50mL) and brine (50mL), and dried over dried magnesium sulfate. The filtration, and removal of solvent under reduced pressure gave an orange solid. The residue was sonicated in hot ethyl acetate (20mL), left to cool to room temperature and filtered. The solid was washed with fresh ethyl acetate, and dried by suction; this gave a colourless powdered solid (1.55g, 40%) which ^{1}H-NMR confirmed as predominantly the desired **76(1*R*,α*S*)** (by comparison with spectral details for **76(1*S*,α*R*)**).
On the basis of comparing the ^{1}H-NMR spectra of the crude products from iia) and iib), the two were combined, to give a total of 7g of impure **76(1*R*,α*S*)**.

The combined material was suspended in boiling propan-2-ol (50mL) and sufficient dichloromethane (100mL) was added to achieve dissolution. The solution was left loosely covered overnight, to cool slowly to room temperature, while allowing some of the more volatile dichloromethane to evaporate. Filtration gave the pure **76(1*R*,α*S*)** as a colourless crystalline solid (4.1g, 42%), with diastereomeric purity being established by ^{1}H- and ^{13}C-NMR analysis. Several crystals were sent for X-ray analysis, to confirm the assigned stereochemistry of the tetrahydroisoquinoline as **(1*R*,α*S*)**.

Characterisation:

TLC:	*Rf* 0.45 (cyclohexane/ethyl acetate 1:1);
Melting point:	210-211°C;
Optical rotation $[\alpha]_D^{22}$:	–75.1 (c 0.7, chloroform);
^{1}H-NMR ($CDCl_3$):	δ_H 1.44 (3H, d, J = 6.7Hz, tetrahydroisoquinoline CHC***H***$_3$), 1.50 (3H, d, J = 6.9Hz, PhCHC***H***$_3$), 2.67-2.73 (1H, m, ArC***H***$_A$H$_B$CH$_2$), 2.79-2.87 (1H, m, ArCH$_A$***H***$_B$CH$_2$), 3.23-3.30 (1H, m, CH$_2$C***H***$_A$H$_B$N), 3.83 (3H, s, ArOC***H***$_3$), 3.84 (3H, s, ArOC***H***$_3$), 3.91-3.97 (1H, m, CH$_2$CH$_A$***H***$_B$N), 4.73 (1H, d, J = 7.1Hz, N***H***), 4.99-5.09 (2H, m, overlapping tetrahydroisoquinoline C***H***CH$_3$ and PhC***H***CH$_3$), 6.58 (1H, s, Ar***H***-8), 6.59 (1H, s, Ar***H***-5), 7.21-7.26 (1H, m, Ph***H***-4'), 7.30-7.36 (4H, m, Ph***H***-2', -3', -5', -6');
^{13}C-NMR ($CDCl_3$):	δ_C 22.09 (tetrahydroisoquinoline CH***C***H$_3$), 22.63 (PhCH***C***H$_3$), 28.41 (Ar***C***H$_2$CH$_2$), 37.85 (CH$_2$***C***H$_2$N), 50.05 (tetrahydroisoquinoline ***C***HCH$_3$), 50.17 (Ph***C***HCH$_3$), 55.93, 56.03 (2 x ArO***C***H$_3$), 109.85 (***C***$_{Ar}$H-8), 111.36 (***C***$_{Ar}$H-5), 126.12 (***C***$_{Ar}$H-2', ***C***$_{Ar}$H-6'), 126.16 (***C***$_{Ar}$-4a), 127.05 (***C***$_{Ar}$H-4'), 128.58 (***C***$_{Ar}$H-3', ***C***$_{Ar}$H-5'), 130.71 (***C***$_{Ar}$-8a), 144.70 (***C***$_{Ar}$-1'), 147.64 (***C***$_{Ar}$OMe), 147.70 (***C***$_{Ar}$OMe), 156.14 (***C***=O);
MS (EI) *m/z*:	M^+ 354(27), $[M-CH_3]^+$ 339(32), $[M-(C_6H_5CH(CH_3)NHCO+CH_3)]^+$ 192(100);
IR (KBr) ν/cm:	3422 (NH), 1643 (C=O), 1519 (C_{Ar}–C_{Ar}), 1253 (C_{Ar}–OMe);
Microanalysis (C,H,N):	Calculated for $C_{21}H_{26}N_2O_3$: 71.16, 7.39, 7.90; Found: 71.13, 7.18, 7.92.

(*S*)-6,7-Dimethoxy-1-methyl-1,2,3,4-tetrahydroisoquinoline hydrochloride[444] (42*S*)

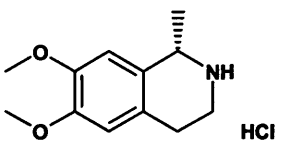

A 2.0M solution of sodium n-butoxide in butan-1-ol was prepared by dissolving sodium spheres (1.15g, 0.05mol) in dry butan-1-ol (25mL) in a flame-dried round-

bottomed flask under argon. **76(1*S*,α*R*)** (3.54g, 0.01mol) was added to the sodium butoxide solution, and the resultant mixture was stirred at reflux; after three hours the reaction, now a clear solution, was allowed to cool to room temperature, before quenching the reaction by pouring into 2.0M aqueous hydrochloric acid (300mL). The solution was washed with ether (100mL); the ether layer was washed with fresh 2.0M aqueous hydrochloric acid (100mL) then discarded. The aqueous layers were combined, basified by the addition of 5.0M aqueous sodium hydroxide (80mL), and the desired product was extracted into dichloromethane (2 x 100mL). The combined dichloromethane extractions were washed with brine (50mL), and dried over dried magnesium sulfate. Filtration and removal of solvent under reduced pressure gave a colourless syrup. The syrup was dissolved in dioxan (10mL); the addition of 4.0M hydrogen chloride in dioxan (5mL, 2.0equivalents) to the stirred solution gave a dense colourless precipitate. The suspension was heated to boiling, and the minimum amount of methanol to dissolve the precipitate was added. The solution was allowed to cool to room temperature; filtration gave a colourless crystalline solid (1.07g, 44%). Refrigeration gave a further crop of colourless crystals (600mg, 25%; total 1.67g. 69%):

Characterisation:

TLC:	*Rf* 0.23 (dichloromethane/ methanol/ 32% $AcOH_{(aq.)}$ 90:9:1);
Melting point:	237-238°C (lit. 238-240°C[444]);
Optical rotation $[\alpha]_D^{20}$:	–26.6 (c 2.1, H_2O) (lit. –25.6 (c 2.1, H_2O[444]);
^{1}H-NMR (D_2O):	δ_H 1.75 (3H, d, J = 6.8Hz, CHC***H***$_3$), 3.04-3.17 (2H, m, ArC***H***$_2$CH$_2$), 3.43-3.50 (1H, m, CH$_2$C***H***$_A$H$_B$N), 3.61-3.68 (CH$_2$CH$_A$***H***$_B$N), 3.87-3.89 (6H, 2 x s overlapping, 2 x ArOC***H***$_3$), 4.64 (1H, quartet, J = 6.8Hz, C***H***CH$_3$), 6.92 (2H, s, Ar***H***-5, Ar***H***-8);
^{13}C-NMR (D_2O):	δ_C 21.74 (CH***C***H$_3$), 27.33 (Ar***C***H$_2$CH$_2$), 41.99 (CH$_2$***C***H$_2$N), 53.89 (***C***HCH$_3$), 58.55 (ArO***C***H$_3$), 58.67 (ArO***C***H$_3$), 112.02 (***C***$_{Ar}$H-8), 114.53 (***C***$_{Ar}$H-5), 126.73 (***C***$_{Ar}$-4a), 128.06 (***C***$_{Ar}$-8a), 150.18 (***C***$_{Ar}$OMe-7), 150.69 (***C***$_{Ar}$OMe-6);
MS (EI) *m/z*:	M^+ 207(18), $[M-CH_3]^+$ 192(100);
IR (KBr) *ν*/cm:	1516 (C_{Ar}–C_{Ar}), 1226 (C_{Ar}–OMe);
Microanalysis (C,H,N):	Calculated for $C_{12}H_{18}NO_2Cl$: 59.14, 7.44, 5.75;

Found: 58.92, 7.30, 5.87.

(*R*)-6,7-Dimethoxy-1-methyl-1,2,3,4-tetrahydroisoquinoline hydrochloride[444] (42*R*)

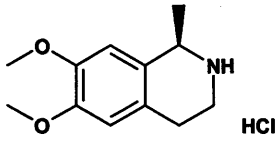

Five equivalents of a 2.0M solution of sodium butoxide in butan-1-ol were prepared by dissolving sodium spheres (1.27g, 0.055mol) in dry butan-1-ol (27.5mL) in a flame-dried 100ml round-bottomed flask under an atmosphere of argon. **76(1*R*,α*S*)** (3.86g, 0.011mol) was added to the solution, and the resulting suspension was stirred at reflux (oil bath temperature of 130°C), with the last of the solid entering solution after 90 minutes. After a further two hours, the solution was cooled to room temperature, and quenched by pouring into 2.0M aqueous hydrochloric acid (100mL). Neutral species were extracted into diethyl ether (100mL); this extraction was washed with 2.0M aqueous hydrochloric acid (100mL), then discarded. The combined aqueous phases were basified with 5.0M aqueous sodium hydroxide, and the desired product was extracted into dichloromethane (2 x 100mL). The combined dichloromethane extractions were washed with brine (50mL), and dried over dried magnesium sulfate. Filtration and removal of the solvent under reduced pressure gave a colourless oil, which was dissolved in dioxan (15mL). 4.0M Hydrogen chloride in dioxan (5.5mL, 2 equivalents) was added to the solution; the resulting suspension was heated to boiling, and methanol was added dropwise until the precipitate dissolved. The solution was hot filtered, and left to cool to room temperature overnight. Filtration, washing with ether and drying at 125°C under vacuum, gave a colourless crystalline solid (1.10g, 41%):

Characterisation:

TLC:	*Rf* 0.23 (dichloromethane/ methanol/ 32% $AcOH_{(aq.)}$ 90:9:1);
Melting point:	239-240°C (lit. 240-242°C[444]);
Optical rotation $[\alpha]_D^{22}$:	+26.6 (c 2.1, H_2O) (lit. +24.1 (c 1.8, H_2O[444]);
^{1}H-NMR (D_2O):	δ_H 1.75 (3H, d, J = 6.8Hz, $CHCH_3$), 3.05-3.17 (2H, m, $ArCH_2CH_2$), 3.43-3.50 (1H, m, $CH_2CH_AH_BN$), 3.62-3.68 ($CH_2CH_AH_BN$), 3.87-3.90 (6H, 2 x s overlapping,

2 x ArOC***H***$_3$), 4.64 (1H, quartet, J = 6.8Hz, C***H***CH$_3$), 6.91 (2H, s, Ar***H***-5, Ar***H***-8);

^{13}C-NMR (D_2O): δ_C 21.74 (CH***C***H$_3$), 27.35 (Ar***C***H$_2$CH$_2$), 42.00 (CH$_2$***C***H$_2$N), 53.90 (***C***HCH$_3$), 58.51 (ArO***C***H$_3$), 58.62 (ArO***C***H$_3$), 111.94 (***C***$_{Ar}$H-8), 114.46 (***C***$_{Ar}$H-5), 126.70 (***C***$_{Ar}$-4a), 128.29 (***C***$_{Ar}$-8a), 150.14 (***C***$_{Ar}$OMe-7), 150.64 (***C***$_{Ar}$OMe-6);

MS (ESI-positive) *m/z*: MH^+ 208(100);

IR (KBr) ν/cm: 1516 (C_{Ar}–C_{Ar}), 1267 (C_{Ar}–OMe);

Microanalysis (C,H,N): Calculated for $C_{12}H_{18}NO_2Cl$: 59.14, 7.44, 5.75;
Found 58.83, 7.27, 5.91.

(*S*)-6,7-Dihydroxy-1-methyl-1,2,3,4-tetrahydroisoquinoline hydrobromide[435] (33*S*):

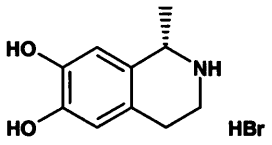

The hydrochloride salt of **42*S*** (900mg, 0.0037mol) was dissolved in 48% aqueous hydrobromic acid (10mL), and stirred at reflux for eighteen hours. The solvent was removed under reduced pressure to give a beige solid; trituration with a hot 1:1 mixture of diethyl ether and propan-2-ol, followed by sonication, refrigeration and filtration, gave the pure catechol as a colourless powdered crystalline solid (570mg, 59%):

Characterisation:

Melting point: 181-182°C (lit. 174-5°C[435]);

Optical rotation $[\alpha]_D^{21}$: –32.0 (c 1.02, methanol) (lit. $[\alpha]_D$ = –30.9 (methanol)[435])

^{1}H-NMR (D_2O): δ_H 1.65 (3H, d, J = 6.8Hz, CHC***H***$_3$), 2.93-3.06 (2H, m, ArC***H***$_2$C***H***$_2$), 3.37-3.44 (1H, m, CH$_2$C***H***$_A$H$_B$N), 3.54-3.61 (1H, m, CH$_2$CH$_A$***H***$_B$N), 4.53 (1H, quartet, J = 6.8Hz, C***H***CH$_3$), 6.75 (1H, s, Ar***H***-8), 6.79 (1H, s, Ar***H***-5);

^{13}C-NMR (D_2O): δ_C 21.60 (CH***C***H$_3$), 27.05 (Ar***C***H$_2$CH$_2$), 42.25 (CH$_2$***C***H$_2$N), 53.79 (***C***HCH$_3$), 116.10 (***C***$_{Ar}$H-8), 118.56 (***C***$_{Ar}$H-5), 126.33 (***C***$_{Ar}$-4a), 128.03 (***C***$_{Ar}$-8a), 145.98 (***C***$_{Ar}$OMe), 146.69 (***C***$_{Ar}$OMe);

MS (EI) *m/z*: M^+ 179(12), $[M\text{-}CH_3]^+$ 164(100);

IR (KBr) *ν*/cm: 3296 (OH str.), 1528 (C_{Ar}–C_{Ar}), 1184 (Ar–OH);

Microanalysis (C,H,N): Calculated for $C_{10}H_{14}NO_2Br$: 46.17, 5.42, 5.38

Found: 45.96, 5.17, 5.47.

(*R*)-6,7-Dihydroxy-1-methyl-1,2,3,4-tetrahydroisoquinoline hydrobromide[435] (33*R*):

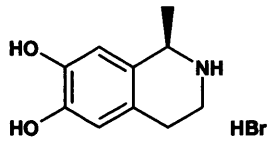

The hydrochloride salt of **42*R*** (550mg, 0.0023mol) was dissolved in 48% aqueous hydrobromic acid (10mL), and stirred at reflux for eighteen hours. Removal of solvent from an aliquot under reduced pressure and analysis by ^{1}H-NMR confirmed the reaction to be complete, by the absence of the peaks at δ_H 3.87-3.90. The solvent was removed from the reaction under reduced pressure to give an off-white solid; sonication in diethyl ether (7.5mL) formed the solid into a finely divided colourless precipitate, which was filtered, wash with fresh diethyl ether and dried under reduced pressure at 100°C for eighteen hours, to give the pure catechol as a colourless powdered solid (600mg, quantitative yield):

Characterisation:

Melting point: 185-186°C (lit. 174-175°C[435]);

Optical rotation $[\alpha]_D^{21}$: +32.0 (c 1.01, methanol) (lit. $[\alpha]_D$ = +30.0 (methanol)[435]);

^{1}H-NMR (D_2O): δ_H 1.63 (3H, d, J = 6.8Hz, CHC***H***$_3$), 2.90-3.05 (2H, m, ArC***H***$_2$C***H***$_2$), 3.35-3.43 (1H, m, $CH_2CH_AH_BN$), 3.52-3.59 (1H, m, $CH_2CH_AH_BN$), 4.53 (1H, quartet, J = 6.8Hz, C***H***CH_3), 6.76 (1H, s, Ar***H***-8), 6.79 (1H, s, Ar***H***-5);

^{13}C-NMR (D_2O): δ_C 21.60 (CH***C***H_3), 27.05 (Ar***C***H_2CH_2), 42.25 (CH_2***C***H_2N), 53.79 (***C***HCH_3), 116.11 (***C***$_{Ar}$H-8), 118.57 (***C***$_{Ar}$H-5), 126.34 (***C***$_{Ar}$-4a), 128.04 (***C***$_{Ar}$-8a), 145.99 (***C***$_{Ar}$OMe), 146.70 (***C***$_{Ar}$OMe);

MS (ESI-positive) *m/z*: MH^+ 180(100);

IR (KBr) *ν*/cm: 3296 (OH str.), 1527 (C_{Ar}–C_{Ar}), 1184 (Ar–OH);

Microanalysis (C,H,N): Calculated for $C_{10}H_{14}NO_2Br$: 46.17, 5.42, 5.38

Found: 45.94, 5.30, 5.64.

2-(4-Chlorophenyl)ethyl isothiocyanate (32):

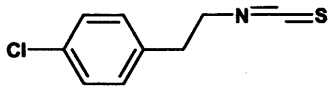

Thiophosgene **41** (15mL, 22.6g, 0.197mol) was dissolved in dry dichloromethane (200mL) with stirring under an atmosphere of nitrogen on ice; a solution of 2-(4-chlorophenyl)ethylamine **40** (30.0g, 0.193mol) and triethylamine (55mL, 40g, 0.395mol) in dry dichloromethane (200mL) was added slowly over 15 minutes. The reaction was stirred for eighteen hours, poured into a 1L separatory funnel and washed consecutively with 0.5M aqueous hydrochloric acid (2 x 200mL) and brine (100mL). The organic phase was dried over dried magnesium sulfate, filtered, and the solvent removed under reduced pressure, to give a red oil. Purification by flash column chromatography (silica, cyclohexane/ ethyl acetate 30:1) gave an orange oil (36.4g, 95%):

Characterisation:

TLC:	*Rf* 0.55 (cyclohexane/ethyl acetate 20:1);
^{1}H-NMR ($CDCl_3$):	δ_H 2.95 (2H, t, J = 6.8Hz, ArCH_2CH_2), 3.71 (2H, t, J = 6.8Hz, CH_2CH_2NCS), 7.15 (2H, dm (AA' of an AA'BB' system), J_{ortho} = 8.3Hz, Ar*H*-2, Ar*H*-6), 7.31 (2H, dm (BB' of an AA'BB' system), J_{ortho} = 8.3Hz, Ar*H*-3, Ar*H*-5);
^{13}C-NMR ($CDCl_3$):	δ_C 35.81 (ArCH_2CH_2), 46.19 (CH_2CH_2NCS), 128.94 (C_{Ar}H-3, C_{Ar}H-5); 130.16 (C_{Ar}H-2, C_{Ar}H-6), 131.16 (br, NCS), 133.08 (C_{Ar}-4), 135.45 (C_{Ar}-1);
MS (EI) *m/z*:	M^+ 197(67), $[M-(CH_2NCS)]^+$ 125(100);
IR (neat) *ν*/cm:	2095 (N=C=S), 1493 (C_{Ar}–C_{Ar});
HRMS	no result by ESI-ionisation; HRMS not possible

(*S*)-*N*-(4-Chlorophenethylthiocarbamoyl)-6,7-dihydroxy-1-methyl-1,2,3,4-tetrahydroisoquinoline (29*S*):

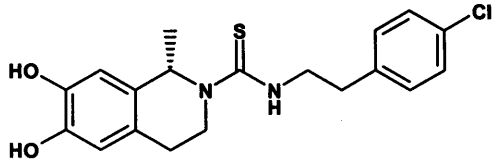

The hydrobromide salt of **33*S*** (420mg, 1.6mmol) was dissolved in dry tetrahydrofuran (15mL), with triethylamine (250μL, 180mg, 1.78mmol). **32** (320mg, 1.6mmol) was added in dry tetrahydrofuran (10mL), and the reaction was stirred for twenty four hours. The reaction was diluted in ethyl acetate (100mL) and washed consecutively with dilute aqueous hydrochloric acid (50mL), water (50mL) and brine (25mL), before drying over dried magnesium sulfate. Filtration and removal of solvent under reduced pressure, followed by purification by flash column chromatography (Biotage 40S, cyclohexane/ethyl acetate 1:1) gave a colourless foamed solid (480mg, 80%), which rapidly discoloured to a pale pink/orange, although the ^{1}H-NMR remained unchanged:

Characterisation:

TLC: *Rf* 0.19 (cyclohexane/ethyl acetate 1:1);

Melting point: amorphous solid;;

Optical rotation $[\alpha]_D^{24}$: +122.7 (c 1.0, chloroform);

^{1}H-NMR ($CDCl_3$): δ_H 1.36 (3H, d, J = 6.8Hz, CHC***H***$_3$), 2.65 (2H, t, J = 6.0Hz, tetrahydroisoquinoline ArC***H***$_2$CH$_2$), 2.94 (2H, t, J = 7.0Hz, 4'-chlorophenyl-C***H***$_2$CH$_2$), 3.34-3.41 (1H, m, tetrahydroisoquinoline CH$_2$C***H***$_A$H$_B$N), 3.86-4.01 (2H, m, CH$_2$C***H***$_2$NH), 4.00-4.10 (1H, br, tetrahydroisoquinoline CH$_2$CH$_A$***H***$_B$N), 5.50-5.65 (1H, br, C***H***CH$_3$), 5.68 (1H, t, J = 5.1Hz, N***H***), 6.52, (1H, s, Ar***H***-8), 6.55 (1H, s, Ar***H***-5), 7.13 (2H, dm (AA' of an AA'BB' system), J_{ortho} = 8.4Hz, Ar***H***-2', Ar***H***-6'), 7.24 (2H, dm (BB' of an AA'BB' system), J_{ortho} = 8.4Hz, Ar***H***-3', Ar***H***-5');

^{13}C-NMR ($CDCl_3$): δ_C 21.27 (CH***C***H$_3$), 27.24 (tetrahydroisoquinoline Ar***C***H$_2$CH$_2$), 34.70 (4'-chlorophenyl-***C***H$_2$CH$_2$), 42.48 (tetrahydroisoquinoline CH$_2$***C***H$_2$N), 46.83 (CH$_2$***C***H$_2$NH), 54.72 (***C***HCH$_3$), 113.40 (***C***$_{Ar}$H-8), 114.85 (***C***$_{Ar}$H-5), 125.91

(C_{Ar}-4a), 128.82 (C_{Ar}H-3', C_{Ar}H-5'), 130.19 (C_{Ar}H-2', C_{Ar}H-6'), 130.26 (C_{Ar}-8a), 132.44 (C_{Ar}Cl-4'), 137.28 (C_{Ar}-1'), 142.50 (C_{Ar}OH), 142.82 (C_{Ar}OH), 179.72 (*C*=S);

MS (ESI-negative) *m/z*: $[M-H]^-$ 375.2(100);

IR (KBr) *ν*/cm: 3408(OH str.), 1522 (C_{Ar}–C_{Ar});

Microanalysis (C,H,N): Calculated for $C_{19}H_{21}N_2O_2SCl$: 60.55, 5.62, 7.43;
Found 60.23, 5.72, 7.35;

HRMS (negative) *m/z*: Calculated for [M-H] $C_{19}H_{20}N_2O_2SCl$: 375.0934;
Found 375.0931.

(*R*)-*N*-(4-Chlorophenethylthiocarbamoyl)-6,7-dihydroxy-1-methyl-1,2,3,4-tetrahydroisoquinoline (29*R*):

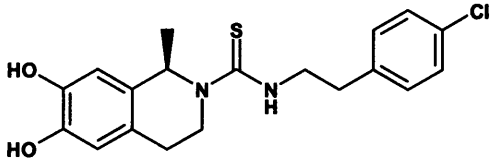

The hydrobromide salt of **33*R*** (1.01g, 3.9mmol) was dissolved in dry tetrahydrofuran (25mL), with triethylamine (820μL, 590mg, 5.8mmol). **32** (770mg, 3.9mmol) was added in dry tetrahydrofuran (5mL), and the reaction was stirred for forty hours at room temperature. The tetrahydrofuran was removed under reduced pressure; the residue was dissolved in ethyl acetate (100mL) and washed consecutively with dilute aqueous hydrochloric acid (50mL), water (50mL) and brine (25mL), before drying over dried magnesium sulfate. The filtration and removal of solvent under reduced pressure followed by flash column chromatography (Biotage 40S, cyclohexane/ethyl acetate 1:1) gave a colourless foamed solid (1.31g, 89%). This foam discoloured rapidly to a pale peach, although the ^{1}H-NMR remained unchanged. While all other characterisation was possible with the foamed solid, it was not possible to obtain a satisfactory microanalysis. However, precipitation of a sample of the foam (250mg) by dissolving in chloroform (4mL) and adding dropwise to a quantity of vigorously stirred cyclohexane (30mL), gave a colourless amorphous solid; this gave a satisfactory microanalysis (C,H,N), and was used for characterisation purposes:

Characterisation:

TLC: *Rf* 0.19 (cyclohexane/ethyl acetate 1:1);

Melting point:	amorphous solid;
Optical rotation $[\alpha]_D^{24}$:	–124.8 (c 1.0, chloroform);
^{1}H-NMR ($CDCl_3$):	δ_H 1.43 (3H, d, J = 6.8Hz, $CHCH_3$), 2.76 (2H, t, J = 6.0Hz, tetrahydroisoquinoline $ArCH_2CH_2$), 2.96 (2H, t, J = 6.9Hz, 4'-chlorophenyl-CH_2CH_2), 3.40-3.47 (1H, m, tetrahydroisoquinoline $CH_2CH_AH_BN$), 3.87-4.03 (2H, m, CH_2CH_2NH), 4.04-4.20 (1H, br, tetrahydroisoquinoline $CH_2CH_AH_BN$), 5.45 (1H, t, J = 5.1Hz, NH), 5.50-5.70 (1H, br, $CHCH_3$), 6.60, (1H, s, ArH-8), 6.62 (1H, s, ArH-5), 7.16 (2H, dm (AA' of an AA'BB' system), J_{ortho} = 8.3Hz, ArH-2', ArH-6'), 7.28 (2H, dm (BB' of an AA'BB' system), J_{ortho} = 8.3Hz, ArH-3', ArH-5');
^{13}C-NMR ($CDCl_3$):	δ_C 21.24 ($CHCH_3$), 27.26 (tetrahydroisoquinoline $ArCH_2CH_2$), 34.68 (4'-chlorophenyl-CH_2CH_2), 42.46 (tetrahydroisoquinoline CH_2CH_2N), 46.85 (CH_2CH_2NH), 54.75 ($CHCH_3$), 113.37 (C_{Ar}H-8), 114.84 (C_{Ar}H-5), 125.87 (C_{Ar}-4a), 128.80 (C_{Ar}H-3', C_{Ar}H-5'), 130.17 (C_{Ar}H-2', C_{Ar}H-6', C_{Ar} -8a), 132.39 (C_{Ar}Cl-4'), 137.22 (C_{Ar}-1'), 142.43 (C_{Ar}OH), 142.75 (C_{Ar}OH), 179.49 (C=S);
MS (ESI-positive) *m/z*:	MH^+ 377(100);
IR (KBr) ν/cm:	3404 (OH str.), 1523 (C_{Ar}–C_{Ar});
Microanalysis (C,H,N):	Calculated for $C_{19}H_{21}N_2O_2SCl$: 60.55, 5.62, 7.43; Found 60.39, 5.75, 7.53;
HRMS (positive) *m/z*:	Calculated for [M+H] $C_{19}H_{22}N_2O_2SCl$: 377.10905; Found 377.10942.

Enantiomers of *N*-(4-chlorophenethylthiocarbamoyl)-6,7-dihydroxy-3-methyl-1,2,3,4-tetrahydroisoquinoline analogues (30*R* and 30*S*)

Resolution of the enantiomers of 2-(3,4-dimethoxy-phenyl)-1-methyl ethylamine (38*R* and 38*S*)

1-(3,4-dimethoxy-phenyl)-propan-2-one O-methyl-oxime (37)

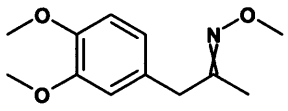

3,4-Dimethoxyphenylacetone **36** (5.0g, 25.8mmol), methoxylamine hydrochloride (2.37g, 28.3mmol) and anhydrous sodium acetate (2.32g, 28.3mmol) were combined in dry methanol (25mL), and stirred under an atmosphere of nitrogen for 18 hours, when the reaction was determined to be complete by TLC (cyclohexane/ethyl acetate 4:1). The mixture was diluted to 200mL with ethyl acetate, and washed with water (2 x 100mL) and brine (50mL), before drying over magnesium sulfate. Filtration, and removal of the solvent under reduced pressure, gave a red oil; purification by flash column chromatography (Biotage 40M cartridge; cyclohexane/ethyl acetate 10:1) gave a mixture of *trans* and *cis* isomers (~5:2 major:minor by ^{1}H-NMR) as a colourless oil (5.3g, 92%):

Characterisation:

TLC: *Rf* 0.55 (cyclohexane/ethyl acetate 4:1);

^{1}H-NMR ($CDCl_3$): δ_H 1.74 (2.2H, s, CC***H***$_3$ *major*), 1.78 (0.8H, s, CC***H***$_3$ *minor*), 3.40 (1.47H, s, ArC***H***$_2$C *major*), 3.61 (0.53H, s, ArC***H***$_2$C *minor*), 3.86 (3H, s, ArOC***H***$_3$), 3.87 (3H, s, ArOC***H***$_3$), 3.89 (3H, s, NOC***H***$_3$), 6.72-6.82 (3H, m, 3 x Ar***H***);

^{13}C-NMR ($CDCl_3$): δ_C 13.46 (C***C***H$_3$, *major*), 19.65 (C***C***H$_3$, *minor*), 34.93 (Ar***C***H$_2$CH, *minor*), 41.71 (Ar***C***H$_2$CH, *major*), 55.83 (1 x ArO***C***H$_3$ *minor*), 55.91 (1 x ArO***C***H$_3$ *major* and 1 x ArO***C***H$_3$), 61.22 (NO***C***H$_3$), 111.30 (***C***$_{Ar}$H *major*), 111.33 (***C***$_{Ar}$H *minor*), 112.08 (***C***$_{Ar}$H, *major*), 112.35 (***C***$_{Ar}$H, *minor*), 121.11 (***C***$_{Ar}$H), 129.16 (***C***$_{Ar}$-1, *minor*), 129.46 (***C***$_{Ar}$-1, *major*), 147.56 (***C***$_{Ar}$OMe-4, *minor*), 147.98 (***C***$_{Ar}$OMe-4, *major*), 149.07 (***C***$_{Ar}$OMe-3), 156.42 (***C***=N, *minor*), 156.77 (***C***=N,

major);

MS (ESI-positive) *m/z*: MH^+ 224(100);

IR (film) *ν*/cm: 1515 (C_{Ar}–C_{Ar}), 1263 (Ar–OCH_3);

HRMS (positive) *m/z*: Calculated for [M+H] $C_{12}H_{18}NO_3$ 224.1287;
Found 224.1287.

2-(3,4-Dimethoxy-phenyl)-1-methylethylamine hydrochloride (38*RS*)

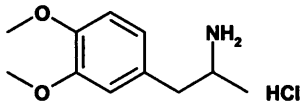

37 (4.8g, 22mmol) was dissolved in 1.0M borane-THF complex in THF, and refluxed under an atmosphere of argon for 24 hours, until TLC (cyclohexane/ethyl acetate 4:1) confirmed that none of the oxime remained. The solution allowed to cool to room temperature, before being chilled on an ice-water bath. 2.0M Aqueous sodium hydroxide (50mL) was cautiously added, followed by methanol (50mL). The reaction was refluxed for a further 24 hours, until none of the borane complexes remained by TLC (cyclohexane/ethyl acetate 4:1; developed in iodoplatinate dip, where borane complexes show up white). The reaction was poured into water (500mL), and products were extracted into diethyl ether (2 x 200mL). The combined ether extractions were washed with fresh water (200mL) and brine (50mL), then dried over magnesium sulfate. Filtration, and the removal of ether under reduced pressure gave a yellow oil, which was dissolved in 50mL 1.0M HCl in dioxan. The solvent was removed under reduced pressure; the residue was suspended in boiling ethyl acetate (200mL); methanol was added until a hazy solution remained; this was hot filtered, then left to cool to room temperature overnight. Filtration gave a colourless crystalline solid, which was washed with ether and dried at 0.1mmHg and 100°C for 24 hours (2.15g, 42%):

Characterisation:

TLC: *Rf* 0.18 (dichloromethane/ methanol/ 32% $AcOH_{(aq.)}$ 90:9:1);

Melting point: 149-150°C (lit. 149-151°C[510]);

^{1}H-NMR (D_2O): δ_H 1.36 (3H, d, J = 6.6Hz, $CHCH_3$), 2.92 (2H, d, J = 7.2Hz, $ArCH_2CH$), 3.62-3.69 (1H, m, CH_2CHCH_3), 3.86-3.89 (6H, 2 x s overlapping, 2 x $ArOCH_3$), 6.90 (1H, dd, J_{ortho} = 8.2Hz, J_{meta} = 1.8Hz, Ar*H*-6), 6.95 (1H, d, J_{meta} = 1.8Hz, Ar*H*-2),

7.00 (1H, d, J_{ortho} = 8.2Hz, Ar***H***-5);

^{13}C-NMR (D_2O): δ_C 20.34 (***C***H_3), 42.51 (***C***H_2), 52.01 (***C***H), 58.49 (2 x ArO***C***H_3), 114.81 ($\boldsymbol{C}_{Ar}$H-5), 115.58 ($\boldsymbol{C}_{Ar}$H-2), 124.86 ($\boldsymbol{C}_{Ar}$H-6), 131.93 ($\boldsymbol{C}_{Ar}CH_2$-1), 150.10 ($\boldsymbol{C}_{Ar}$OMe-4), 151.06 ($\boldsymbol{C}_{Ar}$OMe-3);

^{1}H-NMR (DMSO-d_6): δ_H 1.13 (3H, d, J = 6.5Hz, CHC***H***$_3$), 2.62 (1H, dd, J = 8.6, 13.4Hz, ArC***H***$_A$H$_B$CH), 2.93 (1H, dd, J = 5.5, 13.4Hz, ArCH$_A$***H***$_B$CH), 3.37 (1H, m, ArCH$_2$C***H***CH$_3$), 3.73 (3H, s, ArOC***H***$_3$), 3.75 (3H, s, ArOC***H***$_3$), 6.74 (1H, dd, J = 1.9, 8.1Hz, Ar***H***-6), 6.85 (1H, d, J = 1.9Hz, Ar***H***-2), 6.89 (1H, d, J =8.1Hz, Ar***H***-5), 8.06 (3H, br, RN$^+$***H***$_3$);

^{13}C-NMR (DMSO-d_6): δ_C 17.46 (CH***C***H$_3$), 39.53 (***C***H$_2$, coincident with DMSO and revealed by DEPT experiment), 48.11 (***C***H), 55.37 (ArO***C***H$_3$), 55.40 (ArO***C***H$_3$), 111.77 ($\boldsymbol{C}_{Ar}$H-5), 112.84 ($\boldsymbol{C}_{Ar}$H-2), 121.15 ($\boldsymbol{C}_{Ar}$H-6), 129.18 ($\boldsymbol{C}_{Ar}$-1), 147.53 ($\boldsymbol{C}_{Ar}$OMe-4), 148.63 ($\boldsymbol{C}_{Ar}$OMe-3);MH^+ 196(15), $[M-NH_2]^+$ 179(100);

MS (ESI-positive) *m/z*: MH^+ 196(15), $[M-NH_2]^+$ 179(100);

IR (KBr) *ν*/cm: 1518 (C_{Ar}–C_{Ar}), 1269 (C_{Ar}–O), 1235 (C_{Ar}–O);

Microanalysis (C,H,N): Calculated for $C_{11}H_{17}NO_2$.HCl: 57.02, 7.83, 6.04;
Found 56.69, 7.57, 6.42.

Protocol for the reaction of 38 and *N*-α-(2,4-dinitro-5-fluorophenyl)-*L*-alaninamide (Marfey's reagent, 104*S*)[460]

Following the method of Marfey[460], 0.01mmol of the amine **38** was dissolved in 400μL of a 1% solution of N-α-(2,4-dinitro-5-fluorophenyl)-L-alaninamide **104*S*** in acetone, with 80μL 1.M aqueous sodium bicarbonate, and the mixture was stirred at 40°C for exactly 1 hour, at which time the reaction was neutralised by the addition of 40μL 2.0M $HCl_{(aq)}$. A 10μL aliquot was diluted to 1.0mL in acetonitrile, and the diastereomeric ratio was established by reverse phase analytical HPLC, using either system 3 or system 4.

(*S*)-2-(3,4-dimethoxy-phenyl)-1-methylethylammonium-(*R*)-mandelate (38*S*+103*R*)

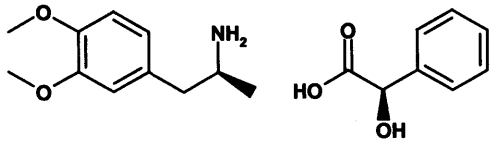

38*RS* (47.0g, 0.241mol) was dissolved in boiling propan-2-ol (1L) with *(R)*-(–)-mandelic acid **103*R*** (36.7g, 0.241mol). The solution was allowed to cool slowly to room temperature overnight, and a colourless crystalline solid was filtered out (70.1g, 0.202mol, 84%, $[\alpha]_D^{26}$ –51.5° (c 1.0, water)). A sample of the diastereomeric salt mixture was converted to the free amine by dissolving in water, basifying with 5M aqueous sodium hydroxide, and extracting into dichloromethane. Reaction with **104*S***[460] and analysis by reverse phase analytical HPLC (system 3) confirmed the amine as racemic.

65.0g of the diastereomeric salt mixture **38*RS*+103*R*** was dissolved in boiling ethyl acetate/methanol 2:1 (1.5L), then left to cool to room temperature. Filtration after 3 hours gave a colourless crystalline solid (24.1g, crop 1). A second filtration after 20 hours gave a second crop of a colourless crystalline solid (11.7g, crop 2). Removal of the solvent from the mother liquor gave a final batch of colourless crystalline material (29.6g). The enantiomeric ratio for each of these crystalline solids was established by the method of Marfey[460], using reverse phase analytical HPLC (system 3); while crop 1 and the mother liquor both appeared to have slight excess of one enantiomer (10% *e.e.*) and were subsequently combined, crop 2 was seen to be much enriched in the opposite enantiomer (80% *e.e.*). Recrystallisation of crop 2 from 450mL ethyl acetate/methanol 2:1, from boiling to room temperature, gave 6.17g of a colourless crystalline solid (crop 2A); the reaction of a freebased sample of this solid with Marfey's reagent confirmed the amine as almost entirely one enantiomer (>97% *e.e.*). A further 24 hours at room temperature yielded a second crop (crop 2B) of 1.65g with a similar *e.e.* (overall yield 18%). Subsequent comparison of the rotation of the free base of the amine with literature precedent[455] identified this as the (*S*)-enantiomer of **38**:

Characterisation:

Melting point: 172-173°C;

Optical rotation $[\alpha]_D^{26}$: –35.1 (c 1.0, water);

^{1}H-NMR (D_2O):	Ammonium ion: δ_H 1.31 (3H, d, J = 6.6Hz, CHC***H***$_3$), 2.90 (2H, d, J = 7.2Hz, ArC***H***$_2$CH), 3.61 (1H, m, CH_2C***H***CH_3), 3.86-3.88 (6H, 2 x s overlapping, 2 x ArOC***H***$_3$), 6.90 (1H, d, J_{ortho} = 8.2Hz, Ar***H***-6), 6.97 (1H, s, Ar***H***-2), 7.05 (1H, d, J_{ortho} = 8.2Hz, Ar***H***-5);
	Mandelate ion: δ_H 4.99 (1H, s, ArC***H***OH), 7.37-7.46 (5H, m, 5 x Ph***H***);
^{13}C-NMR (D_2O):	Ammonium ion: δ_C 20.30 (***C***H_3), 42.50 (***C***H_2), 51.94 (***C***H), 58.43 (ArO***C***H_3), 58.46 (ArO***C***H_3), 114.77 (C_{Ar}H-5), 115.53 (C_{Ar}H-2), 124.87 (C_{Ar}H-6), 131.96 (C_{Ar}-1), 150.09 (C_{Ar}OMe-4), 151.04 (C_{Ar}OMe-3);
	Mandelate ion: δ_C 77.84 (***C***H), 129.86 (2 x C_{Ar}H-2, -6), 130.99 (C_{Ar}H-4), 131.59 (2 x C_{Ar}H-3, -5) 143.37 (C_{Ar}-1), 182.21 (***C***O_2H);
MS (ESI-positive) *m/z*:	MH^+ 196(24), $[MH\text{-}NH_3]^+$ 179(100);
MS (ESI-negative) *m/z*:	$[M\text{-}H]^-$ 151(100);
IR (KBr) ν/cm:	1558 (CO_2^-), 1516 (C_{Ar}–C_{Ar}), 1385 (CO_2^-), 1236 (C–O);
Microanalysis (C,H,N):	Calculated for $C_{19}H_{25}NO_5$: 65.67, 7.25, 4.03;
	Found 65.62, 7.24, 4.16;

(*S*)-2-(3,4-dimethoxy-phenyl)-1-methylethylamine (38*S*)

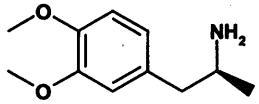

38*S*+103*R* (1g, 2.88mmol) was dissolved in water (75mL); the pH was adjusted to alkalinity by the addition of 5M aqueous sodium hydroxide (3mL, ~5 equivalents). The free base of the amine was extracted into dichloromethane (3 x 50mL). The combined extractions were washed with brine (20mL) and dried over dried magnesium sulfate. Filtration and removal of solvent under reduced pressure gave a colourless crystalline solid (540mg, quantitative). Recrystallisation from n-pentane gave colourless needles (250mg, 46%); reverse phase analytical HPLC (system 4) of the reaction of these needles with Marfey's reagent confirmed them to have an *e.e.* in excess of 99%. Comparison of the optical rotation with the published data[455] confirmed the amine to be the (*S*)-enantiomer:

Characterisation:

Melting point:	67-8°C (literature 39-40°C{Schrecker 1957 16 /id});
Optical rotation $[\alpha]_D^{22}$:	+32.5 (c 4.02, EtOH) (lit. $[\alpha]_D^{21}$ +32.1 (c 3.98, EtOH)[455]);
^{1}H-NMR ($CDCl_3$):	δ_H 1.13 (3H, d, J = 6.3Hz, CHC***H***$_3$), 1.37 (2H, br, N***H***$_2$), 2.44 (1H, dd$_{ABX}$, J_{AB} = 13.4Hz, J_{AX} = 8.3Hz, ArC***H***$_A$H$_B$CH), 2.67 (1H, dd$_{BAX}$, J_{BA} = 13.4Hz, J_{BX} = 5.1Hz, ArCH$_A$***H***$_B$CH), 3.14 (1H, m, ArCH$_A$H$_B$C***H***CH$_3$), 3.86-3.88 (6H, 2 x s, 2 x ArOC***H***$_3$), 6.71-6.75 (2H, m, Ar***H***-2, -6), 6.81 (1H, d, J_{ortho} = 7.9Hz, Ar***H***-5);
^{13}C-NMR ($CDCl_3$):	δ_C 23.58 (***C***H$_3$), 46.20 (***C***H$_2$), 48.53 (***C***H), 55.83 (ArO***C***H$_3$), 55.90 (ArO***C***H$_3$), 111.18 (***C***$_{Ar}$H-5), 112.35 (***C***$_{Ar}$H-2), 121.13 (***C***$_{Ar}$H-6), 132.34 (***C***$_{Ar}$-1), 147.43 (***C***$_{Ar}$OMe-4), 148.79 (***C***$_{Ar}$OMe-3);
MS (ESI-positive) *m/z*:	MH$^+$ 196(100), [M-NH$_2$]$^+$ 179(11);
IR (KBr) *ν*/cm:	1518 (C$_{Ar}$–C$_{Ar}$), 1265 (C$_{Ar}$–O), 1238 (C$_{Ar}$–O);
Microanalysis (C,H,N):	Calculated for $C_{11}H_{17}NO_2$: 67.66, 8.78, 7.17; Found 67.43, 8.53, 7.14.

(*R*)-2-(3,4-dimethoxyphenyl)-1-methylethylammonium-(*S*)-mandelate (38*R*+103*S*)

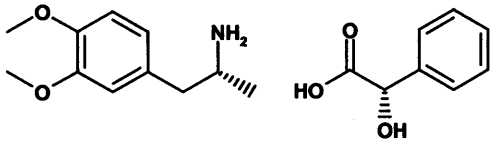

The combined crop 1 crystals and mother liquor (53.7g, 0.152mol) from the resolution of **38*S*** were dissolved in water (1L); the solution was basified by the addition of aqueous sodium hydroxide, and the neutral amine was extracted into dichloromethane (2x500mL). The dichloromethane extractions were combined, and dried initially with a brine wash (200mL), then over dried magnesium sulfate. Filtration, and removal of the solvent under reduced pressure, gave a colourless syrup (~30g, 100%), which was dissolved in boiling propan-2-ol with (*S*)-(+)-mandelic acid **103*S*** (23.5g, 0155mol). The solution was allowed to cool slowly to room temperature overnight, whereupon filtration gave a colourless crystalline solid (50.0g, 0.142mol) $[\alpha]_D^{26}$ +49.0 (c 1.0, water). Resolution was achieved by two further recrystallisations from ethyl acetate/methanol (2:1), which gave **38*R*+103*S*** as

a colourless crystalline solid (yield 8.50g, 20%). The enantiomeric excess of **38*R*** was established as >96% *e.e.* by the method of Marfey[460], using reverse phase analytical HPLC (system 3):

Characterisation:

Melting point:	172-173°C;
Optical rotation $[\alpha]_D^{25}$:	+37.8 (c 1.0, water);
^{1}H-NMR (D_2O):	Ammonium ion: δ_H 1.31 (3H, d, J = 6.6Hz, CHC***H***$_3$), 2.89 (2H, d, J = 7.2Hz, ArC***H***$_2$CH), 3.61 (1H, m, CH_2C***H***CH_3), 3.86-3.88 (6H, 2 x s overlapping, 2 x ArOC***H***$_3$), 6.90 (1H, d, J_{ortho} = 8.2Hz, Ar***H***-6), 6.96 (1H, s, Ar***H***-2), 7.04 (1H, d, J_{ortho} = 8.2Hz, Ar***H***-5); Mandelate ion: δ_H 4.99 (1H, s, ArC***H***OH), 7.37-7.46 (5H, m, 5 x Ph***H***);
^{13}C-NMR (D_2O):	Ammonium ion: δ_C 20.26 (***C***H_3), 42.48 (***C***H_2), 51.91 (***C***H), 58.47 (ArO***C***H_3), 58.50 (ArO***C***H_3), 114.84 (C_{Ar}H-5), 115.61 (C_{Ar}H-2), 124.86 (C_{Ar}H-6), 131.96 (C_{Ar}-1), 150.12 (C_{Ar}OMe-4), 151.07 (C_{Ar}OMe-3); Mandelate ion: δ_C 77.81 (***C***H), 129.83 (2 x C_{Ar}H-2, -6), 130.93 (C_{Ar}H-4), 131.36 (2 x C_{Ar}H-3, -5) 143.42 (C_{Ar}-1), 182.11 (***C***O_2H);
MS (ESI-positive) *m/z*:	MH^+ 196(9), $[MH\text{-}NH_3]^+$ 179(100);
MS (ESI-negative) *m/z*:	$[M\text{-}H]^-$ 151(100);
IR (KBr) ν/cm:	1558 (CO_2^-), 1516 (C_{Ar}–C_{Ar}), 1384 (CO_2^-), 1236 (C–O);
Microanalysis (C,H,N,O):	Calculated for $C_{19}H_{25}NO_5$: 65.69, 7.25, 4.03, 23.03; Found 65.43, 7.30, 4.20, 22.73.

(*R*)-2-(3,4-dimethoxy-phenyl)-1-methylethylamine (38*R*)

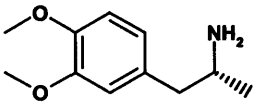

(38*R*+103*S*) (1.2g, 3.46mmol) was dissolved in water (100mL); the solution was basified by the addition of 5M aqueous sodium hydroxide (3mL, ~5 equivalents), and the free base of the amine was extracted into dichloromethane (3 x 50mL). The combined extractions were washed with brine (20mL) and dried over dried

magnesium sulfate. Filtration and removal of solvent under reduced pressure gave a colourless crystalline solid (625mg, 93% yield). Recrystallisation from n-pentane gave colourless needles (360mg, 53%); despite clean NMR spectra and three attempts, a correct elemental analysis was not realised for this enantiomer:

Characterisation:

Melting point:	softened 30-32°C, melted 62-4°C (literature 37-40°C[455]);
Optical rotation $[\alpha]_D^{22}$:	–32.8 (c 4.00, EtOH) (lit. $[\alpha]_D^{22}$ –32.1 (c 4.00, EtOH)[455]);
^{1}H-NMR ($CDCl_3$):	δ_H 1.12 (3H, d, J = 6.3Hz, CHC***H***$_3$), 1.20 (2H, br, N***H***$_2$), 2.44 (1H, dd$_{ABX}$, J_{AB} = 13.4Hz, J_{AX} = 8.3Hz, ArC***H***$_A$H$_B$CH), 2.67 (1H, dd$_{BAX}$, J_{BA} = 13.4Hz, J_{BX} = 5.1Hz, ArCH$_A$***H***$_B$CH), 3.15 (1H, m, ArCH$_A$H$_B$C***H***CH$_3$), 3.86-3.88 (6H, 2 x s, 2 x ArOC***H***$_3$), 6.71-6.75 (2H, m, Ar***H***-2, -6), 6.81 (1H, d, J_{ortho} = 7.9Hz, Ar***H***-5);
^{13}C-NMR ($CDCl_3$):	δ_C 23.58 (***C***H$_3$), 46.20 (***C***H$_2$), 48.53 (***C***H), 55.83 (ArO***C***H$_3$), 55.90 (ArO***C***H$_3$), 111.18 (***C***$_{Ar}$H-5), 112.35 (***C***$_{Ar}$H-2), 121.13 (***C***$_{Ar}$H-6), 132.34 (***C***$_{Ar}$-1), 147.43 (***C***$_{Ar}$OMe-4), 148.79 (***C***$_{Ar}$OMe-3);
MS (EI) *m/z*:	M^+ 195(8), $[MH–CH_3CHNH_2]^+$ 152(100);
IR (KBr) *ν*/cm:	1519 (C_{Ar}–C_{Ar}), 1265 (C_{Ar}–O), 1239 (C_{Ar}–O);
HRMS (positive) *m/z*:	Calculated for [M+H] $C_{11}H_{18}NO_2$: 196.13375; Found 196.13342.

(*S*)-6,7-Dimethoxy-3-methyl-1,2,3,4-tetrahydroisoquinoline (43*S*)

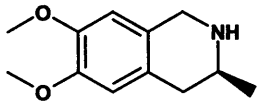

38*S* (1.0g, 5.1mmol) and paraformaldehyde (155mg, 5.1mmol) were dissolved in glacial acetic acid (5mL), and stirred at 40°C for 24 hours. The reaction was poured into water (200mL) and the solution was basified by the addition of 5M aqueous sodium hydroxide (25mL). The product was extracted into dichloromethane (3 x 100mL). The combined dichloromethane extractions were washed with brine (50mL), and dried over dried magnesium sulfate. Filtration, and subsequent removal of solvent under reduced pressure gave a yellow syrup. Purification by flash column chromatography (Biotage 40S, ethyl acetate/methanol/ammonium hydroxide

100:10:1) gave a pale yellow solid (950mg, 90%). Recrystallisation from n-hexane gave a cream coloured crystalline solid (565mg, 53%):

Characterisation:

TLC:	*Rf* 0.25 (dichloromethane/ methanol/ 32% $AcOH_{(aq.)}$ 90:9:1);
Melting point:	70-71°C;
Optical rotation $[\alpha]_D^{21}$:	+141.2 (c 1.01, dichloromethane);
^{1}H-NMR ($CDCl_3$):	δ_H 1.23 (3H, d, J = 6.3Hz, $CHCH_3$), 1.44 (1H, br, N*H*), 2.42 (1H, dd_{ABX}, J_{AB} = 16.0Hz, J_{AX} = 10.5Hz, $ArCH_AH_BCH$), 2.68 (1H, dd_{BAX}, J_{BA} = 16.0Hz, J_{BX} = 3.8Hz, $ArCH_AH_BCH$), 2.95-3.00 (1H, m, $ArCH_AH_BCHCH_3$), 3.83/3.84 (6H, 2 x s (overlapping), 2 x $ArOCH_3$), 3.94 (1H, d_{AB}, J = 15.6Hz, $ArCH_AH_BN$), 4.04 (1H, d_{BA}, J = 15.6Hz, $ArCH_AH_BN$), 6.52 (1H, m, Ar*H*-8), 6.55 (1H, m, Ar*H*-5);
^{13}C-NMR ($CDCl_3$):	δ_C 22.50 (CH_3), 36.80 ($ArCH_2CH$), 48.31 ($ArCH_2NH$), 49.30 (*C*H), 55.92 (2 x $ArOCH_3$), 108.95 (C_{Ar}H-8), 111.88 (C_{Ar}H-5), 126.77 (C_{Ar}-4a), 127.37 (C_{Ar}-8a), 147.27/147.42 (2 x $C_{Ar}OMe$);
MS (ESI-positive) *m/z*:	MH^+ 208.1(100), $[2M+H^+]$ 415.3(9);
IR (KBr) *ν*/cm:	3250 (NH), 1515 (C_{Ar}–C_{Ar}), 1246 (C_{Ar}–OCH_3), 1223 (C_{Ar}–OCH_3);
Microanalysis (C,H,N):	Calculated for $C_{12}H_{17}NO_2$: 69.54, 8.27, 6.76; Found 69.29, 8.11, 6.79.

(*R*)-6,7-Dimethoxy-3-methyl-1,2,3,4-tetrahydroisoquinoline (43*R*)

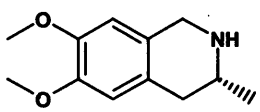

38*R* (1.5g, 7.7mmol) and paraformaldehyde (240mg, 8.0mmol) were dissolved in glacial acetic acid (15mL), and stirred at 40°C for 24 hours. The reaction was poured into 2M aqueous sodium hydroxide (200mL), and the product was extracted into dichloromethane (2 x 100mL). The combined dichloromethane extractions were washed consecutively with water (100mL) and brine (25mL), before drying over dried magnesium sulfate. Filtration, and subsequent removal of solvent under reduced pressure gave the desired product as a virtually pure beige solid (1.50g,

94%). Recrystallisation from n-hexane gave a cream coloured crystalline solid (1.10g, 69%):

Characterisation:

TLC:	*Rf* 0.25 (dichloromethane/ methanol/ 32% $AcOH_{(aq.)}$ 90:9:1);
Melting point:	71-72°C;
Optical rotation $[\alpha]_D^{21}$:	–138.8 (c 1.00, dichloromethane);
^{1}H-NMR ($CDCl_3$):	δ_H 1.24 (3H, d, J = 6.3Hz, CHC***H***$_3$), 1.60 (1H, br, N***H***), 2.44 (1H, dd_{ABX}, J_{AB} = 16.0Hz, J_{AX} = 10.6Hz, ArC***H***$_A$H$_B$CH), 2.69 (1H, dd_{BAX}, J_{BA} = 16.0Hz, J_{BX} = 3.7Hz, ArCH$_A$***H***$_B$CH), 2.97-3.02 (1H, m, ArCH$_A$H$_B$C***H***$_X$H$_3$), 3.83/3.84 (6H, 2 x s (overlapping), 2 x ArOC***H***$_3$), 3.96 (1H, d_{AB}, J = 15.6Hz, ArC***H***$_A$H$_B$N), 4.06 (1H, d_{BA}, J = 15.6Hz, ArCH$_A$***H***$_B$N), 6.53 (1H, m, Ar***H***-8), 6.56 (1H, m, Ar***H***-5);
^{13}C-NMR ($CDCl_3$):	δ_C 22.47 (***C***H$_3$), 36.77 (Ar***C***H$_2$CH), 48.27 (Ar***C***H$_2$NH), 49.31 (***C***H), 55.92 (2 x ArO***C***H$_3$), 108.95 (***C***$_{Ar}$H-8), 111.87 (***C***$_{Ar}$H-5), 126.74 (***C***$_{Ar}$-4a), 127.29 (***C***$_{Ar}$-8a), 147.28/147.43 (2 x ***C***$_{Ar}$OMe);
MS (EI) *m/z*:	M^+ 207(30), $[M–(NHCHCH_3)]^+$ 164(100);
IR (KBr) *ν*/cm:	3250 (NH), 1516 (C_{Ar}–C_{Ar}), 1246 (C_{Ar}–OCH_3), 1223 (C_{Ar}–OCH_3);
Microanalysis (C,H,N):	Calculated for $C_{12}H_{17}NO_2$: 69.54, 8.27, 6.76; Found 69.52, 8.21, 6.85.

Establishing the enantiomeric purity of 42*S* and 42*R*

2.5mg of each of **42*R*** and **42*S*** were combined and dissolved in 0.75mL $CDCl_3$ (+0.03% v/v TMS), and the ^{1}H-NMR spectrum recorded. The chiral solvating agent (*S*)-(+)-1-(9-anthryl)-2,2,2-trifluoroethanol[463;464] ((*S*)-TFAE, **106*S***, 6.7mg, 1 equivalent) was added to the NMR sample, and the ^{1}H-NMR spectrum recorded. A second equivalent of **106*S*** was added, and the ^{1}H-NMR spectrum recorded. Two equivalents of **106*S*** was seen to be sufficient to achieve baseline separation of the signals corresponding to the methyl group of the stereogenic carbon, and the adjacent methylene protons. The experiment was repeated for separate samples of **42*R*** and **42*S***; 5 mg of each were dissolved in 0.75mL $CDCl_3$ (+0.03% v/v TMS), and the ^{1}H-NMR spectrum recorded; **106*S*** (13.4mg, 2 equivalents) was added to each sample,

and the ^{1}H-NMR spectrum recorded. These spectra confirmed the samples of **42*R*** and **42*S*** to be enantiomerically pure, to the limits of analytical detection:

Characterisation:

^{1}H-NMR ($CDCl_3$): **42*RS***

δ_H 1.24 (3H, d, J = 6.3Hz, CHC***H***$_3$), 1.83 (1H, br, N***H***), 2.44 (1H, dd$_{ABX}$, J_{AB} = 16.0Hz, J_{AX} = 10.5Hz, ArC***H***$_A$H$_B$CH), 2.69 (1H, dd$_{BAX}$, J_{BA} = 16.0Hz, J_{BX} = 3.8Hz, ArCH$_A$***H***$_B$CH), 2.96-3.02 (1H, m, ArCH$_A$H$_B$C***H***CH$_3$), 3.83/3.84 (6H, 2 x s (overlapping), 2 x ArOC***H***$_3$), 3.95 (1H, d$_{AB}$, J = 15.6Hz, ArC***H***$_A$H$_B$N), 4.05 (1H, d$_{BA}$, J = 15.6Hz, ArCH$_A$***H***$_B$N), 6.52 (1H, m, Ar***H***-8), 6.56 (1H, m, Ar***H***-5);

^{1}H-NMR ($CDCl_3$): **42*RS*** + 2 equivalents of **106*S***:

δ_H 1.07 (1.5H, d, J = 6.3Hz, CHC***H***$_3$), 1.15 (1.5H, d, J = 6.3Hz, CHC***H***$_3$), 2.13 (0.5H, dd$_{ABX}$, J_{AB} = 16.0Hz, J_{AX} = 10.5Hz, ArC***H***$_A$H$_B$CH), 2.34 (0.5H, dd$_{ABX}$, J_{AB} = 16.0Hz, J_{AX} = 10.5Hz, ArC***H***$_A$H$_B$CH), 2.43 (0.5H, dd$_{BAX}$, J_{BA} = 16.0Hz, J_{BX} = 3.8Hz, ArCH$_A$***H***$_B$CH), 2.55 (0.5H, dd$_{BAX}$, J_{BA} = 16.0Hz, J_{BX} = 3.8Hz, ArCH$_A$***H***$_B$CH), 2.77-2.88 (1H, m, ArCH$_A$H$_B$C***H***CH$_3$), 3.46 (0.5H, d$_{AB}$, J = 15.6Hz, ArC***H***$_A$H$_B$N), 3.70-3.84 (~9.5H, overlapping 4 x s, 3 x d and 1 x br s, 2 x ArOC***H***$_3$, 0.5 x ArC***H***$_A$H$_B$N, 1 x ArCH$_A$***H***$_B$N and 2 x OH (TFAE)), 6.12 (0.5H, s, Ar***H***), 6.26 (0.5H, s, Ar***H***), 6.27 (1H, s, Ar***H***), 6.38 (0.5H, s, Ar***H***), 6.52 (2H, quartet, J = 8.2Hz, ArC***H***(OH)CF$_3$), 7.43-7.53 (8H, m, 4 x Ar***H*** (TFAE)), 7.90-8.00 (6H, m, 3 x Ar***H*** (TFAE)), 8.48 (2H, s, Ar***H***), 9.02 (2H, br, Ar***H***).

^{1}H-NMR ($CDCl_3$) **42*R*** + 2 equivalents of **106*S***:

δ_H 1.15 (3H, d, J = 6.3Hz, CHC***H***$_3$), 2.34 (1H, dd$_{ABX}$, J_{AB} = 16.0Hz, J_{AX} = 10.5Hz, ArC***H***$_A$H$_B$CH), 2.55 (1H, dd$_{BAX}$, J_{BA} = 16.0Hz, J_{BX} = 3.8Hz, ArCH$_A$***H***$_B$CH), 2.81-2.87 (1H, m, ArCH$_A$H$_B$C***H***CH$_3$), 3.47 (1H, d$_{AB}$, J = 15.6Hz, ArC***H***$_A$H$_B$N), 3.70-3.85 (~9H, 2 x s, 1 x d and 1 x br s, 2 x ArOC***H***$_3$, 1 x ArCH$_A$***H***$_B$N and 2 x OH (TFAE)), 6.12 (1H, s, Ar***H***),

6.38 (1H, s, Ar***H***), 6.54 (2H, quartet, J = 8.2Hz, ArC***H***(OH)CF_3), 7.44-7.54 (8H, m, 4 x Ar***H***), 7.90-8.00 (6H, m, 3 x Ar***H***), 8.49 (2H, s, Ar***H***), 9.01 (2H, br, Ar***H***).

^{1}H-NMR ($CDCl_3$) **42*S*** + 2 equivalents of **106*S***:

δ_H 1.06 (3H, d, J = 6.3Hz, CHC***H***$_3$), 2.12 (1H, dd_{ABX}, J_{AB} = 16.0Hz, J_{AX} = 10.5Hz, ArC***H***$_A$H$_B$CH), 2.42 (1H, dd_{BAX}, J_{BA} = 16.0Hz, J_{BX} = 3.8Hz, ArCH$_A$***H***$_B$CH), 2.78-2.84 (1H, m, ArCH$_A$H$_B$C***H***CH$_3$), 3.67-3.83 (1H, d_{AB}, J = 15.6Hz,), 3.70-3.85 (~10H, 2 x s, 2 x d and 1 x br s, 2 x ArOC***H***$_3$, 1 x ArC***H***$_A$H$_B$N, 1 x ArCH$_A$***H***$_B$N and 2 x OH (TFAE)), 6.24 (1H, s, Ar***H***), 6.26 (1H, s, Ar***H***), 6.53 (2H, quartet, J = 8.2Hz, ArC***H***(OH)CF_3), 7.44-7.54 (8H, m, 4 x Ar***H***), 7.90-8.00 (6H, m, 3 x Ar***H***), 8.49 (2H, s, Ar***H***), 9.02(2H, br, Ar***H***).

(*S*)-6,7-Dihydroxy-3-methyl-1,2,3,4-tetrahydroisoquinoline hydrobromide (34*S*)

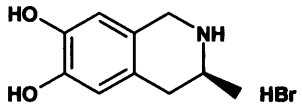

42*S* (675mg, 3.3mmol) was dissolved in 48% hydrobromic acid (10mL), and stirred at reflux for eighteen hours; an aliquot was removed from the reaction, the solvent was removed under reduced pressure, and analysis by ^{1}H-NMR in D_2O confirmed that the reaction was complete, by the absence of signals corresponding to aromatic methoxy groups. The reaction was cooled to room temperature, and the solvent was removed under reduced pressure, to leave a beige foam (850mg, quantitative) that was pure by ^{1}H-NMR. Recrystallisation from methanol/ ethyl acetate (1:1 20mL) gave a beige crystalline solid (135mg, 16% yield), which was used for characterisation:

Characterisation:

Melting point: Softened from 240°C; melted 252-254°C;

Optical rotation $[\alpha]_D^{25}$: +64.4 (c 1.03, water);

^{1}H-NMR (D_2O): (containing 0.75% 3-(trimethylsilyl)propionic-2,2,3,3-d_4 acid)

δ_H 1.46 (3H, d, J = 6.4Hz, CHC***H***$_3$), 2.79 (1H, dd_{ABX}, J_{AB} = 17.2Hz, J_{AX} = 10.6Hz, ArC***H***$_A$H$_B$CH), 3.03 (1H, dd_{BAX}, J_{BA} = 17.2Hz, J_{BX} = 4.6Hz, ArCH$_A$***H***$_B$CH), 3.56-3.65 (1H, m,

	$ArCH_AH_BC\boldsymbol{H}_XCH_3$), 4.26 (2H, s, $ArC\boldsymbol{H}_2N$), 6.73 (1H, m, Ar***H***-8), 6.75 (1H, m, Ar***H***-5);
^{13}C-NMR (D_2O):	(containing 0.75% 3-(trimethylsilyl)propionic-2,2,3,3-d_4 acid) δ_C 20.70 ($\boldsymbol{C}H_3$), 34.69 ($ArCH_2CH$), 46.73 ($Ar\boldsymbol{C}H_2NH$), 52.94 ($\boldsymbol{C}H$), 116.28 ($\boldsymbol{C}_{Ar}H$-8), 118.57 ($\boldsymbol{C}_{Ar}H$-5), 121.95 ($\boldsymbol{C}_{Ar}$-4a), 126.43 ($\boldsymbol{C}_{Ar}$-8a), 145.90/146.75 (2 x $\boldsymbol{C}_{Ar}OH$);
MS (ESI-negative) *m/z*:	$[M–H]^-$ 178.0(10), Br^- 80.9(100);
MS (ESI-positive) *m/z*:	MH^+ 180.0(100);
IR (KBr) *ν*/cm:	3168 (OH str.), 1534 (C_{Ar}–C_{Ar}), 1234 (C_{Ar}–OH);
Microanalysis (C,H,N):	Calculated for $C_{10}H_{14}NO_2Br$: 46.17, 5.42, 5.38; Found 45.58/45.57, 5.16/5.17, 5.46/5.47; Recalculated + 0.17 equivalents of water: 45.70, 5.38, 5.33.

(*R*)-6,7-Dihydroxy-3-methyl-1,2,3,4-tetrahydroisoquinoline hydrobromide (34*R*)

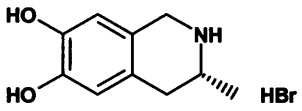

42*R* (1.10g, 5.3mmol) was dissolved in 48% hydrobromic acid (10mL), and stirred at reflux for twenty-four hours; an aliquot was removed from the reaction, the solvent was removed under reduced pressure, and analysis by ^{1}H-NMR in D_2O confirmed that the reaction was complete, by the absence of signals corresponding to aromatic methoxy groups. The reaction was cooled to room temperature, and the solvent was removed under reduced pressure, to leave a beige foam (1.38g, quantitative). ^{1}H-NMR in D_2O confirmed the foam as pure. Recrystallisation from methanol/ ethyl acetate (1:1 20mL) eventually gave a beige microcrystalline solid (55mg, 4% yield), which was used for characterisation:

Characterisation:

Melting point:	242-252°C;
Optical rotation $[\alpha]_D^{22}$:	–62.9 (c 1.00, water);
^{1}H-NMR (D_2O):	(containing 0.75% 3-(trimethylsilyl)propionic-2,2,3,3-d_4 acid) δ_H 1.48 (3H, d, J = 6.4Hz, $CHC\boldsymbol{H}_3$), 2.79 (1H, dd_{ABX}, J_{AB} = 17.2Hz, J_{AX} = 10.6Hz, $ArC\boldsymbol{H}_AH_BCH$), 3.01 (1H, dd_{BAX}, J_{BA} = 17.2Hz, J_{BX} = 4.6Hz, $ArCH_A\boldsymbol{H}_BCH$), 3.54-3.63 (1H, m, $ArCH_AH_BC\boldsymbol{H}_XCH_3$), 4.26 (2H, s, $ArC\boldsymbol{H}_2N$), 6.72 (1H, m,

	Ar***H***-8), 6.74 (1H, m, Ar***H***-5);
^{13}C-NMR (D_2O):	(containing 0.75% 3-(trimethylsilyl)propionic-2,2,3,3-d_4 acid) δ_C 20.68 (***C***H_3), 34.68 (Ar***C***H_2CH), 46.70 (Ar***C***H_2NH), 52.92 (***C***H), 116.31 ($***C***_{Ar}$H-8), 118.60 ($***C***_{Ar}$H-5), 121.98 ($***C***_{Ar}$-4a), 126.44 ($***C***_{Ar}$-8a), 145.93/146.78 (2 x $***C***_{Ar}$OH);
MS (ESI-negative) *m/z*:	$[M–H]^-$ 178.0(10), Br^- 80.9(100);
MS (ESI-positive) *m/z*:	MH^+ 180.0(100);
IR (KBr) *ν*/cm:	3168 (OH str.), 1534 (C_{Ar}–C_{Ar}), 1234 (C_{Ar}–OH);
Microanalysis (C,H,N):	Calculated for $C_{10}H_{14}NO_2Br$: 46.17, 5.42, 5.38; Found 46.02, 5.18, 5.37.

(*S*)-*N*-(4-Chlorophenethylthiocarbamoyl)-6,7-dihydroxy-3-methyl-1,2,3,4-tetrahydroisoquinoline (30*S*):

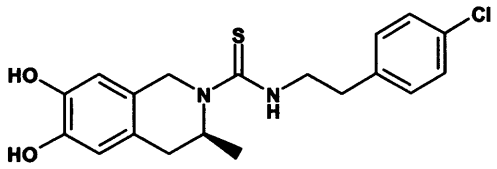

34*S* (750mg, 2.88mmol) was suspended in dry dichloromethane (10mL) with triethylamine (400μL, 291mg, 2.88mmol). Isothiocyanate **32** (570mg, 2.88mmol) was dissolved in dry dichloromethane (5mL) and added to the reaction mixture, which was stirred at room temperature under an atmosphere of argon for eighteen hours. The reaction was diluted to 100mL with dichloromethane and washed consecutively with dilute aqueous hydrochloric acid (2 x 75mL), water (50mL) and brine (25mL), before drying over dried magnesium sulfate. Filtration, and removal of solvent under reduced pressure gave a bright yellow foam; purification by flash column chromatography (Biotage 40S, cyclohexane/ ethyl acetate 2:1) gave a yellow foam, which was dissolved in chloroform (10mL) and precipitated from cyclohexane (50mL), to give a bright yellow amorphous solid. Drying under reduced pressure at 55°C to constant weight gave the product as a finely divided powder, containing ~0.05 equivalents of residual cyclohexane (690mg, 64%):

Characterisation:

Melting point:	amorphous solid;
Optical rotation $[\alpha]_D^{25}$:	–114.5 (*c* 1.04, chloroform);
^{1}H-NMR ($CDCl_3$):	δ_H 0.93 (3H, d, J = 6.6Hz, CHC***H***$_3$), 1.42 (0.6H, s, residual

cyclohexane[504]), 2.40 (1H, dd_{ABX}, J_{AB} = 15.5Hz, J_{AX} = 2.2Hz, ArC***H***$_A$H$_B$CH), 2.87 (1H, dd_{BAX}, J_{BA} = 15.5Hz, J_{BX} = 4.9Hz, ArCH$_A$***H***$_B$CH), 2.93 (2H, t, J = 7.1Hz, 4'-chlorophenyl-C***H***$_2$CH$_2$), 3.84-4.00 (2H, m, 4'-chlorophenyl-CH$_2$C***H***$_2$NH), 4.30 (1H, br d_{AB}, J_{AB} ≈15Hz, ArC***H***$_A$H$_B$N), 4.69 (1H, br d_{AB}, J_{AB} ≈15Hz, ArCH$_A$***H***$_B$N), 4.9-5.1 (1H, br, ArCH$_A$H$_B$C***H***$_X$CH$_3$), 5.69 (1H, t, J = 5.1Hz, N***H***), 5.85-6.15 (2H, br, 2 x ArO***H***), 6.58 (1H, m, Ar***H***-8), 6.62 (1H, m, Ar***H***-5), 7.12 (2H, dm (AA' of an AA'BB' system), J_{ortho} = 8.4Hz, Ar***H***-2', Ar***H***-6'), 7.23 (2H, dm (BB' of an AA'BB' system), J_{ortho} = 8.4Hz, Ar***H***-3', Ar***H***-5');

^{13}C-NMR ($CDCl_3$): δ_C 17.56 (***C***H$_3$), 26.92 (***C***H$_2$, residual cyclohexane[504]), 34.44 (tetrahydroisoquinoline Ar***C***H$_2$CH), 34.66 (4'-chlorophenyl-***C***H$_2$CH$_2$), 46.61 (Ar***C***H$_2$NH), 46.84 (4'-chlorophenyl-CH$_2$***C***H$_2$NH), 49.95 (***C***H), 113.15 (***C***$_{Ar}$H-8), 115.64 (***C***$_{Ar}$H-5), 123.49 (br, ***C***$_{Ar}$-8a), 125.19 (***C***$_{Ar}$-4a), 128.80 (***C***$_{Ar}$H-3', ***C***$_{Ar}$H-5'), 130.17 (***C***$_{Ar}$H-2', ***C***$_{Ar}$H-6'), 132.41 (***C***$_{Ar}$-Cl), 137.25 (***C***$_{Ar}$-1'), 142.55 (***C***$_{Ar}$OH-7), 143.30 (***C***$_{Ar}$OH-6), 179.85 (***C***=S);

MS (ESI-negative) *m/z*: $[M-H]^-$ 375.2(100)/377.2(41);

MS (ESI-positive) *m/z*: MH^+ 377.2(23)/379.2(8),
$[M-(ClC_6H_4CH_2CH_2NHC=S)]^+$ 178.1 (100);

IR (KBr) *ν*/cm: 3361 (OH str.), 1524 (C_{Ar}–C_{Ar});

Microanalysis (C,H,N): Calculated for $C_{19}H_{21}N_2O_2SCl$ + 0.05 equivalents of cyclohexane: 60.81, 5.72, 7.35;
Found 60.56, 5.67, 7.38;

HRMS (positive) *m/z*: Calculated for [M+H] $C_{19}H_{22}N_2O_2SCl$: 377.1091;
Found 377.1097.

(*R*)-*N*-(4-Chlorophenethylthiocarbamoyl)-6,7-dihydroxy-3-methyl-1,2,3,4-tetrahydroisoquinoline (30*R*):

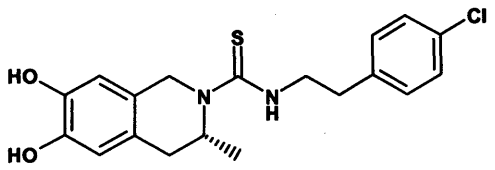

34*R* (1.15g, 4.4mmol) was dissolved in dry *N*,*N*-DMF (10mL) with triethylamine (680μL, 495mg, 4.9mmol, 1.1 equivalents). The reaction was stirred under argon; after five minutes **32** (875mg, 4.4mmol) was dissolved in dry *N*,*N*-DMF (5mL) and added to the reaction mixture. The reaction was stirred at room temperature under an atmosphere of argon for eighteen hours. The reaction was diluted to 250mL with ethyl acetate and washed consecutively with 2M aqueous hydrochloric acid (2 x 100mL), water (100mL) and brine (50mL), before drying over dried magnesium sulfate. Filtration, and removal of solvent under reduced pressure gave an orange syrup; purification by flash column chromatography (Biotage 40M, cyclohexane/ ethyl acetate 2:1) gave a pale yellow foam. The foam was dissolved in chloroform (20mL) and precipitated from 200mL of vigorously stirring cyclohexane (200mL), to give a bright yellow amorphous solid. Drying under reduced pressure at 55°C to constant weight (5 days) gave the product as a finely divided powder, containing ~0.05 equivalents of residual cyclohexane (955mg, 58%):

Characterisation:

Melting point: amorphous solid;

Optical rotation $[\alpha]_D^{25}$: +113.0 (*c* 1.05, $CHCl_3$);

^{1}H-NMR ($CDCl_3$): δ_H 0.94 (3H, d, J = 6.6Hz, CHC***H***$_3$), 1.42 (~0.6H, s, residual cyclohexane[504]), 2.42 (1H, dd$_{ABX}$, J_{AB} = 15.5Hz, J_{AX} = 2.6Hz, ArC***H***$_A$H$_B$CH), 2.86-2.96 (3H overlapping signals, comprising: 2.89 (1H, dd$_{BAX}$, J_{BA} = 15.5Hz, J_{BX} = 5.0Hz, ArCH$_A$***H***$_B$CH), 2.93 (2H, t, J = 7.1Hz, 4'-chlorophenyl-C***H***$_2$CH$_2$)), 3.88-3.98 (2H, m, 4'-chlorophenyl-CH$_2$C***H***$_2$NH), 4.32 (1H, br d$_{AB}$, J_{AB} ≈15Hz, ArC***H***$_A$H$_B$N), 4.69 (1H, br d$_{AB}$, J_{AB} ≈15Hz, ArCH$_A$***H***$_B$N), 4.93-5.07 (1H, br, ArCH$_A$H$_B$C***H***$_X$CH$_3$), 5.65 (1H, t, J = 5.2Hz, N***H***), 5.7-6.0 (2H, br, 2 x ArO***H***), 6.59 (1H, m, Ar***H***-8), 6.63 (1H, m, Ar***H***-5), 7.13 (2H, dm (AA' of an AA'BB' system), J_{ortho} = 8.4Hz,

	Ar***H***-2', Ar***H***-6'), 7.23 (2H, dm (BB' of an AA'BB' system), J_{ortho} = 8.4Hz, Ar***H***-3', Ar***H***-5');
^{13}C-NMR ($CDCl_3$):	δ_C 17.57 (***C***H_3), 26.92 (***C***H_2, residual cyclohexane[504]), 34.47 (tetrahydroisoquinoline Ar***C***H_2CH), 34.65 (4'-chlorophenyl-***C***H_2CH_2), 46.64 (Ar***C***H_2NH), 46.82 (4'-chlorophenyl-CH_2***C***H_2NH), 49.93 (***C***H), 113.13 (C_{Ar}H-8), 115.61 (C_{Ar}H-5), 123.53 (br, C_{Ar}-8a), 125.23 (C_{Ar}-4a), 128.82 (C_{Ar}H-3', C_{Ar}H-5'), 130.18 (C_{Ar}H-2', C_{Ar}H-6'), 132.44 (C_{Ar}-Cl), 137.25 (C_{Ar}-1'), 142.51 (C_{Ar}OH-7), 143.28 (C_{Ar}OH-6), 179.92 (***C***=S);
MS (ESI-negative) *m/z*:	$[M-H]^-$ 375.2 (100);
MS (ESI-positive) *m/z*:	MH^+ 377.1 (100);
IR (KBr) *ν*/cm:	3373 (OH str.), 1524 (C_{Ar}–C_{Ar});
Microanalysis (C,H,N):	Calculated for $C_{19}H_{21}N_2O_2SCl$ + 0.05 equivalents of cyclohexane: 60.81, 5.72, 7.35; Found 60.43, 5.69, 7.40;
HRMS (positive) *m/z*:	Calculated for [M+H] $C_{19}H_{22}N_2O_2SCl$: 377.1085; Found 377.1084.

Enantiomers of the *trans*-diastereomers of N-(4-chlorophenethylthio-carbamoyl)-6,7-dihydroxy-1,3-dimethyl-1,2,3,4-tetrahydroisoquinoline analogues (31(1*R*,3*R*) and 31(1*S*,3*S*))

(*S*)-*N*-Benzyl-2-(3,4-dimethoxyphenyl)-1-methylethylamine (155*S*)

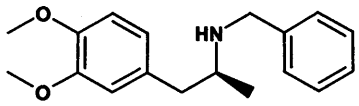

38*S* (10.0g, 0.0513mol) was dissolved in dry methanol (200mL), and chilled to 0°C by stirring on ice under an atmosphere of argon. Benzaldehyde (5.21mL, 5.44g, 0.0513mol) was added in one portion, and the reaction was stirred for 24 hours. TLC (dichloromethane/ methanol/ 32% $AcOH_{(aq.)}$ 90:9:1) confirmed no amine remained. The solution was cooled to –15°C on a salt/ice bath, sodium borohydride (2.91g, 0.077mol, 1.5 equivalents) was added portionwise over fifteen minutes, with accompanying effervescence, and the mixture was left to come to room temperature with stirring for 18 hours. The reaction was poured into 1.0M aqueous sodium hydroxide (500mL), and the product extracted into ethyl acetate (2 x 250mL). The combined extractions were washed with water (200mL) and brine (100mL), then dried over dried magnesium sulfate. Filtration and removal of solvent under reduced pressure, followed by purification by flash column chromatography (Biotage 40M cartridge; cyclohexane/ethyl acetate 1:4) gave a colourless oil (13.4g, 92%):

Characterisation:

TLC: *Rf* 0.50 (dichloromethane/methanol/32% aqueous acetic acid 90:9:1);

Optical rotation $[\alpha]_D^{21}$: +38.4 (c 0.88, dichloromethane);

^{1}H-NMR ($CDCl_3$): δ_H 1.11 (3H, d, J = 6.2Hz, CHC***H***$_3$), 2.58-2.69 (2H, m, ArC***H***$_2$CH), 2.87-2.93 (1H, m, CH_2C***H***CH_3), 3.72 (1H, d_{AB}, J_{AB} = 13.4Hz, PhC***H***$_A$H$_B$NH), 3.82 (3H, s, ArOC***H***$_3$-3), 3.85 (1H, d_{BA}, J_{AB} = 13.4Hz, PhCH$_A$***H***$_B$NH), 3.86 (3H, s, ArOC***H***$_3$-4), 6.65 (1H, d, J_{meta} = 1.8Hz, Ar***H***-2), 6.70 (1H, dd, J_{ortho} = 8.1Hz, J_{meta} = 1.8Hz, Ar***H***-6), 6.79 (1H, d, J_{ortho} = 8.1Hz, Ar***H***-5), 7.17-7.23 (3H, m, Ar***H***-2', Ar***H*** -4', Ar***H*** -6'), 7.24-7.29 (2H, m, Ar***H***-3', Ar***H***-5');

^{13}C-NMR ($CDCl_3$): δ_C 20.24 ($CH\boldsymbol{C}H_3$), 43.27 ($Ar\boldsymbol{C}H_2CH$), 51.25 ($Ph\boldsymbol{C}H_2N$), 53.49 ($CH_2\boldsymbol{C}H(NH)CH_3$), 55.75 ($ArO\boldsymbol{C}H_3$-3), 55.93 ($ArO\boldsymbol{C}H_3$-4), 111.22 ($\boldsymbol{C}_{Ar}H$-5), 112.37 ($\boldsymbol{C}_{Ar}H$-2), 121.26 ($\boldsymbol{C}_{Ar}H$-6), 126.81 ($\boldsymbol{C}_{Ar}H$-4'), 127.98, 128.35 ($\boldsymbol{C}_{Ar}H$-3', $\boldsymbol{C}_{Ar}H$–5' and $\boldsymbol{C}_{Ar}H$-2', $\boldsymbol{C}_{Ar}H$-6'), 132.00 ($\boldsymbol{C}_{Ar}$-1), 140.53 ($\boldsymbol{C}_{Ar}$-1'), 147.50 ($\boldsymbol{C}_{Ar}$OMe-4), 148.86 ($\boldsymbol{C}_{Ar}$OMe-3);

A sample of the oil (500mg, 1.75mmol) was dissolved in dioxan (10mL); to the stirred solution 5.0 equivalents of hydrogen chloride was added, as 4.0M HCl in dioxan (2.2mL). The dense white precipitate formed was filtered and washed with diethyl ether; this precipitate was dissolved in a boiling mixture of propan-2-ol (12mL) and methanol (5mL), hot-filtered, and cooled to room temperature overnight. Filtration gave a colourless crystalline solid (457mg, 82%):

Characterisation:

TLC: *Rf* 0.50 (dichloromethane/ methanol/ 32% $AcOH_{(aq.)}$ 90:9:1);

Melting point: 204°C (sublimed);

Optical rotation $[\alpha]_D^{20}$: +20.7 (c 0.45, ethanol);

^{1}H-NMR ($CDCl_3$): δ_H 1.34 (3H, d, J = 6.5Hz, $CHC\boldsymbol{H}_3$), 2.77 (1H, dd_{ABX}, J_{AB} = 13.1Hz, J_{AX} = 10.7Hz, $ArC\boldsymbol{H}_AH_BCH$), 3.10-3.20 (1H, br m, $CH_2C\boldsymbol{H}CH_3$), 3.42 (1H, dd_{BAX}, J_{BA} = 13.1Hz, J_{BX} = 3.8Hz, $ArCH_A\boldsymbol{H}_BCH$), 3.81 (3H, s, $ArOC\boldsymbol{H}_3$-3), 3.84 (3H, s, $ArOC\boldsymbol{H}_3$-4), 4.01-4.11 (2H, m, $PhC\boldsymbol{H}_2N$), 6.60 (1H, d, J_{meta} = 1.8Hz, Ar***H***-2), 6.65 (1H, dd, J_{ortho} = 8.2Hz, J_{meta} = 1.8Hz, Ar***H***-6), 6.76 (1H, d, J_{ortho} = 8.2Hz, Ar***H***-5), 7.31 (1H, t, J_{ortho} = 7.4Hz, Ar***H***-4'), 7.36-7.41 (2H, m, Ar***H***-3', Ar***H***-5') 7.66 (2H, J_{ortho} = 7.1Hz, Ar***H***-2', Ar***H***-6'), 10.00 (2H, br, $N^+\boldsymbol{H}_2$);

^{13}C-NMR ($CDCl_3$): δ_C 15.85 ($CH\boldsymbol{C}H_3$), 38.72 ($Ar\boldsymbol{C}H_2CH$), 47.92 ($Ph\boldsymbol{C}H_2N$), 54.09 ($CH_2\boldsymbol{C}HCH_3$), 55.87 ($ArO\boldsymbol{C}H_3$), 55.93 ($ArO\boldsymbol{C}H_3$), 111.25 ($\boldsymbol{C}_{Ar}H$-5), 112.35 ($\boldsymbol{C}_{Ar}H$-2), 121.37 ($\boldsymbol{C}_{Ar}H$-6), 128.81 ($\boldsymbol{C}_{Ar}$-1), 129.08 ($\boldsymbol{C}_{Ar}H$-3', $\boldsymbol{C}_{Ar}H$–5'), 129.38 ($\boldsymbol{C}_{Ar}H$-4'), 130.11 ($\boldsymbol{C}_{Ar}$-1'), 130.51 ($\boldsymbol{C}_{Ar}H$-2', $\boldsymbol{C}_{Ar}H$-6'), 147.97 ($\boldsymbol{C}_{Ar}$OMe-4), 148.97 ($\boldsymbol{C}_{Ar}$OMe-3);

MS (ESI-positive) *m/z*: MH^+ 286(100), $[M\text{-}BnNH]^+$ 179(53);

IR (KBr) *ν*/cm: 1518 (C_{Ar}–C_{Ar}), 1268 (Ar–OCH_3), 1021 (ArO–CH_3);

Microanalysis (C,H,N): Calculated for $C_{16}H_{24}NO_2Cl$: 67.17, 7.52, 4.35;
Found 67.12, 7.23, 4.26.

(*R*)-*N*-Benzyl-2-(3,4-dimethoxyphenyl)-1-methylethylamine (155*R*)

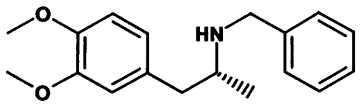

38*R* (4.00g, 0.0205mol) was dissolved in dry methanol (80mL), then cooled to –10°C on a salt/ice bath, with stirring under an atmosphere of nitrogen. Benzaldehyde (2.1mL, 2.18g, 0.0205mol) was added, and the reaction was left to stir for 62 hours, over which time the reaction temperature returned to ambient. The reaction temperature was returned to –10°C, and sodium borohydride (1.16g, 0.0308mol, 1.5 equivalents) was added portionwise over five minutes; the mixture was stirred for four hours. An aliquot of the reaction was partitioned between ethyl acetate and 1M aqueous sodium hydroxide; analysis of the organic phase against the starting primary amine by TLC (dichloromethane/methanol 10:1) confirmed the reaction to be complete. The reaction was poured into 1M aqueous sodium hydroxide (500mL) and the product was extracted into ethyl acetate (2x250mL). The combined organic extractions were washed with water (100mL) and brine (50mL), then dried over dried magnesium sulfate. Filtration, and removal of the solvent under reduced pressure, gave a colourless oil (5.83g, 98%).

Characterisation:

TLC: *Rf* 0.50 (dichloromethane/ methanol/ 32% $AcOH_{(aq.)}$ 90:9:1);

Optical rotation $[\alpha]_D^{21}$: –39.5 (c 0.84, dichloromethane);

^{1}H-NMR ($CDCl_3$): δ_H 1.11 (3H, d, J = 6.2Hz, $CHCH_3$), 2.58-2.70 (2H, m, $ArCH_2CH$), 2.87-2.93 (1H, m, CH_2CHCH_3), 3.72 (1H, d_{AB}, J_{AB} = 13.4Hz, $PhCH_AH_BNH$), 3.82 (3H, s, $ArOCH_3$-3), 3.85 (1H, d_{BA}, J_{AB} = 13.4Hz, $PhCH_AH_BNH$), 3.86 (3H, s, $ArOCH_3$-4), 6.65 (1H, d, J_{meta} = 1.9Hz, Ar*H*-2), 6.70 (1H, dd, J_{ortho} = 8.1Hz, J_{meta} = 1.9Hz, Ar*H*-6), 6.79 (1H, d, J_{ortho} = 8.1Hz, Ar*H*-5), 7.17-7.24 (3H, m, Ar*H*-2', Ar*H* -4', Ar*H* -6'), 7.24-7.30 (2H, m, Ar*H*-3', Ar*H*-5');

^{13}C-NMR ($CDCl_3$): δ_C 20.23 ($CH\boldsymbol{C}H_3$), 43.27 ($Ar\boldsymbol{C}H_2CH$), 51.25 ($Ph\boldsymbol{C}H_2N$), 53.49 ($CH_2\boldsymbol{C}H(NH)CH_3$), 55.80 ($ArO\boldsymbol{C}H_3$-3), 55.93 ($ArO\boldsymbol{C}H_3$-4), 111.22 ($\boldsymbol{C}_{Ar}H$-5), 112.38 ($\boldsymbol{C}_{Ar}H$-2), 121.26 ($\boldsymbol{C}_{Ar}H$-6), 126.81 ($\boldsymbol{C}_{Ar}H$-4'), 127.98, 128.35 ($\boldsymbol{C}_{Ar}H$-3', $\boldsymbol{C}_{Ar}H$–5' and $\boldsymbol{C}_{Ar}H$-2', $\boldsymbol{C}_{Ar}H$-6'), 131.99 ($\boldsymbol{C}_{Ar}$-1), 140.53 ($\boldsymbol{C}_{Ar}$-1'), 147.50 ($\boldsymbol{C}_{Ar}$OMe-4), 148.86 ($\boldsymbol{C}_{Ar}$OMe-3);

A sample of the oil (430mg, 2.21mmol) was dissolved in dioxan (5mL); to the stirred solution was added 5.0 equivalents of hydrogen chloride as 4.0M HCl in dioxan (1.9mL), forming a dense colourless precipitate. The suspension was heated to boiling, and methanol was added dropwise until the precipitate dissolved (~2.5mL); the solution was left to cool to room temperature overnight. Filtration gave a colourless crystalline solid (336mg, 69%):

Characterisation:

TLC: *Rf* 0.54 (dichloromethane/ methanol 10:1);

Melting point: 205°C (sublimed);

Optical rotation $[\alpha]_D^{20}$: –20.8 (c 0.41, ethanol);

^{1}H-NMR ($CDCl_3$): δ_H 1.34 (3H, d, J = 6.5Hz, $CHC\boldsymbol{H}_3$), 2.77 (1H, dd_{ABX}, J_{AB} = 13.2Hz, J_{AX} = 10.7Hz, $ArC\boldsymbol{H}_AH_BCH$), 3.10-3.20 (1H, br m, $CH_2C\boldsymbol{H}CH_3$), 3.42 (1H, dd_{BAX}, J_{BA} = 13.2Hz, J_{BX} = 3.8Hz, $ArCH_A\boldsymbol{H}_BCH$), 3.81 (3H, s, $ArOC\boldsymbol{H}_3$-3), 3.84 (3H, s, $ArOC\boldsymbol{H}_3$-4), 4.01-4.11 (2H, m, $PhC\boldsymbol{H}_2N$), 6.60 (1H, d, J_{meta} = 1.7Hz, Ar***H***-2), 6.65 (1H, dd, J_{ortho} = 8.2Hz, J_{meta} = 1.7Hz, Ar***H***-6), 6.76 (1H, d, J_{ortho} = 8.2Hz, Ar***H***-5), 7.31 (1H, t, J_{ortho} = 7.4Hz, Ar***H***-4'), 7.36-7.40 (2H, m, Ar***H***-3', Ar***H***-5') 7.66 (2H, J_{ortho} = 7.3Hz, Ar***H***-2', Ar***H***-6'), 10.03 (2H, br, $N^+\boldsymbol{H}_2$);

^{13}C-NMR ($CDCl_3$): δ_C 15.90 ($CH\boldsymbol{C}H_3$), 38.77 ($Ar\boldsymbol{C}H_2CH$), 47.94 ($Ph\boldsymbol{C}H_2N$), 54.10 ($CH_2\boldsymbol{C}HCH_3$), 55.91 ($ArO\boldsymbol{C}H_3$), 55.97 ($ArO\boldsymbol{C}H_3$), 111.38 ($\boldsymbol{C}_{Ar}H$-5), 112.47 ($\boldsymbol{C}_{Ar}H$-2), 121.47 ($\boldsymbol{C}_{Ar}H$-6), 128.87 ($\boldsymbol{C}_{Ar}$-1), 129.09 ($\boldsymbol{C}_{Ar}H$-3', $\boldsymbol{C}_{Ar}H$-5'), 129.39 ($\boldsymbol{C}_{Ar}H$-4'), 130.15 ($\boldsymbol{C}_{Ar}$-1'), 130.53 (2 x $\boldsymbol{C}_{Ar}H$-2', $\boldsymbol{C}_{Ar}H$-6'), 148.07 ($\boldsymbol{C}_{Ar}$OMe-4), 149.07 ($\boldsymbol{C}_{Ar}$OMe-3);

MS (ESI-positive) *m/z*: MH^+ 286(45), $[M\text{-}PhCH_2NH]^+$ 179(100);

IR (KBr) *ν*/cm: 1518 (C_{Ar}–C_{Ar}), 1268 (Ar–OCH_3), 1021 (ArO–CH_3);

Microanalysis (C,H,N): Calculated for $C_{16}H_{24}NO_2Cl$: 67.17, 7.52, 4.35;
Found 66.90, 7.40, 4.52.

Ethynyl-4-tolylsulfone (150)[483]

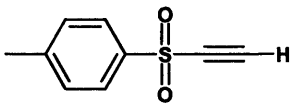

Ethynyl-4-tolylsulfone **150** was synthesised according to the method of Waykole and Paquette[483]. Aluminium chloride (29.4g, 0.22mol) was suspended in dry dichloromethane (200mL), and stirred under an atmosphere of nitrogen. Toluene-4-sulfonyl chloride (41.9g, 0.22mol) was added, and the mixture was stirred for one hour, to give a hazy brown solution. A solution of bis(trimethylsilyl)acetylene (34.0g, 0.20mol) in dry dichloromethane (200mL) was stirred under an atmosphere of nitrogen, and cooled on an ice/water bath; the solution containing the tosyl chloride-aluminium chloride complex was added dropwise, over one hour, to give an orange solution, which was stirred at room temperature for eighteen hours. The now dark brown reaction mixture was poured into a mixture of 2.0M hydrochloric acid (200mL) and ice/water (200mL), stirred for ten minutes, then separated. The organic phase was washed consecutively with water (2 x 250mL), and brine (100mL), before drying over dried magnesium sulfate. Filtration and subsequent solvent removal under reduced pressure gave a brown crystalline solid; purification by flash column chromatography (silica, cyclohexane/ethyl acetate 10:1, to 4:1) and subsequent recrystallisation from ethyl acetate/cyclohexane, gave a beige crystalline solid (yield 24.5g, 68%):

Characterisation:

TLC: *Rf* 0.34 (cyclohexane/ethyl acetate 4:1);

Melting point: 71-72°C (lit. 75°C)[483];

^{1}H-NMR ($CDCl_3$): δ_H 2.48 (3H, s, ArC***H***$_3$), 3.52 (1H, s, C≡C***H***), 7.40 (2H, dm (AA' of an AA'BB' system), J_{ortho} = 8.2Hz, Ar***H***-3, Ar***H***-5), 7.89 (2H, dm (BB' of an AA'BB' system), J_{ortho} = 8.2Hz, Ar***H***-2, Ar***H***-6);
(lit. ($CDCl_3$) δ 2.47 (s, 3H), 3.52 (s, 1H), 7.38 (dd, 2H,

	J = 8.5, 0.6), 7.88 (d, 2H, J = 8.5)[483]);
^{13}C-NMR ($CDCl_3$):	δ_C 21.77 (Ar***C***H$_3$), 80.28 (C≡***C***H), 81.35 (C≡***C***SO$_2$), 127.67 (***C***$_{Ar}$H-2, ***C***$_{Ar}$H-6), 130.13 (***C***$_{Ar}$H-3, ***C***$_{Ar}$H-5), 137.75 (***C***$_{Ar}$SO$_2$), 146.09 (***C***$_{Ar}$CH$_3$);
MS (EI) *m/z*:	M$^+$ 180(100);
IR (KBr) *ν*/cm:	3231 (≡C–H), 2063 (C≡C), 1337 (SO_2), 1155 (SO_2) (lit. (cm^{-1}): 3235, 2013, 1337, 1156[483]);
Microanalysis (C,H):	Calculated for $C_9H_8SO_2$: 59.98, 4.47; Found 60.06/60.09, 4.43/4.57.

_N_-Benzyl-[(_S_)-2-(3,4-dimethoxyphenyl)-1-methylethyl]-_N_-[(_E_)-2-(toluene-4-sulfonyl)vinyl]amine (157_S_)

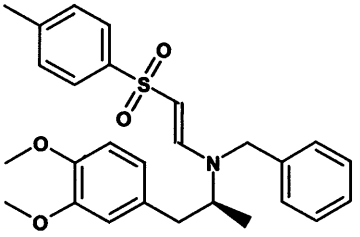

150 (7.9g, 0.044mol) was dissolved in dry dichloromethane (100mL), and added to a chilled (0°C, ice bath) solution of **38*S*** (12.5g, 0.044mol) in dry dichloromethane (250mL) with stirring, under an atmosphere of nitrogen. The resulting solution was stirred for 18 hours. The solvent was removed under reduced pressure, and the residue was dissolved in boiling ethyl acetate (350mL), hot filtered, then cooled to room temperature. Filtration after two hours gave a colourless crystalline solid (16.06g, 78%); a sample of these crystals was sent for X-ray crystallographic analysis. Removal of solvent from the mother liquor under reduced pressure, and purification by flash column chromatography (Biotage 40M, cyclohexane/ ethyl acetate 2:1) gave a further crop of colourless crystalline solid (2.2g, 11%):

Characterisation:

TLC:	*Rf* 0.33 (cyclohexane/ ethyl acetate 2:1)
Melting point:	142°C;
Optical rotation $[\alpha]_D^{22}$:	+117.3 (c 0.55, dichloromethane);
^{1}H-NMR ($CDCl_3$):	δ_H 1.26 (3H, br d, CHC***H***$_3$), 2.39 (3H, s, ArC***H***$_3$), 2.70-2.75 (1H, br, ArC***H***$_A$H$_B$CH), 2.83 (1H, dd$_{BAX}$, J_{BA} = 13.9Hz,

J_{BX} = 8.3Hz, $ArCH_AH_BCH$), 3.56-3.63 (1H, m, $ArCH_2CHCH_3$), 3.75 (3H, s, $ArOCH_3$-3), 3.87 (3H, s, $ArOCH_3$-4), 3.95-4.00 (1H, br d, $PhCH_AH_BN$), 4.20 (1H, d_{AB}, J_{AB} = 16.2Hz, $PhCH_AH_BN$), 4.88-4.92 (1H, br d, SO_2CH=CHN), 6.55 (1H, d, J_{meta} = 1.9Hz, ArH-2), 6.63 (1H, dd, J_{meta} = 1.9Hz, J_{ortho} = 8.1Hz, ArH-6), 6.76 (1H, d, J_{ortho} = 8.1Hz, ArH-5), 7.00 (2H, br, PhH-2', -6'), 7.21-7.25 (5H, m, PhH-3', PhH-4', PhH-5', tosyl ArH-3", tosyl ArH-5" (α to CH_3)), 7.54 (1H, d, J_{trans} = 12.7Hz, SO_2CH=CHN), 7.60 (2H, d, J_{ortho} = 8.0Hz, tosyl ArH-2", tosyl ArH-6" (α to sulfoxide));

^{13}C-NMR ($CDCl_3$): δ_C 19.99 (br, $CHCH_3$), 21.44 ($ArCH_3$), 41.97 (br, $ArCH_2CH$), 52.12 (br, $PhCH_2N$), 55.79 ($ArOCH_3$), 55.86 ($ArOCH_3$), 61.91 (br, CH_2CHCH_3), 94.06 (SO_2CH=CHN), 111.26 (C_{Ar}H-5), 112.08 (C_{Ar}H-2), 121.09 (C_{Ar}H-6), 126.05 (tosyl C_{Ar}H-2", tosyl C_{Ar}H-6" (α to sulfoxide)), 126.81 (br, phenyl C_{Ar}H-2', phenyl C_{Ar}H-6'), 127.51 (phenyl C_{Ar}H-4'), 128.68 (phenyl C_{Ar}H-3', phenyl C_{Ar}H-5'), 129.35 (tosyl C_{Ar}H-3", tosyl C_{Ar}H-5" (α to CH_3)), 130.18 (vanillyl C_{Ar}-1), 135.33 (br, phenyl C_{Ar}-1'), 142.06, 142.12 (tosyl $C_{Ar}CH_3$-4", tosyl $C_{Ar}SO_2$-1"), 147.61 (br, SO_2CH=CHN), 147.78 (C_{Ar}OMe-4), 148.93 (C_{Ar}OMe-3);

MS (ESI-positive) *m/z*: $[M+Na]^+$ 488(100), $[2M+Na]^+$ 953(14);

IR (KBr) ν/cm: 1610 (C=C), 1518 (C_{Ar}–C_{Ar}), 1258 (C_{Ar}–OMe), 1129 (SO_2);

Microanalysis (C,H,N): Calculated for $C_{27}H_{31}NO_4S$: 69.65, 6.71, 3.01;
Found 69.66, 6.78, 3.07.

***N*-Benzyl-[(*R*)-2-(3,4-dimethoxyphenyl)-1-methylethyl]-*N*-[(*E*)-2-(toluene-4-sulfonyl)vinyl]amine (157*R*)**

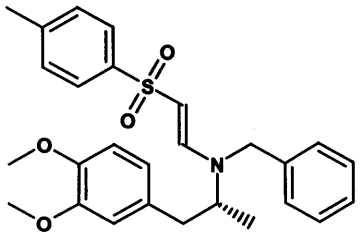

150 (3.7g, 0.0205mol) was dissolved in dry dichloromethane (100mL), and added to a solution of **38*R*** (5.83g, 0.0205mol) in dry dichloromethane (100mL) with stirring, under an atmosphere of nitrogen; the resultant solution was stirred for 2 hours, at which time TLC (dichloromethane/methanol 10:1) confirmed the reaction to be complete. The solvent was removed under reduced pressure, and the residue was dissolved in boiling ethyl acetate (200mL), hot filtered, then left to cool to room temperature over the weekend. Filtration gave a colourless crystalline solid (7.15g, 75%). Removal of solvent from the mother liquor under reduced pressure gave a brown residue; purification by flash column chromatography (Biotage 40S, cyclohexane/ ethyl acetate 2:1) gave a beige solid; recrystallisation gave a colourless crystalline solid (1.31, 14%):

Characterisation:

TLC: *Rf* 0.33 (cyclohexane/ ethyl acetate 2:1);

Melting point: 143°C;

Optical rotation $[\alpha]_D^{21}$: –125.0 (c 0.52, dichloromethane);

^{1}H-NMR ($CDCl_3$): δ_H 1.26 (3H, br d, $CHC\boldsymbol{H}_3$), 2.39 (3H, s, $ArC\boldsymbol{H}_3$), 2.70-2.75 (1H, br, $ArC\boldsymbol{H}_AH_BCH$), 2.83 (1H, dd_{BAX}, J_{BA} = 13.9Hz, J_{BX} = 8.3Hz, $ArCH_A\boldsymbol{H}_BCH$), 3.56-3.63 (1H, m, $ArCH_2C\boldsymbol{H}CH_3$), 3.75 (3H, s, $ArOC\boldsymbol{H}_3$-3), 3.87 (3H, s, $ArOC\boldsymbol{H}_3$-4), 3.95-4.00 (1H, br d, $PhC\boldsymbol{H}_AH_BN$), 4.20 (1H, d_{AB}, J_{AB} = 16.2Hz, $PhCH_A\boldsymbol{H}_BN$), 4.88-4.92 (1H, br d, $SO_2C\boldsymbol{H}$=CHN), 6.55 (1H, d, J_{meta} = 1.9Hz, Ar***H***-2), 6.63 (1H, dd, J_{meta} = 1.9Hz, J_{ortho} = 8.1Hz, Ar***H***-6), 6.76 (1H, d, J_{ortho} = 8.1Hz, Ar***H***-5), 7.00 (2H, br, Ph***H***-2', Ph***H***-6'), 7.21-7.25 (5H, m, Ph***H***-3', Ph***H***-4', Ph***H***-5', tosyl Ar***H***-3", tosyl Ar***H***-5" (α to CH_3)), 7.54 (1H, d, J_{trans} = 12.7Hz,

	$SO_2CH{=}C\boldsymbol{H}N$), 7.60 (2H, d, J_{ortho} = 8.0Hz, tosyl Ar***H***-2", tosyl Ar***H***-6" (α to sulfoxide));
^{13}C-NMR ($CDCl_3$):	δ_C 19.99 (br, $CH\boldsymbol{C}H_3$), 21.44 (Ar$\boldsymbol{C}H_3$), 41.97 (br, Ar$\boldsymbol{C}H_2CH$), 52.12 (br, Ph$\boldsymbol{C}H_2N$), 55.79 (ArO$\boldsymbol{C}H_3$), 55.86 (ArO$\boldsymbol{C}H_3$), 61.91 (br, $CH_2\boldsymbol{C}HCH_3$), 94.06 ($SO_2\boldsymbol{C}H{=}CHN$), 111.26 ($\boldsymbol{C}_{Ar}$H-5), 112.08 ($\boldsymbol{C}_{Ar}$H-2), 121.09 ($\boldsymbol{C}_{Ar}$H-6), 126.05 (tosyl $\boldsymbol{C}_{Ar}$H-2", tosyl $\boldsymbol{C}_{Ar}$H-6" (α to sulfoxide)), 126.81 (br, phenyl $\boldsymbol{C}_{Ar}$H-2', phenyl $\boldsymbol{C}_{Ar}$H-6'), 127.51 (phenyl $\boldsymbol{C}_{Ar}$H-4'), 128.68 (phenyl $\boldsymbol{C}_{Ar}$H-3', phenyl $\boldsymbol{C}_{Ar}$H-5'), 129.35 (tosyl $\boldsymbol{C}_{Ar}$H-3", tosyl $\boldsymbol{C}_{Ar}$H-5" (α to CH_3)), 130.18 (vanillyl $\boldsymbol{C}_{Ar}$-1), 135.33 (br, phenyl $\boldsymbol{C}_{Ar}$-1'), 142.06, 142.12 (tosyl $\boldsymbol{C}_{Ar}CH_3$-4", tosyl $\boldsymbol{C}_{Ar}SO_2$-1"), 147.61 (br, $SO_2CH{=}\boldsymbol{C}HN$), 147.78 ($\boldsymbol{C}_{Ar}$OMe-4), 148.93 ($\boldsymbol{C}_{Ar}$OMe-3);
MS (EI) *m/z*:	M^+ 465(11), $[M\text{-}(3,4\text{-dimethoxybenzyl})]^+$ 314(100);
IR (KBr) ν/cm:	1610 (C=C), 1518 (C_{Ar}–C_{Ar}), 1258 (Ar–OCH_3), 1128 (SO_2);
Microanalysis (C,H,N):	Calculated for $C_{27}H_{31}NO_4S$: 69.65, 6.71, 3.01; Found 69.71, 6.62, 2.87.

(1*R*,3*S*)-2-Benzyl-6,7-dimethoxy-3-methyl-1-(toluene-4-sulfonylmethyl)-1,2,3,4-tetrahydroisoquinoline (158(1*R*,3*S*))

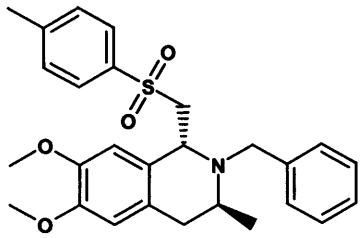

157*S* (18.0g, 0.0387mol) was dissolved in dry dichloromethane (250mL), and cooled with stirring under an atmosphere of nitrogen on a salt/ice bath to –15°C. Trifluoroacetic acid (200mL, 296g, 2.65mol, 68 equivalents) was similarly cooled, then poured into the solution in one portion. The solution immediately changed colour, from colourless to bright yellow. After three hours, the reaction retained a slight yellow colouration. An aliquot (50μL) was neutralised in saturated aqueous sodium bicarbonate (500μL), and products were extracted into diethyl ether. TLC (cyclohexane/ ethyl acetate 2:1) showed no starting material remaining. The reaction was poured into water (1L), and made slightly alkaline (pH ~8) by the cautious,

portionwise addition of solid sodium carbonate (~250g) over thirty minutes. The pH was further basified by the addition of 5.0M aqueous sodium hydroxide (500mL); neutral organic compounds were extracted into dichloromethane (3 x 250mL). The combined extractions were washed consecutively with saturated aqueous sodium bicarbonate (200mL), water (200mL) and brine (100mL), then dried over dried magnesium sulfate. Filtration, and removal of the solvent under reduced pressure gave a peach coloured foam; purification by flash column chromatography (3 x Biotage 40M; cyclohexane/ ethyl acetate 4:1) gave a colourless foam (16.4g, 91%):

Characterisation:

TLC: *Rf* 0.31 (cyclohexane/ ethyl acetate 2:1);

Melting point: amorphous solid;

Optical rotation $[\alpha]_D^{21}$: –8.5 (c 1.02, ethanol);

^{1}H-NMR (CD_2Cl_2): (no TMS) δ_H 1.01 (3H, d, J = 6.6Hz, CHC***H***$_3$), 2.42 (3H, s, ArC***H***$_3$), 2.46-2.58 (2H, m, ArC***H***$_2$CH), 3.12-3.19 (2H, dd_{AB} and m overlapping, J_{AB} = 13.4Hz, PhC***H***$_A$H$_B$N and $CH_2C\boldsymbol{H}CH_3$), 3.24 (1H, dd_{ABX}, J_{AB} = 14.9Hz, J_{AX} = 4.2Hz, tosyl-C***H***$_A$H$_B$CH), 3.67-3.73 (4H, m (overlapping dd_{BAX} (J_{BA} = 15.0Hz, J_{BX} = 7.5Hz) and s, tosyl-CH$_A$***H***$_B$CH and ArOC***H***$_3$), 3.74-3.78 (4H, m (overlapping d_{AB} and s), PhCH$_A$***H***$_B$N and ArOC***H***$_3$), 4.19 (1H, dd_{XAB}, J_{XA} = 4.2Hz, J_{XB} = 7.4Hz, tosyl-CH$_2$C***H***), 6.48 (1H, s, Ar***H***-8), 6.54 (1H, s, Ar***H***-5), 7.22-7.31 (7H, m, Ph***H***-2, Ph***H***-3, Ph***H***-4, Ph***H***-5, Ph***H***-6, tosyl Ar***H***-3", tosyl Ar***H***-5" (α to CH_3)), 7.56 (2H, dm (BB' of an AA'BB' system), J_{ortho} = 8.2Hz, tosyl Ar***H***-2", tosyl Ar***H***-6" (α to sulfoxide));

^{13}C-NMR (CD_2Cl_2): (no TMS) δ_C 18.96 (CH***C***H$_3$), 21.70 (Ar***C***H$_3$), 30.60 (Ar***C***H$_2$CH), 47.54 ($CH_2\boldsymbol{C}HCH_3$), 50.09 (Ph***C***H$_2$N), 56.14 (2 x ArO***C***H$_3$), 56.25 (tosyl-CH$_2$***C***H), 62.77 (tosy-l***C***H$_2$CH), 111.06 (***C***$_{Ar}$H-8), 112.16 (***C***$_{Ar}$H-5), 127.03 (br, ***C***$_{Ar}$-4a or ***C***$_{Ar}$8a), 127.20 (phenyl ***C***$_{Ar}$H-4' + ***C***$_{Ar}$-4a or ***C***$_{Ar}$8a (peak size reduced in DEPT, with respect to adjacent signals), 128.27, 128.35 (***C***$_{Ar}$H-3', ***C***$_{Ar}$H-5' and tosyl ***C***$_{Ar}$H-2", ***C***$_{Ar}$H-6"), 129.87, 130.00 (phenyl ***C***$_{Ar}$H-2', ***C***$_{Ar}$H-6' and tosyl ***C***$_{Ar}$H-3",

	C_{Ar}H-5"), 138.04 (tosyl C_{Ar}-SO_2-1"), 139.84 (phenyl C_{Ar}-1'), 144.66 (tosyl $C_{Ar}CH_3$-4"), 148.32 (C_{Ar}OMe), 148.55 (C_{Ar}OMe);
MS (ESI-positive) *m/z*:	MH^+ 466(100);
IR (KBr) *ν*/cm:	1517 (C_{Ar}–C_{Ar}), 1249 (Ar–OCH_3), 1145cm^{-1} (SO_2);
Microanalysis (C,H,N):	Calculated for $C_{27}H_{31}NO_4S$: 69.65, 6.71, 3.01;
	Found 69.31, 6.71, 3.05.

(1*S*,3*R*)-2-Benzyl-6,7-dimethoxy-3-methyl-1-(toluene-4-sulfonylmethyl)-1,2,3,4-tetrahydroisoquinoline (158(1*S*,3*R*))

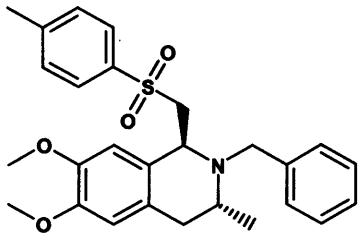

157*R* (8.25g, 0.0177mol) was dissolved in dry dichloromethane (75mL), and cooled with stirring under an atmosphere of nitrogen on a salt/ice bath to –15°C. Trifluoroacetic acid (100mL, 148g, 1.325mol, 75 equivalents) was similarly cooled, then poured into the solution in one portion. An immediate colour change, from colourless to bright yellow, was observed. After two hours, the reaction was poured into water (750mL), and made slightly alkaline (pH ~8) by the cautious, portionwise addition of solid sodium carbonate (~160g) over thirty minutes. Dichloromethane (250mL) was added; the biphasic solution was stirred vigorously for fifteen minutes, then separated. The aqueous phase was extracted with fresh dichloromethane (250mL), the combined dichloromethane extractions were consecutively washed with saturated aqueous sodium hydrogencarbonate (250mL) and saturated aqueous sodium chloride (100mL), then dried over dried magnesium sulfate. Filtration, and removal of the solvent under reduced pressure gave a colourless foam; purification by flash column chromatography (2 x Biotage 40M, cyclohexane/ethyl acetate 4:1) gave a colourless foam (7.57g, 92%):

Characterisation:

TLC:	*Rf* 0.31 (cyclohexane/ ethyl acetate 2:1);
Melting point:	amorphous solid;

Optical rotation $[\alpha]_D^{19}$: –8.5 (c 1.00, ethanol);

^{1}H-NMR (CD_2Cl_2): (no TMS) δ_H 1.02 (3H, d, J = 6.6Hz, CHC***H***$_3$), 2.42 (3H, s, ArC***H***$_3$), 2.45-2.58 (2H, m, ArC***H***$_2$CH), 3.13-3.19 (2H, d_{AB} and m overlapping, J_{AB} = 13.4Hz, PhC***H***$_A$H$_B$N and CH$_2$C***H***CH$_3$), 3.25 (1H, dd_{ABX}, J_{AB} = 14.9Hz, J_{AX} = 4.2Hz, tosyl-C***H***$_A$H$_B$CH), 3.67-3.73 (4H, m (overlapping dd_{BAX} (J_{BA} = 15.0Hz, J_{BX} = 7.5Hz) and s, tosyl-CH$_A$***H***$_B$CH and ArOC***H***$_3$), 3.74-3.78 (4H, m (overlapping d_{AB} and s), PhCH$_A$***H***$_B$N and ArOC***H***$_3$), 4.20 (1H, dd_{XAB}, J_{XA} = 4.2Hz, J_{XB} = 7.4Hz, tosylCH$_2$C***H***), 6.48 (1H, s, Ar***H***-8), 6.54 (1H, s, Ar***H***-5), 7.23-7.31 (7H, m, Ph***H***-2, Ph***H***-3, Ph***H***-4, Ph***H***-5, Ph***H***-6, tosyl Ar***H***-3", tosyl Ar***H***-5" (2 x tosyl Ar***H*** are α to methyl)), 7.56 (2H, dm (BB' of an AA'BB' system), J_{ortho} = 8.2Hz, tosyl Ar***H***-2", tosyl Ar***H***-6" (both α to sulfoxide));

^{13}C-NMR (CD_2Cl_2): (no TMS) δ_C 18.96 (CH***C***H$_3$), 21.71 (Ar***C***H$_3$), 30.60 (Ar***C***H$_2$CH), 47.56 (CH$_2$***C***HCH$_3$), 50.10 (Ph***C***H$_2$N), 56.15 (2 x ArO***C***H$_3$), 56.25 (tosyl-CH$_2$***C***H), 62.77 (tosyl-***C***H$_2$CH), 111.07 (C_{Ar}H-8), 112.17 (C_{Ar}H-5), 127.02 (br, C_{Ar}-4a or 8a), 127.20 (phenyl C_{Ar}H-4' and tetrahydroisoquinoline C_{Ar}-4a or C_{Ar}-8a (peak size reduced in DEPT, with respect to adjacent signals), 128.28, 128.36 (phenyl C_{Ar}H-3', phenyl C_{Ar}H-5', tosyl C_{Ar}H-2", tosyl C_{Ar}H-6"), 129.87, 130.00 (phenyl C_{Ar}H-2', phenyl C_{Ar}H -6', tosyl C_{Ar}H-3", tosyl C_{Ar}H-5"), 138.04 (C_{Ar}-SO$_2$), 139.81 (phenyl C_{Ar}-1'), 144.66 (C_{Ar}-Me), 148.33 (C_{Ar}OMe), 148.56 (C_{Ar}OMe);

MS (ESI-positive) *m/z*: MH^+ 466(100);

IR (KBr) *ν*/cm: 1517 (C_{Ar}–C_{Ar}), 1249 (Ar–OCH$_3$), 1145cm^{-1} (SO$_2$);

Microanalysis (C,H,N): Calculated for $C_{27}H_{31}NO_4S$: 69.65, 6.71, 3.01;
Found 69.81, 6.81, 3.05.

(1*R*,3*S*)-6,7-dimethoxy-3-methyl-1-(toluene-4-sulfonylmethyl)-1,2,3,4-tetra-hydroisoquinoline (159(1*R*,3*S*))

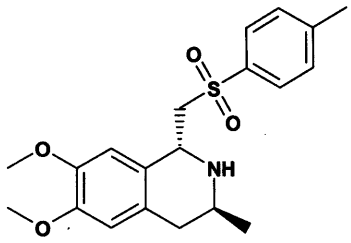

158(1*R*,3*S*) (1.26g, 2.7mmol) was dissolved in methanol (75mL) and stirred. After evacuation and purging with nitrogen (x 2), 270mg of 10% palladium on carbon (~0.27mmol) was added. The mixture was evacuated and left under reduced pressure for five minutes, before an atmosphere of hydrogen was introduced. The reaction was stirred for two hours, after which time TLC confirmed the reaction to be complete. The reaction was evacuated once more, and purged with nitrogen, before filtering through Celite and removing the volatile components under reduced pressure, to give the crude product in quantitative yield, as a colourless crystalline solid. Recrystallisation was achieved by suspending the residue in boiling n-hexane, and gradually adding small amounts of ethyl acetate until a solution was obtained. This was hot-filtered into a little n-hexane, and left to cool overnight. The product crystallised as fine needles (550mg, 54% yield), and these were used for characterisation. A small sample of the compound was crystallised slowly from ethanol, and larger crystals, suitable for X-ray crystallographic analysis, were obtained.

Characterisation:

TLC: *Rf* 0.25 (cyclohexane/ ethyl acetate 1:1);

Melting point: 151-152°C;

Optical rotation $[\alpha]_D^{29}$: +49.6 (c 0.98, ethanol);

^{1}H-NMR ($CDCl_3$): δ_H 1.11 (3H, d, J = 6.1Hz, CHC***H***$_3$), 2.05-2.35 (1H, br, NH), 2.40 (1H, dd_{ABX}, J_{AB} = 16.0Hz, J_{AX} = 10.7Hz, ArC***H***$_A$H$_B$CH$_X$), 2.47 (3H, s, ArC***H***$_3$), 2.60 (1H, dd_{BAX}, J_{BA} = 16.0Hz, J_{BX} = 10.7Hz, ArCH$_A$***H***$_B$CH$_X$), 3.02-3.07 (1H, m, CH$_2$C***H***(NH)CH$_3$), 3.20 (1H, $dd_{A'B'X'}$, $J_{A'B'}$ = 14.6Hz, $J_{A'X'}$ = 2.0Hz, SO$_2$C***H***$_{A'}$H$_{B'}$CH), 3.68 (1H, $dd_{A'B'X'}$, $J_{B'A'}$ = 14.6Hz, $J_{B'X'}$ = 10.2Hz, SO$_2$CH$_{A'}$***H***$_{B'}$CH$_{X'}$), 3.76 (3H,

	s, ArOCH_3-7), 3.81 (3H, s, ArOCH_3-6), 4.61 (1H, br d, CH_2CH(NH)Ar), 6.31 (1H, s, ArH-8), 6.51 (1H, s, ArH-5), 7.39 (2H, d, J_{ortho} = 8.2Hz, ArH-3'and ArH-5'), 7.87 (2H, d, J_{ortho} = 8.2Hz, ArH-2' and ArH-6');
^{13}C-NMR ($CDCl_3$):	δ_C 21.65 (ArCH$_3$), 22.00 (CHCH$_3$), 36.78 (ArCH$_2$CH), 42.61 (CH_2CHCH_3), 51.58 (SO_2CH_2CH), 55.86 (ArOCH$_3$), 56.10 (ArOCH$_3$), 60.57 (SO_2CH_2CH), 109.35 (C_{Ar}H-8), 111.69 (C_{Ar}H-5), 127.05 (C_{Ar}8a), 127.63 (C_{Ar}4a), 128.01 (C_{Ar}H-2', C_{Ar}H-6'), 130.03 (C_{Ar}H-3', C_{Ar}H-5'), 136.92 ($C_{Ar}SO_2$-1'), 144.86 ($C_{Ar}CH_3$-4'), 147.56 (C_{Ar}OMe-7), 148.20 (C_{Ar}OMe-6);
MS (EI) *m/z*:	M^+ 375(20), $[M–CH_2SO_2C_6H_4CH_3]^+$ 206(100);
IR (KBr) *ν*/cm:	3330 (NH), 1522 (C_{Ar}–C_{Ar}), 1370 (SO_2), 1152 (SO_2);
Microanalysis (C,H,N):	Calculated for $C_{20}H_{25}NO_4S$: 63.98, 6.71, 3.73;
	Found 64.03, 6.77, 3.91.

(1*S*,3*S*)-2-Benzyl-6,7-dimethoxy-1,3-dimethyl-1,2,3,4-tetrahydroisoquinoline (167(1*S*,3*S*))

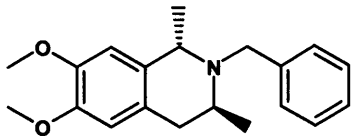

A 1.0M solution of lithium napthalenide was prepared by dissolving naphthalene (12.8g, 0.1mol) in dry THF (100mL), with stirring, under an atmosphere of argon. Lithium wire (2.08g, 0.3mol, 3 equivalents) was added in ~0.5cm pieces, and the mixture was stirred for two hours; the solution changed from colourless to a very dark green within a few minutes of the addition of the lithium wire.

158(1*R*,3*S*) (7.6g, 0.0163mol) was dissolved in dry THF (360mL), and, whilst stirring under an atmosphere of argon, the solution was cooled on a carbon dioxide/ acetone bath to –70°C. The lithium naphthalenide solution was slowly added by syringe (36mL, ~2.2 equivalents) over 10 minutes. During the addition the sulfone solution changed colour, from colourless, via a deepening orange, to dark green. After stirring for one hour, the reaction mixture was poured into 0.5M aqueous hydrochloric acid (400mL) to quench, and the neutral material was extracted into diethyl ether (2 x 100mL). The aqueous layer was basified by the addition of 5.0M

aqueous sodium hydroxide (50mL), and the now neutral amine products were extracted into diethyl ether (3 x 150mL). The second round of ether extractions were combined, washed with brine (100mL) and dried over dried magnesium sulfate. Filtration and removal of solvent under reduced pressure gave a brown oil; purification by flash column chromatography (Biotage 40M cartridge, cyclohexane/ diethyl ether 4:1) gave a colourless syrup (2.80g, 57%).

Characterisation:

TLC:	*Rf* 0.30 (cyclohexane/ ethyl acetate 4:1);
Optical rotation $[\alpha]_D^{22}$:	–43.8 (c 1.21, dichloromethane);
^{1}H-NMR ($CDCl_3$):	δ_H 1.24 (3H, d, J = 6.7Hz, 3-C***H***$_3$), 1.35 (3H, d, J = 6.9Hz, 1-C***H***$_3$), 2.57-2.60 (2H, m, ArC***H***$_2$CH), 3.39-3.46 (2H, d_{AB} and m overlapping, J_{AB} = 14.1Hz, PhC***H***$_A$H$_B$N and CH$_2$C***H***CH$_3$), 3.71 (1H, quartet, J = 6.9Hz, ArC***H***CH$_3$), 3.80-3.85 (7H, m (overlapping d_{BA} and 2 x s), PhCH$_A$***H***$_B$N and 2 x ArOC***H***$_3$), 6.47 (1H, s, Ar***H***-8), 6.56 (1H, s, Ar***H***-5), 7.23 (1H, t, J_{ortho} = 7.2Hz, Ph***H***-4'), 7.28-7.33 (2H, m, Ph***H***-3', Ph***H***-5'), 7.39 (2H, d, J_{ortho} = 7.3Hz, Ph***H***-2', Ph***H***-6');
^{13}C-NMR ($CDCl_3$):	δ_C 18.46 (3-***C***H$_3$), 22.52 (1-***C***H$_3$), 32.12 (Ar***C***H$_2$CH), 46.36 (CH$_2$***C***HCH$_3$), 50.27 (Ph***C***H$_2$N), 55.08 (Ar***C***HCH$_3$), 55.80, (ArO***C***H$_3$), 55.85 (ArO***C***H$_3$), 110.63 (***C***$_{Ar}$H-8), 111.33 (***C***$_{Ar}$H-5), 126.27 (***C***$_{Ar}$-4a), 126.51 (***C***$_{Ar}$H-4'), 128.13 (***C***$_{Ar}$H-3', ***C***$_{Ar}$H-5'), 128.41 (***C***$_{Ar}$H-2', ***C***$_{Ar}$H-6'), 131.14 (***C***$_{Ar}$-8a), 141.01 (***C***$_{Ar}$-1'), 147.13 (***C***$_{Ar}$OMe), 147.24 (***C***$_{Ar}$OMe);
MS (ESI-positive) *m/z*:	MH^+ 312(100);
HRMS (positive) *m/z*:	Calculated for [M+H] $C_{20}H_{25}NO_2$: 312.1964; Found312.1964.

(1*R*,3*R*)-2-Benzyl-6,7-dimethoxy-1,3-dimethyl-1,2,3,4-tetrahydroisoquinoline (167(1*R*,3*R*))

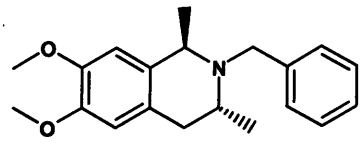

A 1.0M solution of lithium napthalenide in tetrahydrofuran was prepared by dissolving naphthalene (6.41g, 0.05mol) in dry tetrahydrofuran (total volume of

50mL), with stirring, under an atmosphere of argon, in a flame-dried round-bottomed flask. Lithium wire (1.04g, 0.15mol, 3 equivalents) was added portionwise over fifteen minutes, and the mixture was stirred for two hours; the solution changed from colourless to a very dark green within a few minutes of the addition of the lithium wire.

158(1*S*,3*R*) (6.1g, 0.0131mol) was dissolved in dry tetrahydrofuran (290mL), with stirring under an atmosphere of argon; the solution was cooled on a carbon dioxide/ acetone bath to –70°C. The lithium naphthalenide solution was slowly added by syringe (30mL, ~2.2 equivalents) over 10 minutes; during the addition the sulfone solution changed colour, from colourless, via a deep orange, to dark green. After stirring for one hour, the reaction mixture (still dark green), was poured into 0.5M aqueous hydrochloric acid (400mL) to quench; neutral material was extracted into diethyl ether (2 x 100mL). The aqueous layer was basified by the addition of 5.0M aqueous sodium hydroxide (50mL), and the now neutral amine products were extracted into diethyl ether (2 x 200mL). The second round of ether extractions were combined, washed consecutively with water (100mL) and brine (50mL), before drying over dried magnesium sulfate. Filtration and removal of solvent under reduced pressure gave a brown syrup; purification by flash column chromatography (Biotage 40M cartridge, cyclohexane/ diethyl ether 4:1) gave a colourless syrup (1.85g, 45%).

Characterisation:

TLC:	*Rf* 0.30 (cyclohexane/ ethyl acetate 4:1);
Optical rotation $[\alpha]_D^{22}$:	+46.1 (c 1.35, dichloromethane);
^{1}H-NMR ($CDCl_3$):	δ_H 1.23 (3H, d, J = 6.6Hz, 3-C***H***$_3$), 1.35 (3H, d, J = 6.8Hz, 1-C***H***$_3$), 2.57-2.60 (2H, m, ArC***H***$_2$CH), 3.40-3.46 (2H, d_{AB} and m overlapping, J_{AB} = 14.2Hz, PhC***H***$_A$H$_B$N and CH$_2$C***H***CH$_3$), 3.71 (1H, quartet, J = 6.8Hz, ArC***H***CH$_3$), 3.80-3.84 (7H, m (overlapping d_{BA} and 2 x s), PhCH$_A$***H***$_B$N and 2 x ArOC***H***$_3$), 6.47 (1H, s, Ar***H***-8), 6.56 (1H, s, Ar***H***-5), 7.22 (1H, t, J_{ortho} = 7.2Hz, Ph***H***-4'), 7.28-7.32 (2H, m, Ph***H***-3', Ph***H***-5'), 7.38 (2H, d, J_{ortho} = 7.3Hz, Ph***H***-2', Ph***H***-6');
^{13}C-NMR ($CDCl_3$):	δ_C 18.40 (3-***C***H$_3$), 22.51 (1-***C***H$_3$), 32.22 (Ar***C***H$_2$CH), 46.41 (CH$_2$***C***HCH$_3$), 50.36 (Ph***C***H$_2$N), 55.12 (Ar***C***HCH$_3$), 55.84,

(ArO$\boldsymbol{C}$H$_3$), 55.90 (ArO$\boldsymbol{C}$H$_3$), 110.75 ($\boldsymbol{C}_{Ar}$H-8), 111.46 ($\boldsymbol{C}_{Ar}$H-5), 126.33 ($\boldsymbol{C}_{Ar}$-4a), 126.51 ($\boldsymbol{C}_{Ar}$H-4'), 128.14 ($\boldsymbol{C}_{Ar}$H-3', $\boldsymbol{C}_{Ar}$H-5'), 128.40 ($\boldsymbol{C}_{Ar}$H-2', $\boldsymbol{C}_{Ar}$H-6'), 131.24 ($\boldsymbol{C}_{Ar}$-8a), 141.07 ($\boldsymbol{C}_{Ar}$-1'), 147.22 ($\boldsymbol{C}_{Ar}$OMe), 147.32 ($\boldsymbol{C}_{Ar}$OMe);

MS (ESI-positive) *m/z*: MH^+ 312.2(100);

IR (neat) *ν*/cm: 1515 (C_{Ar}–C_{Ar}), 1253 (C_{Ar}–OMe);

HRMS (positive) *m/z*: Calculated for [M+H] $C_{20}H_{26}NO_2$: 312.1964;
Found 312.1964.

(1*S*,3*S*)-6,7-Dimethoxy-1,3-dimethyl-1,2,3,4-tetrahydroisoquinoline (44(1*S*,3*S*))

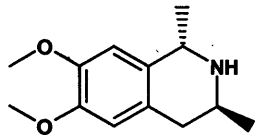

167(1*S*,3*S*) (2.65g, 8.52mmol) was dissolved in dry methanol (100mL); the stirred reaction was evacuated, purged with argon, and 10% palladium on activated carbon (170mg, 0.17mmol, ~2mol%) was added. The stirred suspension was evacuated, stirred for five minutes to thoroughly degas the solution, and placed under an atmosphere of hydrogen. The reaction was left to stir at room temperature for 18 hours. After evacuation, and purging with argon, the reaction mixture was filtered through Celite, and the solvent removed under reduced pressure to give a pale yellow syrup (1.90g, ~quantitative).

Characterisation:

Optical rotation $[\alpha]_D^{20}$: +50.6 (c 1.22, methanol);

^{1}H-NMR ($CDCl_3$): δ_H 1.31 (3H, d, J = 6.3Hz, 3-C$\boldsymbol{H}_3$), 1.52 (3H, d, J = 6.9Hz, 1-C$\boldsymbol{H}_3$), 2.53 (1H, dd_{ABX}, J_{AB} = 16.2Hz, J_{AX} = 9.9Hz, ArC$\boldsymbol{H}_A$H$_B$CH), 2.76 (1H, dd_{BAX}, J_{BA} = 16.2Hz, J = 4.2Hz, ArCH$_A\boldsymbol{H}_B$CH), 3.30-3.40 (1H, m, CH$_2$C$\boldsymbol{H}$CH$_3$), 3.84 (6H, 2 x s overlapping, 2 x ArOC$\boldsymbol{H}_3$), 4.26 (1H, q, J = 6.9Hz, ArC$\boldsymbol{H}$CH$_3$), 6.54 (1H, s, Ar$\boldsymbol{H}$-5), 6.56 (1H, s, Ar$\boldsymbol{H}$-8);

^{13}C-NMR ($CDCl_3$): δ_C 21.32 (3-$\boldsymbol{C}$H$_3$), 23.37 (1-$\boldsymbol{C}$H$_3$), 36.22 (Ar$\boldsymbol{C}$H$_2$CH), 43.41 (CH$_2\boldsymbol{C}$HCH$_3$), 50.46 (Ar$\boldsymbol{C}$HCH$_3$), 55.89 (ArO$\boldsymbol{C}$H$_3$), 56.02 (ArO$\boldsymbol{C}$H$_3$), 109.54 ($\boldsymbol{C}_{Ar}$H-8), 111.60 ($\boldsymbol{C}_{Ar}$H-5), 125.53 ($\boldsymbol{C}_{Ar}$-4a), 130.41 ($\boldsymbol{C}_{Ar}$-8a), 147.51 ($\boldsymbol{C}_{Ar}$OCH$_3$), 147.73 ($\boldsymbol{C}_{Ar}$OCH$_3$);

For full characterisation, the residue was dissolved in dioxan (15mL), and 4.0M hydrogen chloride in dioxan (10mL) was added, with stirring. The resultant suspension was heated to boiling, and sufficient methanol added to leave a hazy solution (~10mL); this was hot filtered, then left to cool to room temperature. Filtration gave a colourless crystalline solid (1.60g, 73%):

Characterisation:

Melting point:	268°C (sublimed);
Optical rotation $[\alpha]_D^{20}$:	+25.3 (c 1.08, dichloromethane);
	+29.0 (c 1.02, water);
^{1}H-NMR (DMSO-d_6):	δ_H 1.39 (3H, d, J = 6.4Hz, 3-C$\boldsymbol{H}_3$), 1.59 (3H, d, J = 6.9Hz, 1-C$\boldsymbol{H}_3$), 2.72 (1H, dd_{ABX}, J_{AB} = 16.8Hz, J_{AX} = 10.1Hz, ArC$\boldsymbol{H}_A$H$_B$CH), 2.95 (1H, dd_{BAX}, J_{BA} = 16.8Hz, J = 4.9Hz, ArCH$_A\boldsymbol{H}_B$CH), 3.62-3.68 (1H, m, CH$_2$C$\boldsymbol{H}$CH$_3$), 3.73-3.74 (6H, 2 x overlapping s, 2 x ArOC$\boldsymbol{H}_3$), 4.46 (1H, q, J = 6.9Hz, ArC$\boldsymbol{H}$CH$_3$), 6.73 (1H, s, Ar$\boldsymbol{H}$-5), 6.83 (1H, s, Ar$\boldsymbol{H}$-8), 9.50-9.85 (2H, br, N$^+\boldsymbol{H}_2$);
^{13}C-NMR (DMSO-d_6):	δ_C 17.74 (3-$\boldsymbol{C}$H$_3$), 20.02 (1-$\boldsymbol{C}$H$_3$), 32.33 (Ar$\boldsymbol{C}$H$_2$CH), 43.71 (CH$_2\boldsymbol{C}$HCH$_3$), 48.88 (Ar$\boldsymbol{C}$HCH$_3$), 55.44 (ArO$\boldsymbol{C}$H$_3$), 55.58 (ArO$\boldsymbol{C}$H$_3$), 109.68 ($\boldsymbol{C}_{Ar}$H-8), 111.49 ($\boldsymbol{C}_{Ar}$H-5), 122.87 ($\boldsymbol{C}_{Ar}$-4a), 125.54 ($\boldsymbol{C}_{Ar}$-8a), 147.62 ($\boldsymbol{C}_{Ar}$OCH$_3$), 148.09 ($\boldsymbol{C}_{Ar}$OCH$_3$);
MS (ESI-positive) *m/z*:	MH$^+$ 222(100);
IR (KBr) *ν*/cm:	1590 (C_{Ar}–C_{Ar}), 1525 (C_{Ar}–C_{Ar}), 1228 (Ar–OCH$_3$);
Microanalysis (C,H,N):	Calculated for $C_{13}H_{20}NO_2Cl$: 60.58, 7.82, 5.43;
	Found 60.41, 7.72, 5.52.

(1*R*,3*R*)-6,7-Dimethoxy-1,3-dimethyl-1,2,3,4-tetrahydroisoquinoline (44(1*R*,3*R*))

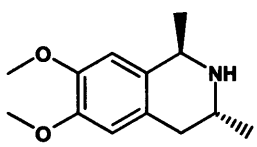

167(1*R*,3*R*) (1.85g, 5.95mmol) was dissolved in dry methanol (75mL); the stirred reaction was evacuated, purged with argon, and 10% palladium on activated carbon (120mg, 1.2mmol, ~20mol%) was added. The stirred suspension was evacuated, before being placed under an atmosphere of hydrogen, and left to stir at room temperature for 18 hours. After evacuation, and purging with argon, the reaction

mixture was analysed by TLC, and, in the absence of starting material, was filtered through Celite, and the solvent removed under reduced pressure to give a pale yellow syrup (1.33g, ~quantitative):

Characterisation:

Optical rotation $[\alpha]_D^{20}$: –50.7 (c 1.39, methanol);

^{1}H-NMR ($CDCl_3$): δ_H 1.25 (3H, d, J = 6.3Hz, 3-C***H***$_3$), 1.47 (3H, d, J = 6.9Hz, 1-C***H***$_3$), 2.45 (1H, dd$_{ABX}$, J_{AB} = 16.2Hz, J_{AX} = 9.9Hz, ArC***H***$_A$H$_B$CH), 2.73 (1H, dd$_{BAX}$, J_{BA} = 16.2Hz, J = 4.2Hz, ArCH$_A$***H***$_B$CH), 3.05 (1H, br, N***H***), 3.26-3.34 (1H, m, CH$_2$C***H***CH$_3$), 3.84 (6H, 2 x s overlapping, 2 x ArOC***H***$_3$), 4.20 (1H, q, J = 6.9Hz, ArC***H***CH$_3$), 6.54 (1H, s, Ar***H***-5), 6.56 (1H, s, Ar***H***-8);

^{13}C-NMR ($CDCl_3$): δ_C 21.87 (3-***C***H$_3$), 23.78 (1-***C***H$_3$), 36.72 (Ar***C***H$_2$CH), 43.09 (CH$_2$***C***HCH$_3$), 50.58 (Ar***C***HCH$_3$), 55.87 (ArO***C***H$_3$), 56.00 (ArO***C***H$_3$), 109.63 (***C***$_{Ar}$H-8), 111.63 (***C***$_{Ar}$H-5), 125.99 (***C***$_{Ar}$-4a), 131.31 (***C***$_{Ar}$-8a), 147.36 (***C***$_{Ar}$OCH$_3$), 147.54 (***C***$_{Ar}$OCH$_3$);

For full characterisation, the residue was dissolved in dioxan (20mL), and 4.0M hydrogen chloride in dioxan (5mL) was added, with stirring. The resultant suspension was heated to boiling, and sufficient methanol added to dissolve the precipitate; the solution was hot filtered into boiling dioxan, then left to cool to room temperature. Filtration gave a colourless crystalline solid (1.14g, 74%):

Characterisation:

Melting point: 264-5°C (sublimed);

Optical rotation $[\alpha]_D^{20}$: –24.3 (c 1.05, dichloromethane);

–28.2 (c 1.02, water);

^{1}H-NMR (DMSO-d$_6$): δ_H 1.38 (3H, d, J = 6.4Hz, 3-C***H***$_3$), 1.58 (3H, d, J = 6.9Hz, 1-C***H***$_3$), 2.71 (1H, dd$_{ABX}$, J_{AB} = 16.9Hz, J_{AX} = 10.0Hz, ArC***H***$_A$H$_B$CH), 2.95 (1H, dd$_{BAX}$, J_{BA} = 16.9Hz, J = 4.6Hz, ArCH$_A$***H***$_B$CH), 3.60-3.70 (1H, m, CH$_2$C***H***CH$_3$), 3.73-3.74 (6H, 2 x overlapping s, 2 x ArOC***H***$_3$), 4.47 (1H, q, J = 6.9Hz, ArC***H***CH$_3$), 6.73 (1H, s, Ar***H***-5), 6.82 (1H, s, Ar***H***-8), 9.45-9.65 (2H, br, N$^+$***H***$_2$);

^{1}H-NMR (D_2O): (containing 0.75% 3-(trimethylsilyl)propionic-*2,2,3,3-d*$_4$,

sodium salt) δ_H 1.47 (3H, d, J = 6.5Hz, 3-C***H***$_3$), 1.66 (3H, d, J = 6.9Hz, 1-C***H***$_3$), 2.82 (1H, dd$_{ABX}$, J_{AB} = 17.4Hz, J_{AX} = 10.1Hz, ArC***H***$_A$H$_B$CH), 3.13 (1H, dd$_{BAX}$, J_{BA} = 17.4Hz, J = 4.9Hz, ArCH$_A$***H***$_B$CH), 3.81-3.87 (7H, m + 2 x s overlapping, CH$_2$C***H***CH$_3$ + 2 x ArOC***H***$_3$), 4.66 (1H, q, J = 6.9Hz, ArC***H***CH$_3$), 6.89-6.90 (2H, 2 x s, Ar***H***-5, Ar***H***-8);

^{13}C-NMR (DMSO-d$_6$): δ_C 17.68 (3-***C***H$_3$), 20.05 (1-***C***H$_3$), 32.31 (Ar***C***H$_2$CH), 43.85 (CH$_2$***C***HCH$_3$), 48.91 (Ar***C***HCH$_3$), 55.47 (ArO***C***H$_3$), 55.61 (ArO***C***H$_3$), 109.68 (***C***$_{Ar}$H-8), 111.50 (***C***$_{Ar}$H-5), 122.92 (***C***$_{Ar}$-4a), 125.58 (***C***$_{Ar}$-8a), 147.61 (***C***$_{Ar}$OCH$_3$), 148.06 (***C***$_{Ar}$OCH$_3$);

^{13}C-NMR (D$_2$O): (containing 0.75% 3-(trimethylsilyl)propionic-*2,2,3,3-d*$_4$, sodium salt) δ_C 20.46 (3-***C***H$_3$), 22.59 (1-***C***H$_3$), 35.15 (Ar***C***H$_2$CH), 47.81 (CH$_2$***C***HCH$_3$), 53.06 (Ar***C***HCH$_3$), 58.58 (ArO***C***H$_3$), 58.68 (ArO***C***H$_3$), 112.25 (***C***$_{Ar}$H-8), 114.52 (***C***$_{Ar}$H-5), 126.22 (***C***$_{Ar}$-4a), 128.15 (***C***$_{Ar}$-8a), 150.23 (***C***$_{Ar}$OCH$_3$), 150.74 (***C***$_{Ar}$OCH$_3$);

MS (ESI-positive) *m/z*: MH$^+$ 222(100);

IR (KBr) *ν*/cm: 1523 (C$_{Ar}$–C$_{Ar}$), 1256 (C$_{Ar}$–OCH$_3$), 1228 (C$_{Ar}$–OCH$_3$);

Microanalysis (C,H,N): Calculated for $C_{13}H_{20}NO_2Cl$: 60.58, 7.82, 5.43;
Found 60.40, 7.62, 5.59.

(1*S*,3*S*)-6,7-Dihydroxy-1,3-dimethyl-1,2,3,4-tetrahydroisoquinoline hydrobromide (35(1*S*,3*S*))

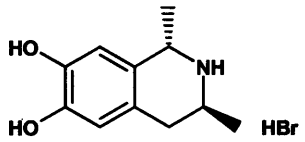

44(1*S*,3*S*) (765mg, 3.0mmol) was dissolved in 48% hydrobromic acid (10mL) and stirred at reflux for 5 hours. ^{1}H-NMR of an aliquot confirmed the reaction was complete; the reaction was cooled to room temperature, and the solvent was removed under reduced pressure. The foam was dissolved in a boiling mixture of propan-2-ol/ ethyl acetate 2:1, hot filtered, and cooled to room temperature. Filtration, and drying for 18 hours at 100°C and 0.1mmHg gave a colourless microcrystalline solid (410mg, 50%):

Characterisation:

Melting point:	209-210°C;
Optical rotation $[\alpha]_D^{22}$:	+16.0 (c 0.51, water);
^{1}H-NMR (DMSO-d_6):	δ_H 1.35 (3H, d, J = 6.4Hz, 3-CH_3), 1.51 (3H, d, J = 6.8Hz, 1-CH_3), 2.61 (1H, dd$_{ABX}$, J_{AB} = 16.8Hz, J_{AX} = 10.0Hz, ArCH_AH$_B$CH), 2.86 (1H, dd$_{BAX}$, J_{BA} = 16.8Hz, J_{BX} = 4.5Hz, ArCH$_A$$H_B$CH), 3.60-3.72 (1H, br m, CH$_2$CHCH$_3$), 4.42-4.52 (1H, br m, ArCHCH$_3$), 6.52 (1H, s, ArH-5), 6.59 (1H, s, ArH-8), 8.94 (1H, s, ArOH-7), 8.95-9.05 (1H, br, N^+H_AH$_B$), 9.06 (1H, s, ArOH-6), 9.10-9.25 (1H, br, N$^+$H$_A$$H_B$);
^{13}C-NMR (DMSO-d_6):	δ_C 17.83 (3-CH$_3$), 20.23 (1-CH$_3$), 32.06 (ArCH$_2$CH), 43.97 (CH$_2$$CHCH_3$), 48.86 (Ar$CHCH_2$), 112.91 ($C_{Ar}$H-8), 114.79 ($C_{Ar}$H-5), 121.09 ($C_{Ar}$-4a), 123.85 ($C_{Ar}$-8a), 144.20 ($C_{Ar}$OH-6), 144.90 ($C_{Ar}$OH-7);
	MS (ESI) *m/z* MH$^+$ 194(100);
MS (ESI-positive) *m/z*:	MH$^+$ 194(100);
IR (KBr) *ν*/cm:	3172 (OH) 1594 (C$_{Ar}$–C$_{Ar}$), 1533 (C$_{Ar}$–C$_{Ar}$), 1241 (C$_{Ar}$–OH);
Microanalysis (C,H,N):	Calculated for $C_{11}H_{16}NO_2Br$: 48.19, 5.88, 5.11;
	Found 48.02, 5.71, 5.51.

(1*R*,3*R*)-6,7-Dihydroxy-1,3-dimethyl-1,2,3,4-tetrahydroisoquinoline hydrobromide (35(1*R*,3*R*))

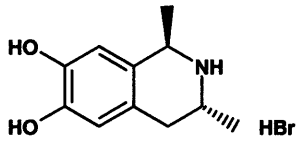

44(1*R*,3*R*) (280mg, 1.09mmol) was dissolved in 48% aqueous hydrobromic acid (5mL), and stirred at reflux for six hours. Removal of solvent under reduced pressure and analysis by ^{1}H-NMR confirmed the reaction to be complete (no signals corresponding to the methoxy substituents apparent in the spectrum). The reaction was cooled to room temperature, and the solvent removed under reduced pressure, to give a pale brown foam. The foam was suspended in hot ethyl acetate; methanol was added, with heating, until the foam dissolved; the solution was allowed to cool to room temperature, before refrigeration for 24 hours. At this time there had been no crystallisation, so diethyl ether was added until the solution became hazy; the

solution was refrigerated for a further 24 hours. Filtration gave a colourless crystalline solid (165mg, 55%):

Characterisation:

Melting point: 220-221°C;

Optical rotation $[\alpha]_D^{21}$: –16.1 (c 0.49, water);

^{1}H-NMR (DMSO-d_6): δ_H 1.35 (3H, d, J = 6.4Hz, 3-C***H***$_3$), 1.51 (3H, d, J = 6.8Hz, 1-C***H***$_3$), 2.60 (1H, dd$_{ABX}$, J_{AB} = 16.8Hz, J_{AX} = 10.0Hz, ArC***H***$_A$H$_B$CH), 2.86 (1H, dd$_{BAX}$, J_{BA} = 16.8Hz, J_{BX} = 4.5Hz, ArCH$_A$***H***$_B$CH), 3.60-3.72 (1H, br m, CH$_2$C***H***CH$_3$), 4.42-4.52 (1H, br m, ArC***H***CH3), 6.52 (1H, s, Ar***H***-5), 6.59 (1H, s, Ar***H***-8), 8.94 (1H, s, ArO***H***-7), 8.95-9.05 (1H, br, N$^+$***H***$_A$H$_B$), 9.06 (1H, s, ArO***H***-6), 9.10-9.25 (1H, br, N$^+$H$_A$***H***$_B$);

^{13}C-NMR (DMSO-d_6): δ_C 17.83 (3-***C***H$_3$), 20.23 (1-***C***H$_3$), 32.06 (Ar***C***H$_2$CH), 43.97 (CH$_2$***C***HCH$_3$), 48.86 (Ar***C***HCH$_2$), 112.90 (***C***$_{Ar}$H-8), 114.79 (***C***$_{Ar}$H-5), 121.09 (***C***$_{Ar}$-4a), 123.85 (***C***$_{Ar}$-8a), 144.20 (***C***$_{Ar}$OH-6), 144.90 (***C***$_{Ar}$OH-7);

MS (ESI-positive) *m/z*: MH$^+$ 194(100);

IR (KBr) *ν*/cm: 3171 (OH) 1594 (C$_{Ar}$–C$_{Ar}$), 1533 (C$_{Ar}$–C$_{Ar}$), 1241 (C$_{Ar}$–OH);

Microanalysis (C,H,N): Calculated for $C_{11}H_{16}NO_2Br$: 48.19, 5.88, 5.11;
Found 47.84, 5.73, 5.09.

(1*S*,3*S*)-*N*-(4-Chlorophenethylthiocarbamoyl)-6,7-dihydroxy-1,3-dimethyl-1,2,3,4-tetrahydroisoquinoline (31(1*S*,3*S*))

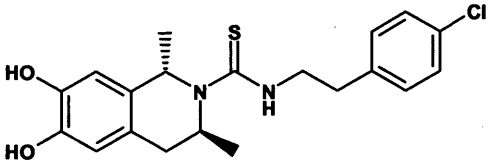

35(1*S*,3*S*) (1.07g, 3.90mmol) was dissolved in dry *N*,*N*-DMF (10mL) with triethylamine (600μL, 437mg, 4.30mmol, 1.1 equivalents). **32** (800mg, 4.10mmol, 1.05 equivalents) was dissolved in dry *N*,*N*-DMF (5mL) and added to the solution. The resulting solution was stirred at room temperature under an atmosphere of argon for eighteen hours. The reaction was diluted to 150mL with ethyl acetate, and washed consecutively with 2M hydrochloric acid (2 x 50mL), water (100mL) and brine (50mL), before drying over dried magnesium sulfate. Filtration, and removal of

solvent under reduced pressure gave a pale brown syrup. Purification by flash column chromatography (Biotage 40M cartridge; cyclohexane/ethyl acetate 3:1) gave a colourless foamed solid (1.32g, 87%). The foam was dissolved in chloroform (5mL) and precipitated from cyclohexane (100mL), to give a colourless powdered solid; drying at high vacuum at room temperature for seven days (to constant weight) gave 1.18g of material, containing 0.25 equivalents of cyclohexane (effective molecular weight 411.97, yield 73%):

Characterisation:

TLC:	*Rf* 0.49 (cyclohexane/ ethyl acetate 1:1);
Melting point:	amorphous solid;
Optical rotation $[\alpha]_D^{21}$:	–114.4 (c 0.52, dichloromethane);
^{1}H-NMR ($CDCl_3$):	δ_H 0.77 (3H, d, J = 6.3Hz, 3-C***H***$_3$), 1.34 (3H, d, J = 6.5Hz, 1-C***H***$_3$), 2.42 (1H, dd$_{ABX}$, J_{AB} = 15.1Hz, J_{AX} = 1.7Hz, tetrahydroisoquinoline ArC***H***$_A$H$_B$CH), 2.90-3.02 (2H, m, 4'-chlorophenyl-C***H***$_2$CH$_2$), 3.15 (1H, dd$_{BAX}$, J_{BA} = 15.1Hz, J_{BX} = 4.7Hz, tetrahydroisoquinoline ArCH$_A$***H***$_B$CH), 3.86-3.94 (1H, m, 4'chlorophenyl-CH$_2$C***H***$_A$H$_B$NH), 3.99-4.07 (1H, m, 4'-chlorophenyl-CH$_2$CH$_A$***H***$_B$NH), 4.40-4.55 (1H, br, CH$_2$C***H***(N)CH$_3$), 5.35-5.50 (1H, br, ArC***H***(N)CH$_3$), 5.57 (1H, br t, J = 5.0Hz, N***H***), 6.20-6.40 (2H, br, 2 x ArO***H***), 6.69 (1H, s, Ar***H***-5), 6.71 (1H, s, Ar***H***-8), 7.16 (2H, dm (AA' of an AA'BB' system), J_{ortho} = 8.4Hz, Ar***H***-2', -6'), 7.26 (2H, dm (BB' of an AA'BB' system), J_{ortho} = 8.4Hz, Ar***H***-3' and –5');
^{13}C-NMR ($CDCl_3$):	δ_C 18.43 (3-***C***H$_3$), 23.32 (1-***C***H$_3$), 34.20 (Ar***C***H$_2$CH), 34.52 (4'-chlorophenyl-***C***H$_2$CH$_2$), 46.87 (4'-chlorophenyl-CH$_2$***C***H$_2$NH), 50.63 (br, CH$_2$***C***H(N)CH$_3$), 55.45 (br, Ar***C***H(N)CH$_3$), 113.44 (***C***$_{Ar}$H-5), 115.86 (***C***$_{Ar}$H-8), 124.95 (***C***$_{Ar}$-4a), 128.88 (2 x ***C***$_{Ar}$-2', -6'), 130.14 (2 x ***C***$_{Ar}$H-3', -5'), 130.66 (***C***$_{Ar}$-8a), 132.50 (***C***$_{Ar}$Cl), 137.22 (***C***$_{Ar}$-1'), 142.52 (***C***$_{Ar}$OH), 143.15 (***C***$_{Ar}$OH), 178.78 (***C***=S);
MS (ESI-positive) *m/z*:	MH$^+$ 391(100), 393(37);
IR (KBr) *ν*/cm:	3419 (OH) 1517 (C$_{Ar}$–C$_{Ar}$), 1128 (C$_{Ar}$–OH);
HRMS (positive) *m/z*:	Calculated for $C_{22}H_{24}N_2O_2SCl$ [M+H]: 391.1247;

Found 391.1251.

HPLC — System 1: retention time = 4.88 minutes;
System 2: retention time = 7.46 minutes.

(1*R*,3*R*)-*N*-(4-Chlorophenethylthiocarbamoyl)-6,7-dihydroxy-1,3-dimethyl-1,2,3,4-tetrahydroisoquinoline (31(1*R*,3*R*))

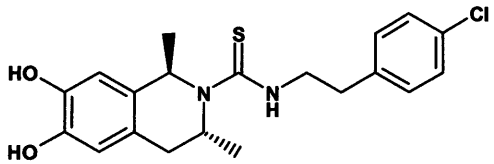

35(1*R*,3*R*) (1.07g, 3.9mmol) was dissolved in dry *N,N*-DMF (10mL). Triethylamine (600µL, 437mg, 4.3mmol) was added to the stirred solution, followed by a solution of **32** (800mg, 4.1mmol) in dry *N,N*-DMF (5mL). The reaction was stirred at room temperature under argon for 48 hours, then diluted with ethyl acetate (200mL) and washed consecutively with 0.1M hydrochloric acid (2 x 100mL), water (50mL) and brine (20mL), before drying over dried magnesium sulfate. Filtration and removal of solvent under reduced pressure gave a colourless foam; the foam was dissolved in chloroform (15mL) and precipitated from vigorously stirred cyclohexane (200mL), to give a finely divided colourless amorphous solid (1.25g, 82% yield). Although initially pure by ^{1}H-NMR, the successful removal of residual solvent by prolonged drying at 70°C and 0.1mmHg introduced a trace impurity, visible in the ^{1}H-NMR as doublets at δ_H 1.31 and 1.48, and a triplet at δ_H 3.71. Comparison with ^{1}H-NMR of **35(1*R*,3*S*)** confirmed the impurity was not a diastereomer, and the impurity was not apparent in the either analytical HPLC trace.

Characterisation:

TLC: *Rf* 0.50 (cyclohexane/ ethyl acetate 1:1);

Melting point: amorphous solid;

Optical rotation $[\alpha]_D^{21}$: +114.1 (c 0.54, dichloromethane);

^{1}H-NMR ($CDCl_3$): δ_H 0.79 (3H, d, J = 6.3Hz, 3-C***H***$_3$), 1.36 (3H, d, J = 6.6Hz, 1-C***H***$_3$), 2.44 (1H, dd$_{ABX}$, J_{AB} = 15.1Hz, J_{AX} = 2.0Hz, tetrahydroisoquinoline ArC***H***$_A$H$_B$CH), 2.93-3.02 (2H, m, 4'-chlorophenyl-C***H***$_2$CH$_2$), 3.18 (1H, dd$_{BAX}$, J_{BA} = 15.1Hz, J_{BX} = 4.8Hz, tetrahydroisoquinoline ArCH$_A$***H***$_B$CH), 3.89-3.96 (1H, m, 4'chlorophenyl-CH$_2$C***H***$_A$H$_B$NH), 3.99-4.06 (1H,

	m, 4'-chlorophenyl-$CH_2CH_A\boldsymbol{H}_BNH$), 4.38-4.58 (1H, br, $CH_2C\boldsymbol{H}(N)CH_3$), 5.20-5.55 (4H, broad overlapping signals (including t, J = 5.0Hz), N***H***, ArC***H***$(N)CH_3$, 2 x ArO***H***), 6.68 (1H, s, Ar***H***-5), 6.70 (1H, s, Ar***H***-8), 7.17 (2H, dm (AA' of an AA'BB' system), J_{ortho} = 8.4Hz, Ar***H***-2', -6'), 7.28 (2H, dm (BB' of an AA'BB' system), J_{ortho} = 8.4Hz, Ar***H***-3' and -5');
^{13}C-NMR ($CDCl_3$):	δ_C 18.43 (3-$\boldsymbol{C}H_3$), 23.37 (1-$\boldsymbol{C}H_3$), 34.27 (Ar$\boldsymbol{C}H_2CH$), 34.54 (4'-chlorophenyl-$\boldsymbol{C}H_2CH_2$), 46.84 (4'-chlorophenyl-$CH_2\boldsymbol{C}H_2NH$), 50.53 (br, $CH_2\boldsymbol{C}H(N)CH_3$), 55.44 (br, Ar$\boldsymbol{C}H(N)CH_3$), 113.44 ($\boldsymbol{C}_{Ar}$H-5), 115.79 ($\boldsymbol{C}_{Ar}$H-8), 125.05 ($\boldsymbol{C}_{Ar}$-4a), 128.91 (2 x $\boldsymbol{C}_{Ar}$-2', -6'), 130.16 (2 x $\boldsymbol{C}_{Ar}$H-3', -5'), 130.85 ($\boldsymbol{C}_{Ar}$-8a), 132.55 ($\boldsymbol{C}_{Ar}$Cl), 137.30 ($\boldsymbol{C}_{Ar}$-1'), 142.42 ($\boldsymbol{C}_{Ar}$OH), 143.11 ($\boldsymbol{C}_{Ar}$OH), 179.05 ($\boldsymbol{C}$=S);
MS (APCI) *m/z*:	MH^+ 391.0 (100);
IR (KBr) *ν*/cm:	3386 (OH + NH) 1518 (C_{Ar}–C_{Ar}), 1127 (C_{Ar}–OH);
HRMS (positive) *m/z*:	Calculated for $C_{20}H_{24}N_2O_2SCl$ [M+H]: 391.1242; Found 391.1241.
HPLC	System 1: retention time = 4.90 minutes; System 2: retention time = 7.49 minutes

Enantiomers of the cis-diastereomers of N-(4-chlorophenethylthio-carbamoyl)-6,7-dihydroxy-1,3-dimethyl-1,2,3,4-tetrahydroisoquinoline analogues (31(1*R*,3*S*) and 31(1*S*,3*R*))

(1*S*,3*S*)-6,7-dimethoxy-3-methyl-1-(toluene-4-sulfonylmethyl)-1,2,3,4-tetra-hydroisoquinoline hydrochloride (159(1*S*,3*S*))

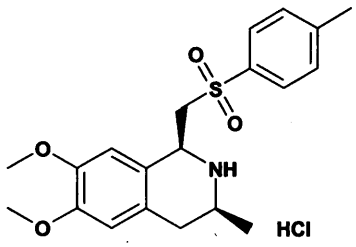

38*S* (1.12g, 5.7mmol) was dissolved in dry dichloromethane (10mL), and stirred on an ice/water bath under an atmosphere of dry argon. **150** (1.033g, 5.7mmol) was dissolved in dry dichloromethane (5mL), and added to the amine solution. After 30 minutes, thin layer chromatography confirmed the absence of starting materials. The reaction solution was cooled to –10°C on a salt/ice bath, and cold (–10°C) trifluoroacetic acid (18mL, ~40 equivalents) was added in one portion. After two hours at –10°C, the reaction was poured into 400mL of a 1:1 mixture of dichloromethane and water. The TFA was neutralised by the cautious, portionwise addition of solid sodium hydrogen carbonate (30g, 0.357mol). The phases were separated, and the aqueous phase was washed with fresh dichloromethane (100mL). The combined organic extractions were washed consecutively with water (100mL) and brine (50mL), before drying over dried magnesium sulfate. Filtration, and the removal of volatile components under reduced pressure gave a beige foam. Two chromatographic purifications (Biotage 40M, cyclohexane/ ethyl acetate 1:2, then Biotage 40S, cyclohexane/ ethyl acetate 1:2 of the impure fractions) gave the desired compound as a colourless glass (950mg, 44% yield), which resisted all attempts at crystallisation. Some of the colourless glass (370mg) was dissolved in methanol (5mL), precipitated by the addition of excess 4.0M hydrogen chloride in dioxan (500μL), filtered and dried, to give a colourless powdered solid. This was dried under high vacuum (0.1mmHg) at 100°C for four hours, to give 350mg.

Characterisation:

TLC: free base *Rf* 0.27 (cyclohexane/ ethyl acetate 1:4);

Melting point: 238-239°C;

Optical rotation $[\alpha]_D^{29}$: +25.4 (c 0.5, water);

^{1}H-NMR (DMSO-d_6): (no TMS; referenced to DMSO at 2.50ppm)

δ_H 1.47 (3H, d, J = 6.3Hz, CHC***H***$_3$), 2.43 (3H, s, ArC***H***$_3$), 2.81 (1H, dd$_{ABX}$, J_{AB} = 16.6Hz, J_{AX} = 3.6Hz, ArC***H***$_A$H$_B$CH$_X$), 3.03 (1H, dd$_{BAX}$, J_{BA} = 16.6Hz, J_{BX} = 11.9Hz, ArCH$_A$***H***$_B$CH$_X$), 3.41-3.55 (1H, br, CH$_2$C***H***(NH)CH$_3$), 3.65 (3H, s, ArOC***H***$_3$-7), 3.73 (3H, s, ArOC***H***$_3$-6), 4.14 (1H, dd$_{A'B'X'}$, $J_{A'B'}$ = 15.1Hz, $J_{A'X'}$ = 4.1Hz, SO$_2$C***H***$_{A'}$H$_{B'}$CH), 4.36 (1H, dd$_{A'B'X'}$, $J_{B'A'}$ = 15.1Hz, $J_{B'X'}$ = 6.4Hz, SO$_2$CH$_{A'}$***H***$_{B'}$CH$_{X'}$), 4.96-5.04 (1H, br, CH$_2$C***H***(NH)Ar), 6.75-6.76 (2H, 2 x s overlapping, Ar***H***-5 and Ar***H***-8), 7.49 (2H, d, J_{ortho} = 8.2Hz, Ar***H***-3' and Ar***H***-5'), 7.95 (2H, d, J_{ortho} = 8.2Hz, Ar***H***-2' and Ar***H***-6');

^{13}C-NMR (DMSO-d_6): (no TMS; referenced to DMSO at39.52)

δ_C 18.39 (CH***C***H$_3$), 21.10 (Ar***C***H$_3$), 32.23 (Ar***C***H$_2$CH), 50.30 (CH$_2$***C***HCH$_3$), 50.64 (SO$_2$CH$_2$***C***H), 55.52/55.56 (2 x ArO***C***H$_3$), 58.25 (SO$_2$***C***H$_2$CH), 109.58 (***C***$_{Ar}$H-8), 111.55 (***C***$_{Ar}$H-5), 121.23 (***C***$_{Ar}$8a), 125.25 (***C***$_{Ar}$4a), 128.03 (***C***$_{Ar}$H-2', ***C***$_{Ar}$H-6'), 129.94 (***C***$_{Ar}$H-3', ***C***$_{Ar}$H-5'), 136.05 (***C***$_{Ar}$SO$_2$-1'), 145.12 (***C***$_{Ar}$CH$_3$-4'), 147.76 (***C***$_{Ar}$OMe-7), 148.40 (***C***$_{Ar}$OMe-6);

MS (EI) *m/z*: M^+ 375(21), $[M–CH_2SO_2C_6H_4CH_3]^+$ 206(100);

IR (KBr) *ν*/cm: 2992 (NH_2^+), 1525 (C_{Ar}–C_{Ar}), 1229 (C_{Ar}–OMe), 1152 (SO_2);

Microanalysis (C,H,N): Calculated for $C_{20}H_{25}NO_4S.HCl$: 58.31, 6.36, 3.40;
Found 58.31, 6.33, 3.59.

_N_-Acetyl-2-(3,4-dimethoxy-phenyl)-1-methyl ethylamine (170*RS*)

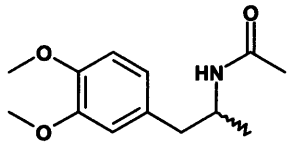

38*RS* (2.5g, 0.0108mol) was dissolved in dry dichloromethane (50mL) under an atmosphere of dry argon, by the addition of triethylamine (3.32mL, 2.42g, 0.024mol, 2.2 equivalents) in one portion. The solution was cooled on an ice bath, before the

dropwise addition of a solution of acetyl bromide (800μL, 1.33g, 0.0108mol) in dry dichloromethane (5mL) over ten minutes. The reaction was stirred for forty-eight hours.

The reaction was diluted to 250mL with dichloromethane, and washed consecutively with dilute aqueous hydrochloric acid (2 x 200mL), water (200mL) and brine (50mL), before drying over dried magnesium sulfate. Filtration and removal of solvent under reduced pressure gave a colourless crystalline solid; recrystallisation from ethyl acetate/ n-hexane gave fine colourless needles (1.75g, 68%):

Characterisation:

TLC:	*Rf* 0.7 (dichloromethane/ methanol 10:1);
Melting point:	89°C;
^{1}H-NMR ($CDCl_3$):	δ_H 1.11 (3H, d, J = 6.6Hz, CHC***H***$_3$), 1.93 (3H, s, C(=O)C***H***$_3$), 2.64 (1H, dd$_{ABX}$, J_{AB} = 13.6Hz, J_{AX} = 7.8Hz, ArC***H***$_A$H$_B$CH), 2.79 (1H, dd$_{BAX}$, J_{BA} = 13.6Hz, J_{BX} = 5.6Hz, ArCH$_A$***H***$_B$CH), 3.86-3.87 (6H, 2 x s overlapping, ArOC***H***$_3$-4 (δ_H 3.86), ArOC***H***$_3$-3 (δ_H 3.87)), 4.18-4.28 (1H, m, CH$_2$C***H***(NH)CH$_3$), 6.68-6.71 (2H, m, 2 x Ar***H***-2, -6), 6.80 (1H, d, J_{ortho} = 8.1Hz, Ar***H***-5);
^{13}C-NMR ($CDCl_3$):	δ_C 19.97 (CH***C***H$_3$), 23.53 (C(=O)***C***H$_3$), 42.04 (Ar***C***H$_2$CH), 46.17 (***C***H), 55.91 (2 x ArO***C***H$_3$), 111.19 (***C***$_{Ar}$H-5), 112.58 (***C***$_{Ar}$H-2), 121.44 (***C***$_{Ar}$H-6), 130.58 (***C***$_{Ar}$-1), 147.71 (***C***$_{Ar}$OMe-4), 148.89 (***C***$_{Ar}$OMe-3), 169.27 (***C***=O);
MS (ESI-positive) *m/z*:	MH$^+$ 238.1(10), [M+Na]$^+$ 260.1(100);
IR (KBr) *ν*/cm:	3315 (NH), 1639 (C(=O)NH), 1264 (C$_{Ar}$–OMe);
Microanalysis (C,H,N):	Calculated for $C_{13}H_{19}NO_3$: 65.80, 8.07, 5.90; Found 65.68/65.73, 7.87/8.03, 5.86/5.88.

6,7-Dimethoxy-1,3-dimethyl-3,4-dihydroisoquinoline (171*RS*)

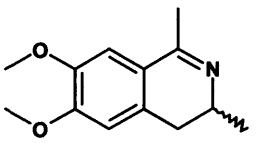

170*RS* (1.75g, 0.0074mol) was dissolved in warm toluene (20mL); phosphorous oxychloride (1.75mL, 2.89g, 0.0189mol, ~2.5 equivalents) was added, and the solution was refluxed for five hours with stirring under an atmosphere of argon. The

solution was cooled, and poured into a vigorously stirring 0.5M aqueous solution of sodium hydroxide (250mL). The product was extracted into diethyl ether (200mL); the ether phase was washed consecutively with water (200mL) and brine (20mL), and dried over dried magnesium sulfate. Filtration and removal of solvent under reduced pressure gave a beige crystalline solid. Initial purification by flash column chromatography (Biotage 40M, dichloromethane/ methanol 50:1 to 25:1) gave a colourless crystalline solid (1.0g, 62%). For characterisation purposes this solid was dissolved in boiling n-hexane (20mL); subsequent cooling to room temperature yielded an off-white crystalline solid (550mg, 34%):

Characterisation:

TLC:	*Rf* 0.3 (dichloromethane/ methanol 10:1);
Melting point:	78-79°C;
^{1}H-NMR ($CDCl_3$):	δ_H 1.37 (3H, d, J = 6.8Hz, CHC***H***$_3$), 2.37 (3H, d, J = 1.9Hz, CC***H***$_3$), 2.42 (1H, dd$_{ABX}$, J_{AB} = 15.6Hz, J_{AX} = 12.7Hz, ArC***H***$_A$H$_B$CH), 2.66 (1H, dd$_{BAX}$, J_{BA} = 15.6Hz, J_{BX} = 5.3Hz, ArCH$_A$***H***$_B$CH), 3.48-3.54 (1H, m, CH$_2$C***H***CH$_3$), 3.90-3.92 (6H, 2 x s overlapping, 2 x ArOC***H***$_3$), 6.67 (1H, s, Ar***H***-5), 7.00 (1H, s, Ar***H***-8);
^{13}C-NMR ($CDCl_3$):	δ_C 22.05 (CH***C***H$_3$), 23.46 (C***C***H$_3$), 33.19 (***C***H$_2$), 52.05 (CH$_2$***C***HCH$_3$), 55.97 (O***C***H$_3$), 56.26 (O***C***H$_3$), 109.09 (***C***$_{Ar}$H-8), 110.44 (***C***$_{Ar}$H-5), 122.31 (***C***$_{Ar}$-8a), 131.00 (***C***$_{Ar}$-4a), 147.46 (***C***$_{Ar}$OMe-7), 150.90 (***C***$_{Ar}$OMe-6), 162.66 (C$_{Ar}$***C***(CH$_3$)=N);
MS (ESI-positive) *m/z*:	MH$^+$ 220.1(100);
IR (KBr) *ν*/cm:	1604 (C=N), 1512 (C$_{Ar}$–C$_{Ar}$), 1216 (C$_{Ar}$–OMe);
Microanalysis (C,H,N):	Calculated for $C_{13}H_{17}NO_2$: 71.21, 7.81, 6.39; Found 71.10, 7.79, 6.37.

Product ratio of the diastereomers of 44, as synthesised from 38*RS* by the Pictet-Spengler tetrahydroisoquinoline synthesis with acetaldehyde

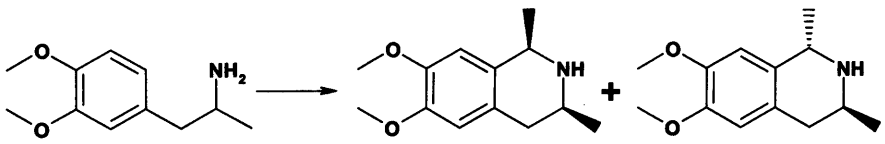

38*RS* (500mg, 2.15mmol) was dissolved in water (10mL); acetaldehyde (1.1mL, 946mg, 21.5mmol, 10 equivalents) was added, followed by 37% aqueous

hydrochloric acid (2.15mL). The solution was stirred at reflux for eighteen hours. Analysis by ^{1}H-NMR in DMSO-d_6 confirmed the reaction to be approximately 50% completed. A further 1.1mL of acetaldehyde and 2.15mL of 37% hydrochloric acid were added, and the reaction was stirred at reflux for a further twenty four hours. The reaction was again analysed by ^{1}H-NMR, and found to be complete. The excess reagents and solvent were removed under reduced pressure, to leave a greyish black solid. ^{1}H-NMR spectroscopy in DMSO-d_6 showed a 3:1 mixture of diastereomers. Comparison with the ^{1}H-NMRs in DMSO-d_6 of the hydrochloride salts of the *cis*-diastereomer **44(1*R*,3*S*)** and the *trans*-diastereomer **44(1*R*,3*R*)** confirmed the product mixture to be an approximately 3:1 *cis*:*trans* mixture of the anticipated tetrahydroisoquinolines.

Product ratio of the diastereomers of 44, as synthesised by the reduction of 171*RS* with sodium borohydride

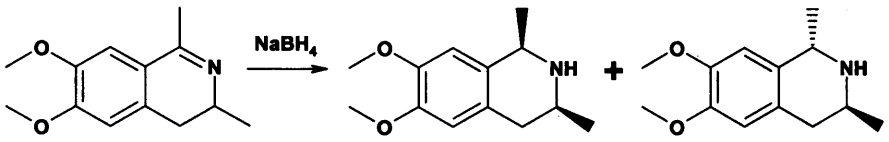

171*RS* (125mg, 0.57mmol) was dissolved in dry methanol (5mL). Sodium borohydride (87mg, 2.3mmol, 4.0 equivalents) was added in one portion, and the reaction was stirred for eighteen hours at room temperature. The reaction was quenched with 0.5M aqueous sodium hydroxide; the products were extracted into dichloromethane (2 x 25mL). The combined dichloromethane extractions were washed consecutively with water (20mL) and brine (5mL), before drying over dried magnesium sulfate. Filtration and solvent removal under reduced pressure gave an off white crystalline solid. The residue was dissolved in dioxan (5mL); 4.0M hydrogen chloride in dioxan was added (0.5mL, 2.0mmol, ~4 equivalents) to give a dense precipitate. The precipitate was dissolved by the addition of methanol (1mL); the solvents and excess hydrogen chloride were removed under reduced pressure to leave an ochre solid (~150mg, quantitative). Analysis of the solid by ^{1}H-NMR in DMSO-d_6 confirmed an approximate 6:1 ratio of products. Eventual comparison with the ^{1}H-NMRs in DMSO-d_6 of the hydrochloride salts of the *cis*-diastereomer **44(1*R*,3*S*)** and the *trans*-diastereomer **44(1*R*,3*R*)** confirmed the product mixture to be an approximately 6:1 *cis*:*trans* mixture of the anticipated tetrahydroisoquinolines.

(*S*)-*N*-Acetyl-2-(3,4-dimethoxy-phenyl)-1-methyl ethylamine (170*S*)

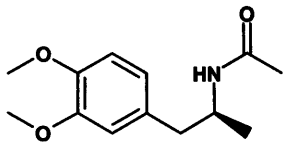

38*S* (5.08g, 0.0261mol) was dissolved in dichloromethane (75mL) with triethylamine (4.0mL, 2.90g, 0.0287mol), and stirred under argon. The solution was cooled to –15°C on a salt/ice bath; acetyl bromide (1.93mL, 3.21g, 0.0261mol) in dry dichloromethane (25mL) was added dropwise over 15 minutes, and the reaction was left to stir for 1 hour. TLC (dichloromethane/methanol/32% aqueous acetic acid 90:9:1) showed no starting amine remaining. The reaction was diluted to 300mL with dichloromethane, and washed consecutively with 0.5M aqueous hydrochloric acid (100mL), water (100mL) and brine (50mL), then dried over dried magnesium sulfate. Filtration, and removal of the solvent under reduced pressure gave a colourless crystalline solid (5.95g, 96%). Recrystallisation from n-hexane/ethyl acetate (275mL/200mL; boiling to room temperature) gave a colourless fibrous solid (3.75g, 61%), and refrigeration gave a second crop of fibres (850mg, 14%). The removal of solvent under reduced pressure gave a colourless crystalline solid (1.30g, 21%). Characterisation is for crop 1:

Characterisation:

TLC:	*Rf* 0.55 (dichloromethane/ methanol/ 32% $AcOH_{(aq)}$ 90:9:1);
Melting point:	109°C;
Optical rotation $[\alpha]_D^{21}$:	–4.4 (c 0.55, ethanol)
^{1}H-NMR ($CDCl_3$):	δ_H 1.11 (3H, d, J = 6.6Hz, CHC***H***$_3$), 1.93 (3H, s, C(=O)C***H***$_3$), 2.63 (1H, dd$_{ABX}$, J_{AB} = 13.6Hz, J_{AX} = 7.4Hz, ArC***H***$_A$H$_B$CH), 2.80 (1H, dd$_{BAX}$, J_{BA} = 13.6Hz, J_{BX} = 5.6Hz, ArCH$_A$***H***$_B$CH), 3.86 (6H, 2 x s overlapping, 2 x ArOC***H***$_3$), 4.19-4.26 (1H, m, CH$_2$C***H***(NH)CH$_3$), 7.72 (1H, br, N***H***), 6.69-6.71 (2H, d + s overlapping, Ar***H***-2, -6), 6.80 (1H, d, J_{ortho} = 8.6Hz, Ar***H***-5);
^{13}C-NMR ($CDCl_3$):	δ_C 19.97 (CH***C***H$_3$), 23.52 (C(=O)***C***H$_3$), 42.04 (Ar***C***H$_2$CH), 46.17 (***C***H), 55.91 (2 x ArO***C***H$_3$), 111.19 (***C***$_{Ar}$H-5), 112.58 (***C***$_{Ar}$H-2), 121.44 (***C***$_{Ar}$H-6), 130.59 (***C***$_{Ar}$-1), 147.71 (***C***$_{Ar}$OMe-3), 148.89 (***C***$_{Ar}$OMe-4), 169.28 (***C***=O);
MS (EI) *m/z*:	M^+ 237(24), 178(100);

IR (KBr) ν/cm: 3315 (NH), 1635 (C(=O)NH), 1520 (C_{Ar}–C_{Ar}), 1263 (C_{Ar}–OMe)

Microanalysis (C,H,N): Calculated for $C_{13}H_{19}NO_3$: 65.80, 8.07, 5.90;
Found 65.89, 8.15, 5.79.

(*R*)-*N*-Acetyl-2-(3,4-dimethoxy-phenyl)-1-methylethylamine (170*R*)

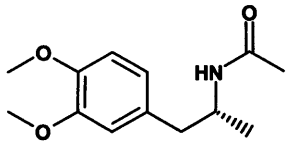

38*R* (2.50g, 0.0128mol) was dissolved in dichloromethane (50mL) with triethylamine (2.0mL, 1.46g, 0.0144mol), and stirred under argon. The solution was cooled to –15°C on a salt/ice bath; acetyl bromide (950µL, 1.58g, 0.0128mol) in dry dichloromethane (10mL) was added dropwise over 10 minutes, and the reaction was left to stir for 2 hours. TLC (dichloromethane/methanol 10:1) showed no starting amine remaining. The reaction was diluted to 200mL with dichloromethane, and washed consecutively with 0.5M aqueous hydrochloric acid (50mL), water (50mL) and brine (25mL), then dried over dried magnesium sulfate. Filtration, and removal of the solvent under reduced pressure gave a colourless crystalline solid (2.92g, 96%). Recrystallisation from n-hexane/ethyl acetate (275mL/200mL; boiling to room temperature) gave a colourless fibrous solid (crop 1, 1.25g, 41%); refrigeration of the supernatant gave a further crop of colourless fibres (crop 2, 540mg, 18%); removal of solvent from the supernatant gave a colourless crystalline solid (1.07g, 35%). ^{1}H-NMR revealed crop 1 and the supernatant residue to contain trace impurities; crop 2 was dried at 100°C/ 0.1mmHg under reduced pressure for 18 hours to characterise:

Characterisation:

TLC: *Rf* 0.44 (dichloromethane/methanol 10:1);

Melting point: 109°C;

Optical rotation $[\alpha]_D^{21}$: +4.4 (c 0.54, ethanol);

^{1}H-NMR ($CDCl_3$): δ_H 1.11 (3H, d, J = 6.6Hz, CHC***H***$_3$), 1.93 (3H, s, C(=O)C***H***$_3$), 2.63 (1H, dd$_{ABX}$, J_{AB} = 13.6Hz, J_{AX} = 7.4Hz, ArC***H***$_A$H$_B$CH), 2.80 (1H, dd$_{BAX}$, J_{BA} = 13.6Hz, J_{BX} = 5.6Hz, ArCH$_A$***H***$_B$CH), 3.86 (6H, 2 x s overlapping, 2 x ArOC***H***$_3$), 4.19-4.26 (1H, m, CH$_2$C***H***(NH)CH$_3$), 7.72 (1H, br, N***H***), 6.69-6.71 (2H, d + s

	overlapping, Ar***H***-2, -6), 6.80 (1H, d, J_{ortho} = 8.6Hz, Ar***H***-5);
^{13}C-NMR ($CDCl_3$):	δ_C 19.97 (CH***C***H_3), 23.52 (C(=O)***C***H_3), 42.04 (Ar***C***H_2CH), 46.17 (***C***H), 55.91 (2 x ArO***C***H_3), 111.19 ($\boldsymbol{C}_{Ar}$H-5), 112.58 ($\boldsymbol{C}_{Ar}$H-2), 121.44 ($\boldsymbol{C}_{Ar}$H-6), 130.59 ($\boldsymbol{C}_{Ar}$-1), 147.71 ($\boldsymbol{C}_{Ar}$OMe-3), 148.89 ($\boldsymbol{C}_{Ar}$OMe-4), 169.28 (***C***=O);
MS (EI) *m/z*:	M^+ 237(20), 178(100);
IR (KBr) *ν*/cm:	3315 (NH), 1636 (C(=O)NH), 1520 (C_{Ar}–C_{Ar}), 1263 (C_{Ar}–OMe);
Microanalysis (C,H,N):	Calculated for $C_{13}H_{19}NO_3$: 65.80, 8.07, 5.90;
	Found 65.60/65.65, 7.88/7.83, 5.63/5.79.

(*S*)-6,7-Dimethoxy-1,3-dimethyl-3,4-dihydroisoquinoline (171*S*)

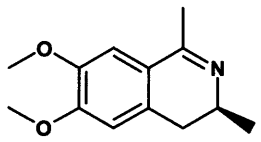

170*S* (5.6g, 0.0236mol) was dissolved in dry toluene (100mL) with phosphorous oxychloride (5.62mL, 9.24g, 0.060mol) and refluxed under an atmosphere of nitrogen for three hours. An aliquot was partitioned between 1M aqueous sodium hydroxide and ethyl acetate, and TLC of the ethyl acetate layer (dichloromethane/methanol 10:1) showed the reaction to be complete. The oil bath was removed, and the reaction was allowed to cool to room temperature before pouring into 1.0M aqueous sodium hydroxide (500mL). The product was extracted into ethyl acetate (2 x 250mL); the combined organic extractions were washed with water (200mL) and brine (50mL), then dried over dried magnesium sulfate. Filtration and removal of solvent under reduced pressure gave a brown solid; flash column chromatography (Biotage 40M cartridge, dichloromethane/methanol 50:1) gave an orange crystalline solid (4.40g, 85%); recrystallisation of this solid from boiling n-hexane (120mL) with a few drops of ethyl acetate after refrigeration gave a pale pink crystalline solid (3.64g, 70%):

Characterisation:

TLC:	*Rf* 0.40 (dichloromethane/methanol 50:1);
Melting point:	98°C;
Optical rotation $[\alpha]_D^{20}$:	–11.8 (c 0.56, dichloromethane);

^{1}H-NMR ($CDCl_3$):	δ_H 1.37 (3H, d, J = 6.8Hz, CHC***H***$_3$), 2.37 (3H, s, CC***H***$_3$), 2.42 (1H, dd$_{ABX}$, J_{AB} = 15.6Hz, J_{AX} = 12.7Hz, ArC***H***$_A$H$_B$CH), 2.66 (1H, dd$_{BAX}$, J_{BA} = 15.6Hz, J_{BX} = 5.3Hz, ArCH$_A$***H***$_B$CH), 3.45-3.58 (1H, m, CH$_2$C***H***CH$_3$), 3.91-3.92 (6H, 2 x s overlapping, 2 x ArOC***H***$_3$), 6.67 (1H, s, Ar***H***-5), 7.00 (1H, s, Ar***H***-8);
^{13}C-NMR ($CDCl_3$):	δ_C 22.06 (CH***C***H$_3$), 23.48 (C***C***H$_3$), 33.19 (***C***H$_2$), 52.06 (CH$_2$***C***HCH$_3$), 55.98 (O***C***H$_3$), 56.27 (O***C***H$_3$), 109.09 (***C***$_{Ar}$H-8), 110.44 (***C***$_{Ar}$H-5), 122.32 (***C***$_{Ar}$-8a), 131.01 (***C***$_{Ar}$-4a), 147.46 (***C***$_{Ar}$OMe-7), 150.90 (***C***$_{Ar}$OMe-6), 162.67 (C$_{Ar}$***C***(CH$_3$)=N);
MS (EI) *m/z*:	M^+ 219(100), $[M\text{-}CH_3]^+$ 204(73);
IR (KBr) *ν*/cm:	1604 (C=N), 1512 (C$_{Ar}$–C$_{Ar}$) , 1216 (C$_{Ar}$–OCH$_3$);
Microanalysis (C,H,N):	Calculated for $C_{13}H_{17}NO_2$: 71.21, 7.81, 6.39;
	Found 71.09, 7.73, 6.41.

(*R*)-6,7-Dimethoxy-1,3-dimethyl-3,4-dihydroisoquinoline (171*R*)

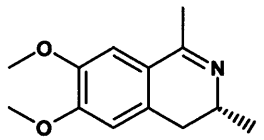

170*R* (2.65g, 0.0112mol) was dissolved in warm toluene (20mL); phosphorous oxychloride (2.65mL, 4.37g, 0.0286mol) was added, and the solution was refluxed for four hours with stirring under an atmosphere of nitrogen. A 100μL aliquot was partitioned between ethyl acetate and 1.0M aqueous sodium hydroxide (1mL of each); analysis of the organic phase by TLC (dichloromethane/methanol 10:1) revealed the reaction to be complete. The solution was cooled, and poured into a vigorously stirring 1.0M aqueous solution of sodium hydroxide. The product was extracted into ethyl acetate (2 x 250mL); the combined organic phase were washed with water (100mL), then brine (50mL), and dried over dried magnesium sulfate. Filtration and removal of solvent under reduced pressure gave a dark orange crystalline solid; this solid was dissolved in boiling n-hexane (50mL) containing ethyl acetate (3mL), hot filtered and refrigerated to give a beige crystalline solid (1.75g, 71%):

Characterisation:

TLC:	*Rf* 0.3 (dichloromethane/methanol 10:1);

Melting point:	97-98°C;
Optical rotation $[\alpha]_D^{21}$:	+12.5 (c 0.53, dichloromethane);
^{1}H-NMR ($CDCl_3$):	δ_H 1.37 (3H, d, J = 6.8Hz, CHC***H***$_3$), 2.37 (3H, s, CC***H***$_3$), 2.42 (1H, dd$_{ABX}$, J_{AB} = 15.6Hz, J_{AX} = 12.7Hz, ArC***H***$_A$H$_B$CH), 2.66 (1H, dd$_{BAX}$, J_{BA} = 15.6Hz, J_{BX} = 5.3Hz, ArCH$_A$***H***$_B$CH), 3.49-3.53 (1H, m, CH$_2$C***H***CH$_3$), 3.90-3.92 (6H, 2 x s overlapping, 2 x ArOC***H***$_3$), 6.67 (1H, s, Ar***H***-5), 7.00 (1H, s, Ar***H***-8);
^{13}C-NMR ($CDCl_3$):	δ_C 22.06 (CH***C***H$_3$), 23.48 (C***C***H$_3$), 33.19 (***C***H$_2$), 52.06 (CH$_2$***C***HCH$_3$), 55.98 (O***C***H$_3$), 56.27 (O***C***H$_3$), 109.08 (***C***$_{Ar}$H-8), 110.44 (***C***$_{Ar}$H-5), 122.32 (***C***$_{Ar}$-8a), 131.01 (***C***$_{Ar}$-4a), 147.46 (***C***$_{Ar}$OMe-7), 150.90 (***C***$_{Ar}$OMe-6), 162.67 (C$_{Ar}$***C***(CH$_3$)=N);
MS (EI) *m/z*:	M^+ 219(100), $[M\text{-}CH_3]^+$ 204(75);
IR (KBr) *ν*/cm:	1570 (C=N), 1512 (C$_{Ar}$–C$_{Ar}$), 1216 (C$_{Ar}$–OMe), 1061 (C$_{Ar}$–OMe);
Microanalysis (C,H,N):	Calculated for $C_{13}H_{17}NO_2$: 71.21, 7.81, 6.39; Found 70.88/71.09, 7.56/7.75, 6.22/6.16.

(1*R*,3*S*)-6,7-Dimethoxy-1,3-dimethyl-1,2,3,4-tetrahydroisoquinoline hydrochloride (44(1*R*,3*S*))

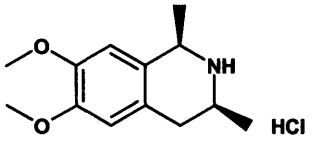

The procedure was adapted from a literature protocol. for the reductive amination of aldehydes and ketones with sodium triacetoxyborohydride[503]. **171*S*** (4.0g, 0.0183mol) was dissolved in 1,2-dichloroethane (50mL) with acetic acid (1.06mL, 1.10g, 0.0183mol). Sodium triacetoxyborohydride (95%, 6.12g, 0.0274mol, 1.5 equivalents) was added in one portion, and the mixture was stirred under nitrogen for 18 hours. An aliquot was worked up by partitioning between 0.5mL each of diethyl ether and 1.0M aqueous sodium hydroxide; removal of solvent from the organic phase under reduced pressure and subsequent analysis by ^{1}H-NMR showed there to be no **171*S*** remaining, and the reaction was assumed to be complete. The reaction was poured into 1.0M aqueous sodium hydroxide (500mL), and the product was extracted into diethyl ether (2 x 250mL). The combined ether extractions were washed with water (100mL) and brine (50mL), then dried over dried magnesium

sulfate. Filtration, and removal of the solvent under reduced pressure gave a brown syrup; this syrup was dissolved in dioxan (50mL), and stirred while 4.0M HCl in dioxan was added. After stirring for fifteen minutes, the solvent was removed from the suspension, and the resulting colourless solid was analysed by ^{1}H-NMR. The product was confirmed as predominantly one diastereomer (90% *d.e.*). The solid was dissolved in boiling methanol (50mL), and hot 1,4-dioxan was added portionwise until hazy (~50mL). Methanol was added in 1mL portions until the haziness was gone. The solution was hot filtered, and left to cool to room temperature. Filtration after 18 hours gave a colourless crystalline solid (crop1, 2.28g); a second crop of colourless crystal was also collected (crop 2, 950mg). ^{1}H-NMR confirmed these crops to be diastereomerically pure, and they were combined (3.23g, 69% yield):

Characterisation:

Melting point:	274-275°C (sublimed);
Optical rotation $[\alpha]_D^{19}$:	+96.9 (c 0.51, water);
^{1}H-NMR (D_2O):	(containing 0.75% 3-(trimethylsilyl)propionic-2,2,3,3-d_4 acid, sodium salt) δ_H 1.58 (3H, d, J = 6.5Hz, 3-C***H***$_3$), 1.78 (3H, d, J = 6.8Hz, 1-C***H***$_3$), 2.94-3.08 (2H, m (2 x dd overlapping), ArC***H***$_2$CH), 3.51-3.58 (1H, m, CH_2C***H***CH_3), 3.87-3.89 (6H, 2 x s, 2 x ArOC***H***$_3$), 4.58 (1H, quartet, J = 6.8Hz, ArC***H***CH_3), 6.87 (1H, s, Ar***H***-5), 6.91 (1H, s, Ar***H***-8);
^{13}C-NMR (D_2O):	(containing 0.75% 3-(trimethylsilyl)propionic-2,2,3,3-d_4 acid, sodium salt) δ_C 21.12, 21.16 (1-, 3-***C***H_3), 35.79 (Ar***C***H_2CH), 53.24 (CH_2***C***HCH_3), 55.41 (Ar***C***HCH_3), 58.49 (ArO***C***H_3), 58.63 (ArO***C***H_3), 111.33 (C_{Ar}H-8), 114.27 (C_{Ar}H-5), 127.19 (C_{Ar}-4a), 127.73 (C_{Ar}-8a), 150.17 (C_{Ar}-OMe), 150.65 (C_{Ar}-OMe);
MS (EI) *m/z*:	M^+ 221(15), $[M-CH_3]^+$ 206(100);
IR (KBr) *ν*/cm:	1524 (C_{Ar}–C_{Ar}), 1254 (C_{Ar}–OMe), 1226 (C_{Ar}–OMe);
Microanalysis (C,H,N):	Calculated for $C_{13}H_{20}NO_2Cl$: 60.58, 7.82, 5.43; Found 60.47, 7.57, 5.49.

(1*S*,3*R*)-6,7-Dimethoxy-1,3-dimethyl-1,2,3,4-tetrahydroisoquinoline hydrochloride (44(1*S*,3*R*))

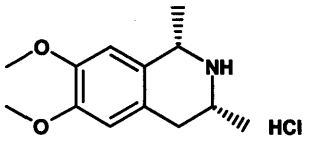

171*R* (5.0g, 22.8mmol) was dissolved in 1,2-dichloroethane (60mL) with acetic acid (1.32mL, 1.37g, 22.8mmol). Sodium triacetoxyborohydride[503] (95%, 7.26g, 34.2mmol, 1.5 equivalents) was added, and the mixture was stirred under a nitrogen atmosphere for 18 hours. An aliquot was partitioned between 0.5mL each of ethyl acetate and 1.0M aqueous sodium hydroxide, and the organic phase was analysed by TLC to confirm that the reaction was complete.

The reaction mixture was poured into 1.0M aqueous sodium hydroxide (500mL), and the product was extracted into diethyl ether (2 x 250mL). The combined ether extractions were washed with fresh water (250mL) and brine (50mL), then dried over dried magnesium sulfate. Filtration, and subsequent removal of solvent under reduced pressure gave an off-white crystalline solid. The residue was dissolved in dioxan (50mL), and 4.0M HCl in dioxan (10mL) was added to the vigorously stirring solution. The solvent was removed from the resultant suspension, to give a colourless solid. Analysis by ^{1}H-NMR showed a diastereomeric ratio of 20:1 **44(1*S*,3*R*):44(1*R*,3*R*)**. Recrystallisation from methanol/dioxan (x2) gave pure **44(1*S*,3*R*)** as a colourless crystalline solid (2.65g, 45% isolated yield):

Characterisation:

Melting point: 275-276°C (sublimed);

Optical rotation $[\alpha]_D^{22}$ –95.2(c 0.50, water);

^{1}H-NMR (D_2O): (containing 0.75% 3-(trimethylsilyl)propionic-2,2,3,3-d_4 acid, sodium salt) δ_H 1.55 (3H, d, J = 6.5Hz, 3-C***H***$_3$), 1.75 (3H, d, J = 6.8Hz, 1-C***H***$_3$), 2.96 (1H, dd$_{ABX}$, J_{AB} = 17.2Hz, J_{AX} = 11.7Hz, ArC***H***$_A$H$_B$CH), 3.05 (1H, dd$_{BAX}$, J_{BA} = 17.2Hz, J_{BX} = 4.7Hz, ArCH$_A$***H***$_B$CH), 3.52-3.58 (1H, m, CH$_2$C***H***CH$_3$), 3.87-3.88 (6H, 2 x s, 2 x ArOC***H***$_3$), 4.58 (1H, quartet, J = 6.8Hz, ArC***H***CH$_3$), 6.88 (1H, s, Ar***H***-5), 6.91 (1H, s, Ar***H***-8);

^{13}C-NMR (D_2O): (containing 0.75% 3-(trimethylsilyl)propionic-2,2,3,3-d_4 acid,

sodium salt) δ_C 21.08, 21.16 (1-, 3-***C***H_3), 35.79 (Ar***C***H_2CH), 53.23 (CH_2***C***HCH_3), 55.40 (Ar***C***HCH_3), 58.48 (ArO***C***H_3), 58.61 (ArO***C***H_3), 111.33 ($\boldsymbol{C}_{Ar}$H-8), 114.27 ($\boldsymbol{C}_{Ar}$H-5), 127.22 ($\boldsymbol{C}_{Ar}$-4a), 127.76 ($\boldsymbol{C}_{Ar}$-8a), 150.14 ($\boldsymbol{C}_{Ar}$-OMe), 150.62 ($\boldsymbol{C}_{Ar}$-OMe);

MS (ESI positive) *m/z*: MH^+ 222(100);

IR (KBr) *ν*/cm: 1524 (C_{Ar}–C_{Ar}), 1254 (C_{Ar}–OMe), 1226 (C_{Ar}–OMe);

Microanalysis (C,H,N): Calculated for $C_{13}H_{19}NO_2$.HCl: 60.58, 7.82, 5.43;
Found 60.44, 7.73, 5.49.

(1*R*,3*S*)-6,7-Dihydroxy-1,3-dimethyl-1,2,3,4-tetrahydroisoquinoline hydrobromide (35(1*R*,3*S*))

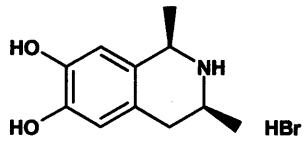

44(1*R*,3*S*) (1.00g, 3.9mmol) was dissolved in 48% hydrobromic acid (15mL) and stirred at reflux for eighteen hours. The solution was cooled to room temperature, and the solvent removed from a 50μL aliquot under reduced pressure for analysis by ^{1}H-NMR in CD_3OD, to confirm the absence of starting material. The solvent was removed from the reaction under reduced pressure, and the pale brown foam was recrystallised from propan-2-ol to give, after drying under high vacuum at 150°C to constant weight, a colourless crystalline solid (885mg, 84% yield), which ^{1}H-NMR revealed to still contain a trace amount of propan-2-ol (~0.35 mol%, 0.08% by mass):

Characterisation:

Melting point: 213-4°C;

Optical rotation $[\alpha]_D^{23}$: +77.9 (c 1.00, ethanol);

^{1}H-NMR (DMSO-d_6): (no TMS) δ_H 1.36 (3H, d, J = 6.4Hz, 3-C***H***$_3$), 1.54 (3H, d, J = 6.7Hz, 1-C***H***$_3$), 2.72 (1H, dd_{ABX}, J_{AB} = 16.8Hz, J_{AX} = 11.8Hz, ArC***H***$_A$H$_B$CH), 2.81 (1H, dd_{BAX}, J_{BA} = 16.8Hz, J_{BX} = 4.5Hz, ArCH$_A$***H***$_B$CH), 3.44-3.50 (1H, m, 3-***H***), 4.43 (1H, q, J = 6.7Hz, 1-***H***), 6.53 (1H, s, Ar***H***-5), 6.66 (1H, s, Ar***H***-8), 8.65 (1H, vbr s, N^+***H***), 8.89 (1H, br s, ArO***H***-7), 9.04

(1H, br s, ArO***H***-6), 9.19 (1H, vbr s, N^+***H***);

^{13}C-NMR (DMSO-d_6): (no TMS) δ_C 18.37, 18.53 (1-***C***H_3, 3-***C***H_3), 32.68 (***C***H_2), 49.42 (***C***H-3), 51.45 (***C***H-1), 112.15 (C_{Ar}H-8), 114.75 (C_{Ar}H-5), 122.08 (C_{Ar}-4a), 123.57 (C_{Ar}-8a), 144.28 (C_{Ar}OH-6), 144.83 (C_{Ar}OH-7);

MS (EI) *m/z*: M^+ 193(10), $[M\text{-}CH_3]^+$ 178(100);

IR (KBr) *ν*/cm: 3398 (C_{Ar}–OH), 3293 (C_{Ar}–OH), 1526 (C_{Ar}–C_{Ar});

Microanalysis (C,H,N): Calculated for $C_{11}H_{16}NO_2Br$: 48.19, 5.88, 5.11;
Found 48.08, 5.73, 5.27.

(1*S*,3*R*)-6,7-Dihydroxy-1,3-dimethyl-1,2,3,4-tetrahydroisoquinoline hydrobromide (35(1*S*,3*R*))

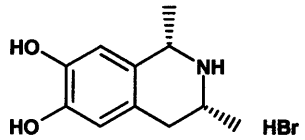

44(1*S*,3*R*) (1.10g, 4.3mmol) was dissolved in 48% hydrobromic acid (10mL) and stirred at reflux. The reaction was followed by removing the solvent from a 50μL aliquot of the reaction under reduced pressure and dissolving the residue in CD_3OD, to monitor the loss of the signals corresponding to $ArOCH_3$ by ^{1}H-NMR. After five hours, the reaction was complete. The reaction was cooled, and the solvent was removed under reduced pressure, to give a brown glass. Recrystallisation from propan-2-ol gave a colourless crystalline solid (840mg, 72%):

Characterisation:

Melting point: 214-5°C

Optical rotation $[\alpha]_D^{21}$: –81.0 (c 0.99, ethanol);

^{1}H-NMR (DMSO-d_6): (+ TMS) δ_H 1.34 (3H, d, J = 6.4Hz, 3-C***H***$_3$), 1.55 (3H, d, J = 6.7Hz, 1-C***H***$_3$), 2.74 (1H, dd_{ABX}, J_{AB} = 16.8z, J_{AX} = 11.8Hz, ArC***H***$_A$H$_B$CH), 2.83 (1H, dd_{BAX}, J_{BA} = 16.8Hz, J_{BX} = 4.5Hz, ArCH$_A$***H***$_B$CH), 3.43-3.53 (1H, br, 3-***H***), 4.38-4.44 (1H, br, 1-***H***), 6.53 (1H, s, Ar***H***-5), 6.65 (1H, s, Ar***H***-8), 8.45-8.65 (1H, v br, N^+***H***), 8.90 (1H, br s, ArO***H***-7), 8.95-9.10 (1H, v br, N^+***H***) overlapping 9.06 (1H, br s, ArO***H***-6);

^{13}C-NMR (DMSO-d_6): (+ TMS) δ_C 18.39, 18.51 (1-***C***H_3, 3-***C***H_3), 32.69 (***C***H_2), 49.48

	(*C*H-3), 51.48 (*C*H-1), 112.18 (C_{Ar}H-8), 114.79 (C_{Ar}H-5), 122.13 (C_{Ar}-4a), 123.60 (C_{Ar}-8a), 144.28 (C_{Ar}OH-6), 144.83 (C_{Ar}OH-7);
MS (EI) *m/z*:	M^+ 193(18), $[M-H]^+$ 192(28), $[M-CH_3]^+$ 178(100);
IR (KBr) *ν*/cm:	3399 (C_{Ar}–OH), 3291 (C_{Ar}–OH), 1525 (C_{Ar}–C_{Ar});
Microanalysis (C,H,N):	Calculated for $C_{11}H_{16}NO_2Br$: 48.19, 5.88, 5.11; Found 48.44, 5.83, 4.98.

(1*R*,3*S*)-*N*-(4-Chlorophenethylthiocarbamoyl)-6,7-dihydroxy-1,3-dimethyl-1,2,3,4-tetrahydroisoquinoline (31(1*R*,3*S*))

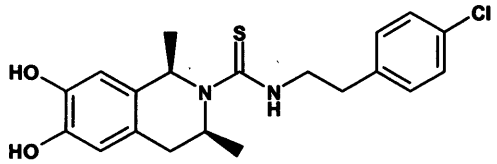

35(1*R*,3*S*) (650mg, 2.4mmol) was dissolved in dry *N*,*N*-DMF (20mL) with triethylamine (370μL, 270mg, 2.7mol). **32** (490mg, 2.5mmol) was added to the reaction in dry *N*,*N*-DMF (5mL), and the reaction was stirred at ambient temperature under argon for eighteen hours. The reaction was diluted to 200mL with ethyl acetate, and washed consecutively with 2M $HCl_{(aq)}$ (2 x 50mL), water (50mL) and brine (20mL), before drying over dried magnesium sulfate. Filtration and under reduced pressure solvent removal gave a beige foam. Purification by flash column chromatography (Biotage 40M, cyclohexane/ ethyl acetate 5:2) gave a pale yellow foam. Precipitation in cyclohexane (100mL) from chloroform (5mL) and drying to constant weight under high vacuum (0.1mmHg) at room temperature gave a pale yellow powdered amorphous solid (660mg, 70%), which ^{1}H-NMR revealed to still contain a trace amount of cyclohexane (~0.15 equivalents, 3.1% by mass):

Characterisation:

TLC:	*Rf* 0.45 (cyclohexane/ethyl acetate 1:1);
Melting point:	amorphous solid;
Optical rotation $[\alpha]_D^{23}$:	–68.2 (c 1.00, dichloromethane);
^{1}H-NMR ($CDCl_3$):	δ_H 1.14 (3H, d, J = 6.7Hz, 3-CH_3), 1.38 (3H, d, J = 7.0Hz, 1-CH_3), 1.43 (1.85H, s, ~0.15eq. cyclohexane), 2.55 (1H, dd_{ABX}, J_{AB} = 15.8Hz, J_{AX} = 5.0Hz, ArC$H_A$$H_B$CH), 2.81 (1H, dd_{BAX}, J_{BA} = 15.8Hz, J_{BX} = 6.2Hz, ArC$H_A$$H_B$CH), 2.96 (2H,

t, J = 7.0Hz, 4'-chlorophenyl-C***H***$_2$CH$_2$), 3.94-4.00 (2H, m, 4'chlorophenyl-CH$_2$C***H***$_2$NH), 4.85-4.95 (1H, br, CH$_2$C***H***(N)CH$_3$), 5.20-6.00 (4H, comprising overlapping signals: 5.20-6.00 (2H, 2 x v br, 2 x ArO***H***), 5.50-5.60 (1H, br, ArC***H***(N)CH$_3$), 5.65 (1H, br t, J = 5.1Hz, N***H***)), 6.55 (1H, s, Ar***H***-5), 6.57 (1H, s, Ar***H***-8), 7.15 (2H, dm (AA' of an AA'BB' system), J_{ortho} = 8.4Hz, Ar***H***-2', -6'), 7.26 (2H, dm (BB' of an AA'BB' system), J_{ortho} = 8.4Hz, Ar***H***-3' and -5');

^{13}C-NMR ($CDCl_3$): δ_C 20.37 (3-***C***H$_3$), 21.65 (1-***C***H$_3$), 26.93 (cyclohexane), 34.29 (Ar***C***H$_2$CH), 34.55 (4'-chlorophenyl-***C***H$_2$CH$_2$), 47.00 (CH$_2$***C***H$_2$NH), 49.27 (CH$_2$***C***H(N)CH$_3$), 53.52 (br, Ar***C***H(N)CH$_3$), 112.97 (***C***$_{Ar}$H-8), 115.12 (***C***$_{Ar}$H-5), 124.14 (***C***$_{Ar}$-4a), 128.87 (***C***$_{Ar}$-3', ***C***$_{Ar}$-5'), 129.32 (br, ***C***$_{Ar}$-8a), 130.18 (***C***$_{Ar}$-2', ***C***$_{Ar}$-6'), 132.50 (***C***$_{Ar}$Cl-4'), 137.25 (***C***$_{Ar}$-1'), 142.54 (***C***$_{Ar}$OH), 143.01 (***C***$_{Ar}$OH), 179.70 (***C***=S);

IR (KBr) ν/cm: 3308 (C$_{Ar}$–OH), 1524 (C$_{Ar}$–C$_{Ar}$), 1273 (C$_{Ar}$–O);

HRMS (positive) *m/z*: Calculated for $C_{20}H_{24}N_2O_2SCl$ [M+H]: 391.1241;
Found 391.1242;
Calculated for $C_{20}H_{23}N_2O_2SClNa$ [M+Na]: 413.1061;
Found 413.1061;

HPLC System 1: retention time = 5.95 minutes;
System 2: retention time = 8.20 minutes.

(1*S*,3*R*)-*N*-(4-Chlorophenethylthiocarbamoyl)-6,7-dihydroxy-1,3-dimethyl-1,2,3,4-tetrahydroisoquinoline (31(1*S*,3*R*)):

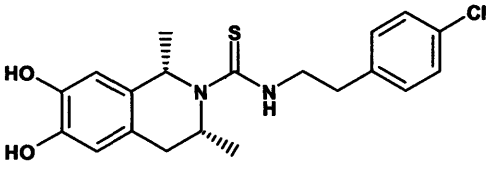

35(1*S*,3*R*) (500mg, 1.8mmol) was dissolved in dry *N*,*N*-DMF (10mL). Triethylamine (280μL, 203mg, 2.0mmol) was added to the reaction, followed by **32** (395mg, 2.0mmol) in dry *N*,*N*-DMF (5mL). The reaction was stirred at ambient temperature under argon for eighteen hours. The reaction was diluted to 150mL with ethyl acetate, and washed consecutively with 2M HCl$_{(aq)}$ (2 x 50mL), water (50mL) and

brine (10mL), before drying over dried magnesium sulfate. Filtration and the removal of solvent under reduced pressure gave a beige foam. Purification by flash column chromatography (Biotage 40M, cyclohexane/ ethyl acetate 2:1) gave a pale colourless foam, which was dissolved in chloroform (4mL), and precipitated by dropwise addition to vigorously stirring cyclohexane (75mL). Drying to constant weight under high vacuum (0.1mmHg) at room temperature gave a pale yellow powdered amorphous solid (570mg, 80%), which ^{1}H-NMR revealed to still contain ~0.5 equivalents of cyclohexane (10% by mass, effective MW 433.02, 72% yield):

Characterisation:

TLC:	*Rf* 0.45 (cyclohexane/ ethyl acetate 1:1);
Melting point:	amorphous solid;
Optical rotation $[\alpha]_D^{23}$:	+60.5 (c 1.01, dichloromethane);
^{1}H-NMR ($CDCl_3$):	δ_H 1.15 (3H, d, J = 6.7Hz, 3-C***H***$_3$), 1.39 (3H, d, J = 7.0Hz, 1-C***H***$_3$), 1.43 (6H, s, 0.5eq. cyclohexane), 2.56 (1H, dd$_{ABX}$, J_{AB} = 15.8Hz, J_{AX} = 5.0Hz, ArC***H***$_A$H$_B$CH), 2.83 (1H, dd$_{BAX}$, J_{BA} = 15.8Hz, J_{BX} = 6.2Hz, ArCH$_A$***H***$_B$CH), 2.96 (2H, t, J = 7.0Hz, 4'-chlorophenyl-C***H***$_2$CH$_2$), 3.94-4.00 (2H, m, 4'chlorophenyl-CH$_2$C***H***$_2$NH), 4.85-4.95 (1H, br, CH$_2$C***H***(N)CH$_3$), 5.20-6.00 (4H, comprising overlapping signals: 5.20-6.00 (2H, 2 x v br, 2 x ArO***H***), 5.55-5.65 (1H, br, ArC***H***(N)CH$_3$), 5.62 (1H, br t, J = 5.1Hz, N***H***)), 6.55 (1H, s, Ar***H***-5), 6.58 (1H, s, Ar***H***-8), 7.15 (2H, dm (AA' of an AA'BB' system), J_{ortho} = 8.4Hz, Ar***H***-2', -6'), 7.26 (2H, dm (BB' of an AA'BB' system), J_{ortho} = 8.4Hz, Ar***H***-3' and -5');
^{13}C-NMR ($CDCl_3$):	δ_C 20.37 (3-***C***H$_3$), 21.66 (1-***C***H$_3$), 26.93 (cyclohexane), 34.30 (Ar***C***H$_2$CH), 34.54 (4'-chlorophenyl-***C***H$_2$CH$_2$), 46.99 (CH$_2$***C***H$_2$NH), 49.26 (CH$_2$***C***H(N)CH$_3$), 53.51 (br, Ar***C***H(N)CH$_3$), 112.96 (***C***$_{Ar}$H-8), 115.09 (***C***$_{Ar}$H-5), 124.18 (***C***$_{Ar}$-4a), 128.88 (***C***$_{Ar}$-3', ***C***$_{Ar}$-5'), 129.35 (br, ***C***$_{Ar}$-8a), 130.17 (***C***$_{Ar}$-2', ***C***$_{Ar}$-6'), 132.51 (***C***$_{Ar}$Cl-4'), 137.24 (***C***$_{Ar}$-1'), 142.46 (***C***$_{Ar}$OH), 142.95 (***C***$_{Ar}$OH), 179.74 (***C***=S);
MS (ESI-negative) *m/z*:	[M–H]$^-$ 389.1(100), 391.2(46) Cl isotope pattern;
IR (KBr) *ν*/cm:	3308 (NH, OH), 1524 (thioamide), 1273 (C$_{Ar}$–O);

HRMS (positive) *m/z*:	Calculated for $C_{20}H_{24}N_2O_2SCl$ [M+H]: 391.1247;
	Found 391.1247;
HPLC	System 1: retention time = 5.94 minutes;
	System 2: retention time = 8.07 minutes.

Biology – in vitro assays

Materials:

The **culture medium** was prepared from minimum essential medium alpha (MEM-α) without ribonucleosides and deoxyribonucleosides and supplemented with 10% foetal bovine serum (FBS), plus geneticin selective antibiotic (G418) at 0.5mg/mL final concentration, penicillin at 100units/mL final concentration and streptomycin at 100μg/mL final concentration. All components of the cell culture medium were *ex*-Invitrogen.

HEPES-buffered HBSS was Hank's balanced salt solution (HBSS, *ex*-Invitrogen), buffered to pH 7.4 by the addition of 4-(2-hydroxyethyl)-1-piperazineethanesulfonic acid (HEPES) at a 10mM concentration.

The **loading buffer for the agonist assay** was a solution of fluo-4-AM (*ex*-Cambridge Bioscience, 50μg in 20mL) and 0.01% pluronic F-127 (*ex*-Cambridge Bioscience) in HEPES-buffered HBSS.

The **loading buffer for the antagonist assay** was a 2μM solution of fura-2/AM (*ex*-Molecular Probes) and 0.01% pluronic F-127 (*ex*-Cambridge Bioscience) in HEPES-buffered HBSS.

Methods - General

Preparation of cells:

40,000 Chinese hamster ovary cells (CHO) per well, expressing either the human or rat orthologue of TRPV1, were seeded overnight in 100μL cell culture medium. The medium was removed and the cells were washed with 100μL of HBSS, before 50μL of the loading buffer was added to each well. After 60 minutes, the loading buffer was removed and the cells in each well were washed with 100μL HBSS.

Methods – Agonist Assay

Preparation of test compound solutions:

From an original 10mM DMSO stock solution, test compounds were diluted to 2mM, with further serial dilutions in DMSO being made using a Biomek 2000 on plates holding micronics tubes, to give final concentrations of 3.0, 1.0, 0.3, 0.1, 0.03, 0.01, 0.003, 0.001, 0.0003 and 0.0001mM respectively. 24μL of each DMSO stock solution, and, for control purposes, 24μL of DMSO, was diluted with 376μL of HBSS, to give final concentrations of 180, 60, 18.0, 6.0, 1.8, 0.6, 0.18, 0.6, 0.018,

and 0.006μM (plus control), with a DMSO concentration of 6%. A control solution of 6% DMSO in HBSS was also prepared.

Agonist Assay

100μL of HBSS was added to each well. The plates with loaded cells were placed in a Molecular Devices Flexstation, and stimulated by light at 485 nm. Emissions were measured at 535 nm measured (with a 530 nm cut off), with the fluorescence measured at 5 second intervals over 60 seconds (13 readings). After 17 seconds (four basal readings) the agonist activity of the test compounds was determined by the addition of 20μL of each of the 6% DMSO stock solutions to wells containing the loaded cells, to give final concentrations on the assay plate of 30, 10, 3.0, 1.0, 0.3, 0.1, 0.03, 0.01, 0.003 and 0.001μM, and a final DMSO concentration of 1%.

Methods - Antagonist Assay

Preparation of test compound solutions:

From an original 10mM DMSO stock solution, test compounds were diluted to 2mM, with further serial dilutions in DMSO being made using a Biomek 2000 on plates holding micronics tubes, to give final concentrations of 2.0, 0.667, 0.2, 0.0667, 0.02, 0.00667, 0.002, 0.000667, 0.0002 and 0.0000667mM respectively.

12μL of each DMSO stock solution was diluted with 388μL of HBSS, to give concentrations of 60, 20, 6.0, 2.0, 0.6, 0.2, 0.06, 0.02, 0.006 and 0.002μM, with a DMSO concentration of 3%. A control solution of 3% DMSO in HBSS was also prepared.

Antagonist Assay

50μL of HBSS was added to each well, followed by 50μL of the test compound solutions, to give final concentrations on the assay plate of 30, 10, 3.0, 1.0, 0.3, 0.1, 0.03, 0.01, 0.003 and 0.001μM, and a final DMSO concentration of 1.5%. Low and high control wells, containing 50μL of HBSS plus 50μL of the control solution of 3% DMSO in HBSS, were prepared. The plates were light stimulated at 340nm and 380nm and emissions at 520nm measured at 5 second intervals over 60 seconds (13 readings).

vs. capsaicin

At 17 seconds (after four basal readings), 20μL of 0.3μM capsaicin in HEPES-buffered HBSS (plus 1.67% DMSO) was injected onto the cells (0.05μM final concentration). For the low control wells, just 1.67% DMSO in HEPES-buffered HBSS was added.

vs. low pH

At 17 seconds (after four basal readings), 20μL of 60mM 2-(*N*-morpholino)ethane sulfonic acid (MES) in HBSS was injected onto the cells (10mM MES final concentration, 5.75 final pH). For the low control wells 20 μL of HEPES-buffered HBSS at pH 7.4 was added.

BIBLIOGRAPHY

1. Melzack, R.; Wall, P. D. *The Challenge of Pain*; Penguin: London, 1988.
2. Schweitzer, A. *On the Edge of the Primaeval Forest*; Adam & Charles Black: London, 1953.
3. Mann, R. D. *The History of the Management of Pain*; The Parthenon Publishing Group: Carnforth, Lancs., 1988.
4. Lipton, S. *Br.Med.Bull.* **1991**, *47*, i-iv.
5. Sherrington, C. S. *The Integrative Actions of the Nervous System*; Scribner: New York, 1906.
6. Woolf, C. J. *Br.Med.Bull.* **1991**, *47*, 523-533.
7. Scholz, J.; Woolf, C. J. *Nat.Neurosci.* **2002**, *5*, 1062-1067.
8. Bear, M. F.; Connors, B. W.; Paradiso, M. A. *Neuroscience: Exploring the Brain*; Lippincott, Williams and Wilkins: Baltimore, 2001; Chapter 12, pp 396-435.
9. Fox, A. J. *Pain and Neurogenic Inflammation*; Birkhäuser Verlag: Basle, Switzerland, 1999, pp 1-22.
10. Johnson, K. O. *Curr.Opin.Neurobiol.* **2001**, *11*, 455-461.
11. Kruger, L.; Perl, E. R.; Sedivec, M. J. *J.Comp.Neurol.* **1981**, *198*, 137-154.
12. Darian-Smith, I.; Johnson, K. O.; LaMotte, C.; Kenins, P.; Shigenaga, Y.; Ming, V. C. *J.Neurophysiol.* **1979**, *42*, 1316-1331.
13. Darian-Smith, I.; Johnson, K. O.; LaMotte, C.; Shigenaga, Y.; Kenins, P.; Champness, P. *J.Neurophysiol.* **1979**, *42*, 1297-1315.
14. Raja, S.; Meyer, R.; Campbell, J. *Anesthesia: Biologic Foundations*; Lippincott-Raven: New York, 1997, pp 515-530.
15. Darian-Smith, I.; Johnson, K. O.; Dykes, R. *J.Neurophysiol.* **1973**, *36*, 325-346.

16. Hensel, H.; Andres, K. H.; von During, M. *Pflugers Archiv.European Journal Of Physiology* **1974**, *352*, 1-10.

17. Szallasi, A.; Blumberg, P. M. *Neuroscience (Oxford, United Kingdom)* **1989**, *30*, 515-520.

18. Blumberg, P. M.; Szallasi, A.; Acs, G. *Capsaicin in the Study of Pain*; Academic Press Inc.: San Diego, 1993; Chapter 3, pp 45-62.

19. Szallasi, A.; Jonassohn, M.; Acs, G.; Biro, T.; Acs, P.; Blumberg, P. M.; Sterner, O. *Br.J.Pharmacol.* **1996**, *119*, 283-290.

20. Szallasi, A.; Biro, T.; Szabo, T.; Modarres, S.; Petersen, M.; Klusch, A.; Blumberg, P. M.; Krause, J. E.; Sterner, O. *Br.J.Pharmacol.* **1999**, *126*, 1351-1358.

21. Thresh, J. C. *The Pharmaceutical Journal and Transactions* **1876**, *7*, 21.

22. Thresh, J. C. *The Pharmaceutical Journal and Transactions* **1876**, *7*, 259-260.

23. Thresh, J. C. *The Pharmaceutical Journal and Transactions* **1876**, *7*, 473.

24. Thresh, J. C. *The Pharmaceutical Journal and Transactions* **1877**, *8*, 187-188.

25. Högyes, A. *Arch.Exp.Path.Pharmak* **1878**, *9*, 117.

26. Szolcsanyi, J. *Capsaicin in the Study of Pain*; Academic Press Inc.: San Diego, 1993; Chapter 1, pp 1-26.

27. Toh, C. C.; Lee, T. S.; Kiang, A. K. *British Journal of Pharmacology and Chemotherapy* **1955**, *10*, 175-182.

28. de Lille, J.; Ramirez, E. *Anales inst.biol.(Mex.)* **1935**, *6*, 23-37.

29. Porszasz, J.; GYORGY, L.; Porszasz-Gibiszer, K. *Acta Physiol.Hung.* **1955**, *8*, 61-76.

30. Porszasz, J.; Such, G.; Porszasz-Gibiszer, K. *Acta Physiol.Acad.Sci.Hung.* **1957**, *12*, 189-205.

31. Issekutz, B.; Lichtneckert, I.; Nagy, H. *Arch.Int.Pharmacodyn.Ther.* **1950**, *81*, 35-46.

32. Issekutz, B., Jr.; Lichtneckert, I.; Winter, M. *Arch.Int.Pharmacodyn.Ther.* **1950**, *83*, 319-326.

33. Jancsó-Gábor, A.; Szolcsányi, J.; Jancsó, N. *Journal of Physiology (Cambridge, United Kingdom)* **1970**, *208*, 449-459.

34. Jancsó-Gábor, A.; Szolcsányi, J.; Jancsó, N. *Journal of Physiology (Cambridge, United Kingdom)* **1970**, *206*, 495-507.

35. Jancsó, N. *Adademischer Verlag Budapest* **1955**, 468.

36. Szolcsanyi, J. *Neuropeptides (Amsterdam, Netherlands)* **2004**, *38*, 377-384.

37. Jancsó, N.; Jancsó-Gábor, A. *Naunyn-Schmiedebergs Archiv fuer Experimentelle Pathologie und Pharmakologie* **1959**, *236*, 142-145.

38. Jancsó, N.; Jancsó-Gábor, A.; Takats, I. *Acta Physiol.Acad.Sci.Hung.* **1961**, *19*, 113-132.

39. Jancsó, N.; Jancsó-Gábor, A.; Szolcsányi, J. *Br.J.Pharmacol.* **1967**, *31*, 138-151.

40. Jancsó, G.; Király, E.; Jancsó-Gábor, A. *Nature (London, United Kingdom)* **1977**, *270*, 741-743.

41. Hayes, A. G.; Tyers, M. B. *Brain Res.* **1980**, *189*, 561-564.

42. Marsh, S. J.; Stansfeld, C. E.; Brown, D. A.; Davey, R.; McCarthy, D. *Neuroscience (Oxford, United Kingdom)* **1987**, *23*, 275-289.

43. Holzer, P. *Adv.Exp.Med.Biol.* **1991**, *298*, 3-16.

44. Burgess, P. R.; Perl, E. R. *J.Physiol.(Lond).* **1967**, *190*, 541-562.

45. Perl, E. R. *J.Physiol.(Lond).* **1968**, *197*, 593-615.

46. Lynn, B.; Carpenter, S. E. *Brain Res.* **1982**, *238*, 29-43.

47. Seno, N.; Dray, A. *Neuroscience* **1993**, *55*, 563-569.

48. Fitzgerald, M.; Lynn, B. *J.Physiol.(Lond).* **1977**, *265*, 549-563.

49. Bessou, P.; Perl, E. R. *J.Neurophysiol.* **1969**, *32*, 1025-1043.

50. Adriaensen, H.; Gybels, J.; Handwerker, H. O.; Van Hees, J. *J.Neurophysiol.* **1983**, *49*, 111-122.

51. Szolcsanyi, J.; Anton, F.; Reeh, P. W.; Handwerker, H. O. *Brain Res.* **1988**, *446*, 262-268.

52. McMahon, S.; Koltzenburg, M. *Pain* **1990**, *43*, 269-272.

53. Szolcsanyi, J.; Bartho, L. *Naunyn-Schmiedeberg's Archives of Pharmacology* **1978**, *305*, 83-90.

54. Kenins, P. *Neurosci.Lett.* **1982**, *29*, 83-88.

55. Szolcsanyi, J. *Journal of Physiology (Cambridge, United Kingdom)* **1987**, *388*, 9-23.

56. Baumann, T. K.; Simone, D. A.; Shain, C. N.; LaMotte, R. H. *J.Neurophysiol.* **1991**, *66*, 212-227.

57. Bear, M. F.; Connors, B. W.; Paradiso, M. A. *Neuroscience: Exploring the Brain*; Lippincott, Williams and Wilkins: Baltimore, 2001; Chapter 3, pp 50-72.

58. Stryer, L. *Biochemistry*; Freeman: 1988; Chapter 12, pp 283-312.

59. Singer, S. J.; Nicolson, G. L. *Science (Washington, DC, United States)* **1972**, *175*, 720-731.

60. Hille, B. *Ion Channels in Excitable Membranes*; Sinauer Associates, Inc.: Sunderland, Mass., 2001; Chapter 2, pp 25-60.

61. Skou, J. C. *News Physiol Sci* **1992**, *7*, 95-100.

62. Carafoli, E. *Physiol.Rev.* **1991**, *71*, 129-153.

63. Bear, M. F.; Connors, B. W.; Paradiso, M. A. *Neuroscience: Exploring the Brain*; Lippincott, Williams and Wilkins: Baltimore, 2001; Chapter 4, pp 73-97.

64. Hille, B. *Ion Channels in Excitable Membranes*; Sinauer Associates, Inc.: Sunderland, Mass., 2001.

65. Hodgkin, A. L.; Huxley, A. F. *Journal of Physiology, London* **1952**, *117*, 500-544.

66. Wood, J. N.; Winter, J.; James, I. F.; Rang, H. P.; Yeats, J.; Bevan, S. *J.Neurosci.* **1988**, *8*, 3208-3220.

67. Bleakman, D.; Brorson, J. R.; Miller, R. J. *Br.J.Pharmacol.* **1990**, *101*, 423-431.

68. Docherty, R. J.; Robertson, B.; Bevan, S. *Neuroscience (Oxford, United Kingdom)* **1991** , *40*, 513-521.

69. Szolcsanyi, J.; Jancso-Gabor, A. *Arzneimittelforschung.* **1975**, *25*, 1877-1881.

70. Oh, U.; Hwang, S. W.; Kim, D. *J.Neurosci.* **1996**, *16*, 1659-1667.

71. Bevan, S.; Hothi, S.; Hughes, G.; James, I. F.; Rang, H. P.; Shah, K.; Walpole, C. S. J.; Yeats, J. C. *Br.J.Pharmacol.* **1992**, *107*, 544-552.

72. Walpole, C. S. J.; Bevan, S.; Bovermann, G.; Boelsterli, J. J.; Breckenridge, R.; Davies, J. W.; Hughes, G. A.; James, I.; Oberer, L. *J.Med.Chem.* **1994**, *37*, 1942-1954.

73. Caterina, M. J.; Schumacher, M. A.; Tominaga, M.; Rosen, T. A.; Levine, J. D.; Julius, D. *Nature* **1997**, *389*, 816-824.

74. Hayes, P.; Meadows, H. J.; Gunthorpe, M. J.; Harries, M. H.; Duckworth, D. M.; Cairns, W.; Harrison, D. C.; Clarke, C. E.; Ellington, K.; Prinjha, R. K.;

Barton, A. J.; Medhurst, A. D.; Smith, G. D.; Topp, S.; Murdock, P.; Sanger, G. J.; Terrett, J.; Jenkins, O.; Benham, C. D.; Randall, A. D.; Gloger, I. S.; Davis, J. B. *Pain* **2000**, *88*, 205-215.

75. McIntyre, P.; McLatchie, L. M.; Chambers, A.; Phillips, E.; Clarke, M.; Savidge, J.; Toms, C.; Peacock, M.; Shah, K.; Winter, J.; Weerasakera, N.; Webb, M.; Rang, H. P.; Bevan, S.; James, I. F. *Br.J.Pharmacol.* **2001**, *132*, 1084-1094.

76. Jordt, S. E.; Julius, D. *Cell (Cambridge, MA, United States)* **2002**, *108*, 421-430.

77. Savidge, J.; Davis, C.; Shah, K.; Colley, S.; Phillips, E.; Ranasinghe, S.; Winter, J.; Kotsonis, P.; Rang, H.; McIntyre, P. *Neuropharmacology* **2002**, *43*, 450-456.

78. Gavva, N. R.; Klionsky, L.; Qu, Y.; Shi, L.; Tamir, R.; Edenson, S.; Zhang, T. J.; Viswanadhan, V. N.; Toth, A.; Pearce, L. V.; Vanderah, T. W.; Porreca, F.; Blumberg, P. M.; Lile, J.; Sun, Y.; Wild, K.; Louis, J. C.; Treanor, J. J. S. *J.Biol.Chem.* **2004**, *279*, 20283-20295.

79. Correll, C. C.; Phelps, P. T.; Anthes, J. C.; Umland, S.; Greenfeder, S. *Neurosci.Lett.* **2004**, *370*, 55-60.

80. Montell, C.; Birnbaumer, L.; Flockerzi, V.; Bindels, R. J.; Bruford, E. A.; Caterina, M. J.; Clapham, D. E.; Harteneck, C.; Heller, S.; Julius, D.; Kojima, I.; Mori, Y.; Penner, R.; Prawitt, D.; Scharenberg, A. M.; Schultz, G.; Shimizu, N.; Zhu, M., X *Mol.Cell* **2002**, *9*, 229-231.

81. Caterina, M. J.; Rosen, T. A.; Tominaga, M.; Brake, A. J.; Julius, D. *Nature* **1999**, *398*, 436-441.

82. Xu, H.; Ramsey, I. S.; Kotecha, S. A.; Moran, M. M.; Chong, J. A.; Lawson, D.; Ge, P.; Lilly, J.; Silos-Santiago, I.; Xie, Y.; DiStefano, P. S.; Curtis, R.; Clapham, D. E. *Nature* **2002**, *418*, 181-186.

83. Peier, A. M.; Reeve, A. J.; Andersson, D. A.; Moqrich, A.; Earley, T. J.; Hergarden, A. C.; Story, G. M.; Colley, S.; Hogenesch, J. B.; McIntyre, P.; Bevan, S.; Patapoutian, A. *Science (Washington, DC, United States)* **2002**, *296*, 2046-2049.

84. Smith, G. D.; Gunthorpe, M. J.; Kelsell, R. E.; Hayes, P. D.; Reilly, P.; Facer, P.; Wright, J. E.; Jerman, J. C.; Walhin, J. P.; Ooi, L.; Egerton, J.; Charles, K. J.; Smart, D.; Randall, A. D.; Anand, P.; Davis, J. B. *Nature (London, United Kingdom)* **2002**, *418*, 186-190.

85. Liedtke, W.; Choe, Y.; Marti-Renom, M. A.; Bell, A. M.; Denis, C. S.; Sali, A.; Hudspeth, A. J.; Friedman, J. M.; Heller, S. *Cell (Cambridge, Massachusetts)* **2000**, *103*, 525-535.

86. Wissenbach, U.; Bodding, M.; Freichel, M.; Flockerzi, V. *FEBS Lett.* **2000**, *485*, 127-134.

87. Strotmann, R.; Harteneck, C.; Nunnenmacher, K.; Schultz, G.; Plant, T. D. *Nature cell biology* **2000**, *2*, 695-702.

88. Clapham, D. E. *Nature (London, United Kingdom)* **2003**, *426*, 517-524.

89. Moran, M. M.; Xu, H.; Clapham, D. E. *Curr.Opin.Neurobiol.* **2004**, *14*, 362-369.

90. Clapham, D. E.; Runnels, L. W.; Strubing, C. *Nature Reviews Neuroscience* **2001**, *2*, 387-396.

91. Cosens, D. J.; Manning, A. *Nature* **1969**, *224*, 285-287.

92. Montell, C.; Jones, K.; Hafen, E.; Rubin, G. *Science (Washington, DC, United States)* **1985**, *230*, 1040-1043.

93. Montell, C.; Rubin, G. M. *Neuron* **1989**, *2*, 1313-1323.

94. Hardie, R. C.; Minke, B. *Neuron* **1992**, *8*, 643-651.

95. Palmer, C. P.; Zhou, X. L.; Lin, J.; Loukin, S. H.; Kung, C.; Saimi, Y. *Proc.Natl.Acad.Sci.U.S.A.* **2001**, *98*, 7801-7805.

96. Denis, V.; Cyert, M. S. *J.Cell Biol.* **2002**, *156*, 29-34.

97. Zhou, X. L.; Batiza, A. F.; Loukin, S. H.; Palmer, C. P.; Kung, C.; Saimi, Y. *Proc.Natl.Acad.Sci.U.S.A.* **2003**, *100*, 7105-7110.

98. Colbert, H. A.; Smith, T. L.; Bargmann, C. I. *J.Neurosci.* **1997**, *17*, 8259-8269.

99. Wes, P. D.; Chevesich, J.; Jeromin, A.; Rosenberg, C.; Stetten, G.; Montell, C. *Proc.Natl.Acad.Sci.U.S.A.* **1995**, *92*, 9652-9656.

100. Zitt, C.; Zobel, A.; Obukhov, A. G.; Harteneck, C.; Kalkbrenner, F.; Lueckhoff, A.; Schultz, G. *Neuron* **1996**, *16*, 1189-1196.

101. Zhu, X.; Jiang, M.; Peyton, M.; Boulay, G.; Hurst, R.; Stefani, E.; Birnbaumer, L. *Cell (Cambridge, Massachusetts)* **1996**, *85*, 661-671.

102. Harteneck, C.; Plant, T. D.; Schultz, G. *Trends Neurosci.* **2000**, *23*, 159-166.

103. Phillips, A. M.; Bull, A.; Kelly, L. E. *Neuron* **1992**, *8*, 631-642.

104. Zhu, X.; Chu, P. B.; Peyton, M.; Birnbaumer, L. *FEBS Lett.* **1995**, *373*, 193-198.

105. Clapham, D. E.; Montell, C.; Schultz, G.; Julius, D. *Pharmacol.Rev.* **2003**, *55*, 591-596.

106. Lux, S. E.; John, K. M.; Bennett, V. *Nature (London, United Kingdom)* **1990**, *344*, 36-42.

107. Bear, M. F.; Connors, B. W.; Paradiso, M. A. *Neuroscience: Exploring the Brain*; Lippincott, Williams and Wilkins: Baltimore, 2001; Chapter 5, pp 98-129.

108. Battaglia, G.; Rustioni, A. *J.Comp.Neurol.* **1988**, *277*, 302-312.

109. Jeftinija, S.; Jeftinija, K.; Liu, F.; Skilling, S. R.; Smullin, D. H.; Larson, A. *Neurosci.Lett.* **1991**, *125*, 191-194.

110. Kangrga, I.; Randic, M. *Brain Res.* **1991**, *553*, 347-352.

111. Skilling, S. R.; Smullin, D. H.; Beitz, A. J.; Larson, A. A. *J.Neurochem.* **1988**, *51*, 127-132.

112. Jessell, T. M.; Yoshioka, K.; Jahr, C. E. *J.Exp.Biol.* **1986**, *124*, 239-258.

113. Dougherty, P. M.; Palecek, J.; Paleckova, V.; Sorkin, L. S.; Willis, W. D. *J.Neurosci.* **1992**, *12*, 3025-3041.

114. Wilcox, G. L. *Proceedings of the 6th World Congress on Pain*; Elsevier: Amsterdam, 1991, pp 97-117.

115. Ueda, M.; Kuraishi, Y.; Satoh, M. *Neurosci.Lett.* **1993**, *155*, 179-182.

116. Ueda, M.; Kuraishi, Y.; Sugimoto, K.; Satoh, M. *Neurosci.Res.* **1994**, *20*, 231-237.

117. Hokfelt, T.; Kellerth, J. O.; Nilsson, G.; Pernow, B. *Science (Washington, DC, United States)* **1975**, *190*, 889-890.

118. Gibson, S. J.; Polak, J. M.; Bloom, S. R.; Wall, P. D. *J.Comp.Neurol.* **1981**, *201*, 65-79.

119. Duggan, A. W.; Hendry, I. A.; Morton, C. R.; Hutchison, W. D.; Zhao, Z. Q. *Brain Res.* **1988**, *451*, 261-273.

120. Yaksh, T. L.; Jessell, T. M.; Gamse, R.; Mudge, A. W.; Leeman, S. E. *Nature (London, United Kingdom)* **1980**, *286*, 155-157.

121. Kuraishi, Y.; Hirota, N.; Sato, Y.; Hanashima, N.; Takagi, H.; Satoh, M. *Neuroscience (Oxford, United Kingdom)* **1989**, *30*, 241-250.

122. Todd, A. J.; Puskar, Z.; Spike, R. C.; Hughes, C.; Watt, C.; Forrest, L. *J.Neurosci.* **2002**, *22*, 4103-4113.

123. Henry, J. L. *Brain Res.* **1976**, *114*, 439-451.

124. Randic, M.; Miletic, V. *Brain Res.* **1977**, *128*, 164-169.

125. Ma, Q. P.; Woolf, C. J. *J.Physiol.(Lond).* **1995**, *486 (Pt 3)*, 769-777.

126. Traub, R. J. *Pain* **1996**, *67*, 151-161.

127. Henry, J. L.; Yashpal, K.; Pitcher, G. M.; Chabot, J. G.; Coderre, T. J. *J.Neurosci.* **1999**, *19*, 6588-6598.

128. Mantyh, P. W.; Rogers, S. D.; Honore, P.; Allen, B. J.; Ghilardi, J. R.; Li, J.; Daughters, R. S.; Lappi, D. A.; Wiley, R. G.; Simone, D. A. *Science* **1997**, *278*, 275-279.

129. Theriault, E.; Otsuka, M.; Jessell, T. *Brain Res.* **1979**, *170*, 209-213.

130. Gamse, R.; Jancsó, G.; Király, E. Intracisternal capsaicin: a novel approach for studying nociceptive sensory neurons. Chahl, L. A.; Szolcsányi, J.; Lembeck, F., eds. Antidromic Vasodilatation Neurogenic Inflammation, Satellite Symposium. 93-110. 1984. Budapest, Hungary, Akadémiai Kiadó. Ref Type: Conference Proceeding

131. Hua, X. Y.; Saria, A.; Gamse, R.; Theodorsson-Norheim, E.; Brodin, E.; Lundberg, J. M. *Neuroscience (Oxford, United Kingdom)* **1986**, *19*, 313-319.

132. Saria, A.; Gamse, R.; Petermann, J.; Fischer, J. A.; Theodorsson-Norheim, E.; Lundberg, J. M. *Neurosci.Lett.* **1986**, *63*, 310-314.

133. Morton, C. R.; Hutchison, W. D. *Neurosci.Lett.* **1990**, *117*, 319-324.

134. Cridland, R. A.; Henry, J. L. *Neuropeptides (Edinburgh, United Kingdom)* **1988**, *11*, 23-32.

135. Neugebauer, V.; Ruemenapp, P.; Schaible, H.-G. *Neuroscience (Oxford)* **1996**, *71*, 1095-1109.

136. Sun, R. Q.; Lawand, N. B.; Willis, W. D. *Pain* **2003**, *104*, 201-208.

137. Sun, R. Q.; Lawand, N. B.; Lin, Q.; Willis, W. D. *J.Neurophysiol.* **2004**, *92*, 320-326.

138. Oku, R.; Satoh, M.; Fujii, N.; Otaka, A.; Yajima, H.; Takagi, H. *Brain Res.* **1987**, *403*, 350-354.

139. Cridland, R. A.; Henry, J. L. *Neurosci.Lett.* **1989**, *102*, 241-246.

140. Del Bianco, E.; Santicioli, P.; Tramontana, M.; Maggi, C. A.; Cecconi, R.; Geppetti, P. *Brain Res.* **1991**, *566*, 46-53.

141. Wess, J. *Pharmacol.Ther.* **1998**, *80*, 231-264.

142. Strader, C. D.; Fong, T. M.; Tota, M. R.; Underwood, D. *Annu.Rev.Biochem.* **1994**, *63*, 101-132.

143. Kar, S.; Quirion, R. *J.Comp.Neurol.* **1995**, *354*, 253-281.

144. Yung, K. K. L. *Neuroreport* **1998**, *9*, 1639-1644.

145. Merskey, H.; Bogduk, N. *Classification of chronic pain*; IASP Press: Seattle, 1994; pp 210-213.

146. Dray, A. *Br.J.Anaesth.* **1995**, *75*, 125-131.

147. Levine, J. D.; Reichling, D. B. *Textbook of Pain*; Chuchill Livingstone: London, 1999; Chapter 2.

148. Omote, K.; Kawamata, T.; Kawamata, M.; Namiki, A. *Brain Res.* **1998**, *787*, 161-164.

149. Holzer, P. *Neuroscience (Oxford, United Kingdom)* **1988**, *24* , 739-768.

150. Holzer, P. *Pharmacol.Rev.* **1991**, *43*, 143-201.

151. Lawson, S. N. *Prog.Brain Res.* **1996**, *113*, 369-385.

152. Brain, S. D.; Williams, T. J.; Tippins, J. R.; Morris, H. R.; MacIntyre, I. *Nature (London, United Kingdom)* **1985**, *313*, 54-56.

153. Brain, S. D.; Williams, T. J. *Br.J.Pharmacol.* **1985**, *86*, 855-860.

154. Brain, S. D.; Williams, T. J. *Nature (London, United Kingdom)* **1988**, *335*, 73-75.

155. Brain, S. D.; Williams, T. J. *Br.J.Pharmacol.* **1989**, *97*, 77-82.

156. Pedersen-Bjergaard, U.; Nielsen, L. B.; Jensen, K.; Edvinsson, L.; Jansen, I.; Olesen, J. *Peptides* **1989**, *10*, 1147-1152.

157. Pedersen-Bjergaard, U.; Nielsen, L. B.; Jensen, K.; Edvinsson, L.; Jansen, I.; Olesen, J. *Peptides* **1991**, *12*, 333-337.

158. Krause, J. E.; Takeda, Y.; Hershey, A. D. *J.Invest.Dermatol.* **1992**, *98*, 2S-7S.

159. Maggi, C. A. *Prog.Neurobiol.* **1995**, *45*, 1-98.

160. Kilo, S.; Harding-Rose, C.; Hargreaves, K. M.; Flores, C. M. *Pain* **1997**, *73*, 201-207.

161. Dray, A. *Pain Reviews* **1994**, *1*, 153-171.

162. Campos, M. M.; Calixto, J. B. *Neuropeptides* **2000**, *34*, 314-322.

163. Rang, H. P.; Bevan, S.; Dray, A. *Br.Med.Bull.* **1991**, *47*, 534-548.

164. Holzer, P. *General Pharmacology: The Vascular System* **1998**, *30*, 5-11.

165. Steen, K. H.; Reeh, P. W.; Anton, F.; Handwerker, H. O. *J.Neurosci.* **1992**, *12*, 86-95.

166. Issberner, U.; Reeh, P. W.; Steen, K. H. *Neurosci.Lett.* **1996**, *208*, 191-194.

167. Steranka, L. R.; Manning, D. C.; DeHaas, C. J.; Ferkany, J. W.; Borosky, S. A.; Connor, J. R.; Vavrek, R. J.; Stewart, J. M.; Snyder, S. H. *Proc.Natl.Acad.Sci.U.S.A.* **1988**, *85*, 3245-3249.

168. Bevan, S. J. *Textbook of Pain* ; Chuchill Livingstone: London, 1999; Chapter 3.

169. Lang, E.; Novak, A.; Reeh, P. W.; Handwerker, H. O. *J.Neurophysiol.* **1990**, *63*, 887-901.

170. Lynn, B. *Trends Neurosci.* **1991**, *14*, 95.

171. Sann, H.; Pierau, F. K. *Zeitschrift fuer Rheumatologie* **1998**, *57*, 8-13.

172. Caterina, M. J.; Leffler, A.; Malmberg, A. B.; Martin, W. J.; Trafton, J.; Petersen-Zeitz, K. R.; Koltzenburg, M.; Basbaum, A., I; Julius, D. *Science* **2000**, *288*, 306-313.

173. Davis, J. B.; Gray, J.; Gunthorpe, M. J.; Hatcher, J. P.; Davey, P. T.; Overend, P.; Harries, M. H.; Latcham, J.; Clapham, C.; Atkinson, K.; Hughes, S. A.; Rance, K.; Grau, E.; Harper, A. J.; Pugh, P. L.; Rogers, D. C.; Bingham, S.; Randall, A.; Sheardown, S. A. *Nature* **2000**, *405*, 183-187.

174. Bevan, S.; Yeats, J. *J.Physiol.(Lond).* **1991**, *433*, 145-161.

175. Bevan, S.; Forbes, C. A.; Winter, J. *J.Physiol.(Lond).* **1993**, *459*, 401P.

176. Baumann, T. K.; Burchiel, K. J.; Ingram, S. L.; Martenson, M. E. *Pain* **1996**, *65*, 31-38.

177. Bevan, S.; Geppetti, P. *Trends Neurosci.* **1994**, *17*, 509-512.

178. Petersen, M.; LaMotte, R. H. *Pain* **1993**, *54*, 37-42.

179. Kress, M.; Fetzer, S.; Reeh, P. W.; Vyklicky, L. *Neurosci.Lett.* **1996**, *211*, 5-8.

180. Tominaga, M.; Caterina, M. J.; Malmberg, A. B.; Rosen, T. A.; Gilbert, H.; Skinner, K.; Raumann, B. E.; Basbaum, A., I; Julius, D. *Neuron* **1998**, *21*, 531-543.

181. Jordt, S. E.; Tominaga, M.; Julius, D. *Proc.Natl.Acad.Sci.U.S.A.* **2000**, *97*, 8134-8139.

182. Hwang, S. W.; Cho, H.; Kwak, J.; Lee, S. Y.; Kang, C. J.; Jung, J.; Cho, S.; Min, K. H.; Suh, Y. g.; Kim, D.; Oh, U. *Proc.Natl.Acad.Sci.U.S.A.* **2000**, *97*, 6155-6160.

183. Devane, W. A.; Hanus, L.; Breuer, A.; Pertwee, R. G.; Stevenson, L. A.; Griffin, G.; Gibson, D.; Mandelbaum, A.; Etinger, A.; Mechoulam, R. *Science (Washington, DC, United States)* **1992**, *258*, 1946-1949.

184. Bisogno, T.; Melck, D.; Bobrov, M. Y.; Gretskaya, N. M.; Bezuglov, V. V.; De Petrocellis, L.; Di Marzo, V. *Biochem.J.* **2000**, *351*, 817-824.

185. Smart, D.; Jerman, J. C. *Trends Pharmacol.Sci.* **2000**, *21*, 134.

186. Smart, D.; Gunthorpe, M. J.; Jerman, J. C.; Nasir, S.; Gray, J.; Muir, A. I.; Chambers, J. K.; Randall, A. D.; Davis, J. B. *Br.J.Pharmacol.* **2000**, *129*, 227-230.

187. Huang, S. M.; Bisogno, T.; Trevisani, M.; Al Hayani, A.; De Petrocellis, L.; Fezza, F.; Tognetto, M.; Petros, T. J.; Krey, J. F.; Chu, C. J.; Miller, J. D.; Davies, S. N.; Geppetti, P.; Walker, J. M.; Di Marzo, V. *Proc.Natl.Acad.Sci.U.S.A.* **2002**, *99*, 8400-8405.

188. Zygmunt, P. M.; Petersson, J.; Andersson, D. A.; Chuang, H. h.; Sorgard, M.; Di Marzo, V.; Julius, D.; Hogestatt, E. D. *Nature (London)* **1999**, *400*, 452-457.

189. Akerman, S.; Kaube, H.; Goadsby, P. J. *Br.J.Pharmacol.* **2004**, *142*, 1354-1360.

190. O'Sullivan, S. E.; Kendall, D. A.; Randall, M. D. *Br.J.Pharmacol.* **2004**, *141*, 803-812.

191. Kress, M.; Reeh, P. W.; Vyklicky, L. *Neurosci.Lett.* **1997**, *224*, 37-40.

192. Vyklicky, L.; Knotkova-Urbancova, H.; Vitaskova, Z.; Vlachova, V.; Kress, M.; Reeh, P. W. *J.Neurophysiol.* **1998**, *79*, 670-676.

193. Linhart, O.; Obreja, O.; Kress, M. *Neuroscience (Oxford, United Kingdom)* **2003**, *118*, 69-74.

194. Chuang, H. h.; Prescott, E. D.; Kong, H.; Shields, S.; Jordt, S. E.; Basbaum, A. I.; Chao, M. V.; Julius, D. *Nature* **2001**, *411*, 957-962.

195. Tang, H. B.; Inoue, A.; Oshita, K.; Nakata, Y. *Eur.J.Pharmacol.* **2004**, *498*, 37-43.

196. Kirschstein, T.; Busselberg, D.; Treede, R.-D. *Neurosci.Lett.* **1997**, *231*, 33-36.

197. Nagy, I.; Rang, H. *Neuroscience (Oxford)* **1998**, *88*, 995-997.

198. Kirschstein, T.; Greffrath, W.; Busselberg, D.; Treede, R. D. *J.Neurophysiol.* **1999**, *82*, 2853-2860.

199. Raja, S. N.; Campbell, J. N.; Meyer, R. A. *Brain* **1984**, *107 (Pt 4)*, 1179-1188.

200. Ali, Z.; Meyer, R. A.; Campbell, J. N. *Pain* **1996**, *68*, 401-411.

201. Simone, D. A.; Baumann, T. K.; Collins, J. G.; LaMotte, R. H. *Brain Res.* **1989**, *486*, 185-189.

202. Woolf, C. J.; King, A. E. *J.Neurosci.* **1990**, *10*, 2717-2726.

203. Woolf, C. J.; Doubell, T. P. *Curr.Opin.Neurobiol.* **1994**, *4* , 525-534.

204. Coderre, T. J.; Melzack, R. *J.Neurosci.* **1992**, *12*, 3665-3670.

205. Koltzenburg, M.; Lundberg, L. E. R.; Torebjork, H. E. *Pain* **1992**, *51*, 207-219.

206. Magerl, W.; Wilk, S. H.; Treede, R. D. *Pain* **1998**, *74*, 257-268.

207. Mendell, L. M. *Exp.Neurol.* **1966**, *16*, 316-332.

208. Schouenborg, J.; Sjolund, B. H. *J.Neurophysiol.* **1983**, *50*, 1108-1121.

209. Urban, L.; Thompson, S. W. N.; Dray, A. *Trends Neurosci.* **1994**, *17*, 432-438.

210. Mayer, M. L.; Westbrook, G. L.; Guthrie, P. B. *Nature (London, United Kingdom)* **1984**, *309*, 261-263.

211. Gamse, R.; Molnar, A.; Lembeck, F. *Life Sci.* **1979**, *25*, 629-636.

212. Price, D. D.; Hu, J. W.; Dubner, R.; Gracely, R. H. *Pain* **1977**, *3*, 57-68.

213. Smith, T. E.; Chong, M. S. *Hosp.Med.* **2000**, *61*, 760-766.

214. Melzack, R.; Wall, P. D. *Science* **1965**, *150*, 971-979.

215. Mayer, D. J.; Wolfle, T. L.; Akil, H.; Carder, B.; Liebeskind, J. C. *Science* **1971**, *174*, 1351-1354.

216. Liebeskind, J. C.; Guilbaud, G.; Besson, J. M.; Oliveras, J. L. *Brain Res.* **1973**, *50*, 441-446.

217. Richardson, D. E.; Akil, H. *J.Neurosurg.* **1977**, *47*, 184-194.

218. Richardson, D. E.; Akil, H. *J.Neurosurg.* **1977**, *47*, 178-183.

219. Tyce, G. M.; Yaksh, T. L. *J.Physiol.(Lond).* **1981**, *314*, 513-529.

220. Cui, M.; Feng, Y.; McAdoo, D. J.; Willis, W. D. *J.Pharmacol.Exp.Ther.* **1999**, *289*, 868-876.

221. Roberts, M. H. *Prog.Brain Res.* **1988**, *77*, 329-338.

222. Sawynok, J.; Reid, A. *Behav.Brain Res.* **1995**, *73*, 63-68.

223. Alhaider, A. A.; Wilcox, G. L. *J.Pharmacol.Exp.Ther.* **1993**, *265*, 378-385.

224. Zemlan, F. P.; Behbehani, M. M.; Murphy, R. M. *Prog.Brain Res.* **1988**, *77*, 349-355.

225. Furst, S. *Brain Res.Bull.* **1999**, *48*, 129-141.

226. Millan, M. J. *Progress in Neurobiology (Oxford, United Kingdom)* **2002**, *66*, 355-474.

227. Coggeshall, R. E.; Carlton, S. M. *Brain Research Reviews* **1997**, *24*, 28-66.

228. Hammond, D. L. *Handbook of Experimental Pharmacology* **1997**, *130*, 361-383.

229. Dickenson, A. H.; Chapman, V.; Green, G. M. *Gen.Pharmacol.* **1997**, *28*, 633-638.

230. Barber, R. P.; Vaughn, J. E.; Roberts, E. *Brain Res.* **1982**, *238*, 305-328.

231. Carlton, S. M.; Hayes, E. S. *J.Comp.Neurol.* **1990**, *300*, 162-182.

232. Millan, M. J. *Prog.Neurobiol.* **1999**, *57*, 1-164.

233. Bowery, N. G.; Malcangio, M. g-Aminobutyric acid and pain. 249-264. 1999.
Ref Type: Conference Proceeding

234. Margeta-Mitrovic, M.; Mitrovic, I.; Riley, R. C.; Jan, L. Y.; Basbaum, A. I. *J.Comp.Neurol.* **1999**, *405*, 299-321.

235. Charles, K. J.; Evans, M. L.; Robbins, M. J.; Calver, A. R.; Leslie, R. A.; Pangalos, M. N. *Neuroscience (Oxford, United Kingdom)* **2001**, *106*, 447-467.

236. Rajendra, S.; Lynch, J. W.; Schofield, P. R. *Pharmacol.Ther.* **1997**, *73*, 121-146.

237. Todd, A. J.; Sullivan, A. C. *J.Comp.Neurol.* **1990**, *296*, 496-505.

238. Dumba, J. S.; Irish, P. S.; Anderson, N. L.; Westrum, L. E. *Brain Res.* **1998**, *806*, 16-25.

239. Todd, A. J.; Watt, C.; Spike, R. C.; Sieghart, W. *J.Neurosci.* **1996**, *16*, 974-982.

240. Hughes, J.; Smith, T. W.; Kosterlitz, H. W.; Fothergill, L. A.; Morgan, B. A.; Morris, H. R. *Nature (London, United Kingdom)* **1975**, *258*, 577-579.

241. Millan, M. J. *Handbook of Experimental Pharmacology* **1993**, *104/II*, 127-162.

242. Millan, M. J. *Trends Pharmacol.Sci.* **1990**, *11*, 70-76.

243. Millan, M. J. *Pain* **1986**, *27*, 303-347.

244. Dickenson, A. H. *Proceedings of the 7th World Congress on Pain*; IASP Press: Seattle, 1994.

245. Meunier, J. C.; Mollereau, C.; Toll, L.; Suaudeau, C.; Moisand, C.; Alvinerie, P.; Butour, J. L.; Guillemot, J. C.; Ferrara, P.; Monsarrat, B.; + *Nature* **1995**, *377*, 532-535.

246. Reinscheid, R. K.; Nothacker, H. P.; Bourson, A.; Ardati, A.; Henningsen, R. A.; Bunzow, J. R.; Grady, D. K.; Langen, H.; Monsma, F. J., Jr.; Civelli, O. *Science (Washington, D.C.)* **1995**, *270*, 792-794.

247. Sawynok, J.; Doak, G.; Poon, A. *Drug Development Research* **1998**, *45*, 304-311.

248. Ralevic, V.; Burnstock, G. *Pharmacol.Rev.* **1998**, *50*, 413-492.

249. Olah, M. E.; Stiles, G. L. *Pharmacol.Ther.* **2000**, *85*, 55-75.

250. Choca, J. I.; Green, R. D.; Proudfit, H. K. *J.Pharmacol.Exp.Ther.* **1988**, *247*, 757-764.

251. Salter, M. W.; De Koninck, Y.; Henry, J. L. *Progress in Neurobiology (Oxford, United Kingdom)* **1993**, *41*, 125-156.

252. Karlsten, R.; Post, C.; Hide, I.; Daly, J. W. *Neurosci.Lett.* **1991**, *121*, 267-270.

253. Reeve, A. J.; Dickenson, A. H. *Br.J.Pharmacol.* **1995**, *116*, 2221-2228.

254. Morton, C. R.; Hutchison, W. D.; Hendry, I. A.; Duggan, A. W. *Brain Res.* **1989**, *488*, 89-96.

255. Morton, C. R.; Hutchison, W. D.; Hendry, I. A. *Neuropeptides (Edinburgh, United Kingdom)* **1988**, *12*, 189-197.

256. Decker, M. W.; Meyer, M. D. *Biochem.Pharmacol.* **1999**, *58*, 917-923.

257. Decker, M. W.; Meyer, M. D.; Sullivan, J. P. *Expert Opinion on Investigational Drugs* **2001**, *10*, 1819-1830.

258. Eisenach, J. C. *Life Sci.* **1999**, *64*, 549-554.

259. Levesque, H.; Lafont, O. *La Revue de medecine interne / fondee ...par la Societe nationale francaise de medecine interne* **2000**, *21 Suppl 1* , 8s-17s.

260. Vane, J. R.; Botting, R. M. *Postgraduate Medical Journal, Supplement* **1990**, *66*, S2-S17.

261. Jourdier, S. *Chem.Br.* **1999**, *35*, 33-35.

262. Vane, J. R. *Nature: New biology* **1971**, *231*, 232-235.

263. Henry, D. A. *Bailliere's clinical rheumatology* **1988**, *2*, 425-454.

264. Rang, H. P.; Dale, M. M.; Ritter, J. M. *Pharmacology*; Churchill Livingstone: 1996; Chapter 11, pp 214-245.

265. Kujubu, D. A.; Fletcher, B. S.; Varnum, B. C.; Lim, R. W.; Herschman, H. R. *J.Biol.Chem.* **1991**, *266*, 12866-12872.

266. Vane, J. R.; Bakhle, Y. S.; Botting, R. M. *Annu.Rev.Pharmacol.Toxicol.* **1998**, *38*, 97-120.

267. Fletcher, B. S.; Kujubu, D. A.; Perrin, D. M.; Herschman, H. R. *J.Biol.Chem.* **1992**, *267*, 4338-4344.

268. O'Banion, M. K.; Sadowski, H. B.; Winn, V.; Young, D. A. *J.Biol.Chem.* **1991**, *266*, 23261-23267.

269. Seibert, K.; Masferrer, J. L. *Receptor* **1994**, *4*, 17-23.

270. Seibert, K.; Zhang, Y.; Leahy, K.; Hauser, S.; Masferrer, J.; Perkins, W.; Lee, L.; Isakson, P. *Proc.Natl.Acad.Sci.U.S.A.* **1994**, *91*, 12013-12017.

271. Seibert, K.; Zhang, Y.; Leahy, K.; Hauser, S.; Masferrer, J.; Isakson, P. *Adv.Exp.Med.Biol.* **1997**, *400A*, 167-170.

272. Beiche, F.; Scheuerer, S.; Brune, K.; Geisslinger, G.; Goppelt-Struebe, M. *FEBS Lett.* **1996**, *390*, 165-169.

273. Vane, J. *Nature* **1994**, *367*, 215-216.

274. Luong, C.; Miller, A.; Barnett, J.; Chow, J.; Ramesha, C.; Browner, M. F. *Nat.Struct.Biol.* **1996**, *3*, 927-933.

275. Kurumbail, R. G.; Stevens, A. M.; Gierse, J. K.; McDonald, J. J.; Stegeman, R. A.; Pak, J. Y.; Gildehaus, D.; Miyashiro, J. M.; Penning, T. D.; Seibert, K.; Isakson, P. C.; Stallings, W. C. *Nature (London)* **1996**, *384*, 644-648.

276. Kurumbail, R. G.; Stevens, A. M.; Gierse, J. K.; McDonald, J. J.; Stegeman, R. A.; Pak, J. Y.; Gildehaus, D.; Miyashiro, J. M.; Penning, T. D.; Seibert, K.; Isakson, P. C.; Stallings, W. C. *Nature (London)* **1997**, *385*, 555.

277. Penning, T. D.; Talley, J. J.; Bertenshaw, S. R.; Carter, J. S.; Collins, P. W.; Docter, S.; Graneto, M. J.; Lee, L. F.; Malecha, J. W.; Miyashiro, J. M.; Rogers, R. S.; Rogier, D. J.; Yu, S. S.; Anderson, G. D.; Burton, E. G.; Cogburn, J. N.; Gregory, S. A.; Koboldt, C. M.; Perkins, W. E.; Seibert, K.; Veenhuizen, A. W.; Zhang, Y. Y.; Isakson, P. C. *J.Med.Chem.* **1997**, *40*, 1347-1365.

278. Prasit, P.; Wang, Z.; Brideau, C.; Chan, C.-C.; Charleson, S.; Cromlish, W.; Ethier, D.; Evans, J. F.; Ford-Hutchinson, A. W.; Gauthier, J. Y.; Gordon, R.; Guay, J.; Gresser, M.; Kargman, S.; Kennedy, B.; Leblanc, Y.; Leger, S.; Mancini, J.; O'Neill, G. P.; Ouellet, M.; Percival, M. D.; Perrier, H.; Riendeau, D.; Rodger, I.; Tagari, P.; Therien, M.; Vickers, P.; Wong, E.; Xu, L.-J.; Young, R. N.; Zamboni, R.; Boyce, S.; Rupniak, N.; Forrest, M.; Visco, D.; Patrick, D. *Bioorg.Med.Chem.Lett.* **1999**, *9*, 1773-1778.

279. Ding, C.; Jones, G. *IDrugs* **2002**, *5*, 1168-1172.

280. Capone, M. L.; Tacconelli, S.; Sciulli, M. G.; Patrignani, P. *International Journal of Immunopathology and Pharmacology* **2003**, *16*, 49-58.

281. Frantz, S. *Nature Reviews Drug Discovery* **2004**, *3*, 899-900.

282. Couzin, J. *Science (Washington, DC, United States)* **2004**, *306*, 384-385.

283. Dorey, E. *Chemistry & Industry (London, United Kingdom)* **2004**, 6.

284. Botting, R. *J.Physiol.Pharmacol.* **2000**, *51*, 609-618.

285. Mitchell, J. A.; Akarasereenont, P.; Thiemermann, C.; Flower, R. J.; Vane, J. R. *PNAS* **1993**, *90*, 11693-11697.

286. Chandrasekharan, N. V.; Dai, H.; Roos, K. L. T.; Evanson, N. K.; Tomsik, J.; Elton, T. S.; Simmons, D. L. *PNAS* **2002**, *99*, 13926-13931.

287. Simmons, D. L.; Botting, R. M.; Robertson, P. M.; Madsen, M. L.; Vane, J. R. *PNAS* **1999**, *96*, 3275-3280.

288. Eastwood, D. *International Congress and Symposium Series - Royal Society of Medicine* **2000**, *246*, 69-78.

289. Sora, I.; Takahashi, N.; Funada, M.; Ujike, H.; Revay, R. S.; Donovan, D. M.; Miner, L. L.; Uhl, G. R. *Proc.Natl.Acad.Sci.U.S.A.* **1997**, *94* , 1544-1549.

290. Kowaluk, E. A.; Arneric, S. P.; Williams, M. *Emerging Drugs* **1998**, *3*, 1-37.

291. Williams, M.; Kowaluk, E. A.; Arneric, S. P. *J.Med.Chem.* **1999**, *42*, 1481-1500.

292. Cauffield, J. S. Treatment Options in Neuropathic Pain. U.S.Pharmacist 25. 2000. Jobson Publishing LLC.
Ref Type: Electronic Citation

293. Cox, J. M.; Pappagallo, M. *Expert Review of Neurotherapeutics* **2001**, *1*, 81-91.

294. Max, M. B.; Lynch, S. A.; Muir, J.; Shoaf, S. E.; Smoller, B.; Dubner, R. *New Engl.J.Med.* **1992**, *326*, 1250-1256.

295. Max, M. B. *Ann.Neurol.* **1994**, *35 Suppl*, S50-S53.

296. Watson, C. P. *J.Pain Symptom Manage.* **1994**, *9*, 392-405.

297. Korzeniewska-Rybicka, I.; P³aŸnik, A. *Pharmacology Biochemistry and Behavior* **1998**, *59*, 331-338.

298. Baños, J. E.; Sánchez, G.; Berrendero, F.; Maldonado, R. *Mini-Reviews in Medicinal Chemistry* **2003**, *3*, 719-727.

299. McQuay, H.; Carroll, D.; Jadad, A. R.; Wiffen, P.; Moore, A. *BMJ (Clinical Research Ed.)* **1995**, *311*, 1047-1052.

300. Johnson, F. N.; Johnson, R. D.; Armer, M. L. *Reviews in Contemporary Pharmacotherapy* **2001**, *12*, 125-211.

301. Huckle, R. *Current Opinion in Investigational Drugs (Thomson Scientific)* **2004**, *5*, 82-89.

302. Kowaluk, E. A.; Arneric, S. P. *Annu.Rep.Med.Chem.* **1998**, *33*, 11-20.

303. Gillen, C.; Maul, C. *Expert Review of Neurotherapeutics* **2002**, *2*, 691-702.

304. Hogyes, E. *Orv.Hetil.* **2000**, *141*, 739-740.

305. Micko, K. *Zeitschrift fur Untersuchung der Nahrungs- und Genussmittel sowie der Gebrauchs* **1898**, *1*, 818-829.

306. Micko, K. *Zeitschrift fur Untersuchung der Nahrungs- und Genussmittel sowie der Gebrauchs* **1899**, *2*, 411-412.

307. Nelson, E. K. *J.Am.Chem.Soc.* **1919**, *41*, 1115-1121.

308. Nelson, E. K. *J.Am.Chem.Soc.* **1919**, *41*, 2121-2130.

309. Nelson, E. K. *J.Am.Chem.Soc.* **1920**, *42*, 597-599.

310. Nelson, E. K.; Dawson, L. E. *J.Am.Chem.Soc.* **1923**, *45*, 2179-2181.

311. Spath, E.; Darling, S. F. *Ber.* **1930**, *63B*, 737-743.

312. Crombie, L.; Dandegaonker, S. H.; Simpson, K. B. *Journal of the Chemical Society, Abstracts* **1955**, 1025-1027.

313. Walpole, C. S.; Wrigglesworth, R.; Bevan, S.; Campbell, E. A.; Dray, A.; James, I. F.; Perkins, M. N.; Reid, D. J.; Winter, J. *J.Med.Chem.* **1993**, *36*, 2362-2372.

314. Walpole, C. S.; Wrigglesworth, R.; Bevan, S.; Campbell, E. A.; Dray, A.; James, I. F.; Masdin, K. J.; Perkins, M. N.; Winter, J. *J.Med.Chem.* **1993**, *36*, 2373-2380.

315. Walpole, C. S.; Wrigglesworth, R.; Bevan, S.; Campbell, E. A.; Dray, A.; James, I. F.; Masdin, K. J.; Perkins, M. N.; Winter, J. *J.Med.Chem.* **1993**, *36*, 2381-2389.

316. Lapworth, A.; Royle, F. A. *Journal of the Chemical Society, Abstracts* **1919**, *115*, 1109-1116.

317. Jones, E. C. S.; Pyman, F. L. *Journal of the Chemical Society, Abstracts* **1925**, *127*, 2588-2598.

318. Ott, E.; Zimmermann, K. *Ann* **1921**, *425*, 314-337.

319. Ott, E.; Eichler, F.; Ludemann, O.; Heimann, H. *Ber.* **1922**, *55B*, 2653-2663.

320. Kobayashi, S. *Scientific Papers of the Institute of Physical and Chemical Research (Japan)* **1927**, *6*, 166-184.

321. Szeki, T. *Arch.Pharm.* **1930**, *268*, 151-157.

322. Newman, A. A. *Chemical Products and Chemical News* **1953**, *16*, 343-345.

323. Newman, A. A. *Chemical Products and Chemical News* **1953**, *16*, 379-382.

324. Newman, A. A. *Chemical Products and Chemical News* **1953**, *16*, 413-417.

325. Newman, A. A. *Chemical Products and Chemical News* **1953**, *16*, 467-471.

326. Newman, A. A. *Chemical Products and Chemical News* **1954**, *17*, 14-18.

327. Newman, A. A. *Chemical Products and Chemical News* **1954**, *17*, 102-106.

328. Jessell, T. M.; Iversen, L. L.; Cuello, A. C. *Brain Res.* **1978**, *152*, 183-188.

329. Gamse, R.; Petsche, U.; Lembeck, F.; Jancsó, G. *Brain Res.* **1982**, *239*, 447-462.

330. Bear, M. F.; Connors, B. W.; Paradiso, M. A. *Neuroscience: Exploring the Brain*; Lippincott, Williams and Wilkins: Baltimore, 2001; Chapter 2.

331. Hayes, A. G.; Hawcock, A. B.; Hill, R. G. *Life Sci.* **1984**, *35*, 1561-1568.

332. Hayes, A. G.; Oxford, A.; Reynolds, M.; Shingler, A. H.; Skingle, M.; Smith, C.; Tyers, M. B. *Life Sci.* **1984**, *34*, 1241-1248.

333. Hayes, A. G.; Skingle, M.; Tyers, M. B. *Neuropharmacology* **1981**, *20*, 505-511.

334. Winter, J.; Bevan, S.; Campbell, E. A. *Br.J.Anaesth.* **1995**, *75*, 157-168.

335. Porszasz, J.; Jancso, N. *Acta Physiol.Acad.Sci.Hung.* **1959**, *16*, 299-306.

336. Cholewinski, A.; Burgess, G. M.; Bevan, S. *Neuroscience (Oxford, United Kingdom)* **1993**, *55*, 1015-1023.

337. Koplas, P. A.; Rosenberg, R. L.; Oxford, G. S. *J.Neurosci.* **1997**, *17*, 3525-3537.

338. Docherty, R. J.; Yeats, J. C.; Bevan, S.; Boddeke, H. W. G. M. *Pfluegers Archiv* **1996**, *431*, 828-837.

339. Jung, J.; Shin, J. S.; Lee, S. Y.; Hwang, S. W.; Koo, J.; Cho, H.; Oh, U. *J.Biol.Chem.* **2004**, *279*, 7048-7054.

340. Mohapatra, D. P.; Nau, C. *J.Biol.Chem.* **2003**, *278*, 50080-50090.

341. Bhave, G.; Hu, H. J.; Glauner, K. S.; Zhu, W.; Wang, H.; Brasier, D. J.; Oxford, G. S.; Gereau, R. W., IV *PNAS* **2003**, *100*, 12480-12485.

342. Zhang, W. Y.; Li Wan, P. A. *Eur.J.Clin.Pharmacol.* **1994**, *46*, 517-522.

343. Mason, L.; Moore, R. A.; Derry, S.; Edwards, J. E.; McQuay, H. J. *BMJ [British Medical Journal]* **2004**, *328*, 991-994.

344. Robbins, W. R.; Staats, P. S.; Levine, J.; Fields, H. L.; Allen, R. W.; Campbell, J. N.; Pappagallo, M. *Anesth Analg* **1998**, *86*, 579-583.

345. Acs, G.; Biro, T.; Acs, P.; Modarres, S.; Blumberg, P. M. *J.Neurosci.* **1997**, *17*, 5622-5628.

346. Wender, P. A.; Jesudason, C. D.; Nakahira, H.; Tamura, N.; Tebbe, A. L.; Ueno, Y. *J.Am.Chem.Soc.* **1997**, *119*, 12976-12977.

347. Hegyes, P.; Foldeak, S. *Acta Physica et Chemica* **1974**, *20*, 115-120.

348. Szolcsanyi, J.; Jancso-Gabor, A. *Arzneimittelforschung.* **1976**, *26*, 33-37.

349. Lee, S. S.; Sohn, Y. W.; Yoo, E. S.; Kim, K. H. *J.Toxicol.Sci.* **1991**, *16*, 3-20.

350. Janusz, J. M.; Buckwalter, B. L.; Young, P. A.; LaHann, T. R.; Farmer, R. W.; Kasting, G. B.; Loomans, M. E.; Kerckaert, G. A.; Maddin, C. S. *J.Med.Chem.* **1993**, *36*, 2595-2604.

351. Chen, I. J.; Yang, J. M.; Yeh, J. L.; Wu, B. N.; Lo, Y. C.; Chen, S. J. *Eur.J.Med.Chem.* **1992**, *27*, 187-192.

352. Wrigglesworth, R.; Walpole, C. S.; Bevan, S.; Campbell, E. A.; Dray, A.; Hughes, G. A.; James, I.; Masdin, K. J.; Winter, J. *J.Med.Chem.* **1996**, *39*, 4942-4951.

353. Berman, Elizabeth F., Buckwalter, Brian, Cupps, Thomas L., and Gardner, Joseph H. EP Patent 206609, 1986 **1986** , 33.

354. Gardner, Joseph H., Kasting, Gerald B., Cupps, Thomas L., Echler, Richard S., and Gibson, Thomas W. EP Patent 282127, 1988 **1988**, 44.

355. Park, No Sang, Ha, Deok Chan, Choi, Joong Kwon, Kim, Hyun Sook, Hong, Mi Sook, Lim, Hee Jong, and Lee, Kwang Sook EP Patent 525360, 1992 **1993**, 32.

356. Park, No Sang, Jung, Young Sik, Seong, Churl Min, Lee, Jong Cheol, Choi, Jin Li, Choi, Seung Won, Choi, Yeon Joo, and Lee, Kwang Sook EP Patent 721939, 1996 **1996**, 13.

357. Lee, J.; Park, S. U.; Kim, J. Y.; Kim, J. K.; Lee, J.; Oh, U.; Marquez, V. E.; Beheshti, M.; Wang, Q. J.; Modarres, S.; Blumberg, P. M. *Bioorg.Med.Chem.Lett.* **1999**, *9*, 2909-2914.

358. Lee, Jeewoo, Oh, Uhtaek, Park, Young Ho, Suh, Young ger, Park, Hyeung geun, and Kim, Hee Doo WO Patent 2000050387, 2000 **2000**, 54.

359. Lee, J. *Bioorg.Med.Chem.* **2001**, *9*, 19-32.

360. Lee, J.; Lee, J.; Kang, M. S.; Kim, K. P.; Chung, S. J.; Blumberg, P. M.; Yi, J. B.; Park, Y. H. *Bioorg.Med.Chem.* **2002**, *10*, 1171-1179.

361. Lee, J.; Kim, S. Y.; Park, S.; Lim, J. O.; Kim, J. M.; Kang, M.; Lee, J.; Kang, S. U.; Choi, H. K.; Jin, M. K.; Welter, J. D.; Szabo, T.; Tran, R.; Pearce, L. V.; Toth, A.; Blumberg, P. M. *Bioorg.Med.Chem.* **2004**, *12*, 1055-1069.

362. *The Merck Index*; Merck & Co.,Inc.: Rahway, N.J., U.S.A., 1989.

363. Maggi, C. A.; Patacchini, R.; Santicioli, P.; Giuliani, S.; Geppetti, P.; Meli, A. *Neurosci.Lett.* **1988**, *88*, 201-205.

364. Maggi, C. A.; Santicioli, P.; Geppetti, P.; Parlani, M.; Astolfi, M.; Pradelles, P.; Patacchini, R.; Meli, A. *Eur.J.Pharmacol.* **1988**, *154*, 1-10.

365. Amann, R.; Lembeck, F. *Eur.J.Pharmacol.* **1989**, *161*, 227-229.

366. Maggi, C. A.; Bevan, S.; Walpole, C. S. J.; Rang, H.; Giuliani, S. *Br.J.Pharmacol.* **1993**, *108*, 801-805.

367. Docherty, R. J.; Yeats, J. C.; Piper, A. S. *Br.J.Pharmacol.* **1997**, *121*, 1461-1467.

368. Reid, G.; Babes, A.; Pluteanu, F. *Journal of Physiology (Cambridge, United Kingdom)* **2002**, *545*, 595-614.

369. Liu, L.; Simon, S. A. *Neurosci.Lett.* **1997**, *228*, 29-32.

370. Gill, C. H.; Randall, A.; Bates, S. A.; Hill, K.; Owen, D.; Larkman, P. M.; Cairns, W.; Yusaf, S. P.; Murdock, P. R.; Strijbos, P. J. L. M.; Powell, A. J.; Benham, C. D.; Davies, C. H. *Br.J.Pharmacol.* **2004**, *143*, 411-421.

371. Yamamura, H.; Ugawa, S.; Ueda, T.; Nagao, M.; Shimada, S. *J.Biol.Chem.* **2004**, *279*, 44483-44489.

372. Perkins, M. N.; Campbell, E. A. *Br.J.Pharmacol.* **1992**, *107* , 329-333.

373. Santos, A. R. S.; Calixto, J. B. *Neurosci.Lett.* **1997**, *235* , 73-76.

374. Sakurada, T.; Matsumura, T.; Moriyama, T.; Sakurada, C.; Ueno, S.; Sakurada, S. *Pharmacol.Biochem.Behav.* **2003**, *75*, 115-121.

375. Walker, K. M.; Urban, L.; Medhurst, S. J.; Patel, S.; Panesar, M.; Fox, A. J.; McIntyre, P. *J.Pharmacol.Exp.Ther.* **2003**, *304*, 56-62.

376. Phillips, E.; Reeve, A.; Bevan, S.; McIntyre, P. *J.Biol.Chem.* **2004**, *279*, 17165-17172.

377. Chen, I. J.; Lo, Y. C.; Lo, W. J.; Yeh, J. L.; Wu, B. N. *General Pharmacology: The Vascular System* **1997**, *29*, 387-395.

378. Wahl, P.; Foged, C.; Tullin, S.; Thomsen, C. *Mol.Pharmacol.* **2001**, *59*, 9-15.

379. Seabrook, G. R.; Sutton, K. G.; Jarolimek, W.; Hollingworth, G. J.; Teague, S.; Webb, J.; Clark, N.; Boyce, S.; Kerby, J.; Ali, Z.; Chou, M.; Middleton, R.; Kaczorowski, G.; Jones, A. B. *J.Pharmacol.Exp.Ther.* **2002**, *303*, 1052-1060.

380. Toth, A.; Blumberg, P. M.; Chen, Z.; Kozikowski, A. P. *Mol.Pharmacol.* **2004**, *65*, 282-291.

381. Lee, J. *Bioorg.Med.Chem.* **2001**, *9*, 1713-1720.

382. Park, H. g.; Park, M. K.; Choi, J. Y.; Choi, S. H.; Lee, J.; Suh, Y. g.; Oh, U.; Lee, J.; Kim, H. D.; Park, Y. H.; Jeong, Y. S.; Choi, J. K.; Jew, S. S. *Bioorg.Med.Chem.Lett.* **2003**, *13*, 197-200.

383. Park, H. g.; Park, M. K.; Choi, J. Y.; Choi, S. H.; Lee, J.; Park, B. s.; Kim, M. G.; Suh, Y. g.; Cho, H.; Oh, U.; Lee, J.; Kim, H. D.; Park, Y. H.; Koh, H. J.; Lim, K. M.; Moh, J. H.; Jew, S. S. *Bioorg.Med.Chem.Lett.* **2003**, *13*, 601-604.

384. Lee, J.; Lee, J.; Kang, M.; Shin, M.; Kim, J. M.; Kang, S. U.; Lim, J. O.; Choi, H. K.; Suh, Y. g.; Park, H. g.; Oh, U.; Kim, H. D.; Park, Y. H.; Ha, H. J.; Kim, Y. H.; Toth, A.; Wang, Y.; Tran, R.; Pearce, L. V.; Lundberg, D. J.; Blumberg, P. M. *J.Med.Chem.* **2003**, *46*, 3116-3126.

385. Suh, Young ger, Oh, Uh Taek, Kim, Hee Doo, Lee, Jee woo, Park, Hyeung geun, Park, Ok Hui, Lee, Yong Sil, Park, Young Ho, Joo, Yung Hyup, Choi, Jin Kyu, Lim, Kyung Min, Kim, Sun Young, Kim, Jin Kwan, Koh, Hyun Ju, Moh, Joo Hyun, Jeong, Yeon Su, Yi, Jung Bum, and Oh, Young Im WO Patent 2002016318, 2001 **2002**, 245.

386. Wang, Y.; Szabo, T.; Welter, J. D.; Toth, A.; Tran, R.; Lee, J.; Kang, S. U.; Suh, Y. g.; Blumberg, P. M.; Lee, J. *Mol.Pharmacol.* **2002**, *62*, 947-956.

387. Wang, Y.; Szabo, T.; Welter, J. D.; Toth, A.; Tran, R.; Lee, J.; Kang, S. U.; Suh, Y. g.; Blumberg, P. M.; Lee, J. *Mol.Pharmacol.* **2003**, *63*, 958.

388. Suh, Y. g.; Lee, Y. S.; Min, K. H.; Park, O. H.; Seung, H. S.; Kim, H. D.; Park, H. G.; Choi, J. Y.; Lee, J.; Kang, S. W.; Oh, U. T.; Koo, J. Y.; Joo, Y. H.; Kim, S. Y.; Kim, J. K.; Park, Y. H. *Bioorg.Med.Chem.Lett.* **2003**, *13*, 4389-4393.

389. Lee, J.; Kang, S. U.; Lim, J. O.; Choi, H. K.; Jin, M. K.; Toth, A.; Pearce, L. V.; Tran, R.; Wang, Y.; Szabo, T.; Blumberg, P. M. *Bioorg.Med.Chem.* **2004**, *12*, 371-385.

390. Valenzano, K. J.; Grant, E. R.; Wu, G.; Hachicha, M.; Schmid, L.; Tafesse, L.; Sun, Q.; Rotshteyn, Y.; Francis, J.; Limberis, J.; Malik, S.; Whittemore, E. R.; Hodges, D. *J.Pharmacol.Exp.Ther.* **2003**, *306*, 377-386.

391. Pomonis, J. D.; Harrison, J. E.; Mark, L.; Bristol, D. R.; Valenzano, K. J.; Walker, K. *J.Pharmacol.Exp.Ther.* **2003**, *306*, 387-393.

392. Bakthavatchalam, Rajagopal WO Patent 2002008221, 2001 **2002**, 209.

393. Kyle, Donald J., Sun, Qun, Tafesse, Laykea, Zhang, Chongwu, and Zhou, Xiaoming WO Patent 2004002983, 2003 **2004**, 287.

394. Balan, Chenera, Bo, Yunxin, Dominguez, Celia, Fotsch, Christopher H., Gore, Vijay K., Ma, Vu Van, Norman, Mark H., Ognyanov, Vassil I., Qian, Yi xin, Wang, Xianghong, Xi, Ning, and Xu, Shimin WO Patent 2004035549, 2003 **2004**, 259.

395. Swanson, D. M.; Dubin, A. E.; Shah, C.; Nasser, N.; Chang, L.; Dax, S. L.; Jetter, M.; Breitenbucher, J. G.; Liu, C.; Mazur, C.; Lord, B.; Gonzales, L.; Hoey, K.; Rizzolio, M.; Bogenstaetter, M.; Codd, E. E.; Lee, D. H.; Zhang, S. P.; Chaplan, S. R.; Carruthers, N. I. *J.Med.Chem.* **2004**, *ASAP article*, ACS.

396. Thompson, Mervyn and Wyman, Paul Adrian WO Patent 2002072536, 2002 **2002**, 18.

397. Rami, H. K.; Thompson, M.; Wyman, P.; Jerman, J. C.; Egerton, J.; Brough, S.; Stevens, A. J.; Randall, A. D.; Smart, D.; Gunthorpe, M. J.; Davis, J. B. *Bioorg.Med.Chem.Lett.* **2004**, *14*, 3631-3634.

398. Rami, Harshad Kantilal, Thompson, Mervyn, and Wyman, Paul Adrian WO Patent 2002090326, 2002 **2002**, 23.

399. Rami, Harshad Kantilal, Thompson, Mervyn, and Wyman, Paul Adrian WO Patent 2003022809, 2002 **2003**, 57.

400. Davis, John Beresford and Winchester, Wendy Joyce WO Patent 2004024154, 2003 **2004**, 17.

401. Bountra, Charanjit, Davis, John Beresford, Rami, Harshad Kantilal, and Thompson, Mervyn WO Patent 2004056394, 2003 **2004**, 58.

402. Bakthavatchatam, Rajagopal, Blum, Charles A., Brielmann, Harry L., Caldwell, Timothy M., and De Lombaert, Stephane WO Patent 2003062209, 2003 **2003**, 294.

403. Bakthavatchalam, Rajagopal, Blum, Charles A., Brielmann, Harry, Caldwell, Timothy M., De Lombaert, Stephane, Hodgetts, Kevin J., and Zheng, Xiaozhang WO Patent 2004055004, 2003 **2004**, 113.

404. Bakthavatchalam, Rajagopal, Blum, Charles A., Brielmann, Harry, Caldwell, Timothy M., De Lombaert, Stephane, Hodgetts, Kevin J., and Zheng, Xiaozhang WO Patent 2004055003, 2003 **2004**, 226.

405. Culshaw, Andrew James, Dziadulewicz, Edward Karol, Hallett, Allan, and Hart, Terance William WO Patent 2004033435, 2003 **2004**, 40.

406. Doherty, E. M.; Fotsch, C.; Bo, Y.; Chakrabarti, P. P.; Chen, N.; Gavva, N.; Han, N.; Kelly, M. G.; Kincaid, J.; Klionsky, L.; Liu, Q.; Ognyanov, V. I.; Tamir, R.; Wang, X.; Zhu, J.; Norman, M. H.; Treanor, J. J. S. *J.Med.Chem.* ACS.

407. Bo, Yunxin Y., Chakrabarti, Partha P., Chen, Ning, Doherty, Elizabeth M., Fotsch, Christopher H., Han, Nianhe, Kelly, Michael G., Liu, Qingyian, Norman, Mark Henry, Wang, Xianghong, Zhu, Jiawang, and Ognyanov, Vassil WO Patent 2003049702, 2002 **2003**, 611.

408. Gunthorpe, M. J.; Rami, H. K.; Jerman, J. C.; Smart, D.; Gill, C. H.; Soffin, E. M.; Hannan, S. L.; Lappin, S. C.; Egerton, J.; Smith, G. D.; Worby, A.; Howett, L.; Owen, D.; Nasir, S.; Davies, C. H.; Thompson, M.; Wyman, P. A.; Randall, A. D.; Davis, J. B. *Neuropharmacology* **2004**, *46*, 133-149.

409. Gunthorpe, M. J.; Rami, H. K.; Jerman, J. C.; Smart, D.; Gill, C. H.; Soffin, E. M.; Hannan, S. L.; Lappin, S. C.; Egerton, J.; Smith, G. D.; Worby, A.; Howett, L.; Owen, D.; Nasir, S.; Davies, C. H.; Thompson, M.; Wyman, P. A.; Randall, A. D.; Davis, J. B. *Neuropharmacology* **2004**, *46*, 905.

410. Tafesse, L.; Sun, Q.; Schmid, L.; Valenzano, K. J.; Rotshteyn, Y.; Su, X.; Kyle, D. J. *Bioorg.Med.Chem.Lett.* **2004**, *14*, 5513-5519.

411. Eliel, E. L.; Wilen, S. H.; Mander, L. N. *Stereochemistry of Organic Compounds*; John Wiley and Sons, Inc.: New York, 1994; Chapter 3, pp 49-70.

412. Cahn, R. S.; Ingold, C.; Prelog, V. *Angew.Chem., Intern.Ed.Engl.* **1966**, *5*, 385-415.

413. Prelog, V.; Helmchen, G. *Angew.Chem.Int.Ed.Engl.* **1982**, *21* , 567-583.

414. Eliel, E. L.; Wilen, S. H.; Mander, L. N. *Stereochemistry of Organic Compounds*; John Wiley and Sons, Inc.: New York, 1994; Chapter 5, pp 101-152.

415. Pictet, A.; Spengler, T. *Chem.Ber.* **1911**, *44*, 2030-2036.

416. Rozwadowska, M. D. *Heterocycles* **1994**, *39*, 903-931.

417. Chrzanowska, M.; Rozwadowska, M. D. *Chemical Reviews (Washington, DC, United States)* **2004**, *104*, 3341-3370.

418. Bischler, A.; Napieralski, B. *Chem.Ber.* **1893**, *26*, 1903-1908.

419. Pomeranz, C. *Monatshefte fur Chemie* **1893**, *14*, 116-119.

420. Fritsch, P. *Chem.Ber.* **1893**, *26*, 419-422.

421. Fritsch, P. *Liebigs Ann.Chem.* **1895**, *286*, 1-26.

422. Pomeranz, C. *Monatshefte fur Chemie* **1894**, *15*, 299-306.

423. Pomeranz, C. *Monatshefte fur Chemie* **1897**, *18*, 1-5.

424. Bobbitt, J. M.; Kiely, J. M.; Khanna, K. L.; Ebermann, R. *J.Org.Chem.* **1965**, *30*, 2247-2250.

425. Whaley, W. M.; Govindachari, T. R. *Organic Reactions (New York)* **1951**, *VI*, 74-150.

426. Whaley, W. M.; Govindachari, T. R. *Organic Reactions (New York)* **1951**, *VI*, 151-190.

427. Gensler, W. J. *Organic Reactions (New York)* **1951**, *VI*, 191-206.

428. Berger, U.; Dannhardt, G.; Wiegrebe, W. *Archiv der Pharmazie (Weinheim, Germany)* **1983**, *316*, 182-189.

429. Schlittler, E.; Muller, J. *Helv.Chim.Acta* **1948**, *31*, 914-924.

430. Bobbitt, J. M.; Khanna, K. L.; Kiely, J. M. *Chemistry & Industry (London, United Kingdom)* **1964**, 1950-1951.

431. Henry, T. A. *The Plant Alkaloids*; J & A Churchill Ltd.: London, 1949, pp 154-328.

432. Lundstrom, J. *The Alkaloids*; Academic Press: New York, 1983; Chapter 6, pp 255-327.

433. Bringmann, G. *The Alkaloids*; Academic Press, Inc.: Orlando, Florida, 1986; Chapter 3, pp 141-184.

434. Brossi, A.; Focella, A.; Teitel, S. *Helv.Chim.Acta* **1972**, *55*, 15-21.

435. Teitel, S.; O'Brien, J.; Brossi, A. *J.Med.Chem.* **1972**, *15*, 845-846.

436. Brossi, A.; Focella, A.; Teitel, S. *J.Med.Chem.* **1973**, *16*, 418-420.

437. Teitel, S.; O'Brien, J.; Pool, W.; Brossi, A. *J.Med.Chem.* **1974**, *17*, 134-137.

438. Collins, M. A. *The Alkaloids*; Academic Press: New York, 1983; Chapter 7, pp 329-358.

439. Bembenek, M. E.; Abell, C. W.; Chrisey, L. A.; Rozwadowska, M. D.; Gessner, W.; Brossi, A. *J.Med.Chem.* **1990**, *33*, 147-152.

440. Craig, P. N.; Nabenhauer, F. P.; Williams, P. M.; Macko, E.; Toner, J. *J.Am.Chem.Soc.* **1952**, *74*, 1316-1317.

441. Kaufman, T. S. *Tetrahedron: Asymmetry* **2004**, *15*, 1203-1237.

442. Spath, E.; Dengel, F. *Ber.* **1938**, *71B*, 114-119.

443. Polniaszek, R. P.; Kaufman, C. R. *J.Am.Chem.Soc.* **1989**, *111*, 4859-4863.

444. Schoenenberger, B.; Brossi, A. *Helv.Chim.Acta* **1986**, *69*, 1486-1497.

445. Bringmann, G.; Geisler, J. P. *Synthesis* **1989**, 608-610.

446. Nordlander, J. E.; Payne, M. J.; Njoroge, F. G.; Balk, M. A.; Laikos, G. D.; Vishwanath, V. M. *J.Org.Chem.* **1984**, *49*, 4107-4111.

447. Curphey, T. J. *J.Org.Chem.* **1979**, *44*, 2805-2807.

448. West, C. T.; Donnelly, S. J.; Kooistra, D. A.; Doyle, M. P. *J.Org.Chem.* **1973**, *38*, 2675-2681.

449. Nordlander, J. E.; Njoroge, F. G.; Payne, M. J.; Warman, D. *J.Org.Chem.* **1985**, *50*, 3481-3484.

450. Jones, J. *Amino Acid and Peptide Synthesis*; Oxford University Press: Oxford, 1992.

451. Sykes, P. *A Guidebook to Mechanism in Organic Chemistry*; Longman: London, 1986.

452. Buckley, T. F., III; Rapoport, H. *J.Am.Chem.Soc.* **1981**, *103*, 6157-6163.

453. McClure, D. E.; Arison, B. H.; Jones, J. H.; Baldwin, J. J. *J.Org.Chem.* **1981**, *46*, 2431-2433.

454. Weinges, K.; Graab, G. *Chemiker-Zeitung, Chemische Apparatur* **1970**, *94*, 728.

455. Schrecker, A. W. *J.Org.Chem.* **1957**, *22*, 33-35.

456. Schrecker, A. W.; Hartwell, J. L. *J.Am.Chem.Soc.* **1957**, *79* , 3827-3831.

457. Beckett, A. H.; Kirk, G.; Sharpen, A. J. *Tetrahedron* **1965**, *21*, 1489-1493.

458. Beckett, A. H.; Casy, A. F. *Journal of the Chemical Society, Abstracts* **1955**, 900-904.

459. Eliel, E. L.; Wilen, S. H.; Mander, L. N. *Stereochemistry of Organic Compounds*; John Wiley & Sons, Inc.: New York, 1994; Chapter 7, pp 297-464.

460. Marfey, P. *Carlsberg Res.Commun.* **1984**, *49*, 591-596.

461. Marfey, P.; Ottesen, M. *Carlsberg Res.Commun.* **1984**, *49*, 585-590.

462. B'Hymer, C.; Montes-Bayon, M.; Caruso, J. A. *Journal of Separation Science* **2003**, *26*, 7-19.

463. Eliel, E. L.; Wilen, S. H. *Stereochemistry of Organic Compounds*; Wiley Interscience: New York, 1994; Chapter 6, pp 231-236.

464. Pirkle, W. H.; Hoover, D. J. *Topics in Stereochemistry* **1982**, *13*, 263-331.

465. Govindachari, T. R.; Parthasarathy, P. C. *Indian J.Chem.* **1970**, *8*, 567-569.

466. Bringmann, G.; Kinzinger, L.; Ortmann, T.; De Souza, N. J. *Phytochemistry* **1994**, *35*, 259-261.

467. Bringmann, G.; Jansen, J. R.; Rink, H. P. *Angewandte Chemie* **1986**, *98*, 917-919.

468. Bringmann, G.; Weirich, R.; Reuscher, H.; Jansen, J. R.; Kinzinger, L.; Ortmann, T. *Liebigs Ann.Chem.* **1993**, 877-888.

469. Grunewald, G. L.; Caldwell, T. M.; Li, Q.; Criscione, K. R. *Bioorg.Med.Chem.* **1999**, *7*, 869-880.

470. Solladie, G. *Synthesis* **1981**, 185-196.

471. Lee, A. W. M.; Chan, W. H.; Tao, Y.; Lee, Y. K. *Journal of the Chemical Society, Perkin Transactions 1: Organic and Bio-Organic Chemistry (1972-1999)* **1994**, 477-481.

472. Lee, A. W. M.; Chan, W. H.; Lee, Y. K. *Tetrahedron Lett.* **1991**, *32*, 6861-6864.

473. Andersen, K. K. *J.Org.Chem.* **1964**, *29*, 1953-1956.

474. Klunder, J. M.; Sharpless, K. B. *J.Org.Chem.* **1987**, *52*, 2598-2602.

475. Kosugi, H.; Kitaoka, M.; Tagami, K.; Takahashi, A.; Uda, H. *J.Org.Chem.* **1987**, *52*, 1078-1082.

476. Evans, D. A.; Faul, M. M.; Colombo, L.; Bisaha, J. J.; Clardy, J.; Cherry, D. *J.Am.Chem.Soc.* **1992**, *114*, 5977-5985.

477. Evans, D. A.; Mathre, D. J.; Scott, W. L. *J.Org.Chem.* **1985**, *50*, 1830-1835.

478. Gage, J. R.; Evans, D. A. *Org.Synth.* **1990**, *68*, 77-82.

479. Youn, J. H.; Herrmann, R. *Tetrahedron Lett.* **1986**, *27*, 1493-1494.

480. Dominguez, E.; Lete, E.; Badia, M. D.; Villa, M. J.; Castedo, L.; Dominguez, D. *Tetrahedron* **1987**, *43*, 1943-1948.

481. Eliel, E. L.; Wilen, S. H.; Mander, L. N. *Stereochemistry of Organic Compounds*; John Wiley and Sons, Inc.: New York, 1994; Chapter 11, p 727.

482. Anakabe, E.; Badia, D.; Carrillo, L.; Vicario, J. L. *Recent Research Developments in Organic Chemistry* **2001**, *5*, 63-75.

483. Waykole, L.; Paquette, L. A. *Org.Synth.* **1989**, *67*, 149-156.

484. Cossu, S.; De Lucchi, O.; Durr, R. *Synth.Commun.* **1996**, *26* , 4597-4601.

485. Davis, A. P.; Whitham, G. H. *Journal of the Chemical Society, Chemical Communications* **1980**, 639-640.

486. Chan, W.; Lee, A. W. M.; Jiang, L. *Tetrahedron Lett.* **1995**, *36*, 715-718.

487. Williams, D. H.; Fleming, I. *Spectroscopic Methods in Organic Chemistry*; McGraw-Hill: Maidenhead, Berkshire, 1995.

488. Trost, B. M.; Weber, L.; Strege, P.; Fullerton, T. J.; Dietsche, T. J. *J.Am.Chem.Soc.* **1978**, *100*, 3426-3435.

489. Clayton, S. C.; Regan, A. C. *Tetrahedron Lett.* **1993**, *34*, 7493-7496.

490. Otten, A.; Namyslo, J. C.; Stoermer, M.; Kaufmann, D. E. *European Journal of Organic Chemistry* **1998**, 1997-2001.

491. Giblin, G. M. P.; Jones, C. D.; Simpkins, N. S. *Journal of the Chemical Society, Perkin Transactions 1: Organic and Bio-Organic Chemistry* **1998**, 3689-3698.

492. Lee, G. H.; Choi, E. B.; Lee, E.; Pak, C. S. *Tetrahedron Lett.* **1993**, *34*, 4541-4542.

493. Pascali, V.; Umani-Ronchi, A. *Journal of the Chemical Society, Chemical Communications* **1973**, 351.

494. Bremner, J.; Julia, M.; Launay, M.; Stacino, J. P. *Tetrahedron Lett.* **1982**, *23*, 3265-3266.

495. Keck, G. E.; Savin, K. A.; Weglarz, M. A. *J.Org.Chem.* **1995**, *60*, 3194-3204.

496. Bucher, C. B.; Heimgartner, H. *Helv.Chim.Acta* **1996**, *79*, 1903-1915.

497. Fieser, M.; Fieser, L. F. *Reagents for Organic Synthesis, Vol. 2*; Wiley-Interscience: New York, 1969; p 288.

498. Trost, B. M.; Cossy, J.; Burks, J. *J.Am.Chem.Soc.* **1983**, *105*, 1052-1054.

499. Yu, J.; Cho, H. S.; Chandrasekhar, S.; Falck, J. R.; Mioskowski, C. *Tetrahedron Lett.* **1994**, *35*, 5437-5440.

500. Klyne, W.; Prelog, V. *Experientia* **1960**, *16*, 521-523.

501. Hore, P. *Nuclear Magnetic Resonance*; Oxford University Press: Oxford, 1995; Chapter 2, pp 8-21.

502. Hoye, T. R.; Chen, M. *Tetrahedron Lett.* **1996**, *37*, 3099-3100.

503. Abdel-Magid, A. F.; Carson, K. G.; Harris, B. D.; Maryanoff, C. A.; Shah, R. D. *J.Org.Chem.* **1996**, *61*, 3849-3862.

504. Gottlieb, H. E.; Kotlyar, V.; Nudelman, A. *J.Org.Chem.* **1997**, *62*, 7512-7515.

505. Eliel, E. L.; Wilen, S. H.; Mander, L. N. John Wiley and Sons, Inc.: New York, 1994; Chapter 1, pp 1-10.

506. Olefirowicz, E. M.; Eliel, E. L. *J.Org.Chem.* **1997**, *62*, 9154-9158.

507. Gee, K. R.; Brown, K. A.; Chen, W.-N. U.; Bishop-Stewart, J.; Gray, D.; Johnson, I. *Cell Calcium* **2000**, *27*, 97-106.

508. Grynkiewicz, G.; Poenie, M.; Tsien, R. Y. *J.Biol.Chem.* **1985**, *260*, 3440-3450.

509. http:; bloch.anu.edu.au/hmbc.html. Australian National University NMR Centre . 2005.
Ref Type: Electronic Citation

510. Dumpis, M. A.; Kudryashova, N. I.; Veresova, M. A. *J.Org.Chem.USSR (Engl.Transl.)* **1989**, *25*, 1332-1337.

APPENDIX 1: X-ray crystal co-ordinate data

(*R*)-2-((*S*)-1-phenylethyl)carbamoyl-6,7-dimethoxy-1-methyl-1,2,3,4-tetrahydroisoquinoline, 71(1*R*,α*S*)

Table 1. Bond Lengths (Å) and Angles (°)

O(1)-C(15)	1.231(2)	O(2)-C(11)	1.374(2)
O(2)-C(25)	1.418(2)	O(3)-C(10)	1.371(2)
O(3)-C(26)	1.422(2)	N(4)-C(15)	1.362(2)
N(4)-C(6)	1.461(2)	N(4)-C(14)	1.460(2)
N(5)-C(15)	1.368(2)	N(5)-C(16)	1.455(2)
C(6)-C(7)	1.504(2)	C(7)-C(8)	1.517(2)
C(8)-C(13)	1.384(2)	C(8)-C(9)	1.398(2)
C(9)-C(10)	1.378(2)	C(10)-C(11)	1.406(2)
C(11)-C(12)	1.379(2)	C(12)-C(13)	1.406(2)
C(13)-C(14)	1.526(2)	C(14)-C(23)	1.528(2)
C(16)-C(17)	1.519(2)	C(16)-C(24)	1.529(2)
C(17)-C(18)	1.381(2)	C(17)-C(22)	1.397(2)
C(18)-C(19)	1.390(2)	C(19)-C(20)	1.374(3)
C(20)-C(21)	1.372(3)	C(21)-C(22)	1.386(3)

C(11)-O(2)-C(25)	116.5(1)	C(10)-O(3)-C(26)	116.3(1)
C(15)-N(4)-C(6)	118.8(1)	C(15)-N(4)-C(14)	126.6(1)
C(6)-N(4)-C(14)	114.5(1)	C(15)-N(5)-C(16)	120.3(1)
N(4)-C(6)-C(7)	109.6(1)	C(6)-C(7)-C(8)	110.4(1)
C(13)-C(8)-C(9)	119.1(1)	C(13)-C(8)-C(7)	121.3(1)
C(9)-C(8)-C(7)	119.5(1)	C(10)-C(9)-C(8)	121.5(1)
O(3)-C(10)-C(9)	124.6(1)	O(3)-C(10)-C(11)	116.0(1)
C(9)-C(10)-C(11)	119.4(1)	O(2)-C(11)-C(12)	124.9(1)
O(2)-C(11)-C(10)	115.9(1)	C(12)-C(11)-C(10)	119.2(1)
C(11)-C(12)-C(13)	121.2(1)	C(8)-C(13)-C(12)	119.4(1)
C(8)-C(13)-C(14)	122.4(1)	C(12)-C(13)-C(14)	118.2(1)
N(4)-C(14)-C(13)	110.0(1)	N(4)-C(14)-C(23)	111.0(1)
C(13)-C(14)-C(23)	112.2(1)	O(1)-C(15)-N(4)	121.7(1)
O(1)-C(15)-N(5)	120.6(1)	N(4)-C(15)-N(5)	117.7(1)
N(5)-C(16)-C(17)	113.8(1)	N(5)-C(16)-C(24)	108.5(1)
C(17)-C(16)-C(24)	111.1(1)	C(18)-C(17)-C(22)	117.7(1)
C(18)-C(17)-C(16)	123.4(1)	C(22)-C(17)-C(16)	118.9(1)
C(17)-C(18)-C(19)	121.2(2)	C(20)-C(19)-C(18)	120.3(2)
C(19)-C(20)-C(21)	119.4(2)	C(22)-C(21)-C(20)	120.6(2)
C(21)-C(22)-C(17)	120.8(2)		

Table 2. Atomic Coordinates

atom	x	y	z	U(eq)
O(1)	.0035(2)	.4612(1)	.78491(5)	.0611(3)
O(2)	.0156(2)	1.0006(1)	1.04133(4)	.0581(3)
O(3)	.3054(2)	1.0726(1)	.98911(5)	.0616(3)
N(4)	-.0564(2)	.6268(1)	.84364(5)	.0493(3)
N(5)	-.1233(2)	.4145(1)	.86822(5)	.0510(3)
C(6)	.0177(2)	.7194(2)	.80386(6)	.0508(3)
C(7)	.1788(2)	.7841(2)	.82910(6)	.0521(3)
C(8)	.1355(2)	.8333(1)	.88730(5)	.0445(3)
C(9)	.2455(2)	.9264(2)	.91180(6)	.0482(3)
C(10)	.2061(2)	.9789(1)	.96330(6)	.0471(3)
C(11)	.0512(2)	.9384(1)	.99186(6)	.0468(3)
C(12)	-.0537(2)	.8430(1)	.96883(6)	.0464(3)
C(13)	-.0123(2)	.7890(1)	.91649(5)	.0424(3)
C(14)	-.1357(2)	.6845(1)	.89350(6)	.0450(3)
C(15)	-.0569(2)	.4996(1)	.82980(6)	.0434(3)
C(16)	-.1278(2)	.2775(1)	.85585(7)	.0482(3)
C(17)	-.3024(2)	.2329(1)	.82952(6)	.0443(3)
C(18)	-.4504(2)	.3113(2)	.82328(7)	.0541(3)
C(19)	-.6091(2)	.2646(2)	.8006(1)	.0661(4)
C(20)	-.6211(3)	.1388(2)	.78333(8)	.0692(5)
C(21)	-.4742(3)	.0602(2)	.78795(8)	.0655(4)
C(22)	-.3159(2)	.1059(2)	.81082(7)	.0545(3)
C(23)	-.3239(2)	.7352(2)	.88127(8)	.0615(4)
C(24)	-.0885(3)	.2034(2)	.9097(1)	.0676(5)
C(25)	-.1610(3)	.9884(2)	1.06259(8)	.0705(5)
C(26)	.4509(3)	1.1240(3)	.9578(1)	.0783(6)

U(eq) is defined as 1/3 the trace of the Uij tensor.

2. (1*R*,3*S*)-6,7-dimethoxy-3-methyl-1-(toluene-4-sulfonylmethyl)-1,2,3,4-tetrahydroisoquinoline hydrochloride 159(1*R*,3*S*),

Table 1. Bond lengths (Å)

molecule A		molecule B	
S(1)-O(2)	1.426(3)	S(31)-O(32)	1.430(3)
S(1)-O(3)	1.430(4)	S(31)-O(33)	1.440(3)
S(1)-C(17)	1.766(3)	S(31)-C(47)	1.770(3)
S(1)-C(16)	1.774(3)	S(31)-C(46)	1.785(3)
O(4)-C(12)	1.367(4)	O(34)-C(42)	1.363(5)
O(4)-C(23)	1.420(4)	O(34)-C(53)	1.417(6)
O(5)-C(11)	1.366(4)	O(35)-C(41)	1.369(4)
O(5)-C(24)	1.411(5)	O(35)-C(54)	1.404(6)
N(6)-C(15)	1.453(4)	N(36)-C(45)	1.455(4)
N(6)-C(7)	1.487(5)	N(36)-C(37)	1.478(5)
C(7)-C(25)	1.510(5)	C(37)-C(55)	1.503(5)
C(7)-C(8)	1.511(5)	C(37)-C(38)	1.519(5)
C(8)-C(9)	1.504(4)	C(38)-C(39)	1.511(5)
C(9)-C(14)	1.377(4)	C(39)-C(44)	1.384(4)
C(9)-C(10)	1.415(4)	C(39)-C(40)	1.399(5)
C(10)-C(11)	1.371(4)	C(40)-C(41)	1.356(6)
C(11)-C(12)	1.405(4)	C(41)-C(42)	1.403(5)
C(12)-C(13)	1.383(4)	C(42)-C(43)	1.382(5)
C(13)-C(14)	1.402(4)	C(43)-C(44)	1.392(5)
C(14)-C(15)	1.523(4)	C(44)-C(45)	1.526(4)
C(15)-C(16)	1.555(4)	C(45)-C(46)	1.553(4)
C(17)-C(18)	1.372(6)	C(47)-C(48)	1.370(4)
C(17)-C(22)	1.383(4)	C(47)-C(52)	1.383(4)
C(18)-C(19)	1.365(7)	C(48)-C(49)	1.384(5)
C(19)-C(20)	1.386(6)	C(49)-C(50)	1.378(6)
C(20)-C(21)	1.373(6)	C(50)-C(51)	1.394(6)
C(20)-C(26)	1.507(6)	C(50)-C(56)	1.505(6)
C(21)-C(22)	1.374(5)	C(51)-C(52)	1.384(5)

Table 2. Atomic coordinates (U(eq) is defined as 1/3 the trace of the Uij tensor)

atom	x	y	z	U(eq)
S(1)	.1006(1)	.23602(4)	.54114(5)	.0666(2)
O(2)	.3392(5)	.2355(2)	.5174(2)	.100(1)
O(3)	.0296(7)	.2820(1)	.5970(2)	.095(1)
O(4)	-.2153(4)	.1775(1)	.1138(2)	.0679(5)
O(5)	-.5818(4)	.2399(1)	.0678(2)	.0753(6)
N(6)	-.1062(6)	.3478(1)	.4235(2)	.0675(7)
C(7)	-.3656(7)	.3581(2)	.4250(2)	.0700(8)
C(8)	-.4658(7)	.3651(1)	.3318(2)	.0670(7)
C(9)	-.3936(5)	.3148(1)	.2761(2)	.0551(5)
C(10)	-.5285(5)	.3010(1)	.1975(2)	.0590(6)
C(11)	-.4632(5)	.2562(1)	.1447(2)	.0577(6)
C(12)	-.2617(5)	.2221(1)	.1696(2)	.0555(6)
C(13)	-.1285(5)	.2355(1)	.2462(2)	.0552(5)
C(14)	-.1956(5)	.2814(1)	.2999(2)	.0530(5)
C(15)	-.0509(5)	.2910(1)	.3863(2)	.0570(6)
C(16)	-.0928(5)	.2367(1)	.4447(2)	.0580(6)
C(17)	.0417(6)	.1670(2)	.5879(2)	.0607(6)
C(18)	.1928(8)	.1208(2)	.5765(4)	.093(1)
C(19)	.151(1)	.0680(2)	.6148(5)	.106(2)
C(20)	-.0448(8)	.0590(2)	.6618(3)	.076(1)
C(21)	-.1918(7)	.1062(2)	.6723(2)	.0710(8)
C(22)	-.1521(6)	.1604(2)	.6364(2)	.0657(7)
C(23)	-.0174(6)	.1409(2)	.1385(3)	.0718(8)
C(24)	-.7627(8)	.2778(2)	.0327(3)	.086(1)
C(25)	-.408(1)	.4117(2)	.4797(3)	.105(2)
C(26)	-.085(1)	.0003(2)	.7041(4)	.110(2)
S(31)	.5879(1)	.08375(3)	.90786(4)	.0546(2)
O(32)	.8353(4)	.0771(1)	.9333(2)	.0743(6)
O(33)	.4836(5)	.0451(1)	.8413(2)	.0758(6)
O(34)	.3445(7)	.0833(2)	1.3465(2)	.102(1)
O(35)	.0131(7)	.0071(2)	1.3577(2)	.100(1)
N(36)	.4534(5)	-.0370(1)	.9973(2)	.0670(6)
C(37)	.1984(6)	-.0496(1)	.9772(2)	.0676(7)
C(38)	.1018(6)	-.0688(1)	1.0618(3)	.0702(8)
C(39)	.1751(5)	-.0274(1)	1.1360(2)	.0614(6)
C(40)	.0575(6)	-.0297(2)	1.2123(2)	.0706(8)
C(41)	.1185(7)	.0062(2)	1.2808(2)	.075(1)
C(42)	.3016(6)	.0475(2)	1.2759(2)	.0707(8)
C(43)	.4207(6)	.0496(2)	1.2012(2)	.0637(7)
C(44)	.3590(5)	.0124(1)	1.1312(2)	.0559(6)
C(45)	.4936(5)	.0161(1)	1.0495(2)	.0573(6)
C(46)	.4285(5)	.0751(1)	1.0023(2)	.0516(5)
C(47)	.5402(5)	.1574(1)	.8727(2)	.0540(5)
C(48)	.7133(6)	.1987(2)	.8921(2)	.0685(7)
C(49)	.6821(8)	.2554(2)	.8601(3)	.083(1)
C(50)	.4811(8)	.2708(2)	.8085(3)	.081(1)
C(51)	.3068(7)	.2281(2)	.7903(2)	.077(1)
C(52)	.3341(6)	.1712(2)	.8223(2)	.0662(7)
C(53)	.529(1)	.1255(3)	1.3448(4)	.125(3)
C(54)	-.161(1)	-.0355(3)	1.3695(4)	.117(2)
C(55)	.166(1)	-.0960(2)	.9077(3)	.094(1)
C(56)	.451(2)	.3320(2)	.7714(5)	.133(3)

3. Benzyl-[(*S*)-2-(3,4-dimethoxy-phenyl)-1-methylethyl]-[(*E*)-2-(toluene-4-sulfonyl)-vinyl]-amine 157*S*:

Table 1. Bond Lengths (Å) and angles (°)

S(1)-O(2)	1.437(4)	S(1)-O(3)	1.445(4)
S(1)-C(13)	1.725(5)	S(1)-C(7)	1.777(5)
O(4)-C(27)	1.359(6)	O(4)-C(30)	1.437(7)
O(5)-C(26)	1.375(7)	O(5)-C(31)	1.404(7)
N(6)-C(14)	1.331(6)	N(6)-C(15)	1.455(6)
N(6)-C(22)	1.477(6)	C(7)-C(12)	1.385(7)
C(7)-C(8)	1.371(7)	C(8)-C(9)	1.369(8)
C(9)-C(10)	1.400(9)	C(10)-C(11)	1.372(8)
C(10)-C(32)	1.496(9)	C(11)-C(12)	1.371(7)
C(13)-C(14)	1.344(6)	C(15)-C(16)	1.511(7)
C(16)-C(21)	1.368(8)	C(16)-C(17)	1.376(7)
C(17)-C(18)	1.374(9)	C(18)-C(19)	1.353(9)
C(19)-C(20)	1.37(1)	C(20)-C(21)	1.382(9)
C(22)-C(23)	1.530(7)	C(22)-C(33)	1.526(7)
C(23)-C(24)	1.496(7)	C(24)-C(29)	1.374(7)
C(24)-C(25)	1.388(7)	C(25)-C(26)	1.382(7)
C(26)-C(27)	1.404(7)	C(27)-C(28)	1.388(8)
C(28)-C(29)	1.383(8)		

O(2)-S(1)-O(3)	118.6(3)	O(2)-S(1)-C(13)	109.3(2)
O(3)-S(1)-C(13)	107.5(3)	O(2)-S(1)-C(7)	106.5(2)
O(3)-S(1)-C(7)	105.7(2)	C(13)-S(1)-C(7)	108.8(2)
C(27)-O(4)-C(30)	116.8(5)	C(26)-O(5)-C(31)	117.4(4)
C(14)-N(6)-C(15)	119.9(4)	C(14)-N(6)-C(22)	119.8(4)
C(15)-N(6)-C(22)	118.6(4)	C(12)-C(7)-C(8)	119.5(5)
C(12)-C(7)-S(1)	119.5(4)	C(8)-C(7)-S(1)	121.1(4)
C(7)-C(8)-C(9)	120.9(5)	C(8)-C(9)-C(10)	120.8(5)
C(11)-C(10)-C(9)	117.0(5)	C(11)-C(10)-C(32)	122.6(6)
C(9)-C(10)-C(32)	120.4(6)	C(10)-C(11)-C(12)	123.0(5)
C(7)-C(12)-C(11)	118.9(5)	C(14)-C(13)-S(1)	119.0(4)
C(13)-C(14)-N(6)	127.7(5)	N(6)-C(15)-C(16)	115.8(4)
C(21)-C(16)-C(17)	118.3(5)	C(21)-C(16)-C(15)	122.9(5)
C(17)-C(16)-C(15)	118.7(5)	C(16)-C(17)-C(18)	121.2(6)
C(19)-C(18)-C(17)	120.2(6)	C(18)-C(19)-C(20)	119.6(6)
C(21)-C(20)-C(19)	120.3(7)	C(16)-C(21)-C(20)	120.4(6)
N(6)-C(22)-C(23)	111.1(4)	N(6)-C(22)-C(33)	111.5(4)
C(23)-C(22)-C(33)	113.1(4)	C(24)-C(23)-C(22)	113.8(4)
C(29)-C(24)-C(25)	117.8(5)	C(29)-C(24)-C(23)	122.1(5)
C(25)-C(24)-C(23)	120.0(5)	C(26)-C(25)-C(24)	121.8(5)
O(5)-C(26)-C(25)	124.2(5)	O(5)-C(26)-C(27)	115.9(5)
C(25)-C(26)-C(27)	119.9(5)	O(4)-C(27)-C(28)	125.8(5)
O(4)-C(27)-C(26)	116.0(5)	C(28)-C(27)-C(26)	118.1(5)
C(29)-C(28)-C(27)	120.8(5)	C(24)-C(29)-C(28)	121.6(5)

Table 2. Atomic coordinates and equivalent isotropic displacement parameters ($Å^2$)

atom	x	y	z	U(eq)
S(1)	-.0001(2)	.2364(1)	.24502(6)	.0659(4)
O(2)	.1071(4)	.3197(3)	.2592(2)	.084(1)
O(3)	.0541(6)	.1687(3)	.2018(2)	.091(1)
O(4)	-.2862(6)	.2809(3)	.4658(2)	.079(1)
O(5)	-.1014(6)	.4318(3)	.4338(2)	.079(1)
N(6)	-.3759(5)	.4268(3)	.2237(2)	.052(1)
C(7)	-.0186(6)	.1615(4)	.3055(2)	.058(1)
C(8)	.010(1)	.2015(4)	.3569(2)	.077(2)
C(9)	.002(1)	.1426(5)	.4032(2)	.087(2)
C(10)	-.0376(8)	.0403(5)	.3993(2)	.074(2)
C(11)	-.0668(7)	.0026(4)	.3474(3)	.071(1)
C(12)	-.0586(7)	.0605(4)	.3006(2)	.063(1)
C(13)	-.1976(7)	.2808(4)	.2272(2)	.062(1)
C(14)	-.2356(6)	.3775(3)	.2374(2)	.051(1)
C(15)	-.5198(7)	.3720(4)	.2014(2)	.055(1)
C(16)	-.5077(7)	.3436(3)	.1411(2)	.057(1)
C(17)	-.6105(8)	.2683(4)	.1214(2)	.075(2)
C(18)	-.608(1)	.2413(5)	.0666(3)	.100(2)
C(19)	-.507(1)	.2909(6)	.0306(3)	.112(3)
C(20)	-.406(1)	.3669(7)	.0492(3)	.113(3)
C(21)	-.403(1)	.3919(5)	.1047(2)	.088(2)
C(22)	-.4020(6)	.5307(3)	.2435(2)	.058(1)
C(23)	-.5204(8)	.5329(4)	.2934(2)	.067(1)
C(24)	-.4658(7)	.4659(4)	.3398(2)	.057(1)
C(25)	-.3126(7)	.4829(4)	.3661(2)	.059(1)
C(26)	-.2540(7)	.4201(4)	.4074(2)	.059(1)
C(27)	-.3517(8)	.3376(4)	.4243(2)	.064(1)
C(28)	-.5051(8)	.3212(4)	.3980(2)	.070(1)
C(29)	-.5592(7)	.3839(4)	.3560(2)	.068(1)
C(30)	-.370(1)	.1873(5)	.4775(3)	.096(2)
C(31)	.013(1)	.5017(5)	.4114(3)	.091(2)
C(32)	-.049(1)	-.0232(6)	.4502(3)	.116(3)
C(33)	-.459(1)	.5999(4)	.1968(2)	.076(2)

U(eq) is defined as 1/3 the trace of the Uij tensor.

APPENDIX 2: ^{1}H-NMR spectra for the resolved stereoisomers of 29, 30 and 31

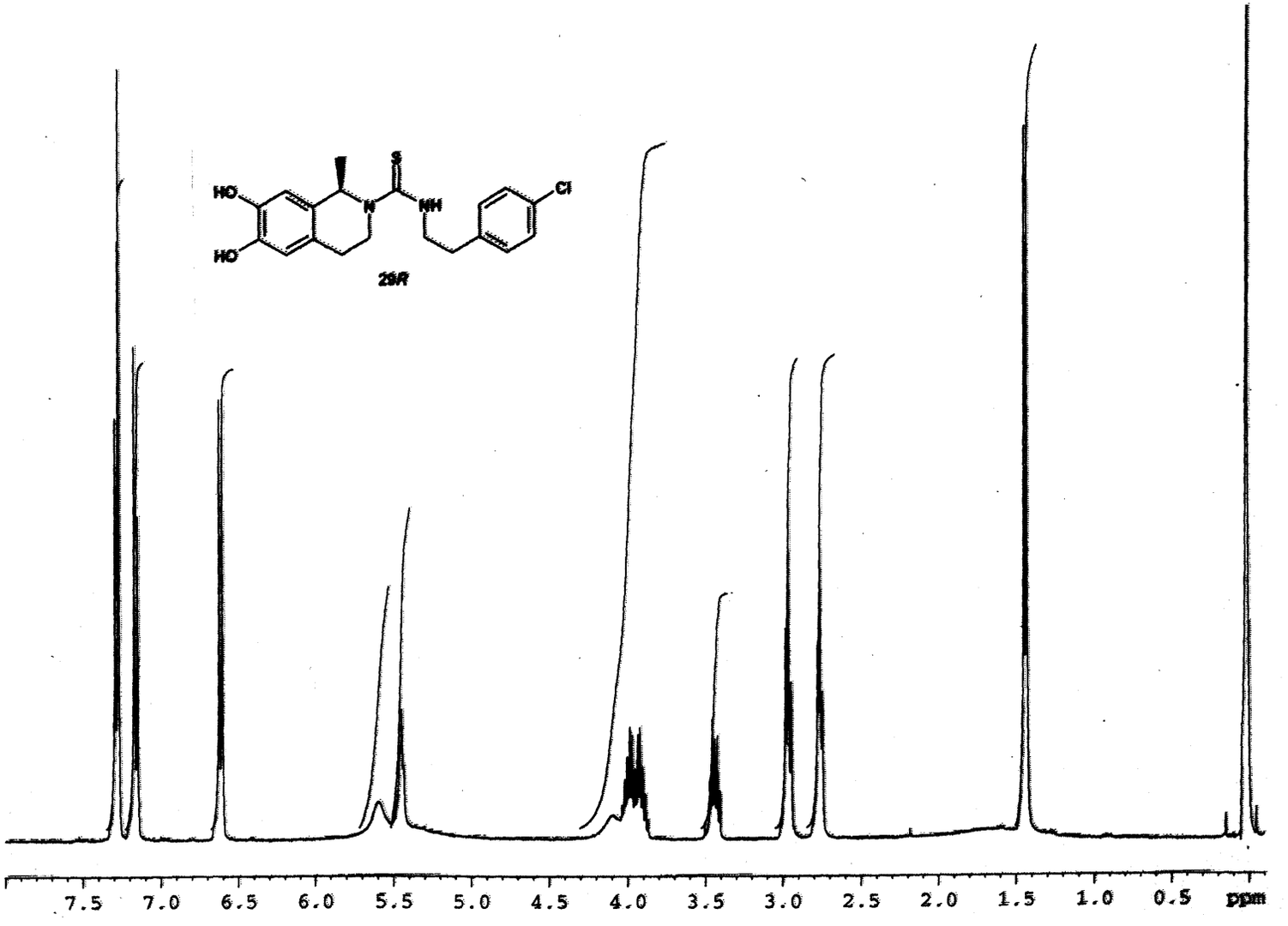
HO
HO
N
S
NH
Cl
2S/R
7.5
7.0
6.5
6.0
5.5
5.0
4.5
4.0
3.5
3.0
2.5
2.0
1.5
1.0
0.5
ppm

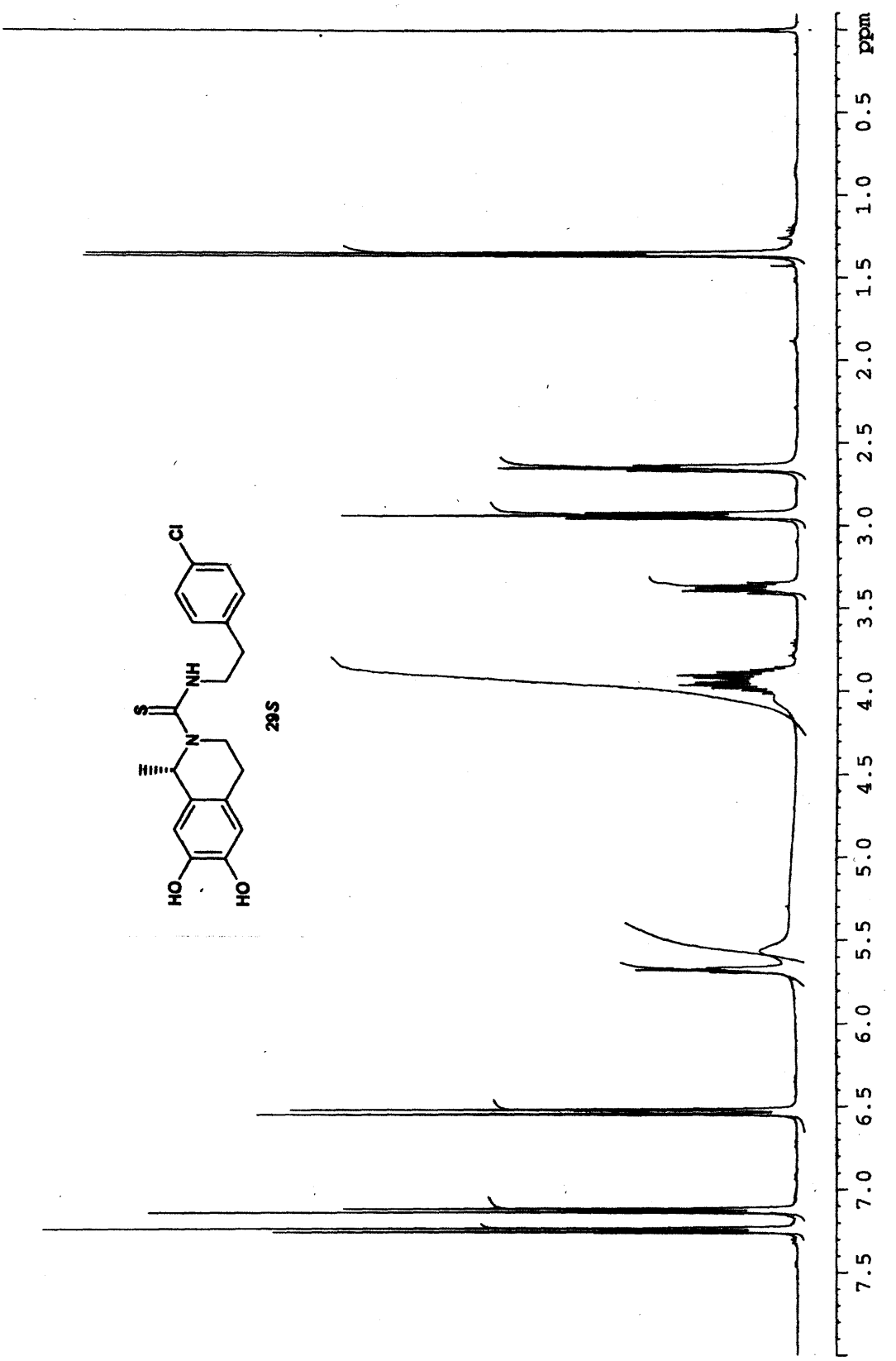
Cl
NH
S
N
HO
HO
29S
7.5
7.0
6.5
6.0
5.5
5.0
4.5
4.0
3.5
3.0
2.5
2.0
1.5
1.0
0.5
ppm

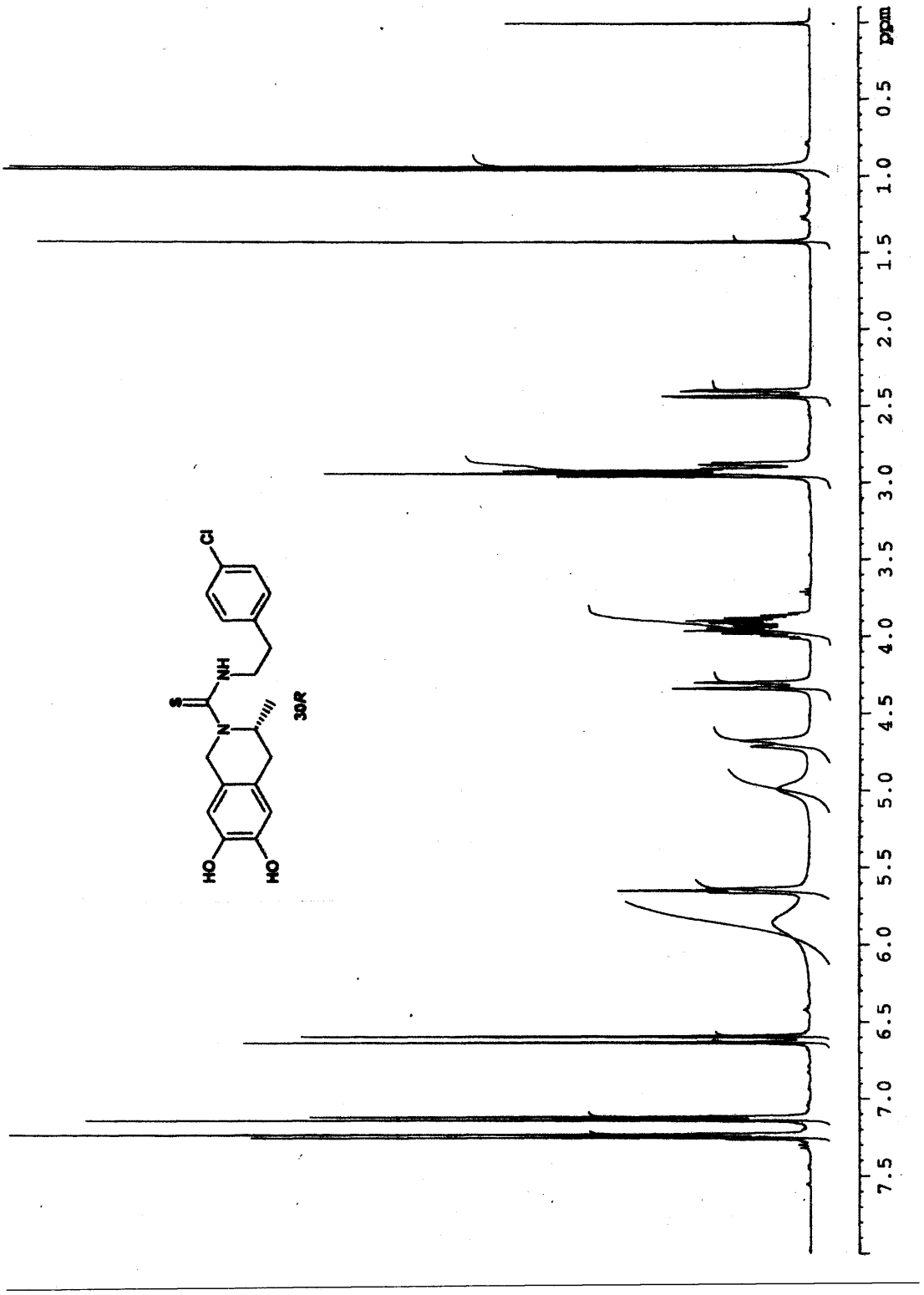
Cl
NH
S
N
HO
HO
30R
7.5
7.0
6.5
6.0
5.5
5.0
4.5
4.0
3.5
3.0
2.5
2.0
1.5
1.0
0.5
ppm

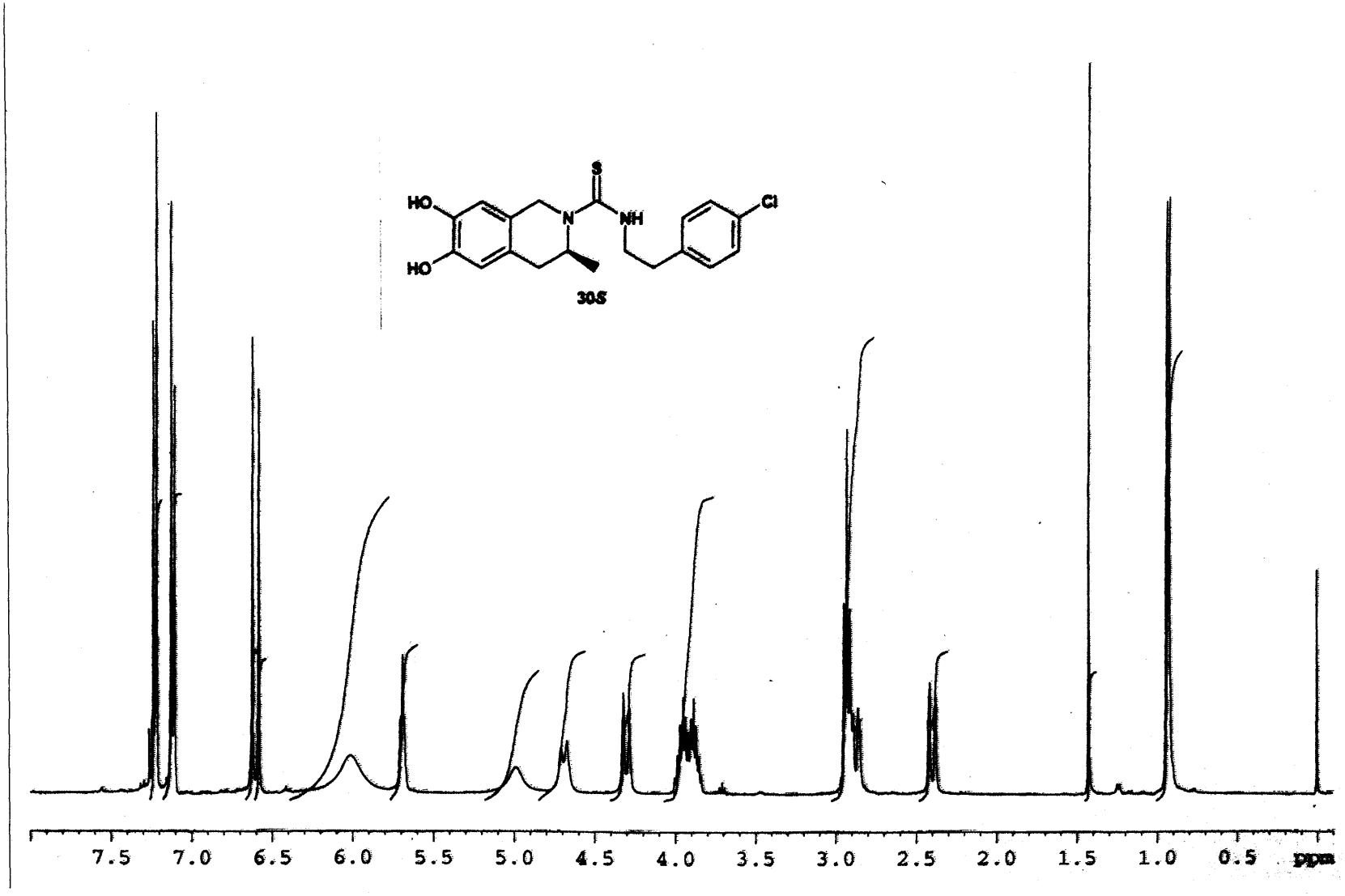
HO
HO
N
S
NH
Cl
30S
7.5
7.0
6.5
6.0
5.5
5.0
4.5
4.0
3.5
3.0
2.5
2.0
1.5
1.0
0.5
ppm

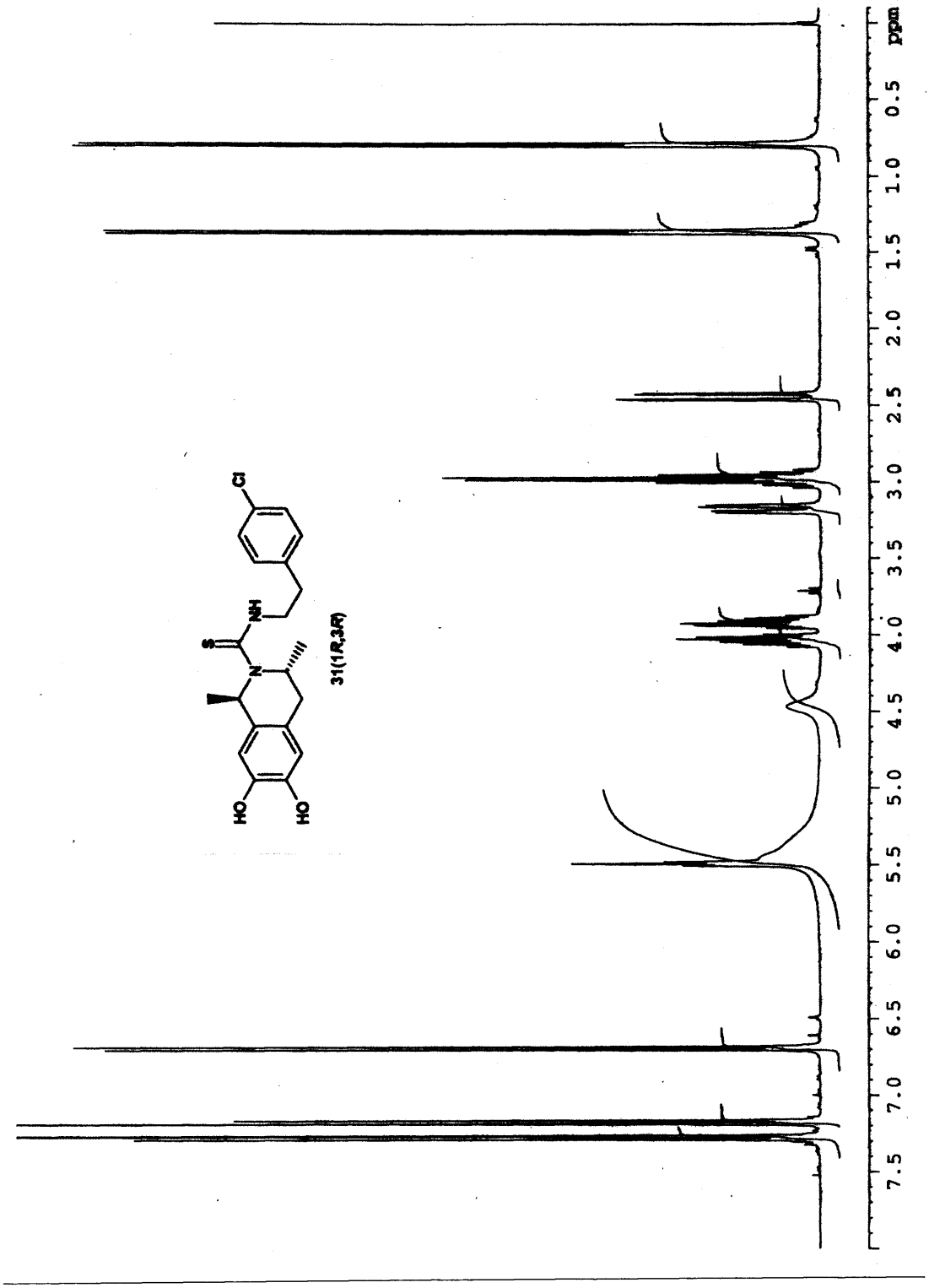
Cl
NH
S
N
HO
HO
31(1R,3R)
7.5
7.0
6.5
6.0
5.5
5.0
4.5
4.0
3.5
3.0
2.5
2.0
1.5
1.0
0.5
ppm

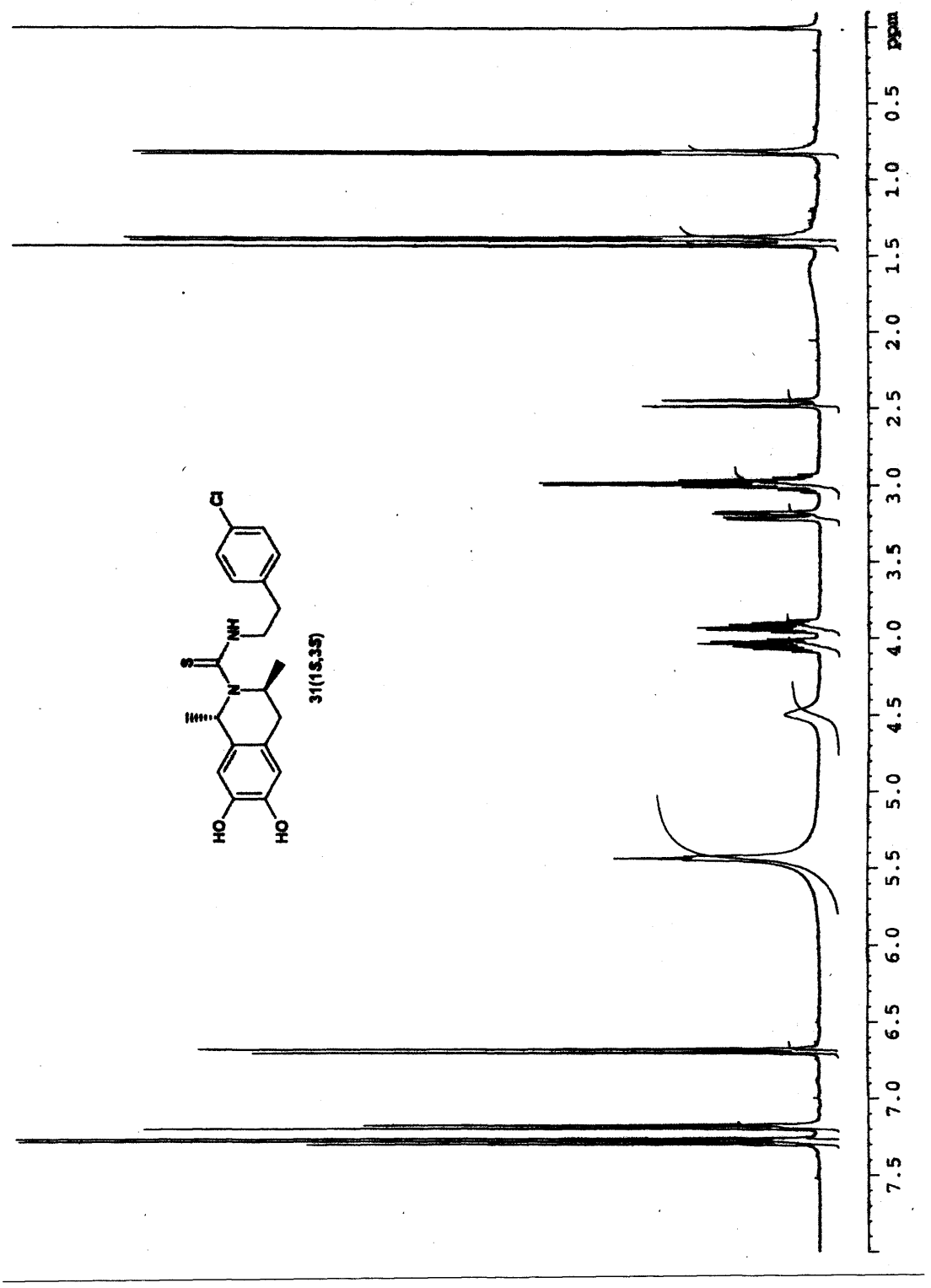
Cl
NH
S
N
HO
HO
31(1S,3S)
7.5
7.0
6.5
6.0
5.5
5.0
4.5
4.0
3.5
3.0
2.5
2.0
1.5
1.0
0.5
ppm

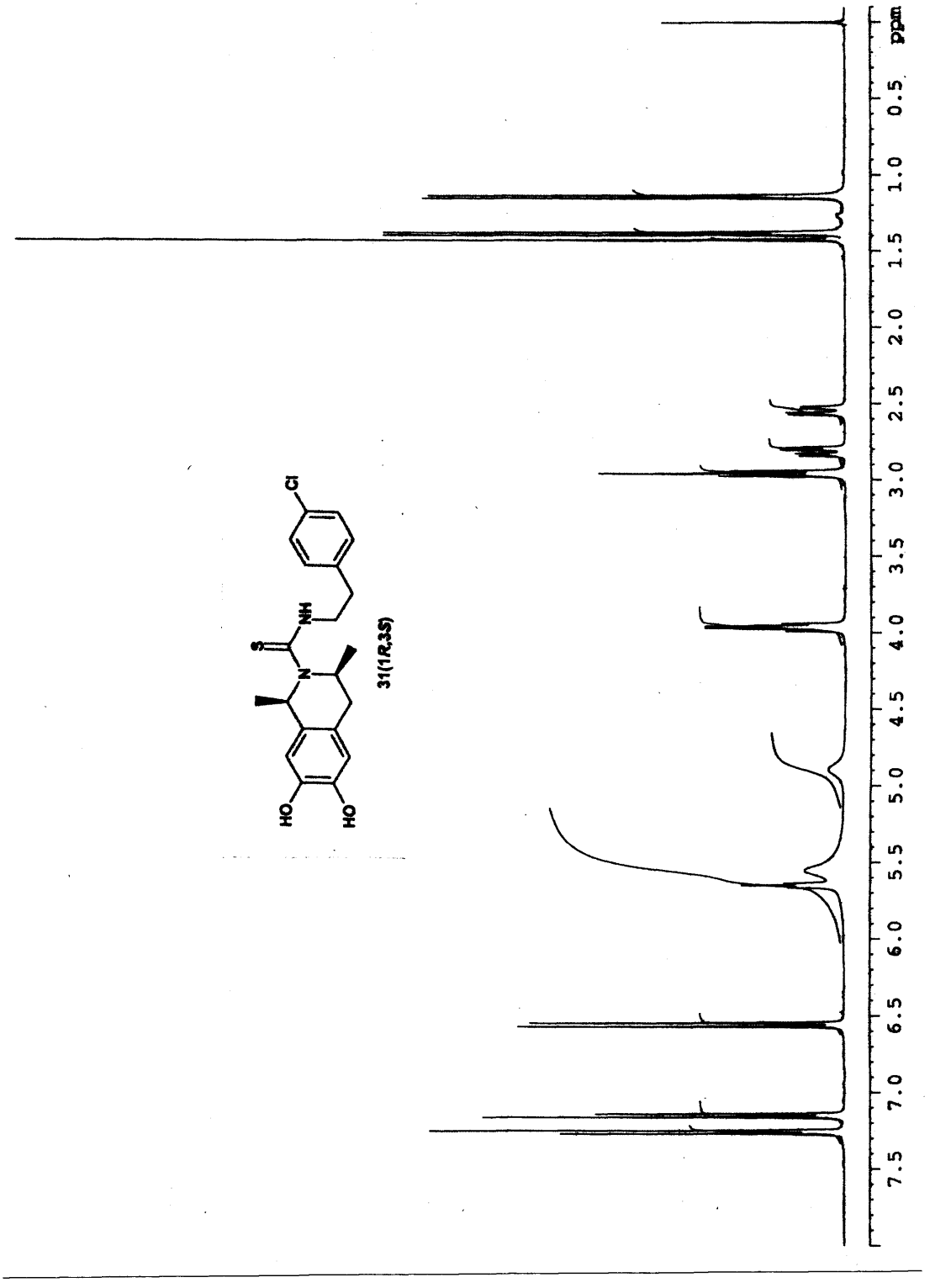
Cl
NH
S
N
HO
HO
31(1R,3S)
7.5
7.0
6.5
6.0
5.5
5.0
4.5
4.0
3.5
3.0
2.5
2.0
1.5
1.0
0.5
ppm

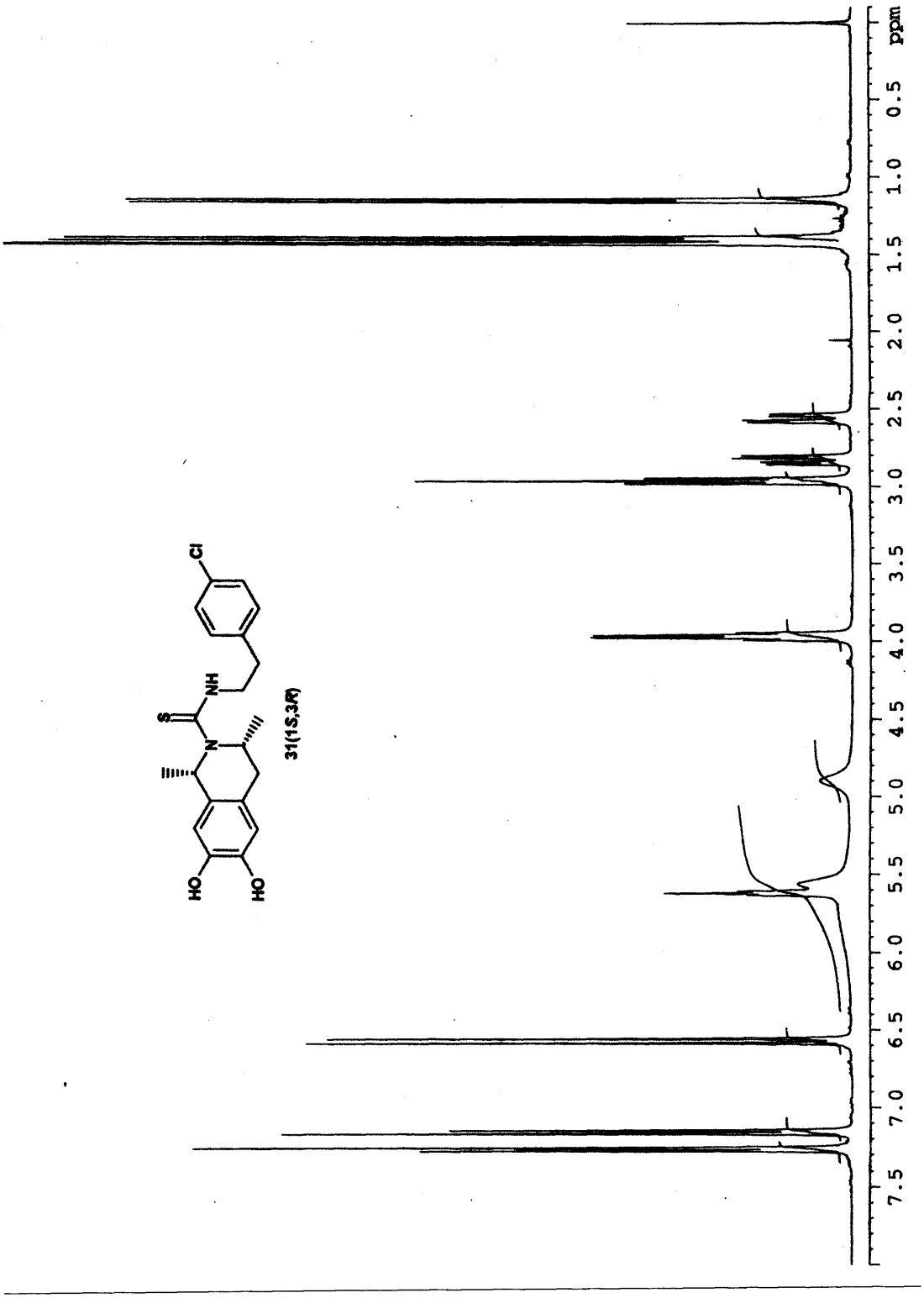
Cl
NH
S
N
HO
HO
31(1S,3R)
7.5
7.0
6.5
6.0
5.5
5.0
4.5
4.0
3.5
3.0
2.5
2.0
1.5
1.0
0.5
ppm

APPENDIX 3: ^{13}C-NMR spectra for the resolved stereoisomers of 29, 30 and 31

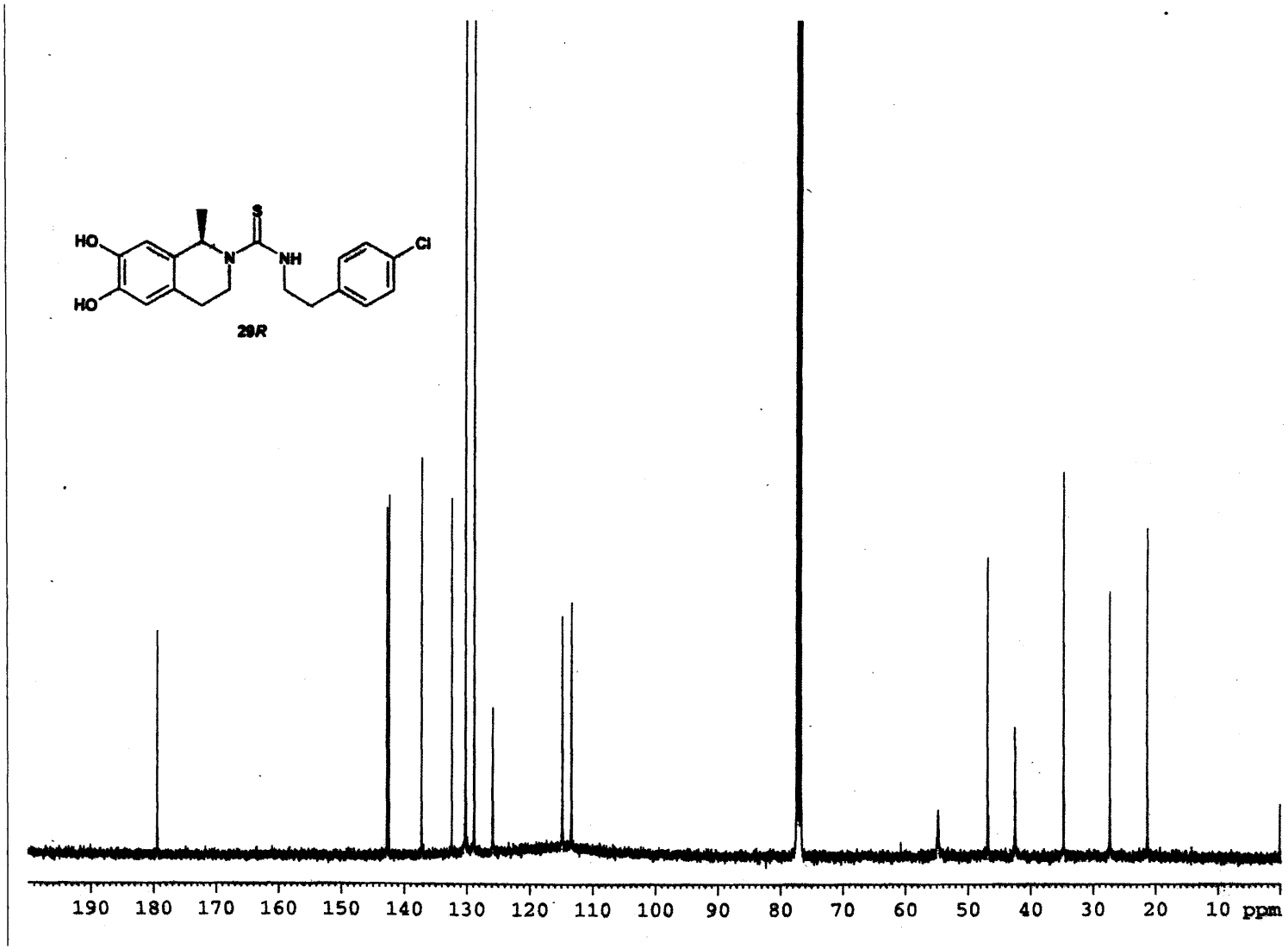
HO
HO
N
S
NH
Cl
29R
190 180 170 160 150 140 130 120 110 100 90 80 70 60 50 40 30 20 10 ppm

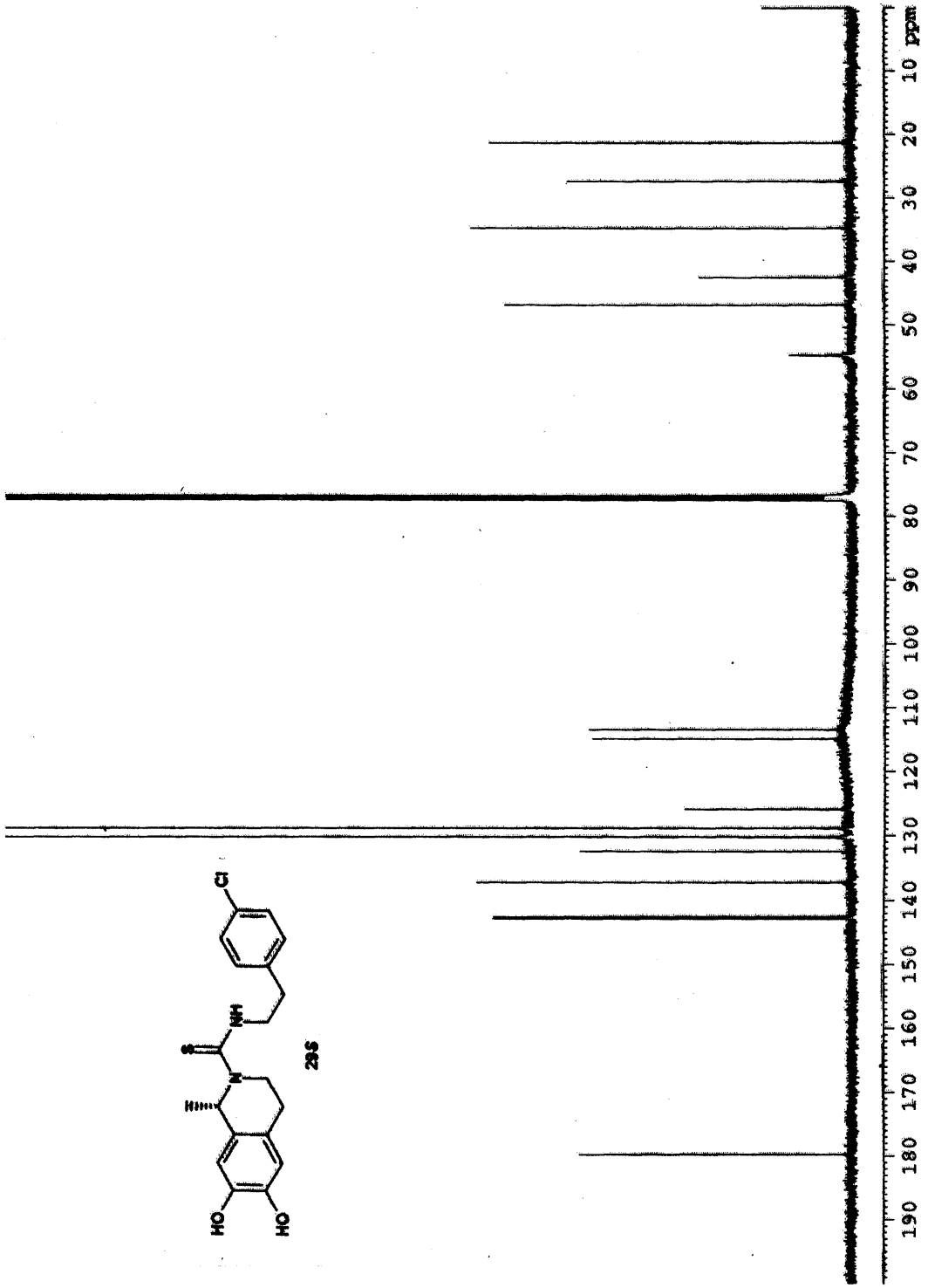
Cl
NH
N
HO
HO
296
ppm
10
20
30
40
50
60
70
80
90
100
110
120
130
140
150
160
170
180
190

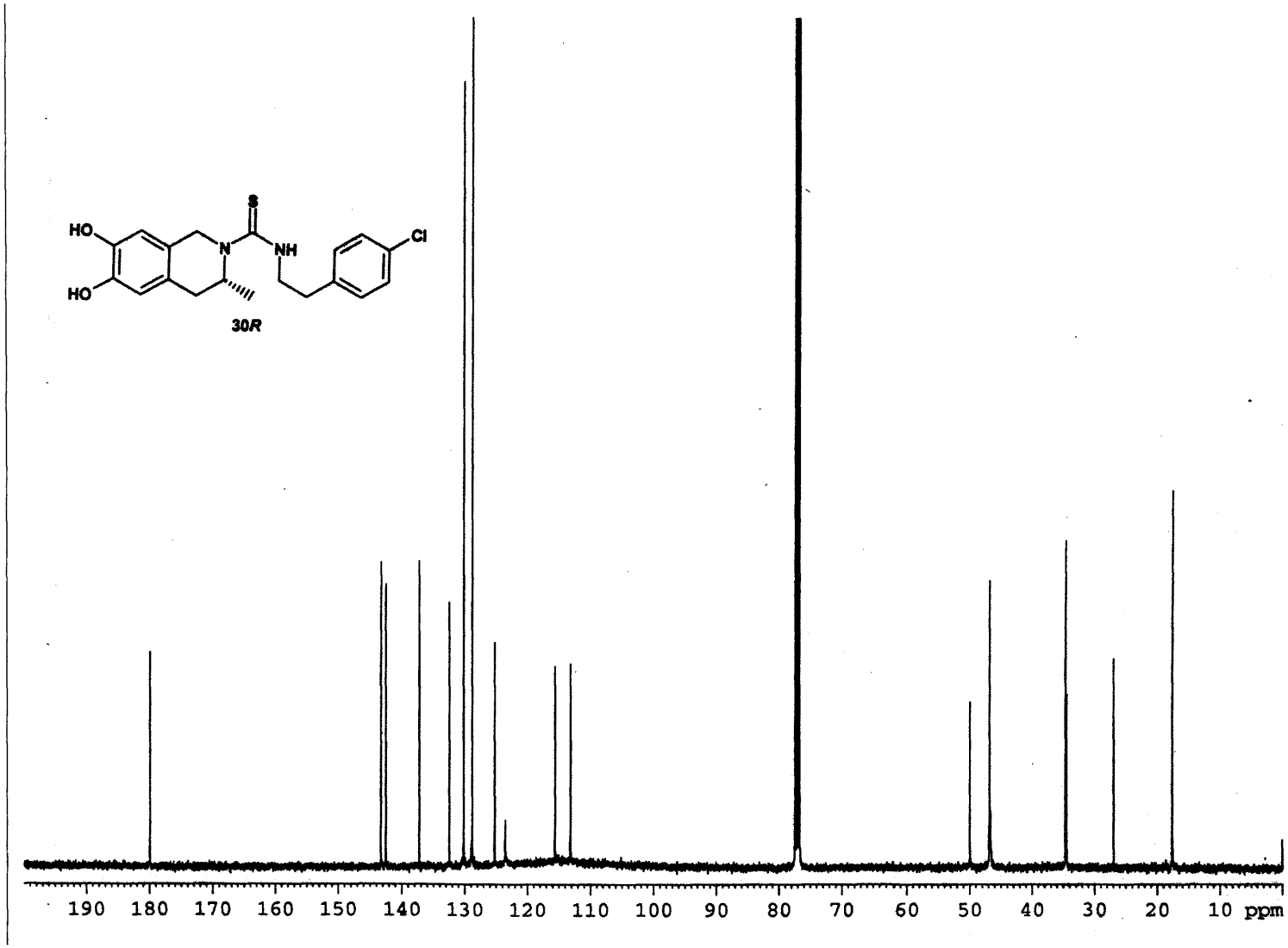
HO
HO
N
S
NH
Cl
30R
190 180 170 160 150 140 130 120 110 100 90 80 70 60 50 40 30 20 10 ppm

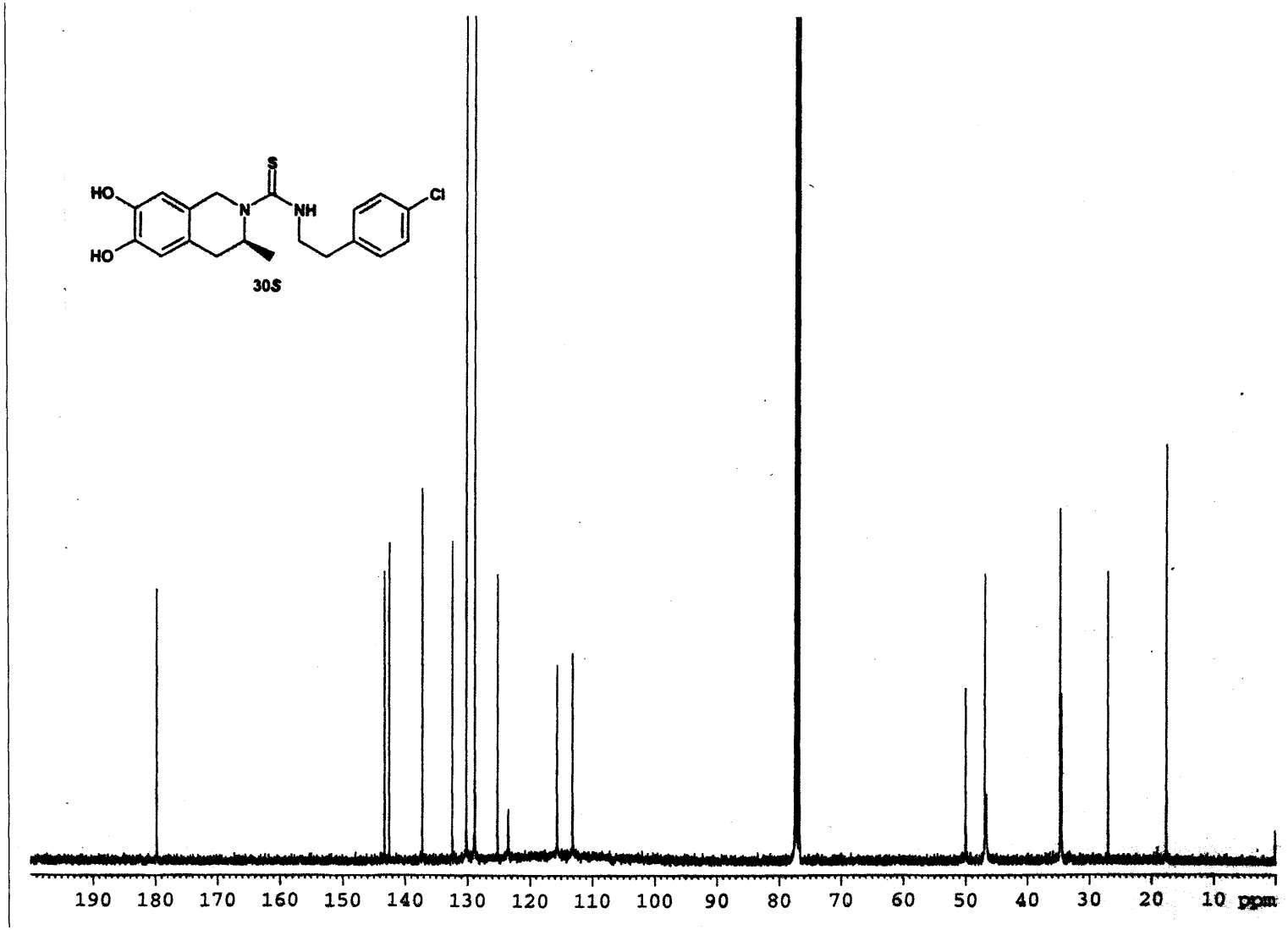
HO
HO
N
S
NH
Cl
30S
190 180 170 160 150 140 130 120 110 100 90 80 70 60 50 40 30 20 10 ppm

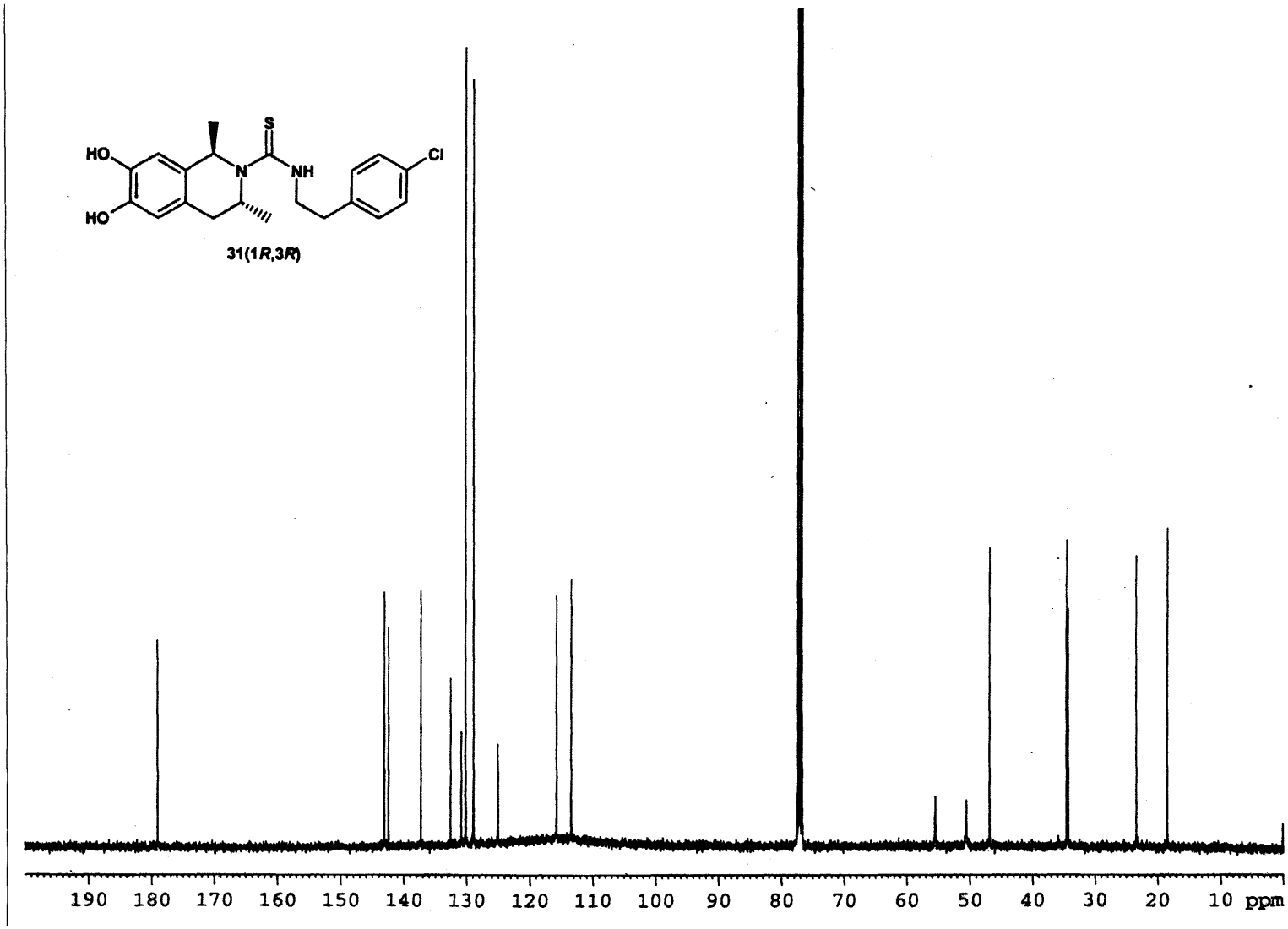
HO
HO
N
S
NH
Cl
31(1R,3R)
190 180 170 160 150 140 130 120 110 100 90 80 70 60 50 40 30 20 10 ppm

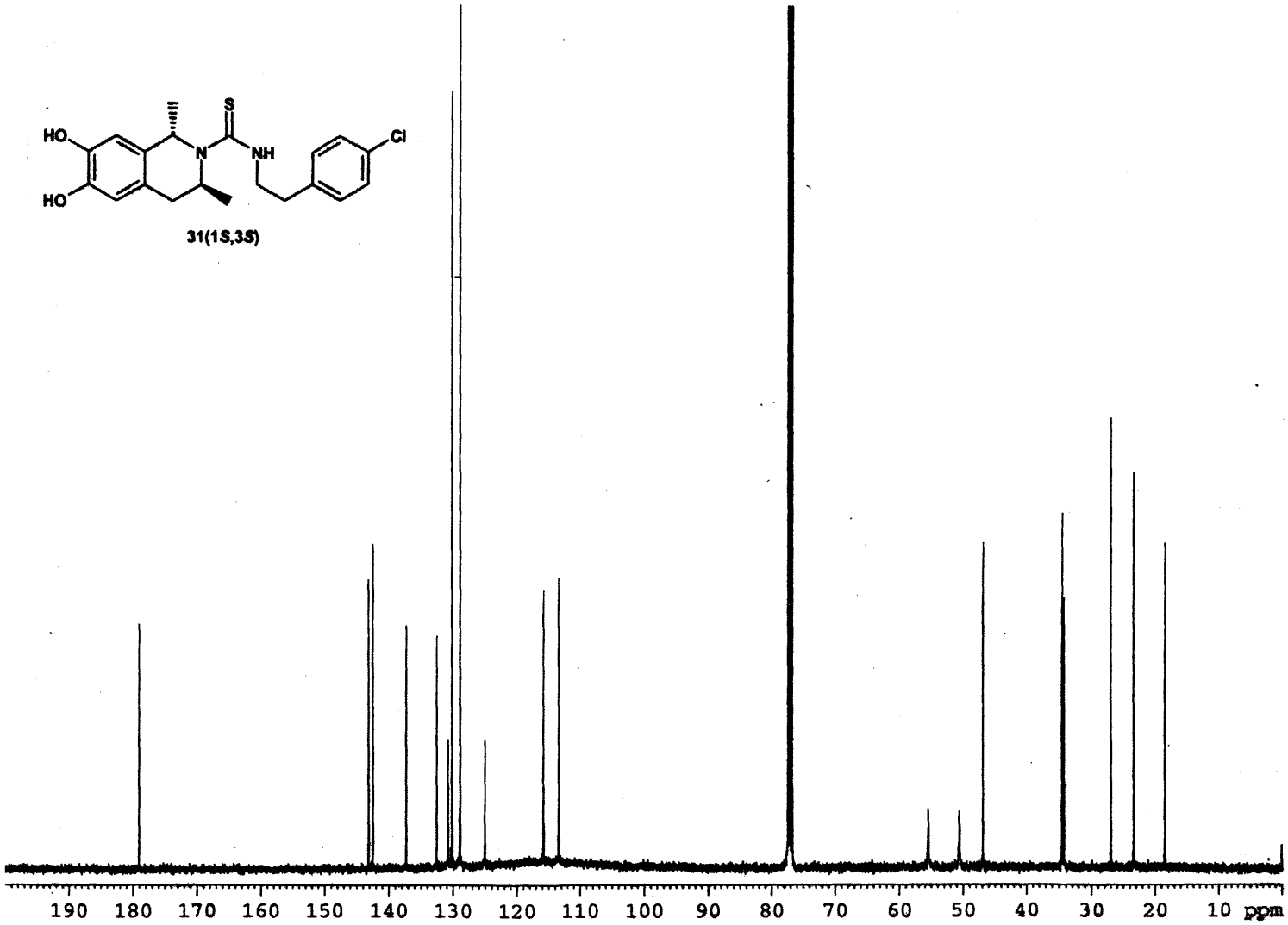
HO
HO
S
N
NH
Cl
31(1S,3S)
190 180 170 160 150 140 130 120 110 100 90 80 70 60 50 40 30 20 10 ppm

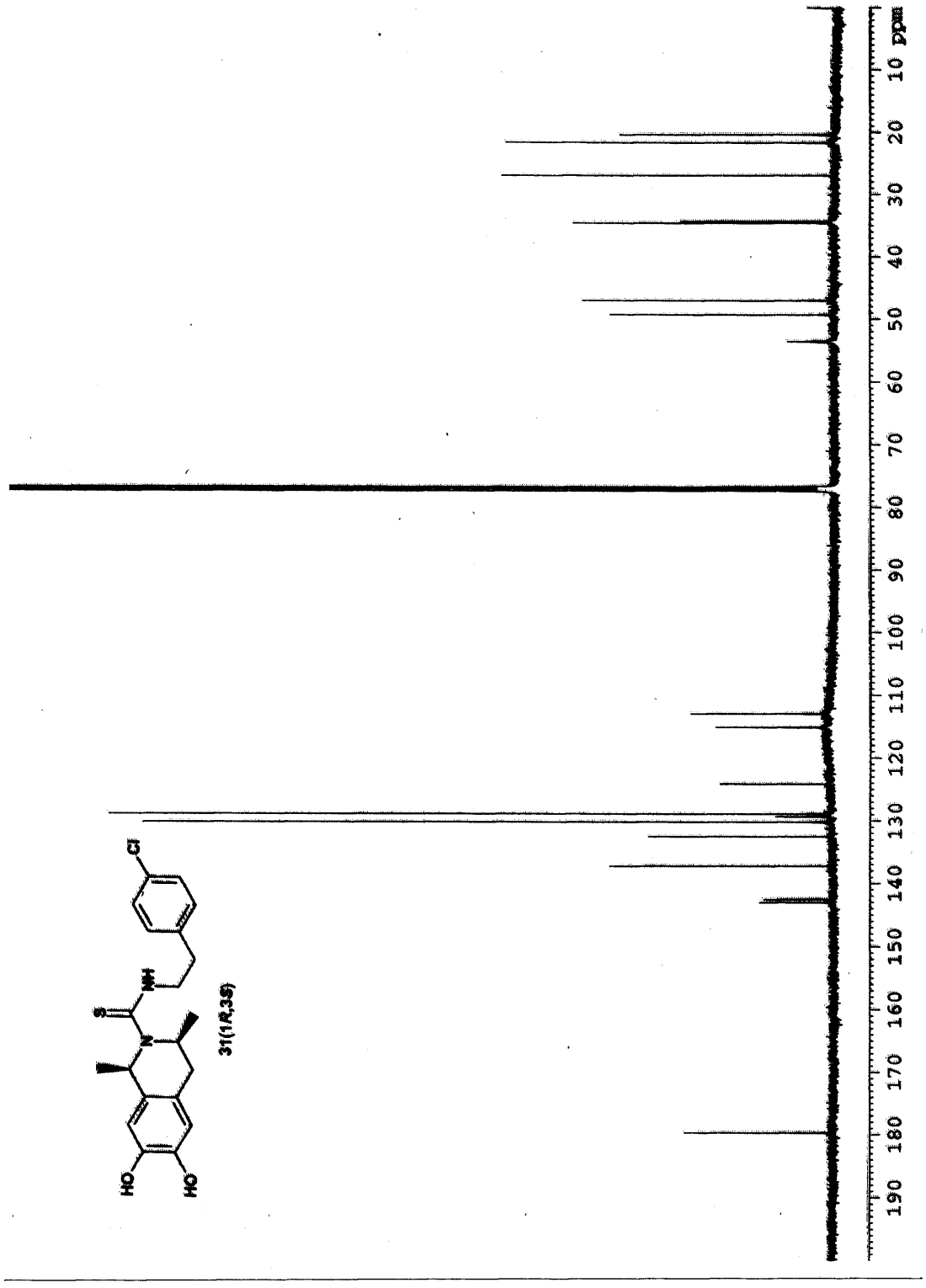
Cl
NH
S
N
HO
HO
31(1R,3S)
190 180 170 160 150 140 130 120 110 100 90 80 70 60 50 40 30 20 10 ppm

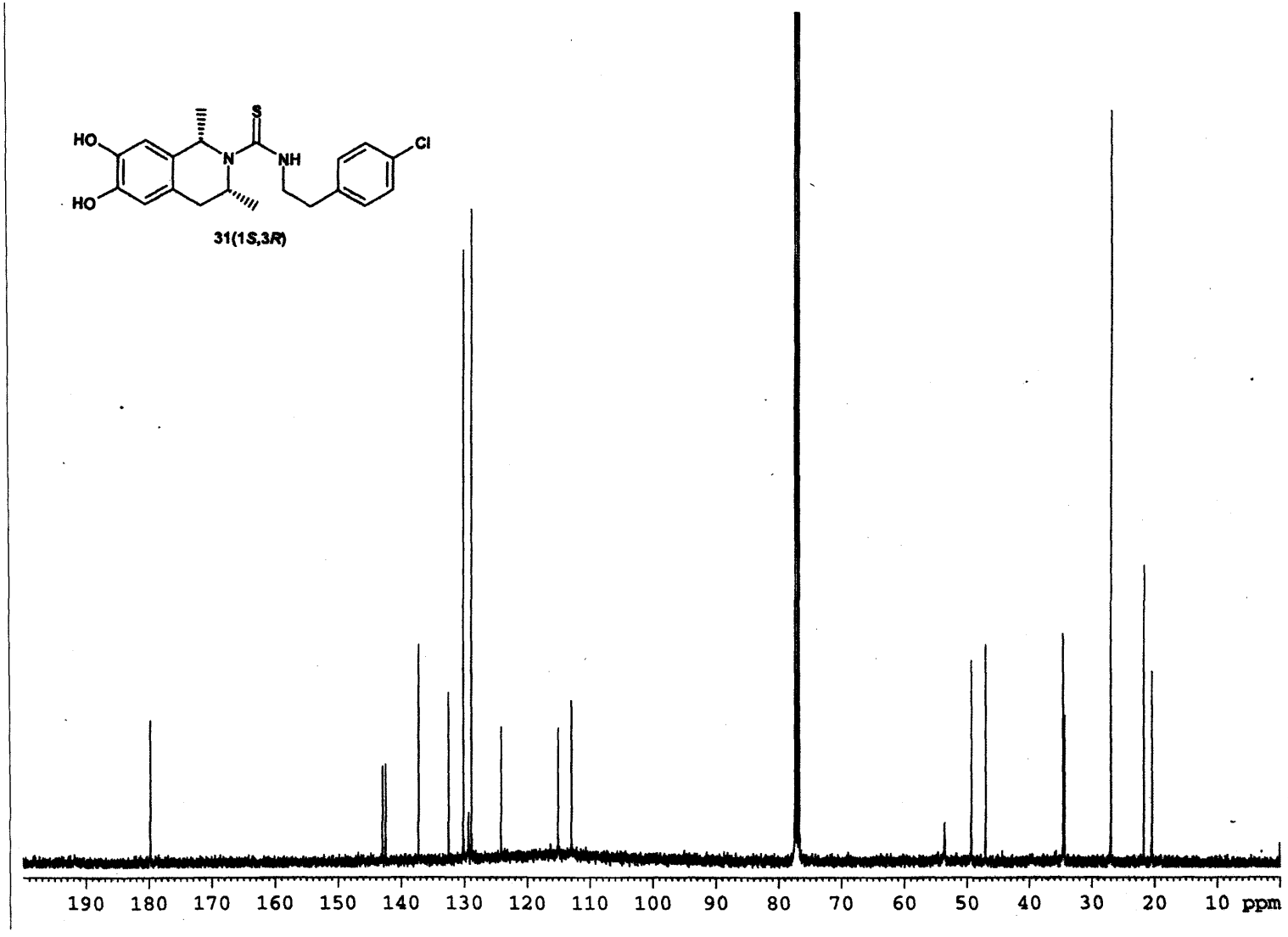
HO
HO
N
S
NH
Cl
31(1S,3R)
190 180 170 160 150 140 130 120 110 100 90 80 70 60 50 40 30 20 10 ppm